

Groundwater Model Poverty Bay Flats, Gisborne

Groundwater Modelling of the Poverty Bay Flats – Turanganui a Kiwa (Gisborne)

Report

3D FEFLOW Groundwater Model Poverty Bay Flats, Gisborne

Client:

WGA NZ

Wallbridge Gilbert Aztec New Zealand Pty LTD
15 Fitzherbert Street, Gisborne 4010

Gisborne District Council (GDC), New Zealand

Contractor:



Westheim • Berlin • Stuttgart • Passau

Joachim-Friedrich-Straße 48
10711 Berlin, Germany

AQUASOIL Ref.: AS210425

Berlin, 24/10/2022

Reviewed: Peter Schäz

Contents

1.	Executive Summary	20
2.	Introduction	21
2.1.	Background	21
2.2.	GDC Project Objectives	22
2.3.	Basic Data used for model setup, calibration, validation and scenarios.....	23
2.4.	Workflow from model setup to scenario runs.....	24
2.5.	Documentation	25
3.	Development and setup of the 3D groundwater model	27
3.1.	Basis of the groundwater flow model: 3D geological model and conceptual hydrogeological model (WGA).....	27
3.2.	Model area and horizontal discretization	29
3.3.	3D geometry model and vertical discretization	36
3.4.	Hydraulic properties and boundary conditions.....	47
3.4.1.	Hydraulic properties.....	47
3.4.2.	Hydraulic boundary conditions	53
3.4.3.	Spatially distributed groundwater recharge from rainfall	57
3.5.	Monitoring bores	59
4.	Calibration, validation and verification of the 3D groundwater model.....	64
4.1.	Steady State Calibration	64
4.1.1.	Parameters	64
4.1.2.	Results.....	65
4.2.	Sensitivity analyses for model parameters	72
4.2.1.	Parameters	72
4.2.2.	Results.....	72
4.3.	Transient Calibration (2008-2015) and Validation (2016-2021).....	76
4.3.1.	Parameters	76
4.3.2.	Results.....	79
4.4.	Simulation MAR-Trials 2017-2020	94
4.4.1.	Parameters	94
4.4.2.	Results.....	94
4.5.	Groundwater Age Simulation (residence times)	95
4.5.1.	Parameters	95

4.5.2.	Results	96
4.6.	Electrical conductivity simulation of MAR-Trials 2017 - 2020	96
4.6.1.	Parameters	96
4.6.2.	Results	96
4.7.	Additional transient simulation showing effect of additional evapotranspiration in summer ...	97
4.7.1.	Parameters	97
4.7.2.	Results	98
4.8.	Additional simulations with respect to artesian potential in the south eastern Matokitoki aquifer.....	99
4.8.1.	Parameters	99
4.8.2.	Results of steady state simulations	100
4.8.3.	Results of the transient simulation.....	104
4.8.4.	Evaluation of the results	108
4.9.	Summary of Calibration, validation and verification of the 3D groundwater model	109
4.10.	Overview of regional groundwater flow processes and remaining uncertainties	111
5.	Scenario Simulations – Groundwater Flow.....	116
5.1.	Scenario 1.1 Baseline (B)	120
5.1.1.	Scenario Parameters	120
5.1.2.	Scenario Results.....	120
5.2.	Scenario 2.1 Baseline + Climate Change (B+CC)	120
5.2.1.	Scenario Parameters	120
5.2.2.	Scenario Results.....	122
5.3.	Scenario 3.1 Natural State + Climate Change (NS)	128
5.3.1.	Scenario Parameters	128
5.3.2.	Scenario Results.....	128
5.4.	Scenario 4.1 Current Allocation Limit V2 + Climate Change	134
5.4.1.	Scenario Parameters	134
5.4.2.	Scenario Results.....	135
5.5.	Scenario 5.1 MAR 600,000 m ³ /season + Climate Change (M1)	141
5.5.1.	Scenario Parameters	141
5.5.2.	Scenario Results.....	143
5.6.	Scenario 7.1 Sustainable Allocation + Climate Change (SA)	149
5.6.1.	Scenario Parameters	149
5.6.2.	Scenario Results.....	151

5.7.	Sensitive locations	157
5.8.	Scenarios Summary	162
6.	Water quality (salinity) simulation	166
6.1.	Poverty Bay Flats Conceptual Groundwater Quality Model (WGA).....	166
6.2.	Model parameterisation for salinity simulation	169
6.3.	Salinity Simulation for the calibration and validation period 2008-2021	176
6.4.	Scenario simulation results	185
6.5.	Salinity simulation summary.....	187
7.	Summary and recommendations	189
8.	Literature	190

Figures

Figure 1-1:	Example for vertical plot view from html file	25
Figure 1-2:	Example for html time-series shown from html file	26
Figure 2-1:	Left: Model area (orange line), rivers/streams/drains (blue lines); Right: Subareas specified by mesh guidance (dash lines), where the red line indicates an approximate model boundary only [1].	30
Figure 2-2:	Left: Supermesh elements (basis for mesh generation); Right: Finite element mesh.	31
Figure 2-3:	Statistics of element sizes of the finite element mesh (histogram on top, percentiles below).	32
Figure 2-4:	Statistics of maximum inner element angles of the finite element mesh (histogram on top, percentiles below).	33
Figure 2-5:	Left: elements around MAR-Trial site; Right: MAR-Trial site GPE066-GPE009-GPE065 in detail.	34
Figure 2-6:	Upper: mesh along coastline before additional refinement; lower: mesh after refinement	35
Figure 2-7:	Overview of lateral distributions / extents of the surface elevation data of the 10 basic units.	37
Figure 2-8:	Scheme of converting the surface elevation grid data into a corresponding 3D FEFLOW geometry model.	39
Figure 2-9:	3D view of the 3D groundwater model built with the 10 hydrogeological units, vertical exaggeration 1:10.	39
Figure 2-10:	3D view of the hydrogeological unit undefined (primary layer 1), vertical exaggeration 1:10.	40
Figure 2-11:	3D view of the hydrogeological unit Te Hapara Sands aquifer (primary layer 2), vertical exaggeration 1:10.	40
Figure 2-12:	3D view of the hydrogeological unit Shallow Fluvial aquifer (primary layer 3), vertical exaggeration 1:10.	41
Figure 2-13:	3D view of the hydrogeological unit Aquitard 1 (primary layer 4), vertical exaggeration 1:10.	41
Figure 2-14:	3D view of the hydrogeological unit Waipaoa aquifer (primary layer 5), vertical exaggeration 1:10.	42
Figure 2-15:	3D view of the hydrogeological unit Aquitard 2 (primary layer 6), vertical exaggeration 1:10.	42
Figure 2-16:	3D view of the hydrogeological unit Makauri aquifer (primary layer 7), vertical exaggeration 1:10.	43
Figure 2-17:	3D view of the hydrogeological unit Aquitard 3 (primary layer 8), vertical exaggeration 1:10.	43



Figure 2-18:	3D view of the hydrogeological unit Matokitoki aquifer (primary layer 9), vertical exaggeration 1:10.	44
Figure 2-19:	3D view of the hydrogeological unit Aquitard 4 (primary layer 10), vertical exaggeration 1:10.	44
Figure 2-20:	3D view of the model bottom eq. to the base of the Quaternary sediments, i.e., the upper surface Basement incl. the base of the hydrogeological unit Aquitard 4 (primary layer 10), vertical exaggeration 1:10.	45
Figure 2-21:	Cross section lines.....	45
Figure 2-22:	Vertical 2D view of North-South cross section 1 (NS-CS#1).....	46
Figure 2-23:	Vertical 2D view of West-East cross section 1 (WE-CS#1).....	46
Figure 2-24:	Vertical 2D view of West-East cross section 2 (WE-CS#2).....	46
Figure 2-25:	Vertical 2D view of West-East cross- section 3 (WE-CS#3).	46
Figure 2-26:	Vertical 2D view of West-East cross section 4 (WE-CS#4).....	47
Figure 2-27:	Overview of hydraulic conductivity of Undefined (left) and Te Hapara Sands + Shallow Fluviatile (right).....	49
Figure 2-28:	Overview of hydraulic conductivity of Aquitard 1 (left) and Waipaoa Aquifer (right).	50
Figure 2-29:	Overview of hydraulic conductivity of Aquitard 2 (left) and Makauri aquifer (right). ..	51
Figure 2-30:	Overview of hydraulic conductivity of Aquitard 3 (left) and Matokitoki aquifer (right).	52
Figure 2-31:	Locations of the transfer boundary condition (3 rd -kind BC shown in green) implemented for Waipaoa River and other local streams and drains (left), along with corresponding riverbed conductance (for flow direction groundwater to surface water) (right).	54
Figure 2-32:	Overview of well boundary conditions () in Te Hapara Sands and Shallow Fluviatile aquifers (left) and Waipaoa aquifer (right).....	56
Figure 2-33:	Overview of well boundary conditions () in Makauri (left) and Matokitoki aquifers (right).....	57
Figure 2-34:	Overview of groundwater recharge from rainfall (left) and climate zonation (right)...	59
Figure 2-35:	Monitoring bores in Te Hapara Sands, Shallow Fluviatile and Unspecified aquifers.	60
Figure 2-36:	Monitoring bores in Waipaoa aquifer.	61
Figure 2-37:	Monitoring bores in Makauri aquifer.	62
Figure 2-38:	Monitoring bores in Matokitoki aquifer.	63
Figure 3-1:	Scatter plot of simulated vs measured water levels, steady state calibration.	68
Figure 3-2:	Simulated GW level contours in Te Hapara Sands/Shallow Fluviatile aquifer (left) and in Makauri aquifer (right), steady state calibration.....	71

Figure 3-3:	Simulated GW levels along the North-South cross section 1 (NS-CS#1), steady state calibration.	71
Figure 3-4:	Scatter plot of simulated vs measured water levels, SSC (left), SSC 5X-TRSF.	74
Figure 3-5:	Scatter plot of simulated vs measured water levels, SSC (left), SSC 1/5X-AQTD. ..	74
Figure 3-6:	Scatter plot of simulated vs measured water levels, SSC (left), SSC 1/5X-WA.	75
Figure 3-7:	Scatter plot of simulated vs measured water levels, SSC (left), SSC 5X-MA (right).	75
Figure 3-8:	Scatter plot of simulated vs measured water levels, SSC (left), SSC 1/5X-MTKA (right).....	75
Figure 3-9:	Abstraction data 2008/2009 - 2020/2021 monthly rates (upper) and annual amounts (lower).	77
Figure 3-10:	Time series of water level records (mRL) Waipaoa river at gauging station 4 (blue), station 3 (light green) and station 8 (purple) used for interpolation.	78
Figure 3-11:	Time series of water level records (mRL) Taruheru river at gauging station 2 (blue), station 1 (light green) and at its estuary (purple) used for interpolation.	78
Figure 3-12:	Rainfall (light blue) and average groundwater recharge (light green) within the recharge period over the model area.	79
Figure 3-13:	Hydraulic-head distribution in the shallow aquifers at the beginning of the calibration/validation period	80
Figure 3-14:	Hydraulic-head distribution in the shallow aquifers at the end of the calibration/validation period	81
Figure 3-15:	Simulated vs measured water levels in Te Hapara Sand aquifer bores, transient calibration+validation.	82
Figure 3-16:	Simulated vs measured water levels in Shallow Fluvatile aquifer bores, transient calibration+validation.	82
Figure 3-17:	Hydraulic-head distribution in the Waipaoa at the beginning of the calibration/validation period	83
Figure 3-18:	Hydraulic-head distribution in the Waipaoa at the end of the calibration/validation period	84
Figure 3-19:	Hydraulic-head distribution in the Makauri aquifer at the beginning of the calibration/validation period	85
Figure 3-20:	Hydraulic-head distribution in the Makauri aquifer at the end of the calibration/validation period	86
Figure 3-21:	Hydraulic-head distribution in the Matokitoki aquifer at the beginning of the calibration/validation period	87
Figure 3-22:	Hydraulic-head distribution in the Matokitoki aquifer at the end of the calibration/validation period	88
Figure 3-23:	Simulated vs measured water levels in Waipaoa aquifer bores, transient calibration+validation.	89


Figure 3-24:	Simulated vs measured water levels in Waipaoa and Makauri aquifer bores (Ferry Road Monitoring), transient calibration+validation.	89
Figure 3-25:	Simulated vs measured water levels in Waipaoa and Makauri aquifer bores (Caesar Road Monitoring), transient calibration+validation.	90
Figure 3-26:	Simulated vs measured water levels in Makauri aquifer bores, transient calibration+validation.	90
Figure 3-27:	Simulated vs measured water levels in Matokitoki aquifer bores, transient calibration+validation.	90
Figure 3-28:	Simulated vs measured water levels in in Te Hapara Sand, Makauri and Matokitoki aquifer bores (Cameron Road Monitoring), transient calibration+validation.	91
Figure 3-29:	Scatter plot of simulated vs measured mean water levels of validation period 2016 – 2021.	92
Figure 3-30:	Histogram of correlation coefficients of simulated and measured water levels in the validation period 2016 – 2021.	92
Figure 3-31:	Scatter plot of scaled Mean Difference and Correlation coefficient of simulated and measured water levels in the validation period 2016 – 2021, classified by the shallow aquifers Te Hapara Sand+Shallow Fluviatile and the deep aquifers Waipaoa, Makauri and Matokitoki.	93
Figure 3-32:	Simulation results comparison with measured data	95
Figure 3-33:	Simulated vs measured electrical Conductivity (EC) of results	97
Figure 3-34:	Location of specified areas with possible evapotranspiration in summer.	98
Figure 3-35:	Simulated vs measured water levels of bore GPD063 in Te Hapara Sand aquifer, transient calibration+validation and transient calibration+validation considering evapotranspiration in the summer period	99
Figure 3-36:	Location of the assumed Hydraulic-head BC  and modified hydraulic conductivity for the Matokitoki aquifer.	100
Figure 3-37:	Scatter plot of simulated vs measured water levels, SSC (left), 1st-BC MTKA 11 mRL.	101
Figure 3-38:	Scatter plot of simulated vs measured water levels, SSC (left), 1st-BC MTKA 10 mRL.	102
Figure 3-39:	Simulated groundwater levels of the Matokitoki aquifer, Steady state calibration SCC.	102
Figure 3-40:	Simulated groundwater levels of the Matokitoki aquifer, Simulation with the 1 st -BC of 11 mRL.	103
Figure 3-41:	Simulated groundwater levels of the Matokitoki aquifer, Steady state simulation with the 1 st -BC of 10 mRL.	104
Figure 3-42:	Simulated vs measured water levels in Matokitoki aquifer bores GPB130 and GPB128, transient calibration+validation and transient simulation with 1st-kind BC 10 mRL.	105

Figure 3-43:	Simulated vs measured water levels in Matokitoki aquifer bores GPB102 and GPB103, transient calibration+validation and transient simulation with 1st-kind BC 10 mRL.	106
Figure 3-44:	Simulated vs measured water levels in Matokitoki aquifer bores GPB117 and GPB118, transient calibration+validation and transient simulation with 1st-kind BC 10 mRL.	107
Figure 3-45:	Simulated vs measured water levels in Matokitoki aquifer bores GPF108 and GPD132, transient calibration+validation and transient simulation with 1st-kind BC 10 mRL.	108
Figure 3-36:	Simulated vs measured water levels of bore GPJ040 in the Shallow Fluviatile aquifer.	109
Figure 3-37:	Simulated vs measured water levels of bore GPF071 in the Makauri aquifer.	110
Figure 4-1:	Difference of simulated groundwater level between scenario 2.1 and scenario 1.1 in the shallow aquifer system	123
Figure 4-2:	Difference of simulated groundwater level between scenario 2.1 and scenario 1.1 in the Waipaoa aquifer.....	124
Figure 4-3:	Difference of simulated groundwater level between scenario 2.1 and scenario 1.1 in the Makauri aquifer	125
Figure 4-4:	Difference of simulated groundwater level between scenario 2.1 and scenario 1.1 in the Matokitoki aquifer.....	126
Figure 4-5:	Comparison of hydraulic head in summer and winter between scenarios 2.1 and 1.1, observation bore GPF035 (Makauri)	127
Figure 4-6:	Comparison of hydraulic head in summer and winter between scenarios 2.1 and 1.1, observation bore GPC100 (Te Hapara Sands)	128
Figure 4-7:	Difference of simulated groundwater level between scenario 3.1 and scenario 2.1 in the shallow aquifer system	129
Figure 4-8:	Difference of simulated groundwater level between scenario 3.1 and scenario 2.1 in the Waipaoa aquifer.....	130
Figure 4-9:	Difference of simulated groundwater level between scenario 3.1 and scenario 2.1 in the Makauri aquifer	131
Figure 4-10:	Difference of simulated groundwater level between scenario 3.1 and scenario 2.1 in the Matokitoki aquifer.....	132
Figure 4-11:	Difference of simulated groundwater level between scenario 3.1 and scenario 2.1 over time, observation bore GPF 159 (Makauri)	133
Figure 4-12:	Comparison of hydraulic head in summer and winter between scenarios 3.1 and 2.1, observation bore GPF159 (Makauri)	133
Figure 4-13:	Comparison of hydraulic head in summer and winter between scenarios 3.1 and 2.1, observation bore GPC097 (Te Hapara Sands)	134

Figure 4-14:	Difference of simulated groundwater level between scenario 4.1 and scenario 2.1 in the shallow aquifer system	136
Figure 4-15:	Difference of simulated groundwater level between scenario 4.1 and scenario 2.1 in the Waipaoa aquifer.....	137
Figure 4-16:	Difference of simulated groundwater level between scenario 4.1 and scenario 2.1 in the Makauri aquifer	138
Figure 4-17:	Difference of simulated groundwater level between scenario 4.1 and scenario 2.1 in the Matokitoki aquifer.....	139
Figure 4-18:	Difference of simulated groundwater level between scenario 4.1 and scenario 2.1 over time, observation bore GPC031 (Te Hapara Sands)	140
Figure 4-19:	Comparison of hydraulic head in summer and winter between scenarios 4.1 and 2.1, observation bore GPC031 (Te Hapara Sands)	140
Figure 4-20:	Comparison of hydraulic head in summer and winter between scenarios 4.1 and 2.1, observation bore GPJ040 (Makauri).....	141
Figure 4-21:	Locations of the 6 MAR bores in scenario 5.1 [15].....	142
Figure 4-22:	Difference of simulated groundwater level between scenario 5.1 and scenario 2.1 in the shallow aquifer system	144
Figure 4-23:	Difference of simulated groundwater level between scenario 5.1 and scenario 2.1 in the Waipaoa aquifer.....	145
Figure 4-24:	Difference of simulated groundwater level between scenario 5.1 and scenario 2.1 in the Makauri aquifer	146
Figure 4-25:	Difference of simulated groundwater level between scenario 5.1 and scenario 2.1 in the Matokitoki aquifer.....	147
Figure 4-26:	Difference of simulated groundwater level between scenario 5.1 and scenario 2.1 over time, observation bore GPE030 (Makauri)	148
Figure 4-27:	Comparison of hydraulic head in summer and winter between scenarios 4.1 and 2.1, observation bore GPE030 (Makauri)	148
Figure 4-28:	Simulated groundwater potential in scenario 5.1 over time, observation bore GPF090 (Makauri).....	149
Figure 4-29:	Difference of simulated groundwater level between scenario 7.1 and scenario 2.1 in the shallow aquifer system	152
Figure 4-30:	Difference of simulated groundwater level between scenario 7.1 and scenario 2.1 in the Waipaoa aquifer.....	153
Figure 4-31:	Difference of simulated groundwater level between scenario 7.1 and scenario 2.1 in the Makauri aquifer	154
Figure 4-32:	Difference of simulated groundwater level between scenario 7.1 and scenario 2.1 in the Matokitoki aquifer.....	155

Figure 4-33:	Simulated groundwater potential in scenario 7.1 and 2.1 over time, observation bore GPC112 (Makauri), current summer level highlighted in green, declining level in scenario 7.1 in red.	156
Figure 4-34:	Comparison of hydraulic head in summer and winter between scenarios 7.1 and 2.1, observation bore GPC112 (Makauri)a.....	156
Figure 4-35:	Sensitive locations as compiled by GDC based on project meetings.	157
Figure 4-36:	Difference between scenario 2.1 and scenario 1.1, GPA003.....	158
Figure 4-37:	Difference between scenario 3.1, 4.1, 5.1, 7.1 and scenario 2.1, GPA003.	158
Figure 4-38:	Difference between scenario 2.1 and scenario 1.1, GPC080.	159
Figure 4-39:	Difference between scenario 3.1, 4.1, 5.1, 7.1 and scenario 2.1, GPC080.	159
Figure 4-40:	Difference between scenario 2.1 and scenario 1.1, GPC029.	160
Figure 4-41:	Difference between scenario 3.1, 4.1, 5.1, 7.1 and scenario 2.1, GPC029.	160
Figure 4-42:	Difference between scenario 2.1 and scenario 1.1, GPB099.....	161
Figure 4-43:	Difference between scenario 3.1, 4.1, 5.1, 7.1 and scenario 2.1, GPB099.	161
Figure 4-44:	Interaction with Waipoa river at the end of the simulation period (summer and winter season) for all scenarios at the end of the simulation period.	165
Figure 5-1:	Initial Cl concentration distribution and concentration of rainfall recharge in Te Hapara Sands aquifer [16].....	167
Figure 5-2:	Initial Cl concentration distribution and concentration of rainfall recharge in Shallow Fluviatile aquifer [16].....	167
Figure 5-3:	Initial distribution of Cl concentration in Waipaoa Aquifer [16].	168
Figure 5-4:	Initial distribution of Cl concentration in Makauri Aquifer [16].....	168
Figure 5-5:	Initial distribution of Cl concentration in Matokitoki Aquifer [16].	169
Figure 5-6:	Initial distribution of Cl concentration and concentration of rainfall recharge assigned to Te Hapara Sands and Shallow Fluviatile aquifers.....	170
Figure 5-7:	Initial distribution of Cl concentration and concentration of rainfall recharge assigned to Waipaoa aquifer.....	171
Figure 5-8:	Initial distribution of Cl concentration assigned to Makauri aquifer.	172
Figure 5-9:	Initial Cl concentration assigned Matokitoki aquifer.	173
Figure 5-10:	Initial distribution of Cl concentration and concentration of rainfall recharge assigned ro User Data RechargeConcentration in the top model layer.....	174
Figure 5-11:	Cl concentration boundary conditions for Makauri Aquifer along its north-western boundary	175
Figure 5-12:	Cl concentration boundary conditions for Aquitard 2 in the north-west, above the Makauri aquifer	176
Figure 5-13:	Simulated vs measured Cl concentrations of selected bores in the Makauri aquifer.	177

Figure 5-14:	Simulated vs measured Cl concentrations of selected bores in the Matokitoki aquifer.....	178
Figure 5-15:	Simulated vs measured Cl concentrations of selected bores in the Waipaoa Aquifer	179
Figure 5-16:	Simulated vs measured Cl concentrations of selected bores in the Te Hapara Sand Aquifer.....	180
Figure 5-17:	Simulated Cl concentrations and groundwater levels on 30 June 2021 in Te Hapara Sands / Shallow Fluviatile aquifer.....	181
Figure 5-18:	Simulated Cl concentrations and groundwater levels on 30 June 2021 in Waipaoa aquifer.....	182
Figure 5-19:	Simulated Cl concentrations and groundwater levels on 30/06/2021 in Makauri aquifer	183
Figure 5-20:	Simulated Cl concentrations and groundwater levels on 30/06/2021 in Matokitoki aquifer	184
Figure 5-21:	Locations of fictive observation points along three transects.....	185
Figure 5-22:	Difference between scenarios 2.1 and 2.1 and scenarios 3.1, 4.1, 5.1, 7.1 and scenario 2.1, Transect2-Obs1.....	186
Figure 5-23:	Simulated chloride concentration in scenarios 1.1-7.1 over time, observation bore GPF035 (Makauri).....	187
Figure A3-1:	Legacy scenarios: Difference between scenarios 2 and 1, shallow aquifers, summer	X
Figure A3-2:	Legacy scenarios: Difference between scenarios 2 and 1, shallow aquifers, winter	XI
Figure A3-3:	Legacy scenarios: Difference between scenarios 2 and 1, Waipaoa aquifer, summer	XII
Figure A3-4:	Legacy scenarios: Difference between scenarios 2 and 1, Waipaoa aquifer, winter	XIII
Figure A3-5:	Legacy scenarios: Difference between scenarios 2 and 1, Makauri aquifer, summer	XIV
Figure A3-6:	Legacy scenarios: Difference between scenarios 2 and 1, Makauri aquifer, winter	XV
Figure A3-7:	Legacy scenarios: Difference between scenarios 2 and 1, Matokitoki aquifer, summer	XVI
Figure A3-8:	Legacy scenarios: Difference between scenarios 2 and 1, Matokitoki aquifer, winter	XVII
Figure A3-9:	Legacy scenarios: Difference between scenarios 3 and 2, shallow aquifers, summer	XIX
Figure A3-10:	Legacy scenarios: Difference between scenarios 3 and 2, shallow aquifers, winter	XX
Figure A3-11:	Legacy scenarios: Difference between scenarios 3 and 2, Waipaoa aquifer, summer	XXI

Figure A3-12:	Legacy scenarios: Difference between scenarios 3 and 2, Waipaoa aquifer, winter	XXII
Figure A3-13:	Legacy scenarios: Difference between scenarios 3 and 2, Makauri aquifer, summer	XXIII
Figure A3-14:	Legacy scenarios: Difference between scenarios 3 and 2, Makauri aquifer, winter	XXIV
Figure A3-15:	Legacy scenarios: Difference between scenarios 3 and 2, Matokitoki aquifer, summer	XXV
Figure A3-16:	Legacy scenarios: Difference between scenarios 3 and 2, Matokitoki aquifer, winter	XXVI
Figure A3-17:	Legacy scenarios: Difference between scenarios 4 and 2, shallow aquifers, summer	XXVIII
Figure A3-18:	Legacy scenarios: Difference between scenarios 4 and 2, shallow aquifers, winter	XXIX
Figure A3-19:	Legacy scenarios: Difference between scenarios 4 and 2, Waipaoa aquifer, summer	XXX
Figure A3-20:	Legacy scenarios: Difference between scenarios 4 and 2, Waipaoa aquifer, winter	XXXI
Figure A3-21:	Legacy scenarios: Difference between scenarios 4 and 2, Makauri aquifer, summer	XXXII
Figure A3-22:	Legacy scenarios: Difference between scenarios 4 and 2, Makauri aquifer, winter	XXXIII
Figure A3-23:	Legacy scenarios: Difference between scenarios 4 and 2, Matokitoki aquifer, summer	XXXIV
Figure A3-24:	Legacy scenarios: Difference between scenarios 4 and 2, Matokitoki aquifer, winter	XXXV
Figure A3-25:	Legacy scenarios: Difference between scenarios 5 and 2, shallow aquifers, summer	XXXVII
Figure A3-26:	Legacy scenarios: Difference between scenarios 5 and 2, shallow aquifers, winter	XXXVIII
Figure A3-27:	Legacy scenarios: Difference between scenarios 5 and 2, Waipaoa aquifer, summer	XXXIX
Figure A3-28:	Legacy scenarios: Difference between scenarios 5 and 2, Waipaoa aquifer, winter	XL
Figure A3-29:	Legacy scenarios: Difference between scenarios 5 and 2, Makauri aquifer, summer	XLI
Figure A3-30:	Legacy scenarios: Difference between scenarios 5 and 2, Makauri aquifer, winter	XLII
Figure A3-31:	Legacy scenarios: Difference between scenarios 5 and 2, Matokitoki aquifer, summer	XLIII

Figure A3-32:	Legacy scenarios: Difference between scenarios 5 and 2, Matokitoki aquifer, winter	XLIV
Figure A3-33:	Legacy scenarios: Difference between scenarios 6 and 2, shallow aquifers, summer	XLVI
Figure A3-34:	Legacy scenarios: Difference between scenarios 6 and 2, shallow aquifers, winter	XLVII
Figure A3-35:	Legacy scenarios: Difference between scenarios 6 and 2, Waipaoa aquifer, summer	XLVIII
Figure A3-36:	Legacy scenarios: Difference between scenarios 6 and 2, Waipaoa aquifer, winter	XLIX
Figure A3-37:	Legacy scenarios: Difference between scenarios 6 and 2, Makauri aquifer, summer ..	L
Figure A3-38:	Legacy scenarios: Difference between scenarios 6 and 2, Makauri aquifer, winter ..	LI
Figure A3-39:	Legacy scenarios: Difference between scenarios 6 and 2, Matokitoki aquifer, summer	LII
Figure A3-40:	Legacy scenarios: Difference between scenarios 6 and 2, Matokitoki aquifer, winter	LIII
Figure A3-41:	Legacy scenarios: Difference between scenarios 7 and 2, shallow aquifers, summer	LV
Figure A3-42:	Legacy scenarios: Difference between scenarios 7 and 2, shallow aquifers, winter	LVI
Figure A3-43:	Legacy scenarios: Difference between scenarios 7 and 2, Waipaoa aquifer, summer	LVII
Figure A3-44:	Legacy scenarios: Difference between scenarios 7 and 2, Waipaoa aquifer, winter	LVIII
Figure A3-45:	Legacy scenarios: Difference between scenarios 7 and 2, Makauri aquifer, summer	LIX
Figure A3-46:	Legacy scenarios: Difference between scenarios 7 and 2, Makauri aquifer, winter ..	LX
Figure A3-47:	Legacy scenarios: Difference between scenarios 7 and 2, Matokitoki aquifer, summer	LXI
Figure A3-48:	Legacy scenarios: Difference between scenarios 7 and 2, Matokitoki aquifer, winter	LXII
Figure A3-49:	Legacy scenarios: Difference between scenarios 8 and 2, shallow aquifers, summer	LXIV
Figure A3-50:	Legacy scenarios: Difference between scenarios 8 and 2, shallow aquifers, winter	LXV
Figure A3-51:	Legacy scenarios: Difference between scenarios 8 and 2, Waipaoa aquifer, summer	LXVI
Figure A3-52:	Legacy scenarios: Difference between scenarios 8 and 2, Waipaoa aquifer, winter	LXVII

Figure A3-53:	Legacy scenarios: Difference between scenarios 8 and 2, Makauri aquifer, summer	LXVIII
Figure A3-54:	Legacy scenarios: Difference between scenarios 8 and 2, Makauri aquifer, winter	LXIX
Figure A3-55:	Legacy scenarios: Difference between scenarios 8 and 2, Matokitoki aquifer, summer	LXX
Figure A3-56:	Legacy scenarios: Difference between scenarios 8 and 2, Matokitoki aquifer, winter	LXXI
Figure A3-57:	Legacy scenarios: Difference between scenarios 9 and 2, shallow aquifers, summer	LXXIII
Figure A3-58:	Legacy scenarios: Difference between scenarios 9 and 2, shallow aquifers, winter	LXXIV
Figure A3-59:	Legacy scenarios: Difference between scenarios 9 and 2, Waipaoa aquifer, summer	LXXV
Figure A3-60:	Legacy scenarios: Difference between scenarios 9 and 2, Waipaoa aquifer, winter	LXXVI
Figure A3-61:	Legacy scenarios: Difference between scenarios 9 and 2, Makauri aquifer, summer	LXXVII
Figure A3-62:	Legacy scenarios: Difference between scenarios 9 and 2, Makauri aquifer, winter	LXXVIII
Figure A3-63:	Legacy scenarios: Difference between scenarios 9 and 2, Matokitoki aquifer, summer	LXXIX
Figure A3-64:	Legacy scenarios: Difference between scenarios 9 and 2, Matokitoki aquifer, winter	LXXX

Tables

Table 2-1:	Basic data used for model setup, calibration, validation and scenario runs.....	23
Table 3-1:	Hydrostratigraphic units [8].	28
Table 3-2:	Basic layers of the 3D geometry model corresponding to the hydrogeological model [9], [10].	37
Table 3-3:	Pre-calibration hydraulic conductivity of the hydrogeological units	47
Table 3-4:	Post-calibration hydraulic conductivity of the modelling hydrogeological units	48
Table 3-5:	Boundary conditions of the hydrogeological units	53
Table 3-6:	Overview of available gauging stations with water level records	55
Table 3-7:	Overview of abstraction and injection bores considered in aquifers within the model area.....	55
Table 3-8:	Station information.....	58
Table 4-1:	Overview of abstraction amounts considered in steady state calibration.....	65
Table 4-2:	Rainfall of the Stations Gisborne EWS and Gisborne Aws May 2011 – April 2012. .	65
Table 4-3:	Statistics of groundwater level records of 79 bores used as targets for steady state calibration	66
Table 4-4:	Statistics of the state steady calibration.	66
Table 4-5:	Comparison of simulated and measured groundwater levels of 79 bores	69
Table 4-6:	Water balance of state steady calibration.....	69
Table 4-7:	Overview of the sensitivity simulations performed based on steady state calibration	72
Table 4-8:	Statistics and water balance error of the state steady calibration and sensitivity simulations.....	73
Table 4-9:	Overview of 88 bores with measured groundwater levels for the transient calibration and validation.....	79
Table 4-10:	Total water balance in the calibration and validation period 2008 – 2021	93
Table 4-10:	Overview of 2017-2019 injection trials details	94
Table 4-11:	Simulation results comparison with NGMP age data	96
Table 4-12:	Statistics and water balance error of the state steady calibration and additional simulations for the Matokitoki aquifer.	101
Table 5-1:	Simplified overview of Scenarios and their specifications.....	116
Table 5-2:	Sea level rise values considered in scenarios with climate change	118
Table 5-3:	Overview of abstraction amounts of the period 2020/21 and scenario 1.1 (Baseline B)	118
Table 5-4:	Overview of abstraction amounts of 3-year draught period 2012/13, 2013/14 and 2014/15.....	120

Table 5-5:	Overview of abstraction amounts of scenario 2.1 Baseline + Climate Change (B+CC)	122
Table 5-6:	Overview of abstraction amounts of scenario 4.1 Current Allocation Limit V2 + Climate Change]	135
Table 5-7:	Overview of the 6 MAR bores considered by scenario 5.1	143
Table 5-8:	Overview of the MAR amount/season with stepwise increase in Scenario 5.1.....	143
Table 5-9:	Overview of abstraction amounts of scenario 7.1 Sustainable Allocation + Climate Change (SA)	151
Table 5-9:	Average water level/hydraulic head changes between the scenarios, summer season.	164
Table 5-10:	Average water level/hydraulic head changes between the scenarios, winter season.	164
Table A1-1:	Comparison of measured and simulated water levels at available monitoring bores, steady state calibration	II
Table A3-1:	Legacy Scenarios: Overview of scenarios.....	VI
Table A3-1:	Legacy Scenarios: Changes of Average of Simulated Water Level (m) between scenarios	VI
Table A3-2:	Legacy Scenarios: Changes of Average of Simulated Water Level (m) between scenarios	VIII

Abbreviations and acronyms

1D / 2D / 3D	one- / two- / three-dimensional
asl	above mean sea level
BC	boundary condition(s)
DEM	Digital Elevation Model
FEFLOW	commercial numerical code (software) of DHI for simulating flow, mass and heat transport processes in the subsurface
GW	groundwater
MAR	managed aquifer recharge
...	

Appendix

A1	Plot style: vertical distribution of hydraulic head and concentration	I
A2	Steady-state calibration: calculated vs. observed hydraulic head	II
A3	Parameter specification of scenario simulations	IV
A4	Scenario simulations: Results of abandoned setups	V

1. Executive Summary

WGA and AQUASOIL were contracted by Gisborne District Council (GDC) to develop a groundwater model for the Poverty Bay Flats. Based on the Conceptual Model [18], AQUASOIL has developed a three-dimensional model including the Shallow Fluvialite, Te Hapara Sands, Waipaoa, Makauri and Matokitoki aquifers. The groundwater model has been calibrated to field data and validated by using additional data sets. The calibrated and validated groundwater model was applied to calculate several predictive scenarios, outlining the possible reaction of the groundwater system to climate change and to a broad range of different groundwater management options under climate-change conditions. The management options include a natural-state scenario (without any groundwater abstraction), a scenario using all allocated abstractions, an option with artificial groundwater replenishment, and a scenario with reduced abstraction. The scenario results can be used to illustrate the reaction of the groundwater system on human activity, and as a basis for discussion and further political decision making. All models and results files have been handed over to GDC for further use.

As one of the major risks for the aquifer system and groundwater use is increasing groundwater salinity, salt transport has been included into the model in an exemplary way, showing the capability of the model to simulate mass transport and illustrating the risks.

Further field work and a further development of the model are recommended in case the model is to be used for decision making with respect to the shallow aquifer system. As a precondition for future predictive simulations on salt transport within the Poverty Bay Flats groundwater system, the role of the western saline aquifer and the salinisation of groundwater in general must be understood better.

2. Introduction

2.1. Background

The Poverty Bay Flats in the Tairāwhiti region of New Zealand has some of the most prime arable land in Aotearoa. It covers an area of some 18,500 ha and is suitable for arable farming, market gardening, horticulture and viticulture. A large portion of the arable land is irrigated in summer season, much of it with water abstracted from the groundwater system.

There are four main aquifers under the Poverty Bay Flats namely the Te Hapara, Waipaoa, Matokitoki and Makauri aquifers. By far the largest abstraction occurs from the latter, with an average of 900,000 m³ being abstracted from the aquifer in the summer irrigation season. There has been a 51% increase in the areas consented for irrigation since 2006 in the region with 7,120 ha now consented to be irrigated, 96% of which is on the Poverty Bay Flats.

The aquifer system is fed mainly from the Waipaoa River and its associated tributaries in a catchment with a combined land area of 2,205 km². Of the 204 current water consents that GDC manages, 197 of these are within the Waipaoa river catchment.

Many of the water sources are considered as over or fully allocated and no new consents are being issued. A waitlist has been established for applicants wishing to apply for a new consent.

A Managed Aquifer Recharge (MAR) trial occurred from 2017 to 2020, to ascertain if the application of MAR for the Makauri aquifer is a feasible solution in reversing/slowing the declining groundwater levels. It is uncertain if an expanded MAR scheme will be given the go-ahead in the future, and in further discussions with the stakeholders and treaty partners it will be determined how and when MAR may be applied in the Poverty Bay Flats.

To try and address the over allocation of the Makauri aquifer, a “paper-based” reduction in the global consented allocations has been implemented. The first stage of this was to reduce the paper-based consented allocations from ~8,000,000 m³ per annum down to ~1,800,000 m³ per annum. The next allocation reduction will occur in 2023 and result in the allocation limit being further reduced to 1,700,000 m³.

As part of the MAR project trial, the Gisborne District Council (GDC) had started an in-house groundwater model project to try and better model the aquifers in the system and to inform the decisions around groundwater management including allocation and the use of MAR. The geological model has been considered almost complete (created in Geomodeller software by GDC staff) at project start, but internal resources were lacking to complete the geological model and to then carry out the development of a numerical flow modelling of the groundwater resources within GDC.

Consequently, WGA and its sub-consultant AQUASOIL were commissioned to finalize the geological model and then produce a groundwater model to quantify the flow and volume of water available in the various Poverty Bay Flats aquifers. The model was supposed to forecast future flow, to accurately evaluate various recharge and withdrawal scenarios. It was also intended to train GDC staff on the use and modifications of the model, so that the model can be used as one of GDC’s analysis tools to help inform groundwater management decisions.

The global intent of the model is to have an accurate and evolvable groundwater model that is accepted not only by GDC, but also iwi and the wider community who rely on both using groundwater and protecting the environmental and cultural values which depend on groundwater.

In the first step, only groundwater flow was to be simulated. However as deteriorating groundwater quality is seen as an additional risk to the groundwater system and its uses, an extension of the objectives to

incorporate groundwater quality (groundwater age simulation to support calibration and as a proof-of-concept for quality simulation in general, and basic salinity simulation) has been agreed on during the modelling process.

2.2. GDC Project Objectives

The following objectives were defined by the client for the modelling process and its outcomes:

The objective of the groundwater model is to use the model to run various exploratory scenarios to help test the model's abilities as well as to help inform decisions around the management and allocation of groundwater resources.

The final output model from is to provide accessibility for future data input, including re-running model scenarios and further calibration and validations of the model as new data is acquired.

Understanding the interaction of groundwater-surface water is important as well as outlining the volumes of water within each aquifer system, the amount of recharge that occurs and the amounts that are abstracted. Estimates of aquifer discharge is also important.

Ultimately, the model is to be used to help inform allocation decisions on sustainable groundwater volumes as they relate to a range of factors including climate change, groundwater pumping, and potential use of MAR.

Gisborne District Council outlined some specific areas that they wanted this modelling project to address:

- Spatial mapping, characterisation and incorporation of GDC datasets

The model will allow the hydrological and geological structures and characteristics of the groundwater systems to be better understood.

- Surface water/groundwater connectivity

Improving our understanding of surface water/groundwater interaction, aquifer and surface water boundaries. The role of groundwater in connecting land use to surface water quantity is not fully understood. This means that current policy, management, and actions may be ineffective. The model must be scalable to assist with determining what factors control and influence water bodies at the regional scale, including Freshwater Management Unit's and water management zones. The model will also determine how water bodies are hydraulically connected.

- Sustainable groundwater use

Sustainable groundwater allocation rates of take and annual volumes and their effects on surface water bodies including springs. Developing and implementing groundwater level limits for the Poverty Bay aquifers. Understanding areas of risk (i.e., saltwater intrusion).

- Managed Aquifer Recharge (MAR)

The model will be used to predict the optimal number of wells, their locations and spacing to achieve the combined goals of injecting a minimum of 600,000 m³ (mainly in winter when excess river water is available), obtaining water level increase and salinity improvements. It will also need to predict the potential for artesian bores in 3rd party bores. Lastly to evaluate potential impacts from injection under pressure (head above ground at injection bore).

- Proving and scaling groundwater solutions

Solutions can be developed that improve the quantity of groundwater i.e. water take efficiency

measures, Managed Aquifer Recharge and enhancing natural recharge mechanisms.

- Future pressures on freshwater resources

Increasing pressures such as population and economic growth, as well as climate change are impacting groundwater availability. Scientific evidence is required for groundwater management and allocation to support future policy/urban planning and adaptation. Management tools and data to respond to pressures on quantity over the medium to long term.

2.3. Basic Data used for model setup, calibration, validation and scenarios

Basic data used for model setup, calibration and validation, and for scenario simulation runs are provided by WGA or/and by GDC and listed with brief description in Table 2-1.

Table 2-1: Basic data used for model setup, calibration, validation and scenario runs.

[i]	Date	Source	Description	Usage
[1]	12.08.2021	WGA	Model and meshing guidance incl. the 1 st model area boundary: Gw model guidance.pptx, Model boundary.dxf	mesh generation
[2]	08.09.2021	WGA	FC_Channel.shp	
[3]	09.09.2021	WGA	SW – Drainage system for model.pptx	
[4]	21.10.2021	WGA	211020_model_boundary.dxf	
[5]	15.09.2021	GDC	Monitored bores: Gisborne WL manual m RL sites.xlsx, Gisborne WL telemetered m RL sites.xlsx	calibration / validation
			GW Manual level / automated records	
[6]			Rainfall: CLI-Rainfall.xlsm	groundwater ex-charge
[7]			Location of gauging site: Gisborne River Flow Sites.xlsx	river/stream BC
	07.12.2021		River level data: Gisborne River Flow Sites.xlsx	
	08.12.2021	WGA	Site datum: SW – Recording site datum estimates.xlsx	
[8]	04.10.2021	WGA	Geological model, conceptual hydrogeology model: WGA210398-RP-HG-0002[A] DRAFT Geological model.docx, WGA210398-RP-HG-0003(A) Conceptual hydrogeological model.docx	model setup, hydraulic parameters
[9]	10.10.2021	WGA	The geol. Model (Outputs from GeoModeller), surface elevations (top/bottom) of the hydrogeological units to be considered by FEFLOW model	model setup, geometries (extents) of aquifers/aquifers
	21.10.2021	WGA	Unit isopachs of the hydrogeological units	
[10]	01.11.2021	WGA	DEM: lidar_resample.asc, 20 m grid spacing	model setup, ground surface
[11]	18.11.2021	GDC	Monthly take data Oct.2008-Jun.2015: JF_ Water Monthly take Spreadsheet 08-2014 A432734_editedV3.xlsx	model setup, steady-state calibration
	03.12.2021		JF_ Water Monthly take Spreadsheet 08-2014 A432734_editedV4.xlsx	
[12]	02.12.2021	MfE NZ	Land use: mfe-lucas-nz-land-use-map-1990-2008-2012-2016-v008-SHP LUCAS NZ Land Use Map 1990 2008 2012 2016 v008 – MfE Data Management GIS Map Data MfE Data Service	model setup, groundwater recharge
[13]	03.12.2021	GDC	Monthly take data Oct.2008-Jun.2015: JF_ Water Monthly take Spreadsheet 08-2014 A432734_editedV4.xlsx	transient calibration

[i]	Date	Source	Description	Usage
[14]	19.01.2022	GDC	Monthly take data Oct.2008-Oct.2021: all_take_data2008-2021_V2.xlsx	transient calibra- (08-15) and valida- tion (16-21)
[15]	08-12.2021	WGA	Email on "GDC Exploratory Scenarios for FEFLOW summer modelling"	scenario definitions / specifications for scenario runs
	08.02.2022	GDC	Email incl. FEFLOW Model Runs.xlsx for scenarios and	
	13.12.2021		locations of 6 potential MAR bores	
	22.02.2022		Specifications for Paper Allocations: Paper allocations_JL_V2.xlsx	
	11.03.2022		FEFLOW Model Scenarios _ 11032022.xlsx: Specifications for scenarios 8 and 9	
[16]	15.03.2022	WGA	Conceptual Groundwater Quality Model: Mail incl. WGA210398-RP-HG-0005A_v1.docx, SWQ - Raw data.xlsm, GWQ database.xlsm	specifications for a primary salinity model
[17]	24.06.2021	DGC/WGA	Golder 2017 Poverty Bay MAR trial Year 1 results.pdf (Golder, 2017), Gisborne MAR Trial 2017-2020 (A2026603).pdf (Golder, 2021)	simulation of MAR- Trials 2017 -2020
[18]	23.02.2022	WGA	Poverty Bay Flats Geological and Conceptual Hydrogeological Models	groundwater model
[19]	21.10.2022	WGA	Poverty Bay Flats Conceptual Groundwater Quality Model–Salinity	salinity modelling
[20]	12.03.2022	Internet	https://environment.govt.nz/assets/Publications/Files/coastal-hazards-guide-final.pdf (MfE NZ, 2017)	sea level rise in climate-change scenarios
[21]	08.02.2022	Internet	Climate change projections and impacts for Tairāwhiti and Hawke's Bay (NIWA, 2020)	climate-change scenarios

References to the basic data are designated as [i] representing the corresponding row i in Table 2-1.

2.4. Workflow from model setup to scenario runs

AQUASOIL's workflow for numerical groundwater flow modelling as applied for this project from model setup to scenario runs consists of the following primary stages:

- Development and setup of a 3D groundwater flow model,
- steady state calibration (incl. parameter sensitivity simulations), transient calibration, validation and verification incl. groundwater age (residence time) simulation and transient electric conductivity simulation for MAR trials 2017-2020 (water quality simulation),
- predictive scenario simulation runs, and
- documentation of results.

2.5. Documentation

This report contains a detailed description of model setup and parameterisation, the calibration process and scenario runs. As most of the value of the work carried out is seen in the actual simulation files and extensive digital outcomes that cannot be fully honoured in a necessarily limited paper/pdf report, all the models and results are available in the additional digital appendix, which is structured as follows:

- DA1: Model input data
- DA2: Model and results files
 - DA2.1: Steady-State calibration and groundwater-age simulation
 - DA2.2: Transient calibration, MAR Trial simulation and EC-simulation of MAR trials
 - DA2.3: Resulting hydraulic head isolines for scenarios in .shp format
- DA3: Time-series plots
 - DA3.1: Transient calibration
 - DA3.2: Scenario runs
- DA4: Vertical plots
 - DA4.1: Steady-state calibration
 - DA4.2: Transient calibration
 - DA4.3: Scenario runs

A description of the vertical plots used throughout this report and provided in DA4 can be found in A1. DA3 and DA4 contain html files in each folder (0_allpngs.html, 0_allhtmls.html) that can be used to easily view the diagrams for different observation bores. Vertical plots are contained in pdf and png format in the digital appendix, time-series diagrams in png and html format, where the latter aren't static diagrams, but allow for zooming/panning and provide tooltips with the actual values.

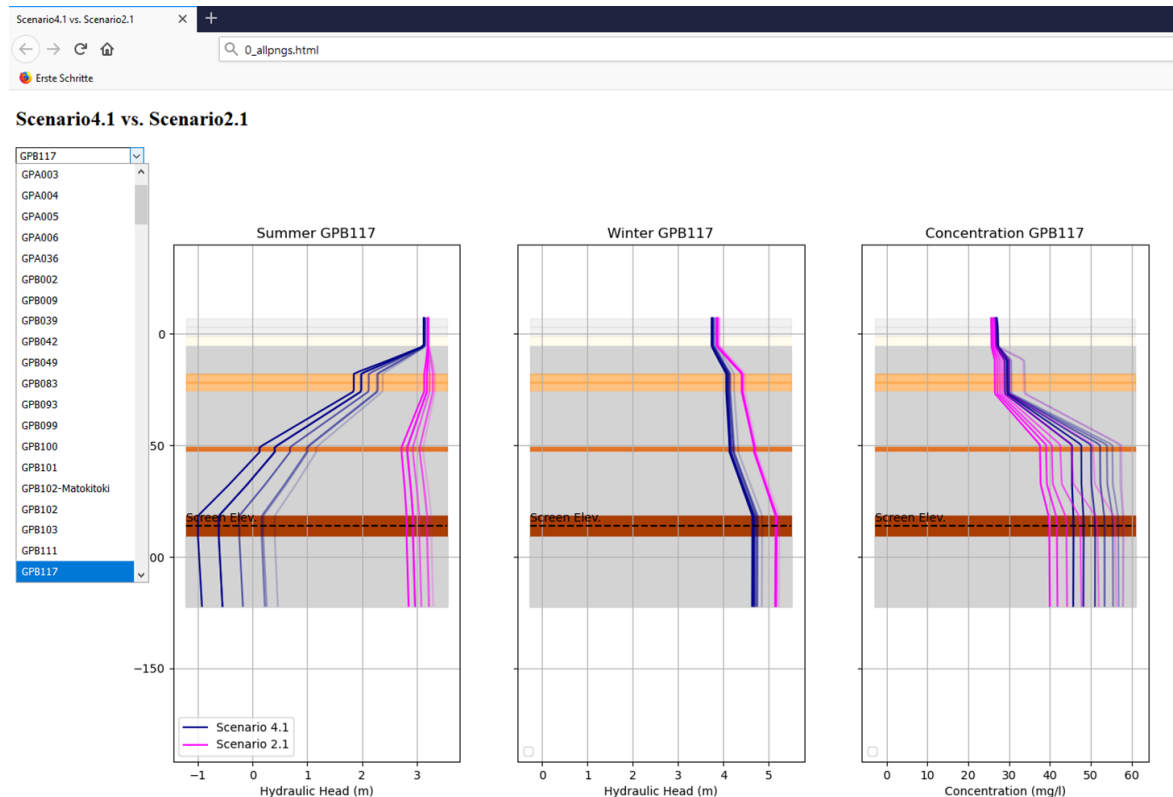


Figure 2-1: Example for vertical plot view from html file

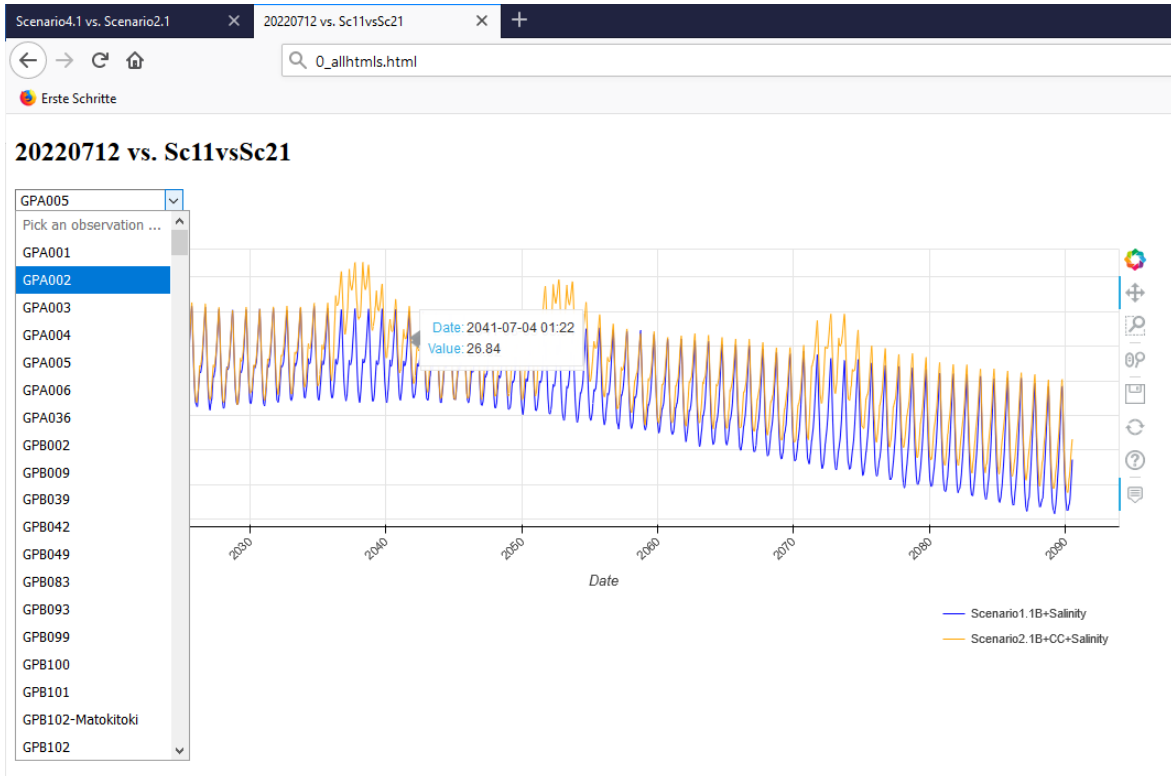


Figure 2-2: Example for html time-series shown from html file

3. Development and setup of the 3D groundwater model

The 3D groundwater model was developed by AQUASOIL using the FEFLOW software (version 7.3), based on the 3D geological model and the conceptual hydrogeological model prepared by WGA [8], [9]. The main stages of model development as implemented here are:

1. Horizontal discretization:
 - generation of a so-called supermesh (geometrical basis for generation of the finite-element mesh) under consideration of the extents of aquifers/aquitards, locations of the relevant rivers, streams and drain courses, and locations of takes in the horizontal direction, and
 - generation of an appropriate 2D finite element mesh considering the geometrical features mentioned above and the meshing guidance [1],
2. Vertical discretization by extending the 2D mesh to a layered 3D model according to the top / bottom surface elevations of the aquifers and aquitards provided by the 3D geological model [8],
3. Assignment of hydraulic parameters and boundary conditions to the 3D groundwater model (material properties such as hydraulic conductivity and storage characteristics of aquifers/aquitards, boundary conditions for rivers/drains and takes, and estimated recharge from rainfall).

3.1. Basis of the groundwater flow model: 3D geological model and conceptual hydrogeological model (WGA)

The 3D geological model and the conceptual hydrogeological model prepared by WGA [8], [9] include 10 hydrostratigraphic units of Quaternary sedimentary deposits in the Poverty Bay Flats. Table 3-1 gives an overview of the 10 hydrostratigraphic or hydrogeological units of aquifers and aquitards, beginning from ground surface down to the interpreted base of the Quaternary sedimentary deposits. None of the aquifers listed in Table 3-1 are continuous across the full extent of the Poverty Bay Flats. In areas where individual aquifers are not present, aquitards defined in Table 3-1 either reach up to the ground or merge with adjacent aquitards with no clear demarcation surface.

The Te Hapara Sand aquifer and the Shallow Fluvatile aquifer interfinger and are both considered to act as unconfined or locally semi-confined aquifers. Their degree of confinement depends on the exact nature of the shallow undifferentiated materials that are present at surface. Any partial confinement has generally been indicated by the analysis of pumping tests returning storativity results that are lower than considered reasonable for unconfined aquifers.

The geological modelling results indicate that the Waipaoa aquifer is predominantly confined except at its northern end where it rises to intersect the Shallow Fluvatile aquifer at the southern end of the Waipaoa River valley. Disconnected gravel horizons at similar elevations to the main Waipaoa aquifer have been interpreted as belonging to this unit, even though they may be hydraulically disconnected. The conceptual split of the Waipaoa aquifer is not relevant to the numerical model as the basic properties of both parts are identical, thus this aquifer is treated as one unit in the following.

The Makauri Aquifer is the primary productive aquifer in the region and is interpreted to be hydraulically connected within its footprint area. Drilling has identified that this aquifer is locally separated into two splits. The upper split is defined as the Makauri aquifer by default; this, however, does vary based on interpretation of the local drillhole logs and elevations of the gravel deposits. The Makauri aquifer is predominantly fully confined, except at its northern end where it rises to potentially meet the Waipaoa and Shallow Fluvatile aquifers [8]. The connection of the Makauri aquifer to the sea is unknown. For the

model, it is assumed that the aquifer does not directly connect to the sea bed and a discharge from the aquifer to the sea is only possible through the overlying aquitards.

Table 3-1: Hydrostratigraphic units [8].

Hydrostratigraphic Unit	Lithological unit	Lithological Description	Aquifer / Aquitard
Undefined	Undifferentiated Shallow Material	Highly variable, predominantly soils, locally includes artificial fill.	Undefined
Te Hapara Sand	Coastal beach and dune sands	Sands, shelly.	Aquifer
Shallow Fluvialite Aquifer	Fluvialite gravel deposits	Sandy silty gravel.	Aquifer
Aquitard 1	Fine grained, low energy coastal flood plain, estuarine, deltaic deposits.	Silts and clays, locally shelly or with wood fragments.	Aquitard
Waipaoa Aquifer	Fluvialite gravel deposits	Sandy silty gravel.	Aquifer
Aquitard 2	Fine grained, low energy coastal flood plain, estuarine, deltaic deposits.	Silts and clays, locally shelly or with wood fragments.	Aquitard
Makauri Aquifer	Fluvialite gravel deposits	Sandy silty gravel.	Aquifer
	Fine grained, low energy coastal flood plain, estuarine, deltaic deposits.	Silts and clays, locally shelly or with wood fragments.	Aquitard ⁽¹⁾
	Fluvialite gravel deposits	Localised lower sandy silty gravel split	Aquifer ⁽²⁾
Aquitard 3	Fine grained, low energy coastal flood plain, estuarine, deltaic deposits.	Silts and clays, locally shelly or with wood fragments.	Aquitard
Matokitoki Aquifer	Buried extension of Waipaoa 1 river terrace.	Fluvialite sandy silty gravel.	Aquifer
	Buried stream valley infill gravel.	Sandy silty gravel.	Aquifer
Aquitard 4	Basal deposits of Poverty Bay sedimentary wedge.	Marine silt, clay.	Aquitard
Basement			

Notes: 1) This aquitard is generally included as part of the Aquitard 3 due to the inconsistent and apparently discontinuous nature of the lower Makauri aquifer split.
2) Interpretation of the continuity, layout and elevation of this aquifer split is problematic from the available drillhole data.

3.2. Model area and horizontal discretization

The model boundary specified by [3] is shown by the orange line in the left figure of Figure 3-1, where blue lines indicate surface water courses of Waipaoa River, Taruheru River (incl. Taruheru Trib), Te Arai River, Waru Stream, Whakaahu Stream, Waikanae Creek and a number of drains in the model area according to the conceptual model. The model area has a size of about 306 km² in total, of which around 70 km² are below the sea.

For a numerical groundwater model, results are calculated at discrete points in space (so-called nodes when using the finite-element technique). Where results are expected to have steeper gradients (in hydraulic head or concentration), a higher density of nodes is desirable to better cover the gradient. Where heads or concentrations are expected to be flat, less nodes are required.

The right figure in Figure 3-1, taken from [1], firstly indicates areas of drawdown during January 2009 irrigation season by blue contours (darker contour indicates greater drawdown). According to [1], areas numbered by 1 to 6 (with dash lines as boundary) mark suggested element size or refinement for horizontal discretization to be performed in the model area as follows:

1. Suggested refinement to ≤ 20 m around main production bores, increasing to 2 m around specific high-demand bores,
2. Suggested refinement to approx. 2 m in a 30 m radius around ASR bore GPE065,
3. Suggested refinement to ≤ 5 m around Waipaoa Augmentation Plant (possible future MAR site),
4. Suggested general refinement to ≤ 20 m around this area as future MAR sites may be chosen here to reduce current apparent saline water movement in Makauri Aquifer from West to East,
5. Suggested general refinement to ≤ 50 m around this area as Matokitoki Aquifer seems to rise steeply, potentially connecting with shallower aquifers in this area. A sensitive area in the southern area of the Flats is to be included as well.,
6. Suggested general refinement to ≤ 50 m around this area where groundwater gradients are steeper than average. The aquifers open out at the lower end of the narrow part of the Waipaoa River Valley. Therefore, an increased refinement is required in the lower valley where the aquifers are merging. Refine to ≤ 20 m at southern end of this area to allow for recharge points suggested by Golder.

To be taken into consideration for mesh generation are also the lateral boundaries of the aquifers Matokitoki, Makauri, Waipaoa, Shallow Fluvial Deposits and Te Hapara Sands as well as bounds of the aquitards separating the aquifers.

The left figure in Figure 3-2 shows the supermesh generated under consideration of extents of aquifers/aquitards, locations of the relevant river, stream and drain courses, and locations of takes in the horizontal direction. In total, there are 173 polygons, 256 points for abstraction bores and 48 polylines for rivers, streams or/and drains. Waipaoa River (incl. wetland/oxbow close to Matawhero) and the part of Taruheru River in the Urban Gisborne are specified by polygons along their river courses.

A finite element mesh was generated, based on the supermesh. The mesh was then locally adapted manually to extents or borders of hydrogeological units (where not included in the supermesh for technical reasons) and smoothed to obtain an even better mesh quality with respect to the stability of the numerical simulation.

The right figure in Figure 3-2 shows the finite element mesh after adapting/smoothing for the horizontal discretisation of the model area. The 2D mesh consists of 100,666 triangular elements and 51,450 nodes in total.

As shown in Figure 3-3, the element diameters vary from 0.1 m to 321 m. About 50 % of the elemental diameters are below 50 m, 80 % less than 100 m. The average diameter of elements is about 79 m.

The maximum inner angles of the elements in most parts of the model are small, with only few elements that are more distorted. The smooth distribution of maximum inner element angles indicates a mesh generation process that is not too much determined by input geometries, and transitions between finer and coarser parts in the mesh are smooth (Figure 3-4).

Figure 3-5 shows the mesh generated for the MAR Trial Site 2017-2020 in detail as an example.

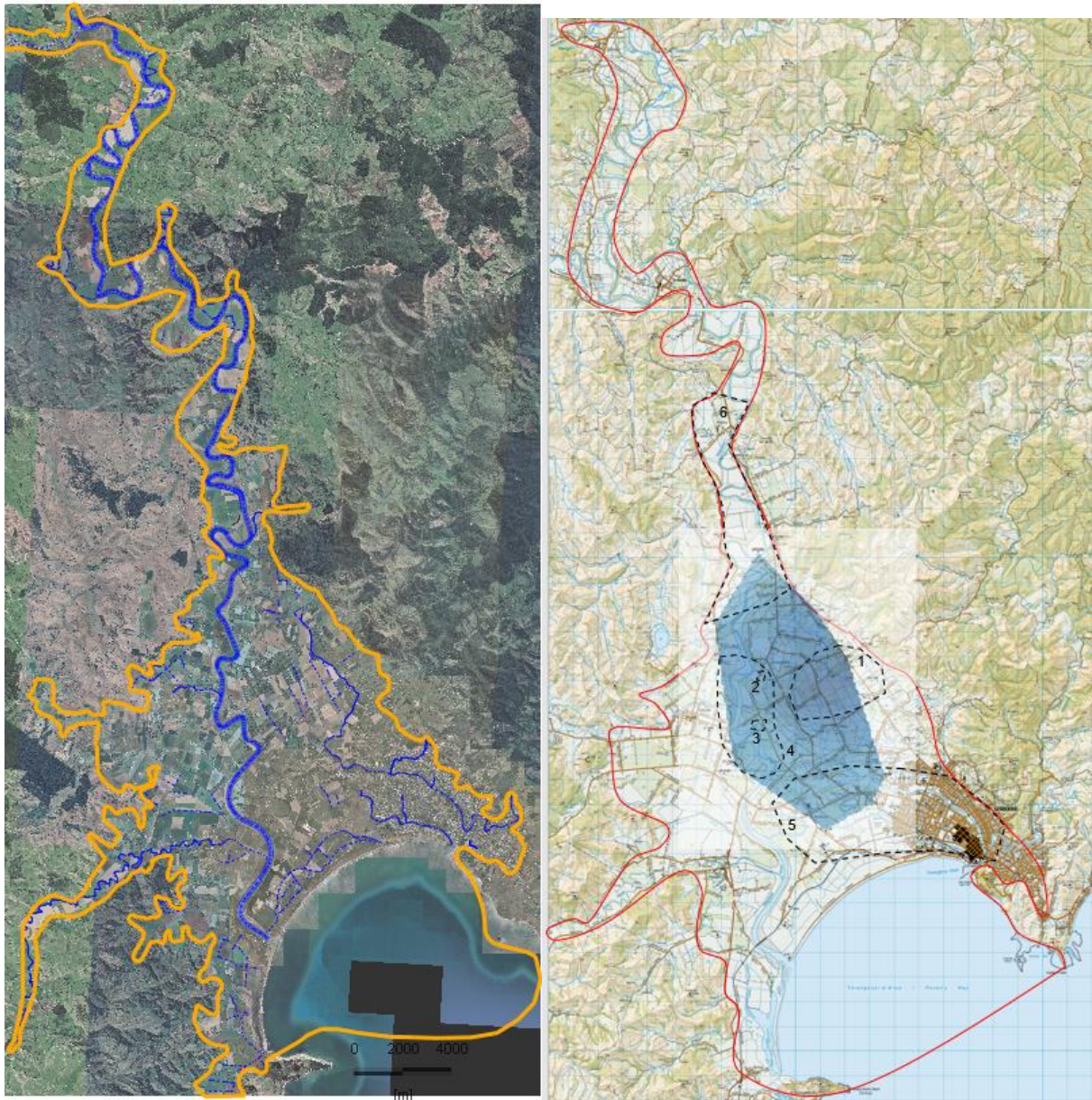


Figure 3-1: Left: Model area (orange line), rivers/streams/drains (blue lines); Right: Subareas specified by mesh guidance (dash lines), where the red line indicates an approximate model boundary only [1].

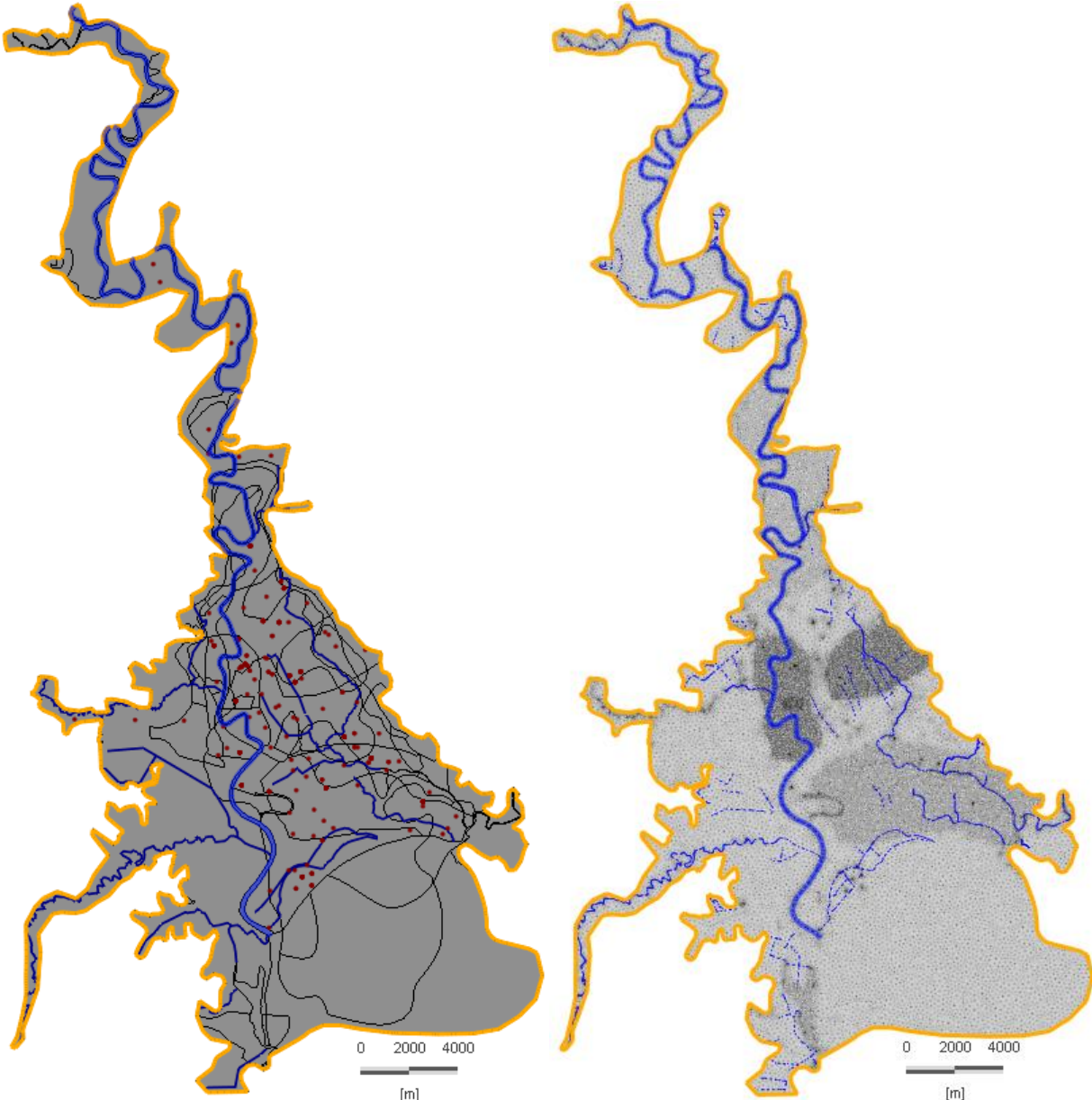


Figure 3-2: Left: Supermesh elements (basis for mesh generation); Right: Finite element mesh.

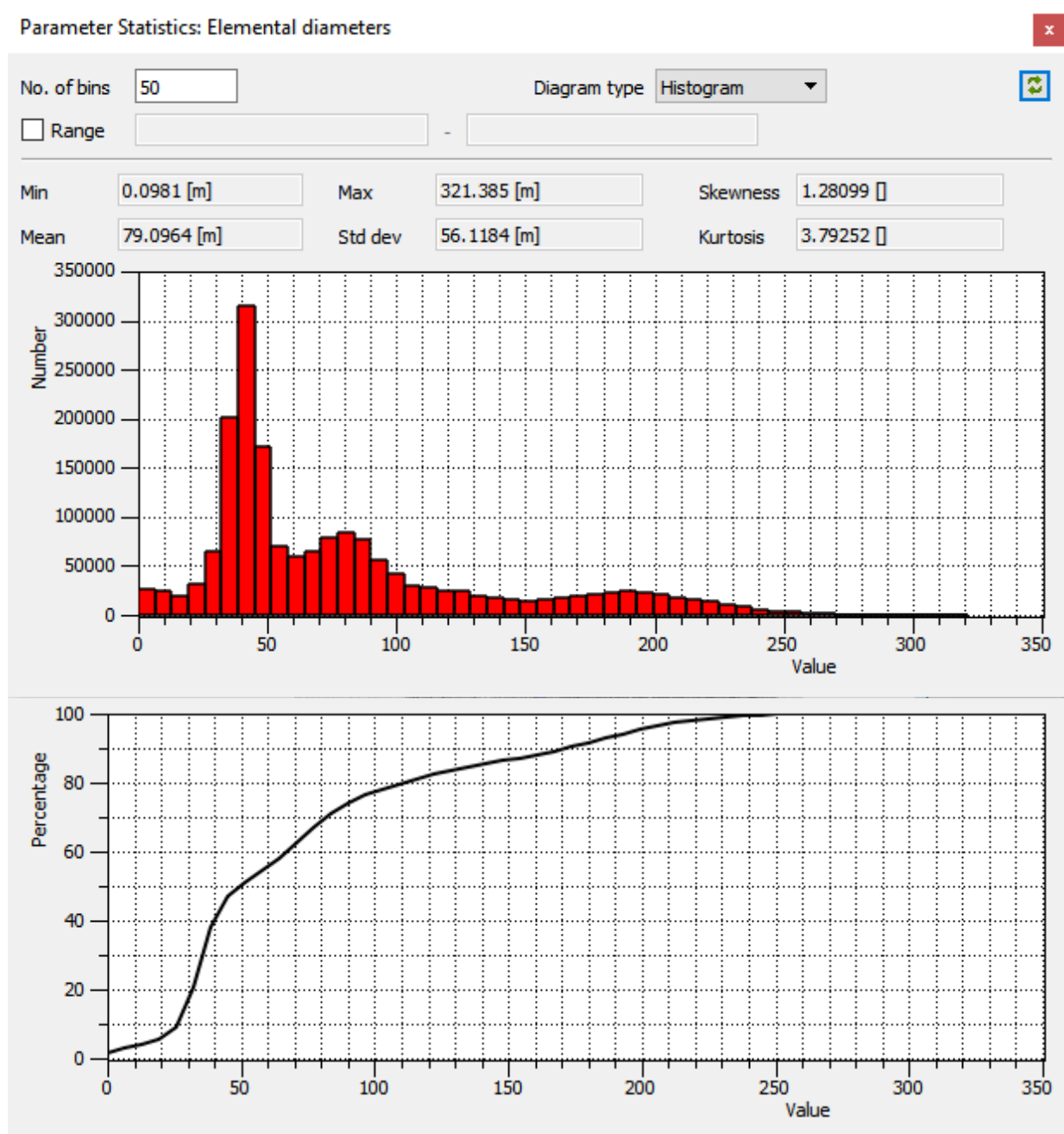


Figure 3-3: Statistics of element sizes of the finite element mesh (histogram on top, percentiles below).

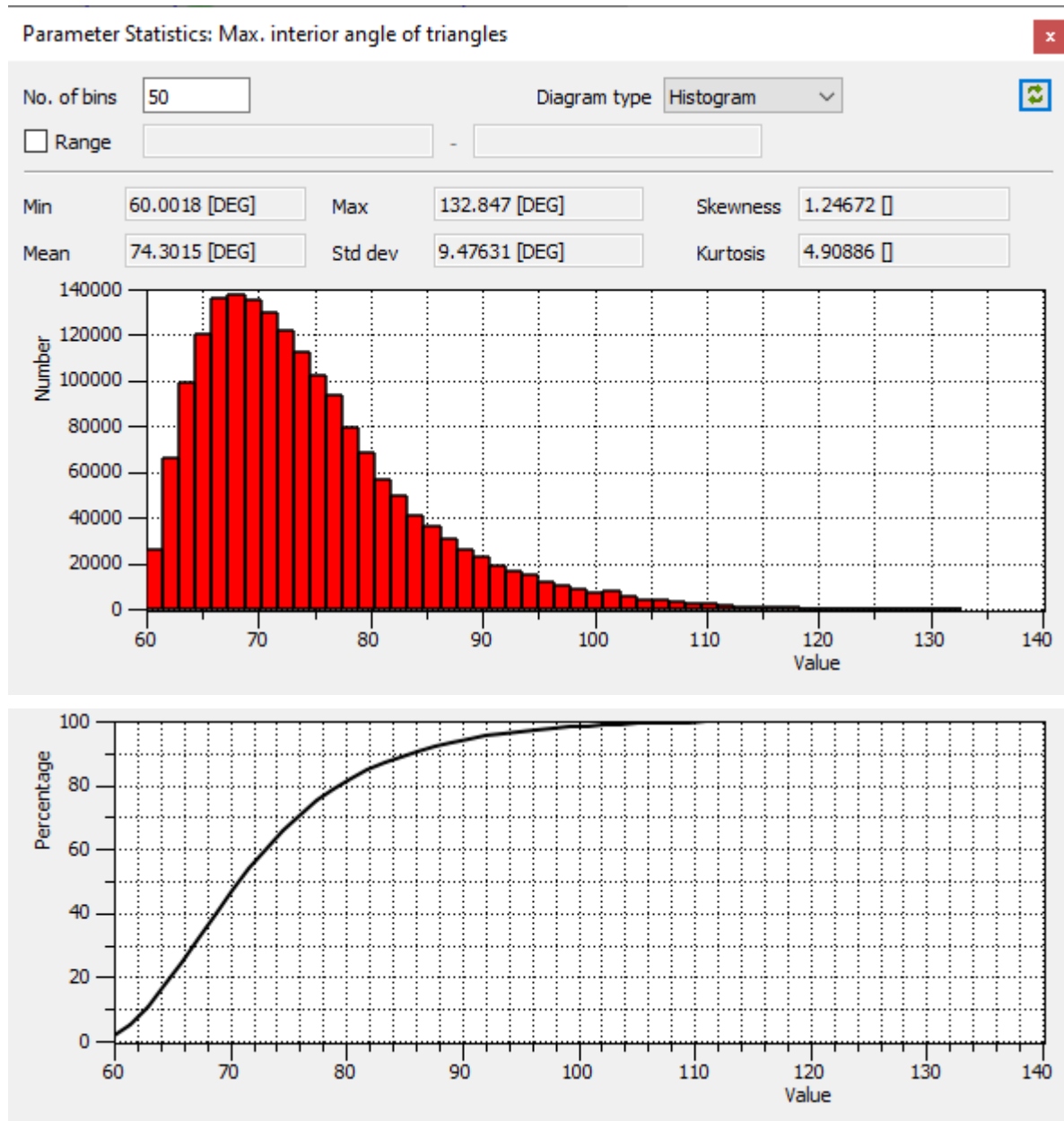


Figure 3-4: Statistics of maximum inner element angles of the finite element mesh (histogram on top, percentiles below).

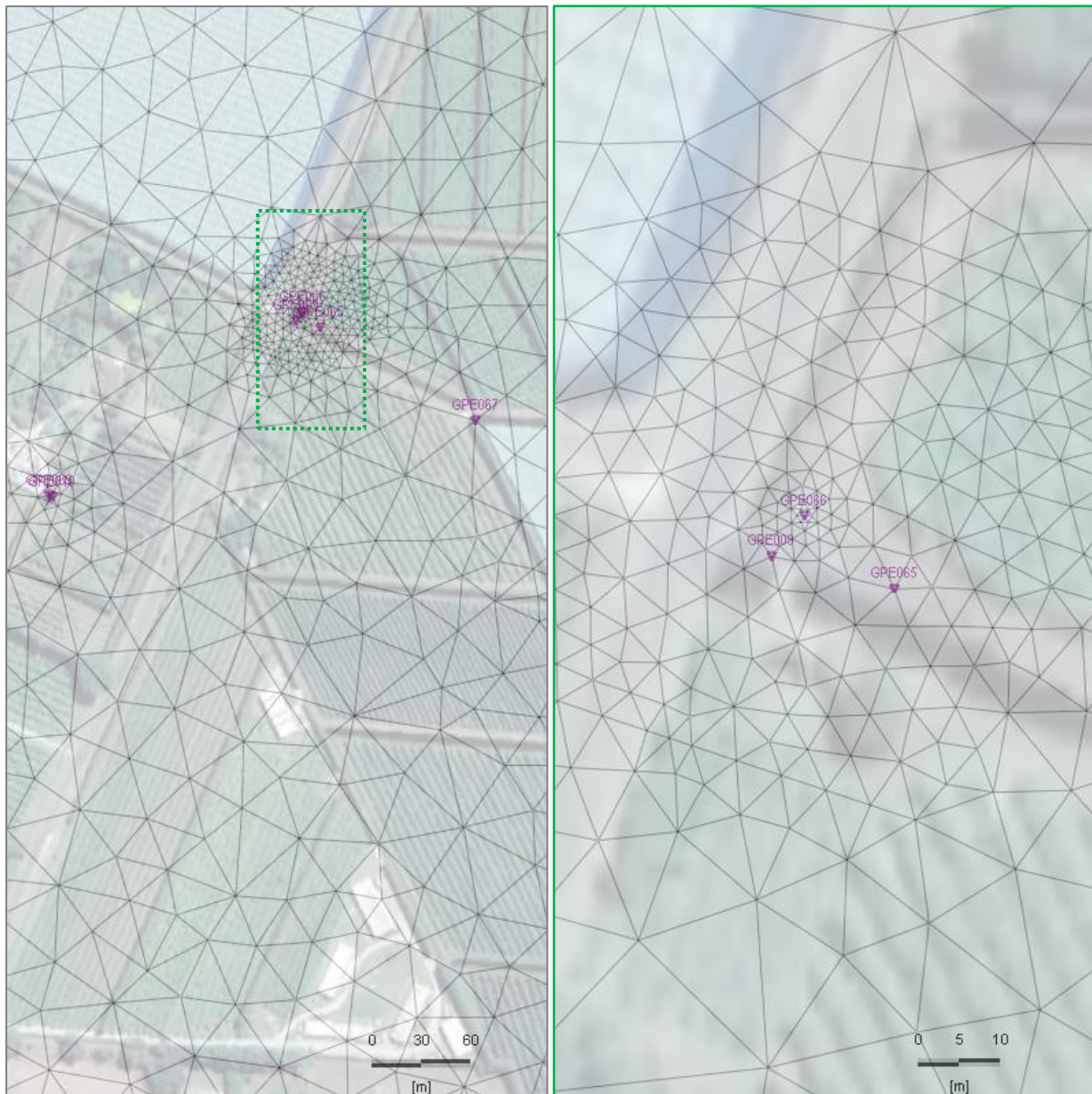


Figure 3-5: Left: elements around MAR-Trial site; Right: MAR-Trial site GPE066-GPE009-GPE065 in detail.

In order to avoid instabilities in the model when simulating salt transport (that had not been originally planned for the model), the mesh has been refined along the coastline in the area where the saltwater-freshwater interface is expected in the shallow aquifers. Transient calibration/validation, scenarios 1.1, 2.1,3.1, 4.1, 5.1 and 7.1 have been simulated based on the refined mesh, all other calculations have been done on the original horizontal discretisation.



Figure 3-6: Upper: mesh along coastline before additional refinement; lower: mesh after refinement

3.3. 3D geometry model and vertical discretization

In order to build a 3D groundwater model for Poverty Bay Flats, the generated 2D finite element mesh is extended geometrically in the vertical according to the 10 hydrogeological units defined by the geological / hydrogeological model [9], [10]. The 10 hydrogeological units (layers) are specified by using 11 surface elevation datasets exported from the geological model as grid data with 20m horizontal resolution. The 11 surface elevation datasets for the 10 hydrogeological units are summarised in Table 3-2 and their laterally spatial distributions / extents are outlined in Figure 3-7 respectively.

It might be important to note that the extents of the Makauri and Matokitoki aquifers are likely to be larger than considered in the hydrogeological model underlying the numerical model described here. The Makauri Aquifer is expected to extend further west, but no geological drilling data is available in this area to enable the extent and thickness of the aquifer to be confidently defined. It is expected to be present due to the presence of drillholes screened at an appropriate elevation for this aquifer within the Te Arai River flats.

The Matokitoki Aquifer extends further to the south than is represented in the hydrogeological and numerical models. However, there are no geological logs from drillholes to the south of the confirmed aquifer extent that were deep enough to intersect the Matokitoki Aquifer. A couple of drillholes to the south were deep enough and are screened in what is interpreted as the Matokitoki Aquifer. However that is insufficient to confidently geologically model the extent and thickness of the aquifer in this area.

Table 3-2: Basic layers of the 3D geometry model corresponding to the hydrogeological model [9], [10].

FEFLOW Model		Geol. Model		Basic Unit-Layer	Hydrogeol. Units	Elevation within the model area (mRL)		Remark
Slice	Model layer	File name (20m Grid)	Layer surface			from	to	
S1		lidar_resample.asc	Groud surface			0.00	189.00	DEM
	Layer 1			1	Undefined			
S2		Gisborne_Final_interfaces_TeHaparaSand.asc	upper surface TeHaparaSand eq. to lower surface Undefined			-48.53	15.91	
	Layer 2			2	Te Hapara Sand Aquifer			
S3		Gisborne_Final_interfaces_ShallowFluvialDeposits	upper surface ShallowFluvialDeposits eq. to lower surface TeHaparaSand / eq. to lower surface undefined			-24.56	21.85	
	Layer 3			3	Shallow Fluviatile Aquifer			
S4		Gisborne_Final_interfaces_Aquitard1.asc	upper surface Aquitard 1 eq. to lower surface ShallowFluviatile / eq. to lower surface TeHaparaSand / eq. to lower surface undefined			-75.06	62.00	
	Layer 4			4	Aquitard 1			
S5		Gisborne_Final_interfaces_WaipaoaGravel.asc	upper surface Waipaoa eq. to lower surface Aquitard 1			-52.30	19.63	distributing in the north
		Gisborne_Final_interfaces_WaipaoaGravel2.asc				-38.79	25.86	distributing in the south
	Layer 5			5	Waipaoa Aquifer			
S6		Gisborne_Final_interfaces_Aquitard2.asc	upper surface Aquitard 2 eq. to lower surface WaipaoaGravel / eq. to lower surface Aquitard 1			-78.96	52.66	
	Layer 6			6	Aquitard 2			
S7		Gisborne_Final_interfaces_MakauriGravel.asc	upper surface MakauriGravel eq. to lower surface Aquitard 2			-91.27	6.11	
	Layer 7			7	Makauri Aquifer			
S8		Gisborne_Final_interfaces_Aquitard3.asc	upper surface Aquitard 3 eq. to lower surface Makauri Gravel			-119.87	47.81	
	Layer 8			8	Aquitard 3			
S9		Gisborne_Final_interfaces_MatokitokiGravel.asc	upper surface MatokitokiGravel eq. to lower surface Aquitard 3			-156.30	5.74	
	Layer 9			9	Matokitoki Aquifer			
S10		Gisborne_Final_interfaces_Aquitard4.asc	upper surface Aquitard 4 eq. to lower surface Matokitoki Gravel / eq. to lower surface Aquitard 3			-183.34	42.48	
	Layer 10			10	Aquitard 4			
S11		Gisborne_Final_interfaces_Basement.asc	upper surface Basement eq. to lower surface Aquitard 4			-238.10	110.03	

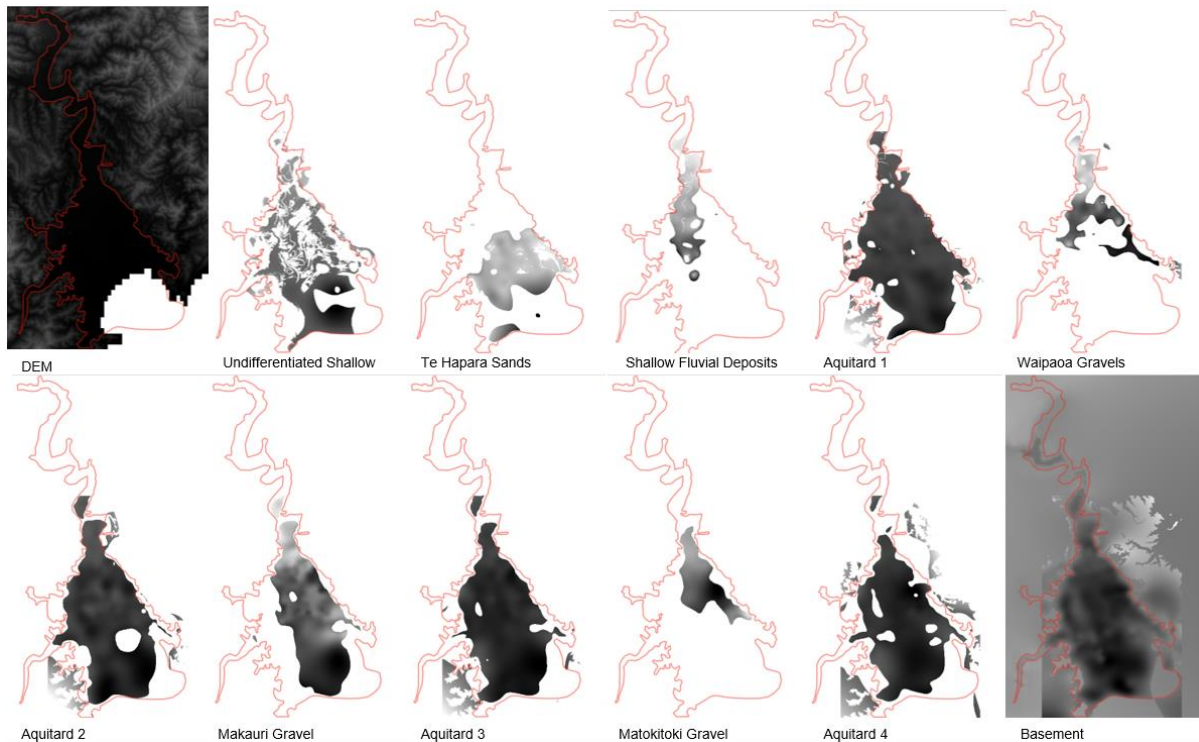


Figure 3-7: Overview of lateral distributions / extents of the surface elevation data of the 10 basic units.

Figure 3-8 illustrates the procedure of converting the 11 surface elevation grid datasets into a corresponding 3D FEFLOW geometry model with 10 primary layers or hydrogeological units. The procedure is briefly described as follows:

1. Importing 11 elevation datasets (gridded surfaces exported from Geomodeller) in a GIS project as grid data,
2. Importing the nodes of the finite element mesh of the FEFLOW model described in chapter 3.2 in the GIS project as point data,
3. Projecting node points of the FEFLOW mesh onto each grid data of the 11 surface elevation data by using GIS-Tool, so as to get appropriate elevation values corresponding the hydrogeological layering for nodes in the data extent, and to assign -99999 (representing no data) for nodes outside of the extent, and further to generate 11 points data or 3D points ready for building a 3D FEFLOW model,
4. Exporting the 11 sets of point data for surface elevations from GIS and importing in FEFLOW as corresponding User Data distributions,
5. Building a 3D geometry model according to the imported surface elevations, progressively from the top layer to bottom layer (ref. Table 3-2) i.e.
 - Slice 1 (S1) for the ground surface,
 - Slice 2 (S2) for the upper surface Te Hapara Sand Aquifer or/and the lower surface Undifferentiated unit,
 - same steps for intermediate hydrogeological units
 - Slice 11 (S11) for upper surface Basement or/and the lower surface Aquitard 4 (= base of Quaternary sedimentary deposits).

The built 3D FEFLOW model with 10 primary hydrogeological layers is shown in Figure 3-9 in a 3D overview. The model top represents the ground surface with elevations ranging from 189 mRL (north) to 0 mRL (south), while the model bottom is specified by the base of the Quaternary/top of bedrock (upper surface Basement) with elevations between 110 mRL and -238 mRL, ref. Figure 3-20 or/and Table 3-2.

The 10 primary hydrogeological layers are shown separately in the following 3D overview figures:

1. Undifferentiated in Figure 3-10,
2. Te Hapara Sands aquifer in Figure 3-11,
3. Shallow Fluvatile aquifer in Figure 3-12,
4. Aquitard 1 in Figure 3-13,
5. Waipaoa aquifer in Figure 3-14,
6. Aquitard 2 in Figure 3-15,
7. Makauri aquifer in Figure 3-16,
8. Aquitard 3 in Figure 3-17,
9. Matokitoki aquifer in Figure 3-18, and
10. Aquitard 4 in Figure 3-19.

Figure 3-21 shows locations of 5 vertical 2D cross-sections in the model area, i.e., one North-South cross section NS-CS#1 and four West-East cross sections WE-CS#1 to WE-CS#4. Figure 3-22, Figure 3-22, Figure 3-24, Figure 3-25 and Figure 3-26 present vertical 2D cross-section views for the 5 2D cross sections that illustrate vertical occurrences or extents of the 10 primary hydrogeological layers crossing the Poverty Bay Flats along the cross sections.

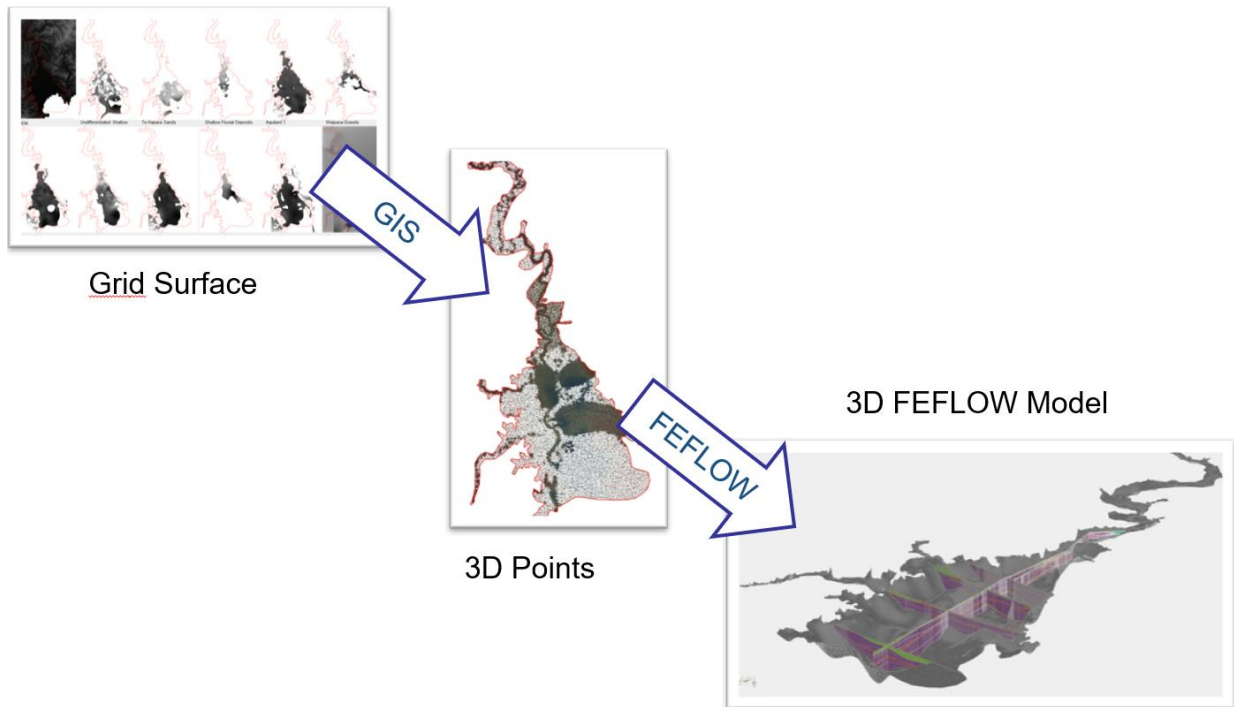


Figure 3-8: Scheme of converting the surface elevation grid data into a corresponding 3D FEFLOW geometry model.

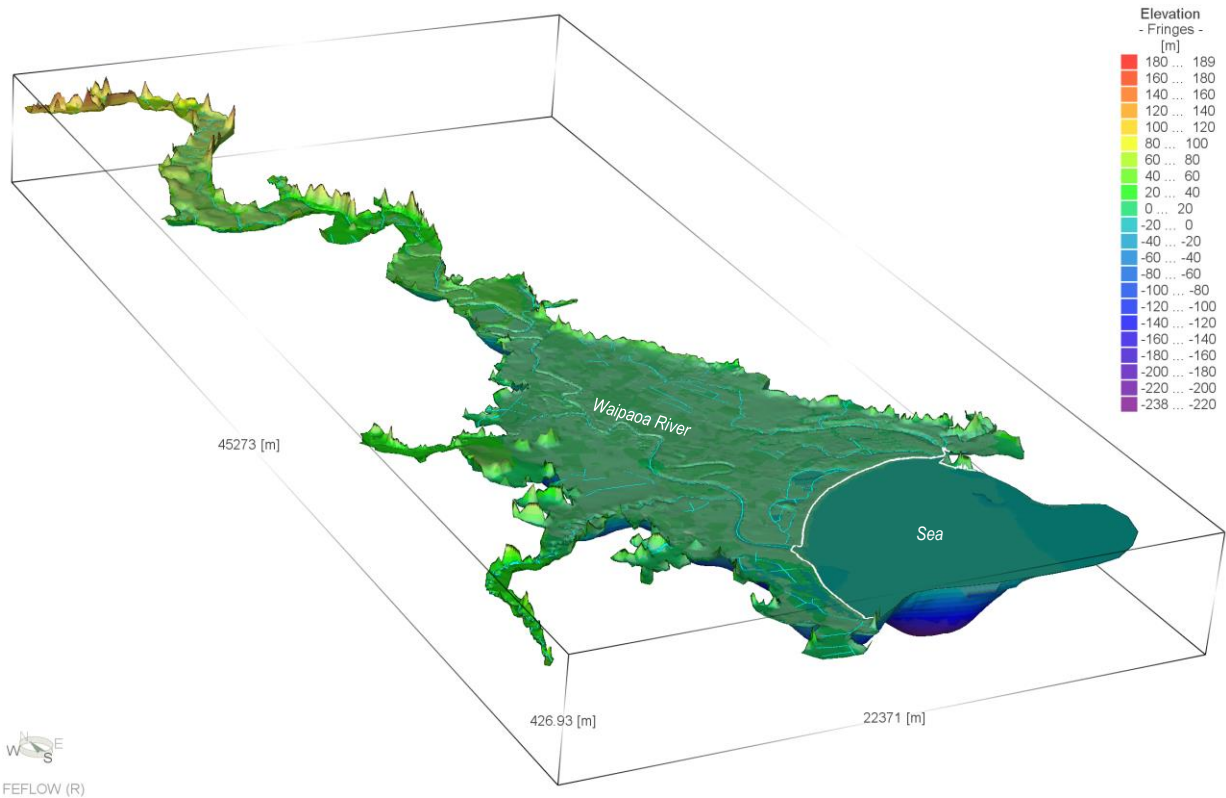


Figure 3-9: 3D view of the 3D groundwater model built with the 10 hydrogeological units, vertical exaggeration 1:10.

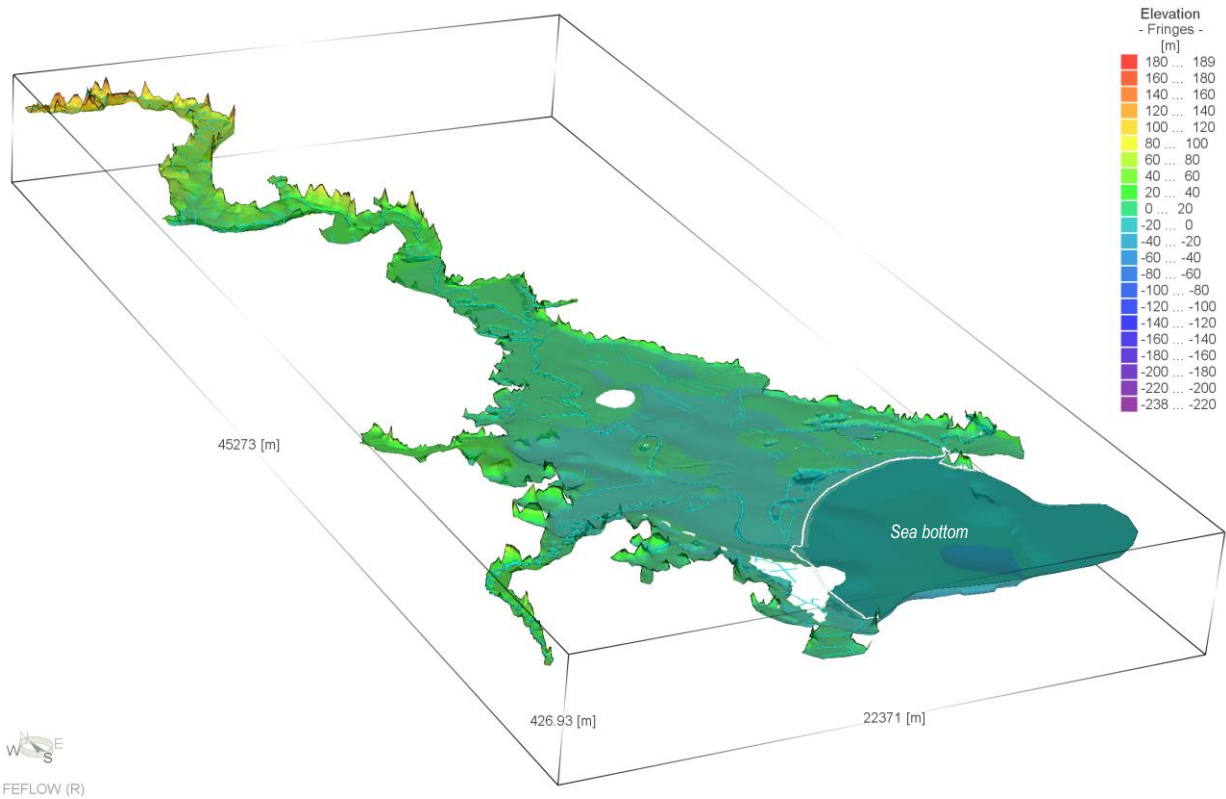


Figure 3-10: 3D view of the hydrogeological unit Undifferentiated (primary layer 1), vertical exaggeration 1:10.

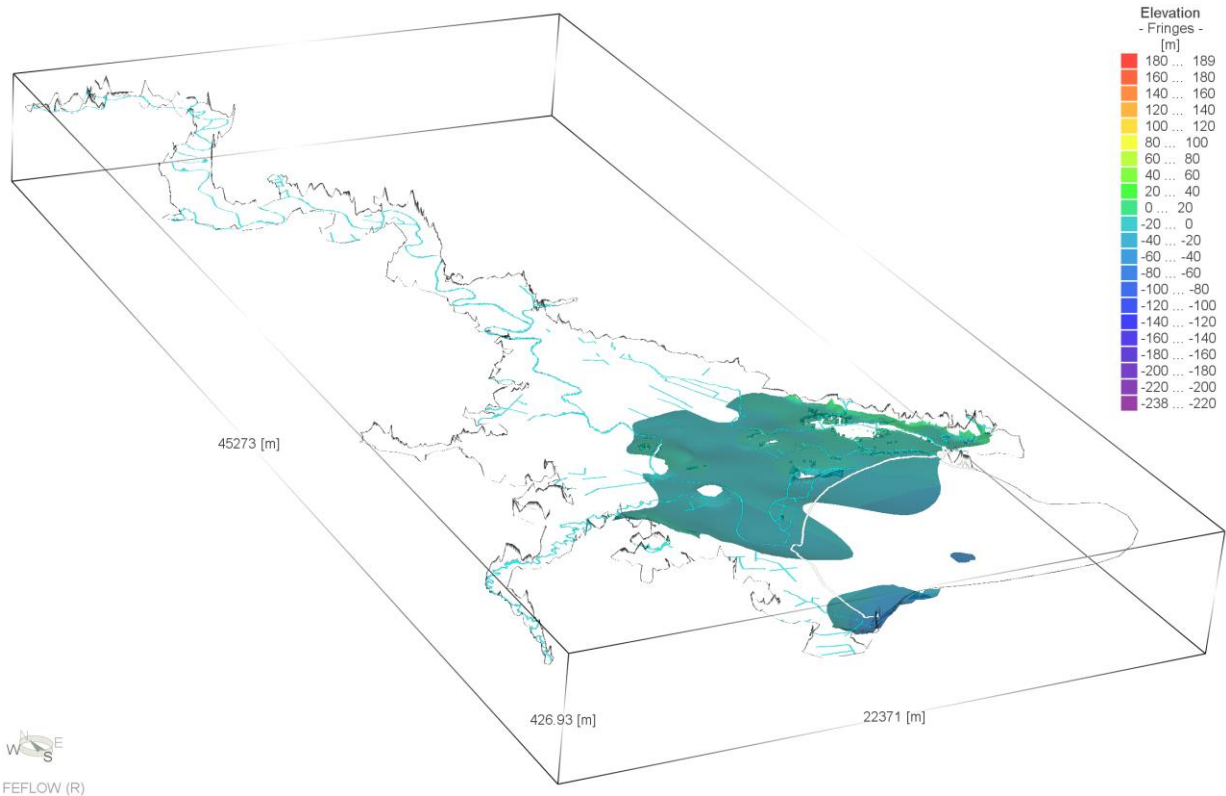


Figure 3-11: 3D view of the hydrogeological unit Te Hapara Sands aquifer (primary layer 2), vertical exaggeration 1:10.

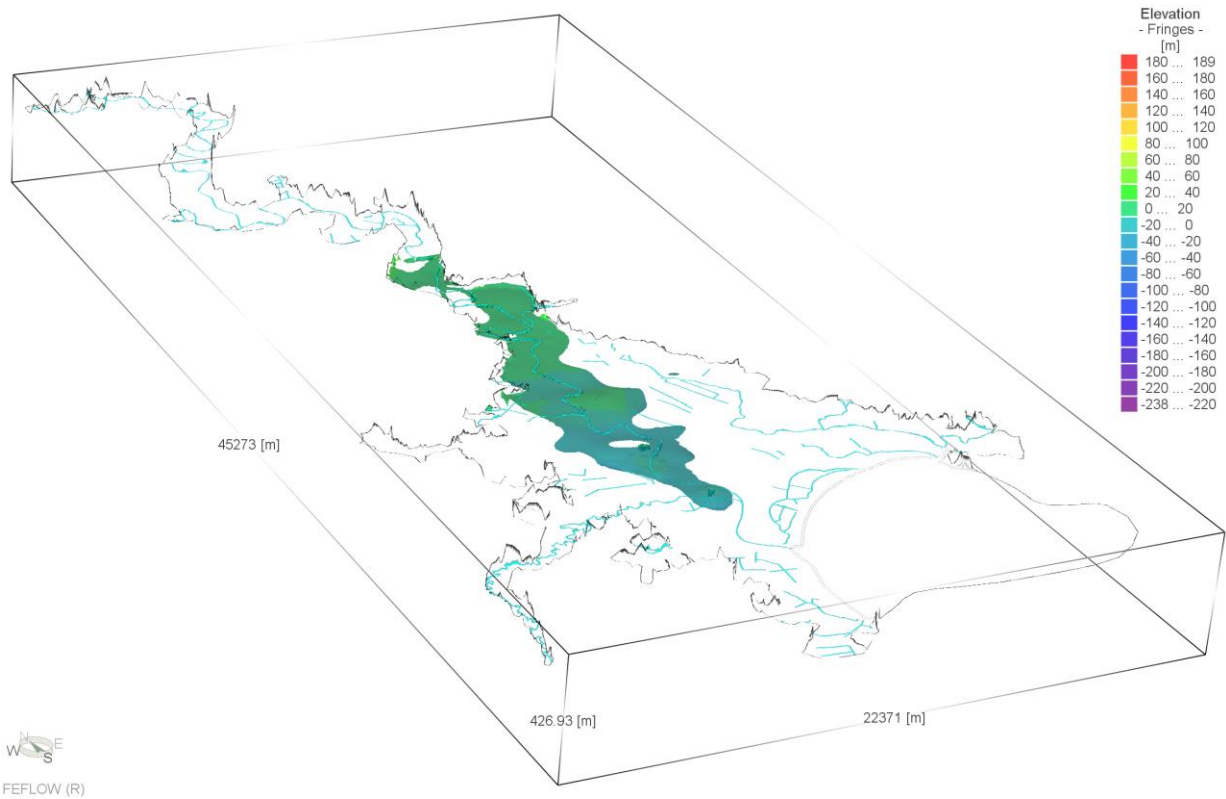


Figure 3-12: 3D view of the hydrogeological unit Shallow Fluvatile aquifer (primary layer 3), vertical exaggeration 1:10.

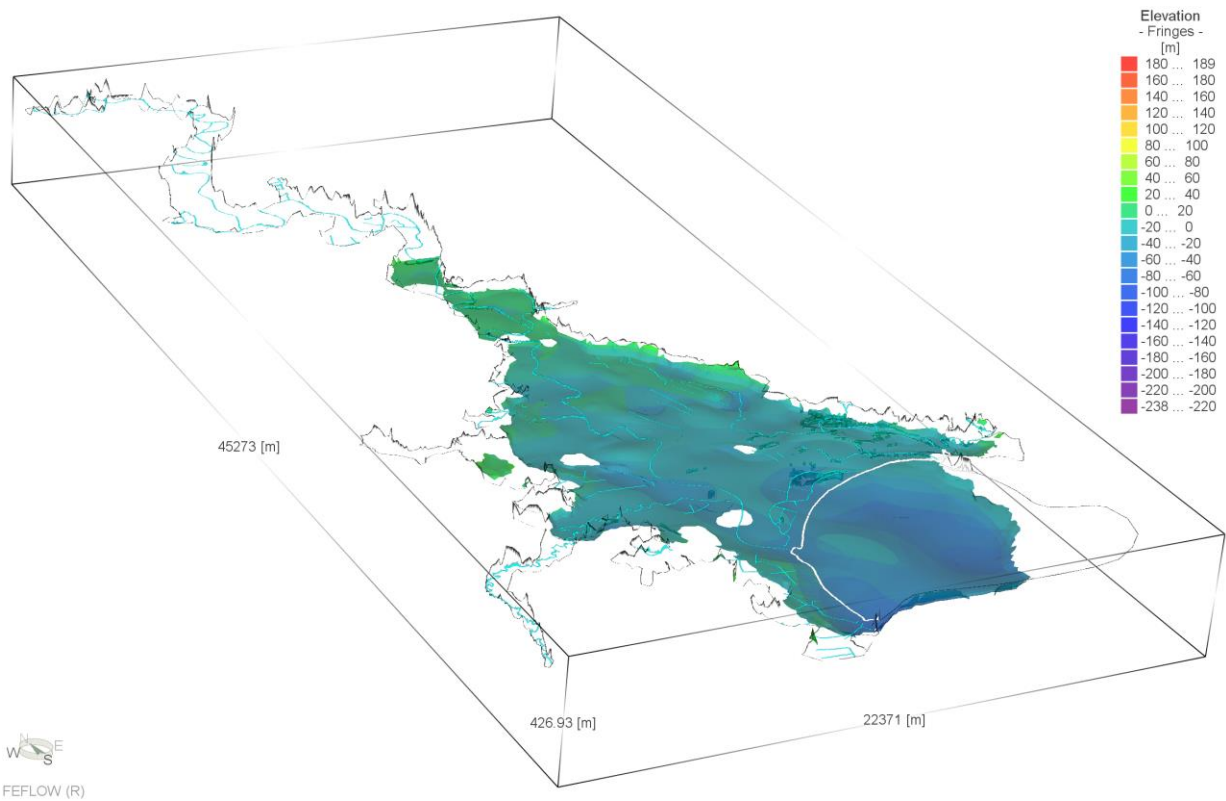


Figure 3-13: 3D view of the hydrogeological unit Aquitard 1 (primary layer 4), vertical exaggeration 1:10.

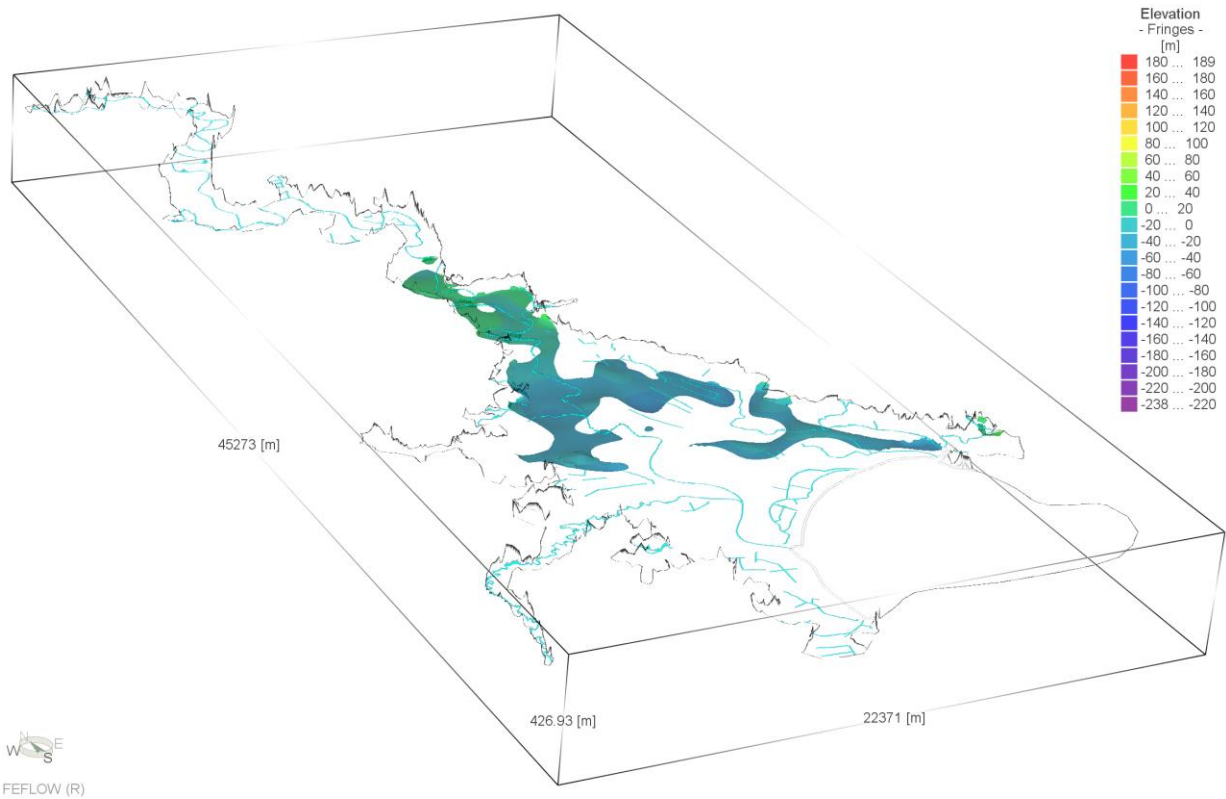


Figure 3-14: 3D view of the hydrogeological unit Waipaoa aquifer (primary layer 5), vertical exaggeration 1:10.

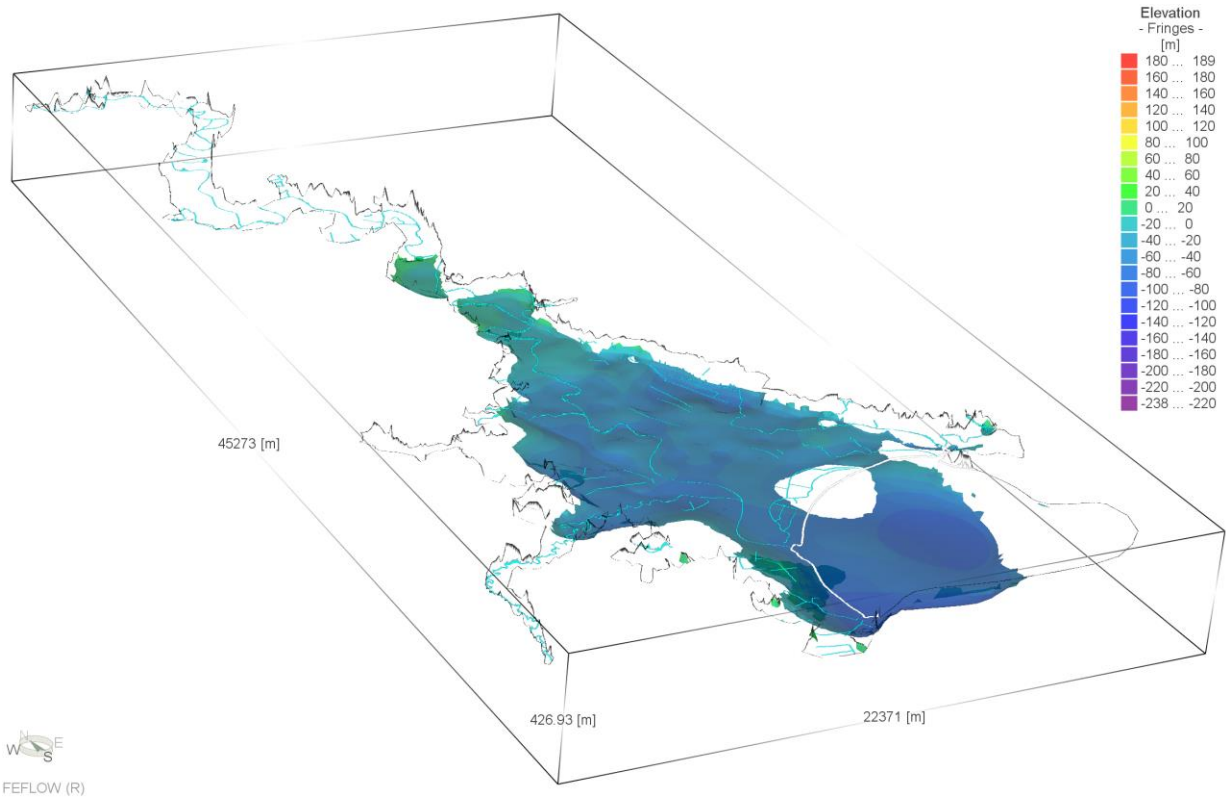


Figure 3-15: 3D view of the hydrogeological unit Aquitard 2 (primary layer 6), vertical exaggeration 1:10.

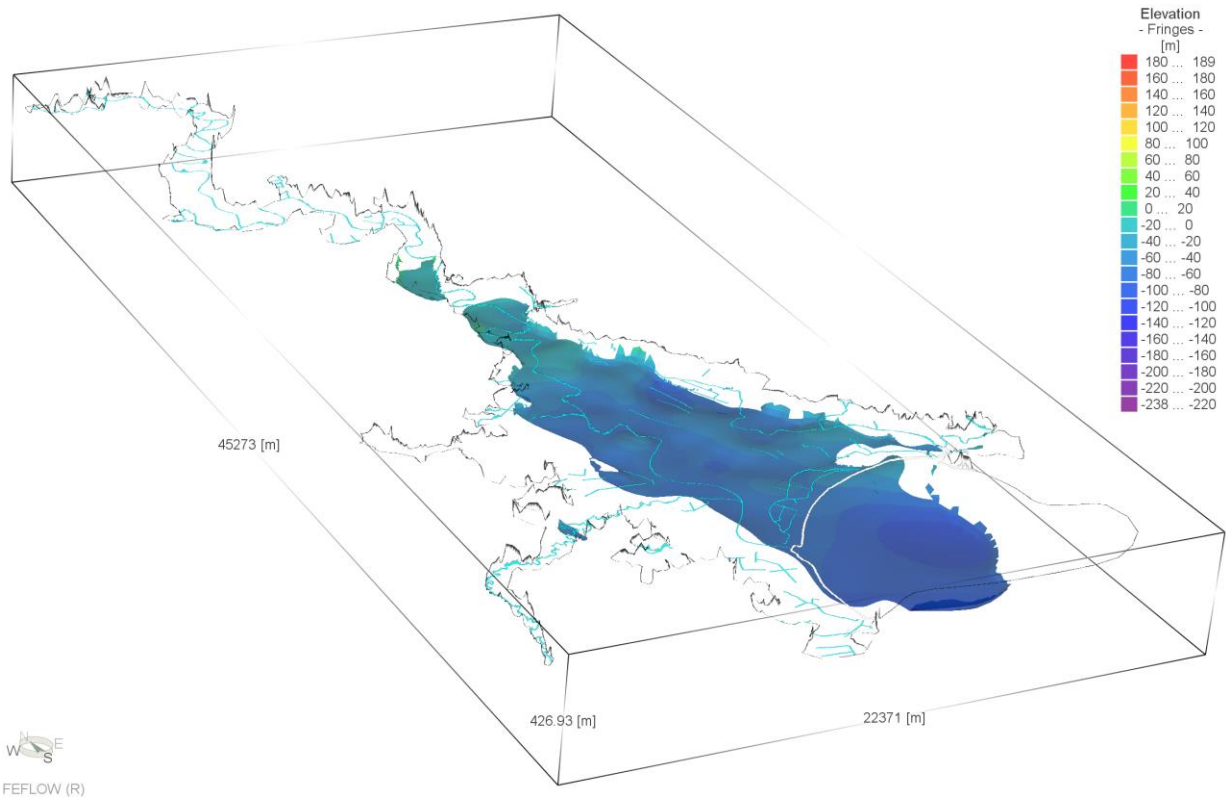


Figure 3-16: 3D view of the hydrogeological unit Makauri aquifer (primary layer 7), vertical exaggeration 1:10.

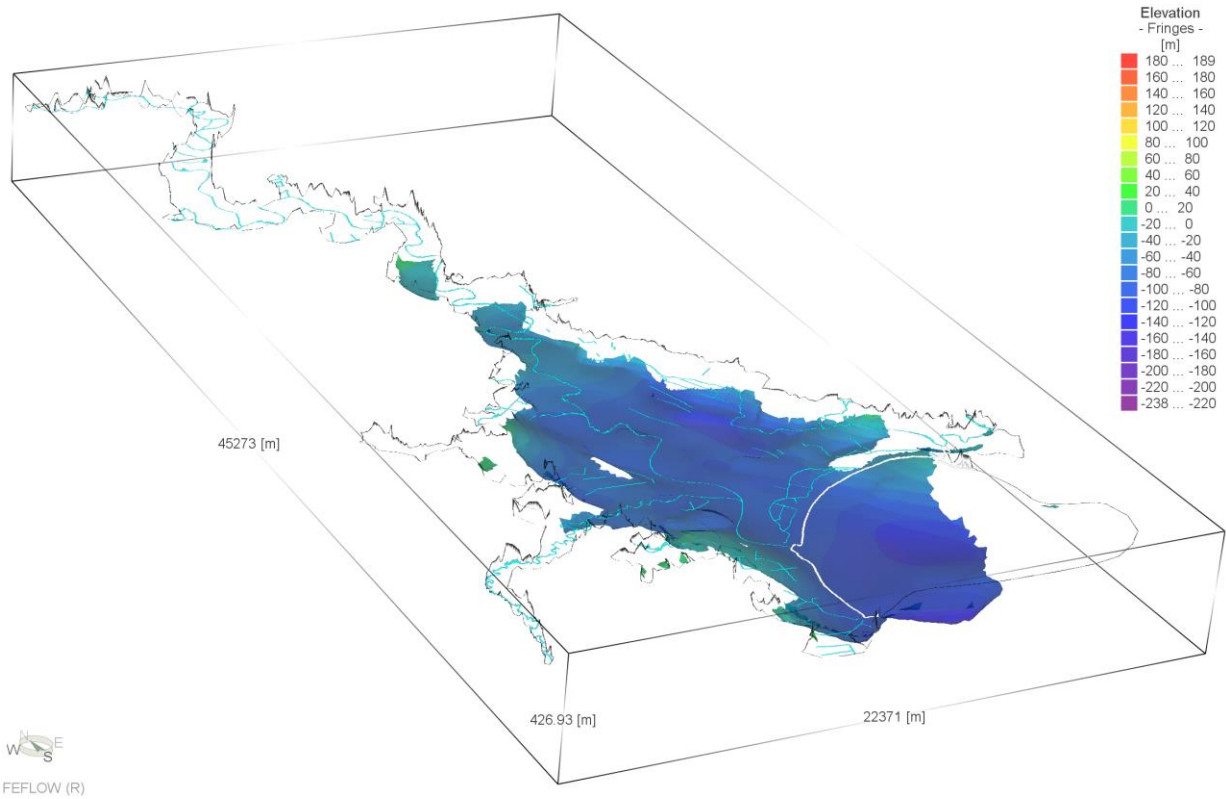


Figure 3-17: 3D view of the hydrogeological unit Aquitard 3 (primary layer 8), vertical exaggeration 1:10.

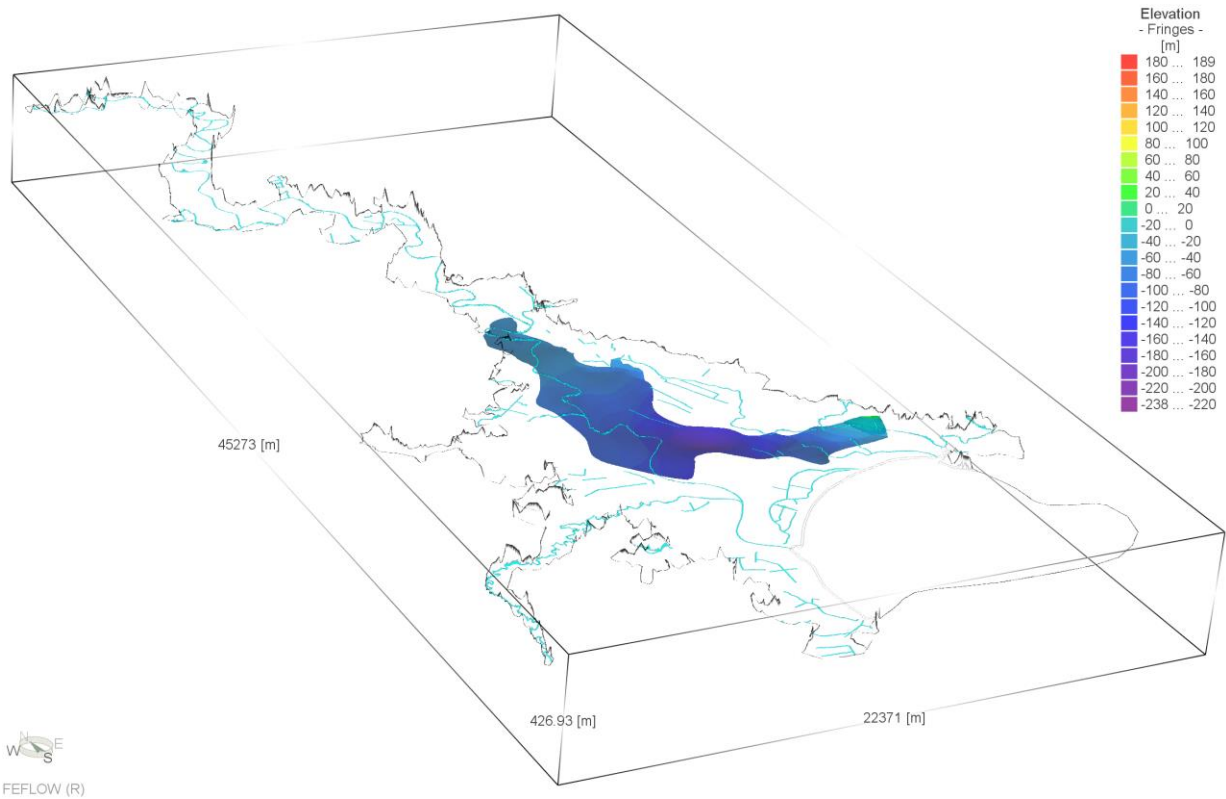


Figure 3-18: 3D view of the hydrogeological unit Matokitoki aquifer (primary layer 9), vertical exaggeration 1:10.

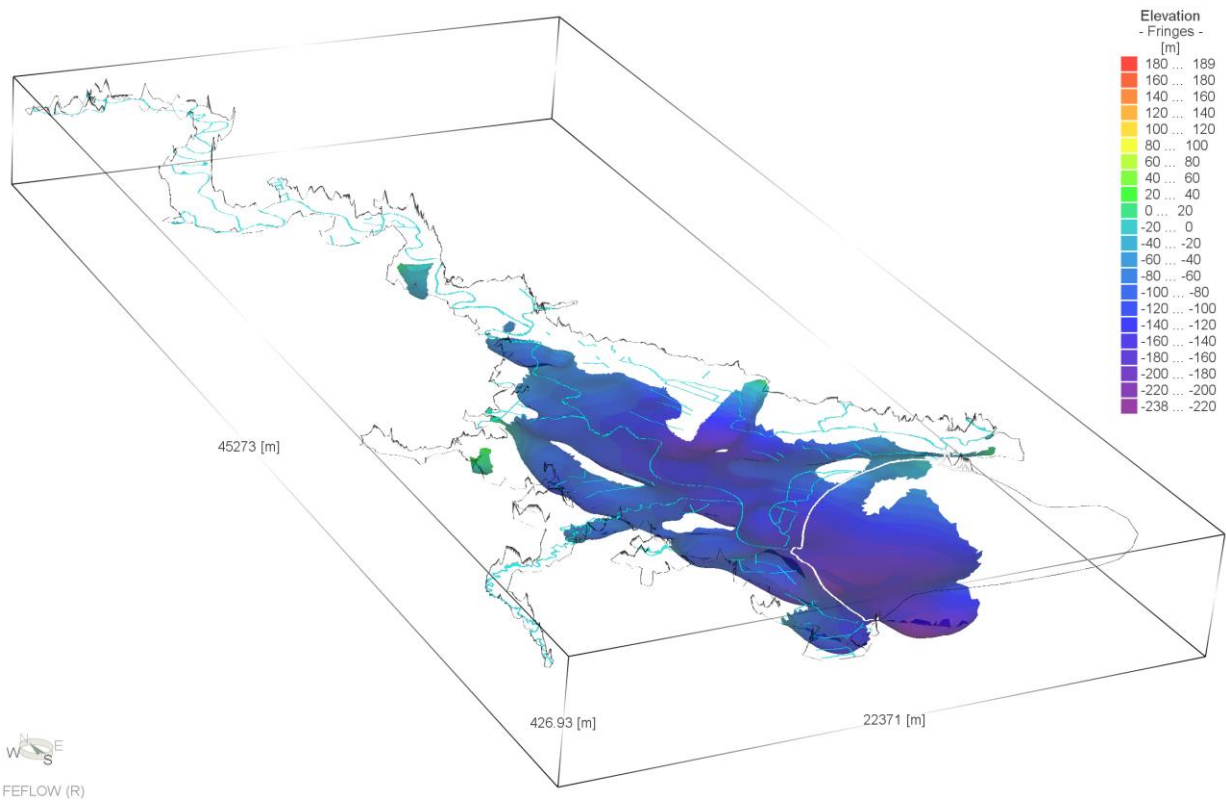


Figure 3-19: 3D view of the hydrogeological unit Aquitard 4 (primary layer 10), vertical exaggeration 1:10.

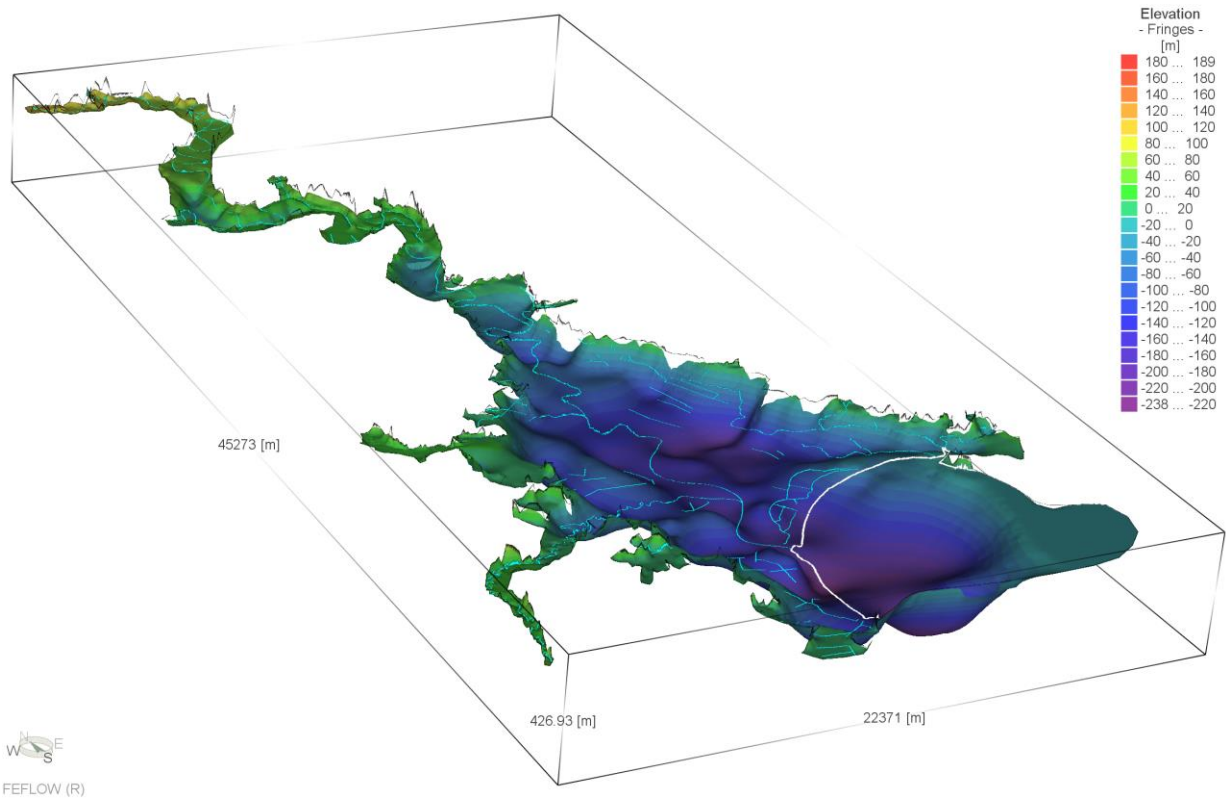


Figure 3-20: 3D view of the model bottom eq. to the base of the Quaternary sediments, i.e., the upper surface Basement incl. the base of the hydrogeological unit Aquitard 4 (primary layer 10), vertical exaggeration 1:10.



Figure 3-21: Cross section lines.

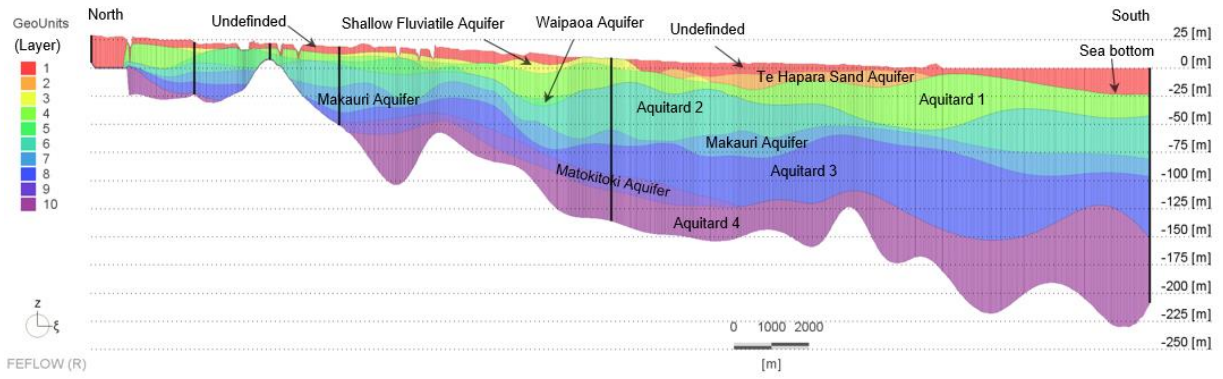


Figure 3-22: Vertical 2D view of North-South cross section 1 (NS-CS#1).

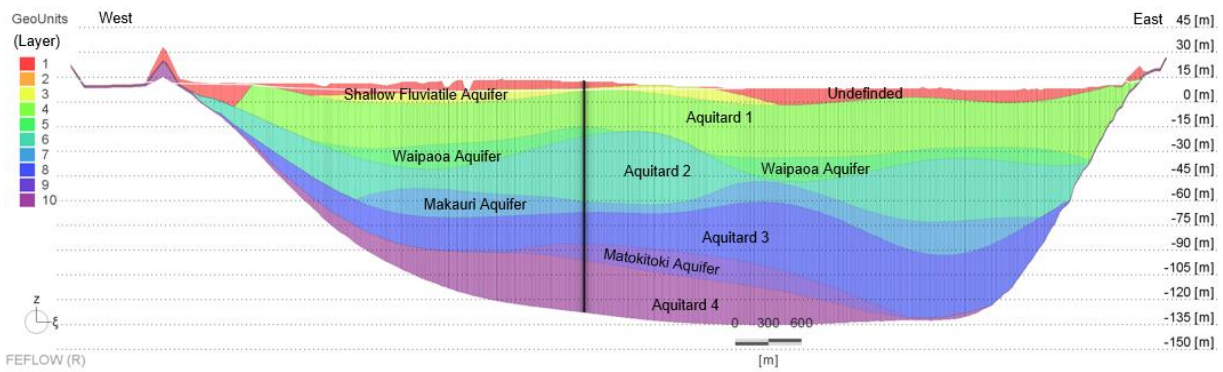


Figure 3-23: Vertical 2D view of West-East cross section 1 (WE-CS#1).

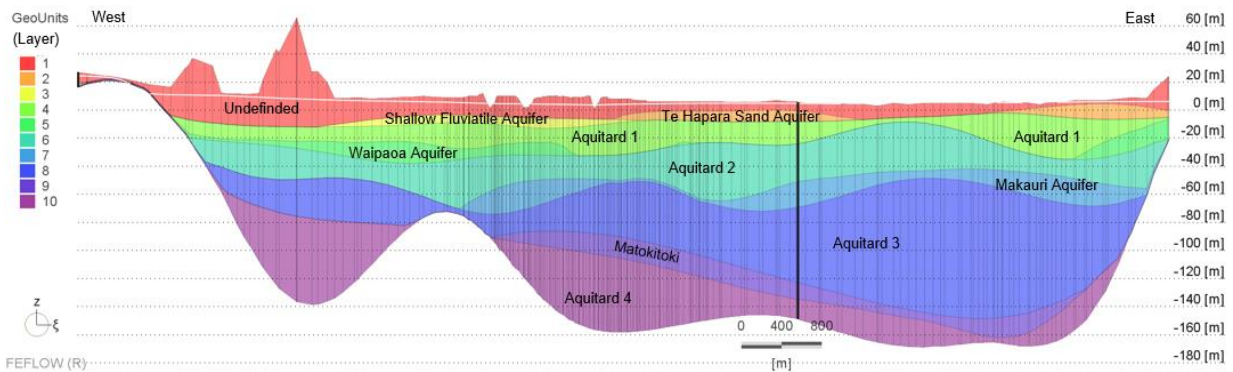


Figure 3-24: Vertical 2D view of West-East cross section 2 (WE-CS#2).

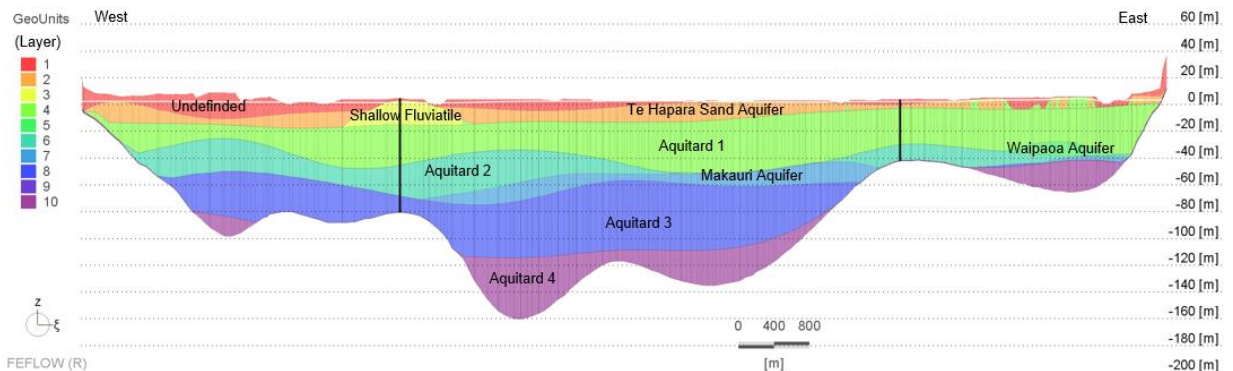


Figure 3-25: Vertical 2D view of West-East cross-section 3 (WE-CS#3).

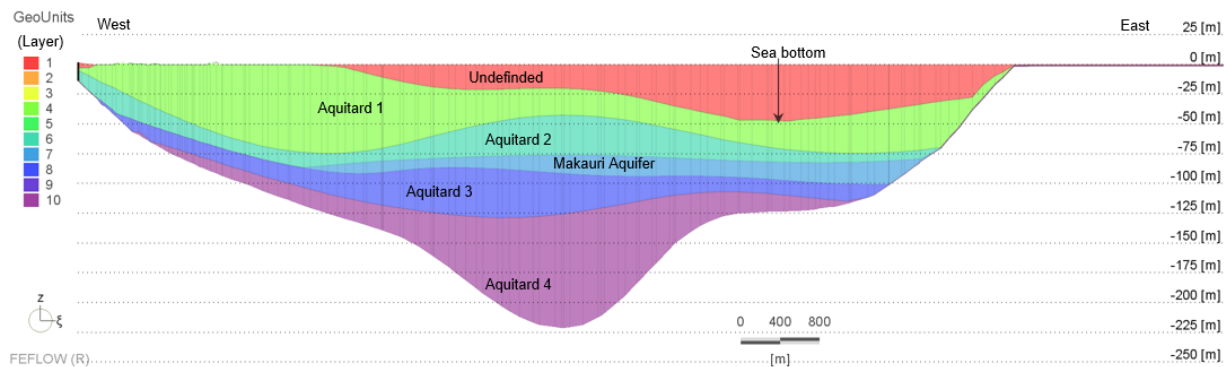


Figure 3-26: Vertical 2D view of West-East cross section 4 (WE-CS#4).

For numerical reasons and also for better modelling vertical flow in the multilayer aquifer-system, the primary 10-layer model is complemented with 8 additional layers for the following aquifers and aquitards by dividing

- primary Layer 1 Undifferentiated into 2 sublayers,
- primary Layer 4 Aquitard 1 into 2 sublayers,
- primary Layer 5 Waipaoa Aquifer into 2 sublayers,
- primary Layer 6 Aquitard 2 into 2 sublayers,
- primary Layer 7 Makauri Aquifer into 3 sublayers,
- primary Layer 8 Aquitard 3 into 2 sublayers,
- primary Layer 9 Matokitoki Aquifer into 2 sublayers.

As a result, the final 3D groundwater model consists of 18 model layers and 19 slices and is composed of 1,811,988 prismatic finite elements and 977,550 nodes in total.

3.4. Hydraulic properties and boundary conditions

Assignment or definition of hydraulic properties and boundary conditions are carried out according to descriptions or/and data base of the Poverty Bay Flats Conceptual Hydrogeological Model [8].

3.4.1. Hydraulic properties

As initial values for model setup, average values derived from pumping tests [8] are specified as hydraulic conductivities of aquifers or aquitards as listed in Table 3-3. Hydraulic conductivity is considered isotropic as the aquifers are all relatively thin.

Table 3-3: Pre-calibration hydraulic conductivity of the hydrogeological units

Aquifer	Initial hydraulic conductivity	
Undifferentiated	8.64 m/d	$1.0 \cdot 10^{-4}$ m/s
Te Hapara Sands aquifer	66.5 m/d	$7.7 \cdot 10^{-4}$ m/s
Shallow Fluvatile aquifer	118.25 m/d	$1.37 \cdot 10^{-3}$ m/s
Aquitard 1:	$8.5 \cdot 10^{-3}$ m/d	$9.84 \cdot 10^{-8}$ m/s
Waipaoa aquifer	88.0 m/d	$1.02 \cdot 10^{-3}$ m/s
Aquitard 2	$8.5 \cdot 10^{-3}$ m/d	$9.84 \cdot 10^{-8}$ m/s
Makauri aquifer	152.0 m/d	$1.76 \cdot 10^{-3}$ m/s

Aquitard 3	8.5*10 ⁻³ m/d	9.84*10 ⁻⁸ m/s
Matokitoki aquifer	38.8 m/d	4.49*10 ⁻⁴ m/s
Aquitard 4	8.5*10 ⁻³ m/d	9.84*10 ⁻⁸ m/s

Hydraulic conductivity has been modified during the calibration procedure where appropriate. Table 3-4 summarises final values of hydraulic conductivity for the hydrogeological units in the model. Spatial distributions of hydraulic conductivity are shown in Figure 3-27 through Figure 3-30 for the hydrogeological units from Undifferentiated to Matokitoki Aquifer.

Table 3-4: Post-calibration hydraulic conductivity of the modelling hydrogeological units

Model Layer	Hydrogeological Units	Hydraulic Conductivity			
		(m/d)		(m/s)	
		from	to	from	to
1 - 2	Undifferentiated *	1.73	172.8	2.0*10 ⁻⁵	2.00*10 ⁻³
3	Te Hapara Sand Aquifer**	6.65	129.6	7.7*10 ⁻⁵	1.50*10 ⁻³
4	Shallow Fluvatile Aquifer	118.25		1.37*10 ⁻³	
5 - 6	Aquitard1	8.5*10 ⁻⁴		9.84*10 ⁻⁹	
7 - 8	Waipaoa Aquifer	17.6	88.0	2.04*10 ⁻⁴	1.02*10 ⁻³
9 - 11	Aquitard2	8.5*10 ⁻⁴		9.84*10 ⁻⁹	
12 - 13	Makauri Aquifer	50.7	304.0	5.86*10 ⁻⁴	3.52*10 ⁻³
14 - 15	Aquitard3	8.5*10 ⁻⁴		9.84*10 ⁻⁹	
16 - 17	Matokitoki Aquifer	38.8	86.4	4.49*10 ⁻⁴	1.00*10 ⁻³
18	Aquitard4	8.5*10 ⁻⁴		9.84*10 ⁻⁹	

* Matawhero/Oxbow Wetland: 172.8 m/d (0.002 m/s)

** Settlements Gisborne: 1.73 m/d (2.0*10⁻⁵ m/s) to 21.6 m/d (2.5*10⁻⁴ m/s)

The phreatic groundwater surface is considered in the 3D groundwater model by using unsaturated flow conditions (Richards' equation). The empirical Modified van Genuchten parametric relationship in FEFLOW is used with following simplified parameters:

- Maximum porosity: 20 %
- Maximum saturation S_s : 100 %
- Residual Saturation S_r : 0,25 %
- Fitting coefficient α : 4,1 [1/m]
- Fitting exponent n : 1,964
- Fitting exponent δ : 1
- Fitting exponent m : 0,509.

It is important to note that a detailed simulation of flow in the unsaturated zone is not intended here; Richards' equation is rather used with simplified parameters to simulate unconfined conditions, as this is typically superior to the other available methods in FEFLOW with respect to model stability and flexibility in application. For confined flow, specific storage $1*10^{-4}$ (1/m) is assigned to the upper aquifers (Undifferentiated, The Hapara Sands, Shallow Fluvatile), $1*10^{-5}$ (1/m) to the aquifers below Aquitard 1.

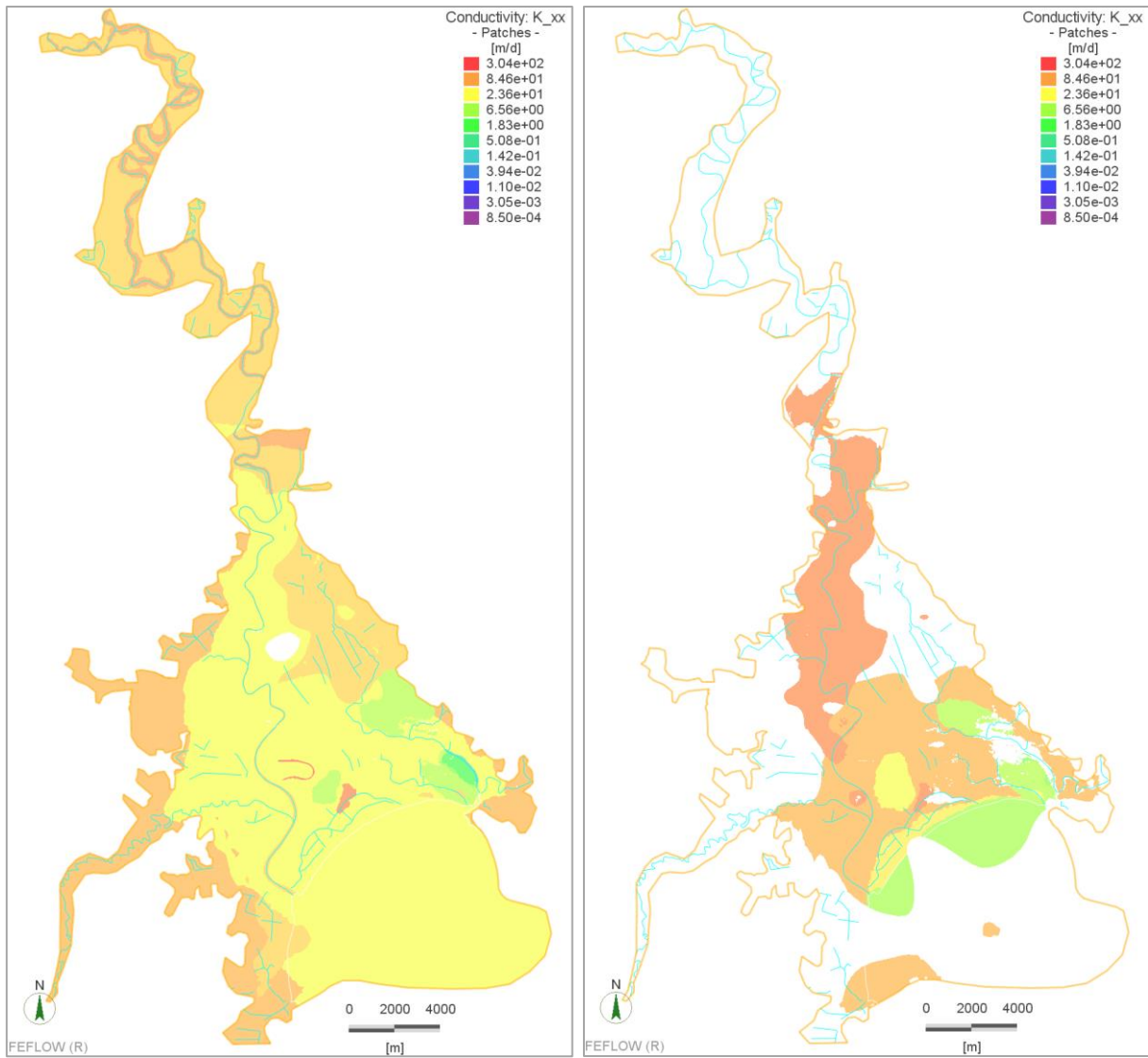


Figure 3-27: Overview of hydraulic conductivity of Undifferentiated (left) and Te Hapara Sands + Shallow Fluviate (right).

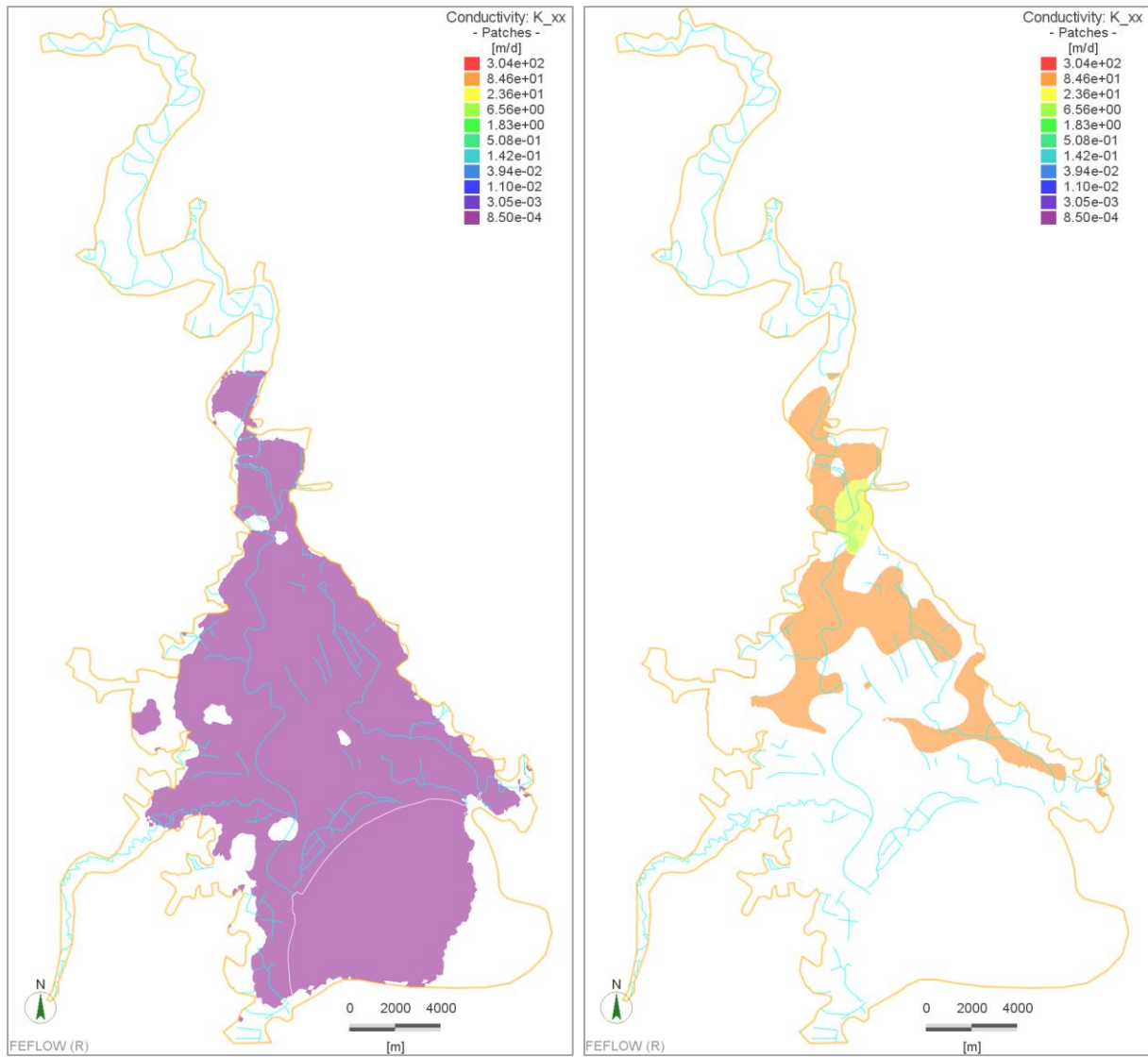


Figure 3-28: Overview of hydraulic conductivity of Aquitard 1 (left) and Waipaoa Aquifer (right).

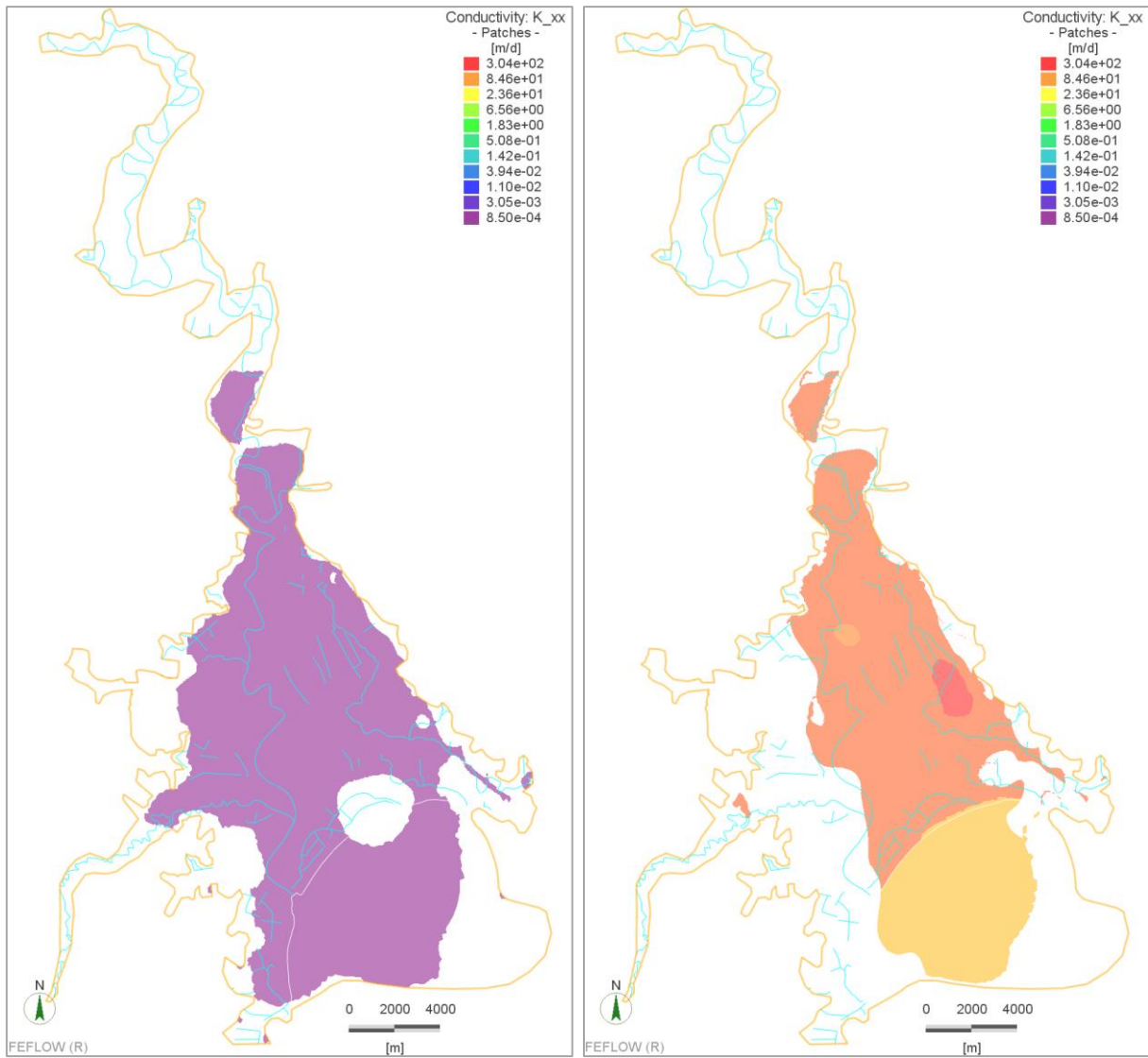


Figure 3-29: Overview of hydraulic conductivity of Aquitard 2 (left) and Makauri aquifer (right).

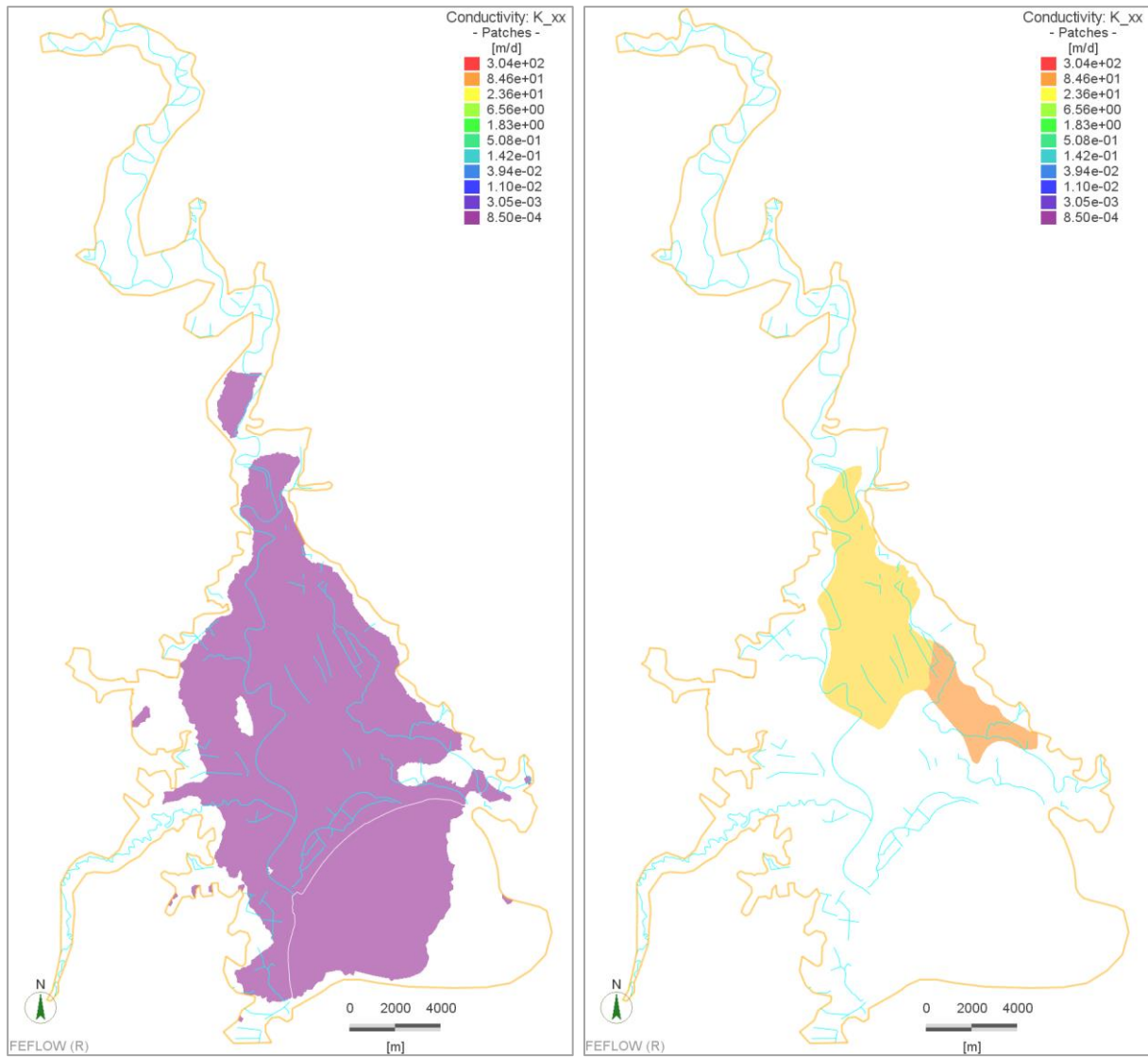


Figure 3-30: Overview of hydraulic conductivity of Aquitard 3 (left) and Matokitoki aquifer (right).

3.4.2. Hydraulic boundary conditions

Table 3-5 gives an overview of all the hydraulic boundary conditions specified, according to [3], for relevant surface water bodies incl. Waipaoa River and sea, and for groundwater usages (takes). All the western and eastern model borders, in case of no boundary condition specified, are assumed to be impermeable for groundwater flow. Lateral inflow to the Matokitoki aquifer has not been considered (see chapter 4.8).

Table 3-5: Boundary conditions of the hydrogeological units

Model Layer	Hydrogeological Unit	Boundary condition for	remark
1 - 2	Undifferentiated	River/Stream/Drains, Sea	on model slice 1-2, sea on slice 3
3	Te Hapara Sands aquifer	Pumping wells	on model slice 3
4	Shallow Fluvial aquifer	Pumping wells	on model slice 3 or 4
5 - 6	Aquitard1		
7 - 8	Waipaoa aquifer	Pumping wells	on model slice 8
9 - 11	Aquitard2		
12 - 13	Makauri aquifer	Takes	on model slice 13
14 - 15	Aquitard3	non	
16 - 17	Matokitoki aquifer	Takes	on model slice 17
18	Aquitard4		

Boundary conditions for surface water bodies

For initial calibration runs, Hydraulic-head boundary conditions (BC), also called 1st-kind or Dirichlet BC, are used for all surface water bodies considered in the model. During calibration, the Hydraulic-head BC is applied only representing the sea, while Fluid-transfer boundary conditions, also called 3rd-kind, Cauchy or river BCs, are defined for rivers, streams and drains, taking into account river-bed clogging.

The definition of a Fluid-transfer BC requires water levels in surface water (h_{sw}) and an additional river-bed conductance parameter with the unit [1/d]. Flow rates through a Fluid-transfer BC are internally calculated in FEFLOW by the following formula

$$Q = \text{Area}_{\text{flowthrough}} * \text{Conductance} * \Delta h,$$

where $\Delta h = h_{sw} - h_{GW}$, i.e., water level difference between surface and ground water at the Fluid-transfer BC.

The transfer rate (riverbed conductance) can be estimated from hydraulic conductivity k and thickness T of a clogging layer in the river bed by

$$\text{Riverbed conductance} = k / T$$

As this parameter is typically fairly unknown, river-bed conductance is generally used as a calibration parameter. Flow through Fluid-transfer BC can be controlled by varying the conductance.

For the Waipaoa river and the part of Taruheru River flowing through the city of Gisborne both conductance for infiltration from the river and baseflow to the river are defined with the same values. For the remaining part of the Taruheru River (incl. Taruheru Trib) and Te Arai River, Waru Stream, Whakaahu Stream, Waikanae Creek and numerous drains that primarily function as drainages from the aquifer system, conductance is only specified for flow from groundwater into the rivers. This prohibits inflow from the

corresponding surface water bodies, making them act as drains only. Figure 3-31 presents an overview of locations of the transfer boundary condition (left) and the corresponding conductance (direction GW to SW) after model calibration (right).

Table 3-6 gives an overview of the available gauging stations with water level records and their locations provided in [7]. The water level records at the gauging stations are used as data points to assign water levels h_{sw} to Fluid-transfer BCs as follows:

1. Assigning recorded water levels h_{sw} to Fluid-transfer BC at nodes corresponding to each gauging location (ref. Figure 3-31),
2. linear interpolation of water levels h_{sw} to Fluid-transfer BC nodes between gauging location nodes.

For Waikanae Creek and drains without water level records, h_{sw} were estimated based on ground surface level or/and groundwater level in the upper aquifers. The estimated h_{sw} for the smaller rivers/creeks/drains are used for steady state calibration and are kept as time-constant for transient calibration and validation.

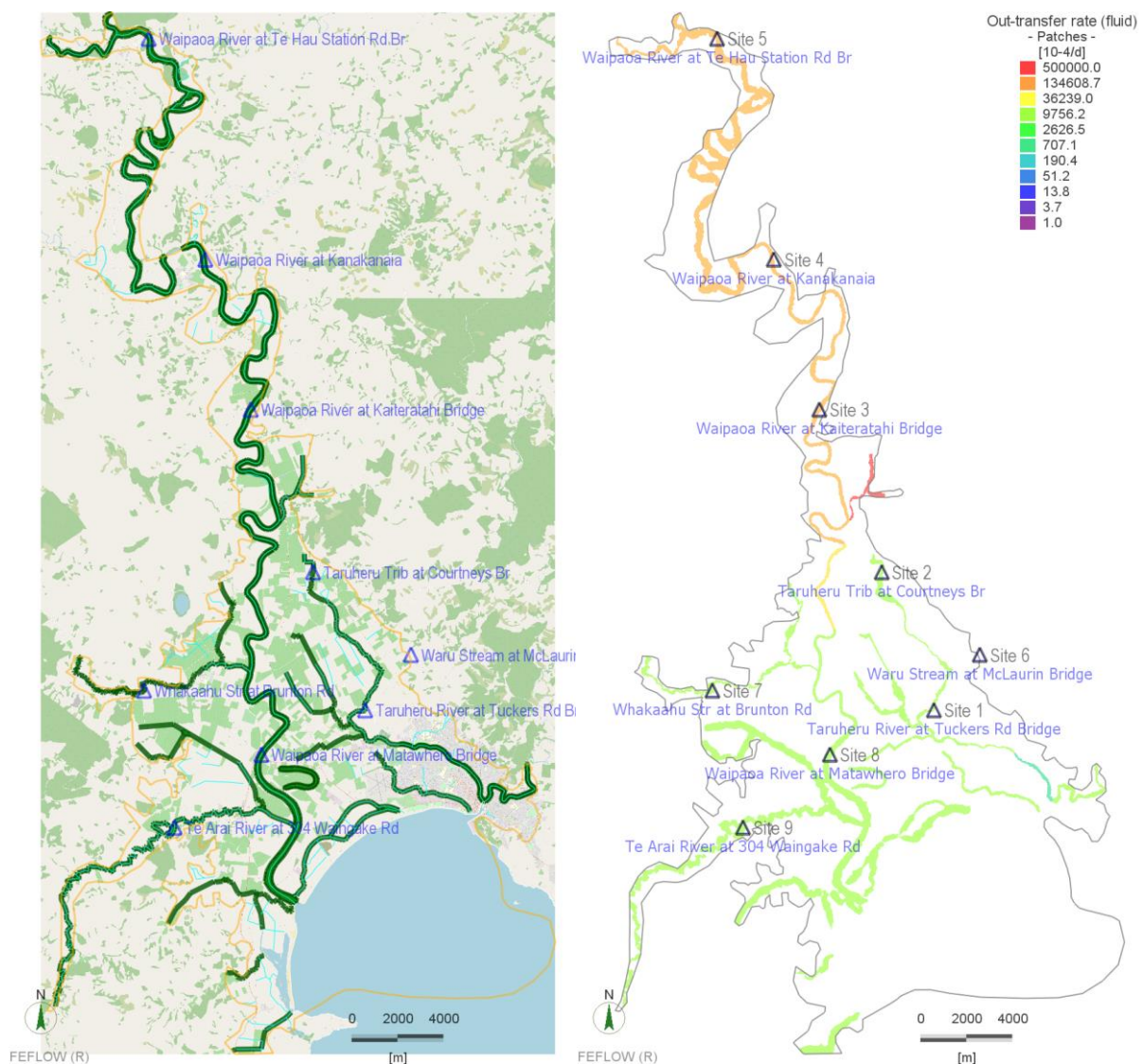


Figure 3-31: Locations of the transfer boundary condition (3rd-kind BC shown in green) implemented for Waipaoa River and other local streams and drains (left), along with corresponding riverbed conductance (for flow direction groundwater to surface water) (right).

Table 3-6: Overview of available gauging stations with water level records

Site ID	River/Stream Name	Location	Measurements		Number of measures	Levels used for steady state calib. (m RL)*
			from	to		
1	Taruhuru River	at Tuckers Rd Bridge	19.01.1981 15:42	29.11.2021 23:42	63812	3.66
2	Taruhuru Trib	at Courtneys Br	01.01.1993 00:00	13.12.2017 07:00	206757	13.23
5	Waipaoa River	at Te Hau Station Rd Br	10.06.2014 15:00	30.11.2021 00:00	63812	78.35
4	Waipaoa River	at Kanakanaia	01.01.1927 12:00	30.11.2021 00:00	574047	30.10
3	Waipaoa River	at Kaiteratahi Bridge	01.01.1989 00:00	28.11.2017 07:00	250601	18.27
8	Waipaoa River	at Matawhero Bridge	01.07.1962 09:52	29.11.2021 23:52	470388	1.15
6	Waru Stream	at McLaurin Bridge	19.09.1995 15:42	02.08.2017 12:42	190837	18.61
7	Whakaahu Str.	at Brunton Rd	31.10.1996 10:00	30.11.2021 00:00	130875	19.21
9	Te Arai River	at 304 Waingake Rd	09.11.2017 10:55	26.11.2021 07:55	35470	2.53

* Mean values of measures in the period of Oct. 2015 – Sept. 2017.

Boundary conditions for groundwater usages / takes

Groundwater usages / takes are implemented by using well boundary conditions (Well BC) corresponding to locations of abstraction or injection (MAR) bores. Table 3-7 shows the Well BC implemented for abstraction and injection bores according to the GDC data [11], [13] - [15]. Locations of the Well BC are presented in Figure 3-31 and Figure 3-32 for upper and lower aquifers respectively.

Table 3-7: Overview of abstraction and injection bores considered in aquifers within the model area

Historical Takes in Aquifer	Sum of Oct.2008- Oct.2021	Annual average	Number of pumping bores	Number of MAR bores
	Amount m ³	m ³ /year		
Makauri aquifer	10,827,035	827,443	39	1 for MAR-trials and 6 for Scenarios
Matokitoki aquifer	776,331	59,330	3	
Shallow Fluviatile	504,431	38,551	17	
Te Hapara Sands	1,381,062	105,546	33	
Waipaoa aquifer	1,104,840	84,436	13	
Sum	14,593,699	1,150,743	105	1 + 6

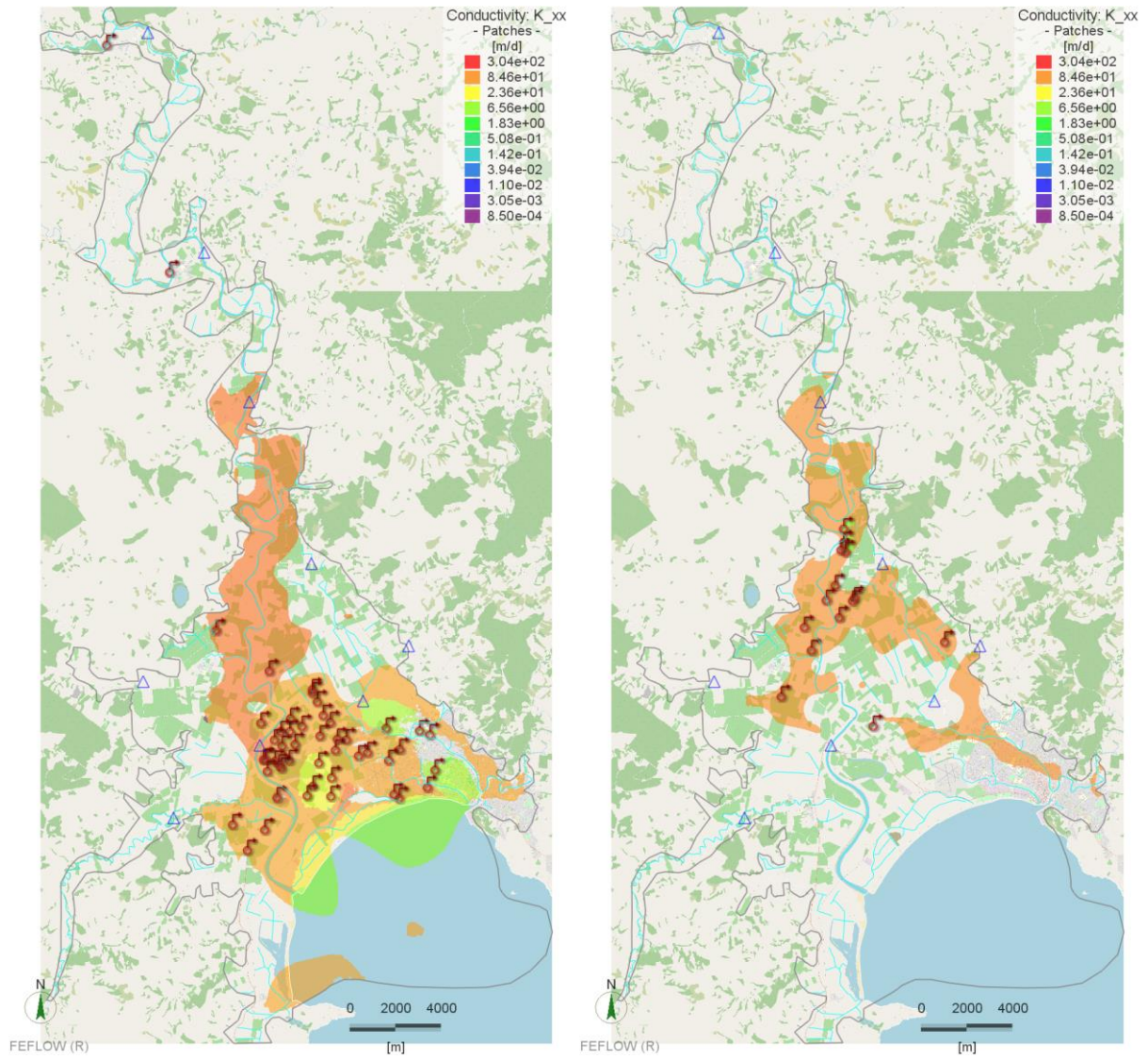



Figure 3-32: Overview of well boundary conditions () in Te Hapara Sands and Shallow Fluvial aquifers (left) and Waipaoa aquifer (right).

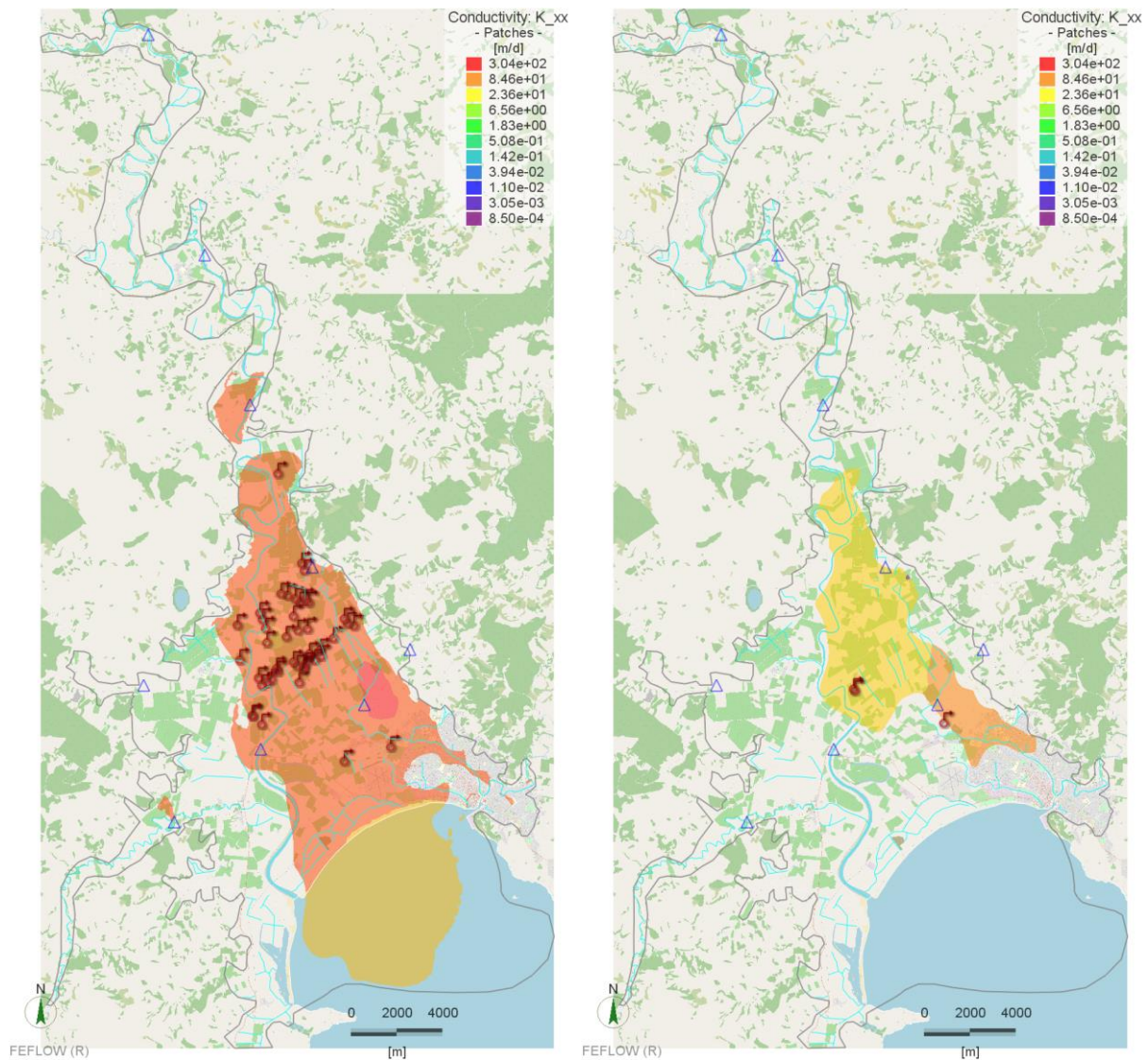


Figure 3-33: Overview of well boundary conditions () in Makauri (left) and Matokitoki aquifers (right).

3.4.3. Spatially distributed groundwater recharge from rainfall

As described in [8], spatially distributed groundwater recharge may result from a combination of rainfall and irrigation infiltration. In general, irrigation is intended to provide sufficient soil moisture to support ideal crop growing conditions. Over-irrigation leading to the excess water recharging shallow aquifers is not considered to be a common situation in the area. Although summer irrigation followed by a significant storm event may result in enhanced short-term recharge to shallow aquifers, this is also not considered to be a significant contributing factor to the groundwater budget for the model.

An initial estimate derived from Golder (2021) [17] indicates rainfall-recharge rates as follows:

- Grassland areas 42 % of winter rainfall Averaging 1.71 mm/day,
- Forest areas 38 % of winter rainfall Averaging 1.55 mm/day,
- Cropped areas 53 % of winter rainfall Averaging 2.15 mm/day,
- Urban areas 27 % of winter rainfall Averaging 1.08 mm/day, and
- Sea/Surface water 0.

These rates were adopted to specify spatially distributed groundwater recharge for groundwater modelling. The implementation of spatially distributed groundwater recharge was performed as follows:

- Generating a spatially varying recharge distribution according to the recharge rates described above and under consideration of LUCAS NZ Land Use Map [12] as primary recharge rates (Q). The primary recharge rates are assigned in FEFLOW as “In/Outflow on top/bottom” in the uppermost model layer,
- Creating a User Data distribution in FEFLOW named ClimateZone in the uppermost model layer, allowing consideration of available rainfall data [6] for the two weather stations Gisborne EWS ($Rainfall_{EWS}$) and Gisborne AWS ($Rainfall_{AWS}$),

Figure 3-34 (left) shows the primary groundwater recharge distributed over the model area, while Figure 3-34 (right) depicts the “User Data” ClimateZone with assigned value 1 in the northern part (station Gisborne EWS), 0 in the southern part (station Gisborne Aws), and interpolated values in an interval between 1 and 0 in the area between the two stations.

- Defining or specifying spatially distributed recharge rates (Q_p) by using the FEFLOW Expression Editor, applying the following calculation formula for each finite element under consideration of its location relative to the two stations:

$$Q_p = Q * (Rainfall_{EWS} * ClimateZone + (1 - ClimateZone) * Rainfall_{AWS})$$

In case of a location north of station Gisborne EWS, the formula calculates spatially distributed recharge (Q_p) using rainfall data of the station Gisborne EWS i.e.

$$Q_p = Q * (Rainfall_{EWS} * 1 + (1 - 1) * Rainfall_{AWS}) = Q * Rainfall_{EWS}$$

or using rainfall data of the station Gisborne Aws for elements south of station Gisborne Aws

$$Q_p = Q * (Rainfall_{EWS} * 0 + (1 - 0) * Rainfall_{AWS}) = Q * Rainfall_{AWS}$$

Technically, rainfall data $Rainfall_{EWS}$ and $Rainfall_{AWS}$ in the formula can be set as constant values or as time series (TS). The available rainfall (daily values) data of the two stations are summarised in Table 3-8.

Table 3-8: Station information

Name	Agent Number	Network Number	Latitude (dec.deg)	Longitude (dec.deg)	Height (m)	Posn_Precision	Observing Authority	Data from	to
Gisborne Ews	24976	D87697	-38.62747	177.9218	12	H	Niwa	14.06.2003	30.06.2021
Gisborne Aws	2810	D87695	-38.6586	177.98513	5	H	Metservice	13.12.1989	30.06.2021

Note: Position precision types are: "W" = based on whole minutes, "T" = estimated to tenth minute, G = derived from gridref, "E" = error cases derived from gridref, H = based on GPS readings (NZGD49), "D" = by definition i.e. grid points.

For transient simulations, only rainfall within the 5-months period from May to September are considered, i.e. one autumn, three winter and one spring month(s).

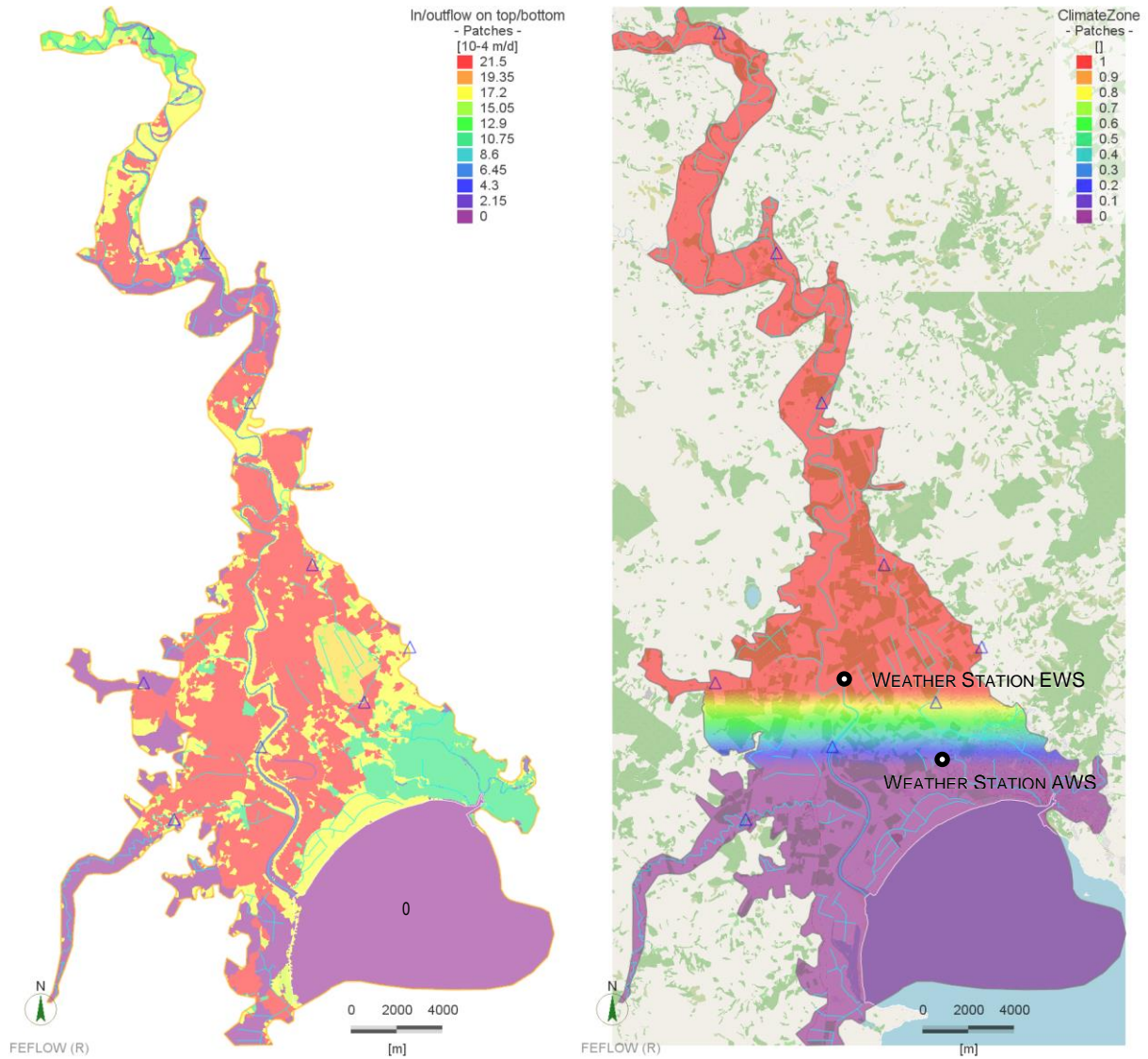


Figure 3-34: Overview of groundwater recharge from rainfall (left) and climate zonation (right).

3.5. Monitoring bores

All known observation bores have been implemented in the model in order to be able to extract results at those locations. In Figure 3-35 through Figure 3-38 the monitoring bores are shown for each aquifer as a reference, for example for diagrams in the digital appendix. Monitoring bores in some cases are outside the respective aquifers, because the underlying geological model does not always represent local conditions perfectly (e. g., small patches of fluvatile sediments not in geological model).

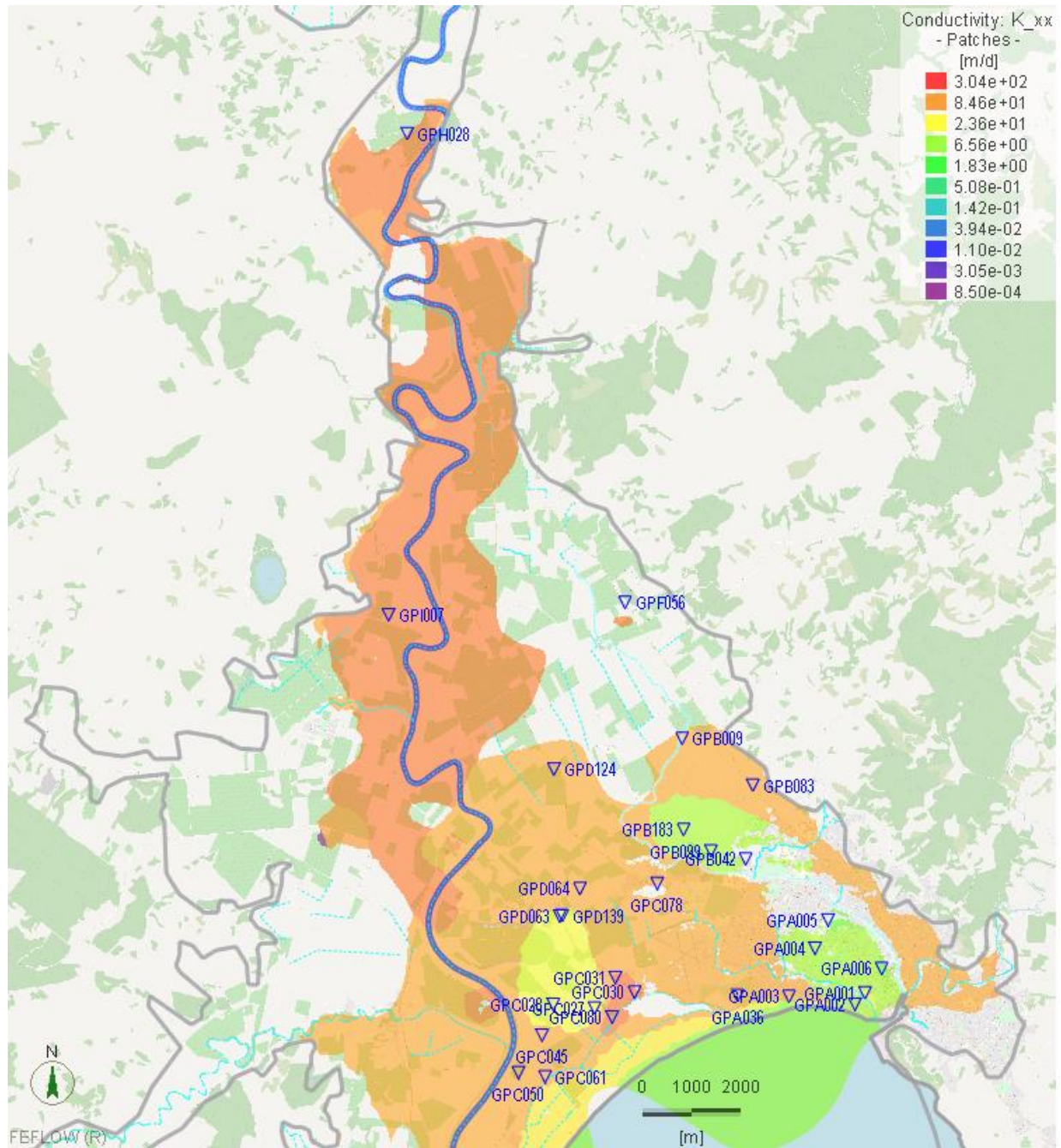


Figure 3-35: Monitoring bores in Te Hapara Sands, Shallow Fluvatile and Undifferentiated aquifers.

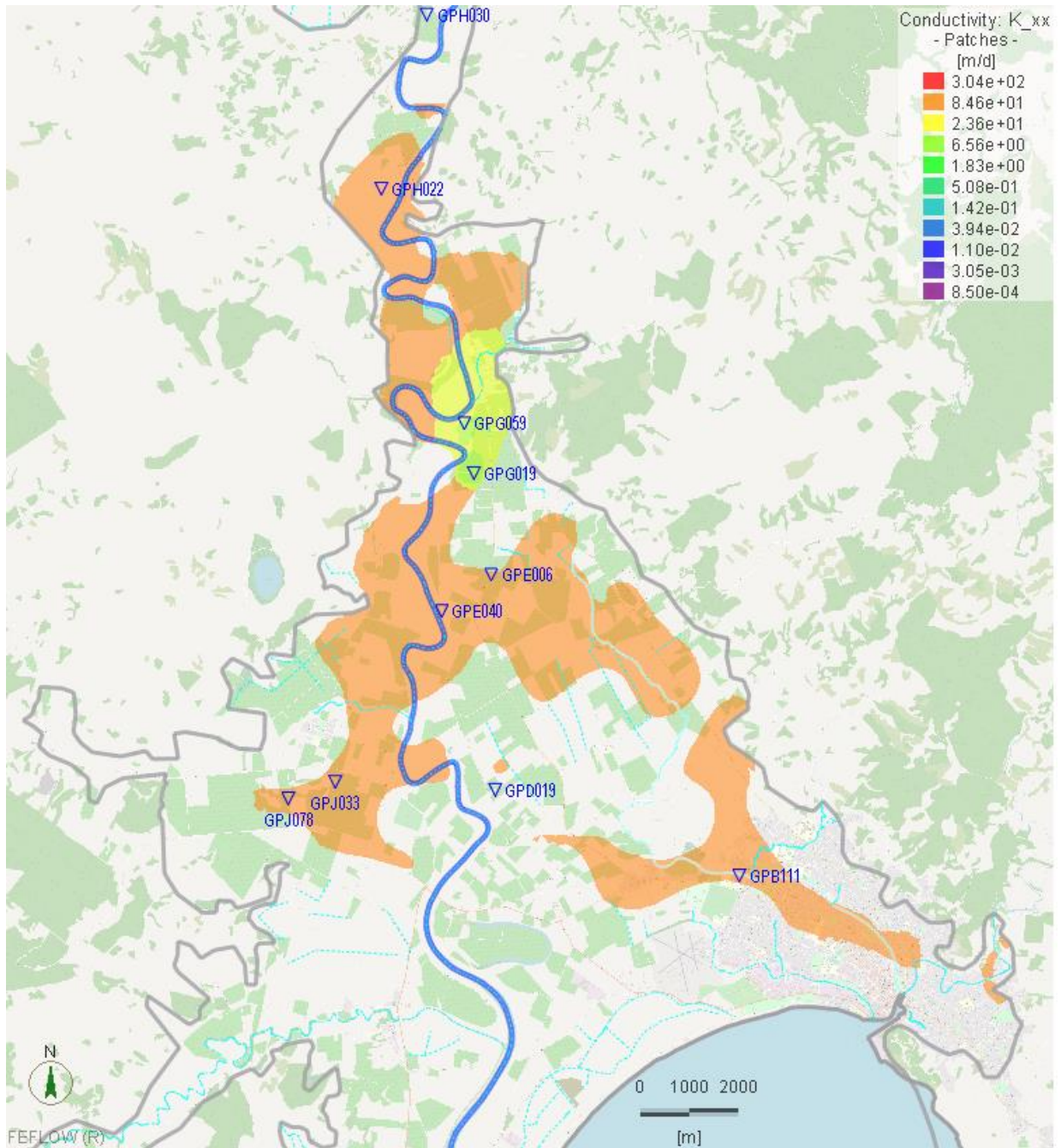


Figure 3-36: Monitoring bores in Waipaoa aquifer.

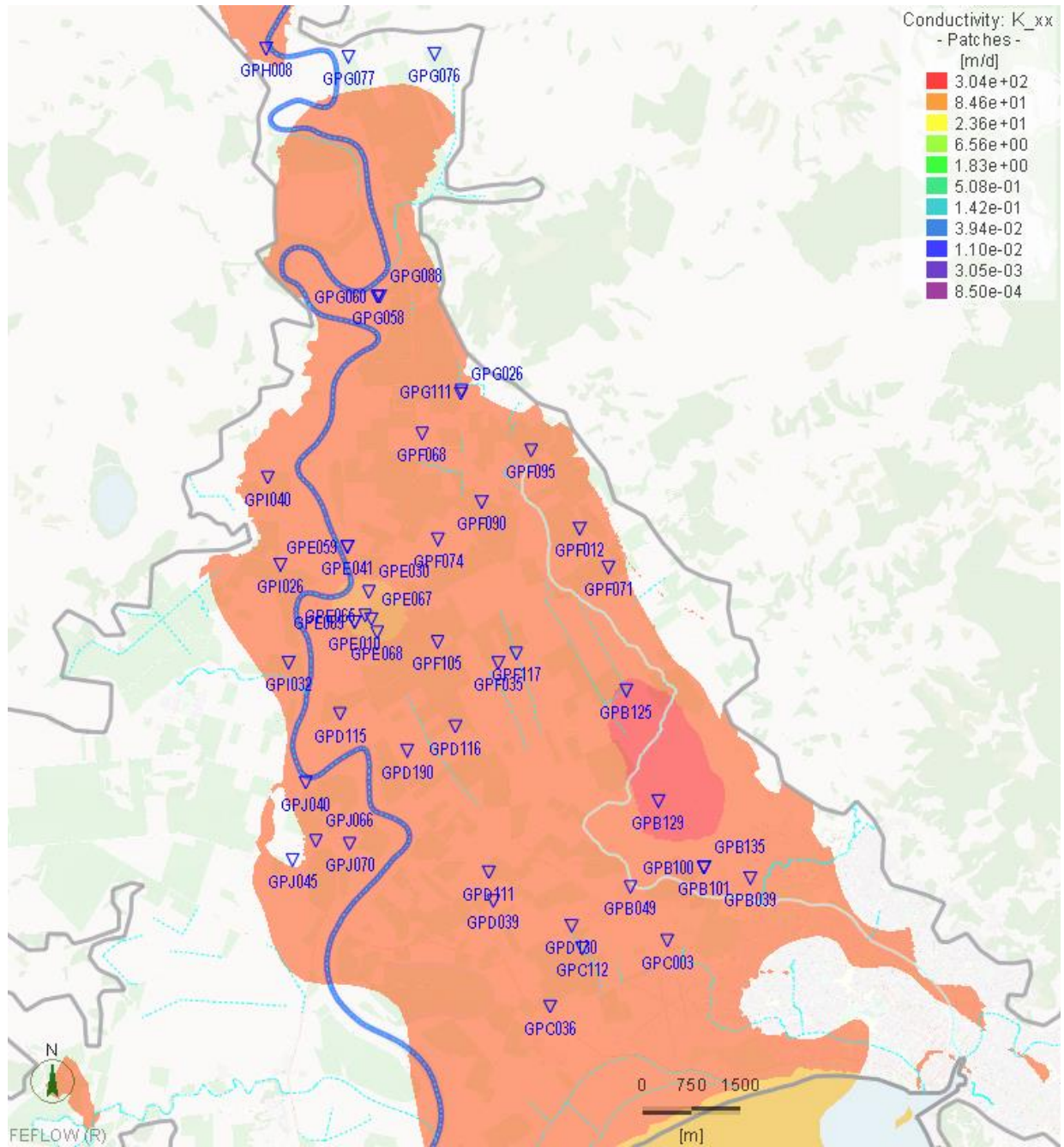


Figure 3-37: Monitoring bores in Makauri aquifer.

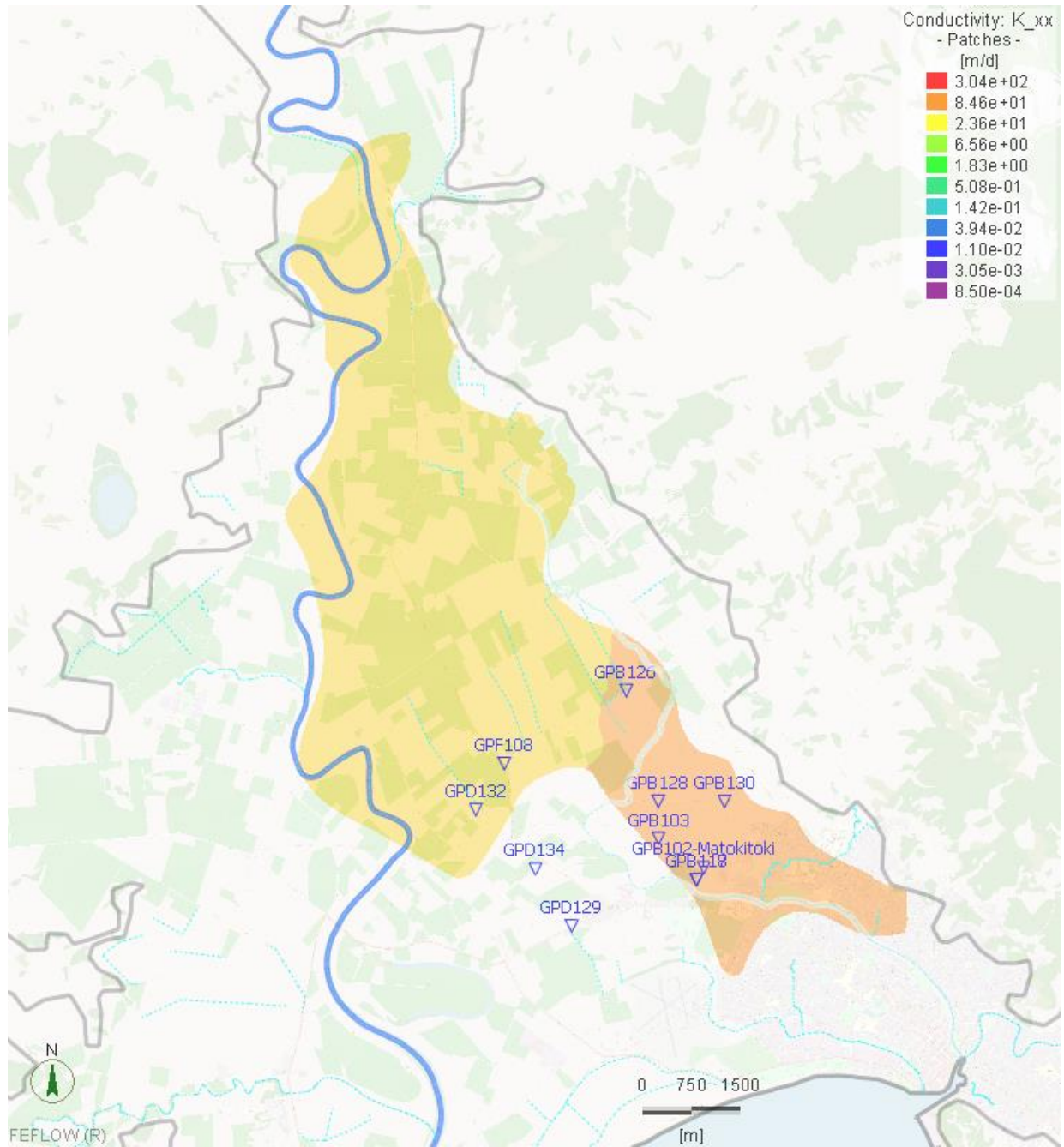


Figure 3-38: Monitoring bores in Matokitoki aquifer.

4. Calibration, validation and verification of the 3D groundwater model

Parameterised with knowledge-based, yet uncertain initial values, the model is not fit to match historical observations. Thus parameters have to be calibrated, i.e., they are adapted within their uncertainty bands in a way that the model can match history. Validation of the parameter set obtained through calibration is achieved by simulating another time period, and for verification groundwater age data are used.

Calibration, validation and verification of the 3D groundwater model Poverty Bay Flats are achieved through a large number of iterative simulation runs, progressively adapting the model to reflect observed groundwater levels and hydraulic potential in the following main steps:

- Steady state calibration,
- Simulations and sensitivity analysis of parameters based on the steady state calibrated model,
- Transient simulation for the period May 1st, 2008 through Oct. 31, 2021 that integrates both the calibration period (2008–2015) and the validation period (2016–2021),
- Transient simulation of the MAR trials 2017 - 2020 as additional hydraulic validation,
- Groundwater-age simulation (residence times) as simplified mass-transport verification,
- Electrical conductivity simulation of MAR trials 2017 - 2020 as mass-transport verification,
- Additional transient runs showing the effect of additional evapotranspiration in areas with a low depth to groundwater during summer.

4.1. Steady State Calibration

The 3D groundwater model Poverty Bay Flats is calibrated first in steady state, with the preliminary aim to model and to assess regional groundwater flow in the Quaternary groundwater system, considering the four aquifer systems (Undifferentiated/Te Hapara Sands/Shallow Fluvialite, Waipaoa, Makauri, Matokitoki). Calibration was performed for steady state hydraulic conditions based on available groundwater level records of 79 observation bores for the period May 2011 through April 2012. The calibration period has been chosen to be as close to natural conditions, hereby keeping the influence of abstraction on the system as low as possible (as this will be considered in transient calibration). Above-mentioned period is the one with the lowest abstraction rate per year in the time frame of available data 2008 – 2021.

Groundwater abstraction data in this period are available for the months of October 2011 - April 2012, abstraction during winter months is assumed to be negligible. According to [11], there were 56 active abstraction bores with a total take amount of about 753,000 m³. Average rainfall of the stations EWS and AWS were 1216 mm in the period May 2011 - April 2012 or/and 444 mm in the months of May - September 2011. During the calibration process hydraulic conductivity values and transfer rates for the Fluid-transfer BC have been manually modified or optimised where necessary to achieve a reasonable correspondence between observed and simulated regional groundwater flow in the Quaternary groundwater system Poverty Bay Flats.

4.1.1. Parameters

Water levels for surface water boundary conditions

- Hydraulic-head BC with 0 mRL for the sea,
- Fluid-transfer BC for rivers, streams and drains with mean values of measures in the period of Oct. 2015 - Sept. 2017 (Table 3-6) as data base (choice of the time period differing from the calibration period as all gauging stations have water level records within this period).

Groundwater usages / takes for well boundary conditions

Groundwater abstractions considered are shown in Table 4-1 for each aquifer and in total.

Table 4-1: Overview of abstraction amounts considered in steady state calibration

Historical Takes in Aquifer	Sum of Oct.2011-Apr.2012	Number of pumping bores	
	Amount m ³		
Makauri Aquifer	598,765	25	
Matokitoki Aquifer	22,297	1	
Shallow Fluvatile	36,921	8	
Te Hapara Sands	40,490	14	
Waipaoa Aquifer	54,361	8	
Sum	752,834	56	

Groundwater recharge from rainfall

Table 4-2 shows rainfall at the Stations Gisborne EWS and Gisborne AWS in the period May 2011 – April 2012, and modelled groundwater recharge in the steady state calibration (ref. Chap. 4.1.2).

Table 4-2: Rainfall of the Stations Gisborne EWS and Gisborne Aws May 2011 – April 2012.

Station	Rainfall (mm)		Recharge steady state calibration (mm)
	May 2011 – April 2012	May - September 2011	
Gisborne EWS	1231	464	
Gisborne AWS	1202	424	
Average	1216	444	245

4.1.2. Results

The model converges well, and – in order to prove that the remaining outer-iteration error after reaching convergence, does not influence simulation results – has been run in quasi-steady state (transient simulation with time-constant conditions) for a long time. The error criterion applied is a relative error criterion of 10^{-3} using the L2/RMS norm. This corresponds to an absolute criterion (also based on RMS) of approx. 0.1 m. The (very small) remaining errors within the bounds of the specified criterion have been spatially checked and are occurring along the steeper gradients on both sides of the Poverty Bay Flats, where the aquifers as well as the entire quaternary valley fills pinch out the remaining material is of low permeability.

The water balance error of the model is about 0.01% and therefore negligible.

So technically the model can be accepted, and its results can be evaluated.

Groundwater level / hydraulic potential

Table 4-3 shows water level statistics for the available 79 bores in the period May 2011 - April 2012. There are 16 bores in Te Hapara Sands, 4 in Shallow Fluviatile, 9 in Waipaoa, 39 in Makauri and 11 in Matokitoki aquifers, respectively. Most of them have counts of measured values between 15 and 20, only 5 bores have less than 5 observations. Measured groundwater level / hydraulic potential ranges from -0.9 mRL to 34.1 mRL, depending on the bore location.

Table 4-3: Statistics of groundwater level records of 79 bores used as targets for steady state calibration

Aquifer	Te Hapara Sands	Shallow Fluviatile	Waipaoa	Makauri	Matokitoki	Total / Overall
Number of bores	16	4	9	39	11	79
Min. (mRL)	-0.42	-0.25	2.49	-0.90	1.72	-0.90
Average of Mean (mRL)	2.25	7.32	10.78	7.94	6.67	6.90
Max. (mRL)	5.65	13.28	26.36	34.09	10.97	34.09
Count of measured values	3 - 20	17 - 20	3 - 20	3 - 20	4 - 18	

The results of the state steady calibration are evaluated by comparison of simulated with mean measured values of each of the 79 bores. Table 4-4 shows the calibration statistics in total. With a low residual mean (0.08 m) and a low scaled RMS Error (4,5 %) less than 5 %, this indicates a good or/and satisfactory calibration in general, meeting Australian groundwater modelling guidelines for calibration (Barnett et al. 2012).

Table 4-4: Statistics of the state steady calibration.

Parameter	Value
Residual Mean (m)	0.08
Absolute Residual Mean (m)	0.99
Residual Standard Deviation (m)	1.52
Sum of Squares (m ²)	181
Root Mean Square (RMS) Error (m)	1.52
Minimum Residual (m)	-5.72
Maximum Residual (m)	4.33
Number of Measures (-)	79
Range in Measures (m)	33.39
Scaled Residual Std. Deviation	4.6%
Scaled Absolute Residual Mean	3.0%
Scaled RMS Error	4.5%
Scaled Residual Mean	0.3%

Figure 4-1 shows a scatter plot of simulated vs measured water levels of the 79 bores with different or/and coloured marks for the shallow aquifers Te Hapara Sands/Shallow Fluviatile and the deep aquifers Waipaoa, Makauri and Matokitoki. Correspondingly,

Table 4-5 gives statistics of minimal (Min. Mean **Measured**), mean (Mean **Measured**), and maximal (Max. Mean **Measured**) values in the upper, minimal (Min. **Simulated**), Mean (Mean. **Simulated**) and maximal (Max. **Simulated**) values in the middle, and statistics of differences **Simulated - Measured** water levels in the lower table part. The scatter plot and the table show that the steady state calibration results fit the measured water levels in the shallow and the deep aquifers with a range from 0.08 (mRL) to 33.47 (mRL) very well.

There are two groups of observation wells that show somewhat larger differences between calculated and observed water levels:

- Groundwater level at observations in the shallow aquifers (Te Hapara Sands, Shallow Fluvial Deposits) in general tend to be calculated too high. Main reason for this is that the model does not consider all drains and subsequently higher water levels build up in areas further away from drains in the model. This effect has been somewhat counterbalanced by slightly increased hydraulic conductivity in such areas; a further artificial increase in hydraulic conductivity could lead to a better matching of observed levels. In this case, however, the underlying model simplification (no local drains) would be substituted by unrealistically high hydraulic conductivity. It is deemed better here to accept the higher groundwater levels, keeping in mind that potentially the model will be refined at a later stage to cover the shallow processes more in detail.
- Groundwater level at observations in the southeastern part of the Matokitoki aquifer tend to be lower than observed in the model. Reason is that the model is lacking some process in the Matokitoki, such as potential lateral inflow from a connected hydrogeological unit. However, as the underlying process is not known and not part of the basic conceptual and hydrogeological models, the groundwater flow model cannot be expected to match the observed hydraulic head in this region.

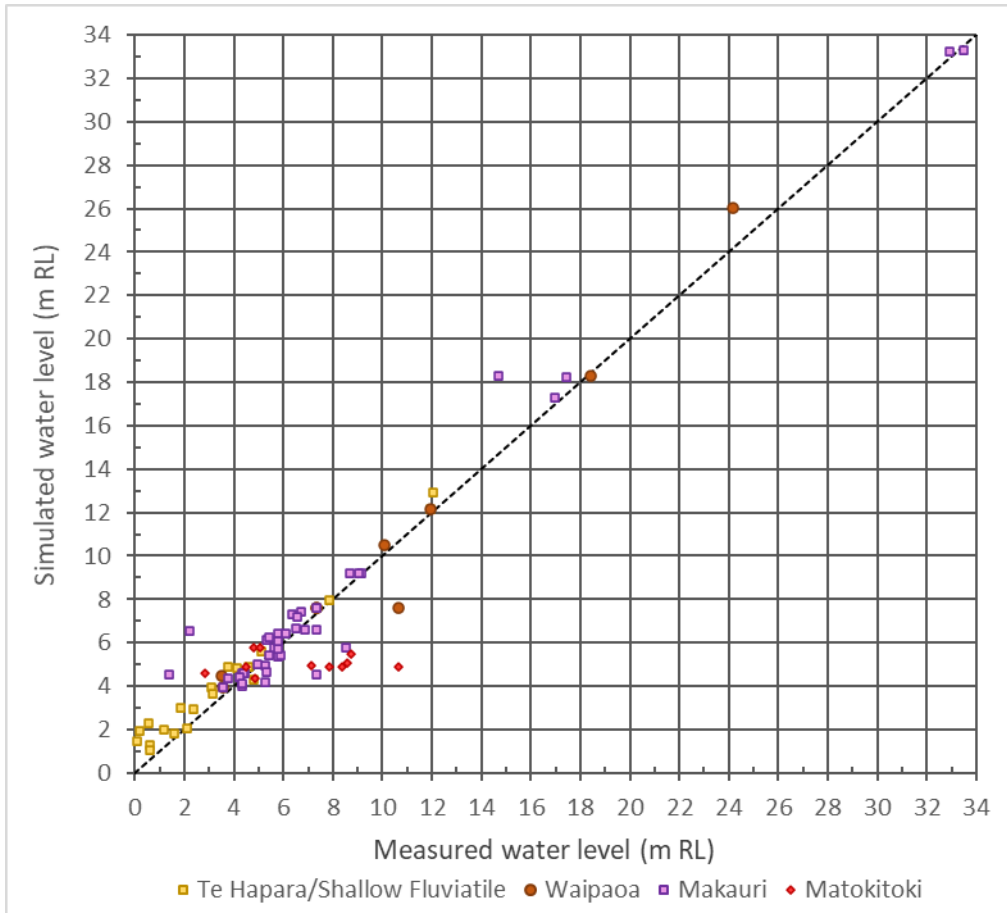


Figure 4-1: Scatter plot of simulated vs measured water levels, steady state calibration.

Table 4-5: Comparison of simulated and measured groundwater levels of 79 bores

Aquifer	Te Hapara Sand	Shallow Fluvialite	Waipaoa	Makauri	Matokitoki	Total / Overall
Number of bores	16	4	9	39	11	79
Min. Mean Measured (mRL)	0.08	3.77	3.51	1.36	2.84	0.08
Average of Mean Measured (mRL)	2.25	7.32	10.78	7.94	6.67	6.90
Max. Mean Measured (mRL)	5.09	12.07	24.16	33.47	10.65	33.47
Min. Simulated (mRL)	1.07	4.88	3.97	4.00	4.36	1.07
Mean Simulated (mRL)	2.95	7.82	10.91	8.20	5.05	6.99
Max. Simulated (mRL)	5.59	12.93	26.04	33.29	5.76	33.29
Min. Simu. - Meas. (m)	-0.48	-0.11	-3.02	-2.80	-5.72	-5.72
Mean Simu. - Meas. (m)	0.70	0.50	0.14	0.26	-1.62	0.08
Max. Simu. - Meas. (m)	1.73	1.11	1.88	4.33	1.78	4.33

Water balance

Table 4-6 shows the water balance of the state steady calibration model summarised for the balance components (or/and boundary condition types) recharge, sea, Waipaoa River, Matawhero wetland, Taruheru River, other river and drains, and groundwater takes. The difference between the total inflow and total outflow amounts to approximately 17 m³/d, that means the water balance error is less than 0.01 % of the total inflow and indicates that the results of steady state calibration are numerically valid. This meets the Australian groundwater modelling guideline (Barnett et al 2012) criterion for water balance of better than 1%.

Table 4-6 and Figure 4-2 show that most of the recharge in the state steady calibration discharged to inland rivers/drains, of which about 52 % to Waipaoa River. Discharges to Sea and through groundwater abstraction amount to about 6 % and 1 % of the recharge only.

Table 4-6: Water balance of state steady calibration

Balance Component / BC	Inflow (m ³ /d)	Outflow (m ³ /d)	Inflow - Outflow (m ³ /d)	Remark
Recharge	158,210	0	158,210	eq. 245.3 mm/year*
Waipaoa River	38,082	119,812	-81,730	
Oxbow / Matawhero wetland	994	4,041	-3,047	
Taruheru River	37	15,537	-15,500	
Other Rivers/Drains	6,245	52,414	-46,169	
Sea	4	9,694	-9,690	
Groundwater takes	0	2,057	-2,057	
Total	203,572	203,555	17	<0.01 % difference

* With respect to the surface area of 235,439,100 m² in the model domain.

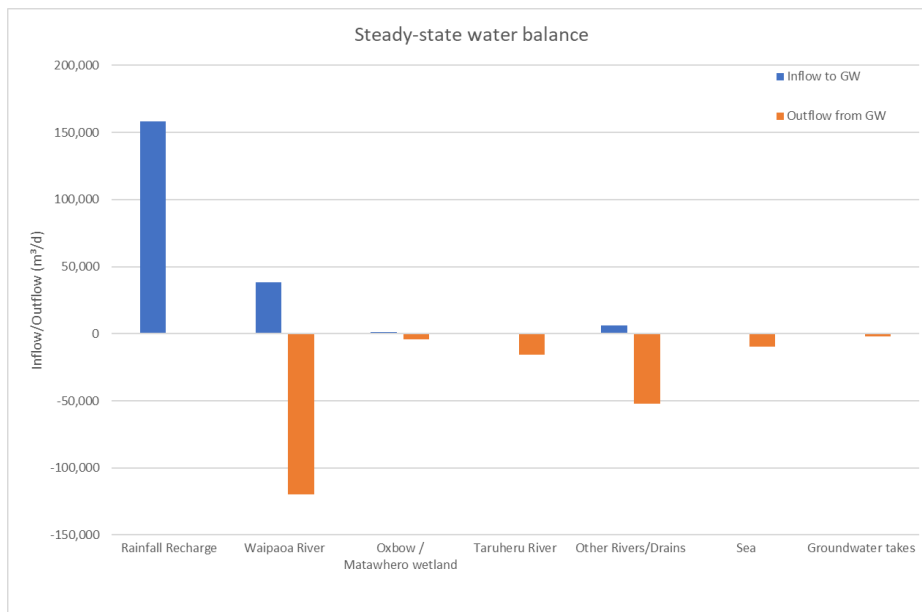


Figure 4-2: Steady-state water balance: inflows and outflows.

In summary, the state steady calibration has been completed with a good and satisfactory fitting of observed and measured water levels. Contours of calculated groundwater levels in the groundwater system Poverty Bay Flats are displayed in Figure 4-3 in 1 m interval for Te Hapara Sands/Shallow Fluvatile and Makauri aquifers, along with the mean measured values of the available bores. According to that, groundwater flow paths in the Poverty Bay Flats direct in general from North to South, showing different flow gradients or patterns with groundwater levels deviating from the general direction in Te Hapara Sands/Shallow Fluvatile (shallow aquifer) and Makauri (deep aquifer):

- Contours in the shallow aquifer are dense (indicating large flow gradients) and show variable flow paths apparently directing to Waipaoa River or other rivers/drains considered as boundary conditions in the groundwater model (reflecting discharges to rivers/drains),
- Contours in the deep aquifers indicate simple flow paths from north to south with clearly smaller flow gradients than in the shallow aquifers,
- Water levels in the shallow aquifers are higher than in the deep aquifer in the northern part of the model, whereas they are lower than in the deep aquifers in the southern part. The different flow patterns or behaviours are illustrated in Figure 4-4 displaying simulated GW levels along the North-South Cross-Section 1 (NS-CS#1, location ref. Figure 3-21). This indicates recharge areas for the deep aquifers mainly in the northern part, while there is a discharge from the deep to the shallow aquifers, the sea resp., in the southern part.

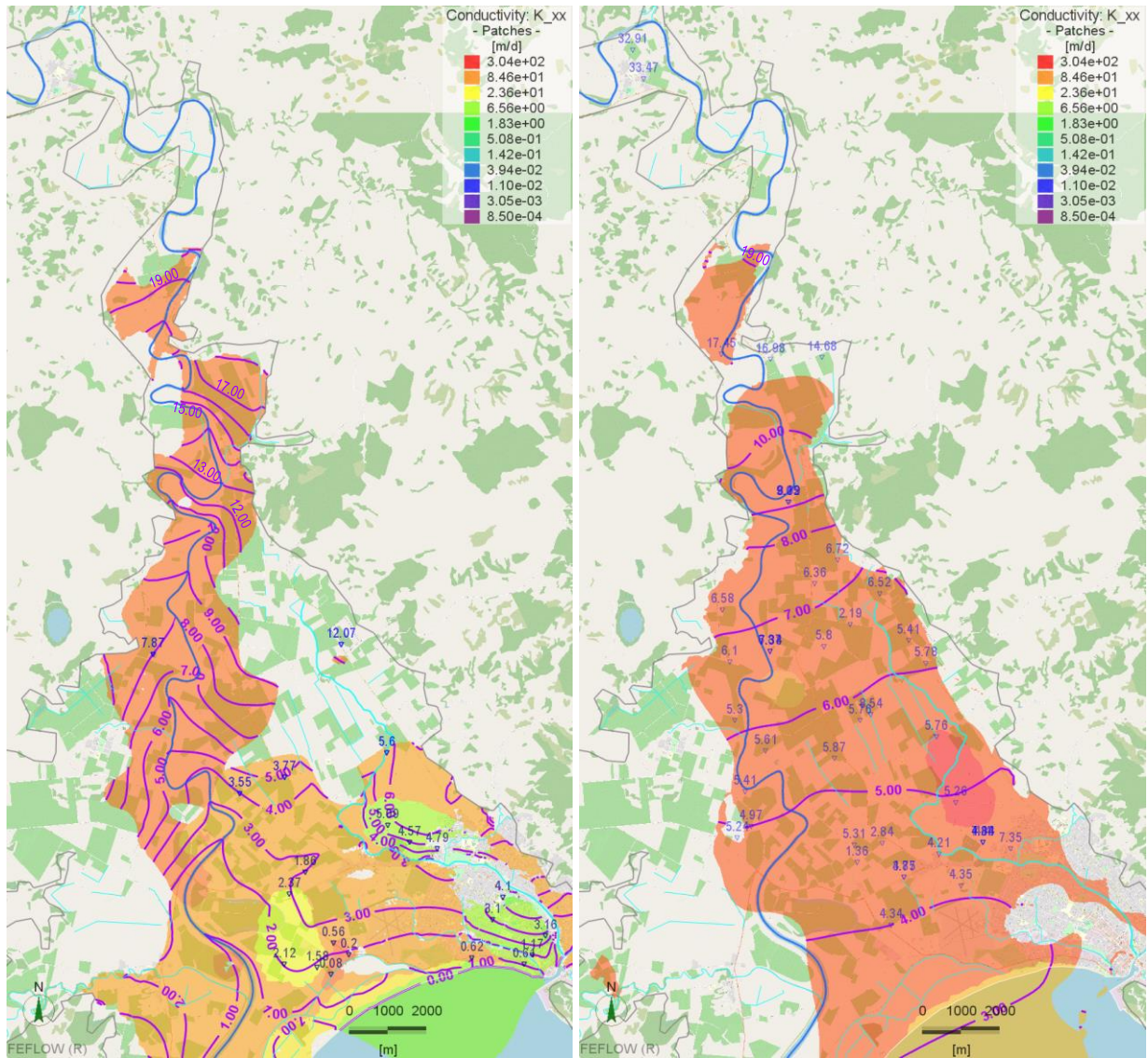


Figure 4-3: Simulated GW level contours in Te Hapara Sands/Shallow Fluvatile aquifer (left) and in Makauri aquifer (right), steady state calibration.

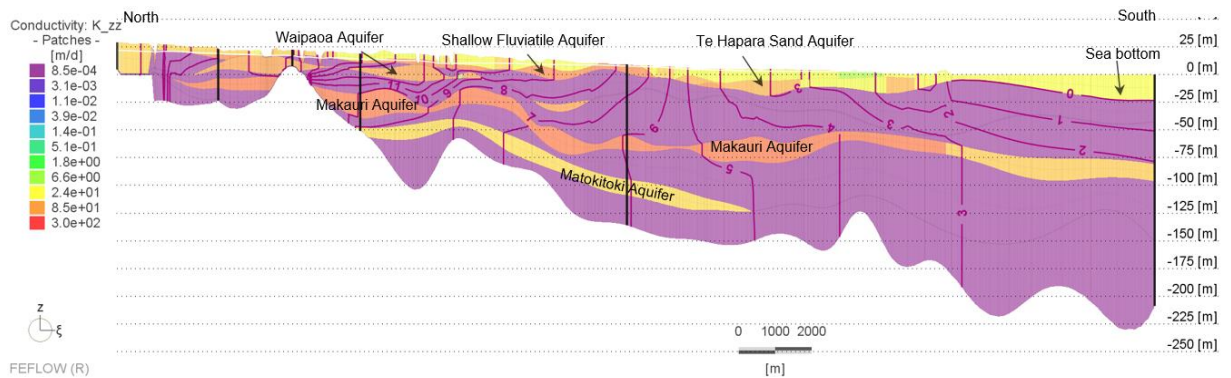


Figure 4-4: Simulated GW levels along the North-South cross section 1 (NS-CS#1), steady state calibration.

4.2. Sensitivity analyses for model parameters

4.2.1. Parameters

Sensitivity analyses were carried out based on the steady state calibration for the model parameters groundwater recharge, hydraulic conductivity of aquitards and aquifers, and conductance for the river/drain boundary conditions, as shown in Table 4-7.

Accordingly, there are 7 parameters or parameter groups considered. For each of the parameter groups two simulations were performed with an increase of the parameter considered to +50 % (recharge) or multiplied by 5 (other properties) or decrease (reduction) -50 % (recharge) or divided by 5 (other properties) in the model domain, i. e., 14 simulations in total.

Table 4-7: Overview of the sensitivity simulations performed based on steady state calibration

Sensitivity Simulation #	Sensitivity Simulation Name	Description	Specifications of parameters changed in comparison with steady state calibration (SSC)						
			Recharge (m ³ /d)	Conductivity of Aquitard 1 - 3	Conductivity of Makauri Aquifer	Conductivity of Waipaoa Aquifer	Conductivity of Undefined + Te Hapara Sands + Shallow Fluvial Aquifers	Conductivity of Matokitoki Aquifer	Transfer Rate (TR) for River-/Drain-BC
0	Steady state calibration (SSC)	Steady State Calibration	158,210						
1a	SSC+50%Recharge	SSC Increase +50% recharge	237,315						
1b	SSC-50%Recharge	SSC decrease 50% recharge	118,658						
2a	SSC 5X-Cond-AQTD	SSC Increase 5X Conductivity of Aquitard		5X SCC					
2b	SSC 1/5X-Cond-AQTD	SSC Reduction 1/5X Conductivity of Aquitard		1/5 X SCC					
3a	SSC 5X-Cond-MA	SSC Increase 5X Conductivity of Makauri Aquifer (MA)			5X SCC				
3b	SSC 1/5X-Cond-MA	SSC Reduction 1/5X Conductivity of Makauri Aquifer (MA)			1/5 X SCC				
4a	SSC 5X-Cond-WA	SSC Increase 5X Conductivity of Waipaoa Aquifer (WA)				5X SCC			
4b	SSC 1/5X-Cond-WA	SSC Reduction 1/5X Conductivity of Waipaoa Aquifer (WA)				1/5 X SCC			
5a	SSC 5X-Cond-UTSA	SSC Increase 5X Conductivity of Undefined+TeHapara+Shallow Aquifers (UTSA)					5X SCC		
5b	SSC 1/5X-Cond-UTSA	SSC Reduction 1/5X Conductivity of Undefined+TeHapara+Shallow Aquifers (UTSA)					1/5 X SCC		
6a	SSC 5X-Cond-MTKA	SSC Increase 5X Conductivity of Matokitoki Aquifer (MTKA)						5X SCC	
6b	SSC 1/5X-Cond-MTKA	SSC Reduction 1/5X Conductivity of Matokitoki Aquifer (MTKA)						1/5 X SCC	
7a	SSC 5X-TRSF	SSC Increase 5X Transfer Rate (TR) for River-/Drain-BC							5X SCC
7b	SSC 1/5X-TRSF	SSC Reduction 1/5X Transfer Rate (TR) for River-/Drain-BC							1/5 X SCC

4.2.2. Results

Since changes of the parameters considered were performed on the whole model domain, evaluation of their sensitivity to simulation results is based mainly on comparison of overall statistics and water balance errors of the sensitivity simulations with that of steady state calibration. The statistics and water balance errors are summarised in Table 4-8. Most of the outcomes reported results with water balance errors < 5% and SRMS results < 5%, thus still meeting the Australian groundwater modelling guideline criteria for a calibrated model (Barnett et al 2012). Nevertheless the change in SRMS gives an indication whether there could have been a better choice for the calibration parameters, and what the overall sensitivity of the model on the parameter in question is.

Sensitivity analysis for groundwater recharge

The Residual Mean of the sensitivity simulations shows, as expected, that increasing or decreasing recharge by 50 % would lead to an apparent over- or underestimation of the measured water levels. The corresponding water balance errors are similar or comparable to that of SSC.

Sensitivity analysis for river-bed conductance

A little under- and an apparent overestimation of the measured water levels are shown by the increasing and decreasing riverbed conductance defined for the rivers/drains respectively. Both the sensitivity simulations show larger water balance errors than that of SSC, implying possible local numerical instability when using the parameter.

Sensitivity simulations for hydraulic conductivity of Undifferentiated, Te Hapara Sands and Shallow Fluvatile (UTSA)

Undifferentiated, Te Hapara Sand and Shallow Fluvatile are three upper hydrogeological units and represent the shallow aquifer system. The sensitivity simulations show that increasing or decreasing their conductivity would lead to apparently under- or overestimation of the measured water levels, and with Scaled RSM Error > 5 %.

Table 4-8: Statistics and water balance error of the state steady calibration and sensitivity simulations.

Parameter	Recharge			Transfer rate		Conductivity of UTSA	
	SSC	SSC+50% Recharge	SSC-50% Recharge	SCC 5X TRSF	SCC 1/5X TRSF	SCC 5X CondUTSA	SCC 1/5X CondUTSA
Residual Mean (m)	0.08	0.61	-0.54	-0.04	0.44	-0.93	2.41
Absolute Residual Mean (m)	0.99	1.26	1.02	0.94	1.16	1.29	2.62
Residual Standard Deviation (m)	1.52	1.53	1.55	1.52	1.53	1.65	2.07
Sum of Squares (m ²)	181	213	211	181	199	280	791
Root Mean Square (RMS) Error (m)	1.52	1.64	1.63	1.51	1.59	1.88	3.16
Minimum Residual (m)	-5.72	-5.08	-6.45	-5.86	-5.30	-6.97	-3.15
Maximum Residual (m)	4.33	4.82	3.71	4.26	4.62	3.33	8.56
Number of Measures (-)	79	79	79	79	79	79	79
Range in Measures (m)	33.39	33.39	33.39	33.39	33.39	33.39	33.39
Scaled Residual Std. Deviation	4.6%	4.6%	4.7%	4.6%	4.6%	4.9%	6.2%
Scaled Absolute Residual Mean	3.0%	3.8%	3.1%	2.8%	3.5%	3.9%	7.8%
Scaled RMS Error	4.5%	4.9%	4.9%	4.5%	4.7%	5.6%	9.5%
Scaled Residual Mean	0.3%	1.8%	-1.6%	-0.1%	1.3%	-2.8%	7.2%
Water balance error	< 0.01%	< 0.01%	< 0.03%	0.19%	3.43%	0.09%	0.82%

Parameter	SSC	Conductivity of aquitards		Conductivity of Waipaoa aquifer		Conductivity of Makauri aquifer		Conductivity of Matokitoki aquifer	
		SCC 5X CondAQTD	SCC 1/5X CondAQTD	SCC 5X CondWA	SCC 1/5X CondWA	SCC 5X CondMA	SCC 1/5X CondMA	SCC 5X CondMTKA	SCC 1/5X CondMTKA
Residual Mean (m)	0.08	0.27	-0.07	0.21	-0.06	-0.01	0.18	0.11	0.05
Absolute Residual Mean (m)	0.99	1.20	1.05	1.06	1.00	1.08	1.12	0.95	1.01
Residual Standard Deviation (m)	1.52	1.71	1.55	1.55	1.56	1.58	1.59	1.44	1.59
Sum of Squares (m ²)	181	234	188	190	191	195	200	163	197
Root Mean Square (RMS) Error (m)	1.52	1.72	1.54	1.55	1.55	1.57	1.59	1.43	1.58
Minimum Residual (m)	-5.72	-5.95	-5.66	-5.69	-5.87	-5.53	-5.66	-5.20	-6.05
Maximum Residual (m)	4.33	5.63	3.67	4.66	4.04	3.78	4.67	4.23	4.37
Number of Measures (-)	79	79	79	79	79	79	79	79	79
Range in Measures (m)	33.39	33.39	33.39	33.39	33.39	33.39	33.39	33.39	33.39
Scaled Residual Std. Deviation	4.6%	5.1%	4.7%	4.6%	4.7%	4.7%	4.8%	4.3%	4.8%
Scaled Absolute Residual Mean	3.0%	3.6%	3.1%	3.2%	3.0%	3.2%	3.4%	2.8%	3.0%
Scaled RMS Error	4.5%	5.2%	4.6%	4.6%	4.7%	4.7%	4.8%	4.3%	4.7%
Scaled Residual Mean	0.3%	0.8%	-0.2%	0.6%	-0.2%	0.0%	0.5%	0.3%	0.1%
Water balance error	< 0.01%	< 0.6%	< 0.07%	0.26%	0.07%	< 0.3%	< 0.16%	< 0.06%	0.07%

Sensitivity simulations for hydraulic conductivity of aquitards

The conductivity changes were performed for all the aquitards at the same time. The sensitivity simulation with the increased conductivity overestimated the measured water levels and shows larger water balance errors than that of SSC. The simulation with the decreased conductivity shows a little underestimation of hydraulic potential but is close to the calibration scenario.

Sensitivity simulations for hydraulic conductivity of Waipaoa aquifer

The sensitivity simulation with increased conductivity in the Waipaoa aquifer overestimates water levels, along with water balance errors larger than that of SSC. The simulation with the decreased conductivity underestimates the water levels a little but is close to the calibration scenario.

Sensitivity simulations for hydraulic conductivity of Makauri aquifer

The simulation with increased conductivity of the Makauri aquifer shows Residual Mean less than that of SSC in total, but not a good fitting to the measured water levels in the Makauri aquifer, ref. Figure 4-8. The simulation with the decreased conductivity overestimates the water levels. Both simulations show water balance errors larger than that of SSC.

Sensitivity simulations for hydraulic conductivity of Matokitoki aquifer

Both sensitivity simulations show a similar fitting to the measured water levels as that of SSC, and with slightly larger water balance errors than that of SSC.

Figure 4-5 through Figure 4-9 show the scatter plots (measured vs. simulated groundwater potential) for all the sensitivity runs.

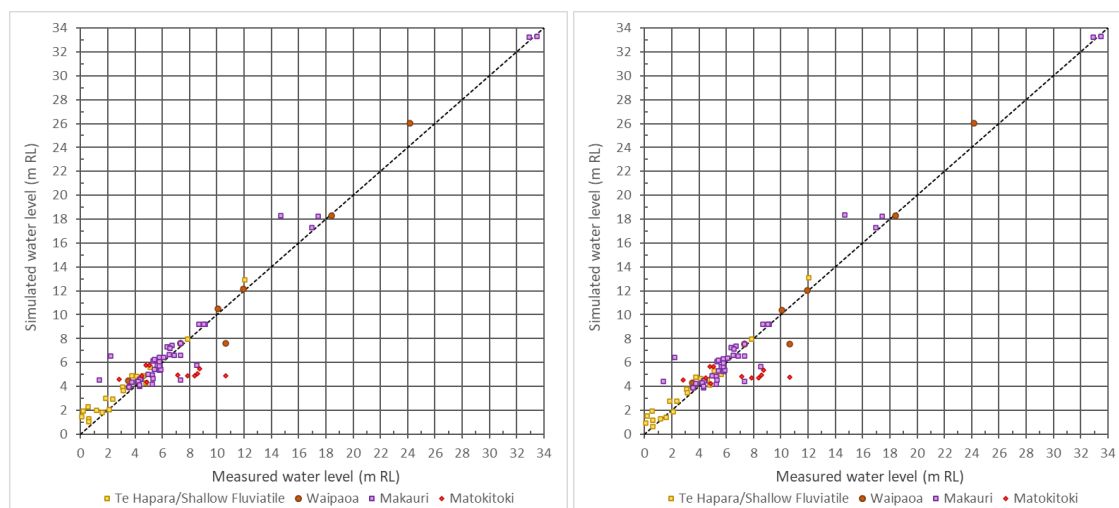


Figure 4-5: Scatter plot of simulated vs measured water levels, SSC (left), SSC 5X-TRSF.

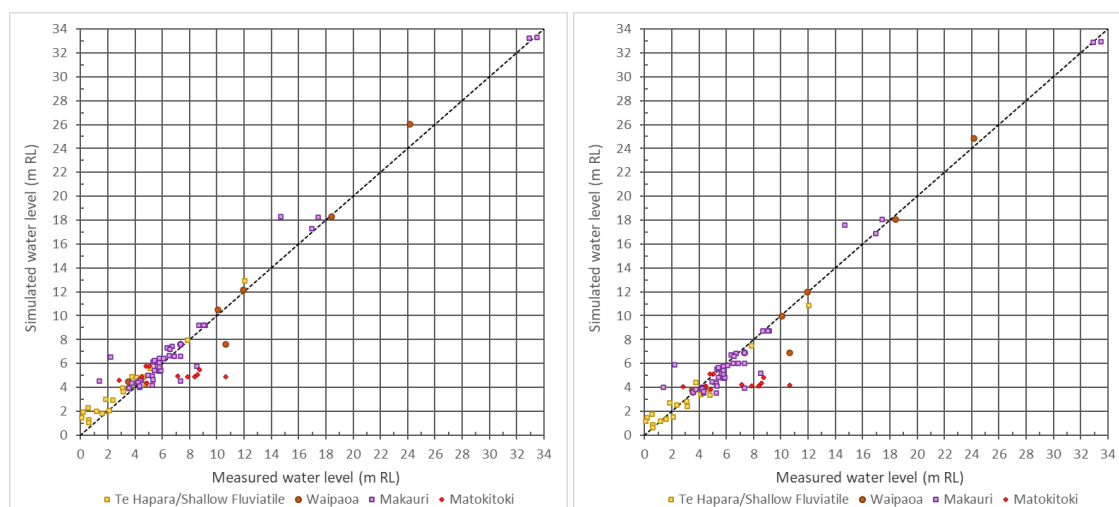


Figure 4-6: Scatter plot of simulated vs measured water levels, SSC (left), SSC 1/5X-AQTD.

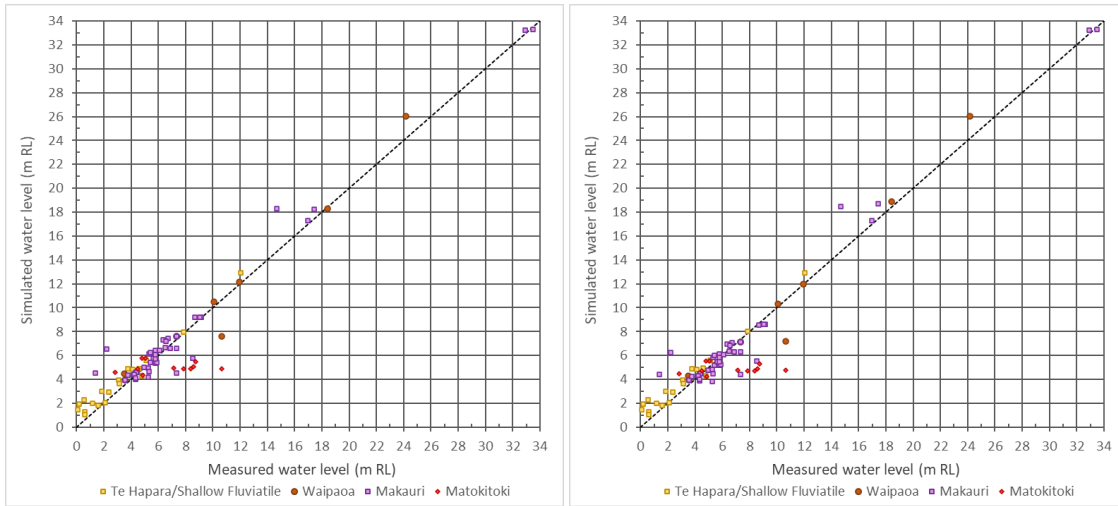


Figure 4-7: Scatter plot of simulated vs measured water levels, SSC (left), SSC 1/5X-WA.

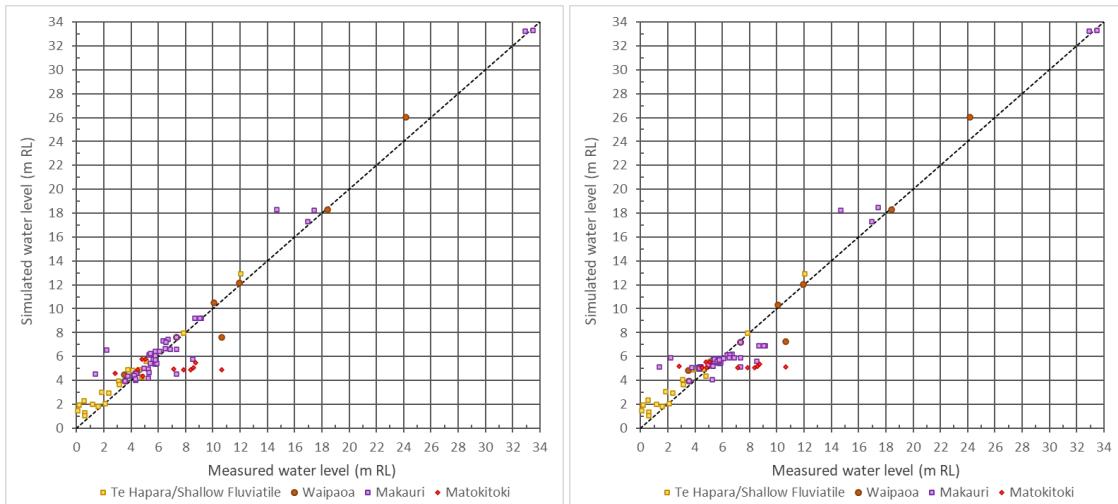


Figure 4-8: Scatter plot of simulated vs measured water levels, SSC (left), SSC 5X-MA (right).

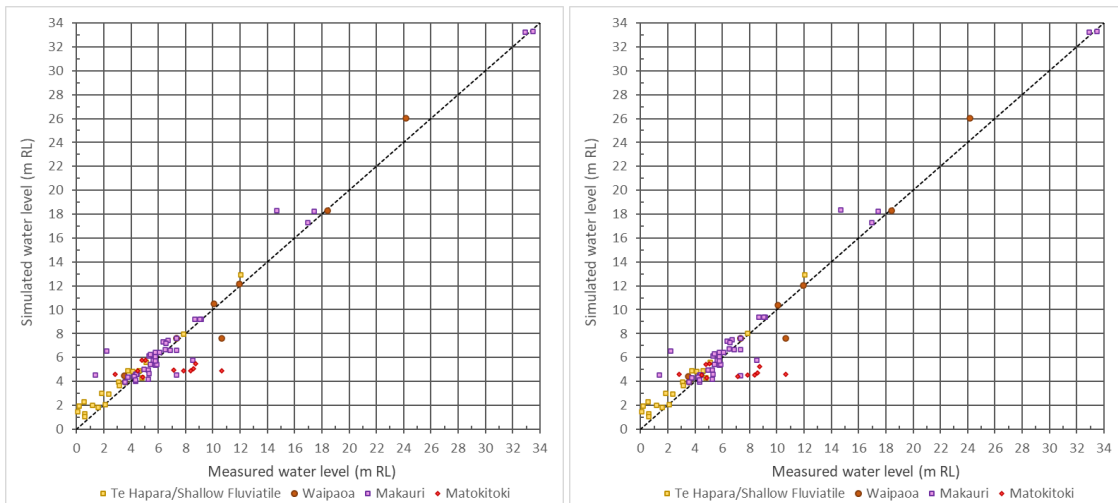


Figure 4-9: Scatter plot of simulated vs measured water levels, SSC (left), SSC 1/5X-MTKA (right).

In summary, sensitivity analysis shows that modifications of the studied parameters in general lead to higher deviation from observed values. As an exception, lowering the hydraulic conductivity of the aquitards as well as of the Waipaoa aquifer produce similar results and thus those parametric configurations

cannot be entirely ruled out. It has to be kept in mind that there is some uncertainty in those two model parameters.

4.3. Transient Calibration (2008-2015) and Validation (2016-2021)

4.3.1. Parameters

The transient calibration is carried out for the period 1 May, 2008 – 30 June 2015 corresponding to the available groundwater abstraction data (2008/2009 - 2014/2015), covering a period of 7 years. After successful transient calibration, the 3D groundwater model is validated for the following period of July 1st, 2015 - Oct 31st, 2021 by using groundwater abstraction data for the period 2015/2016 - 2020/2021. This corresponds to transient validation for a further 6 years. Time-variable parameters used for the transient calibration and validation of the complete period 1 May 2008 – 31 Oct 2021 are summarised as follows:

- time series of pumping rates for the 105 abstraction bores active in the period (monthly values),
- time series of measured water levels (7 day resolution) for the BC representing Waipaoa river, Taruheru river, Whakaahu and Te Arai streams,
- spatially distributed recharge for
 - May - September with constant rates derived from the rainfall data of weather station Gisborne Ews and Gisborne Aws within the 5 months of each year, and
 - October - April with 0 recharge.

Groundwater abstraction - well boundary conditions

The GDC take data [11, 13, 14] were provided for 2008/2009 as take amounts for the period of Oct.2008 - Apr.2009, and thereafter till October 2021 as monthly values of 105 abstraction bores. As mentioned in Chap. 0, each of the 105 abstraction bores has been implemented as a well BC according to its location in an aquifer in the model domain and is identified by its site ID specified in the GDC take database. Accordingly, the given take data of the abstraction bores were prepared as monthly average take rates used for the transient calibration and validation.

As an overview, Figure 4-10 (upper) shows the monthly take rates of the abstraction bores in total, composed by the take amounts from each of the aquifers displayed in different colours, while Figure 4-10 (lower) represents the corresponding total annual amounts in the transient simulation period from 1 May 2008 – 30 June 2021.

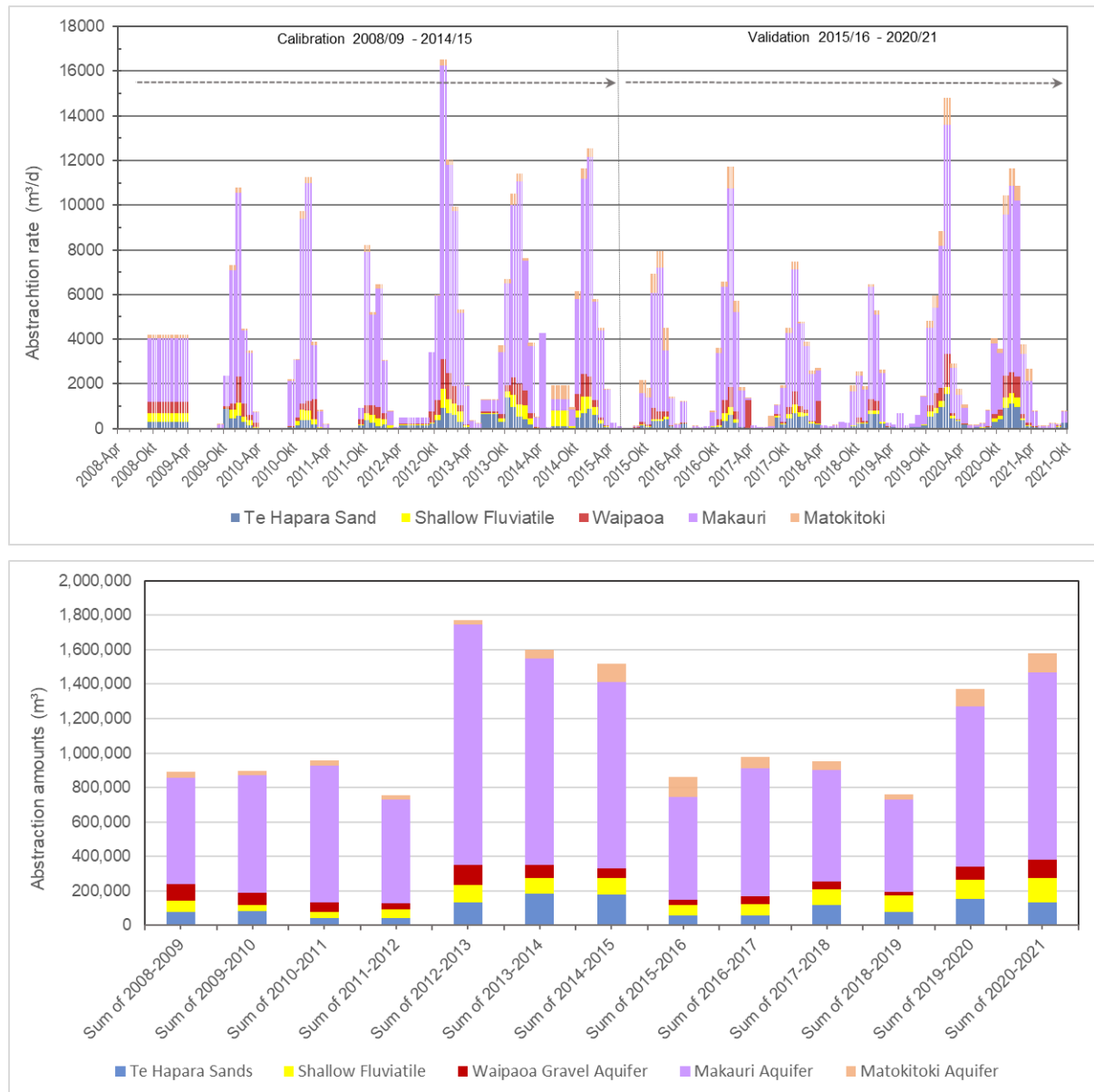


Figure 4-10: Abstraction data 2008/2009 - 2020/2021 monthly rates (upper) and annual amounts (lower).

Water levels for surface water boundary conditions

For the total transient simulation period from May 1st, 2008 - June 30th, 2021, the daily water level records at the gauging stations for the river boundary conditions representing Waipaoa River, Taruheru River, Whakaahu and Te Arai Streams shown in Table 3-6 were resampled on a weekly basis as corresponding time series of water levels. Figure 4-11: Time series of water level records (mRL) Waipaoa river at gauging station 4 (blue), station 3 (light green) and station 8 (purple) used for interpolation.

and Figure 4-12 show the resampled time series of water levels for Waipaoa and Taruheru river, respectively, as an example. The resampled time series were imported into the FEFLOW model and used to linearly interpolate the river water levels along the rivers, ref. Chap. 0.

For Waikanae Creek and other drains without water level records available, the estimated h_{SW} used for steady state calibration are kept as constant for the transient simulation.

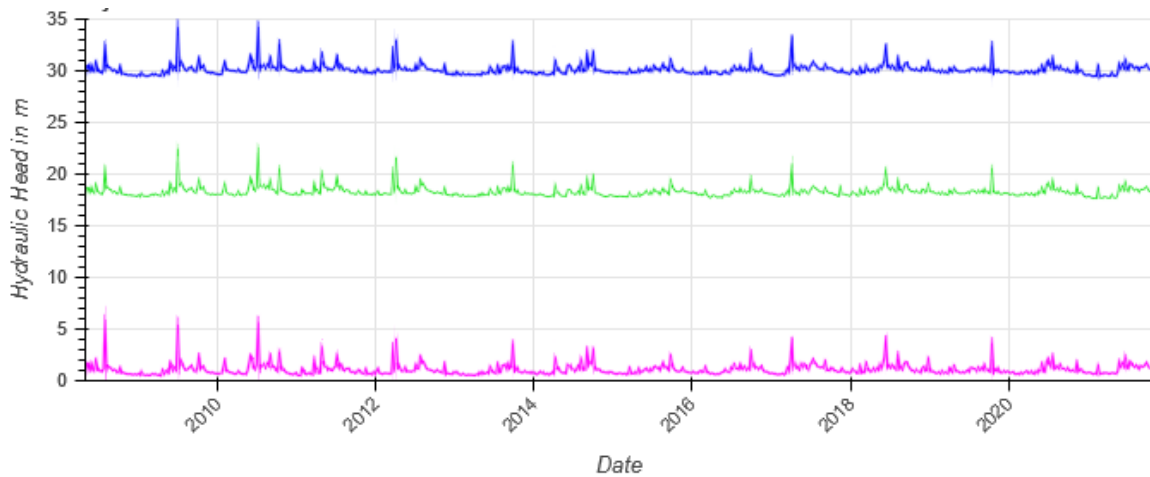


Figure 4-11: Time series of water level records (mRL) Waipaoa river at gauging station 4 (blue), station 3 (light green) and station 8 (purple) used for interpolation.

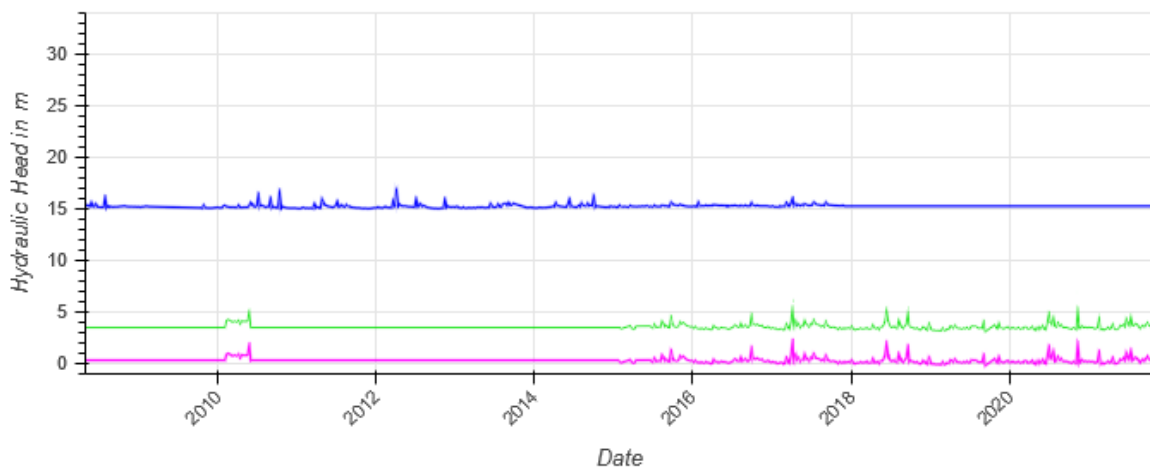


Figure 4-12: Time series of water level records (mRL) Taruheru river at gauging station 2 (blue), station 1 (light green) and at its estuary (purple) used for interpolation.

Groundwater recharge from rainfall

As mentioned in Chap. 3.4.3, only rainfall within the recharge period of May to September (one autumn, three winter and one spring month(s)) were considered as providing recharge for transient simulations. Figure 4-13 shows rainfall (average rainfall of stations Ews and Aws) in the calibration and validation period of May 1st, 2008 - Oct 31st, 2021 for each recharge period as light blue and corresponding recharge as light green bars. Accordingly, the rainfall in the recharge periods considered vary between 185 mm (May-Sept. 2020) and 690 mm (May-Sept. 2009), and with correspondingly estimated recharge ranging from 69 mm to 218 mm.

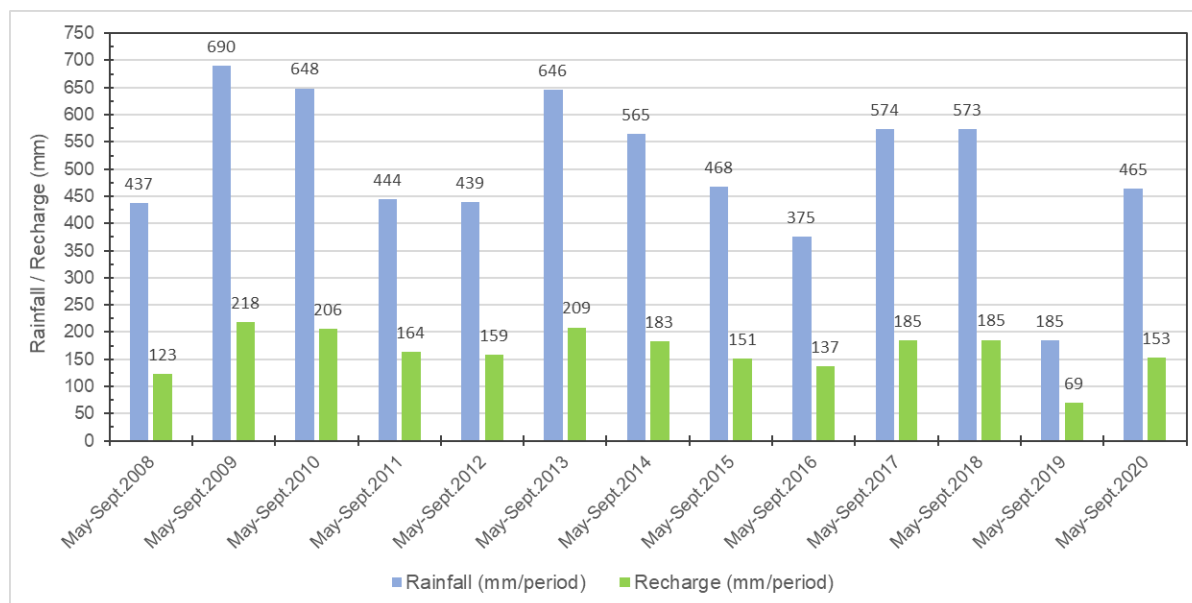


Figure 4-13: Rainfall (light blue) and average groundwater recharge (light green) within the recharge period over the model area.

4.3.2. Results

The transient calibration and validation with the input parameters mentioned above incorporate different stress periods featured by different winter recharges, irrigations seasons in summer months and water levels changes e.g. in main surface water Waipaoa river within the simulation period of 1 May 2008 – 31 October 2021. The results of the transient calibration and validation are evaluated by comparison of simulated with measured groundwater levels of available bores within the simulation period. Table 4-9 gives an overview of 88 bores with groundwater level measures, classified for the aquifers considered. These are 16 and 6 in Te Hapara Sands and Shallow Fluviatile shallow aquifers, 9 in Waipaoa, 46 in Makauri and 11 in Matokitoki deeper aquifers. As shown by the table, not all bores have measures covering the period of 2008 – 2021. Calculated and measured groundwater levels of the transient simulation are presented as curves for all the 88 bores in the digital appendix DA.

In following, transient simulation results will be described and evaluated for selected bores in the shallow and deeper aquifers and with measured values covering the period 2008 – 2021. Thereafter, a statistical evaluation will be undertaken for the outcomes of the validation period 2016 – 2021.

Table 4-9: Overview of 88 bores with measured groundwater levels for the transient calibration and validation

Aquifer	Te Hapara Sand	Shallow Fluviatile	Waipaoa	Makauri	Matokitoki	Total / Overall
Number of bores with measures	16	6	9	46	11	88
Count of measured values	120 - 2424	204 - 270	60 - 2780	14 - 2771	217 - 2435	
The shortest measure series dated from	18.09.2014	05.05.2008	23.04.2021	23.04.2021	31.03.2015	
to	18.06.2021	06.07.2018	21.06.2021	22.06.2021	18.06.2021	
The longest measure series dated from	05.05.2008	05.05.2008	05.05.2008	05.05.2008	05.05.2008	
to	11.06.2021	11.06.2021	11.06.2021	11.06.2021	18.06.2021	
Number of bores with measures in the period 2008 - 2021	15	5	6	30	7	63

Shallow aquifers Te Hapara Sand and Shallow Fluvatile

Figure 4-14 and Figure 4-15 depict the groundwater-level contours at the beginning and end of the calibration and validation period in the shallow aquifers.

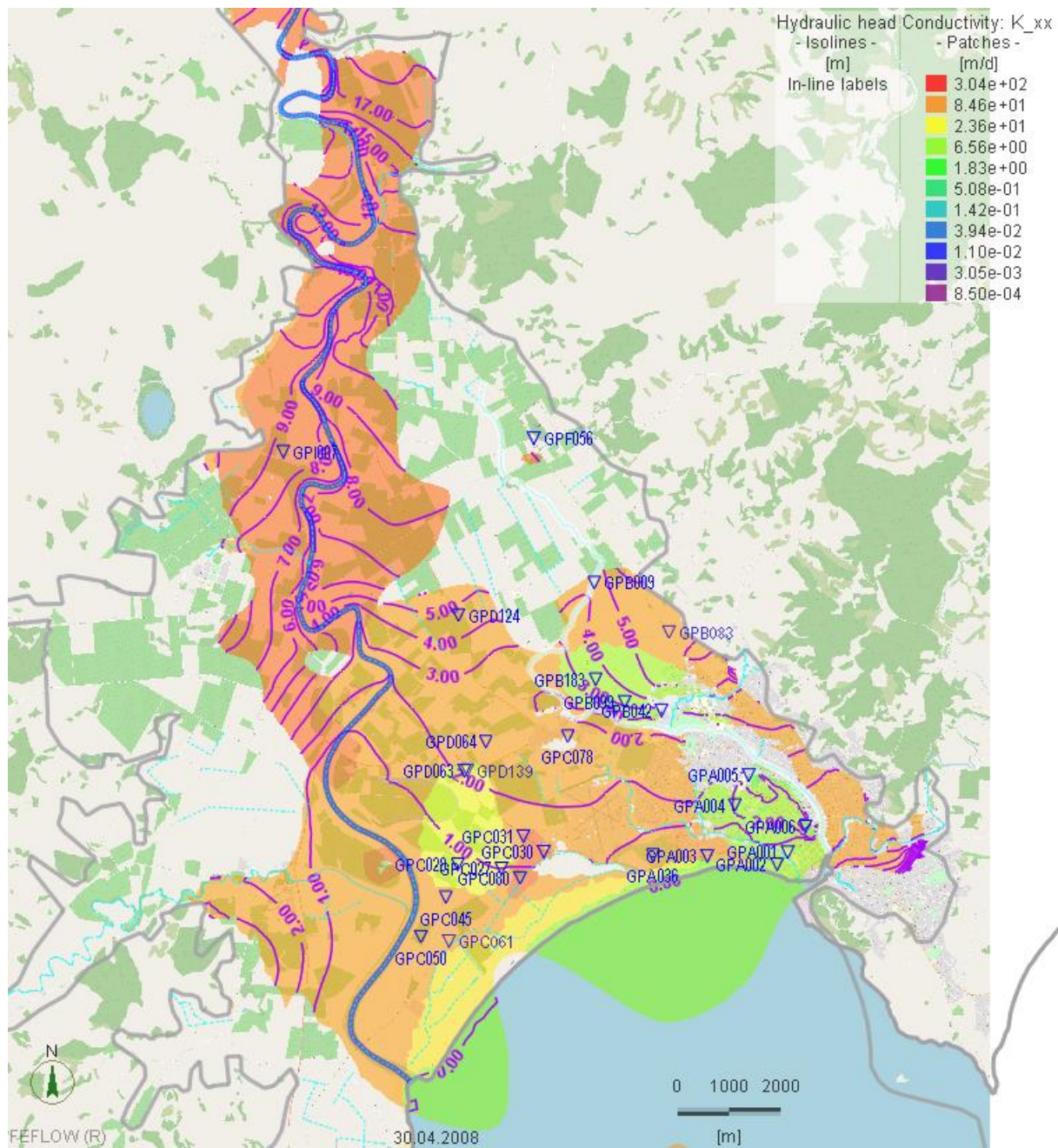


Figure 4-14: Hydraulic-head distribution in the shallow aquifers at the beginning of the calibration/validation period

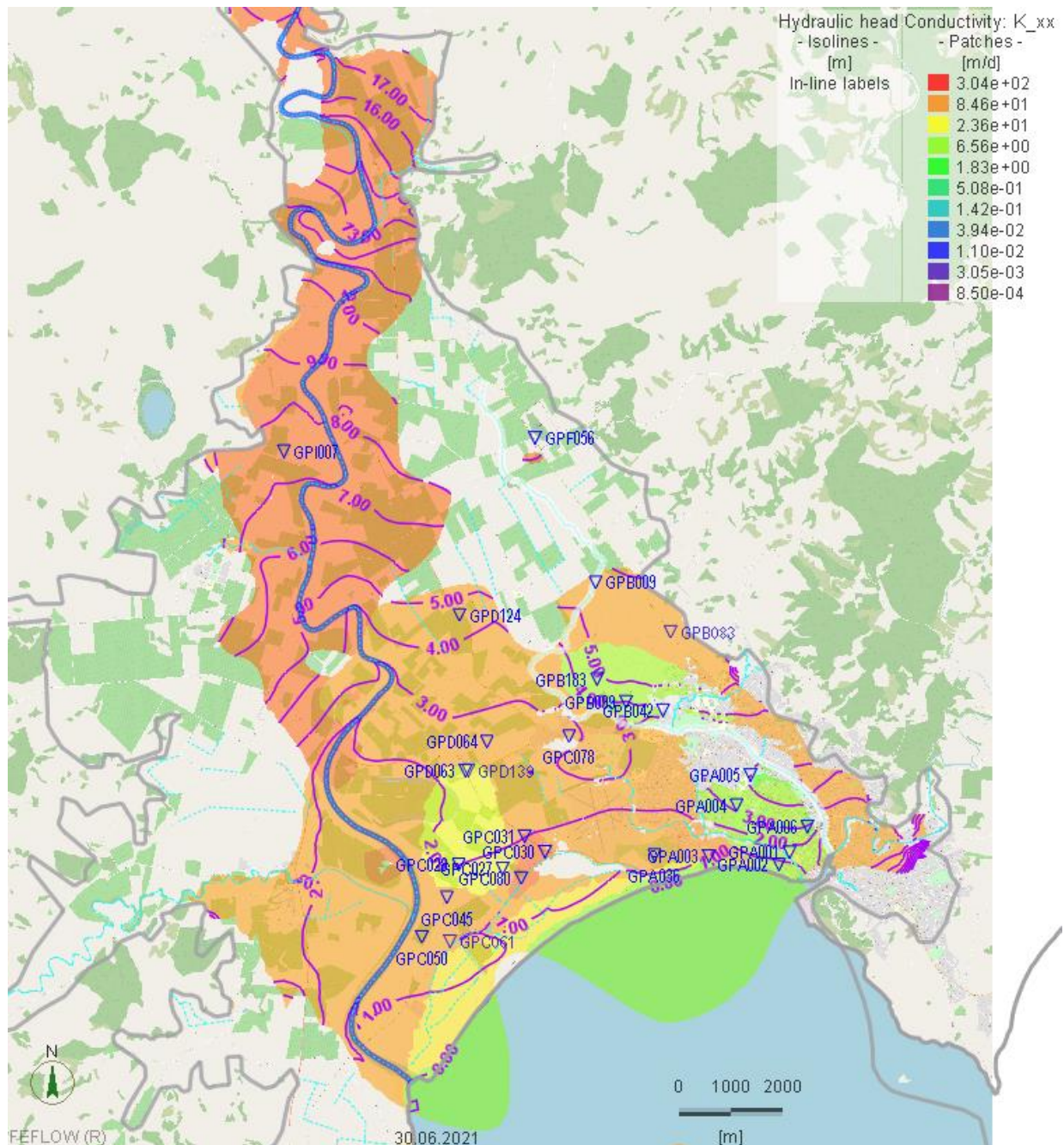


Figure 4-15: Hydraulic-head distribution in the shallow aquifers at the end of the calibration/validation period

Figure 4-16 displays simulated groundwater levels (lines) together with corresponding measurements (point-lines) of 4 bores in the Te Hapara Sand Aquifer: GPD063 is located by Saleyards Road or/and in the north-eastern vicinity of the Oxbow Wetland, while GPA003 by Awapuni Road near to the coast, GPA004 and GPA005 by Stanley Road from south to north in the Gisborne Urban Area.

Figure 4-17 compares simulated (lines) with measured (point-lines) groundwater levels of 3 bores in the Shallow Fluvial Aquifer: GPF056 is located by Back Ormond Road (opposite to Harper Road) in the (north-) eastern, GPI007 by Judd Road in the (north-) western and GPD019 by Bushmere Road in the middle part of the model.

The figures above show that the modelled groundwater levels match and fit well the measurements along with their dynamics over the 2008 – 2021 period in the shallow aquifers.

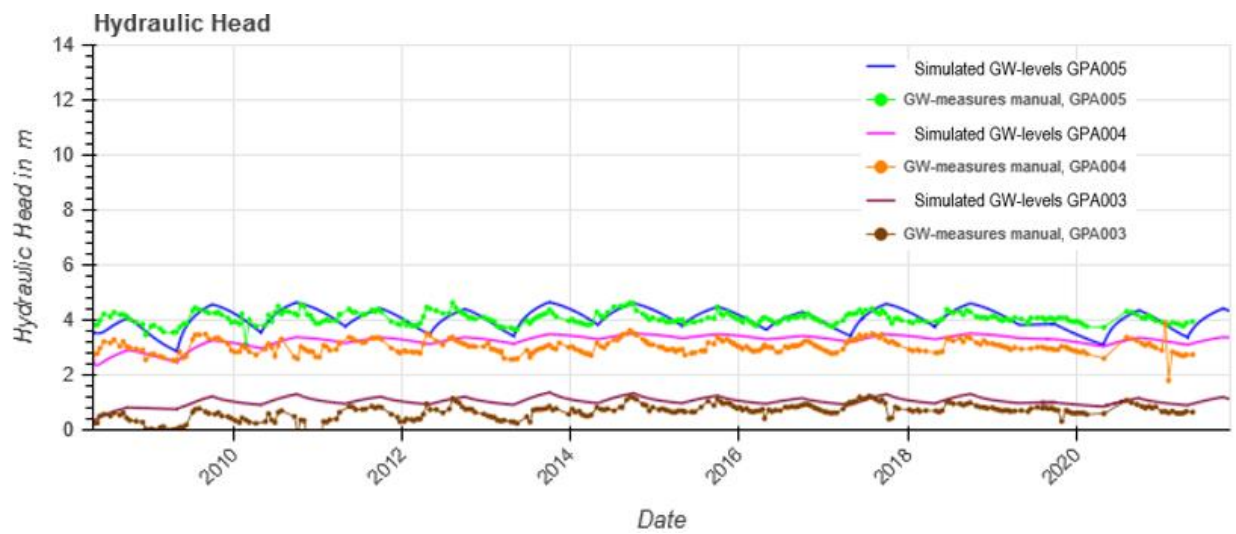
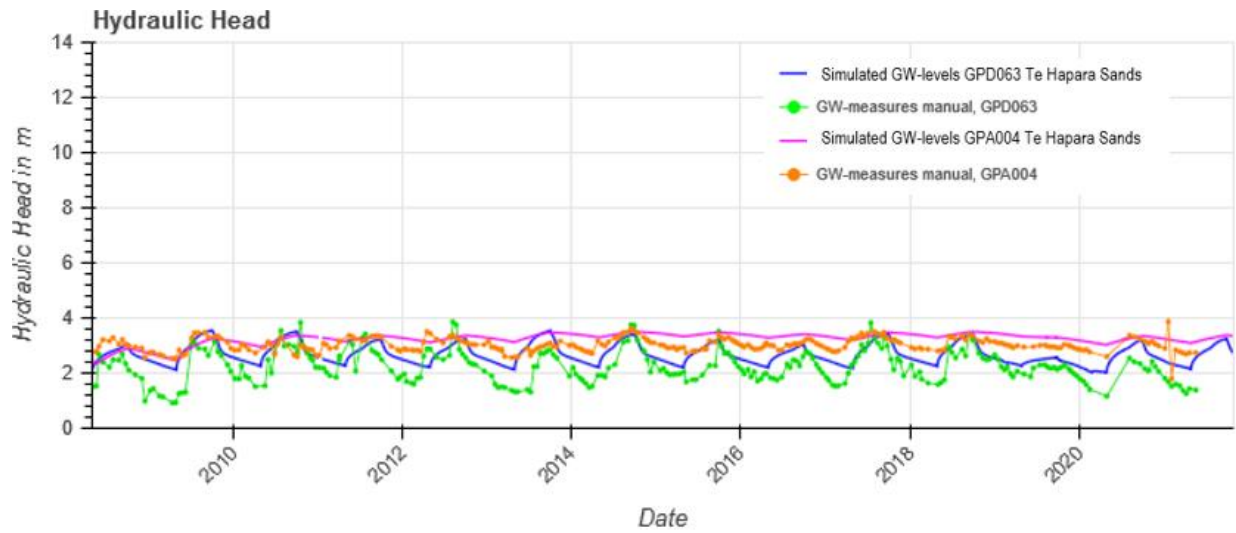


Figure 4-16: Simulated vs measured water levels in Te Hapara Sand aquifer bores, transient calibration+validation.

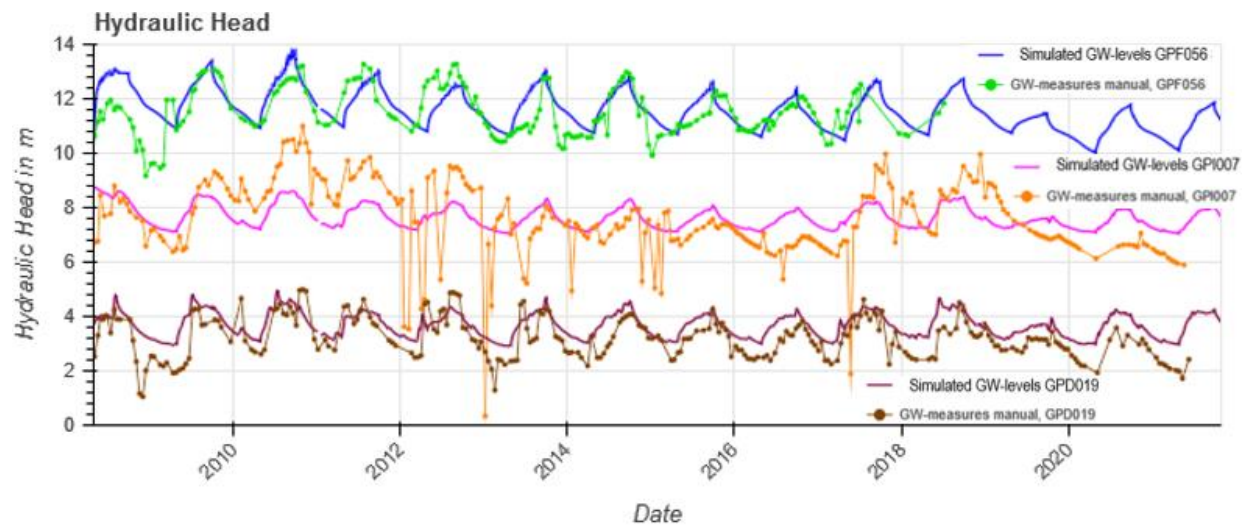


Figure 4-17: Simulated vs measured water levels in Shallow Fluvial aquifer bores, transient calibration+validation.

Deep aquifers Waipaoa, Makauri and Matokitoki

Figure 4-18 and Figure 4-19 depict the groundwater-level contours at the beginning and end of the calibration and validation period in the Waipaoa aquifer.

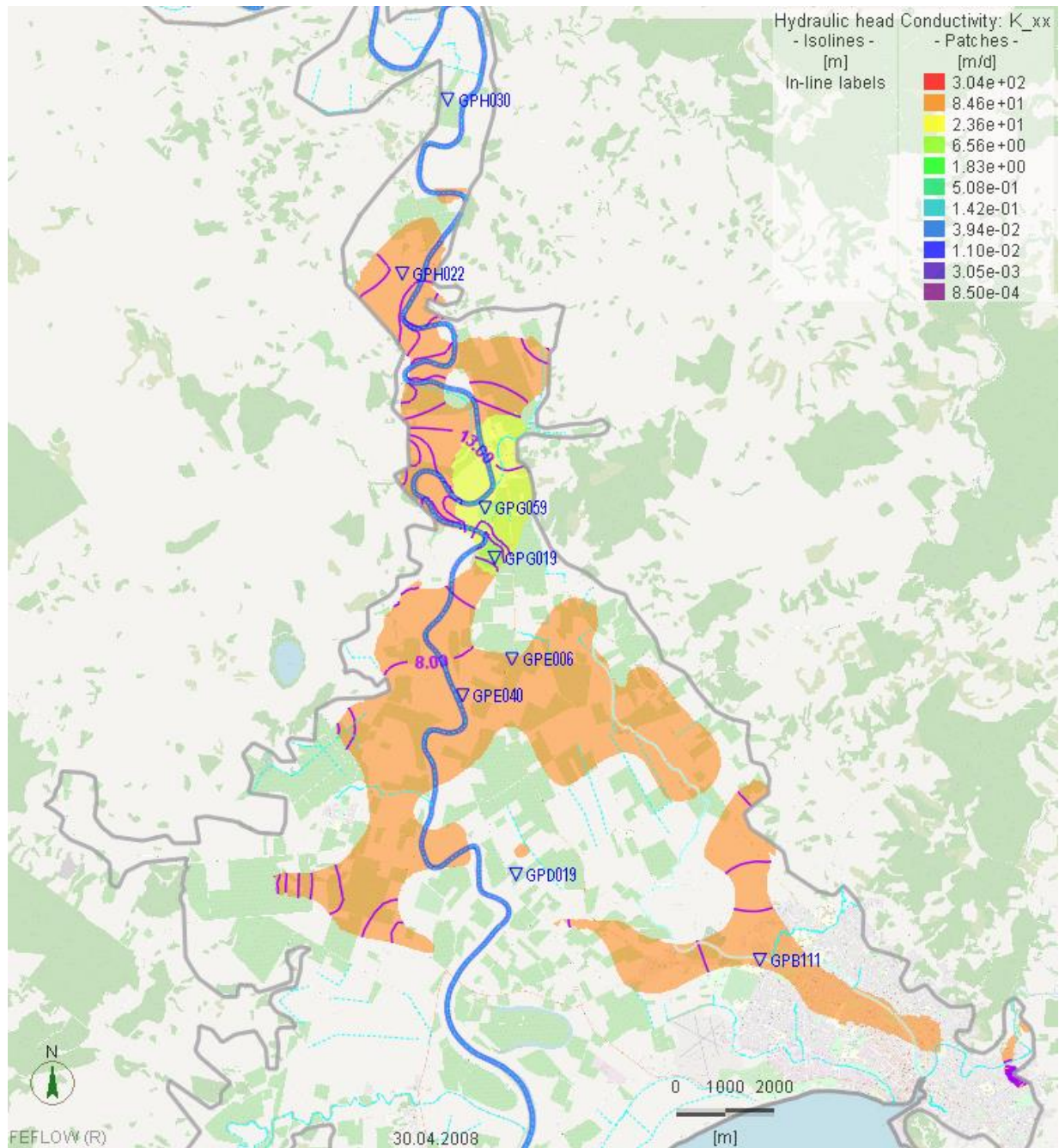


Figure 4-18: Hydraulic-head distribution in the Waipaoa at the beginning of the calibration/validation period

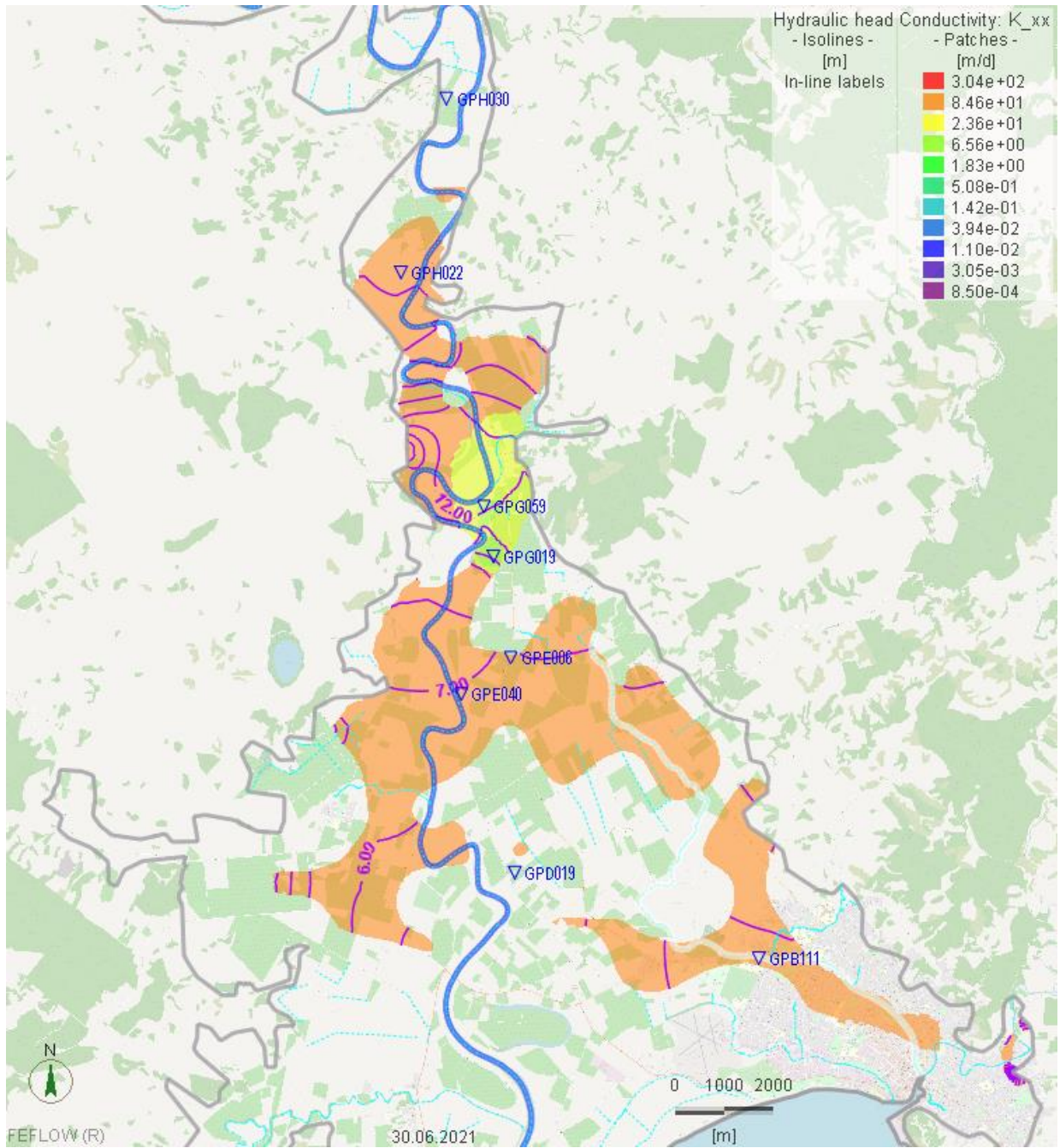


Figure 4-19: Hydraulic-head distribution in the Waipaoa at the end of the calibration/validation period

Figure 4-20 and Figure 4-21 depict the groundwater-level contours at the beginning and end of the calibration and validation period in the Makauri aquifer.

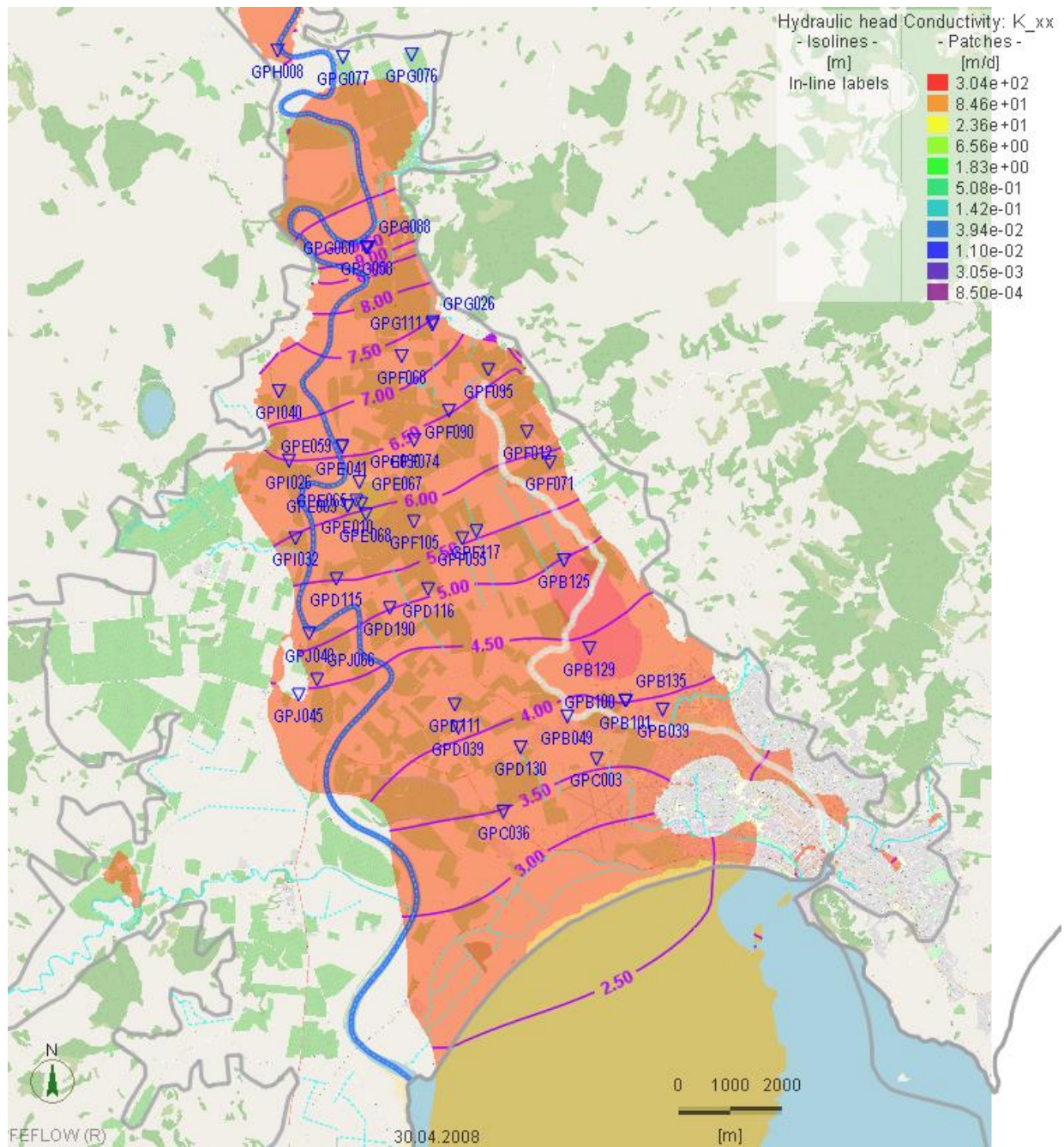


Figure 4-20: Hydraulic-head distribution in the Makauri aquifer at the beginning of the calibration/validation period

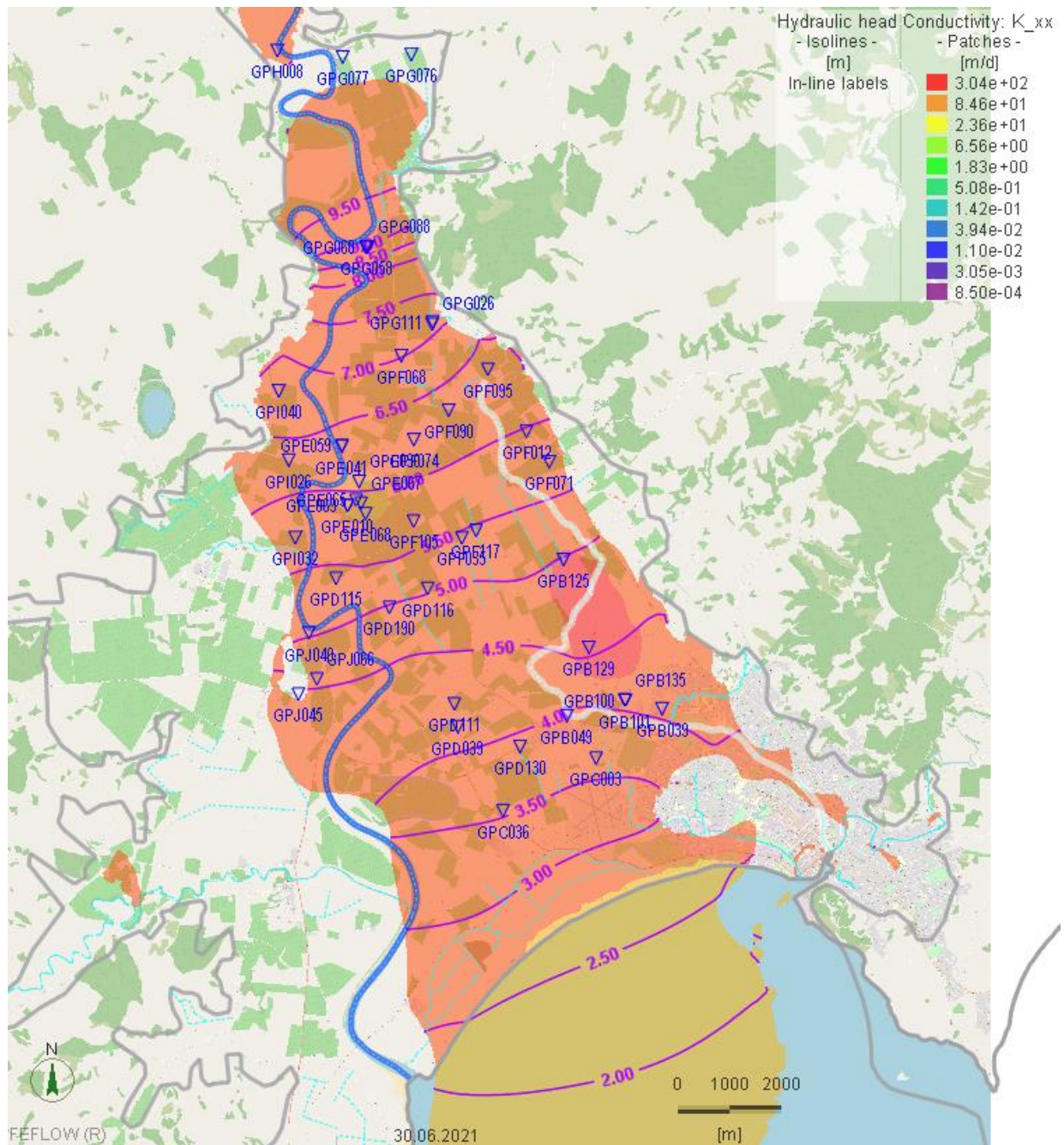


Figure 4-21: Hydraulic-head distribution in the Makauri aquifer at the end of the calibration/validation period

Figure 4-22 and Figure 4-23 depict the groundwater-level contours at the beginning and end of the calibration and validation period in the Makauri aquifer.

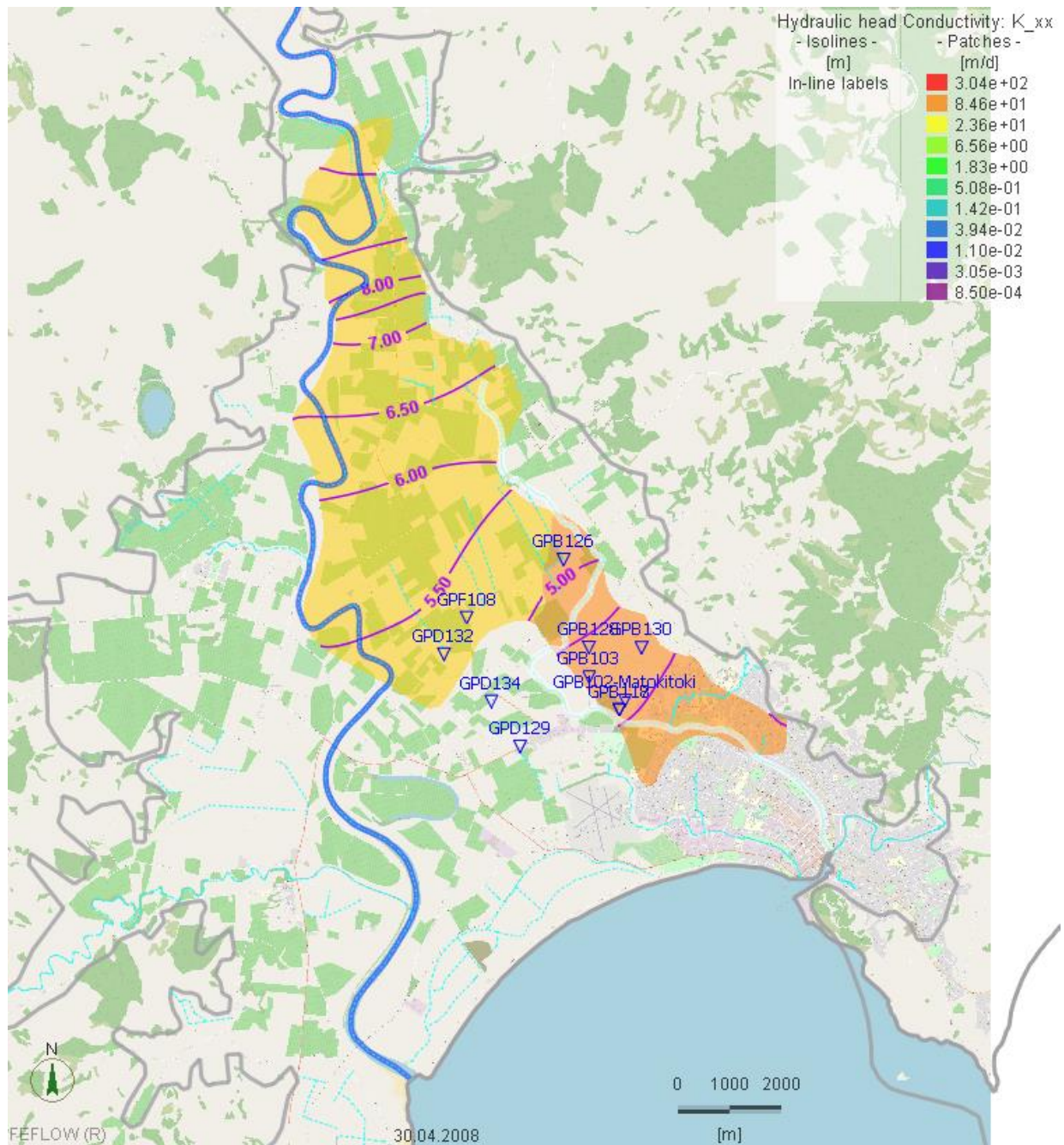


Figure 4-22: Hydraulic-head distribution in the Matokitoki aquifer at the beginning of the calibration/validation period

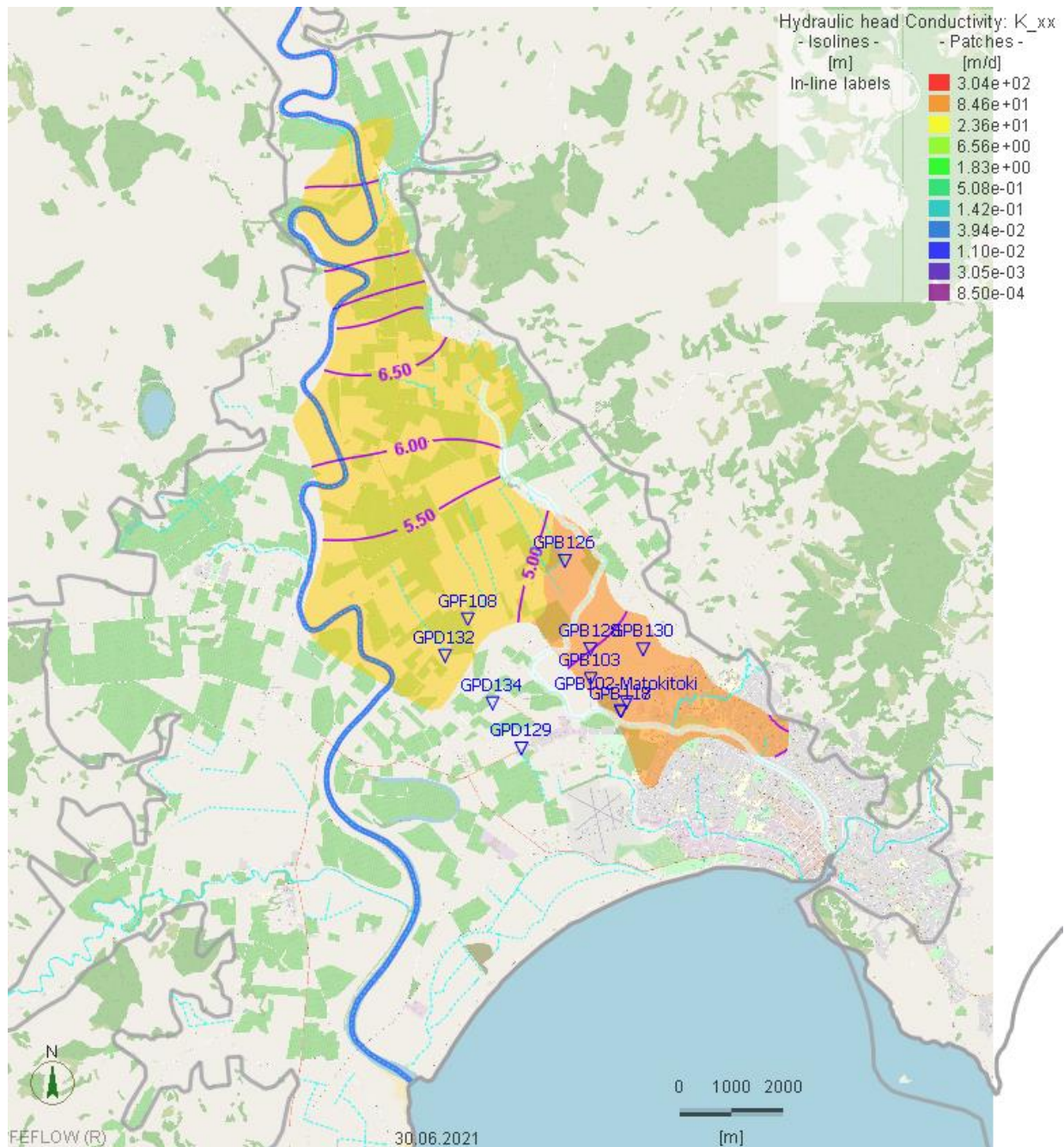


Figure 4-23: Hydraulic-head distribution in the Matokitoki aquifer at the end of the calibration/validation period

Figure 4-24 illustrates good fitting measured groundwater levels of two bores in the Waipaoa Aquifer: GPE040 is a monitoring bore of the Ferry Road Monitoring Site near to the Waipaoa River, representing the north part of the Waipaoa Aquifer. GPB111 is located by Campion Road near to the south bank of the Taruheru River and filtered in the south-east part of the Waipaoa Aquifer.

Figure 4-25 and Figure 4-26 represent good calibration and validation results in monitoring bores of Ferry Road Monitoring Site (GPE032 in the Waipaoa and GPE041 in the Makauri Aquifer) and of Caesar Road Monitoring Site (GPG059 in the Waipaoa and GPG060 in the Makauri Aquifer). The figures show that the calibrated 3D groundwater model Poverty Bay Flats fits well different water levels along with dynamics recorded over the 2008 – 2021 period in and between the Waipaoa and Makauri aquifer.

Figure 4-27 displays good matching measured groundwater levels of two bores in the Makauri Aquifer: GPF074 by Tucker Road and GPJ040 by Eade Road.

Figure 4-28 shows good fitting measured groundwater levels of two bores in the Matokitoki Aquifer, i.e. GPF108 by Kings Road and GPD132 by Bloomfield Road.

Figure 4-29 compares simulated with measured groundwater levels of 3 bores on Cameron Road Monitoring Site: GPB099 in the Te Hapara Sand, GPB100 in the Makauri and GPB102 in the Matokitoki Aquifer. It shows that the model results fit well to the measured values for GPB099 and GPB100. For GPB102, the modelled responses reflect the measured dynamics well, but the measured levels are underestimated by about 3 – 4 m. The measured groundwater levels in the Matokitoki Aquifer on Cameron Road Monitoring Site appear as artesian and higher than that in its overlaying aquifers Makauri and Te Hapara Sand. This points towards a process not covered by the conceptual and hydrogeological models underlying the numerical flow model, such as additional direct inflow into the Matokitoki aquifer.

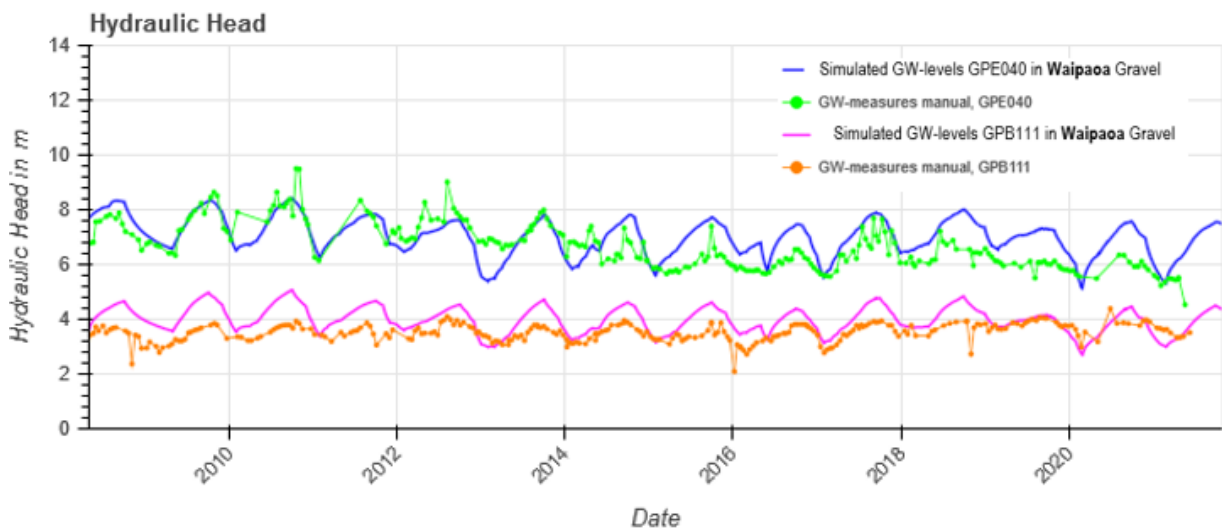


Figure 4-24: Simulated vs measured water levels in Waipaoa aquifer bores, transient calibration+validation.

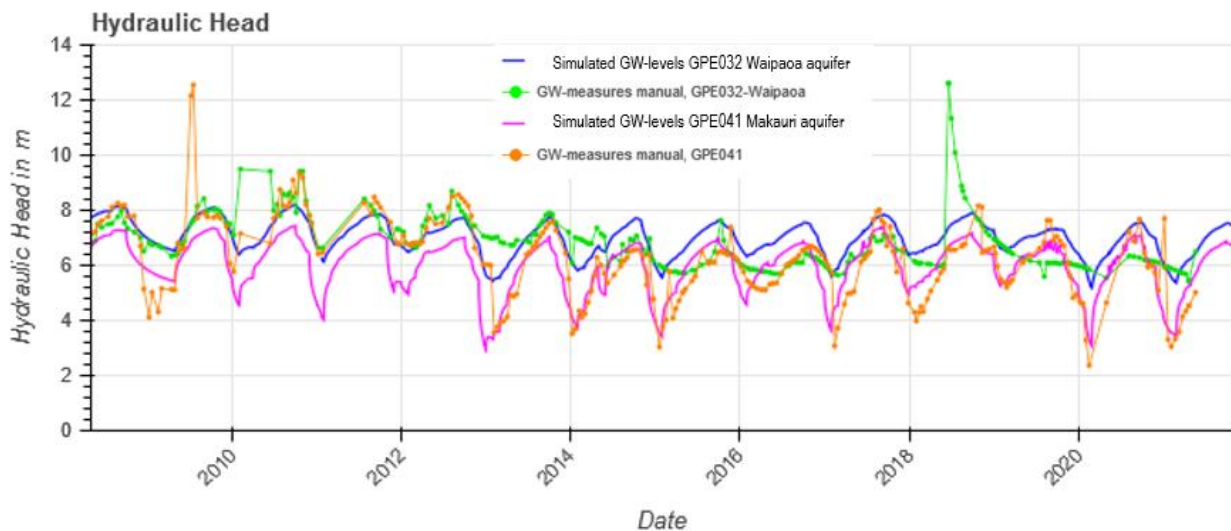


Figure 4-25: Simulated vs measured water levels in Waipaoa and Makauri aquifer bores (Ferry Road Monitoring), transient calibration+validation.

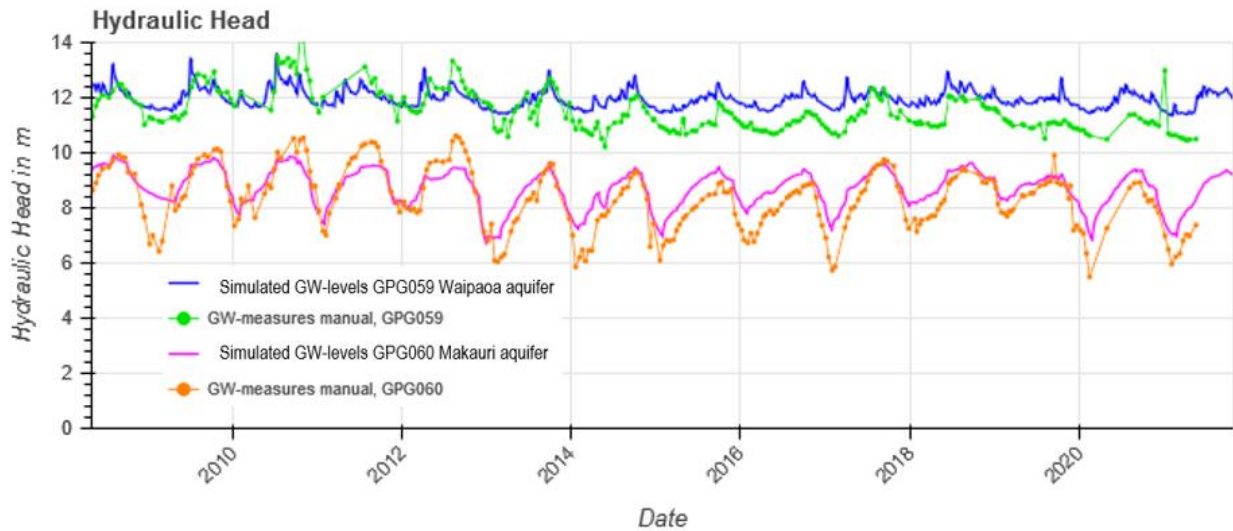


Figure 4-26: Simulated vs measured water levels in Waipaoa and Makauri aquifer bores (Caesar Road Monitoring), transient calibration+validation.

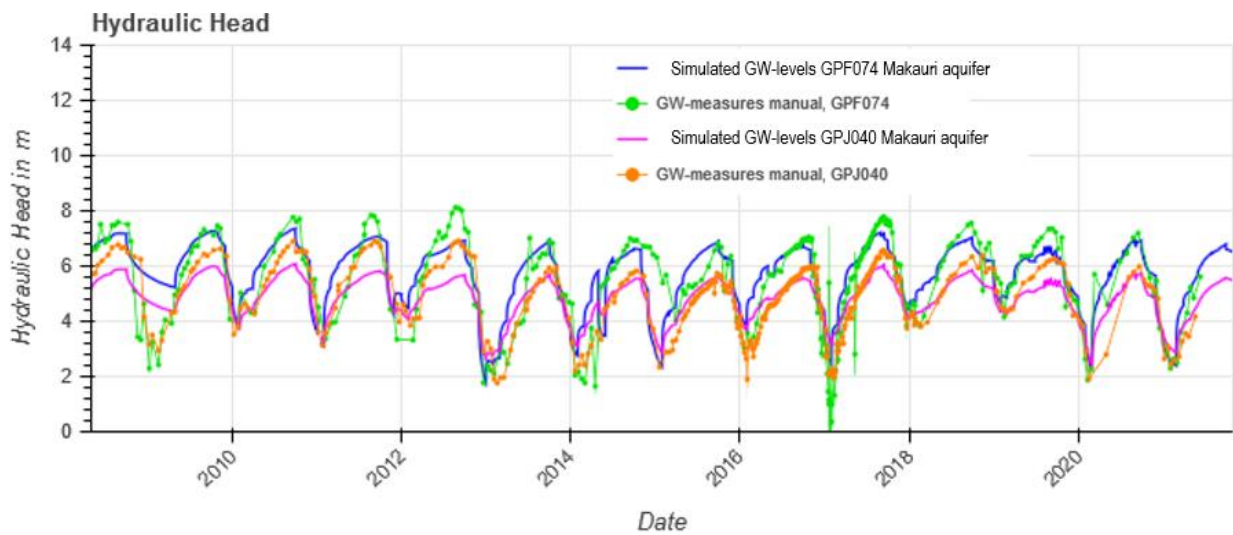


Figure 4-27: Simulated vs measured water levels in Makauri aquifer bores, transient calibration+validation.

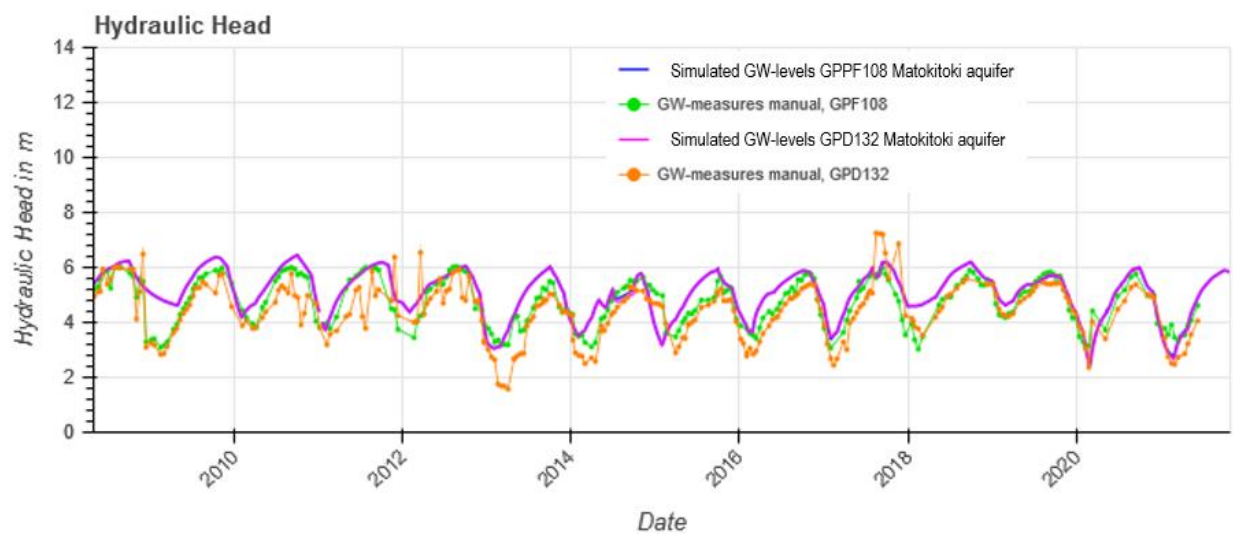


Figure 4-28: Simulated vs measured water levels in Matokitoki aquifer bores, transient calibration+validation.

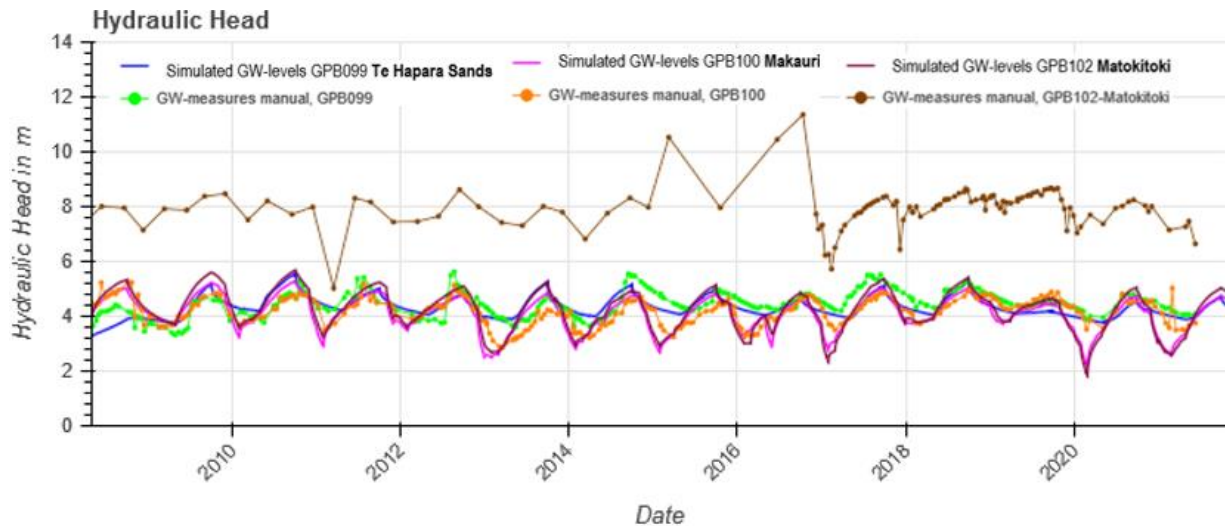


Figure 4-29: Simulated vs measured water levels in Te Hapara Sand, Makauri and Matokitoki aquifer bores (Cameron Road Monitoring), transient calibration+validation.

Statistical evaluation of the validation period 2016 – 2021

Figure 4-30 represents a scatter plot of simulated vs measured means water levels in the validation period 2016 – 2021 for the 88 bores, classified by the shallow aquifers Te Hapara Sand+Shallow Fluvatile and the deep aquifers Waipaoa, Makauri and Matokitoki by different or/and coloured marks. This figure indicates a generally good or/and satisfactory fitting of observed and calculated water levels in the validation period.

Figure 4-31 shows histogram of correlation coefficients of simulated and measured water levels in the validation period. Accordingly, 81% of 88 bores have correlation coefficients above 0.5, of which 48% above 0.75, implying good fittings of groundwater dynamics.

Figure 4-32 displays a scatter plot of scaled mean difference (residual) i.e., the mean residual scaled by difference between the measured maximal and minimal level of each bore and correlation coefficient of simulated and measured water levels in the validation period, classified by the shallow aquifers Te Hapara Sand+Shallow Fluvatile and the deep aquifers Waipaoa, Makauri and Matokitoki. The figure gives a summarised overview on good or/and satisfactory outcomes achieved to fit measured water levels along with their dynamics in the validation period.

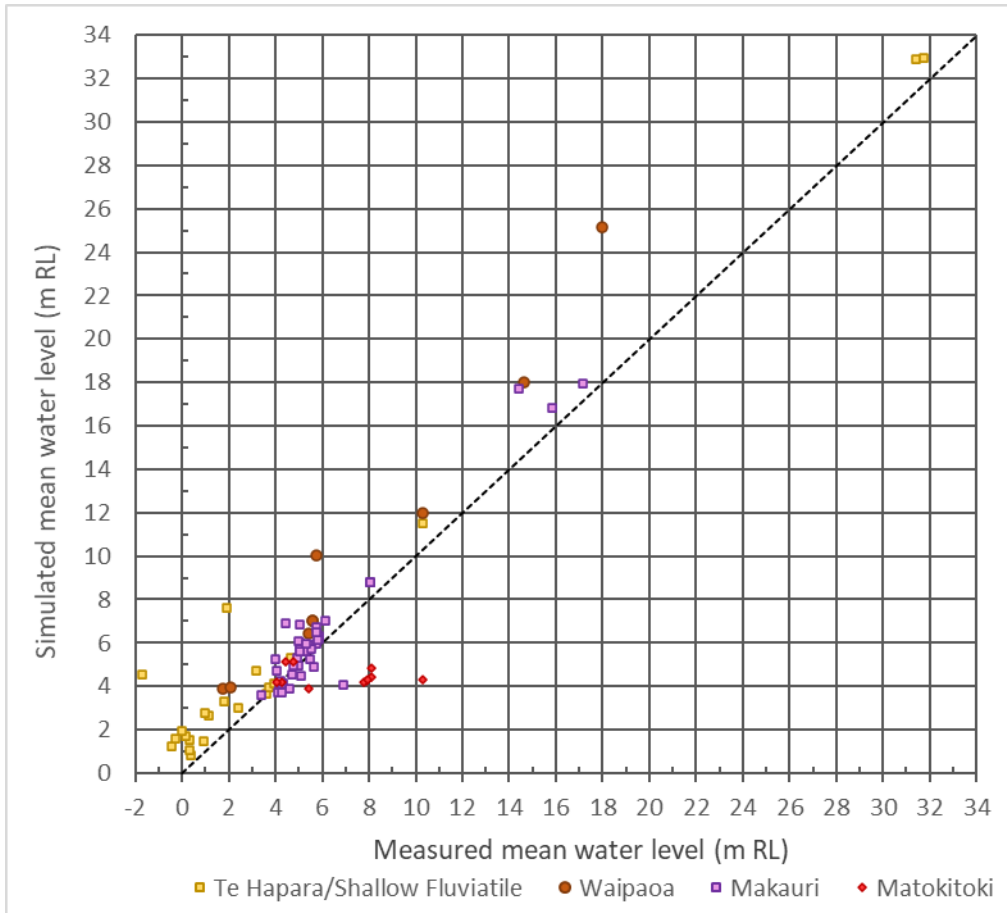


Figure 4-30: Scatter plot of simulated vs measured mean water levels of validation period 2016 – 2021.

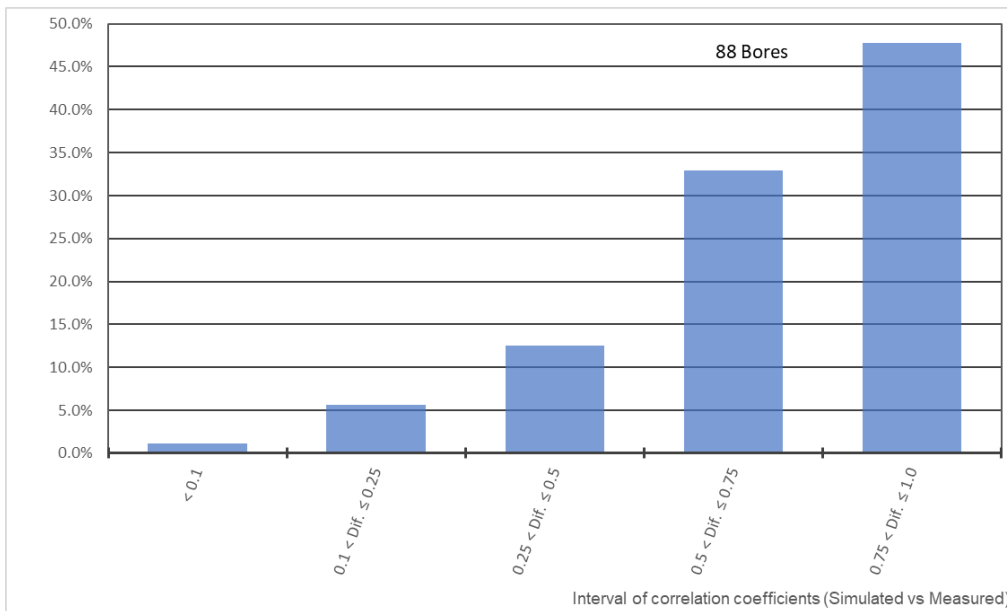


Figure 4-31: Histogram of correlation coefficients of simulated and measured water levels in the validation period 2016 – 2021.

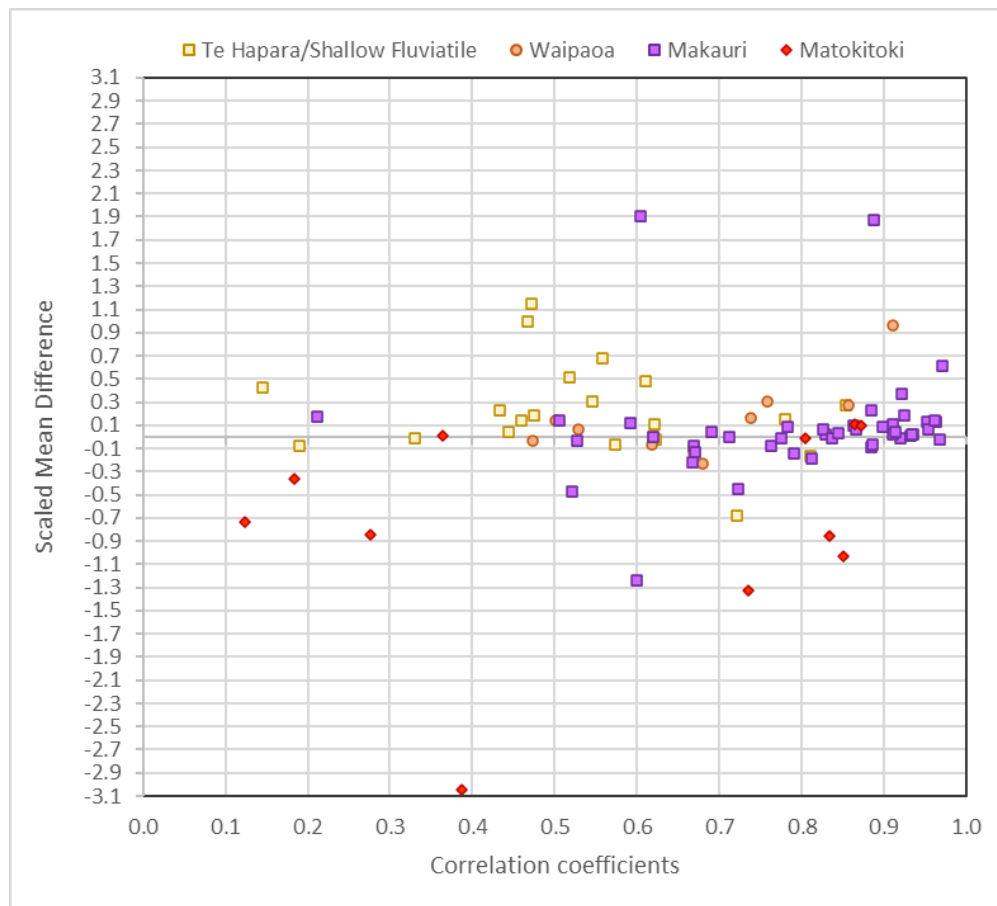


Figure 4-32: Scatter plot of scaled Mean Difference and Correlation coefficient of simulated and measured water levels in the validation period 2016 – 2021, classified by the shallow aquifers Te Hapara Sand+Shallow Fluvialite and the deep aquifers Waipaoa, Makauri and Matokitoki.

Water balance of the calibration and validation period 2008 – 2021

Table 4-10 and Figure 4-33 show the total water balance of the calibration and validation period 2008 – 2021 summarised for the balance components (or/and boundary condition types) recharge, sea, Waipaoa River, Matawhero wetland, Taruheru River, other rivers and drains, and groundwater takes incl. the injection of the MAR trial bore GPE066 in 2017-2020. The difference between the total inflow and total outflow amounts to approximately 5,9 million m³. This indicates, in relation to the total inflows, around 1% for water balance error and storage changes (error and storage change not separated here).

Table 4-10: Total water balance in the calibration and validation period 2008 – 2021

Balance Component / BC	Total Inflow (m ³)	Total Outflow (m ³)	Inflow - Outflow (m ³)	Remark
Recharge	540,189,760	0	540,189,760	Mean 175 mm/year*
Waipaoa River		280,859,224	-280,859,224	
Oxbow / Matawhero wetland		10,927,816	-10,927,816	
Taruheru River		45,846,909	-45,846,909	
Other Rivers/Drains		148,493,574	-148,493,574	
Sea		45,599,952	-45,599,952	
Groundwater MAR Injection (GPE066) and takes	225,507	14,593,699	-14,368,192	
Total	540,415,267	546,321,174	-5,905,907	Imbalance about -1%

* With respect to the surface area of 235,439,100 m² in the model domain.

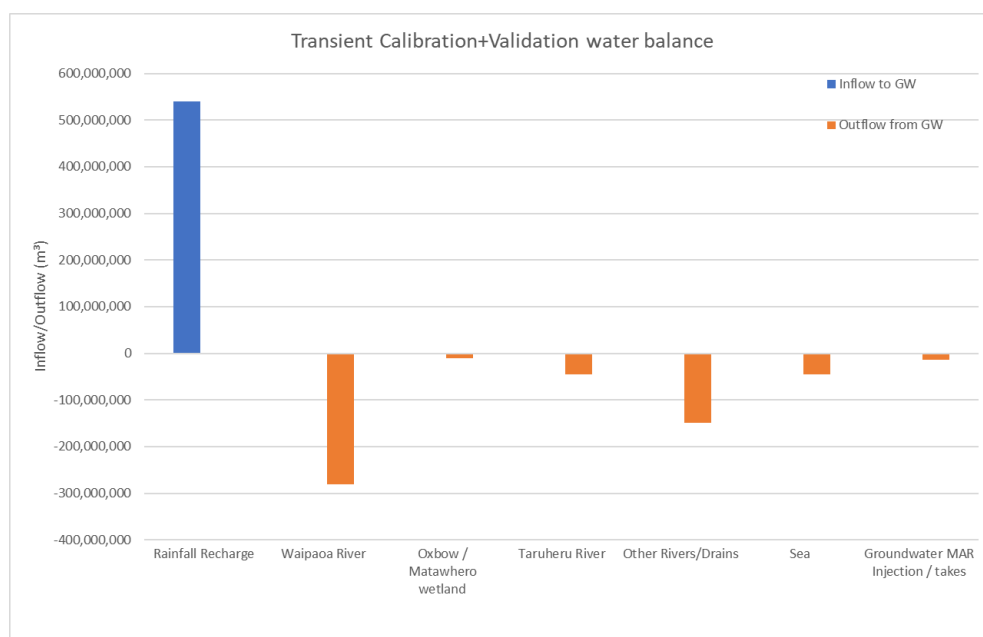


Figure 4-33: Total water balance in the calibration and validation period 2008 – 2021: inflows and outflows.

4.4. Simulation MAR-Trials 2017-2020

4.4.1. Parameters

The MAR-Trials 2017-2020 simulation incorporated the MAR trial bore GPE066 as an injection well-BC in the Makauri Aquifer corresponding to its Location. The simulation started from the transient simulation outcomes of date 30.04.2017 as model initial state, and considered the average injection rates of the MAR trial periods 2017, 2019 and 2020 as inputs as shown in Table 4-11.

4.4.2. Results

Figure 4-34 represents the simulated water levels (blue) compared to the measured values (light green = automatical logger or orange = manual measures) of 4 monitoring bores in the vicinity of the injection Bore GPE066: GPE069 is located with a distance of 190 m south-western to GPE066, while GPE065 with a distance of 14 m, GPE067 124 m and GPE068 334 m south-eastern to GPE066. The figure shows that the simulated responses to the MAR-Trials 2007-2020 match the measured values in the monitoring bores very well, both in levels and dynamics. Peaks are not perfectly matched, though, which can be attributed to the fact that roughly average infiltration flows were used as input to the model, while the actual infiltration was more dynamic. The therefore lower rates in the model lead to a lower hydraulic head during infiltration (the shorter the infiltration periods, the larger the difference).

Table 4-11: Overview of 2017-2019 injection trials details

MAR Trials	Injection Details	Start date / time	Finish date / time	Period (days)	Average injection rate (L/s)	Source
2017	Initial injection trial	12.06.2017 08:44	19.06.2017 03:19	6.77	15.2	Golder 2017 Poverty Bay MAR trial Year 1 results.pdf (Golder, 2017)
	Main injection trial	20.07.2017 09:15	13.09.2017 09:15	52	14.0	
2019	Injection # 1	07.08.2019	12.08.2019	5	14.1	Gisborne MAR Trial 2017-2020
	Injection # 2	17.08.2019	23.08.2019	6	11.3	

	Injection # 3	30.08.2019	05.09.2019	6	16.0	(A2026603).pdf (Golder, 2021)
	Injection # 4	18.09.2019	25.09.2019	7	11.3	
	Injection # 5	03.10.2019	13.10.2019	10	14.5	
2020	Injection # 6	12.05.2020	15.05.2020	3	18.1	
	Injection # 7	22.05.2020	01.06.2020	10	11.2	
	Injection # 8	08.06.2020	18.06.2020	10	6.5	
	Injection # 9	13.07.2020	16.07.2020	3	15.7	
	Injection # 10	27.07.2020	04.09.2020	48*	2.9	
	Injection # 11	12.09.2020	12.10.2020	35*	12.6	* Not continuous on all days

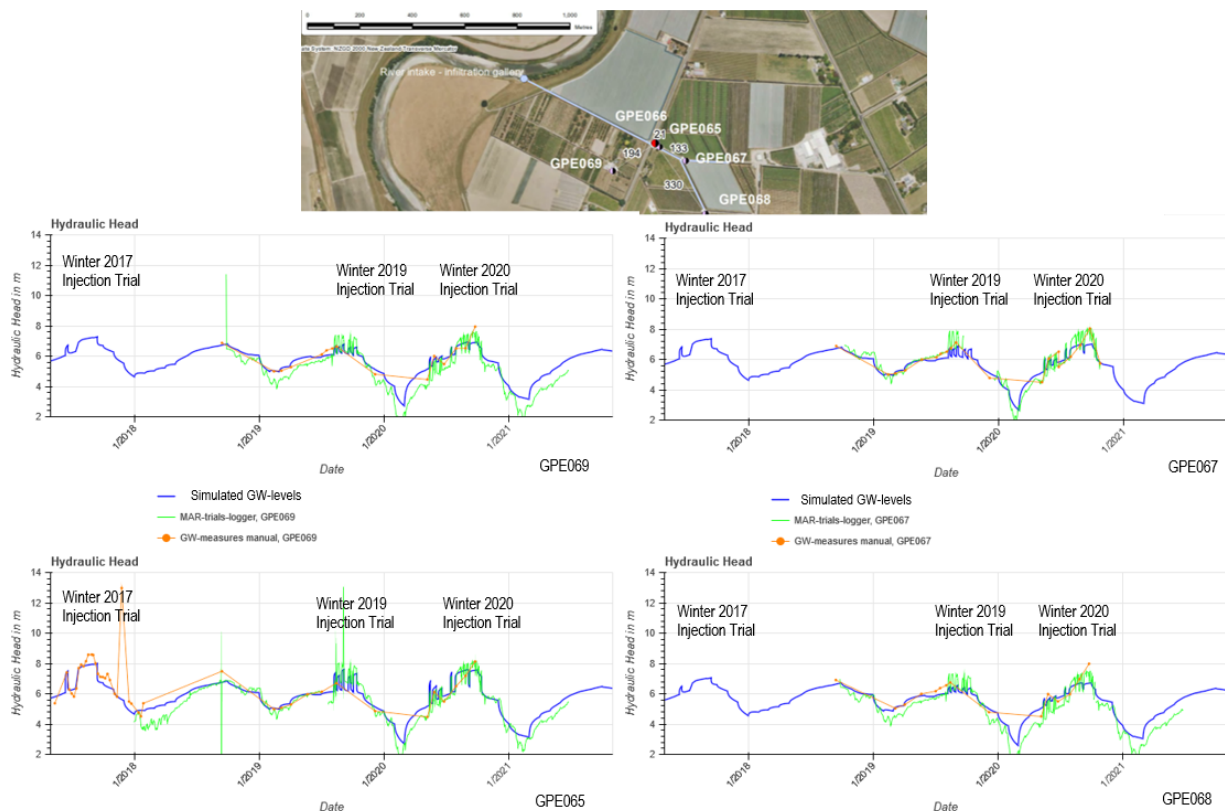


Figure 4-34: Simulation results comparison with measured data

4.5. Groundwater Age Simulation (residence times)

4.5.1. Parameters

Groundwater age simulations have been undertaken as an additional validation or proof of the calibrated 3D groundwater model for simulating flow behaviours and residence times of groundwater in the Quaternary aquifers in the Poverty Bay Flats. Groundwater age simulations require additional parameter (solute) transport porosity and dispersivity, which are specified as followings:

- transport porosity: 0.015 - 0.25 (-) corresponding to hydraulic conductivity of Aquitards/Aquifers
- longitudinal dispersivity: 5 - 50 (m)
- transverse dispersivity: 0,5 - 5 (m).

4.5.2. Results

Table 4-12 shows simulation results (blue) with good matching NGMP age data (green). An exact match is not expected here, among other reasons because of the inherent uncertainty of the underlying age dating methods.

Table 4-12: Simulation results comparison with NGMP age data

Regional Authority	GGW Feature ID	Site	NZTM Easting	NZTM Northing	Exponential Piston Model ratio (%)	Mean Residence Time (years)	Age Simulation (years)	Aquifer
GDC	338	GPB102	2033820	5710963	0.43	185	129	Makauri
GDC	83	GPC031	2031318	5708657	2.6	50	149	Makauri?
GDC	83	GPC031	2031712	5708444	0.43	1	0.2	Te Hapara Sand
GDC	81	GPC062	2030217	5706652	0.43	130	150	Makauri
GDC	81	GPC062	2030254	5706388	0.1	15	2	Te Hapara Sand
GDC	82	GPE006	2029193	5716763	0.38	44	32	Makauri
GDC	80	GPD130	2031636	5710162	0.43	170	116	Makauri
GDC	79	GPF090	2030247	5716709	0.43	125	35	Makauri

4.6. Electrical conductivity simulation of MAR-Trials 2017 - 2020

4.6.1. Parameters

The groundwater-age simulation undertaken above is based on steady state solute transport modelling. In contrast, the electrical conductivity (EC) simulation for the MAR trial period 2017 - 2020 is based on transient solute transport modelling. The EC simulation uses the MAR trials 2017-2020 (hydraulic) simulation model described in Cap. 4.4.1 as base, adding additional transport parameters as follows:

- transport porosity: 0.015 - 0.25 (-) corresponding to hydraulic conductivity of aquitards/aquifers
- longitudinal dispersivity: 5 - 50 (m)
- transverse dispersivity: 5 - 5 (m), and
- Mass-concentration BC for the MAR bore GPE066 with constant EC value of **490** mS/cm corresponding to the well-BC with injection water rate
- Initial EC 910 mS/cm for Aquifers Te Hapara/Shallow/Waipaoa and Aquitards 1 and 2
- Initial EC 1320 mS/cm for Makauri / Matokitoki and Aquitards 3 and 4 (Initial EC derived from GDC-data "20220112_GWQ cond and Sal.xlsx").

Initial conditions in particular have been simplified for this run, as the main goal was to simulate the translation and dispersion of the fresh water plume originating in the injection bore.

The EC simulation of MAR trials 2017 - 2020 started from the simulation date 30 April 2017, i.e., equal to the MAR trials 2017-2020 (hydraulic) simulation described above.

4.6.2. Results

Figure 4-35 represents the simulated EC (blue) compared to the measured values (dark lines) of 3 monitoring bores GPE069, GPE067 and GPE068 in the vicinity of the injection bore GPE066. The figure shows

that the simulated EC match the measured values in the monitoring bores GPE069 and GPE067 quite well, especially by the recorded EC dynamics (initial EC is not expected to match perfectly, as uniform values have been used). The simulation outcomes of GPE068 show comparably large differences to the measured values. The intermediate increases in EC in the observation data, however, cannot be reproduced by the model, their source is unknown. GPE068 has the largest distance (334 m) to the MAR bore GPE066 as GPE067 (124 m) and GPE069 (190 m). Its measured EC present yet larger responses than those of GPE067 and GPE069. As both laterally and in flow direction the freshening of the water is reproduced by the model very well, this can be seen as a confirmation of the assumed dispersivity and porosity values.

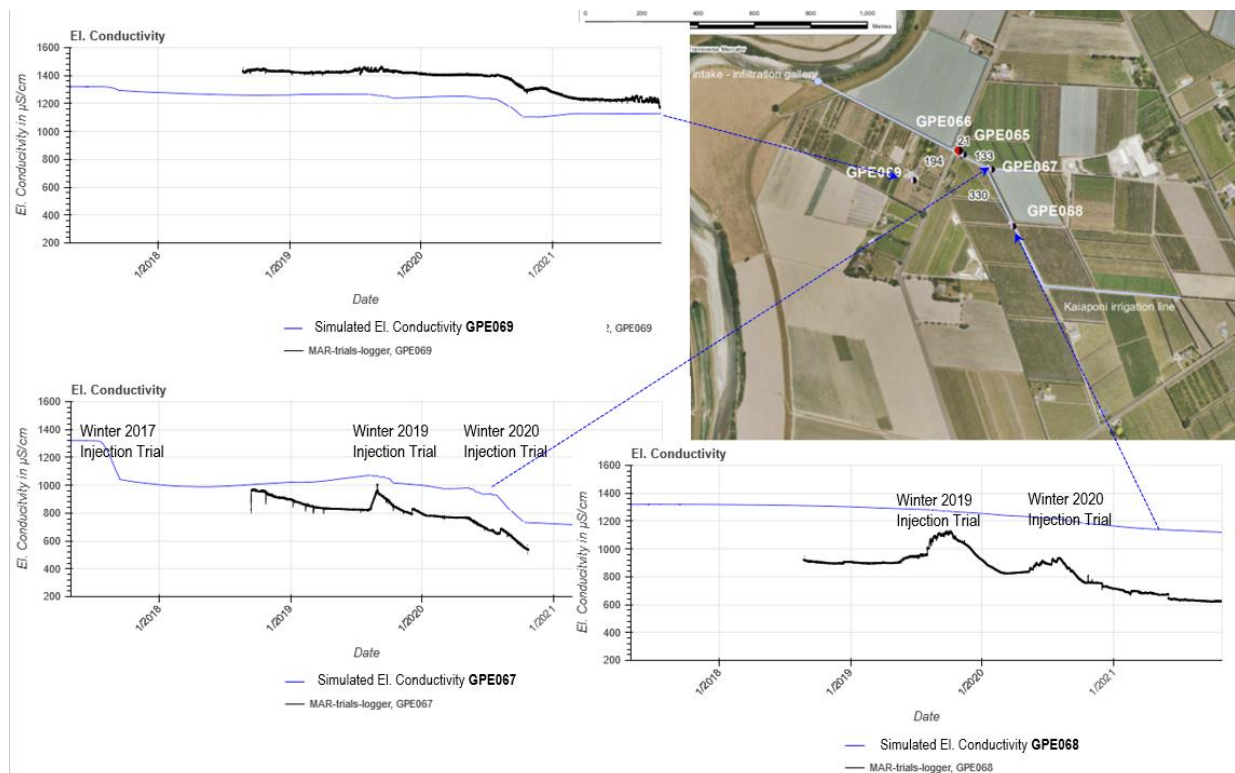


Figure 4-35: Simulated vs measured electrical Conductivity (EC) of results

4.7. Additional transient simulation showing effect of additional evapotranspiration in summer

4.7.1. Parameters

The simulation outcomes of bore GPD063, located in the north-eastern vicinity of the Oxbow Wetland and screened in Te Hapara Sand Aquifer, show that measured groundwater levels in summer appear mostly overestimated by the model (ref. Chap. 4.3.2). In order to understand whether this can be caused by an underestimation of evapotranspiration (by simply assuming rainfall recharge as zero), an additional run of the transient calibration and validation scenario (2008 – 2021) was undertaken. For the run, additional evapotranspiration is considered in summer months

Evapotranspiration is assumed to take place during the summer months December - March in areas with a low depth to groundwater in the unconfined aquifers Te Hapara Sand and Shallow Fluvialite. Figure 4-36 shows the areas where mean depth to groundwater is less than 0.5 m. Evapotranspiration rate is assumed to be 0.2 – 0.5 mm/day.

4.7.2. Results

Figure 4-37 shows the simulated water levels by transient calibration+validation (blue) and transient calibration+validation with evapotranspiration (red) in comparison to measured ones (green) of bore GPD063. The additional simulation run shows a slightly better matching of the observed water levels by considering the assumed evapotranspiration during summer months.

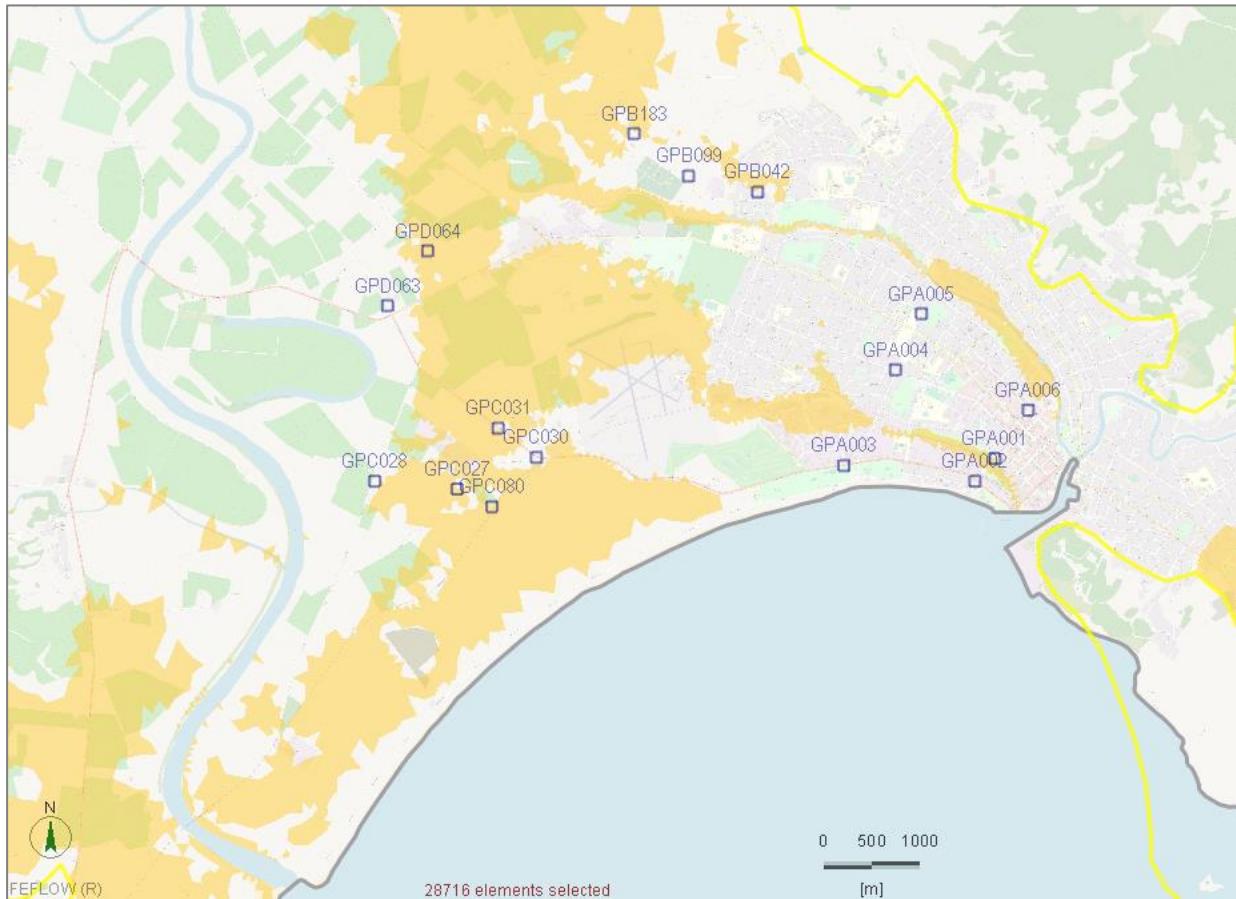


Figure 4-36: Location of specified areas with possible evapotranspiration in summer.

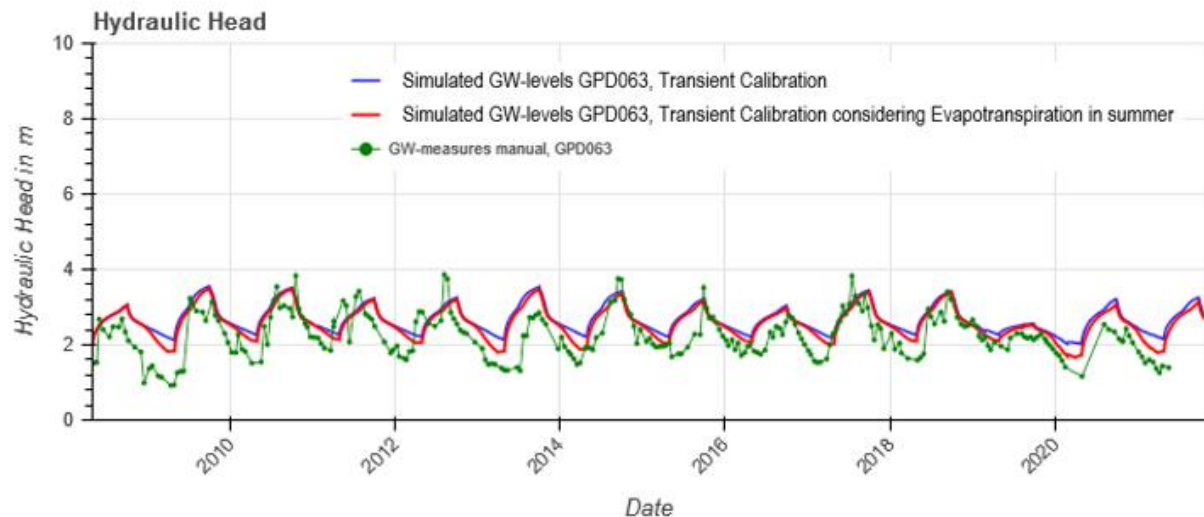


Figure 4-37: Simulated vs measured water levels of bore GPD063 in Te Hapara Sand aquifer, transient calibration+validation and transient calibration+validation considering evapotranspiration in the summer period

4.8. Additional simulations with respect to artesian potential in the south eastern Matokitoki aquifer

Within the iterative calibration process, additional simulations were performed under consideration of lateral inflow from the south-eastern border of the Matokitoki aquifer in order to better match the observed artesian levels in this area. These simulations are not considered as result of the calibration and are not used as basis of scenario runs, as a potential lateral inflow is highly uncertain in its nature and location. At the same time, by neglecting a potential inflow the model is more conservative when it comes to the effects of groundwater abstraction.

4.8.1. Parameters

The lateral inflow was implemented by assuming a fixed hydraulic head along the aquifer boundary (1st-kind BC) in combination with a modified hydraulic conductivity of the Matokitoki aquifer in the area (Figure 4-38). The simulations conducted under the assumed assumptions are

- Steady state simulation with an assumed hydraulic head of 11 mRL for the 1st-kind BC
- Steady state simulation with an assumed hydraulic head of 10 mRL for the 1st-kind BC
- Transient simulation for the period 1 May 2008 – 31 October 2021 with an assumed hydraulic-head of 10 mRL for the 1st-kind BC.

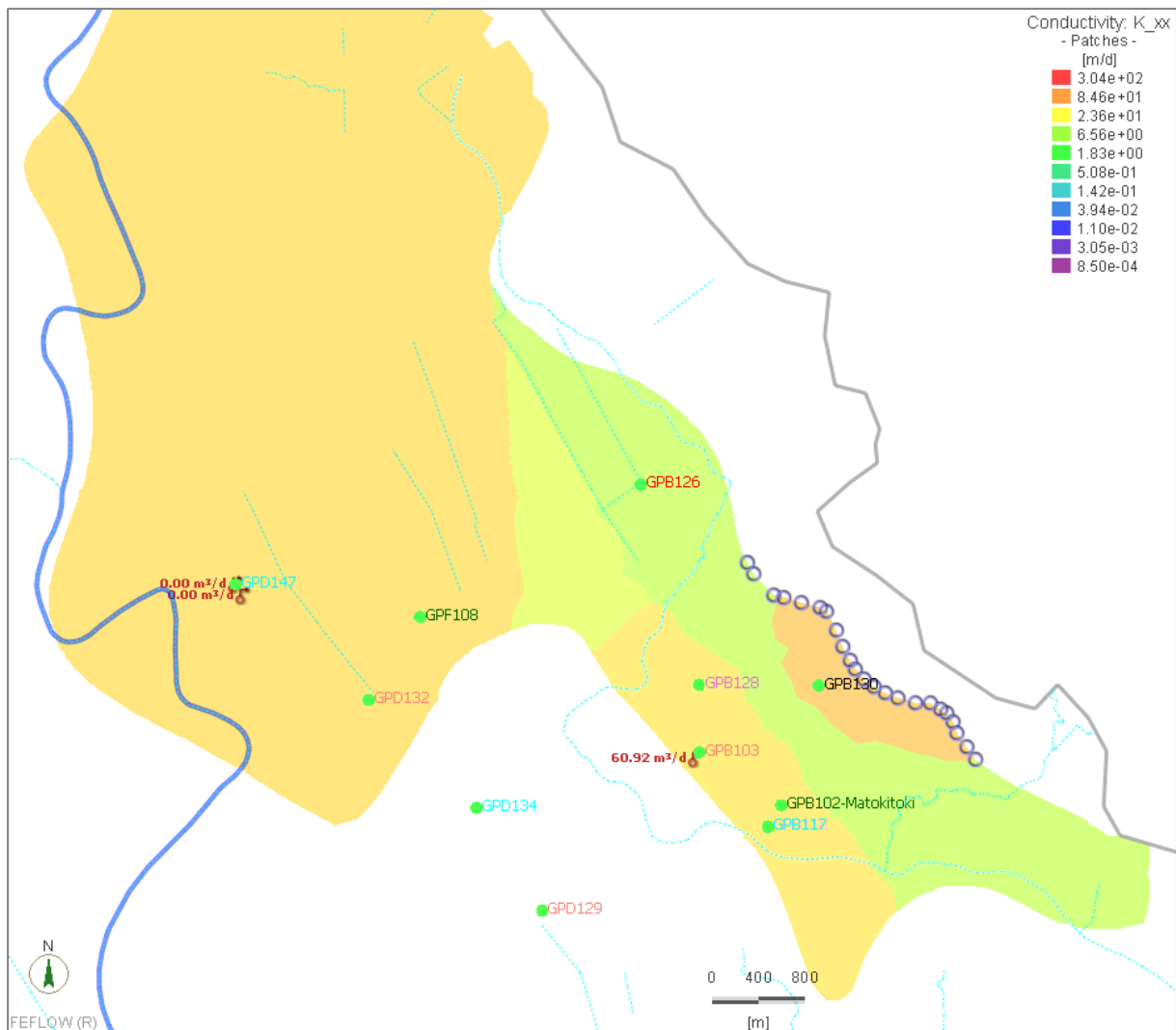



Figure 4-38: Location of the assumed Hydraulic-head BC  and modified hydraulic conductivity for the Matokitoki aquifer.

4.8.2. Results of steady state simulations

Table 4-13 shows overall statistics and water balance errors of the two steady state simulations together with the steady state calibration SCC.

Figure 4-39 and Figure 4-40 show scatter plots of simulated vs measured water levels of the two steady state simulations together with the steady state calibration SCC.

Figure 4-41-Figure 4-43 show simulated groundwater levels in the Matokitoki aquifer, steady state calibration SCC and simulations with the 1st-kind BC of 11 mRL and 10 mRL respectively.

The results show a better fitting of the model results to measured water levels in the south-eastern part of Matokitoki in comparison to the calibration models, along with an overestimation of the hydraulic potential in the northern part of the Matokitoki. At the same time, also water levels in the Makauri aquifer are overestimated. The simulated lateral inflow is in a range between 1653.8 m³/d and 2197.6 m³/d, which is about 27-36 times the abstraction amount (60.9 m³/d) of GPB175, ref. Figure 4-41 or Figure 4-42. The total take amount of the steady state simulations is 2,057 m³/d, ref. Table 4-6.

Table 4-13: Statistics and water balance error of the state steady calibration and additional simulations for the Matokitoki aquifer.

Parameter		1st-BC along the south-eastern border of Matokitoki aquifer		
		Steady State Calibration SSC	1st-kind BC MTKA (11 mRL)	1st-kind BC MTKA (10 mRL)
Simulation				
Residual Mean (m)	0.08	0.77	0.63	
Absolute Residual Mean (m)	0.99	1.02	0.94	
Residual Standard Deviation (m)	1.52	1.19	1.17	
Sum of Squares (m ²)	181	158	139	
Root Mean Square (RMS) Error (m)	1.52	1.41	1.32	
Minimum Residual (m)	-5.72	-2.71	-2.79	
Maximum Residual (m)	4.33	4.87	4.73	
Number of Measures (-)	79	79	79	
Range in Measures (m)	33.39	33.39	33.39	
Scaled Residual Std. Deviation	4.6%	3.6%	3.5%	
Scaled Absolute Residual Mean	3.0%	3.1%	2.8%	
Scaled RMS Error	4.5%	4.2%	4.0%	
Scaled Residual Mean	0.3%	2.3%	1.9%	
Water balance error	< 0.01%	-0.29%	-0.01%	
Simulated inflow by the 1st-kind BC into MTKA		2197.6 (m³/d)	1653.8 (m³/d)	

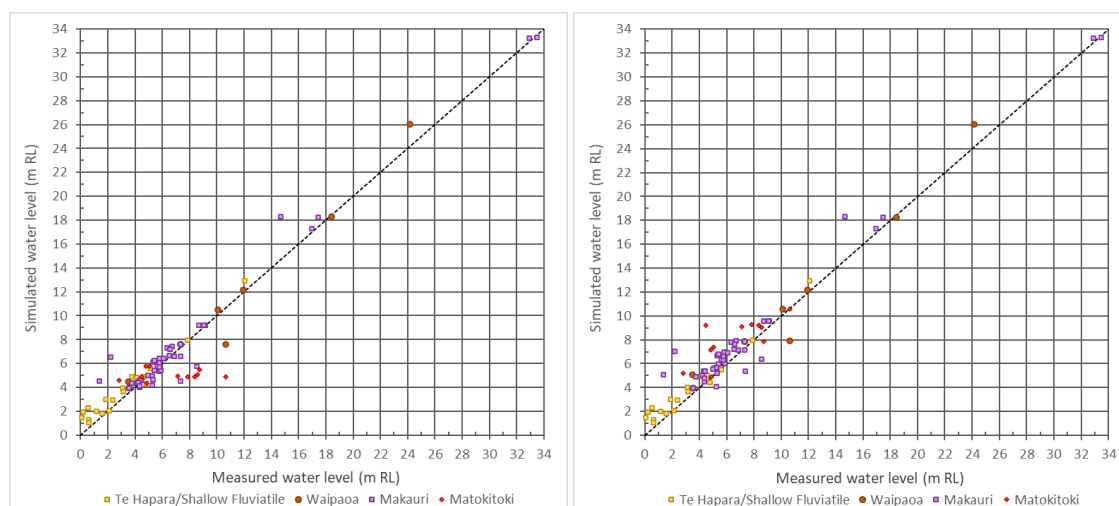


Figure 4-39: Scatter plot of simulated vs measured water levels, SSC (left), 1st-BC MTKA 11 mRL.

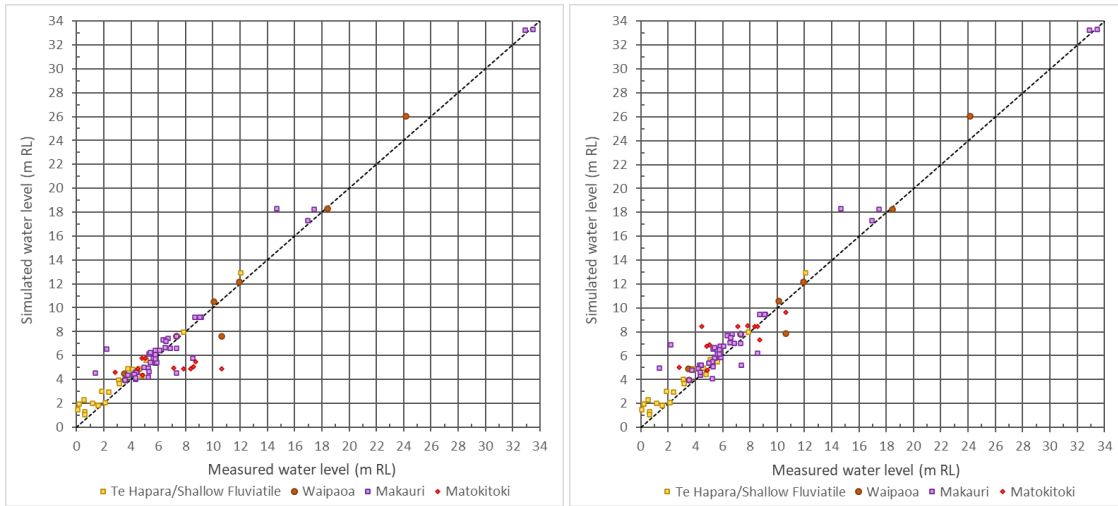


Figure 4-40: Scatter plot of simulated vs measured water levels, SSC (left), 1st-BC MTKA 10 mRL.

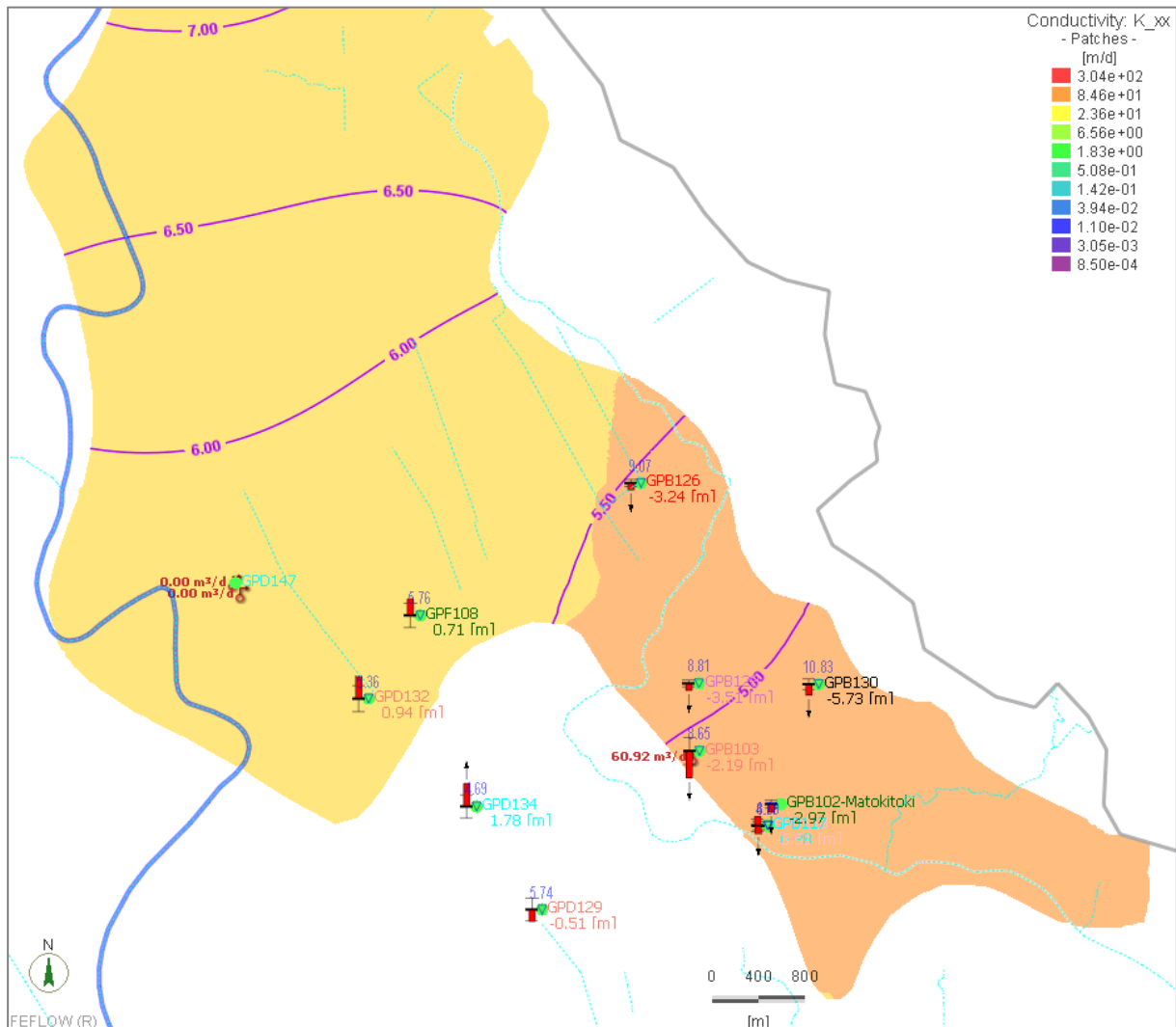


Figure 4-41: Simulated groundwater levels of the Matokitoki aquifer, Steady state calibration SCC.

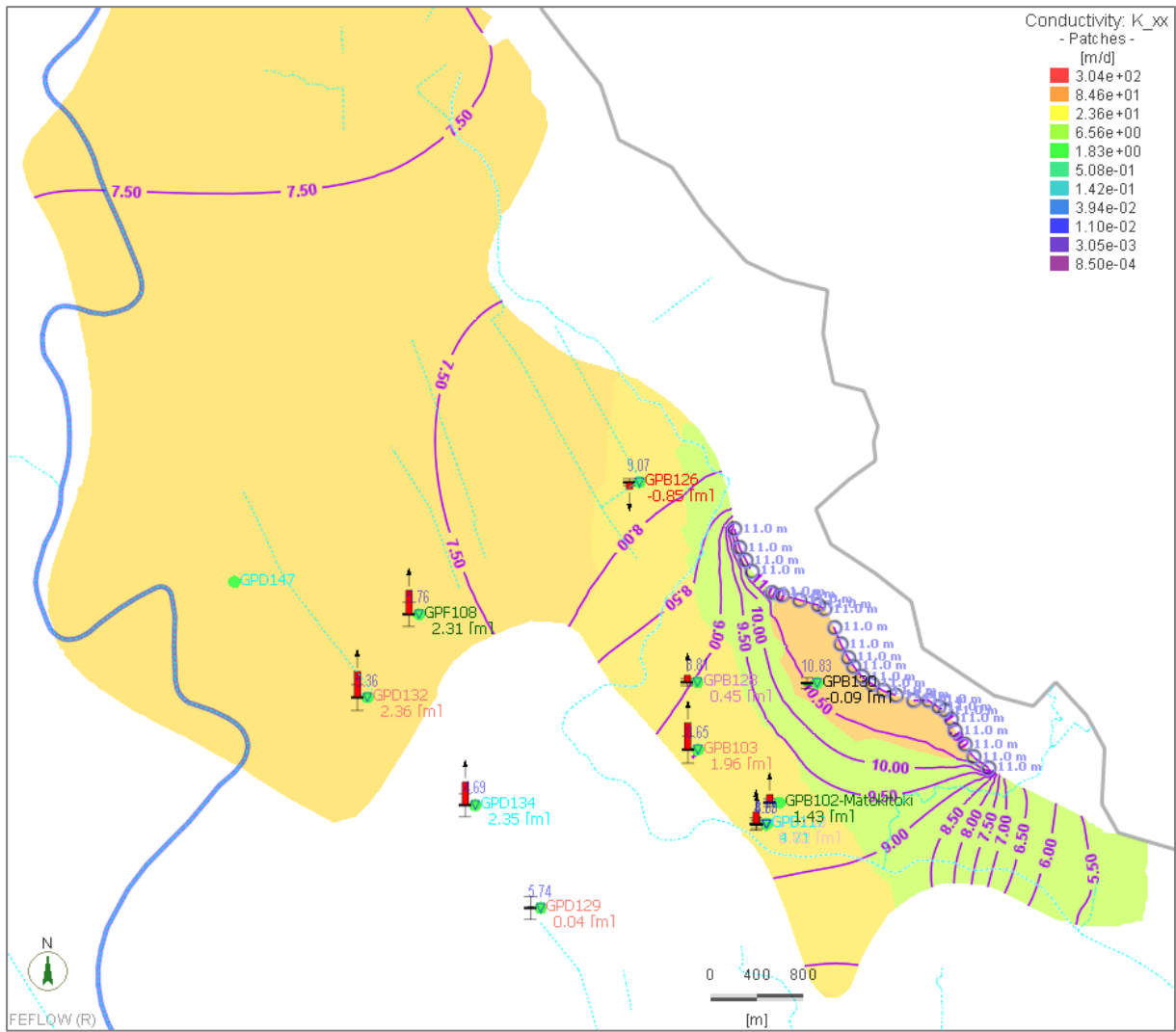


Figure 4-42: Simulated groundwater levels of the Matokitoki aquifer, Simulation with the 1st-BC of 11 mRL.

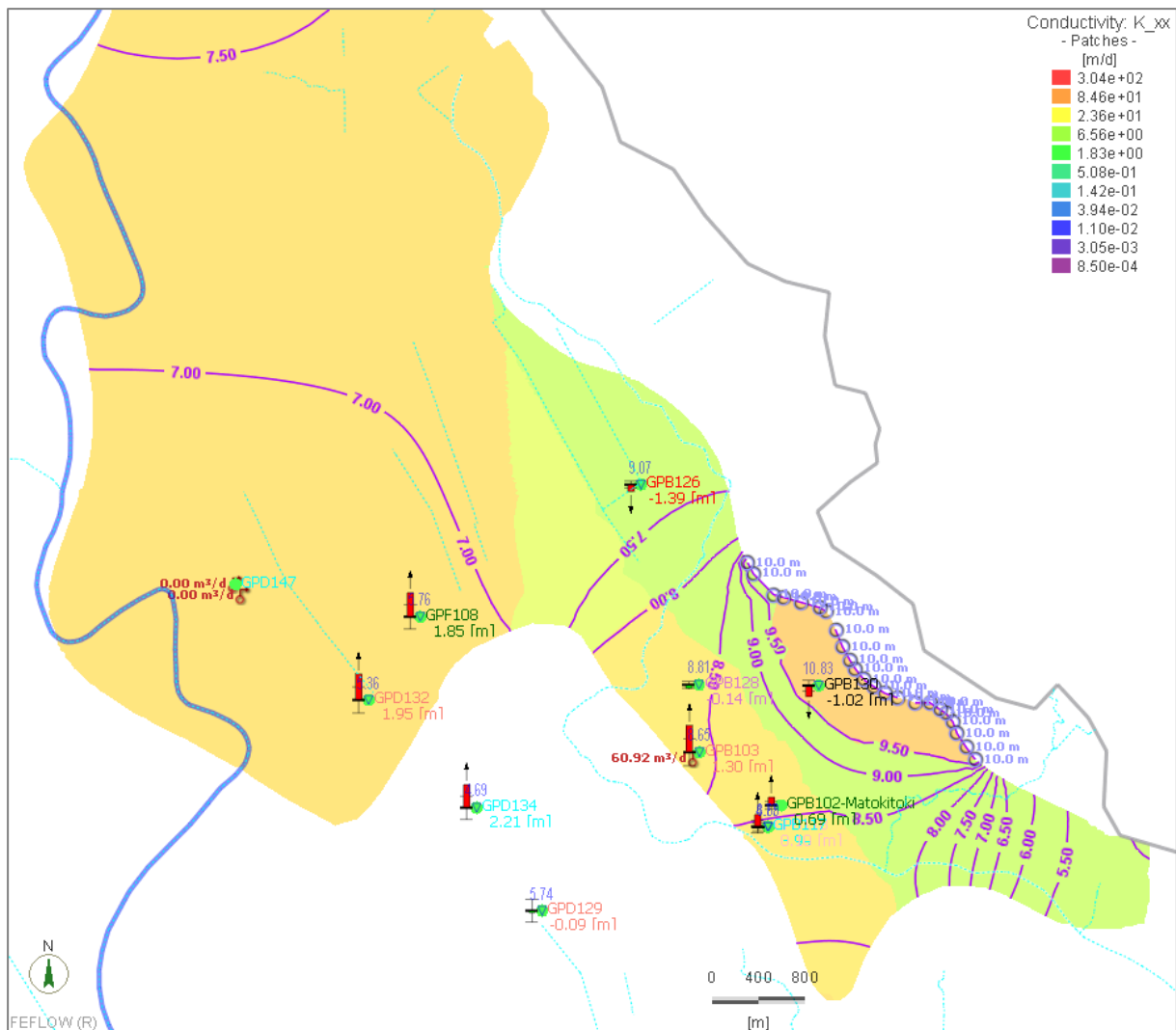


Figure 4-43: Simulated groundwater levels of the Matokitoki aquifer, Steady state simulation with the 1st-BC of 10 mRL.

4.8.3. Results of the transient simulation

In transient – as in the steady-state simulations - hydraulic potential at the observation bores in the south-eastern Matokitoki aquifer is lifted to higher levels by considering a fixed hydraulic head at the boundaries. At the same time, also the response to abstraction from the Matokitoki aquifer at the observation bores in the southeast is closer to the observed behaviour. This points towards an inflow of some sort, though it cannot be placed and quantified on basis of the model results only. The overestimation of water levels towards the northwest points – as in the steady state simulations – towards a hydraulic barrier of some sort that separates the south eastern part of the Matokitoki.

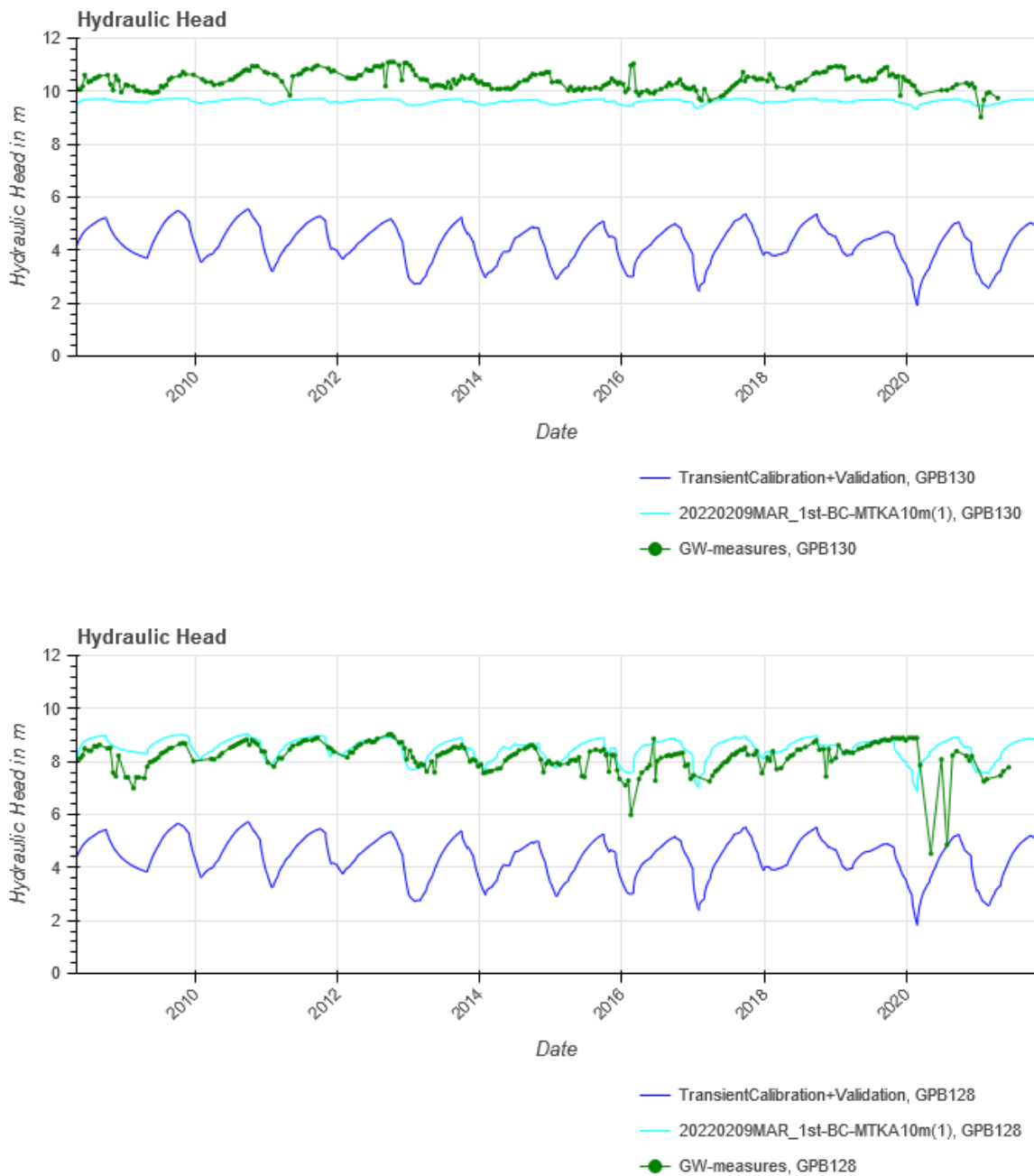


Figure 4-44: Simulated vs measured water levels in Matokitoki aquifer bores GBP130 and GBP128, transient calibration+validation and transient simulation with 1st-kind BC 10 mRL.

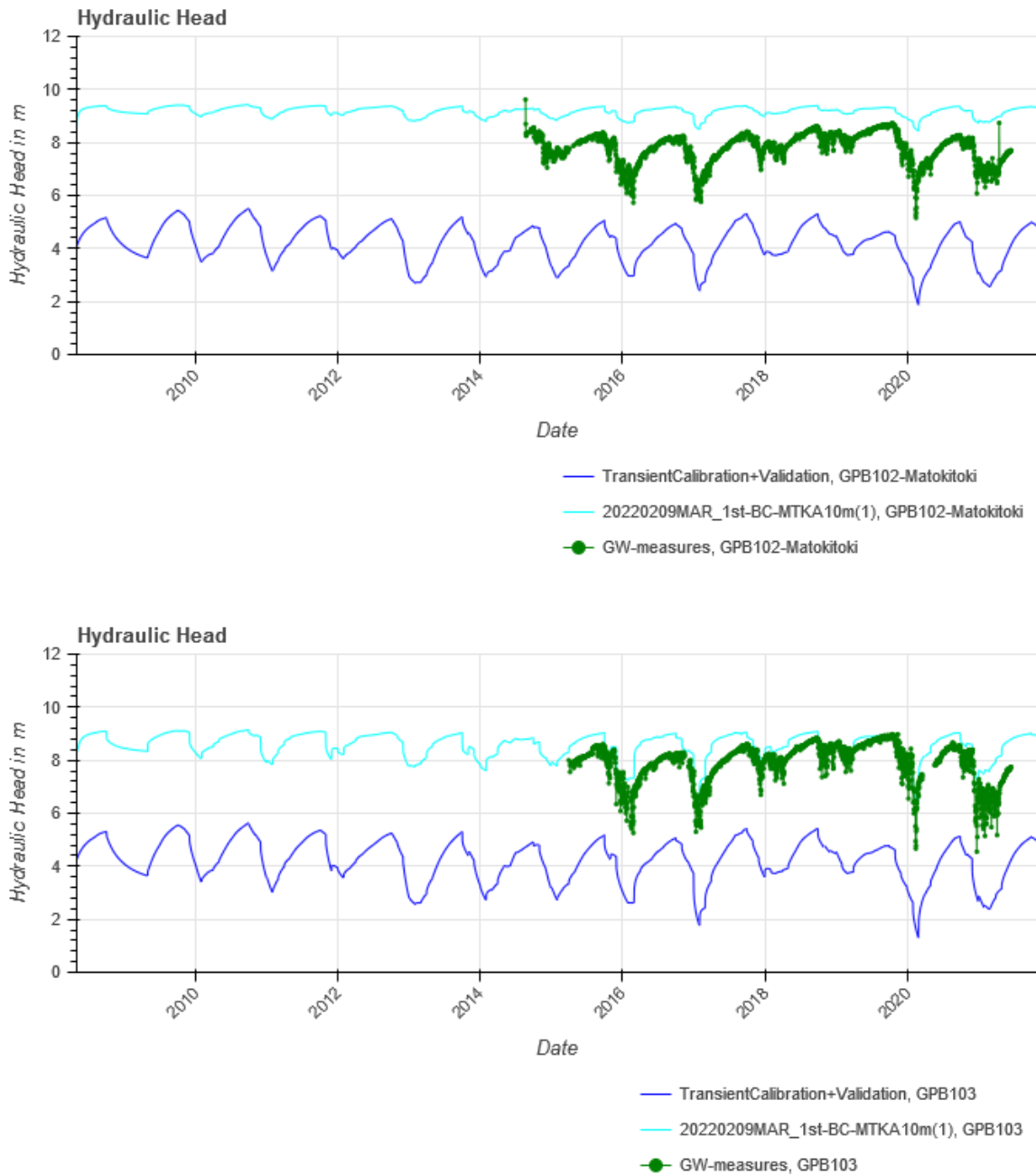


Figure 4-45: Simulated vs measured water levels in Matokitoki aquifer bores GBP102 and GBP103, transient calibration+validation and transient simulation with 1st-kind BC 10 mRL.

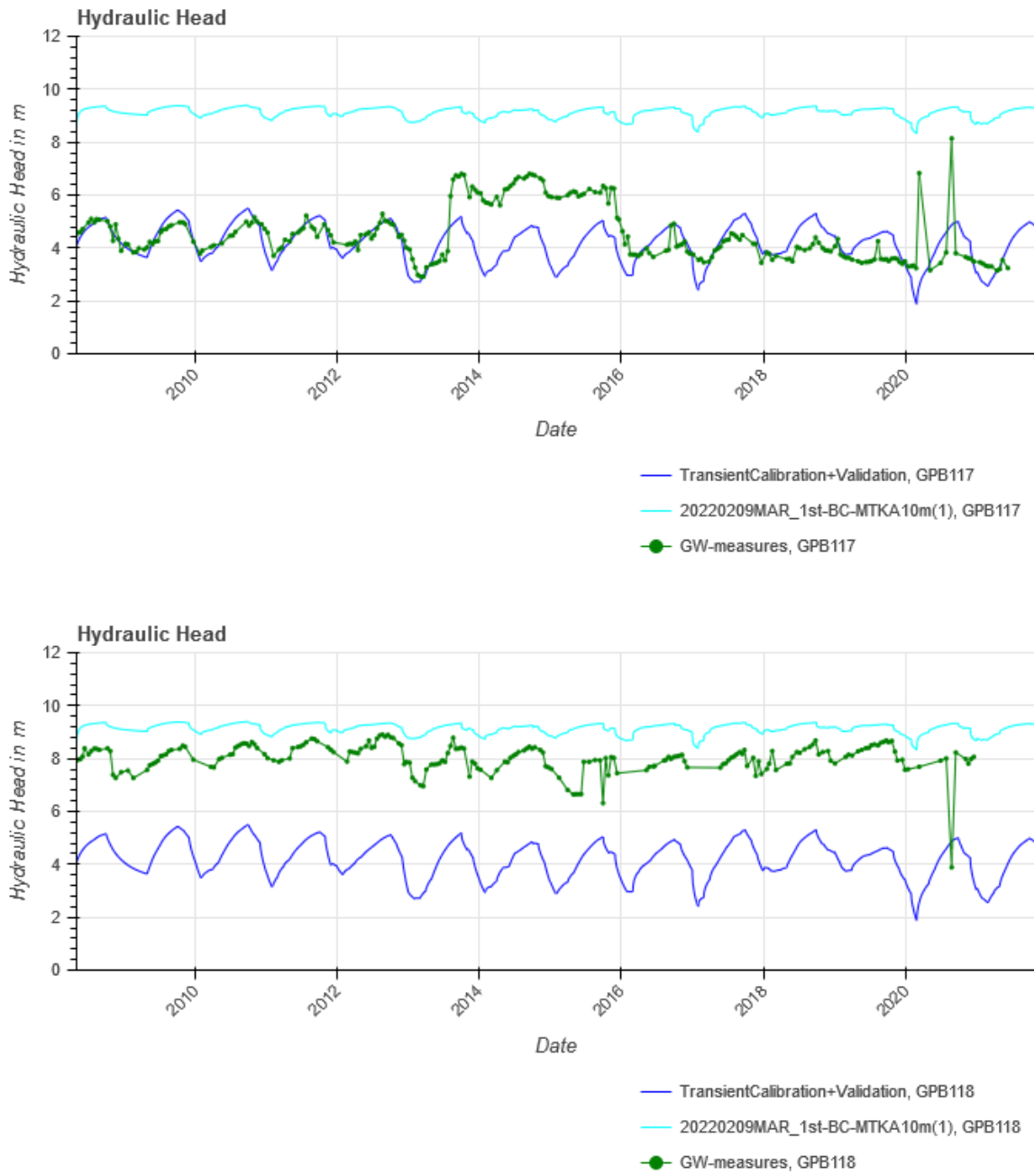


Figure 4-46: Simulated vs measured water levels in Matokitoki aquifer bores GBP117 and GBP118, transient calibration+validation and transient simulation with 1st-kind BC 10 mRL.

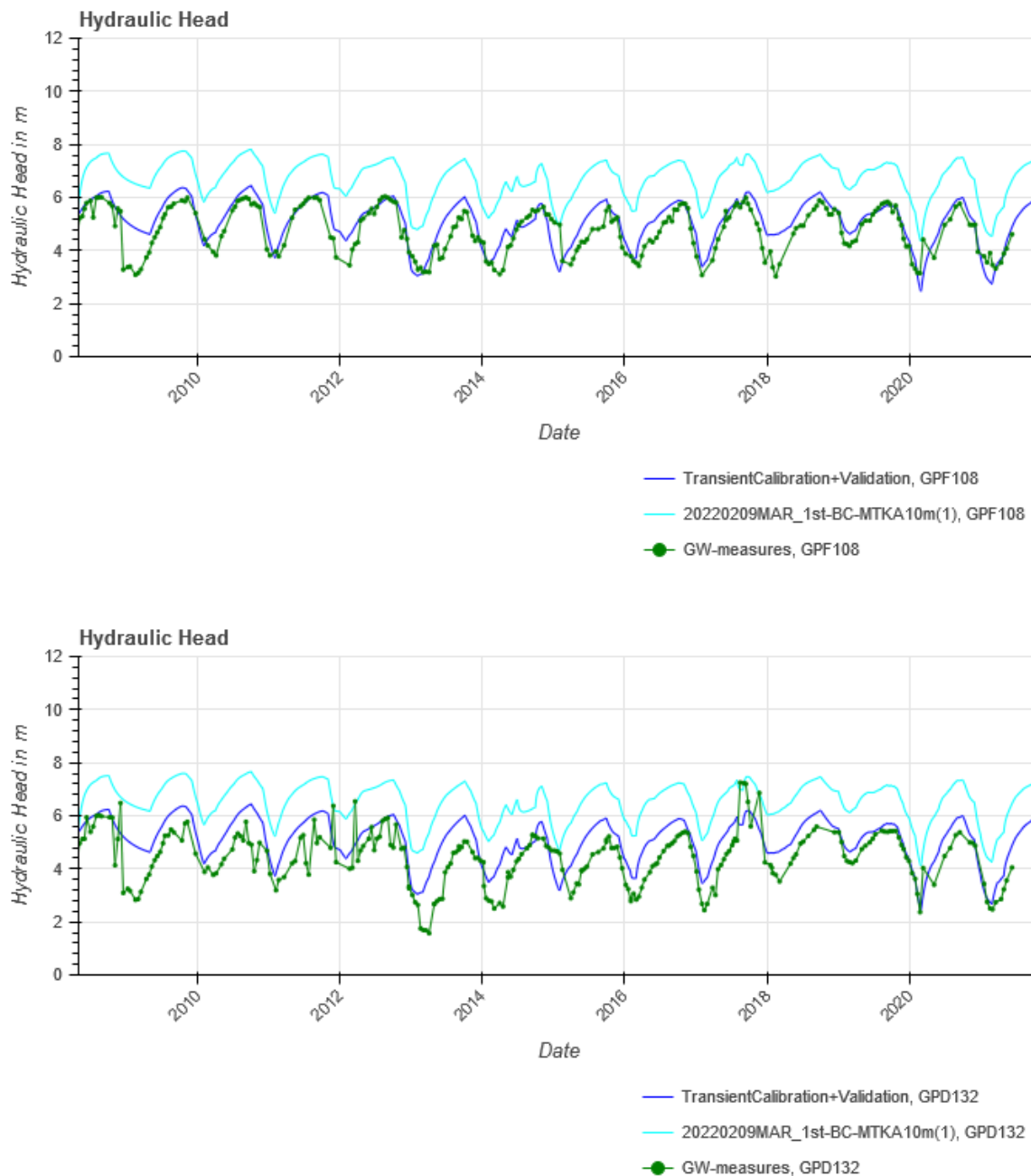


Figure 4-47: Simulated vs measured water levels in Matokitoki aquifer bores GPF108 and GPD132, transient calibration+validation and transient simulation with 1st-kind BC 10 mRL.

4.8.4. Evaluation of the results

Considering the results of the steady state and transient simulations with lateral inflow into the Matokitoki aquifer, it can be stated that applying the fixed water level as a boundary condition alone does not lead to a satisfactory match of the observed conditions. On the one hand, levels further northwest in the aquifer are overestimated, and water levels in the Makauri aquifer are overestimated. Changing hydraulic properties to further improve the residuals (e. g., by adding a low-permeable barrier within the Matokitoki and lowering the hydraulic conductivity in the aquitard separating the Matokitoki and Makauri aquifers) is not considered as an improvement to the model as such changes would move the parameterization away from justifiable parameters, only based on a very simplified and uncertain model property itself (the

boundary inflow). The boundary inflow – if real – is to come from further away with a longer underground passage that is per se unknown. A fixed-head condition has to overestimate the potential inflow and groundwater ability under more stress by far, even if the water levels match the observed ones. For predictive model runs looking for the effect of groundwater abstraction, a conservative approach without any boundary inflow is on the safe side and thus used.

4.9. Summary of Calibration, validation and verification of the 3D groundwater model

The generally very good match of observed and simulated hydraulic head in the steady-state calibration suggests a high level of confidence in the general flow conditions in the multi-aquifer system of the Poverty Bay Flats, except for the not fully known processes in the southeastern part of the Matokitoki aquifer. A specific focus in the assessment of the results needs to be on the vertical differences between the aquifers, as these – more than absolute levels - determine the vertical recharge of the deeper aquifers and the discharge back up into the shallow aquifer systems. The match of the vertical differences is excellent.

Main goal of the transient calibration, plus additional validation period, is to calibrate river-bed conductance and storage parameters (porosity, specific storage). Major stresses with strong temporal variation allowing this calibration are rainfall recharge, river water levels, and – foremost – abstraction from water wells. Figure 4-48 shows the good match between model results and observations for an observation close to Waipaoa River in the Shallow Fluvial Deposits, Figure 4-49 another one in the main abstraction area in the Makauri aquifer.

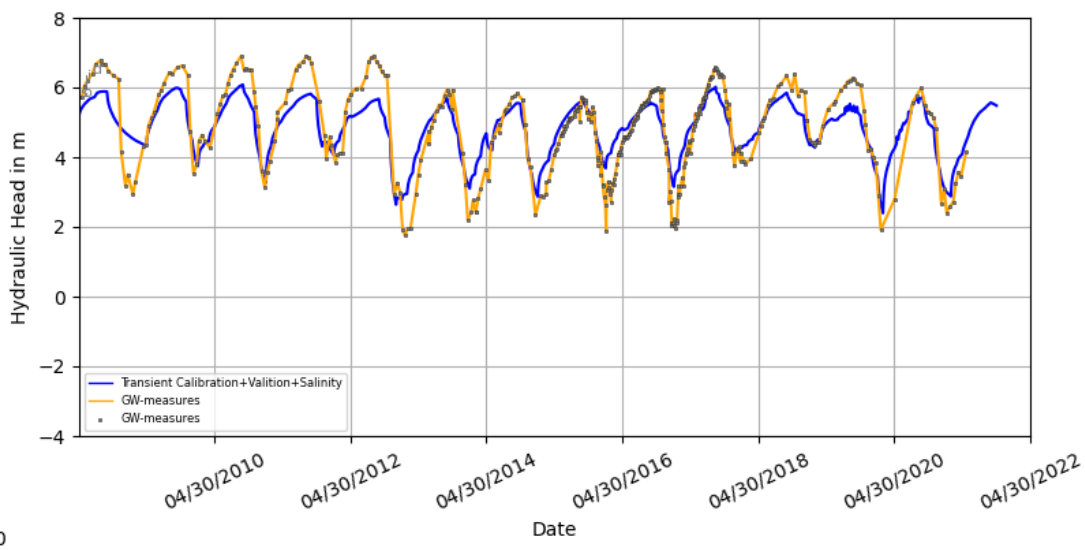


Figure 4-48: Simulated vs measured water levels of bore GPJ040 in the Shallow Fluvial aquifer.

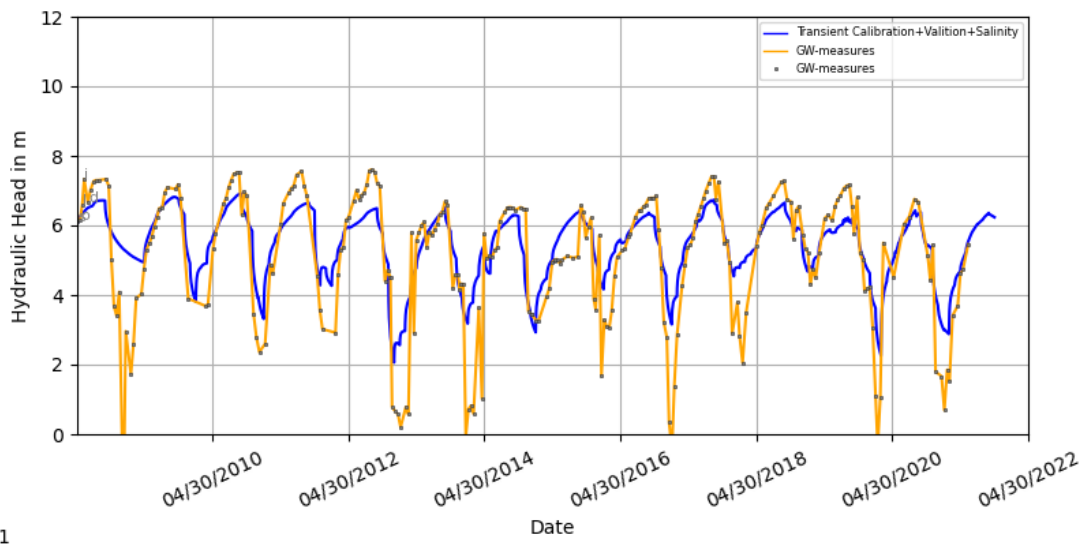


Figure 4-49: Simulated vs measured water levels of bore GPF071 in the Makauri aquifer.

The validation period gives on the one hand a temporally extended set of data to compare to, on the other hand, especially the year 2019 was an exceptionally dry year, providing a period of additional stress to the system that was not contained in the calibration period. Though locally at single observation bores the deviation in the validation period is larger, overall, the match between observation data and simulation results is even better in the validation period than in the calibration period. So, the model is able to also perform well under dry conditions. Within the validation period, the MAR trial infiltration of water during the years from 2017 to 2019 formed an additional stress to the model. The observation data during injection are closely matched.

As the flow processes, especially between the shallow aquifers and the deeper ones, are fairly slow, both steady-state (assuming unlimited time) and transient (covering a relatively short period compared to time needed for groundwater to pass the aquitards) calibration might not be able to catch the temporal scale of the aquitard passage and such the long-term recharge to the lower aquifers correctly. Thus groundwater-age simulation has been performed (in steady state) and the results have been compared to the available results of groundwater-age analyses. The overall match is very good, indicating that also the more long-term processes are represented well in the model.

The separate transport simulation for the MAR trial period confirmed the assumptions for mass-transport dispersivity and porosity as a basis for later transport (salinity simulation).

A test run with evapotranspiration in areas with low depth to groundwater shows that calibration results in those areas may be improved by additionally considering ET. This is taken as a hint for potential future model improvement (calculating groundwater recharge by using a soil-water balance model). Additional ET is not actually implemented, as a number of other influencing factors on water levels in the shallow aquifers is not currently considered (such as transient drain levels, tidal operation of shutters, local drains, etc.), and ET would have to be seen in correspondence with these additional factors that can only be covered by separate recharge modelling.

4.10. Overview of regional groundwater flow processes and remaining uncertainties

As stated in chapter 4.9, the calibrated flow model for the Poverty Bay Flats matches the groundwater level observations as well as additional data, such as groundwater age and observed salinity levels after MAR trial infiltration very well, and sensitivity analysis only leaves minor room for different parameterisation. On this basis, it can be assumed that the underlying flow processes in the catchment are described well by the model, and it seems worthwhile to summarize the flow process as well as the uncertainties that remain. As steady-state calibration has been carried out for a close-to-natural state with respect to groundwater takes (only minor abstraction from the system), the natural state can be distinguished from the influence of groundwater pumping. We are hereby not considering a natural state before drainages, changes to the rivers system, etc. have been put in place, as this is not in the scope of the model.

Natural flow system

Predominant natural groundwater flow in the catchment is north-south in all aquifers except the Matokitoki that shows a different gradient in its south-eastern part. Recharge to the aquifers predominates in the northern part, while the southern part closer to the coastline is characterized by groundwater discharge towards the rivers and drains. Discharge to the sea occurs from the shallow aquifers, the deeper aquifers are assumed to be connected to the sea via the confining units, some discharge occurs here. There is no clear indication from model calibration towards a direct connection of the deeper aquifers to the sea, observed heads could be reasonably matched without such a pathway.

In the vertical between the different aquifers, in general there is downward flow (recharge to the deeper aquifers) in the north and upward flow (discharge from the deeper to the shallower aquifers) in the southern part. This is illustrated by showing to example locations in Figure 4-50. Recharge and discharge depend on the vertical gradient in hydraulic head (difference in head / length of passage through the aquifer).

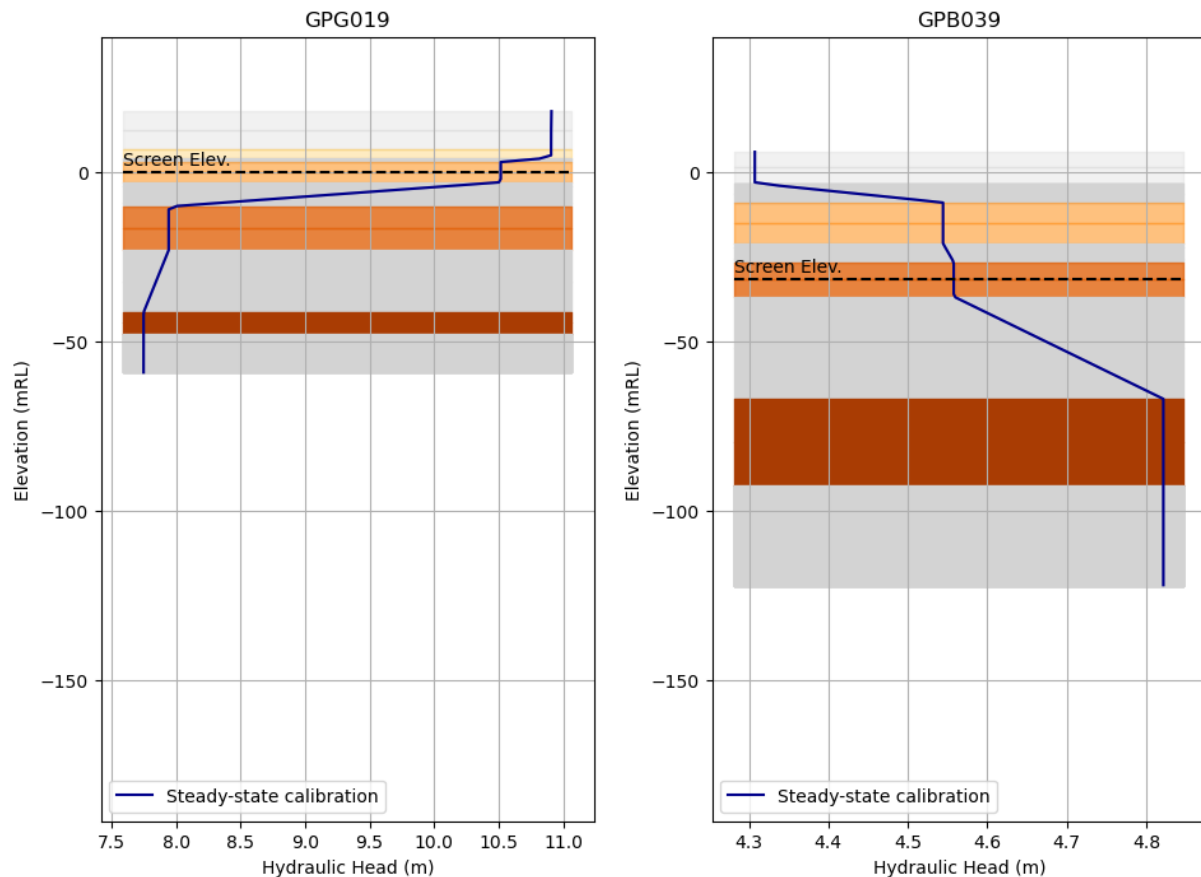


Figure 4-50: Simulated hydraulic head over depth in the northern (GPG019) and southern (GPB039) parts of the model.

Calibration both in steady state and in transient shows a very good agreement between model results and observations with respect to the vertical differences in hydraulic head between the different aquifers. This suggests a high level of confidence in the depiction of the general flow system in the model. Sensitivity analysis for the hydraulic conductivity of the aquitards, however, shows some uncertainty in the parameter, allowing for potentially somewhat lower values.

In general, especially in steady-state calibration, it is difficult to validate recharge from rainfall, as increased rainfall recharge could be balanced by increased hydraulic conductivity and vice versa. In transient calibration, increased rainfall recharge could be balanced by higher storage and/or modified riverbed conductance. Should a higher level of confidence on the detailed processes in the shallow aquifers be desired in the future, it is recommended to calibrate the system using river and drain discharges in addition, and potentially underpinning reliability of groundwater recharge data by performing detailed soil-water balance modelling. With respect to calibration for discharges, it is recommended to measure low-flow discharges to obtain only baseflow. As the main focus during calibration here was on the deeper aquifers, though, the main target for the shallow aquifers was to match hydraulic head to observations, as the groundwater level controls the water exchange between shallow and deep aquifers and thus is of major importance for the behaviour of the deep aquifers.

Major limitations on depicting the natural flow system in the model are related to the knowledge of the spatial and temporal distribution of groundwater recharge, the level of detail of the surface water system, such as neglecting smaller drains, neglecting varying water levels and active/passive operation (tidal shutters) of drains as well as an unknown hydrogeological situation in the south-eastern part of the Matokitoki.

Influence of water abstraction

In transient calibration, there is a very close match of model results and observations with respect to the effects of seasonal abstraction stress, including longer-term variations of abstractions, on the groundwater flow system. Based on this, the model reactions on changes in abstractions are expected to be highly reliable.

Water abstraction from the shallow aquifers lowers the hydraulic potential in these, thus lowering the discharge of groundwater to streams and drains. In the northern part of the Poverty Bay Flats, a lower water table in the shallow aquifers leads to somewhat reduced infiltration to the deeper aquifers (because of a lower vertical gradient), while in the southern part it results in a somewhat increased discharge from the deeper into the shallow aquifers. Abstraction from the deep aquifers lowers the hydraulic potential in these, hereby increasing the infiltration from the upper aquifers into the deeper ones in the north (Figure 4-51) and decreasing discharge from the lower to the upper aquifers in the south (Figure 4-52). It may also happen that the gradient is reversed, i. e., an upward gradient is turned into a downward gradient by deep abstraction (Figure 4-53). As the deeper aquifers are confined and therefore have a much lower storage capacity than the unconfined shallow aquifers, a comparable pumping rate changes hydraulic head by a much larger degree in the deep aquifers compared to the shallow ones. Consequently, abstraction from the deep aquifers changes the vertical flow (recharge to and discharge from deeper aquifers) much more than abstraction from the shallow aquifers.

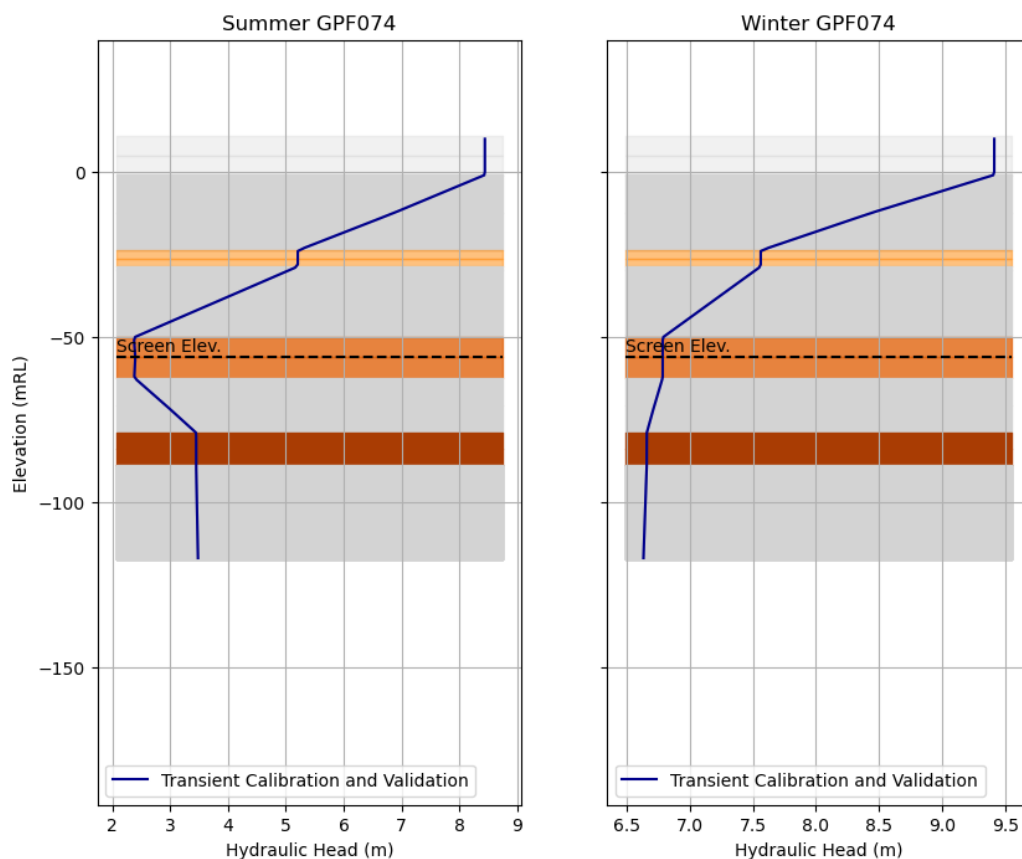


Figure 4-51: Influence of groundwater abstraction: Increased downward gradient in summer caused by abstraction at GPF074.

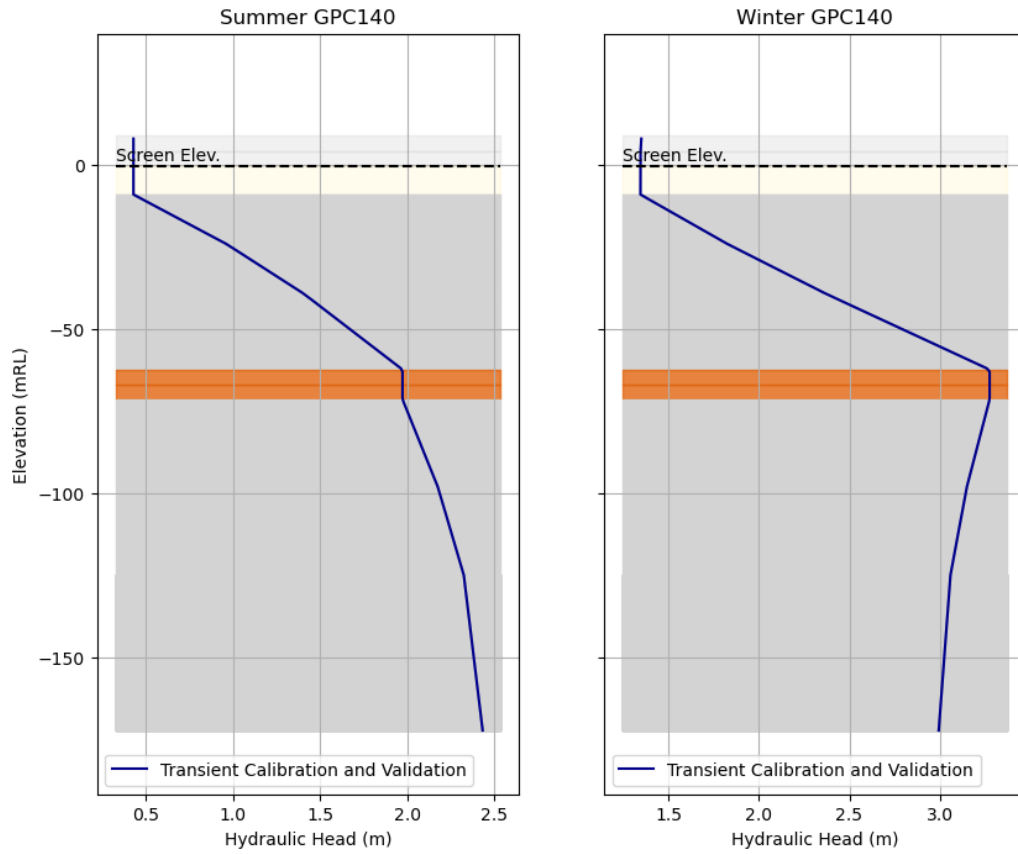


Figure 4-52: Influence of groundwater abstraction: Decreased upward gradient in summer caused by abstraction at GPC140.

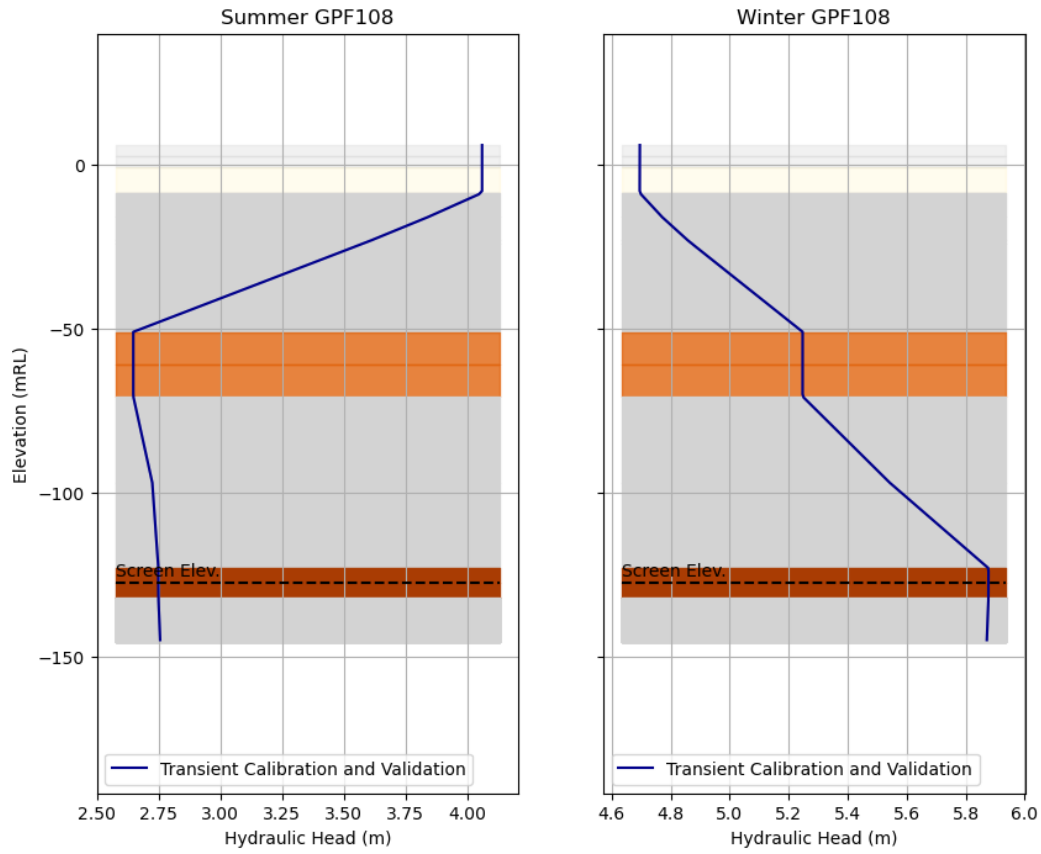


Figure 4-53: Influence of groundwater abstraction: Reversed gradient between summer and winter caused by abstraction at GPF108.

5. Scenario Simulations – Groundwater Flow

The scenario runs are intended to show the expected influence of climate change on the Poverty Bay Flats Groundwater system, as well as the influence of different management options to go against those effects. During project execution and based on the outcome of close interaction between GDC, iwi stakeholders, WGA and AQUASOIL, first one set of scenarios was defined, and the simulations carried out (Scenarios 1-9). Later in the process and based on the results of the first round, a redefinition was decided, and a second set of scenarios 1.1-7.1 was set up and calculated. This chapter contains a description of parameterization, model setup and results for the second set of scenarios, the legacy first set is contained in Appendix 3:

Table 5-1 gives an overview of the 6 scenario definitions for a transient simulation period from July 2021 to June 2090, along with their specifications for water level and quantity modelling, performed with the calibrated and validated 3D groundwater model Poverty Bay Flats.

Table 5-1: Simplified overview of Scenarios and their specifications

Scenario	Basis	Takes	Recharge	River Levels	MAR
#1.1 Baseline (B)	B	B	2017/18	2017/18	-
#2.1 Baseline + Climate Change (B+CC)	B+CC	Stepwise Increase Takes incl.3*3Y-draughts > B	-5% in 2040 -15% in Sept. 2040 - 2090 (RCP4.5)	B + Sea _{RCP4.5}	-
#3.1 Natural State	B+CC	-	B+CC	B+ Sea _{RCP4.5}	-
#4.1 Paper Allocation Current Allocation Limit	B+CC	Stepwise Increase Take Limit incl.3*3Y-draughts > #2.1	B+CC	B+ Sea _{RCP4.5}	-
#5.1 MAR (M1)	B+CC	Same as #2.1	B+CC	B+ Sea _{RCP4.5}	6 MAR bores, Stepwise Increase MAR rate
#7.1 Sustainable Allocation	B+CC	85% of #2.1	B+CC	B+ Sea _{RCP4.5}	-

Accordingly, Scenario 1.1 considers current seasonal metered usage of 1,188,000 m³/year and the average rainfall recharge of the hydrological year 2017/2018. It represents the Baseline (B) without adapting parameters to account for climate change, sea level rise and MAR, see chapter 5.1.

Scenario 2.1 Baseline + Climate Change (B+CC) differs to scenario 1.1 by

- considering a decrease in rainfall recharge due to climate change and a rise of the sea level according to the climate scenario RCP4.5 [21],
- using current seasonal metered usage of 1,188,000 m³/year as the basis for time-variable pumping rates as follows
 - 1,188,000 m³/year till 2029
 - stepwise increase: 5% from 2030, 15% from 2045, 24% from 2060, 33% from 2075 till 2090
 - increased pumping rates in three 3-year draught periods 2035/2036 - 2037/2038, 2050/2051 - 2052/2056 and 2070/2071 - 2072/2073, see chapter. 5.2.

The stepwise increase of abstraction is meant to balance the expected increase in PED [21] in horticulture and agriculture that will lead to an additional irrigation demand.

The same parameters for climate change and sea level rise mentioned above are used for scenario 3.1, scenario 4.1, scenario 5.1 and Scenario 7.1 which all reflect management options based on the

assumption of climate change happening as considered in scenario 2.1.

Scenario 3.1 considers no pumping from groundwater at all and therefore corresponds to a natural state with respect to abstraction. The scenario is carried out under the assumed climate change conditions without any groundwater takes, see chapter 5.3

Scenario 4.1 differs to scenario 2.1 only by using the current allocation limit of 3,980,908 m³/year rather than actual groundwater pumping as the basis for time-variable abstraction amounts specified as follows

- 3,980,908 m³/year till 2029
- stepwise increase: 5% from 2030, 15% from 2045, 24% from 2060 and 33% from 2075 till 2090
- increased pumping rates in three 3-year draught periods 2035/2036 - 2037/2038, 2050/2051 - 2052/2056 and 2070/2071 - 2072/2073, see chapter 5.4.

Scenario 5.1 differs to scenario 2.1 only by additionally considering a stepwise increasing groundwater replenishment (MAR), balancing the stepwise increases in abstraction, see chapter 0.

Scenario 7.1 differs to scenario 2.1 only by a reduction in abstraction to 85% of the ones in scenario 2.1, chapter 5.6. The reduction was chosen to achieve approximately constant groundwater levels/hydraulic heads in the aquifers in the future.

General parameterisation and technical approaches for scenario simulations can be outlined as follows:

- simulation period 1 July 2021 – 30 June 2090
- initial or start water levels = calculated groundwater levels on 30 June 2021 of the calibration und validation simulation 2008 - 2021
- river water levels of 2017/18 (average year) as the basis
- groundwater recharge of 2017/18 from the calibration und validation model for scenario 1.1 and as base for increasing rainfall recharge in scenarios considering climate change
- cyclic repetition of seasonal cycle:
 - seasonal cycle of 2017/18 for river water levels and groundwater recharge
 - seasonal cycle of 2020/21 for groundwater abstraction used as reference for distributing scenario abstraction over time and to the single water wells
 - adaptation of base values (stepwise increase) according to scenario
- extraction of seasonal time series from the calibration model for boundary conditions in FEFLOW by using a Python script
 - takes time period to be used as input
 - reduces time series to selected period and sets the time-series type to ‚cyclic‘
 - allows for different periods for wells and river boundary conditions
 - can deal with time series interpolated in between gauging stations on rivers
- groundwater recharge time series for climate change prepared manually
- additional well boundary condition for the 6 MAR bores

All scenarios use the river water levels of 2017/18 extracted from the calibration und validation model corresponding to the river/stream/drains boundary conditions.

Scenarios with climate change consider time variable parameters for

- the sea boundary condition with the sea level rise as shown in Table 5-2
- the specified decrease in rainfall recharge, i.e., the recharge of 2017/18 of scenario 1.1 modified by a linearly increasing decrease as follows

- 0% - 5% from 2021 to 2040 and remaining 5% thereafter, and additionally
- 5% - 15% decrease in September from 2040 to 2090.

Table 5-2: Sea level rise values considered in scenarios with climate change

Date	Sea level rise (m) of RCP45 [20]	
30.06.2020	0	0 = Calibration+Validation
30.06.2030	0.05	
30.06.2040	0.11	
30.06.2050	0.16	
30.06.2060	0.22	
30.06.2070	0.28	
30.06.2080	0.34	
30.06.2090	0.41	

The period of 1 July 2020 – 30 June 2021 (2020/21) is characterised by a total abstraction of 1,580,189 m³ from 79 active bores in the model area, that is the largest number of seasonal metered take sites throughout the period of data availability. Hence the seasonal cycles of the 2020/21 of the 79 takes are used as reference for distributing scenario abstraction onto monthly take amounts akin to those of 2020/21.

Table 5-3 shows the abstraction amounts of the period 2020/2021 and Scenario Baseline in Te Hapara Sands, Shallow Fluviatile, Waipaoa, Makauri and Matokitoki aquifers as well as in total. The last column represents ratios calculated for each of the aquifers by dividing $\text{Take}_{\text{Baseline}}$ by $\text{Take}_{2020/21}$ correspondingly. Multiplying the ratios to the seasonal cycles of the 2020/21 according to the aquifers (i.e., to take bores in aquifers) respectively, we get the take amounts of Scenario 1.1 converted into seasonal cycles akin to the one of the 2020/21 hydrological year.

Table 5-3: Overview of abstraction amounts of the period 2020/21 and scenario 1.1 (Baseline B)

Abstraction 2020-2021		Scenario Takes in Aquifer	Baseline B		Ratio $\frac{\text{Take}_{\text{Baseline}}}{\text{Takes}_{2020/21}}$
Amount m ³	Number		Amount m ³	Number	
152,175	21	Te Hapara Sands	103,000	21	68%
129,959	14	Shallow Fluviatile	107,000	14	82%
110,793	11	Waipaoa	69,000	11	62%
1,073,812	31	Makauri	847,000	31	79%
113,450	2	Matokitoki	62,000	2	55%
1,580,189	79	Total	1,188,000	79	

Table 5-4 shows the abstraction amounts of the 3-year draught periods 2012/13, 2013/14 and 2014/15 in Te Hapara Sands, Shallow Fluvial, Waipaoa, Makauri and Matokitoki aquifers as well as in total. The last row represents ratios calculated for each of the 3-year draught periods by dividing $Take_{Baseline}$ by $Take_{2012/13}$, $Take_{2013/14}$ and $Take_{2014/15}$ correspondingly. The ratios represent factors being used for increasing pumping amounts in the 1st, 2nd and 3rd draught year respectively.

Table 5-4: Overview of abstraction amounts of 3-year draught period 2012/13, 2013/14 and 2014/15.

Abstraction in Aquifer	Abstraction 2012-2013	Abstraction 2013-2014	Abstraction 2014-2015
Te Hapara Sands	133751	182143	175896
Shallow Fluviatile	99459	93990	97299
Waipaoa	119177	74518	54954
Makauri	1393273	1197537	1083453
Matokitoki	27873	52485	106216
Total	1,773,533	1,600,674	1,517,818
Number of takes	37	40	79
Ratio of total abstraction in each draught year to the one of Baseline	1.49	1.35	1.28

5.1. Scenario 1.1 Baseline (B)

5.1.1. Scenario Parameters

Scenario #1.1 considers current seasonal metered usage of 1,188,000 m³/year cycled yearly same for the whole simulation period 2021 - 2090. It represents the Baseline (B) with the current usage and without considering climate change, sea level rising and MAR.

5.1.2. Scenario Results

- A cyclic/dynamic steady state with equal seasonal variations is reached in the baseline scenario after about 25 years (depending on location in the model area)

5.2. Scenario 2.1 Baseline + Climate Change (B+CC)

Scenario 2.1 is used to calculate the effect of climate change on the groundwater system without any changes in groundwater management. Therefore, it can be used to compare to scenario 1.1 without considering climate change and to all scenarios including different future management options.

5.2.1. Scenario Parameters

Scenario 2.1 Baseline + Climate Change (B+CC) considers

- decrease in rainfall recharge due to climate change
- sea level rise according to the climate scenario RCP4.5
- time variable/increased abstraction specified as follows
 - 1,188,000 m³/year till 2029
 - stepwise increase: 5% from 2030, 15% from 2045, 24% from 2060, 33% from 2075 till 2090
 - increased abstraction in three 3-year draught periods 2035/2036 - 2037/2038, 2050/2051 - 2052/2056 and 2070/2071 - 2072/2073.

The stepwise increase of abstraction is meant to balance the expected increase in PED [21] in horticulture and agriculture that will lead to an additional irrigation demand.

Table 5-5 gives an overview on time variable abstraction amounts of scenario 2.1.

Table 5-5: Overview of abstraction amounts of scenario 2.1 Baseline + Climate Change (B+CC)

Stepwise increased abstraction incl. 3 3-year draught periods scenario 2.1	Increase against to the base abstraction	Hydrological Year	Abstraction amount m ³ /year
no increase till 2029	0	2021/22 - 2028/29	1,188,000
increase 5% from 2030	0.05	2029/30 – 2034/35	1,247,400
		2035/36	1,862,210
		2036/37	1,680,707
		2037/38	1,593,709
		2038/2039 – 2043/44	1,247,400
increase 15% from 2045	0.15	2044/2045 – 2049/50	1,366,200
		2050/51	2,199,181
		2051/52	1,984,835
		2052/53	1,882,094
		2053/54 – 2058/59	1,366,200
increase 24% from 2060	0.24	2059/60 – 2069/70	1,473,120
		2070/71	2,358,799
		2071/72	2,128,896
		2072/73	2,018,698
		2073/74	1,473,120
increase 33% from 2075 till 2090	0.33	2074/2075 – 2089/90	1,580,040

5.2.2. Scenario Results

Based on the reduced rainfall recharge and increased abstraction, groundwater levels are generally lower in this scenario compared to the baseline scenario. This is mostly visible in the aquifers with the largest amount of groundwater abstraction (especially Makauri), and in locations that are clearly influenced by groundwater recharge. An overview of statistical changes in between the different scenarios is shown in chapter 0.

Figure 5-1 through Figure 5-4 show the differences in hydraulic head between scenario 2.1 and scenario 1.1 at the end of the simulation period (year 2089), and therefore indicate the long-term change induced by climate change under the given assumptions. One plot is shown for each of the aquifers.

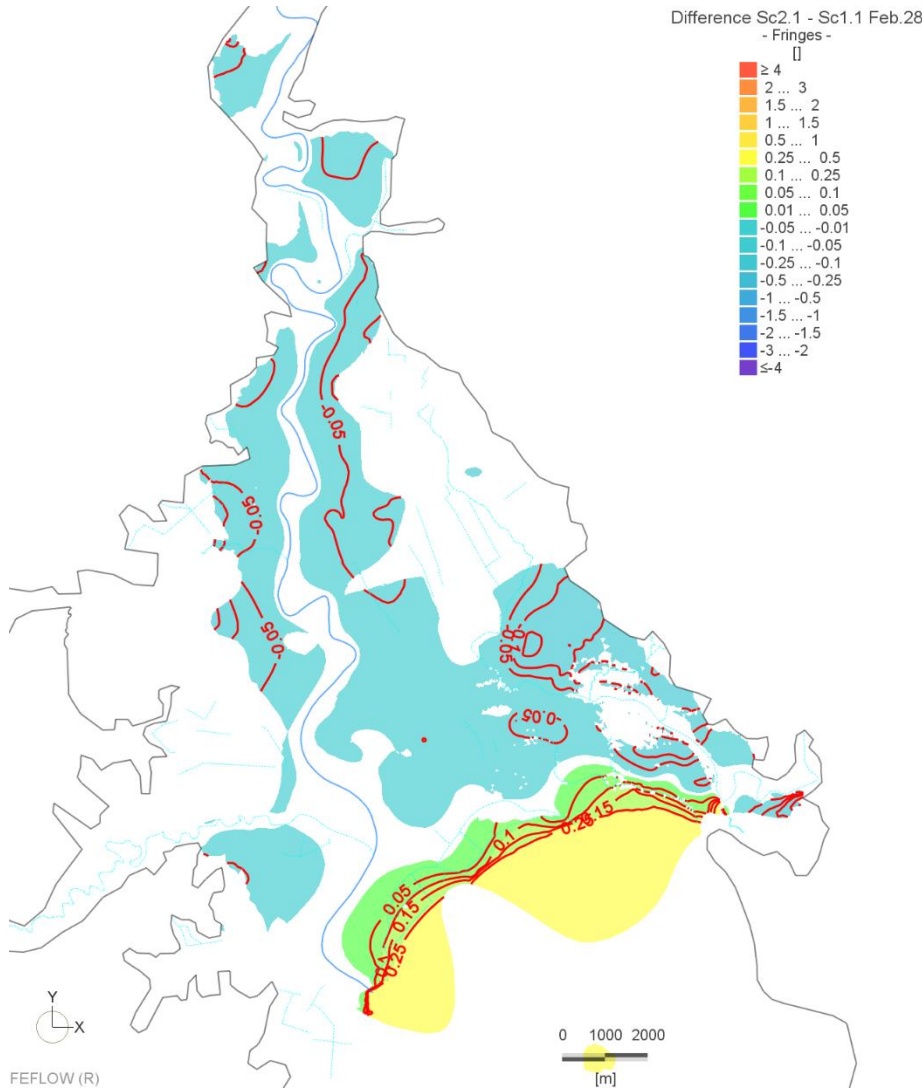


Figure 5-1: Difference of simulated groundwater level between scenario 2.1 and scenario 1.1 in the shallow aquifer system at the end of the simulation period (year 2089)

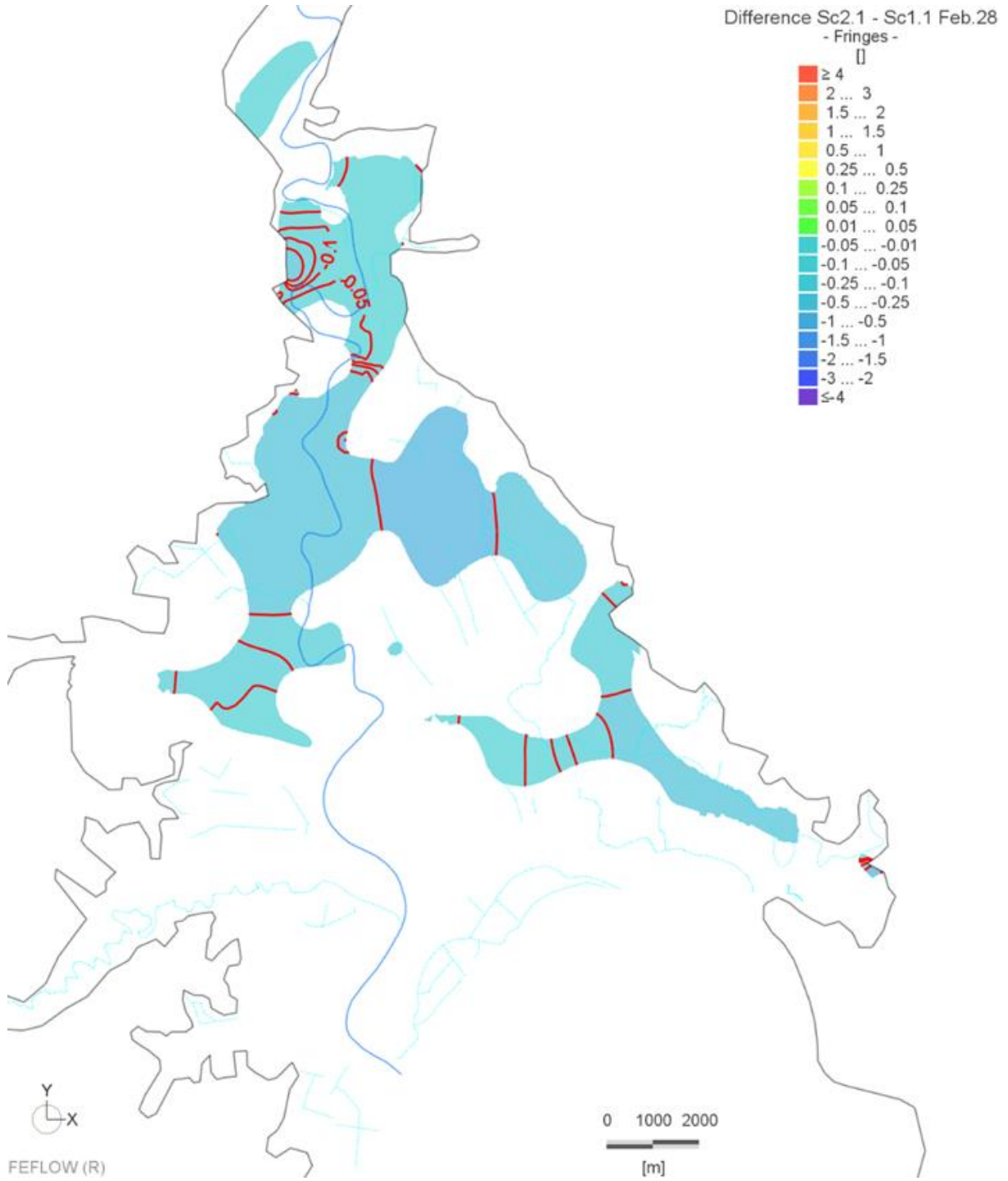


Figure 5-2: Difference of simulated groundwater level between scenario 2.1 and scenario 1.1 in the Waipaoa aquifer at the end of the simulation period (year 2089)

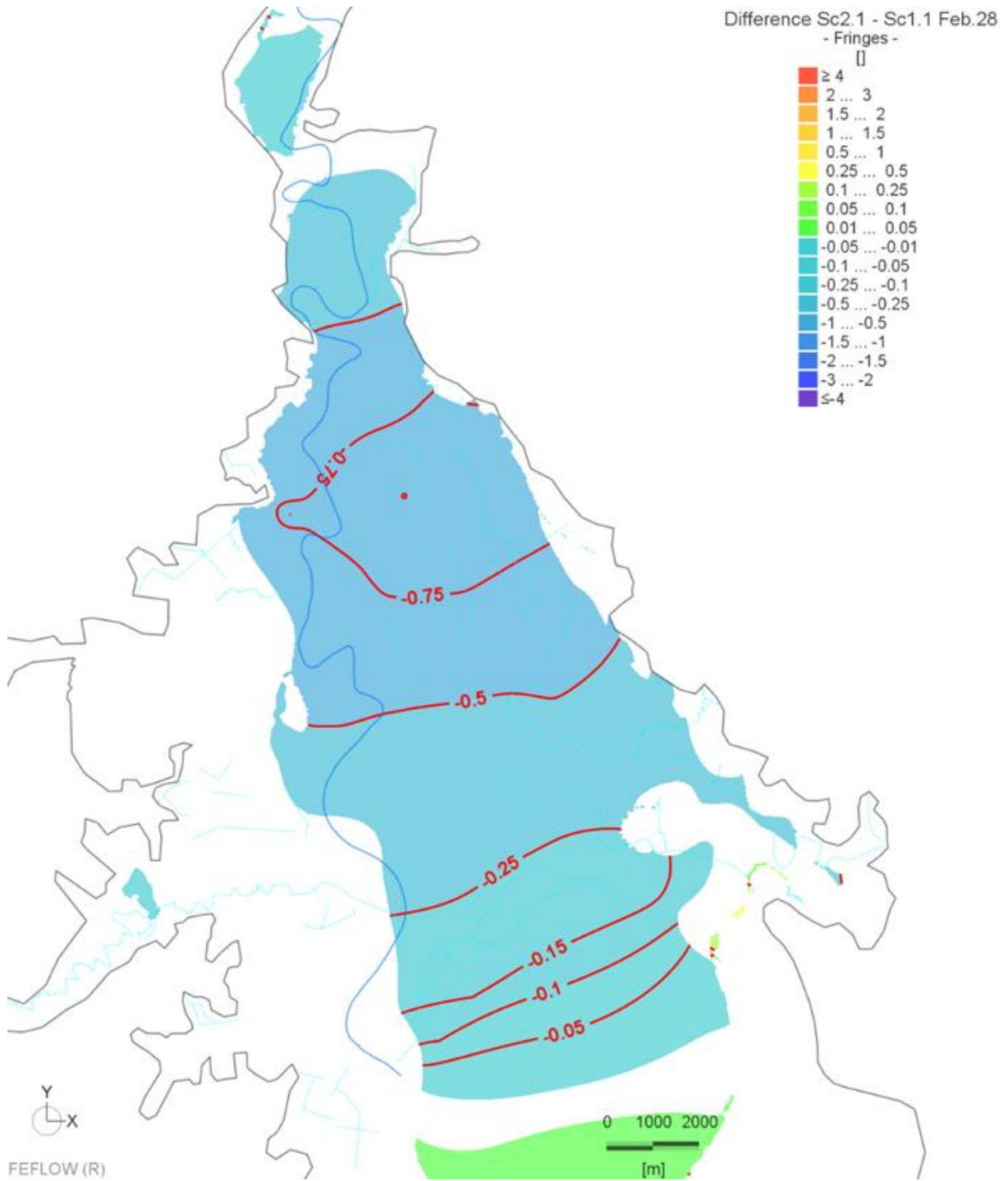


Figure 5-3: Difference of simulated groundwater level between scenario 2.1 and scenario 1.1 in the Makauri aquifer at the end of the simulation period (year 2089)

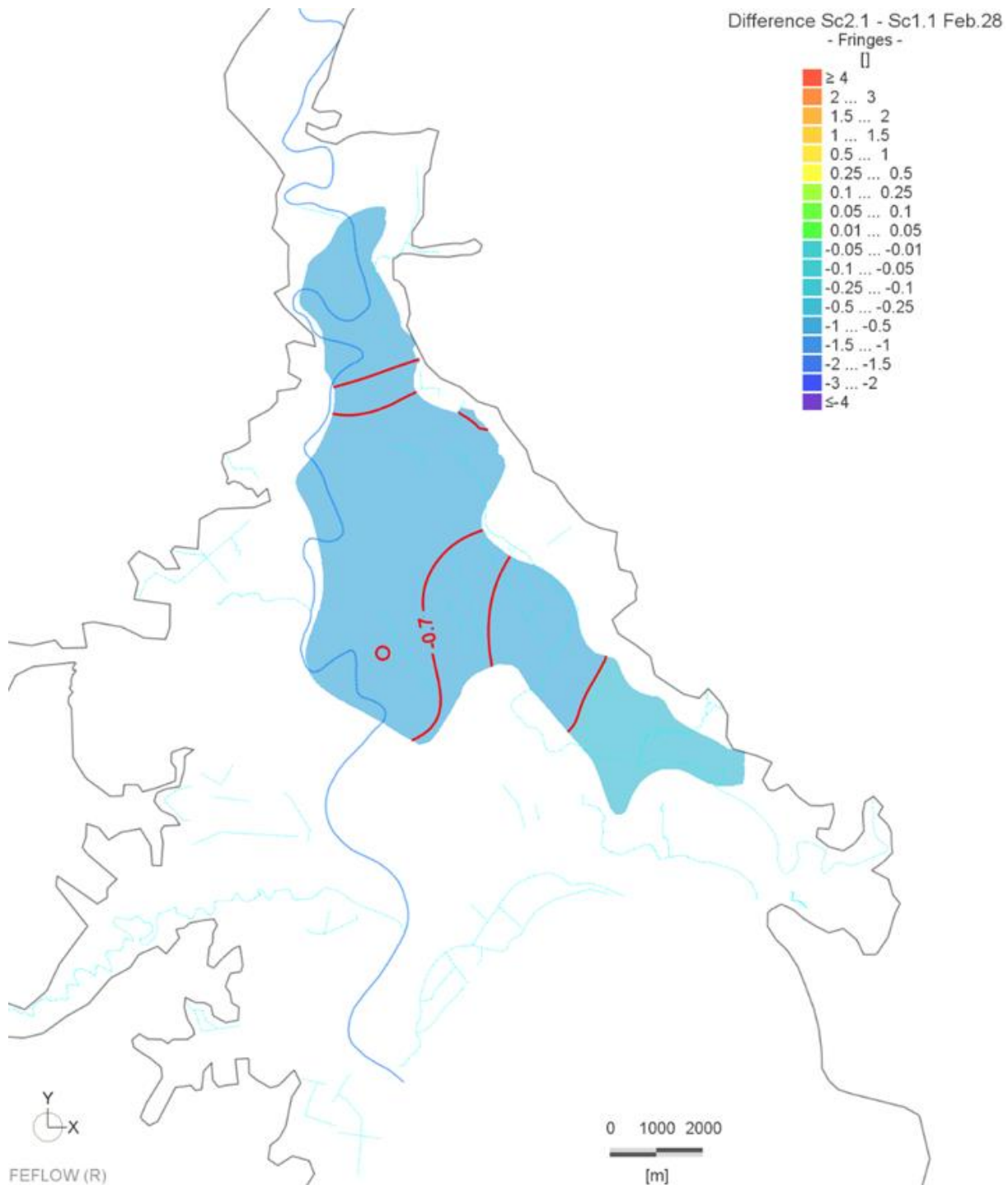


Figure 5-4: Difference of simulated groundwater level between scenario 2.1 and scenario 1.1 in the Matokitoki aquifer at the end of the simulation period (year 2089)

In the following, some aspects of the results in comparison of scenario 2.1 to scenario 1.1 are underpinned by presenting a number of exemplary diagrams, explaining different kind of behaviour in different locations within the model area. A full set of plots, both time-series/time-series differences for observation bores and as well as vertical head plots are available in the digital appendix.

Figure 5-5 shows that at the location of observation bore GPF035 (screened in Makauri aquifer) the consideration of climate-change effects leads to a small reduction in groundwater level in the shallow aquifers in wintertime which can be attributed to the reduction in groundwater recharge from winter rainfalls. The water level drop increases slightly over time, as rainfall recharge reduces. Summer water

levels in the shallow aquifer are lower and do not change with considering climate change as they are solely controlled by stream/drain levels. In the Makauri aquifer, groundwater potentials in winter drop slightly, summer heads decline more, caused by increasing groundwater abstraction over time.

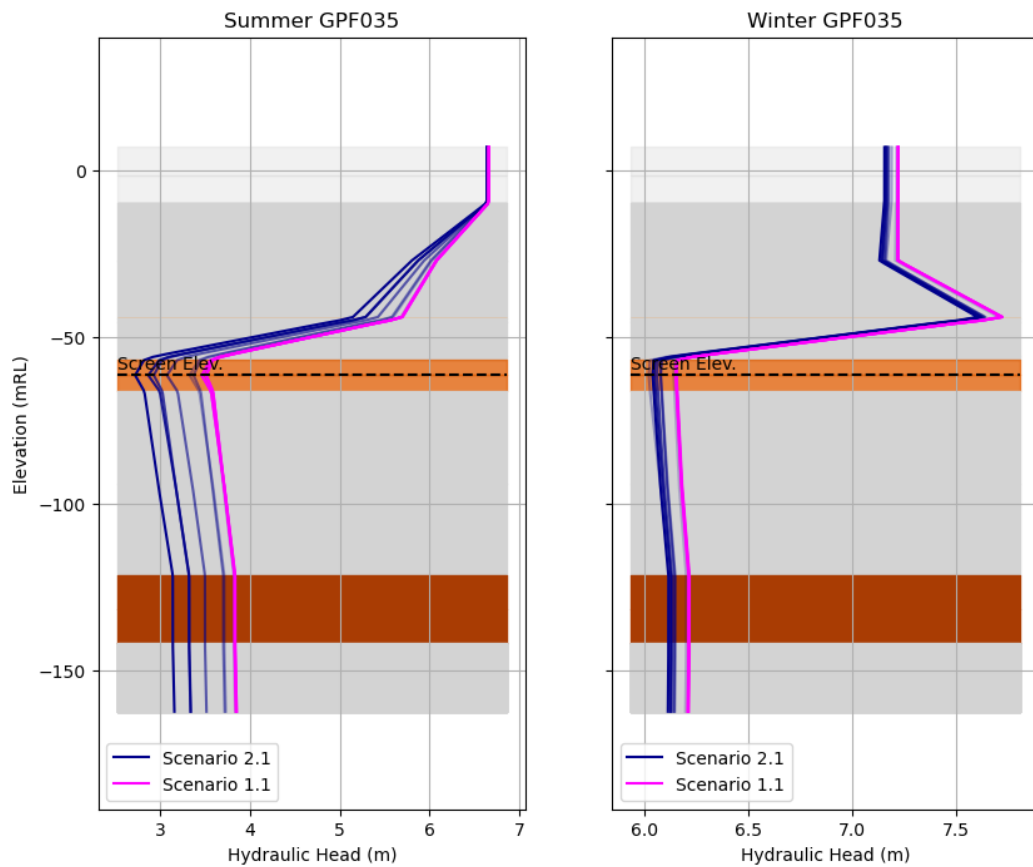


Figure 5-5: Comparison of hydraulic head in summer and winter between scenarios 2.1 and 1.1, observation bore GPF035 (Makauri)

Very close to the coastline, the effect of sea level rise can be seen in the shallow aquifer system. Other than in the reference scenario 1.1, groundwater level rises over time in scenario 2.1 in both winter and summer conditions (Figure 5-6: Comparison of hydraulic head in summer and winter between scenarios 2.1 and 1.1, observation bore GPC100 (Te Hapara Sands)).

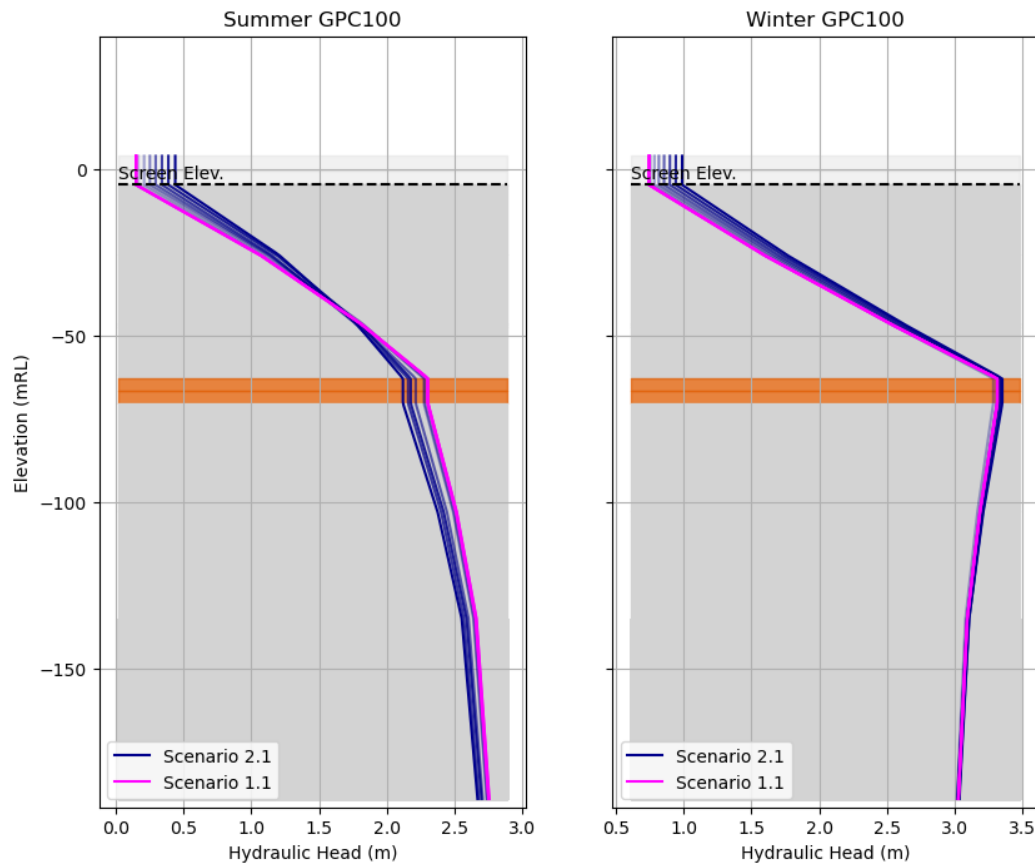


Figure 5-6: Comparison of hydraulic head in summer and winter between scenarios 2.1 and 1.1, observation bore GPC100 (Te Hapara Sands)

5.3. Scenario 3.1 Natural State + Climate Change (NS)

Scenario 3.1 is carried out to illustrate the natural state with respect to pumping. How would the groundwater system react if all pumping was shut off as of now.

5.3.1. Scenario Parameters

Scenario 3.1 considers the climate change parameters for decrease recharge and sea level rise specified above and no groundwater abstraction. With respect to abstraction, it represents a natural state under the climate change assumptions taken for scenario 2.1.

5.3.2. Scenario Results

Based on the lacking groundwater use, groundwater levels are expected to rise compared to the baseline scenario with climate change (scenario 2.1). This is mostly visible in the aquifers with the largest amount of groundwater abstraction (especially Makauri). Groundwater level rise in the shallow aquifers is less predominant as there is a levelling influence of the rivers, streams and drains. An overview of statistical changes in between the different scenarios is shown in chapter 0.

Figure 5-7 through Figure 5-10 show the differences in hydraulic head between scenario 3.1 and scenario 2.1 at the end of the simulation period (year 2089), and therefore indicate the long-term change induced by fully abandoning groundwater abstraction under climate-change conditions. One plot is shown for each of the aquifers.

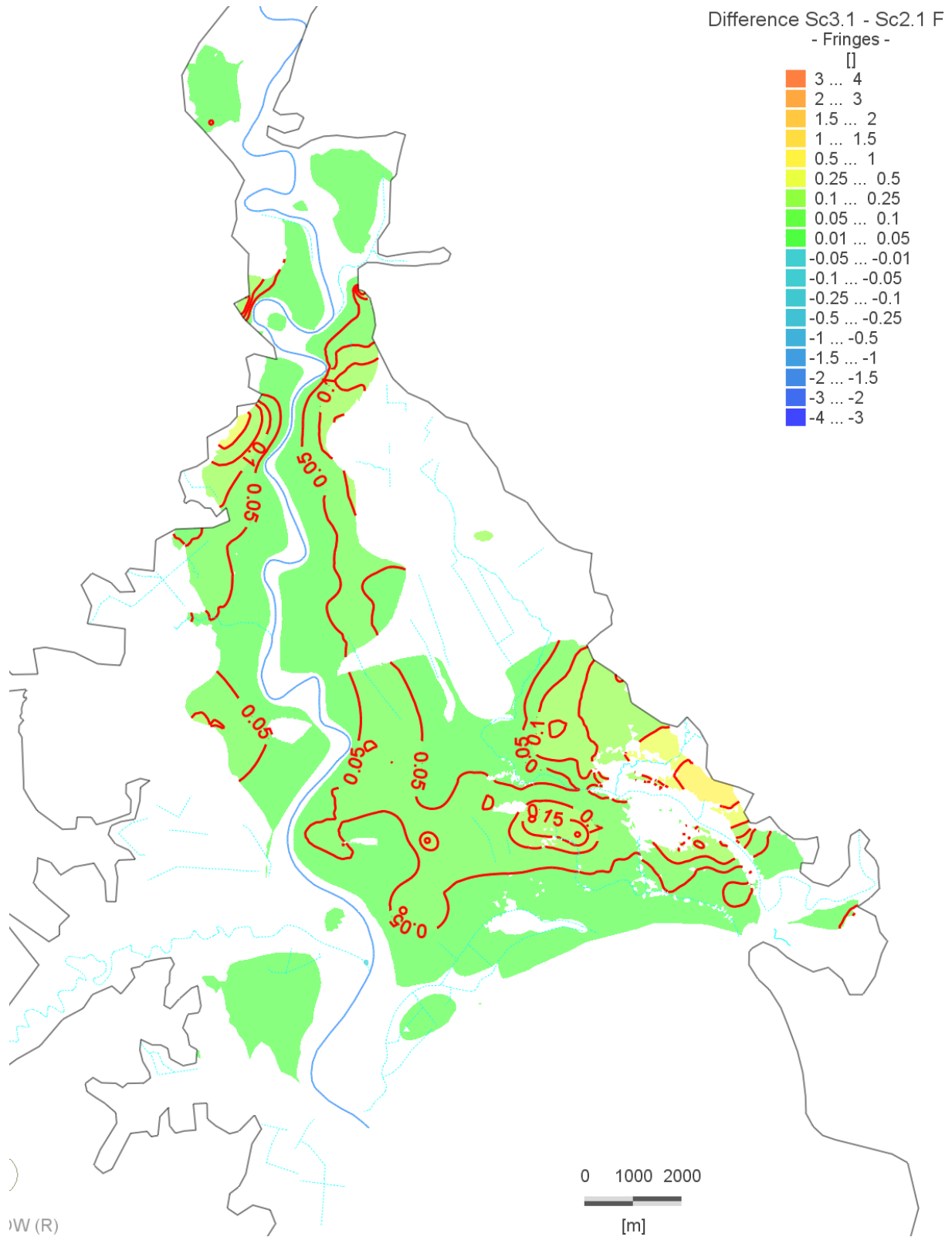


Figure 5-7: Difference of simulated groundwater level between scenario 3.1 and scenario 2.1 in the shallow aquifer system

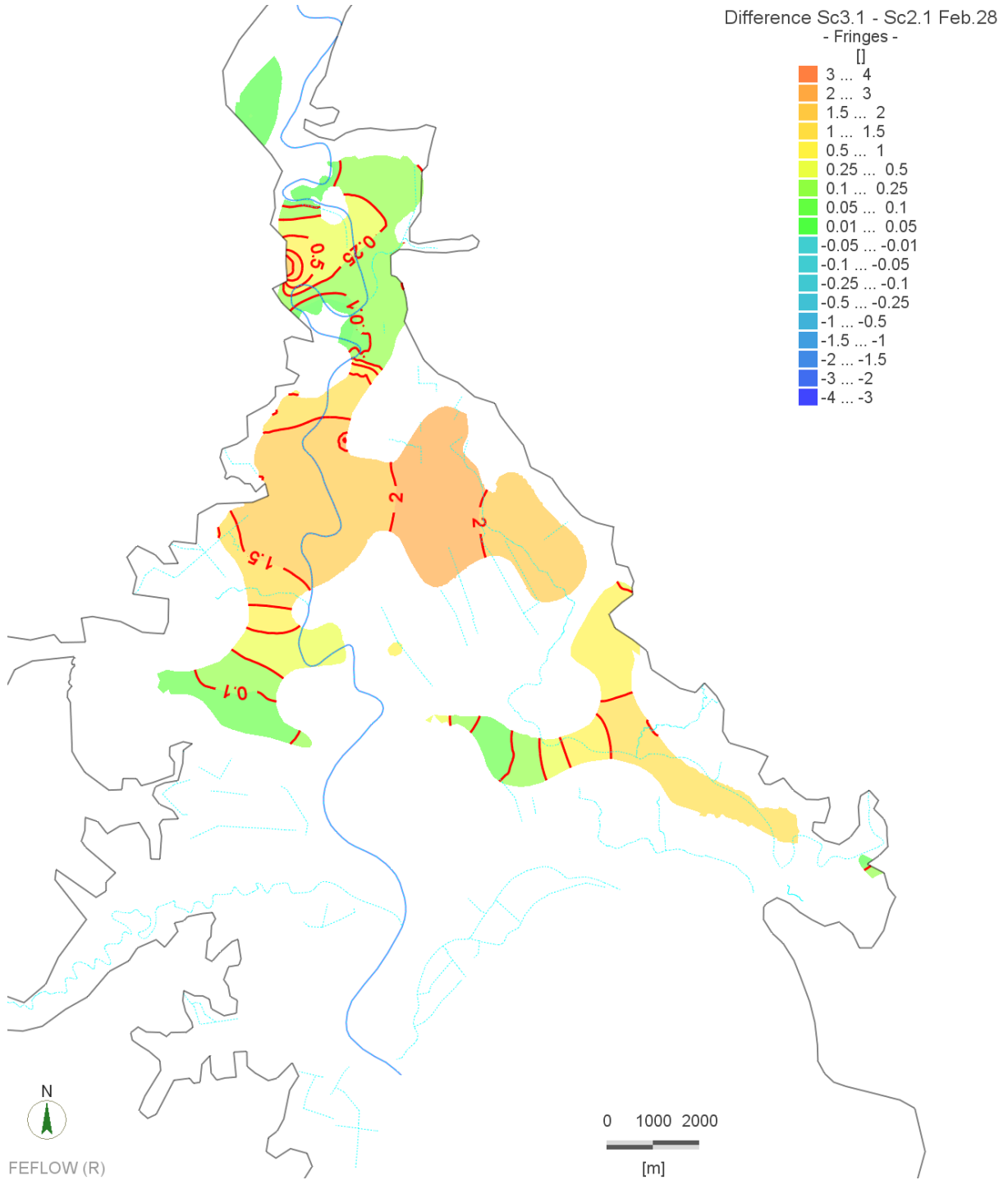


Figure 5-8: Difference of simulated groundwater level between scenario 3.1 and scenario 2.1 in the Waipaoa aquifer

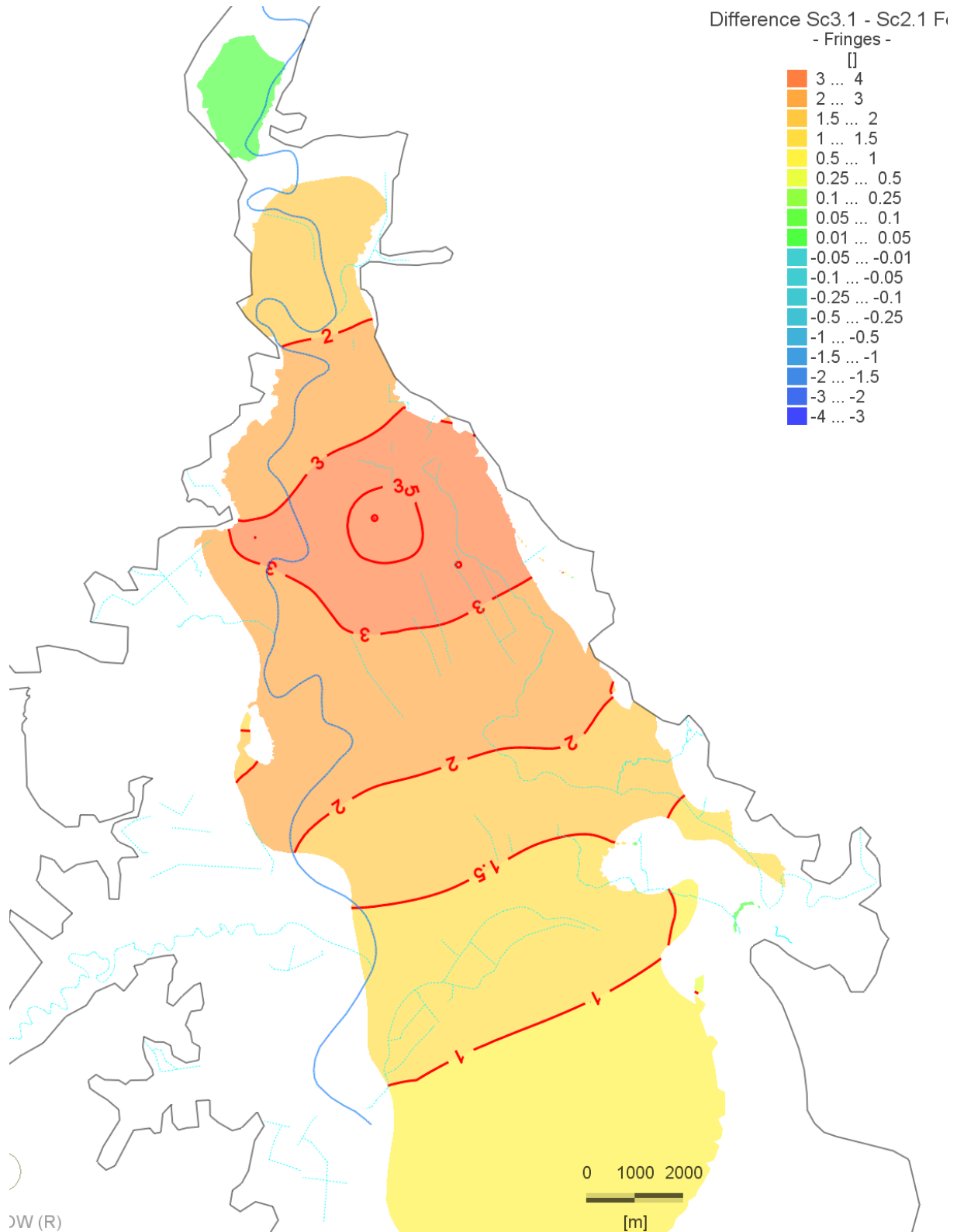


Figure 5-9: Difference of simulated groundwater level between scenario 3.1 and scenario 2.1 in the Makauri aquifer

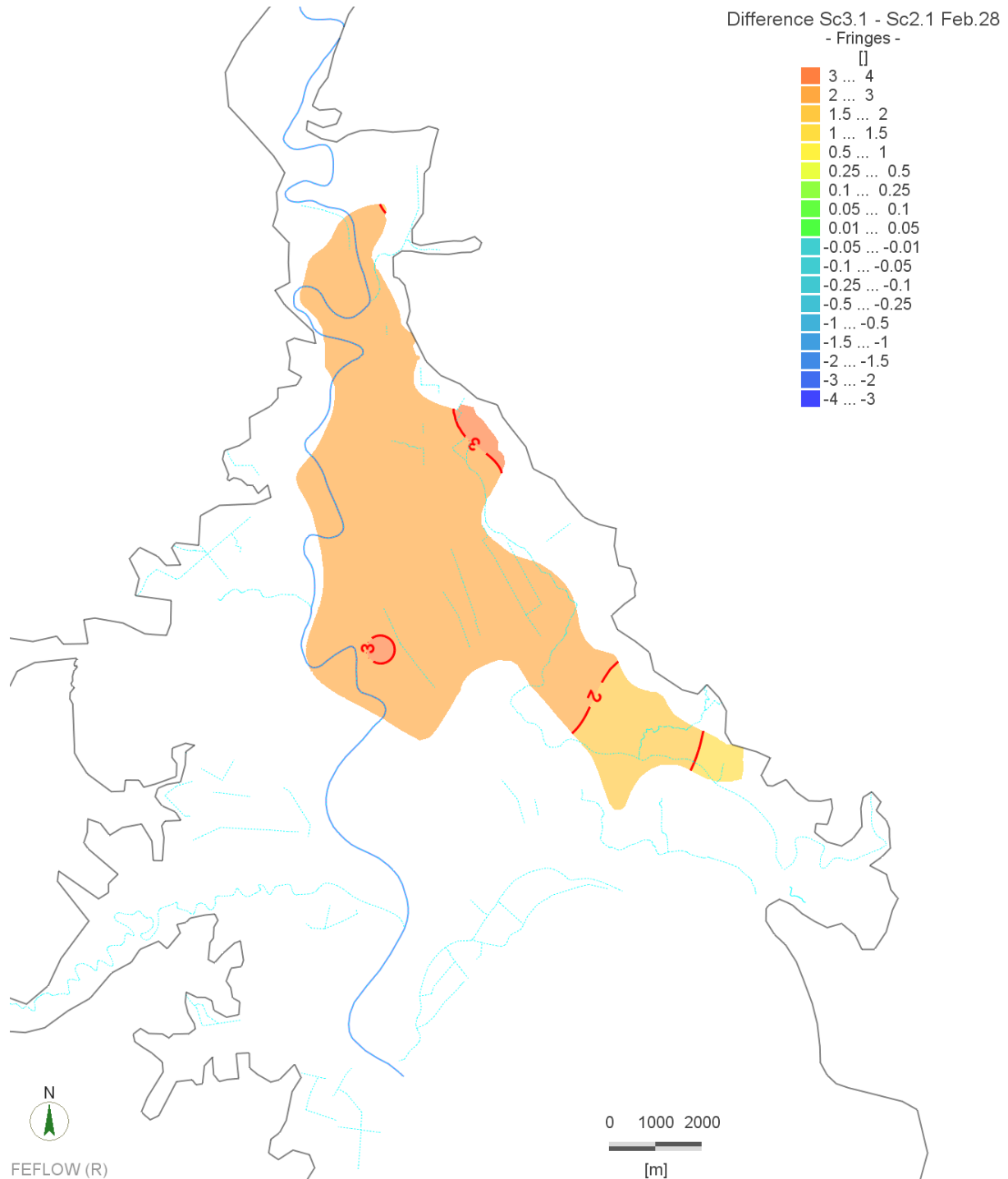


Figure 5-10: Difference of simulated groundwater level between scenario 3.1 and scenario 2.1 in the Matokitoki aquifer

In the following, some aspects of the results in comparison of scenario 3.1 to scenario 2.1 are underpinned by presenting a number of exemplary diagrams, explaining different kind of behaviour in different locations within the model area. A full set of plots, both time-series/time-series differences for observation bores and as well as vertical head plots are available in the digital appendix.

In Figure 5-11 and Figure 5-12 it can be seen that the cease of abstraction leads to an increase of the hydraulic head in the Makauri aquifer (location of bore GPF159) of about 2,50 m to 3,50 m in normal summers (up to about 4,8 m during draught periods). In winter, the increase is only 10 to 20 cm. There is no significant groundwater decline over time anymore (all blue curves in Figure 5-12 close to identical),

even though due to climate change rainfall recharge is subject to a reduction.

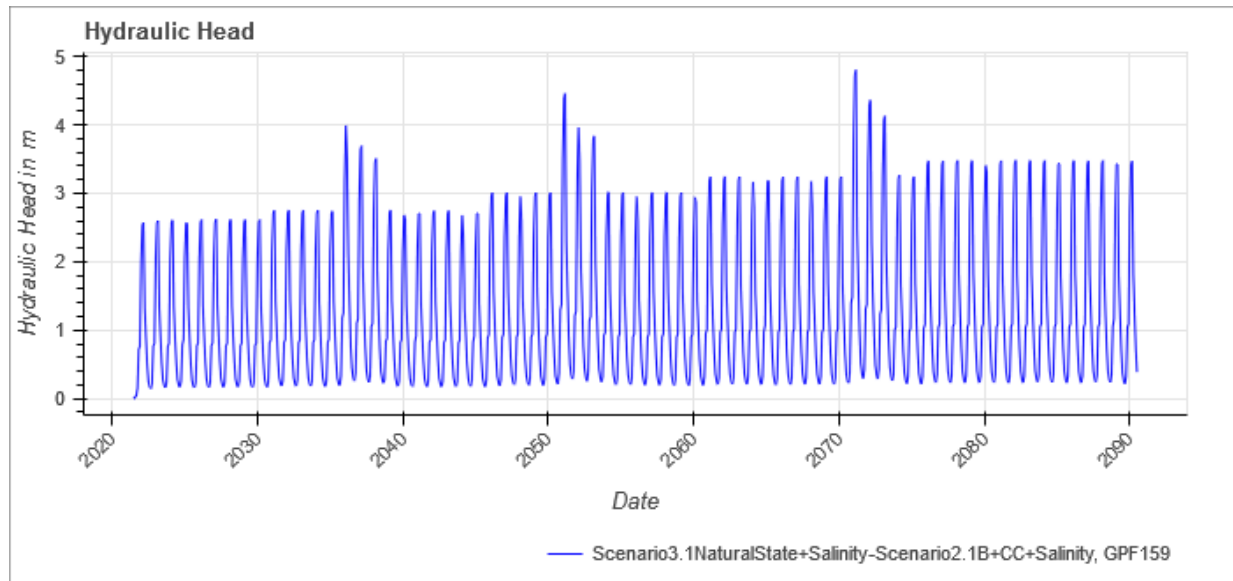


Figure 5-11: Difference of simulated groundwater level between scenario 3.1 and scenario 2.1 over time, observation bore GPF 159 (Makauri)

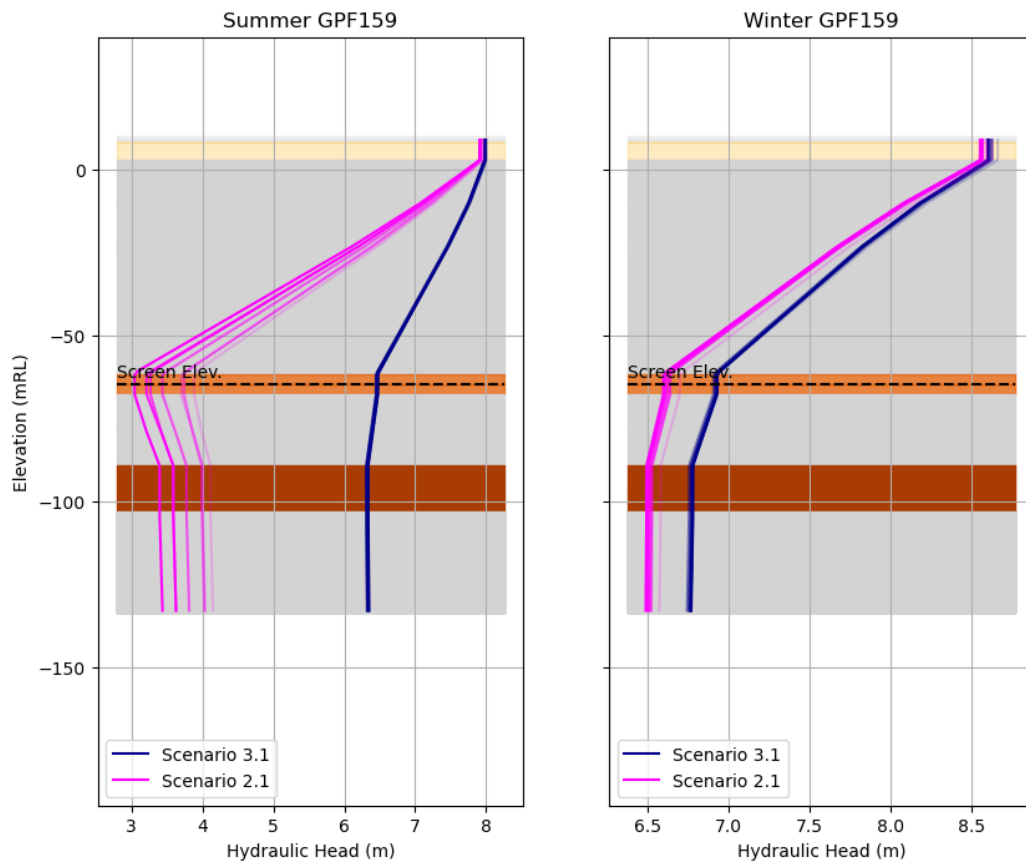


Figure 5-12: Comparison of hydraulic head in summer and winter between scenarios 3.1 and 2.1, observation bore GPF159 (Makauri)

Close to the coastline in the shallow aquifers, there is practically no change in groundwater levels when ceasing abstraction (Figure 5-13).

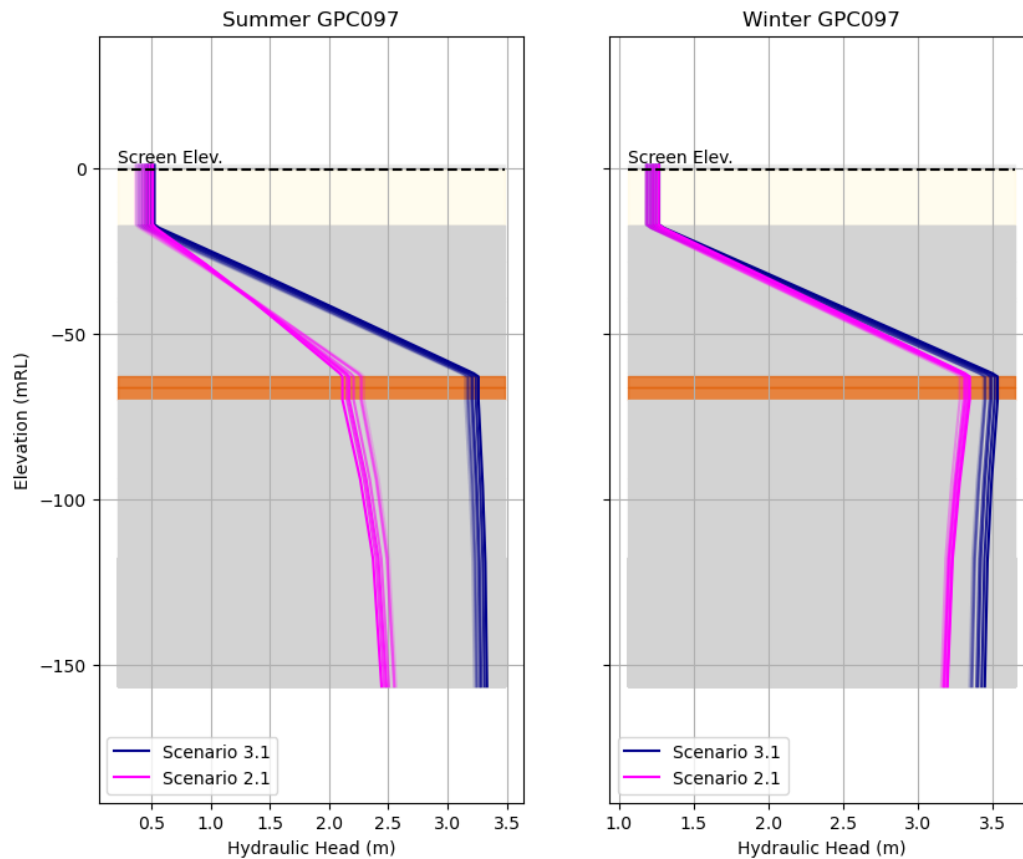


Figure 5-13: Comparison of hydraulic head in summer and winter between scenarios 3.1 and 2.1, observation bore GPC097 (Te Hapara Sands)

5.4. Scenario 4.1 Current Allocation Limit V2 + Climate Change

Scenario 4.1 is conducted to depict the effect of groundwater abstraction at the currently allocated amount, assuming that pumping will also increase to fulfil future demands posed by increasing transpiration of the irrigated crops

5.4.1. Scenario Parameters

The parameter set represents the Current Allocation Limit V2 (GDC 2021 regional rules) [15] considering the climate change conditions as follows:

- recharge decrease due to climate change and sea level rising according to the climate scenario RCP4.5 and
- time variable / increasing abstraction specified as follows
 - 3,980,908 m³/year till 2029, then
 - stepwise increase: 5% from 2030, 15% from 2045, 24% from 2060, 33% from 2075 till 2090 (according to the PED of RCP4.5 converted to percentage increase in average seasonal metered usage)
 - increased abstraction in three 3-year draught periods 2035/2036 - 2037/2038, 2050/2051 - 2052/2056 and 2070/2071 - 2072/2073.

Table 5-6 gives an overview on the time variable abstraction amounts of scenario 4.1.

Table 5-6: Overview of abstraction amounts of scenario 4.1 Current Allocation Limit V2 + Climate Change]

Stepwise increased abstraction incl. 3 3-year draught periods scenario 4.1	Increase against to the base abstraction	Hydrological Year	Abstraction amount m ³ /year
no increase till 2029	0	2021/22 - 2028/29	3,980,908
increase 5% from 2030	0.05	2029/30 – 2034/35	4,179,953
		2035/36	6,240,140
		2036/37	5,631,936
		2037/38	5,340,409
		2038/2039 – 2043/44	4,179,953
increase 15% from 2045	0.15	2044/2045 – 2049/50	4,578,044
		2050/51	7,369,308
		2051/52	6,651,048
		2052/53	6,306,769
		2053/54 – 2058/59	4,578,044
increase 24% from 2060	0.24	2059/60 – 2069/70	4,936,325
		2070/71	7,904,177
		2071/72	7,133,785
		2072/73	6,764,519
		2073/74	4,936,325
increase 33% from 2075 till 2090	0.33	2074/2075 – 2089/90	5,294,607

5.4.2. Scenario Results

Based on the increasing groundwater use, groundwater levels are expected to decline compared to the baseline scenario with climate change (scenario 2.1). This is mostly visible in the aquifers with the largest amount of groundwater abstraction (especially Makauri). Groundwater level decline in the shallow aquifers is less predominant as there is a levelling influence of the rivers, streams and drains. An overview of statistical changes in between the different scenarios is shown in chapter 0.

Figure 5-14 through Figure 5-17 show the differences in hydraulic head between scenario 4.1 and scenario 2.1 at the end of the simulation period (year 2089), and therefore indicate the long-term change induced by fully executing current allocations and rising groundwater abstraction under climate-change conditions. One plot is shown for each of the aquifers.

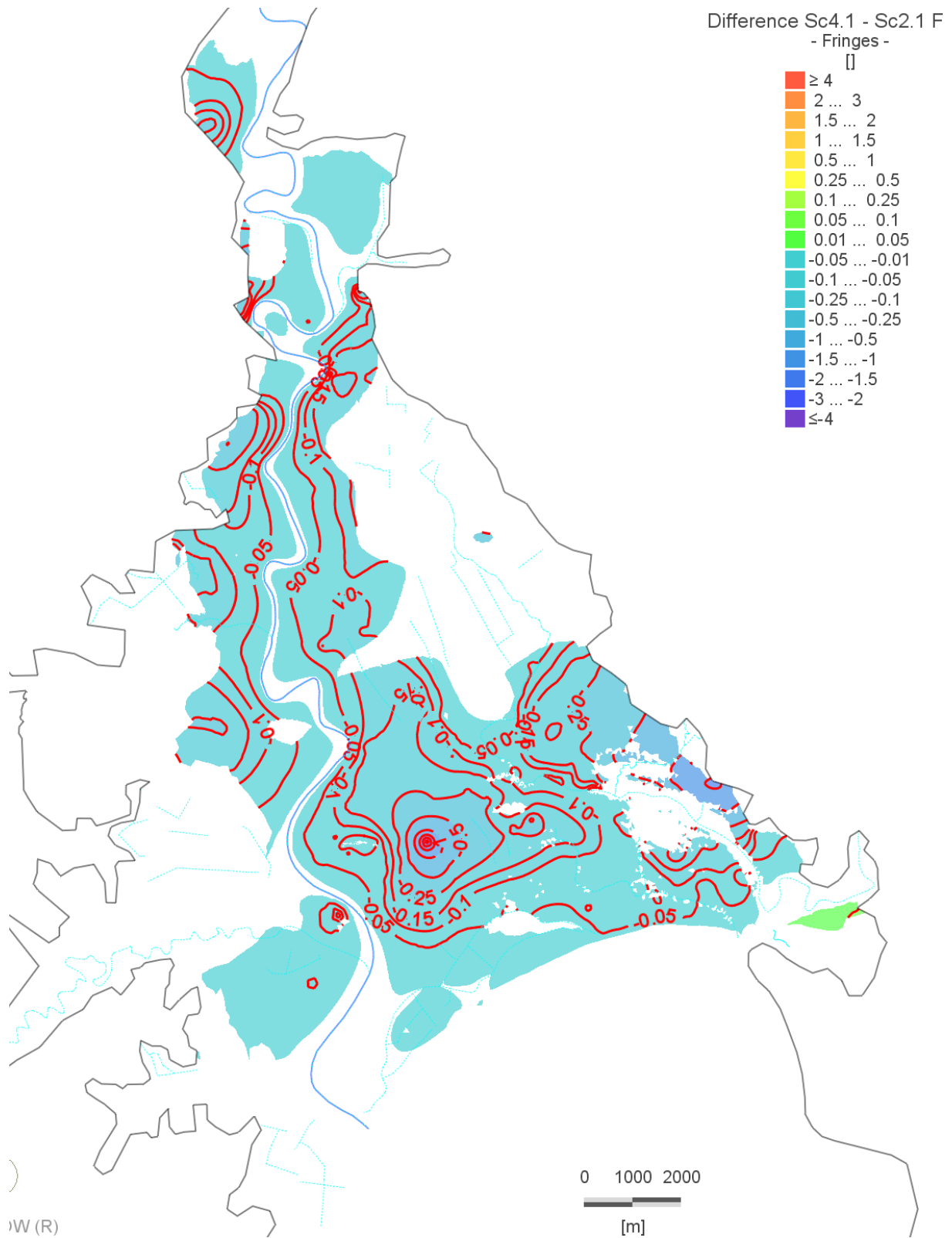


Figure 5-14: Difference of simulated groundwater level between scenario 4.1 and scenario 2.1 in the shallow aquifer system

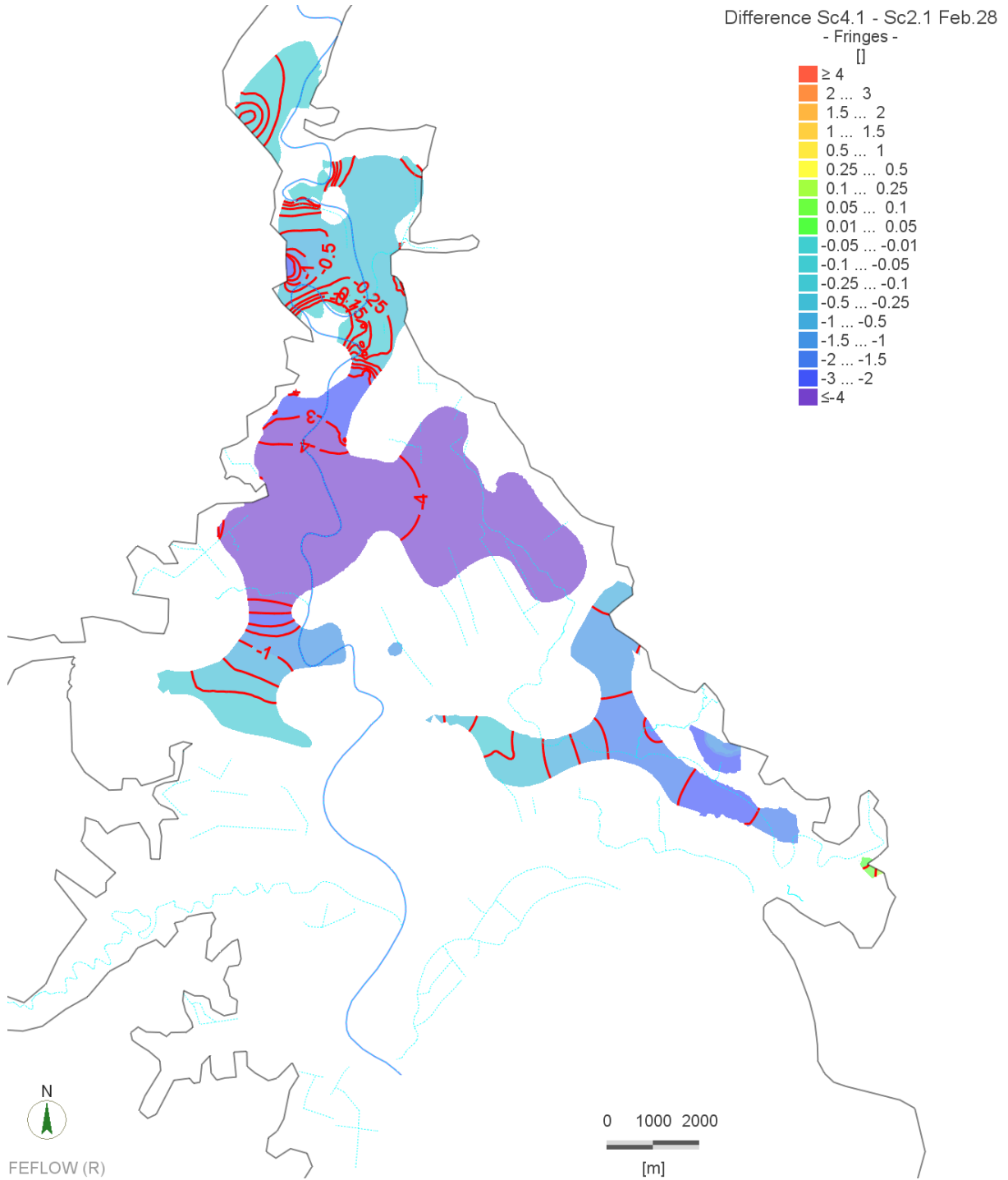


Figure 5-15: Difference of simulated groundwater level between scenario 4.1 and scenario 2.1 in the Waipaoa aquifer

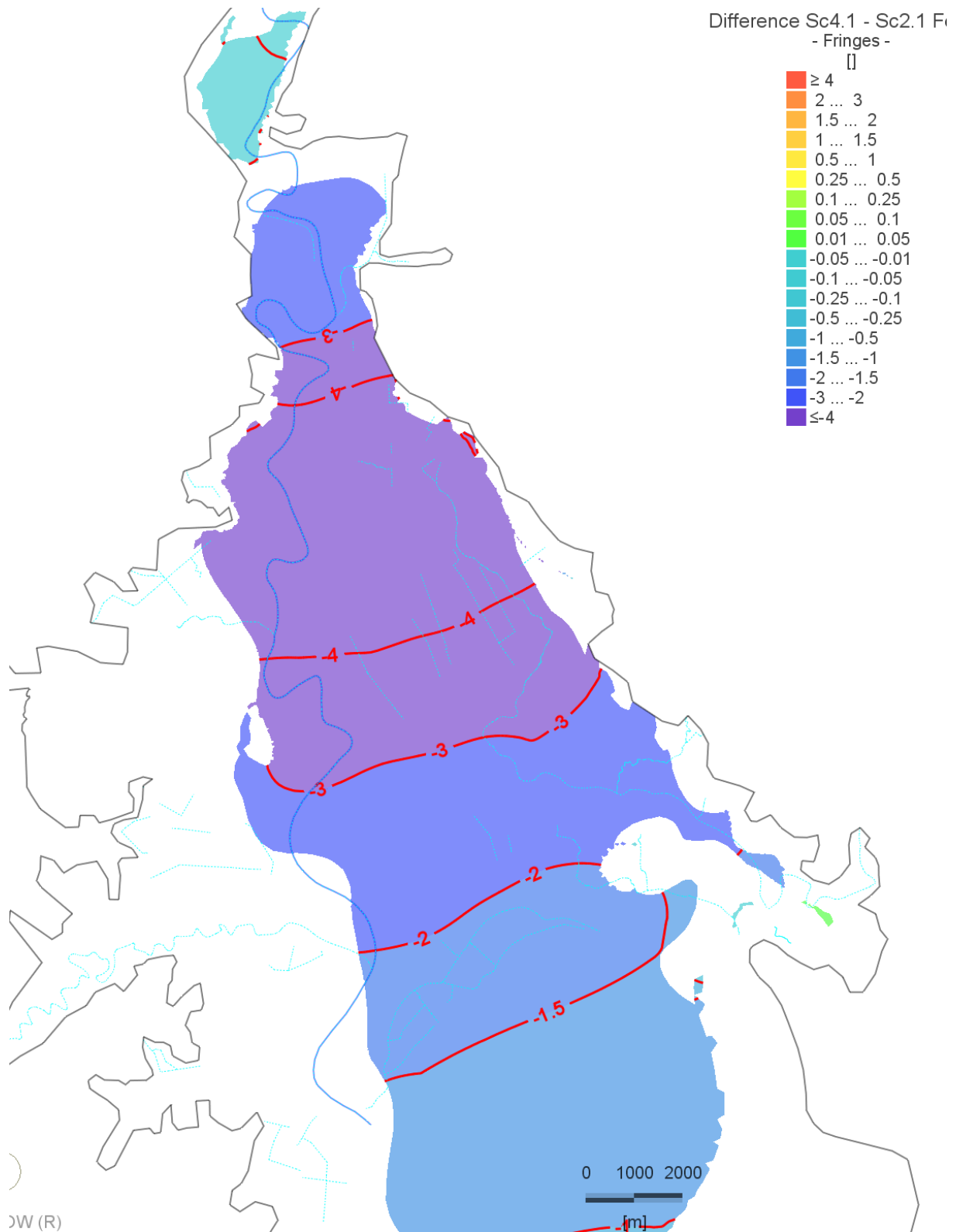


Figure 5-16: Difference of simulated groundwater level between scenario 4.1 and scenario 2.1 in the Makauri aquifer

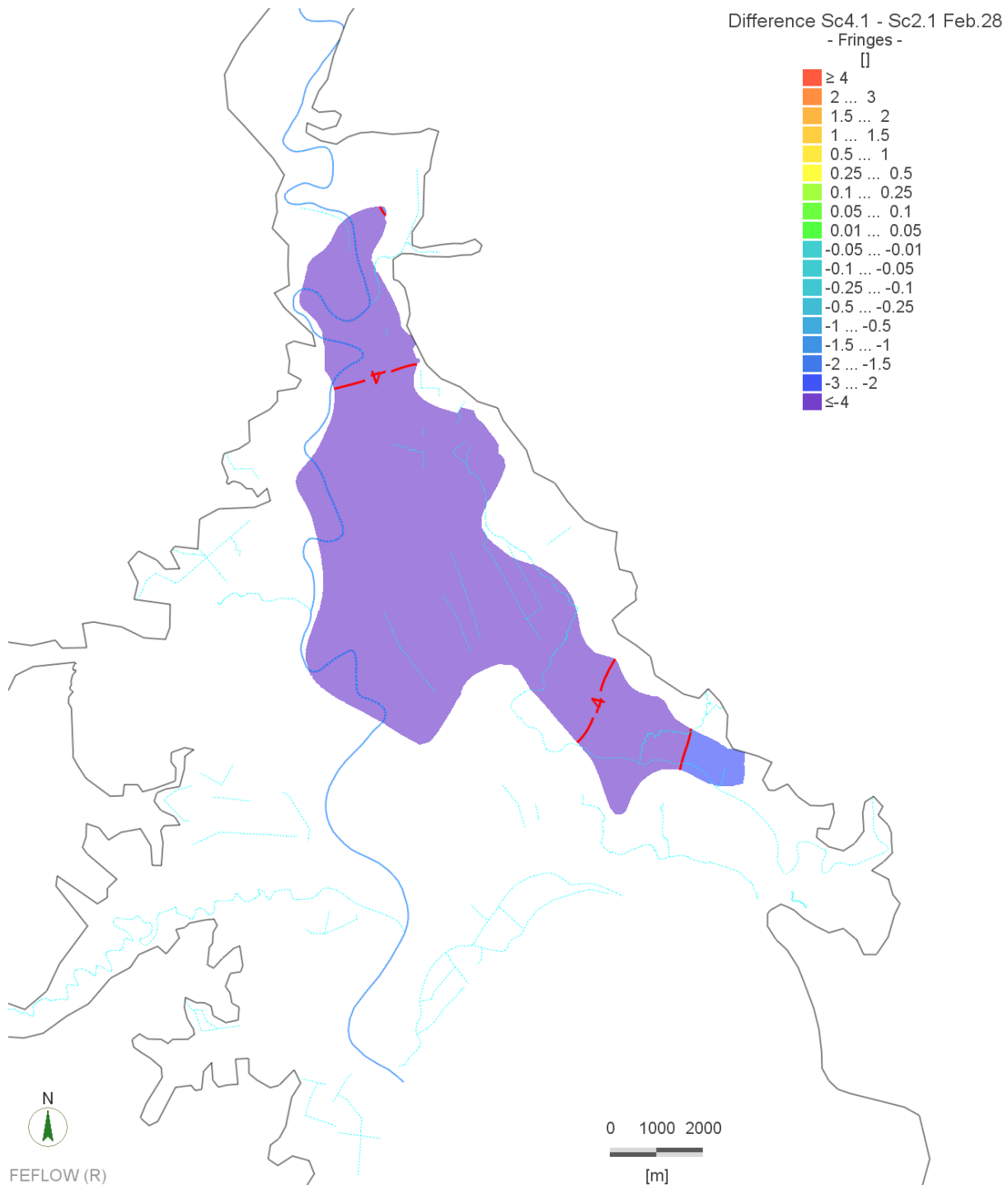


Figure 5-17: Difference of simulated groundwater level between scenario 4.1 and scenario 2.1 in the Matokitoki aquifer

In the following, some aspects of the results in comparison of scenario 4.1 to scenario 2.1 are underpinned by presenting a number of exemplary diagrams, explaining different kind of behaviour in different locations within the model area. A full set of plots, both time-series/time-series differences for observation bores and as well as vertical head plots are available in the digital appendix.

When looking at a bore in the shallow aquifer system (GPC031), it can be seen (Figure 5-18 and Figure 5-19) that groundwater levels decline by about 17 cm in summertime and about 4 cm in wintertime. The draught periods lead to an additional temporary decline in the model. Hydraulic head in the Makauri aquifer at the end of the simulation period in 2089 gets close to sea level – this would pose a high risk for

seawater intrusion. The vertical hydraulic gradient that was upwards in the reference scenario with climate change (scenario 2.1) is reversed because of the strong additional pumping from the Makauri aquifer right from the beginning of the prediction period.

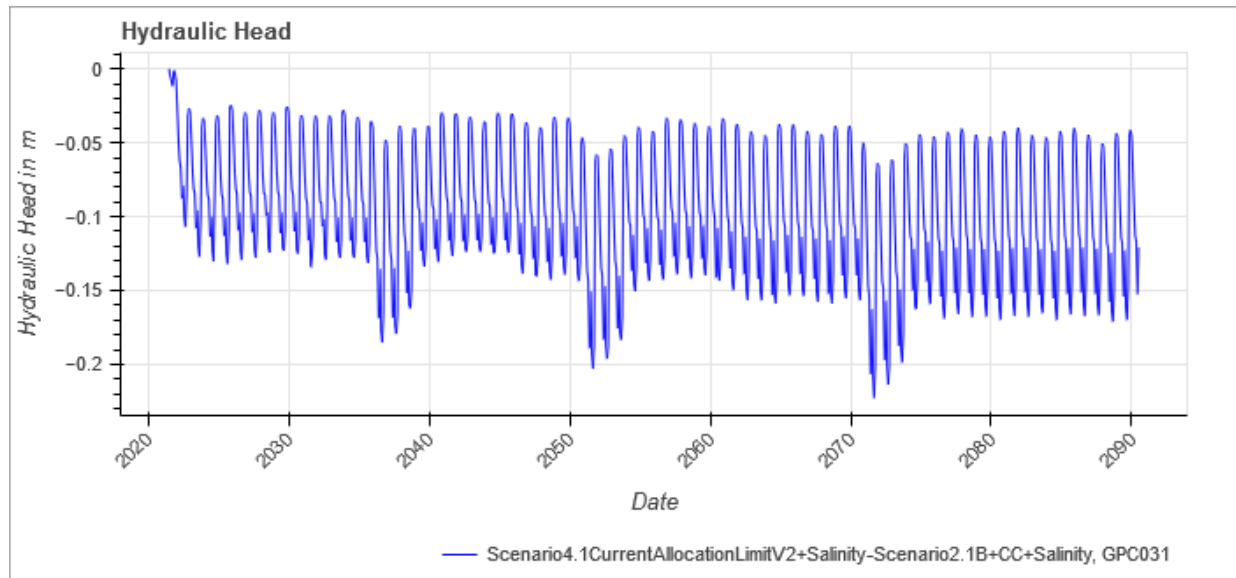


Figure 5-18: Difference of simulated groundwater level between scenario 4.1 and scenario 2.1 over time, observation bore GPC031 (Te Hapara Sands)

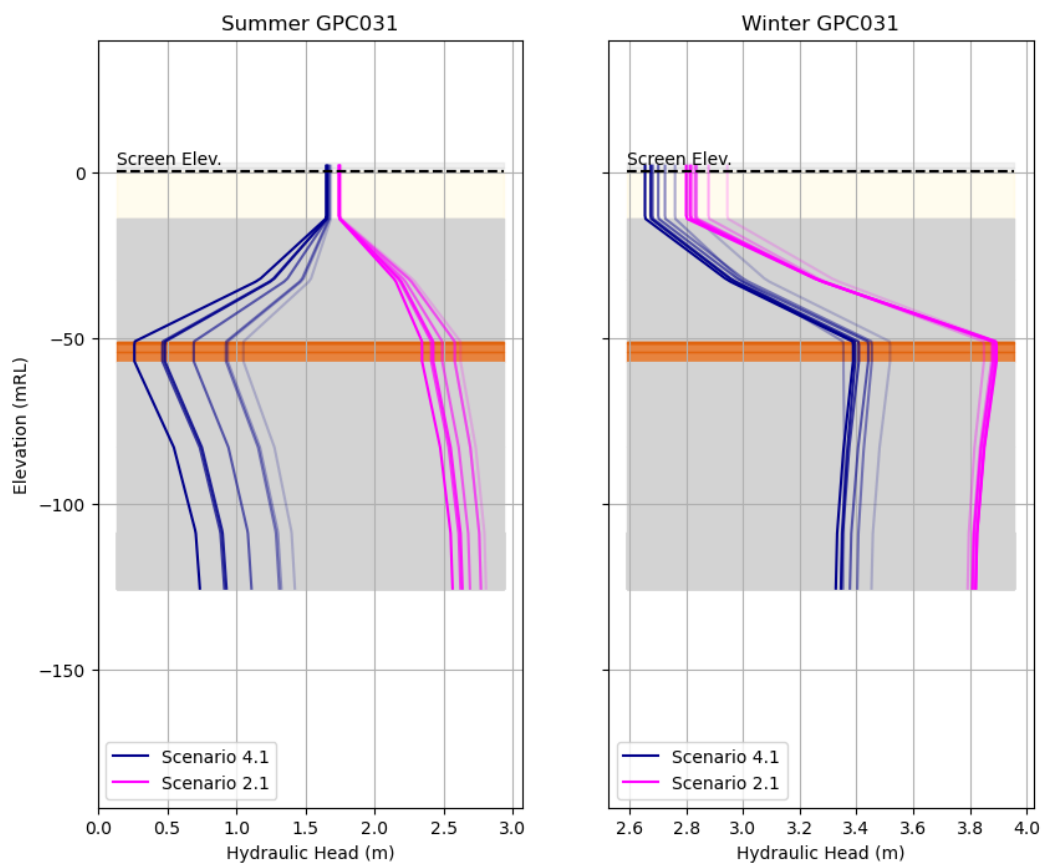


Figure 5-19: Comparison of hydraulic head in summer and winter between scenarios 4.1 and 2.1, observation bore GPC031 (Te Hapara Sands)

Further north, at GPJ040 (Figure 5-20) hydraulic head in the Makauri aquifer in summer is reduced even further, here being below sea level right from the beginning of the period of increased abstraction. In

wintertime, the groundwater potential in the Makauri stays lower than in the reference period, but reduction is far less than in summer. Due to the closeness of GP040 to the Waipaoa River, in the Shallow Fluvial aquifer close to no change in groundwater level is predicted due to the increased groundwater pumping. Once again, the surface water system balances the groundwater level, at the price of reduced baseflow to the rivers and streams or even infiltration from them into groundwater.

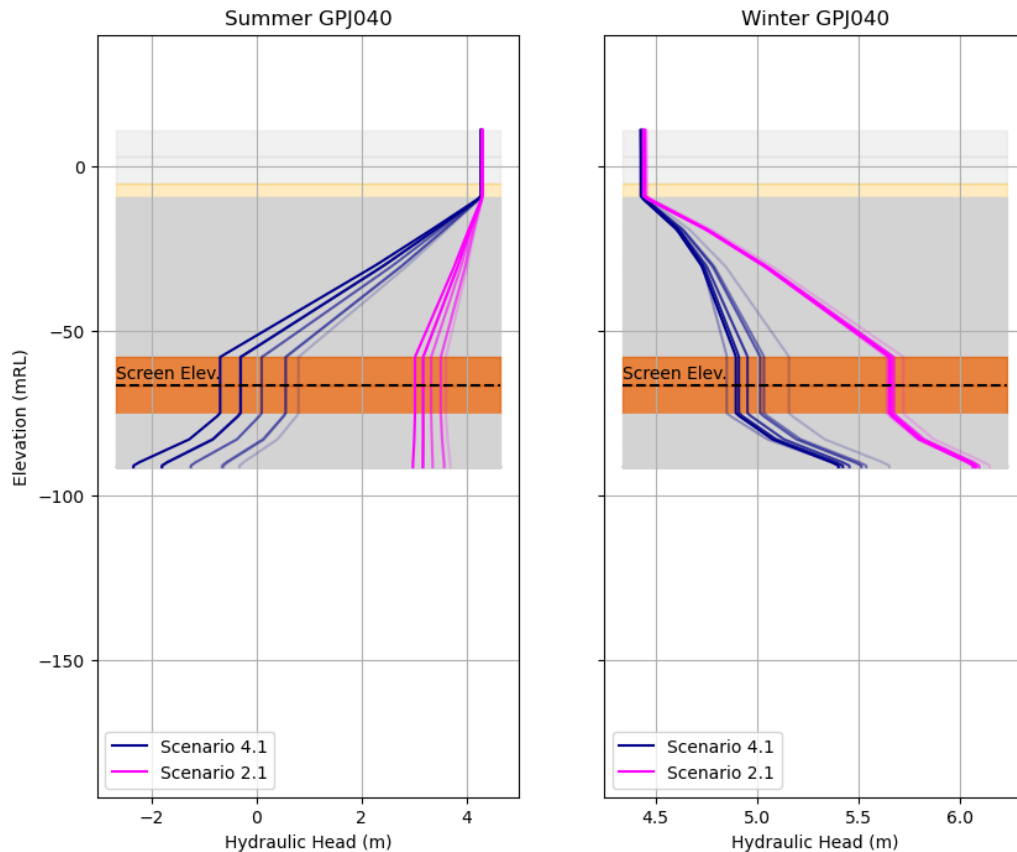


Figure 5-20: Comparison of hydraulic head in summer and winter between scenarios 4.1 and 2.1, observation bore GPJ040 (Makauri)

5.5. Scenario 5.1 MAR 600,000 m³/season + Climate Change (M1)

Scenario 5.1 aims at estimating the effect of replenishing the groundwater system with approximately the amount of water taken from it. MAR is assumed to be into the Makauri aquifer.

5.5.1. Scenario Parameters

Scenario 5.1 incorporates the same input parameters as Scenario 2.1. The only difference between them is that Scenario 5.1 additionally takes into consideration a replenishment scheme with stepwise increase of the amount of water infiltrated into the Makauri aquifer.

Figure 5-21 shows the locations of 6 exemplary MAR injection wells in the Makauri Aquifer (close to Ferry Rd. and Bushmere Rd.). Table 5-7 summarizes their coordinates along with their vertical position and the thickness of the Makauri Aquifer as it is considered in the 3D groundwater model. Numbers in Column “Weighting” are calculated for each injection bore by dividing the aquifer thickness on-site of the bore by the total aquifer thicknesses of 6 bores. The weighting factors are used to allocate a given total MAR amount to MAR bores correspondingly. Column “Injection Amount” represents results of allocating 600,000 m³/season to MAR bore 1 to 6 as average injection rates over a period of 92 days.

The 6 MAR bores are implemented, according to their locations, as injection well BC in the model layer

representing the Makauri aquifer. Temporally, MAR takes place in the period from October to January in three injection stages, separated by two breaks as follows:

- Injection: 1 October - 31 October (31 days)
- Pause: 1 November – 15 November (5 days)
- Injection: 16 November - 16 December (31 days)
- Pause: 17 December – 1 January (16 days)
- Injection: 2 January - 31 January (30 days).

The temporal distribution has been chosen based on time periods with least turbidity in the river, plus the wish to consider breaks in the infiltration to be able to monitor the dynamic reaction of the aquifer in the model. Table 5-8 shows the MAR amount/season beginning with 600,000 m³ till 2029, then a stepwise increase of the infiltration by 5% from 2030, 15% from 2045, 24% from 2060 and 33% from 2075 till 2090, matching the increasing abstraction to cover for increasing PED.

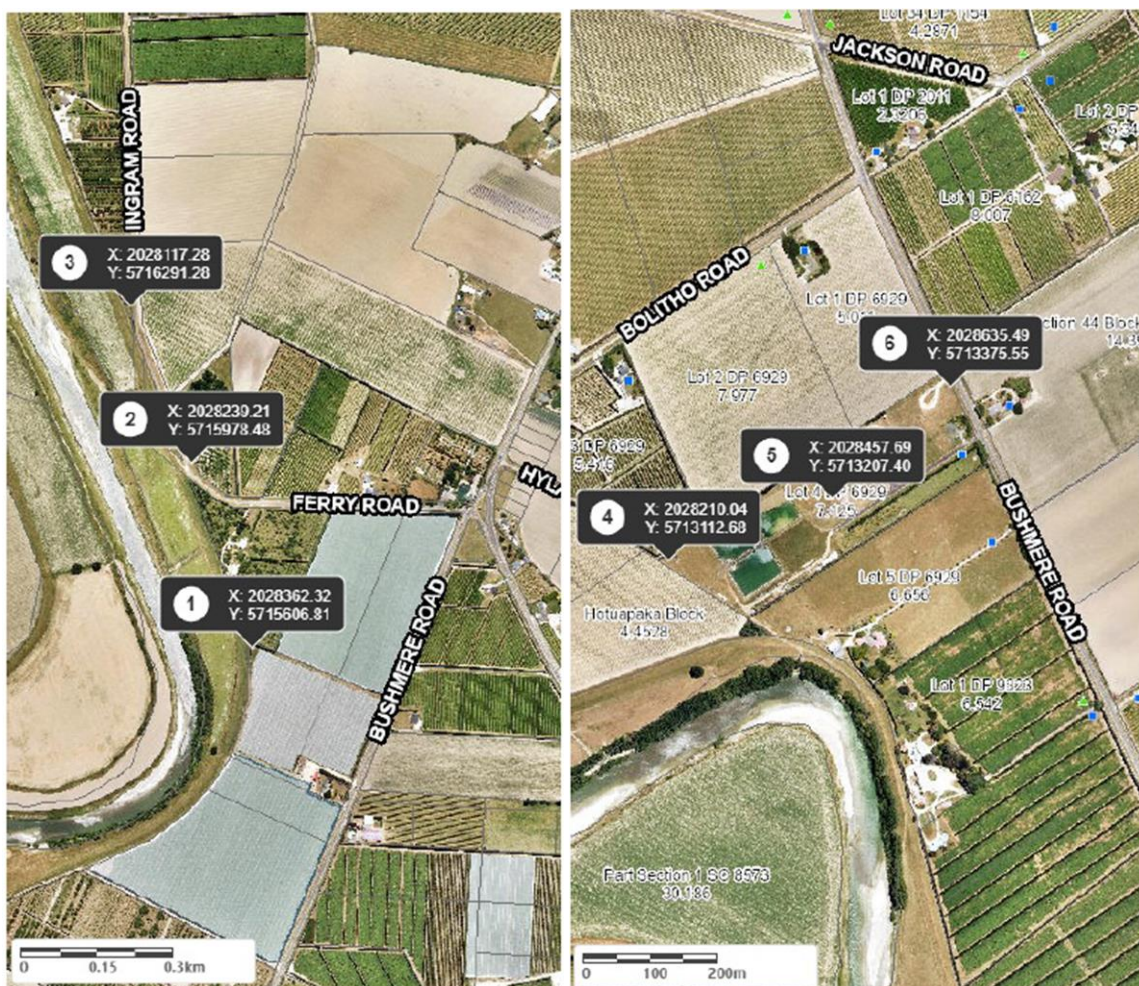


Figure 5-21: Locations of the 6 MAR bores in scenario 5.1 [15]

Table 5-7: Overview of the 6 MAR bores considered by scenario 5.1

MAR bore	Easting	Northing	Location	Depth to Makauri	Ground Surface	Makauri Thickness		Weighting (-) in Model	Injection Amount (m ³ /Season (92d))	Average Injection Rate*	
				(m bgl)	in Modell mRL	(m)	in Model (m)			m ³ /d	L/s
1	2028362.32	5715606.81	667 Bushmere Road (back property)	71	13.50	8	10.0	26%	154538	1679.77	19.44
2	2028239.21	5715978.48	8 Ingram Road	67	13.00	8	9.2	24%	141961	1543.05	17.86
3	2028117.28	5716291.28	73 Ingram Road	67	13.54	4	5.7	15%	87347	949.42	10.99
4	2028210.04	5713112.68	429A Bushmere Road. WWTP	57	10.00	14	9.9	25%	152892	1661.87	19.23
5	2028457.69	5713207.40	429A Bushmere Road. WWTP	61	9.66	6	2.1	5%	32476	353.00	4.09
6	2028635.49	5713375.55	429A Bushmere Road. WWTP	65	10.00	2	2	5%	30786	334.63	3.87

Table 5-8: Overview of the MAR amount/season with stepwise increase in Scenario 5.1

Stepwise increase MAR Scenario 5.1	Increase against to the base MAR	Hydrological Year	MAR amount m ³ /season
no increase till 2029	0	2021/22 - 2028/29	600,000
increase 5% from 2030	0.05	2029/30 - 2043/44	630,000
increase 15% from 2045	0.15	2044/45 - 2058/59	690,000
increase 24% from 2060	0.24	2059/60 - 2073/74	744,000
increase 33% from 2075 till 2090	0.33	2074/75 – 2089/90	798,000

5.5.2. Scenario Results

According to the basic idea of balancing groundwater abstraction by replenishment, groundwater levels are expected to increase compared to the baseline scenario with climate change (scenario 2.1). This is mostly visible in the aquifers with the largest amount of groundwater abstraction (especially Makauri). Groundwater level rise in the shallow aquifers is less predominant as there is a leveling influence of the rivers, streams and drains. An overview of statistical changes in between the different scenarios is shown in chapter 0. The water levels in general are comparable to the ones of scenario 3.1 with no pumping at all.

Figure 5-22 through Figure 5-25 show the differences in hydraulic head between scenario 5.1 and scenario 2.1 at the end of the simulation period (30 June 2090), and therefore indicate the long-term change induced by replenishing the groundwater system in the Makauri aquifer. One plot is shown for each of the aquifers.

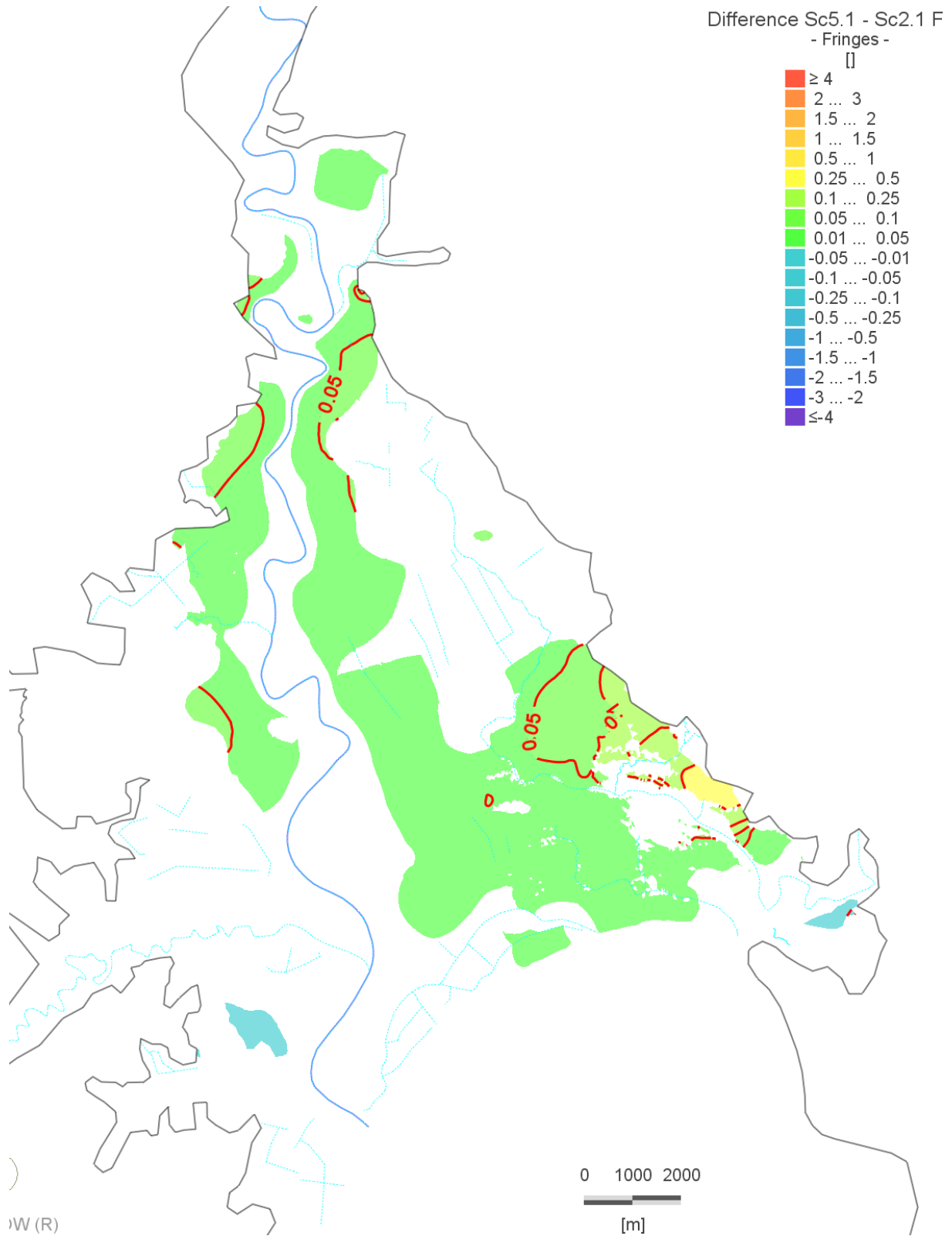


Figure 5-22: Difference of simulated groundwater level between scenario 5.1 and scenario 2.1 in the shallow aquifer system

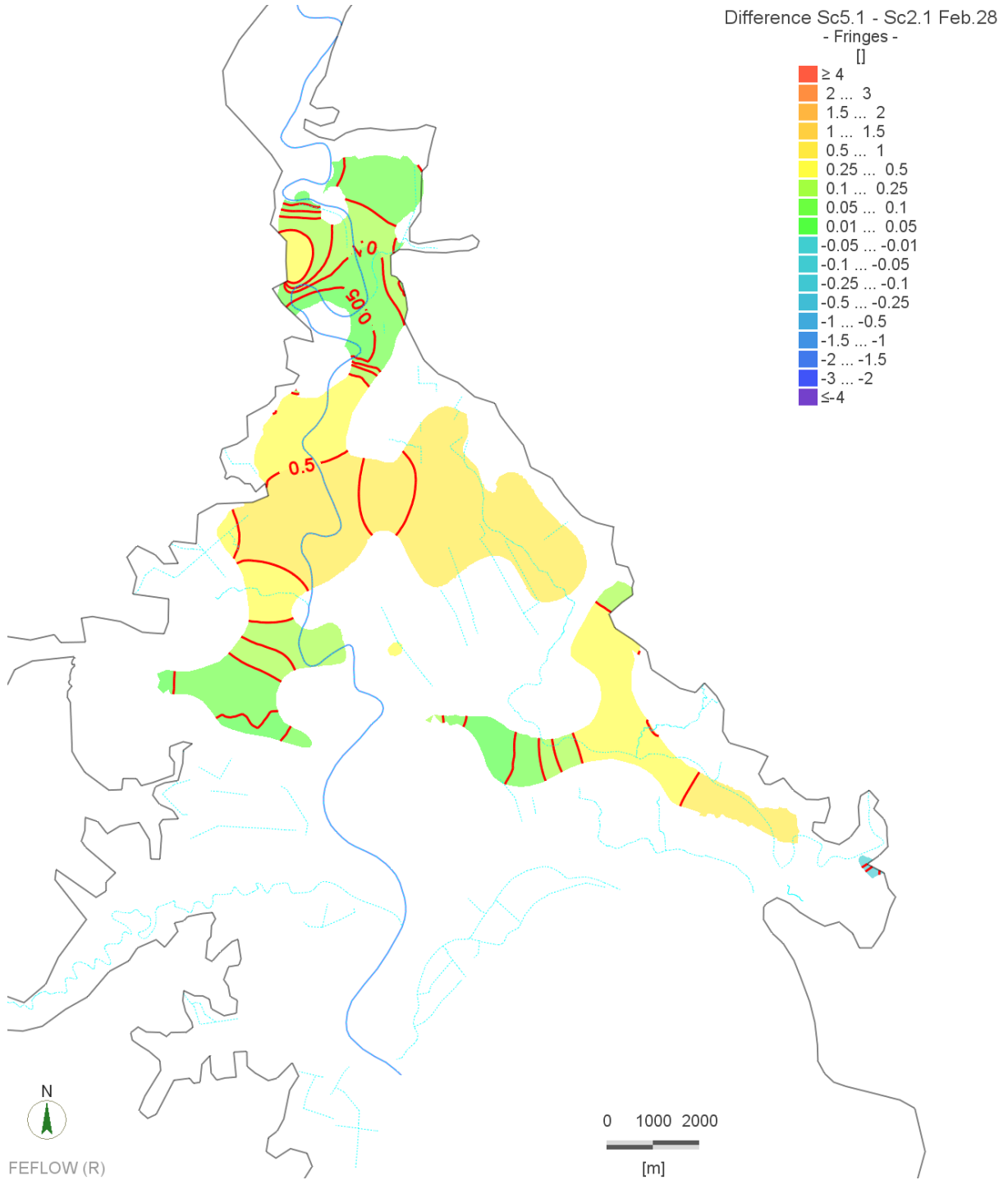


Figure 5-23: Difference of simulated groundwater level between scenario 5.1 and scenario 2.1 in the Waipaoa aquifer

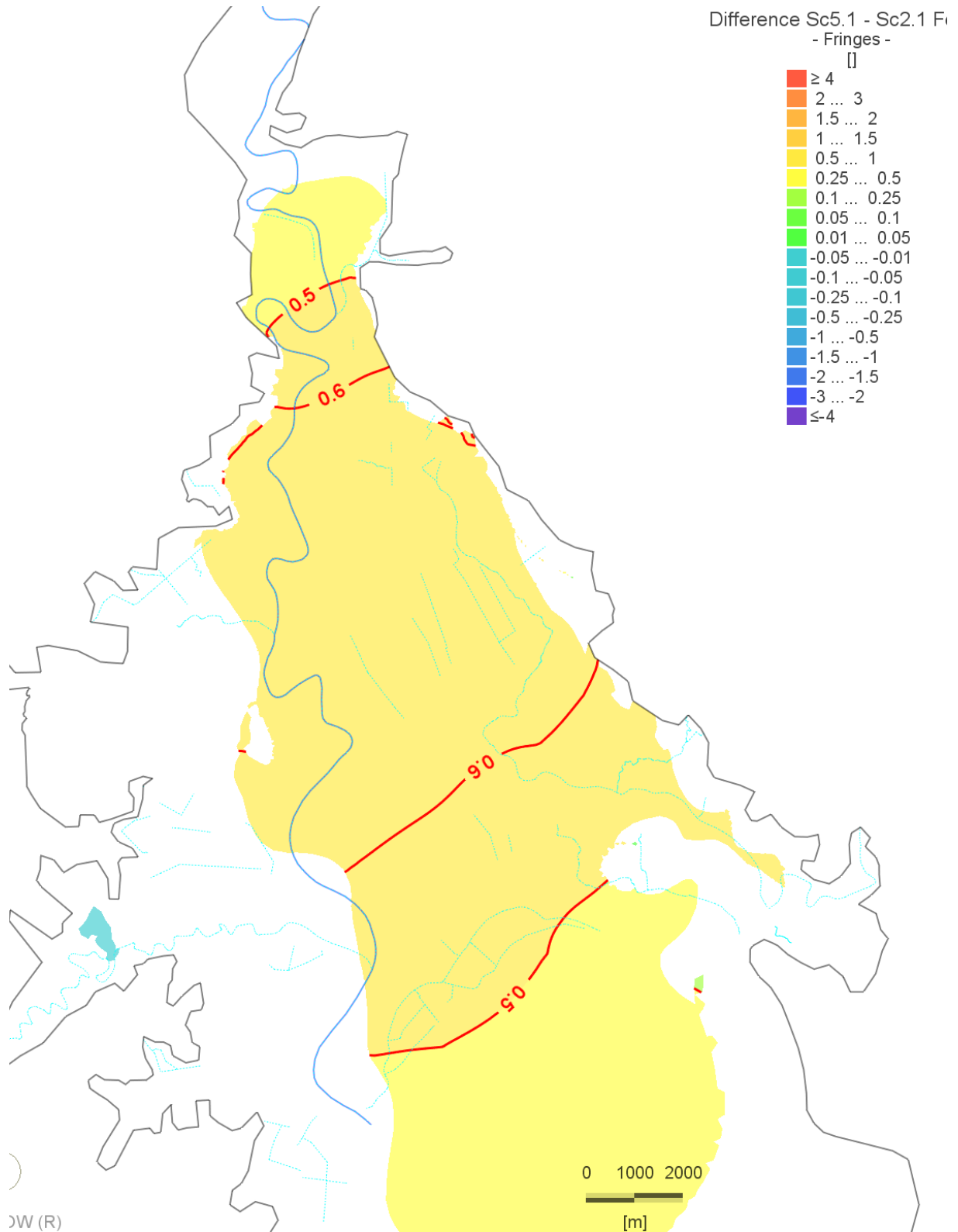


Figure 5-24: Difference of simulated groundwater level between scenario 5.1 and scenario 2.1 in the Makauri aquifer

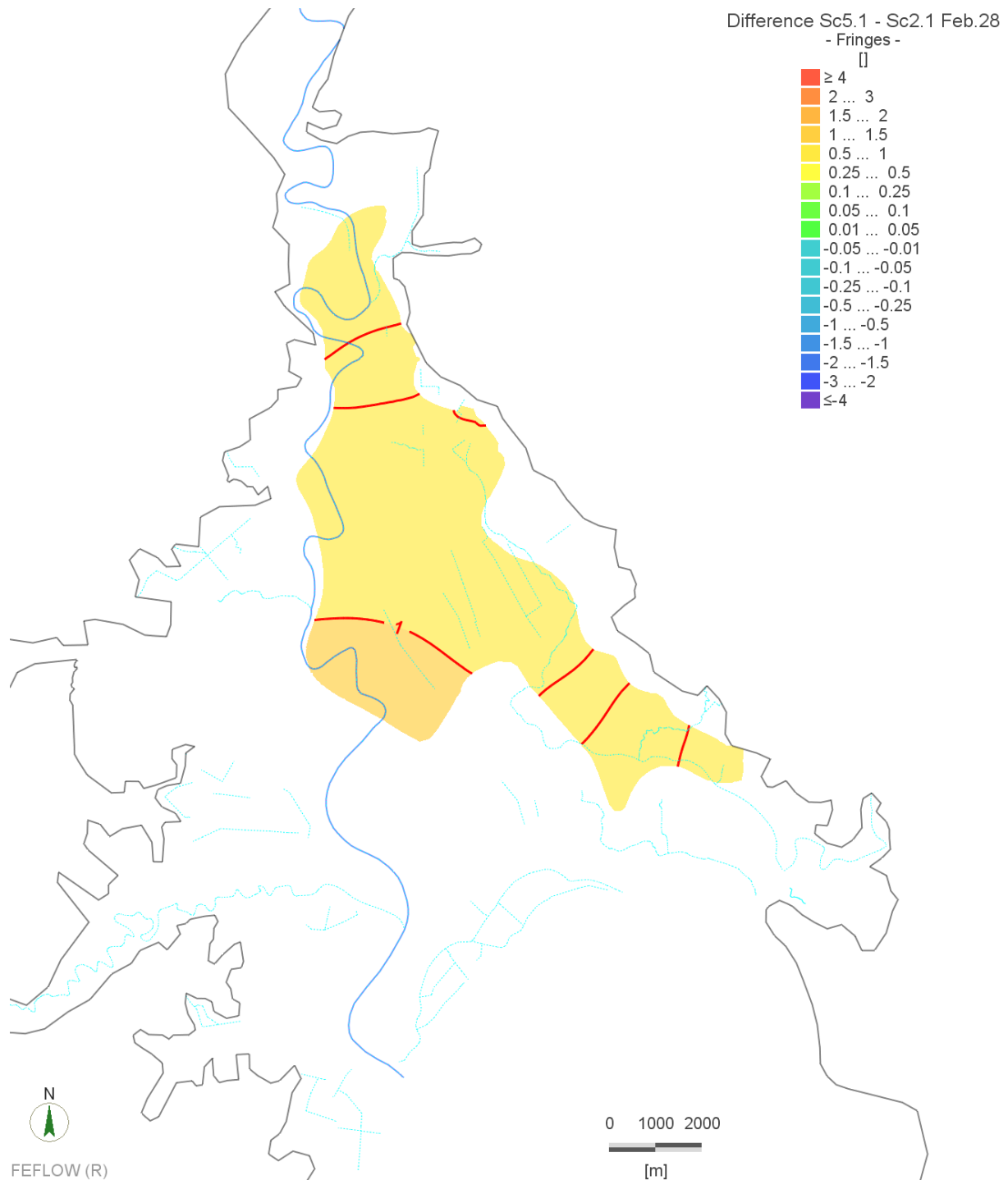


Figure 5-25: Difference of simulated groundwater level between scenario 5.1 and scenario 2.1 in the Matokitoki aquifer

In the following, some aspects of the results in comparison of scenario 5.1 to scenario 2.1 are underpinned by presenting a number of exemplary diagrams, explaining different kind of behaviour in different locations within the model area. A full set of plots, both time-series/time-series differences for observation bores and as well as vertical head plots are available in the digital appendix.

When looking at a bore close to the replenishment site (GPC030), it can be seen (Figure 5-26 and Figure 5-27) that groundwater levels at the end of January (peaks in curves in Figure 5-26) increase with each step of increase in the amount replenished by the MAR system. In winter (lows in curves in Figure 5-26), there is only a slight increase of hydraulic potential in the Makauri aquifer.

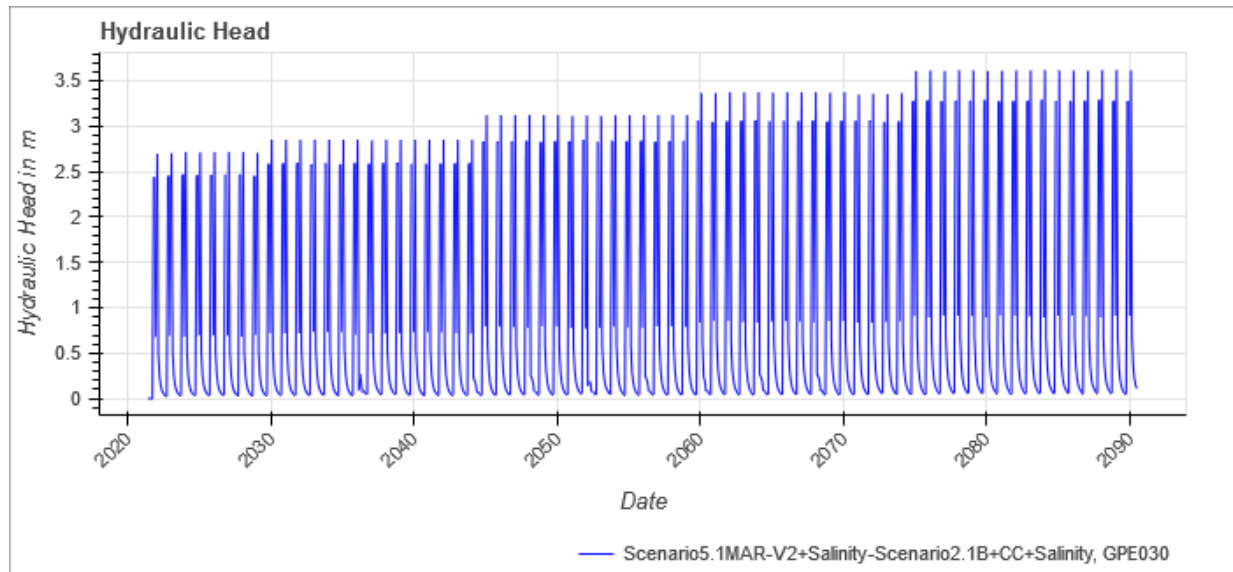


Figure 5-26: Difference of simulated groundwater level between scenario 5.1 and scenario 2.1 over time, observation bore GPE030 (Makauri)

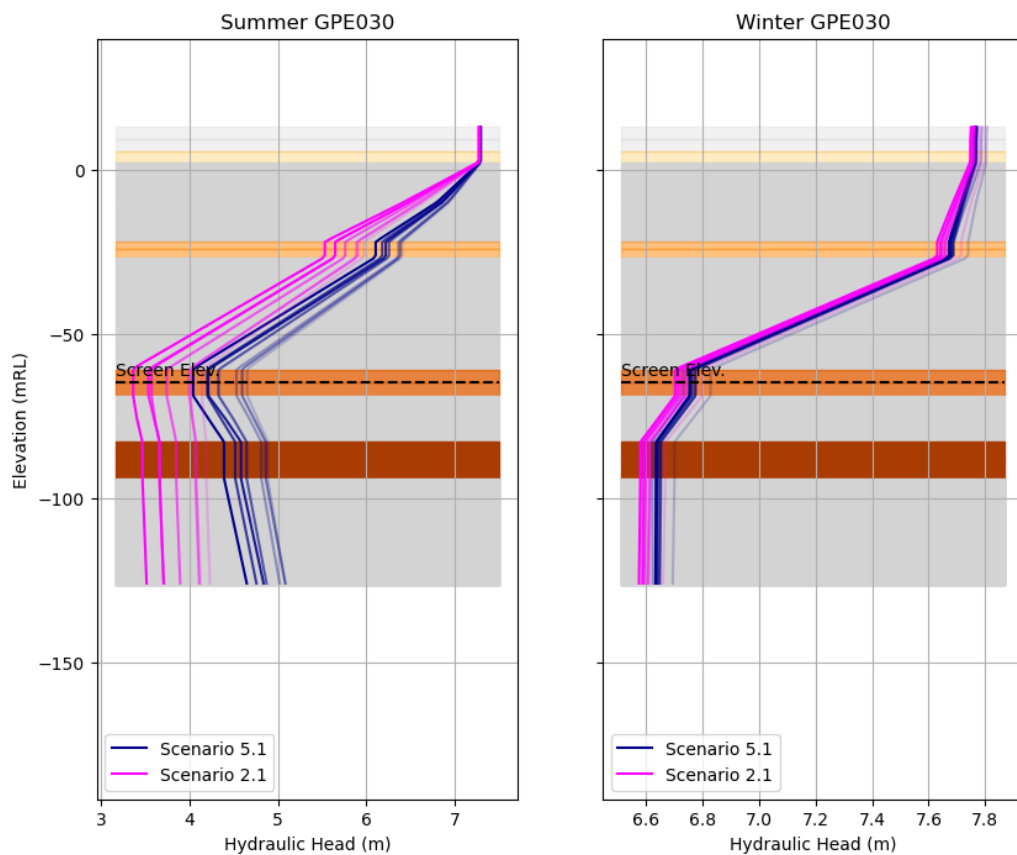


Figure 5-27: Comparison of hydraulic head in summer and winter between scenarios 4.1 and 2.1, observation bore GPE030 (Makauri)

Even though there are clearly higher levels than without MAR, Figure 5-28 shows that while winter levels increase, the summer water levels decline over time with increasing abstraction. This can be attributed on the one hand to the fact that abstraction is not fully balanced by MAR, on the other hand, groundwater replenishment does not occur exactly at the same location and at the same time as abstraction. It would have to be studied more in detail to what degree MAR can balance abstraction under such circumstances, and whether the conditions can be improved by optimising time and location of the replenishment.

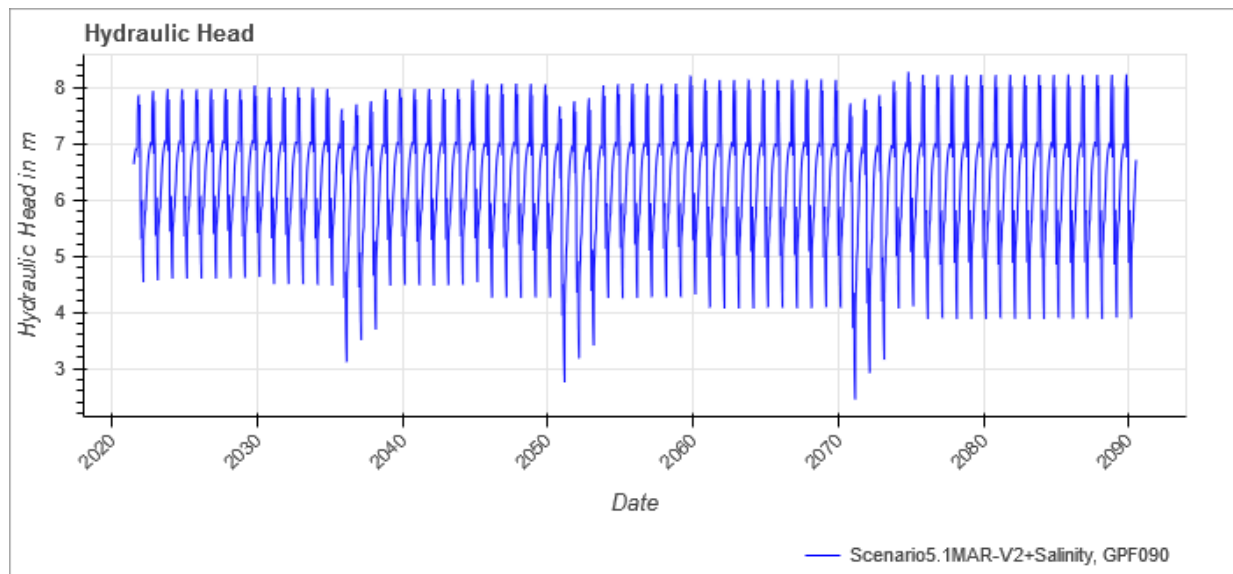


Figure 5-28: Simulated groundwater potential in scenario 5.1 over time, observation bore GPF090 (Makauri)

5.6. Scenario 7.1 Sustainable Allocation + Climate Change (SA)

Scenario 7.1 aims towards identifying an abstraction rate that is sustainable. Defining such a sustainable pumping rate requires a thorough definition with respect to what is to be protected and what changes are still seen as sustainable. These definitions can only be obtained in a political discussion process, involving stakeholders and the community. Therefore, for scenario 7.1 a simplified definition of sustainable has been used.

In scenario 7.1, the amount of abstraction is to be reduced to a degree that groundwater levels and hydraulic potential do not decline below currently observed levels. As groundwater pumping is assumed to increase for climatical reasons, the base level would have to be reduced even more to prohibit drawdowns exceeding the current ones in the future. As for such a scenario definition and immediate reduction of pumping rates, the time horizon at the end of the simulation period (2089) seems way too long, the year 2050 was chosen as a comparison target. This means that an abstraction rate was chosen that allows groundwater levels to stay above the current ones until about 2050 under the assumed climatic conditions.

5.6.1. Scenario Parameters

From a number of simulations, it has been found that at about 85% of the abstractions considered in scenario 2.1 (chapter 5.2) the groundwater potential throughout the aquifers stays above current levels at least until about 2050. Thus, the parameterisation of scenario 7.1 corresponds to the one of scenario 2.1, except that all abstraction rates are cut back by 15%.

Table 5-9 gives an overview on the temporarily variable abstraction amounts of scenario 7.1.

Table 5-9: Overview of abstraction amounts of scenario 7.1 Sustainable Allocation + Climate Change (SA)

Stepwise increased abstraction incl. 3 3-year draught periods scenario 2.1	Increase against to the base abstraction	Hydrological Year	Abstraction amount m ³ /year
no increase till 2029	0	2021/22 - 2028/29	1,009,800
increase 5% from 2030	0.05	2029/30 – 2034/35	1,060,290
		2035/36	1,582,879
		2036/37	1,428,601
		2037/38	1,354,653
		2038/2039 – 2043/44	1,060,290
increase 15% from 2045	0.15	2044/2045 – 2049/50	1,161,270
		2050/51	1,869,304
		2051/52	1,687,110
		2052/53	1,599,780
		2053/54 – 2058/59	1,161,270
increase 24% from 2060	0.24	2059/60 – 2069/70	1,252,152
		2070/71	2,004,979
		2071/72	1,809,562
		2072/73	1,715,893
		2073/74	1,252,152
increase 33% from 2075 till 2090	0.33	2074/2075 – 2089/90	1,343,034

5.6.2. Scenario Results

According to the basic idea of reducing abstraction to prohibit a further groundwater decline, groundwater levels are expected to be approximately the same at the end of the simulation period compared to current time. This means an increase compared to the results of scenario 2.1. An overview of statistical changes in between the different scenarios is shown in chapter 0. The water levels in general are comparable to the ones of scenario 3.1 with no pumping at all.

Figure 5-22 through Figure 5-25 show the differences in hydraulic head between scenario 7.1 and scenario 2.1 at the end of the simulation period (year 2089), and therefore indicate the long-term change induced by a reduction of base groundwater abstraction now. One plot is shown for each of the aquifers.

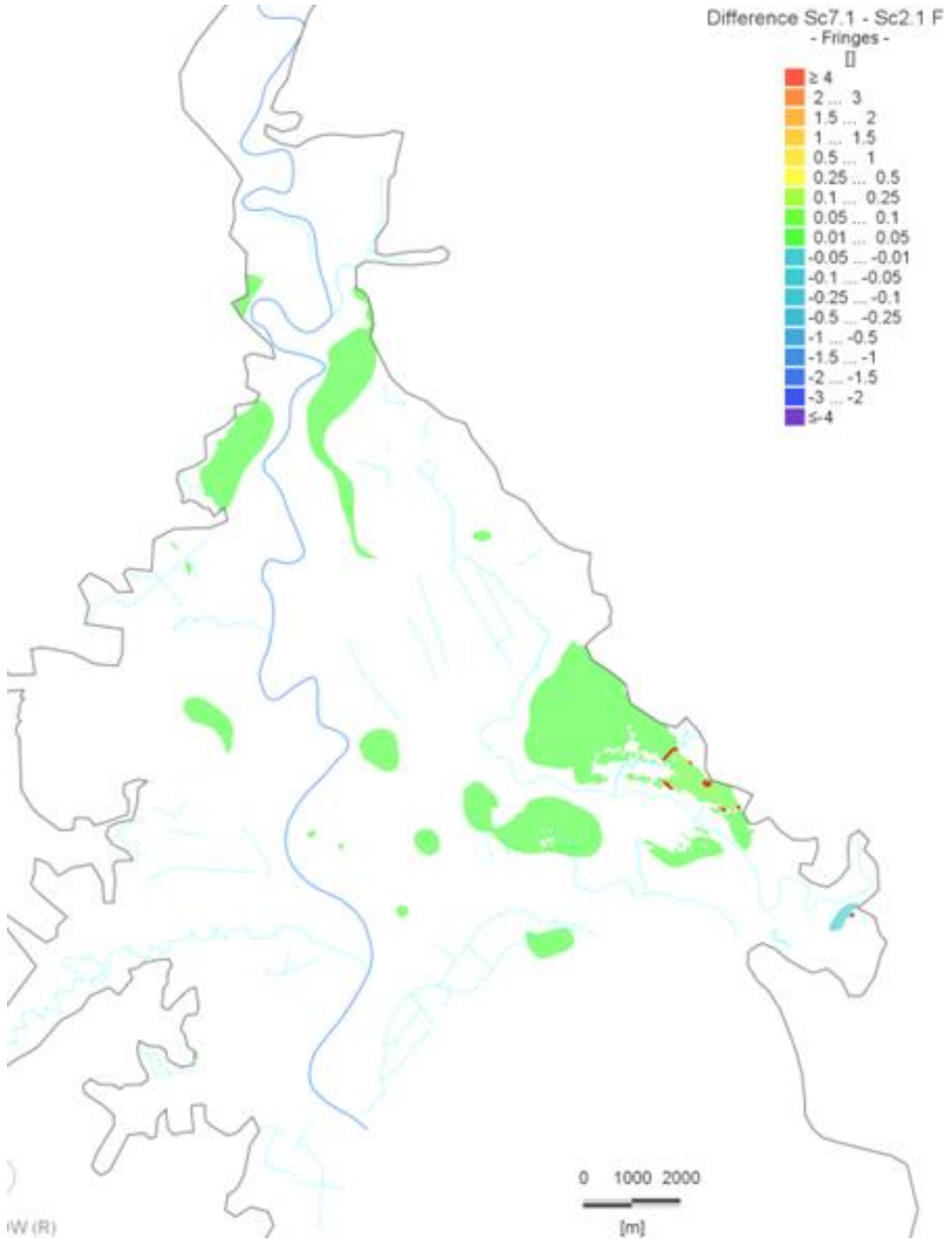


Figure 5-29: Difference of simulated groundwater level between scenario 7.1 and scenario 2.1 in the shallow aquifer system at the end of the simulation period (year 2089)

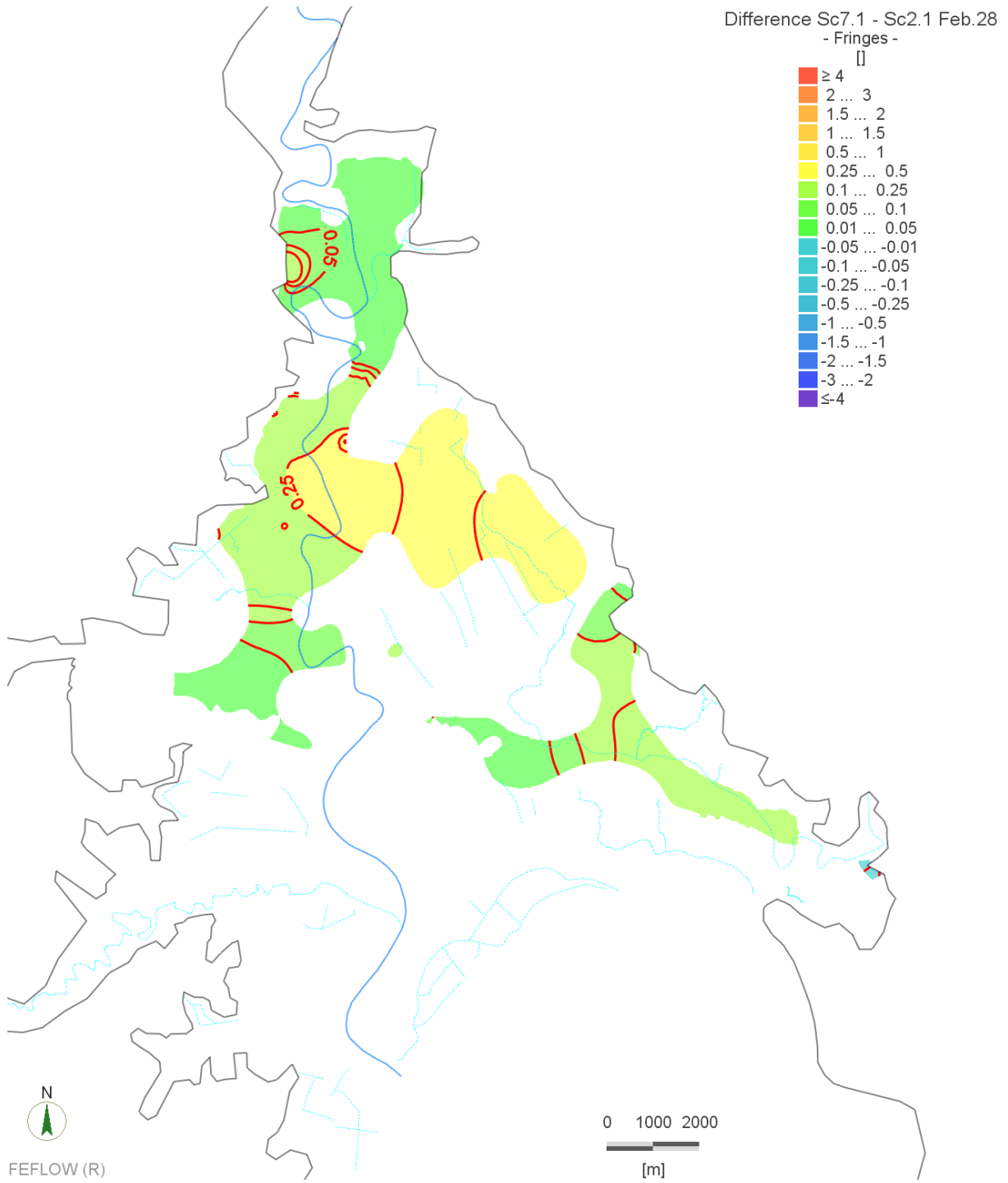


Figure 5-30: Difference of simulated groundwater level between scenario 7.1 and scenario 2.1 in the Waipaoa aquifer at the end of the simulation period (year 2089)

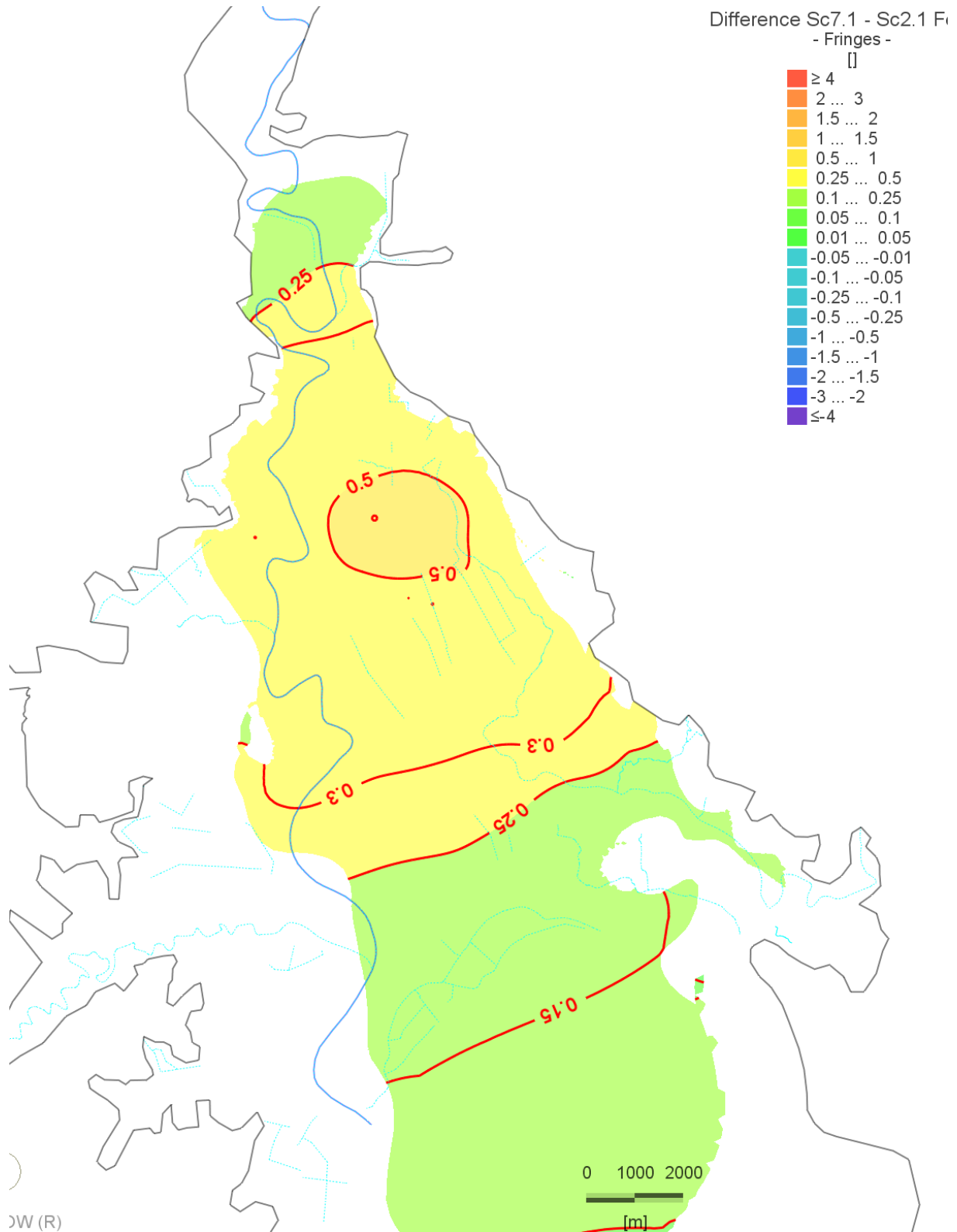


Figure 5-31: Difference of simulated groundwater level between scenario 7.1 and scenario 2.1 in the Makauri aquifer at the end of the simulation period (year 2089)

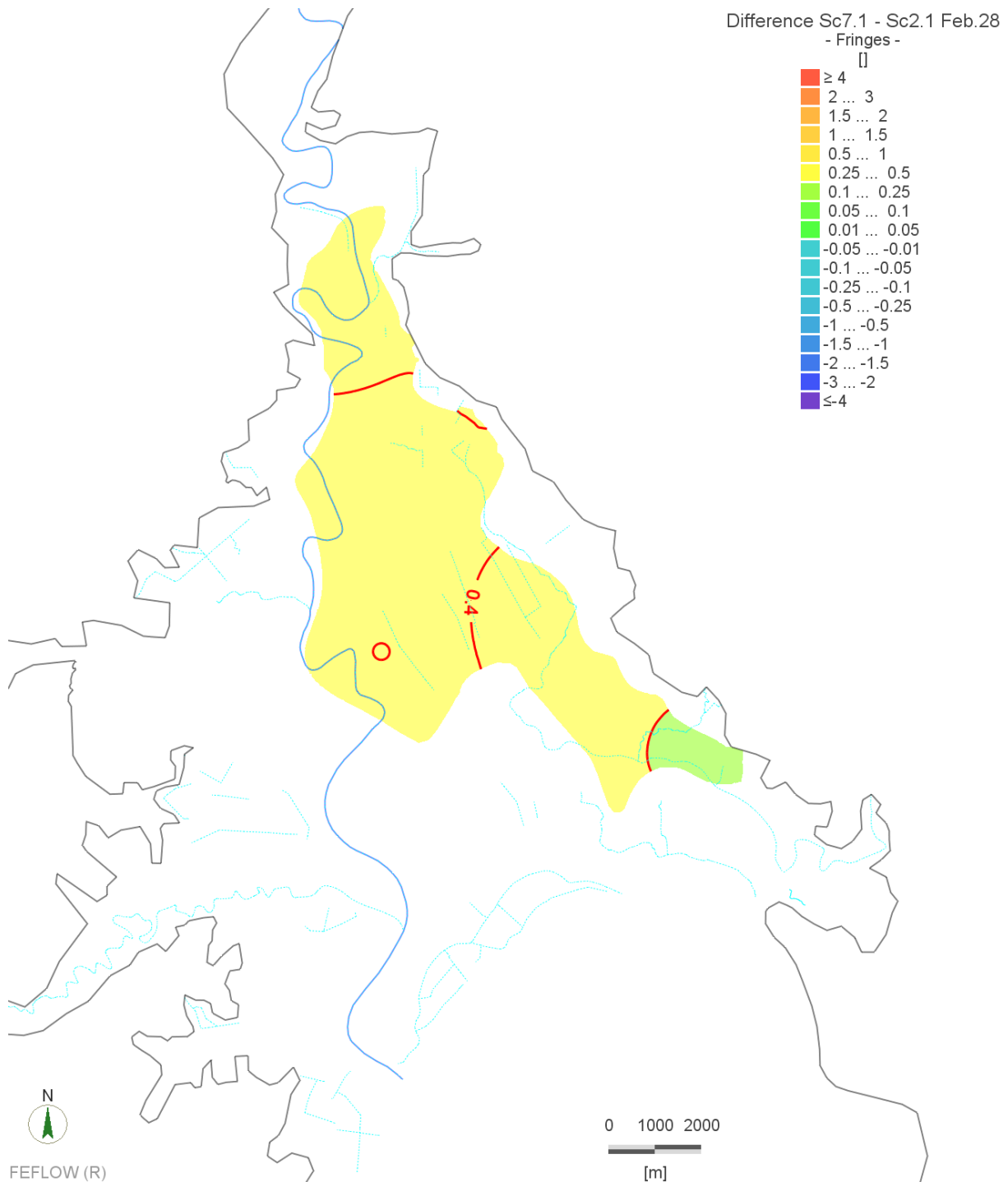


Figure 5-32: Difference of simulated groundwater level between scenario 7.1 and scenario 2.1 in the Matokitoki aquifer at the end of the simulation period (year 2089)

In the following, some aspects of the results in comparison of scenario 7.1 to scenario 2.1 are underpinned by presenting a number of exemplary diagrams, explaining different kind of behaviour in different locations within the model area. A full set of plots, both time-series/time-series differences for observation bores and as well as vertical head plots are available in the digital appendix.

In Figure 5-33 it can be seen that at the location of the observation bore GPC112 in the shallow aquifer system, the summer groundwater levels (approximated by red line) stay above the current level (green line) until 2050, except for draught periods. Due to the further increased amounts of groundwater abstraction to match climatically increasing transpiration of irrigated crops, on the long term even at a

starting level of only 85% of the current pumping rates, summer groundwater potential further declines below the current values (in the example bore about 10 cm below current level in 2089). This is also visible in Figure 5-34, where the most opaque blue line (scenario 7.1, year 2085) is situated to the left of the most transparent magenta line (scenario 2.1, year 2025). Hydraulic head in winter stays higher than the current level in scenario 7.1 throughout the simulation period due to the reduction in abstraction.

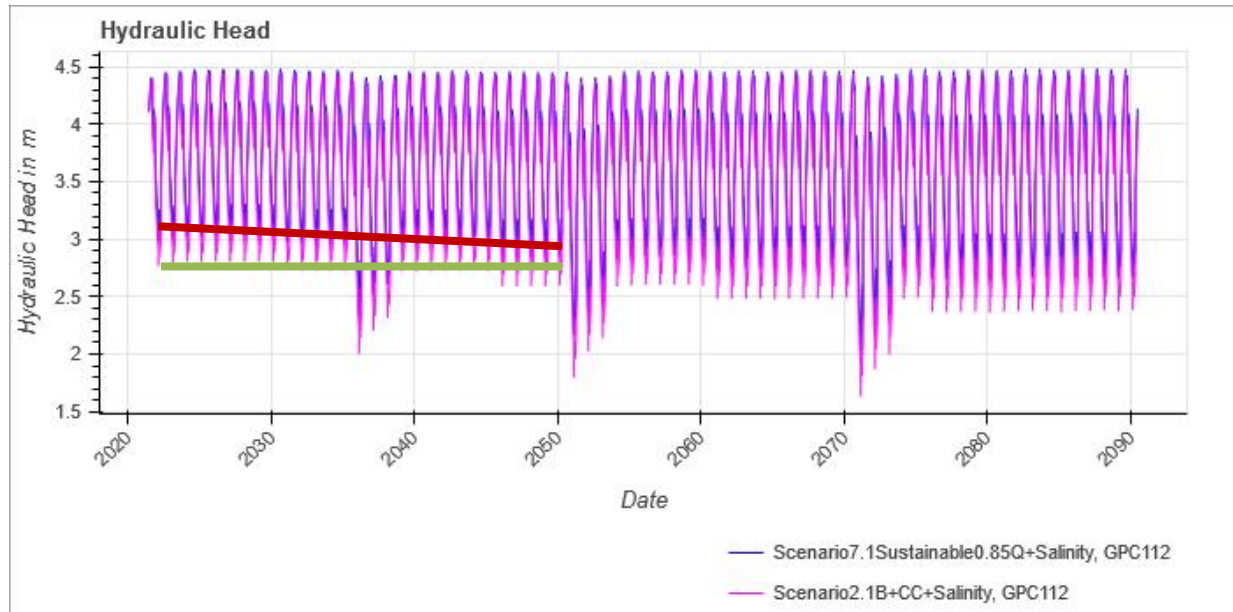


Figure 5-33: Simulated groundwater potential in scenario 7.1 and 2.1 over time, observation bore GPC112 (Makauri), current summer level highlighted in green, declining level in scenario 7.1 in red.

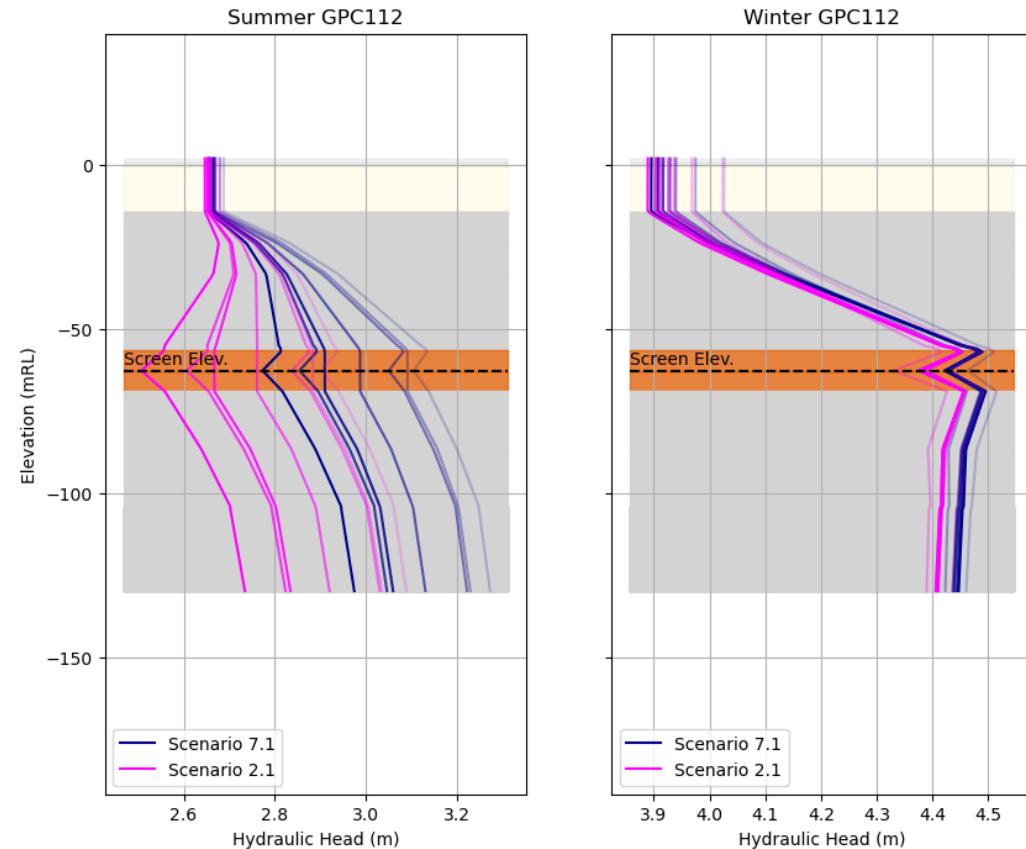


Figure 5-34: Comparison of hydraulic head in summer and winter between scenarios 7.1 and 2.1, observation bore GPC112 (Makauri)

5.7. Sensitive locations

A number of sensitive locations have been identified in a joint process with GDC and iwi stakeholders, which are listed in Figure 5-35.

Categories	Aquifer connection	Surface water connections	Rationale	Status choices
Cultural	Te Hapara Sands	Te Waiohiorore	Has there been a relative change in trend for levels at GPA003?	Likely improved/
		Awapuni Moana Drains	Has there been a relative change in trend for levels at GPC080 and GPC094?	Likely stayed the same/
Surface Water Ecosystems	Shallow Fluvial/Aquifer	Waipaoa River baseflow	<ul style="list-style-type: none"> Has there been a relative change in trend for levels at GPF068 and GPC080? Check changes of outflow to Waipaoa River. 	Likely worsened
		Matawhero Wetland	Can relative changes in trend be presented for the gauge in Matawhero loop? GPC029	
		Taruheru baseflow	<ul style="list-style-type: none"> Has there been a relative change in trend for levels at GPB099? Check changes of outflow to Taruheru River. 	
Salinity	Makauri Aquifer	N/A	Has there been a relative change in trend for salinity at GPD115 and GPJ040?	
	Te Hapara Sands	N/A	Has there been a relative change in trend for salinity at GPC026?	

Figure 5-35: Sensitive locations as compiled by GDC based on project meetings.

The locations can be divided into the following categories:

1. Cultural
2. Surface-water ecosystems
3. Salinity

In the following, the scenario results are discussed for cultural and surface-water ecosystem locations. Salinity changes are discussed in chapter 6.4. It needs to be mentioned that predictions for the shallow aquifer system, especially where closely related to surface water systems are subject to some uncertainty in the model. The surface water system is implemented in a simplified way, and local water levels might strongly be influenced by factors like geometry of the surface water bodies in detail, connection of wetlands to larger streams/ rivers, active or passive management (tidal shutters).

Cultural

The focus for these locations is on the connection of the surface-water and groundwater systems at Te Waiohiorore and the Awapuni Moana Drains.

When we look at the temporal development of the groundwater level at Te Waiohiorore (GPA003), then we can see that considering climate change leads an increase of the groundwater level by about 20 cm by 2090 compared to now (Figure 5-36). This is a direct effect of the sea-level rise considered in all scenarios starting with 2.1. When comparing the scenarios for different management (Figure 5-37) that add modifications in addition to the climate-change conditions considered in 2.1, sea level rise is no more visible as it is common to all these scenarios. Stopping pumping altogether would lead to a rise of about 4 cm, pumping at full allocation to a drop of about 6 cm, MAR and reduced abstraction to close to no change.

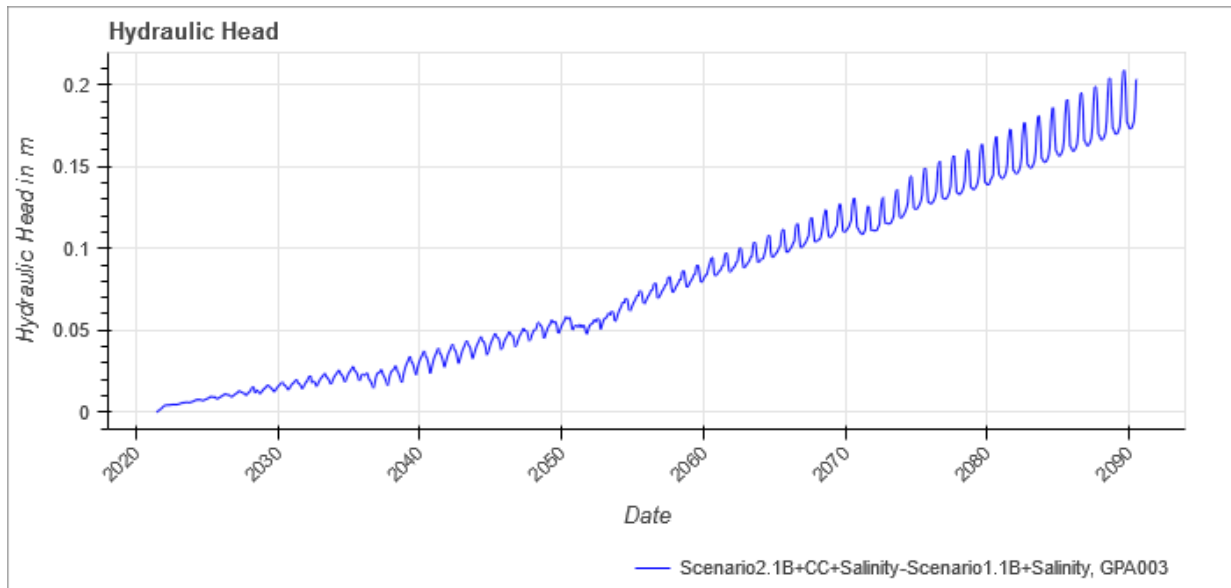


Figure 5-36: Difference between scenario 2.1 and scenario 1.1, GPA003.

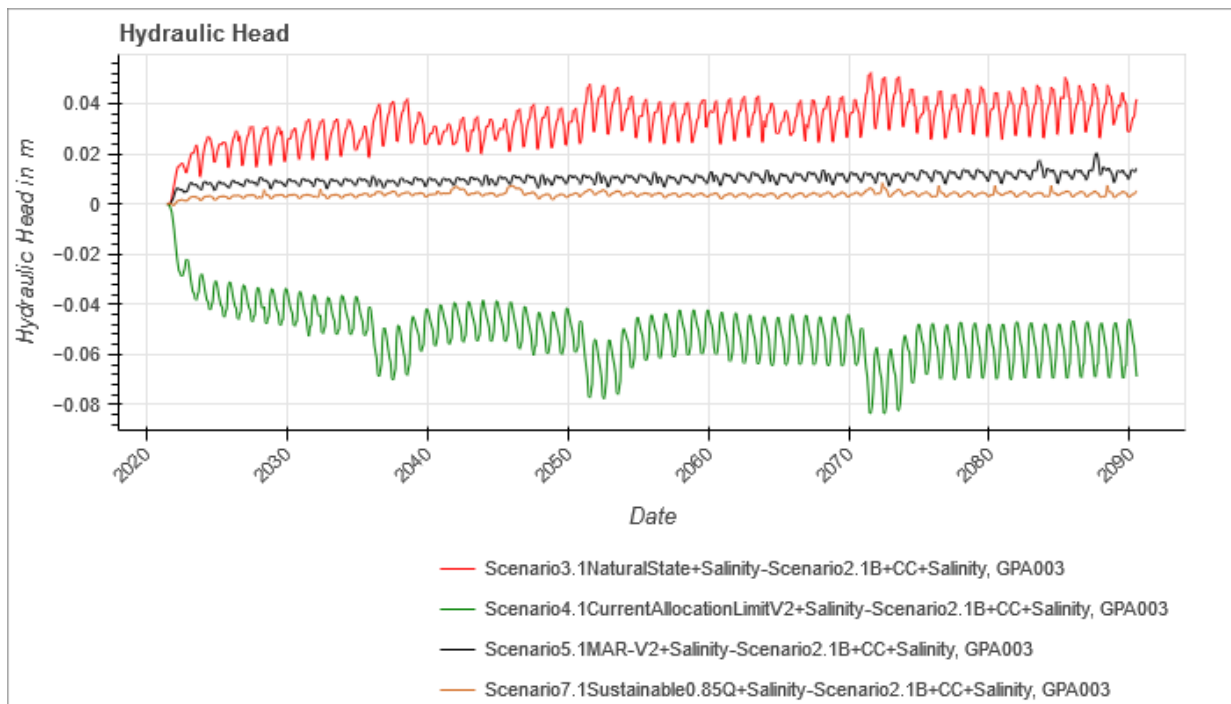


Figure 5-37: Difference between scenario 3.1, 4.1, 5.1, 7.1 and scenario 2.1, GPA003.

North of the Awapuni Moana Drains, considering climate change leads to a decline in groundwater level by about 9 cm in summer, and a very small increase in winter (Figure 5-38). While the increase is probably caused by sea-level rise, the decrease in summer seems to be caused by increasing groundwater abstraction. The management scenarios differ by about 10-15 cm, with pumping at full allocation causing a decline of about 8 cm (up to 10 cm in draught years), and a complete stop to abstraction leading to an increase of groundwater level by about 4 cm (Figure 5-39).

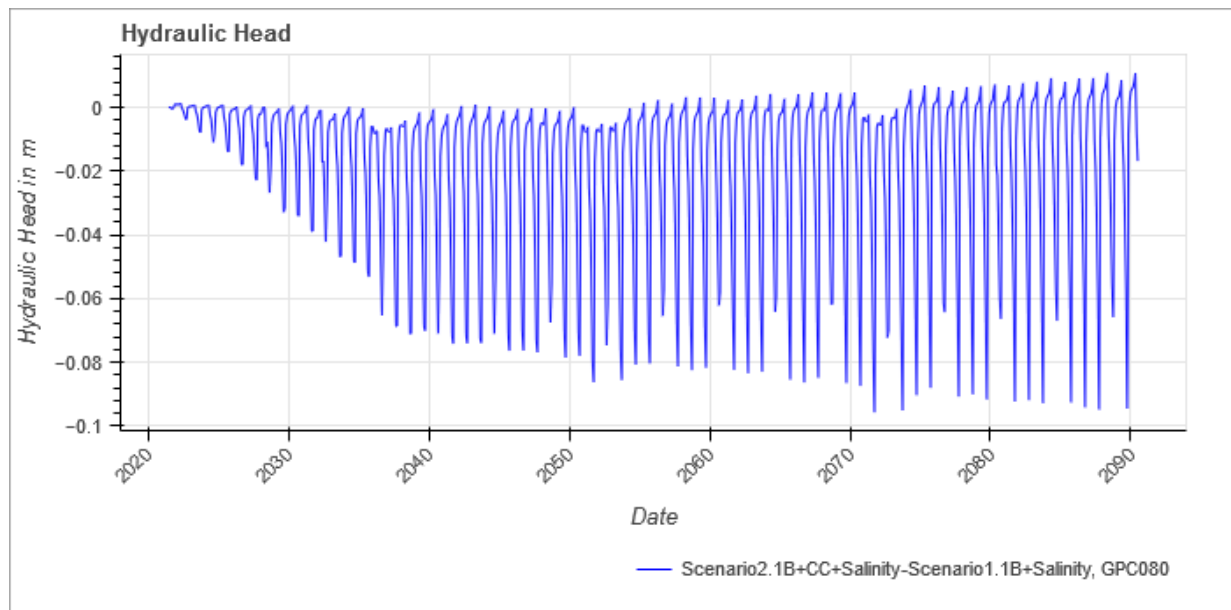


Figure 5-38: Difference between scenario 2.1 and scenario 1.1, GPC080.

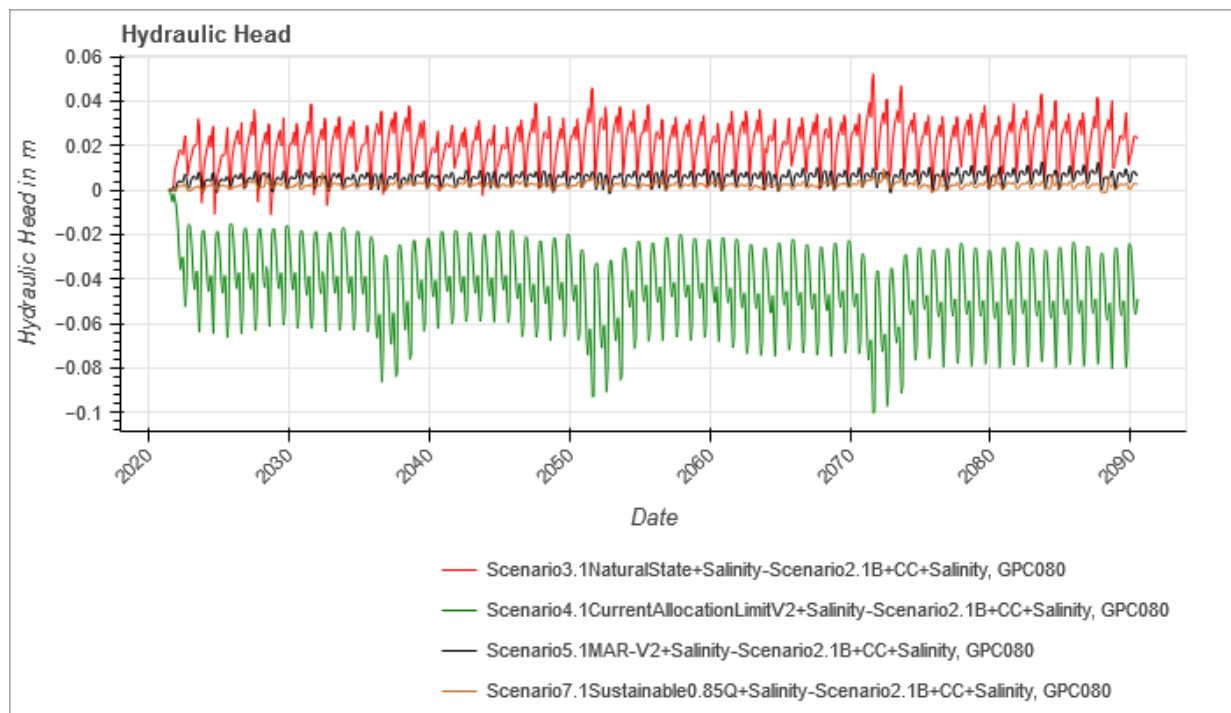


Figure 5-39: Difference between scenario 3.1, 4.1, 5.1, 7.1 and scenario 2.1, GPC080.

Surface-water ecosystems

The effect of the different scenarios at the location of the bore GPC080 have already been described above. The mentioned bore GPE068 is in Makauri and therefore does not have a direct connection to the Waipaoa River.

At Matawhero Wetland (GPC029) climate change as considered in the model causes a very small decline in groundwater levels in winter, but a larger decline in summertime and especially during draught periods (Figure 5-40). Reason is the increased abstraction in this scenario.

Especially the increased abstraction when pumping at full allocated rates causes a large additional

drawdown of about 30 cm at the end of the simulation period, and close to 40 cm during draught periods (Figure 5-41).

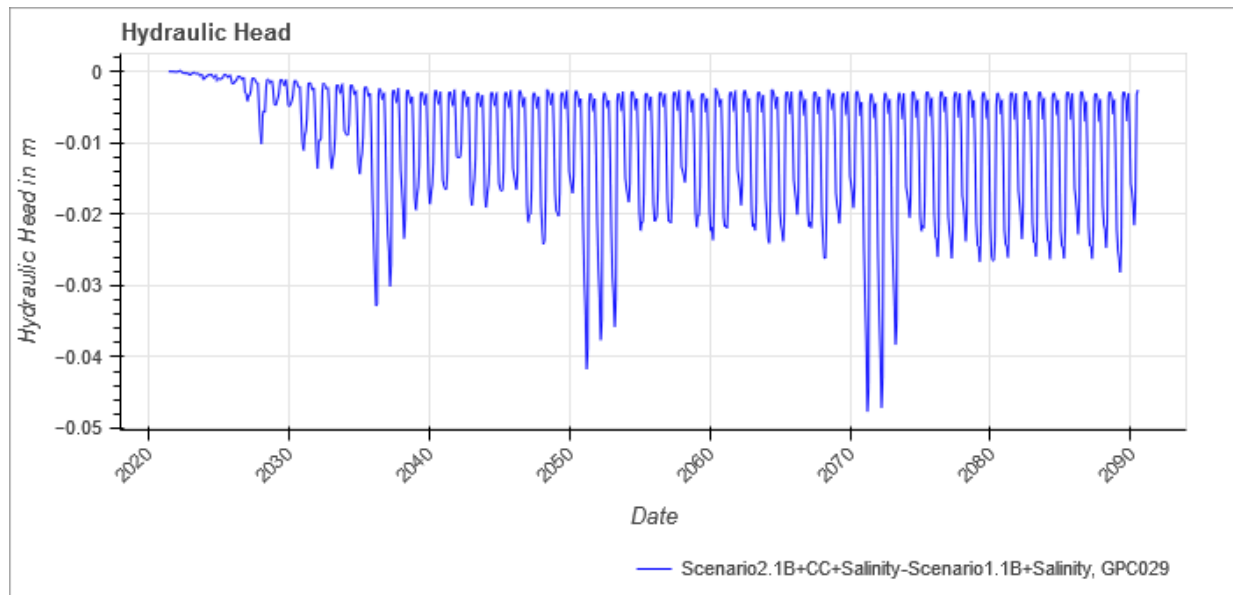


Figure 5-40: Difference between scenario 2.1 and scenario 1.1, GPC029.

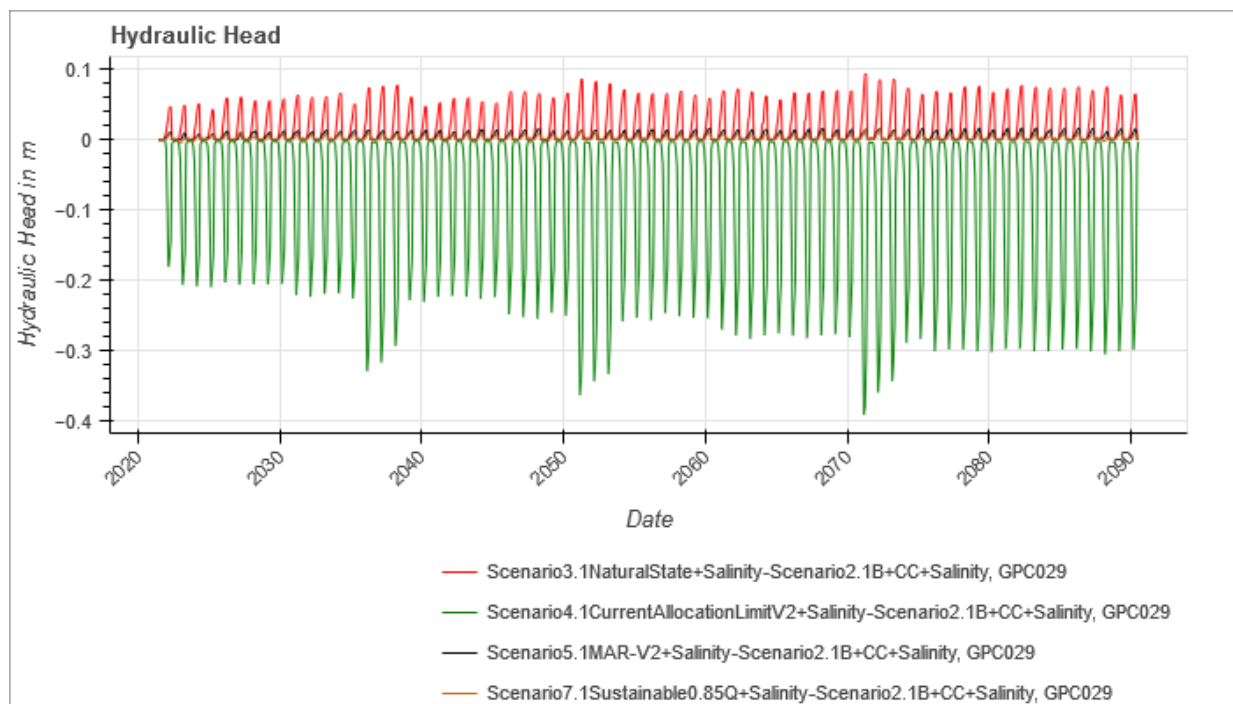


Figure 5-41: Difference between scenario 3.1, 4.1, 5.1, 7.1 and scenario 2.1, GPC029.

At Taruheru River (GPB099), the climate-change scenario shows a decline of groundwater level in the shallow aquifer by about 15 cm (Figure 5-42). The paper-allocation scenario leads to an additional draw-down of about 30 cm in summer (Figure 5-43).

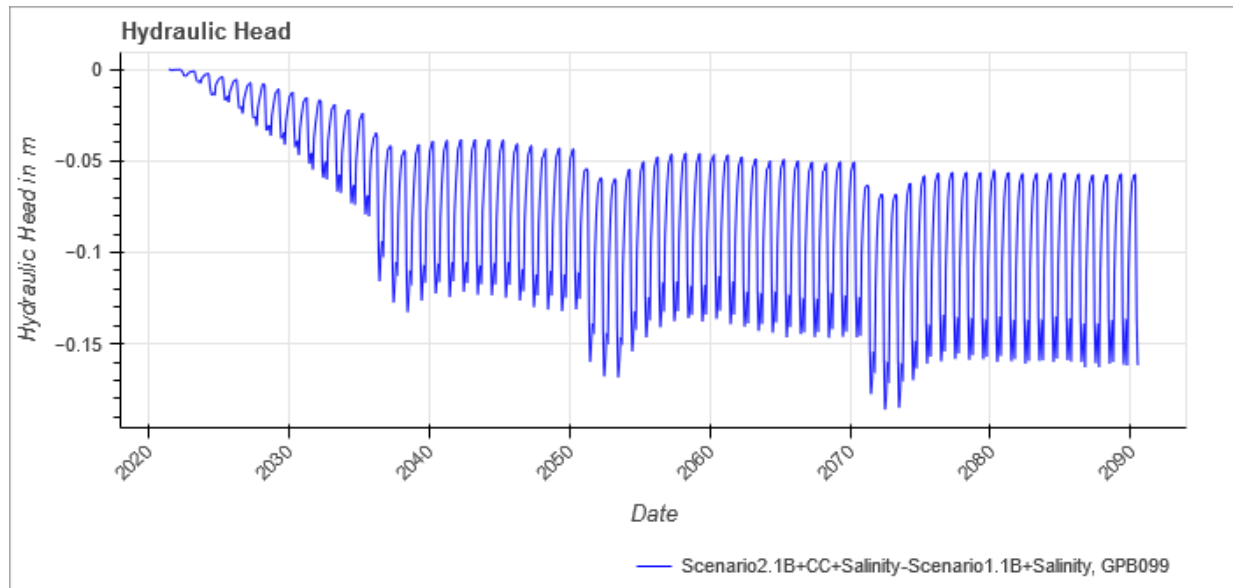


Figure 5-42: Difference between scenario 2.1 and scenario 1.1, GPB099.

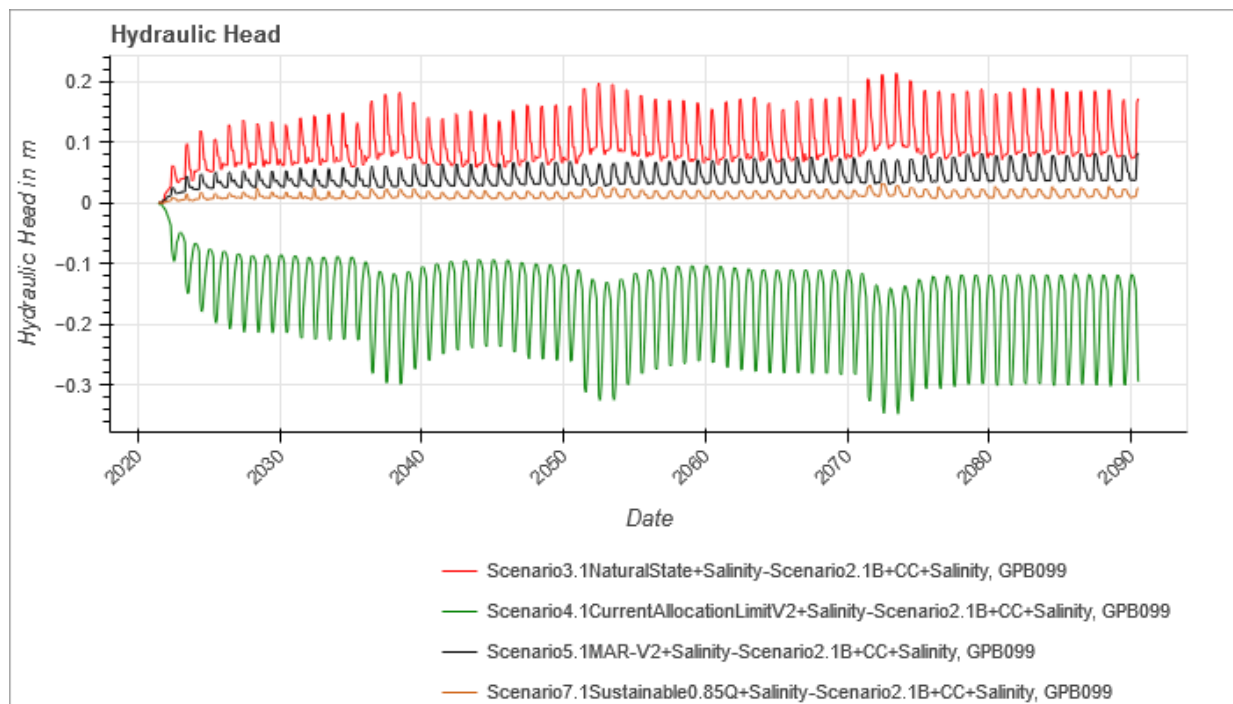


Figure 5-43: Difference between scenario 3.1, 4.1, 5.1, 7.1 and scenario 2.1, GPB099.

The cumulative changes in baseflow to the Waipaoa River are shown in chapter 0, local changes to smaller rivers/streams are not shown here because of the inherent uncertainty due to the necessary simplification of the surface-water system in the current model.

5.8. Scenarios Summary

The scenarios depict forecasts for the future under different circumstances, some of which refer to climate development, others are chosen with respect to aquifer management options. The longer the forecast period, the larger the band of potential deviation from reality – both for the outcomes of the groundwater model and the underlying climate predictions. So rather than taking the scenario results as a precise quantitative prediction of a future reality, they should be seen as indicators on the aquifer reaction under the respective conditions. Those reactions per se are neither good nor bad, which is why in order to be used to support the development of future actions, the scenarios need to be complemented by the formulation of protection and/or management goals against which the scenario results can be compared. For evaluating such goals or targets, the general process understanding as outlined in chapter 0 is of immense importance. So, for example, a lowering of the hydraulic potential in the Makauri aquifer caused by increased abstraction will lead to less upward flow into the shallow aquifers in the southern part of the Poverty Bay Flats (potentially limiting water availability to a wetland), but at the same time it stimulates downward flow in the northern part of the Flats (potentially very slowly increasing freshwater availability in the deep aquifers over time).

In general, the scenario outcomes show that – among the variations considered – groundwater abstraction plays by far the most important role. Removing abstraction (in scenario 3) leads to increasing groundwater potential throughout the model, while considering the full currently allocated abstraction (scenario 4) predicts a further decline in groundwater potential, both in the confined and unconfined aquifers. Even the decline in groundwater levels under climate-change conditions (scenario 2) is predominantly caused by the assumption of additional required abstraction to fulfil increasing water demand for irrigation under the predicted conditions (increasing transpiration from irrigated crops). Changes in rainfall recharge and sea level that are also part of the climate-change predictions have a limited influence on groundwater level in the shallow aquifers. Apart from the per-scenario descriptions above, these relationships can also be seen in

Table 5-10 and Table 5-11 which show the average changes over all calculation nodes between the scenarios (comparing scenario 2.1 to 1.1 and all others to 2.1).

Table 5-10: Average water level/hydraulic head changes between the scenarios, summer season.

Scenario	Scenario Name	Difference of Simulated Average Water Level (m), Summer Season (28 February 2090)					Overall	Remark
		Mato-kitoki	Ma-kauri	Waipaoa	Shallow	Te Hapara Sands		
2.1	B+CC, Climate Change V2, Sc2.1	-0.66	-0.50	-0.32	-0.02	0.05		comp. to Scenario 1.1
3.1	Natural State V2 Sc3.1	2.66	2.18	1.23	0.03	0.05		comp. to Scenario 2.1
4.1	Current Allocation Limit V2, Sc4.1	-4.60	-3.16	-2.95	-0.05	-0.11		comp. to Scenario 2.1
5.1	MAR V2, Sc5.1	0.89	0.58	0.45	0.01	0.02		comp. to Scenario 2.1
7.1	Sustainable V2 with 85% Takes of Sc2.1, Sc7.1	0.40	0.32	0.18	0.00	0.01		comp. to Scenario 2.1

Table 5-11: Average water level/hydraulic head changes between the scenarios, winter season.

Scenario	Scenarios	Difference of Simulated Average Water Level (m), Winter Season (30 September 2089)					Overall	Remark
		Mato-kitoki	Ma-kauri	Waipaoa	Shallow	Te Hapara Sands		
2.1	B+CC, Climate Change	-0.09	-0.05	-0.09	-0.05	0.01		comp. to Scenario 1.1
3.1	Natural State with CC	0.27	0.25	0.14	0.02	0.00		comp. to Scenario 2.1
4.1	A1 Paper Allocation	-0.60	-0.58	-0.35	-0.05	-0.09		comp. to Scenario 2.1
5.1	MAR M1 (600,000 m³)	0.05	0.04	0.03	0.01	0.01		comp. to Scenario 2.1
7.1	Sustainable V2 with 85% Takes of Sc2.1, Sc7.1	0.04	0.04	0.02	0.00	0.00		comp. to Scenario 2.1

The average groundwater levels for scenarios with much higher abstraction rates show the least changes in the shallow aquifers, where surface water has a dampening effect on groundwater levels. However, from Figure 5-44 it can be seen that with climate change considered, but especially in scenario 4.1 with the much higher abstraction the Waipaoa River on average does not receive groundwater anymore, but has a net infiltration into the groundwater system. So, simplifying matters a bit, it can be said that additional

abstraction reduces the baseflow to rivers, streams, and drains, and might even lead to infiltration from surface water. Infiltration is only possible from larger rivers carrying enough water, smaller drains in such a situation may fall dry. The latter has not been evaluated in the model results, as – though technically drains have been designed to be able to fall dry – the level of detail in the upper aquifers does not allow for such local analysis. It would be required to capture the surface-water system more in detail in the model to do such analysis, after doing measurements of low flow in drains and rivers.

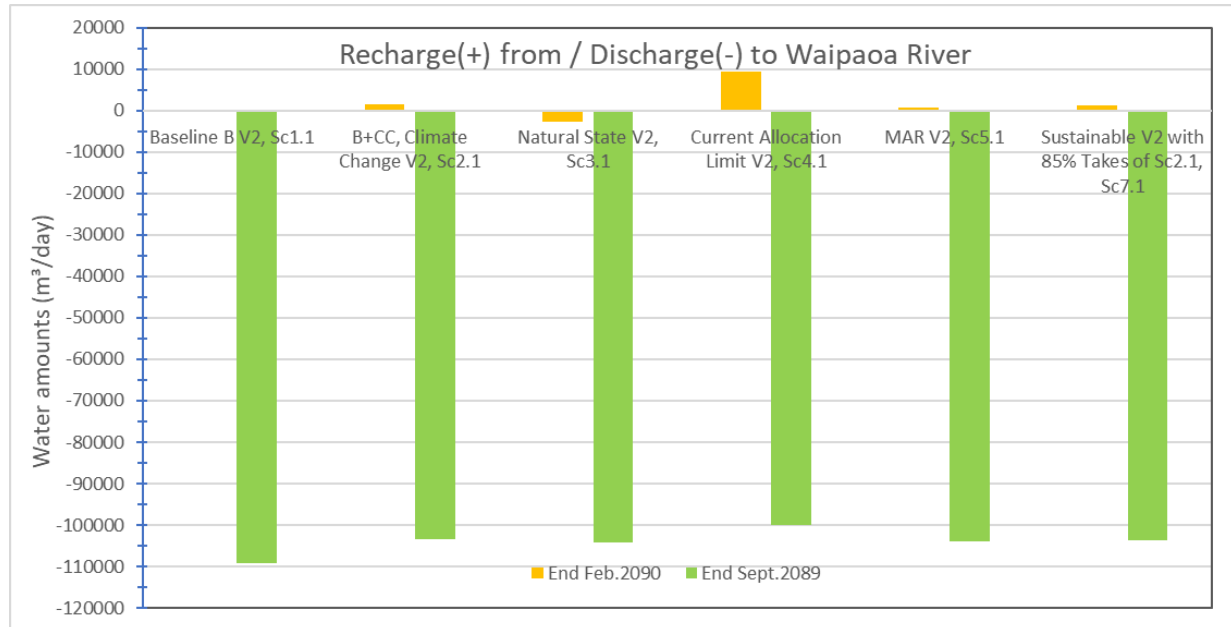


Figure 5-44: Interaction with Waipoa river (summer and winter season) for all scenarios at the end of the simulation period.

There are a number of theoretical courses of action considered in the scenarios to combat declining hydraulic heads in the future:

- Natural state: No abstraction, return to 'natural' state with respect to groundwater abstraction (landscape modifications such as drain construction, river course changes, etc. not reverted)
- Sustainable: Abstraction reduction to a degree that groundwater potential in the Makauri aquifer is not further declining
- MAR: Exemplary groundwater replenishment alternatives in order to balance increased abstractions

The results of the corresponding scenarios show that there are different options to avoid negative impacts on the groundwater system and related protected properties, and the model simulations show their effects in exemplary ways. Additional or alternative measures could be found and potentially tested with the model (such as modifications to management of the shallow aquifers, etc.).

When looking at the sites of cultural importance to iwi, all of the aforementioned scenarios lead to a reduction of the effects of increasing abstraction on local groundwater levels.

6. Water quality (salinity) simulation

Within the Poverty Bay aquifer system, groundwater salinity threatens the current and future use of groundwater for irrigation and drinking water. Major locations of potential water quality deterioration are the western boundary of the Makauri aquifer as considered in the model and along the coastline. Scenario simulations for water quality (salinity) are carried out based on the “Poverty Bay Flats Conceptual Groundwater Quality Model” (WGA [16]). Rather than attempting to provide quantitative predictions of salinity, the main purpose of the salinity scenario simulations is gaining an understanding of possible transport processes. Hereby, it is known in advance that the assumptions of the Conceptual Groundwater Quality Model do not cover all processes involved in causing groundwater salinity and the movement of groundwater of higher salinity. The following chapters describe the basis for the model formulation for Chloride transport as applied within this project.

6.1. Poverty Bay Flats Conceptual Groundwater Quality Model (WGA)

Poverty Bay Flats Conceptual Groundwater Quality Model (WGA [16]) provides, based on the analysis of available monitoring water quality data, a basic concept for numerical modelling of groundwater quality represented by chloride (Cl) concentration. The conceptual model with a limitation to chloride specifies

- Initial Cl concentration distribution in Te Hapara Sands, Shallow Fluviatile, Waipaoa, Makauri and Matokitoki aquifers
- Cl concentration in rainfall recharge in different parts of the shallow aquifers Te Hapara Sand and Shallow Fluviatile
- Average Cl concentration of Waipaoa River (9 mg/l)
- Cl concentration of sea water (20,000 mg/l)
- Simplified assumptions
 - no accumulation, no matrix interaction in aquifer
 - no additional sources of salt (e. g., dissolved from aquitards)
 - no initial chloride concentration in lateral aquitards.

Figure 6-1 through Figure 6-5 outline the initial Cl concentration distribution in Te Hapara Sands, Shallow Fluviatile, Waipaoa, Makauri and Matokitoki Aquifer, along with the corresponding Cl concentration of direct rainfall recharge respectively.

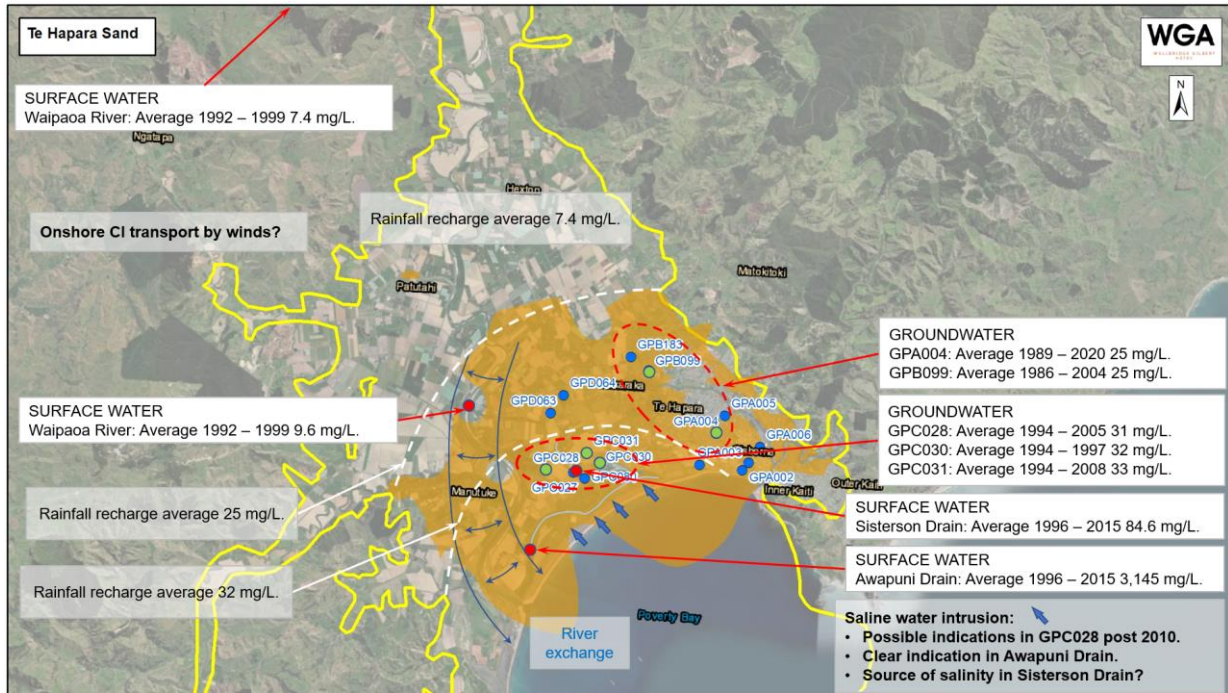


Figure 6-1: Initial Cl concentration distribution and concentration of rainfall recharge in Te Hapara Sands aquifer [16].

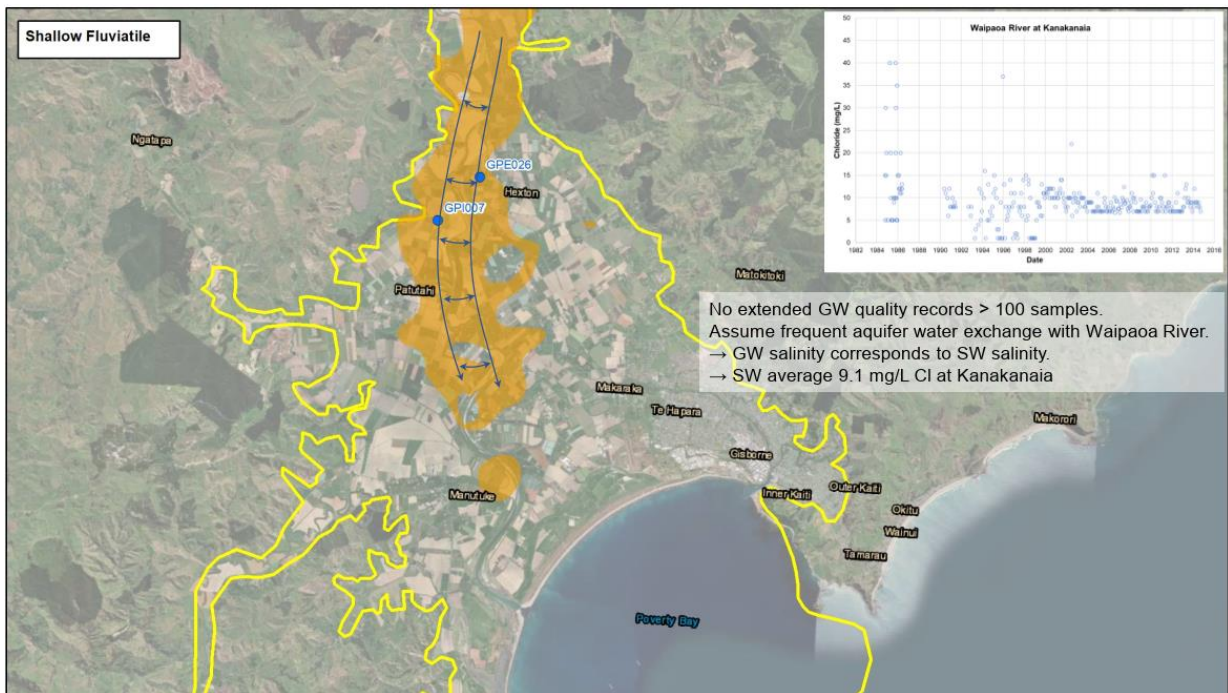


Figure 6-2: Initial Cl concentration distribution and concentration of rainfall recharge in Shallow Fluvatile aquifer [16].

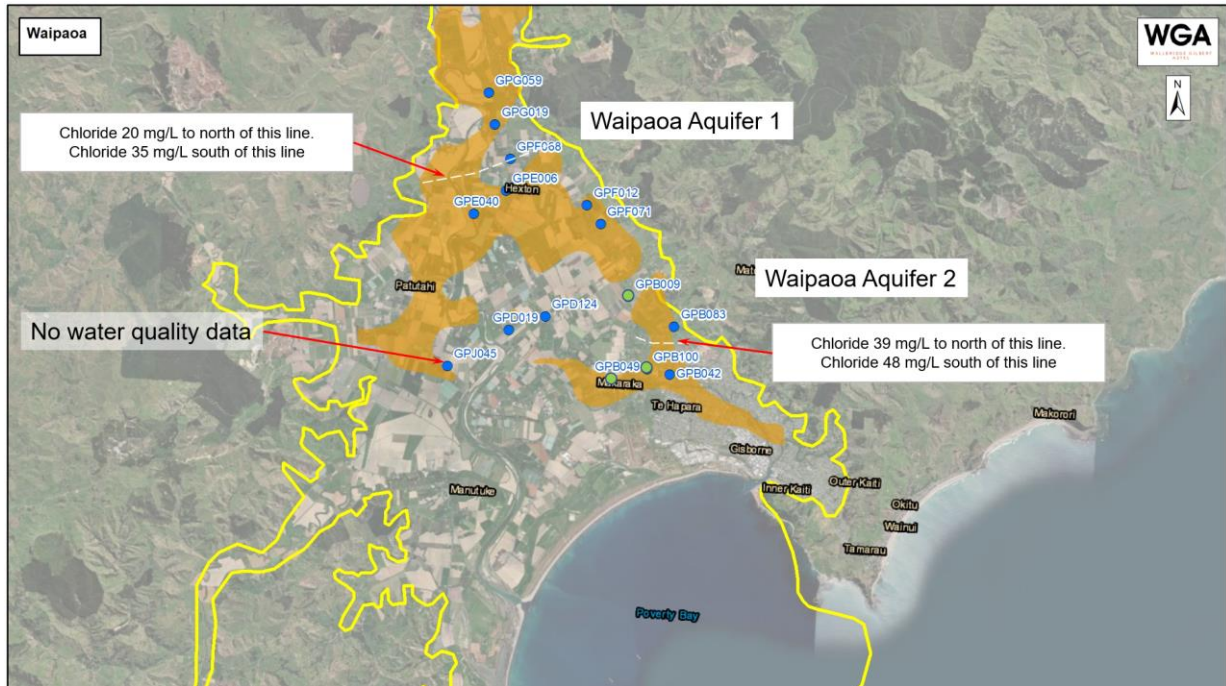


Figure 6-3: Initial distribution of Cl concentration in Waipaoa Aquifer [16].

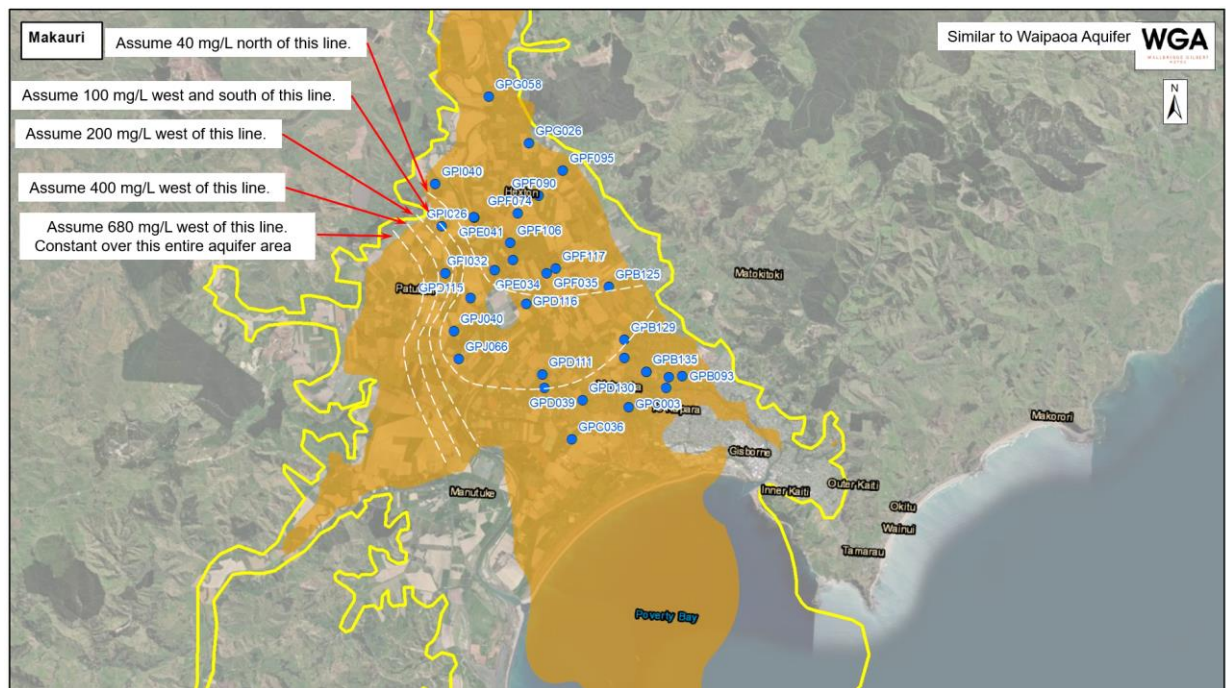


Figure 6-4: Initial distribution of Cl concentration in Makauri Aquifer [16].

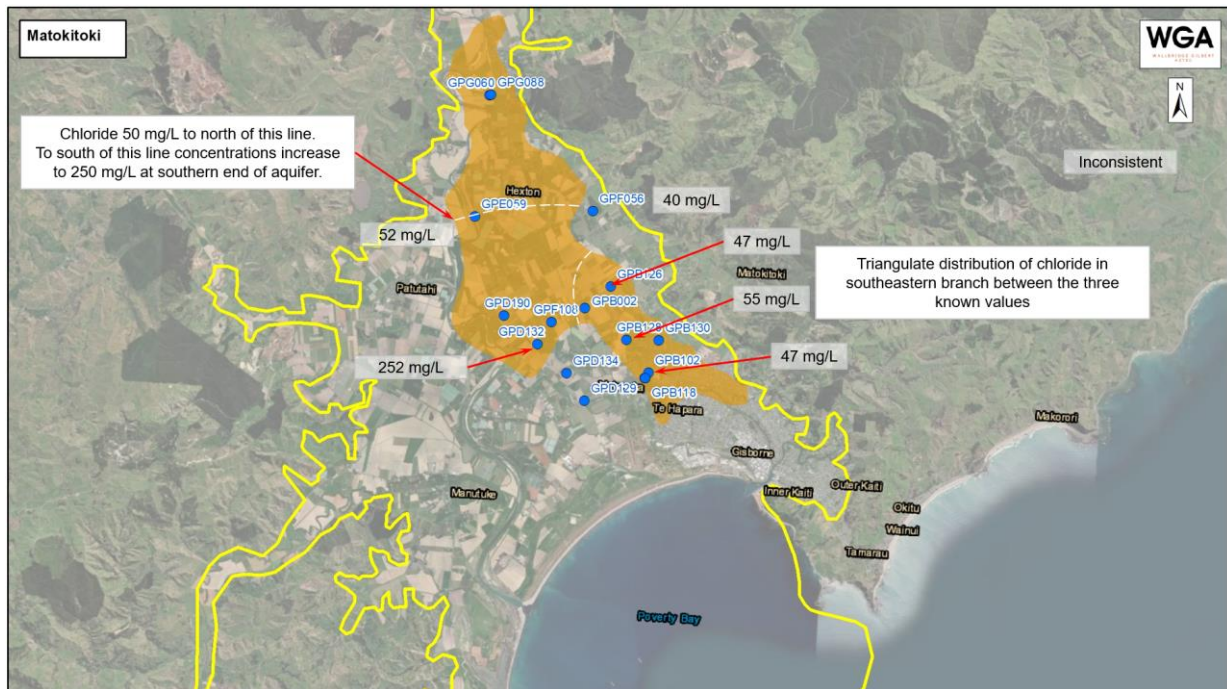


Figure 6-5: Initial distribution of Cl concentration in Matokitoki Aquifer [16].

6.2. Model parameterisation for salinity simulation

Transport porosity and dispersivity

The transport porosity and dispersivity for salinity simulation are the same as that used by the groundwater age simulation described in chapter 4.5.1

Initial Cl concentration and Cl concentration of rainfall recharge

Initial Cl concentration is set up for the aquifers Te Hapara Sands, Shallow Fluvatile, Waipaoa, Makauri and Matokitoki according to the Poverty Bay Flats Conceptual Groundwater Quality Model described above. Figure 6-6 through Figure 6-9 show the initial Cl concentration distributions in these aquifers. All aquitards in the model are assigned with 0 mg/l initial Cl concentration.

As FEFLOW does not directly support the setting of a Cl concentration in rainfall recharge, the following approach is used to nevertheless achieve this (important technical detail for future model application):

- Definition of a User Data distribution called RechargeConcentration in the top model layer with Cl concentration of rainfall recharge (see Figure 6-10) corresponding to the one specified by the Poverty Bay Flats Conceptual Groundwater Quality Model mentioned above.
- The defined RechargeConcentration is applied at run time through a Python script contained in the groundwater model during simulation run in accordance with recharge seasons specified in the groundwater model.

Cl concentration Boundary Conditions

The following Cl concentration boundary conditions are defined:

- Sea with a fixed Cl concentration boundary condition of 20,000 mg/l
- Waipaoa River with 9 mg/l considered only in case of recharge from the river into groundwater, which is controlled or/and realised by the Python script for setting rainfall recharge Cl concentration
- MAR bores with 9 mg/l in scenarios with managed groundwater replenishment, assuming the

infiltration of Waipaoa River water.

With the parameters specified above, test salinity simulations are undertaken for Scenario Baseline+CC (2.1). Evaluation of the outcomes shows a decline of simulated Cl concentrations in the Makauri Aquifer over the simulation period, due to the absence of salinity sources and refreshing by recharge with lower concentrations than that in aquifers.

Consequently, additional Cl concentration boundary conditions are defined as follows

- Cl concentration boundary conditions along the western border of the Makauri Aquifer, assigned with the corresponding initial Cl concentration as shown in Figure 6-10
- Cl concentration boundary conditions on the top of Aquitard 2 in the north-west, above the Makauri Aquifer, assuming the same initial Cl concentration as the one of the Makauri aquifer below, as shown in Figure 6-12.

The two additional Cl concentration boundary conditions can be interpreted as salinity sources there. They are not based on physical evidence and do not directly reflect an underlying physical process.

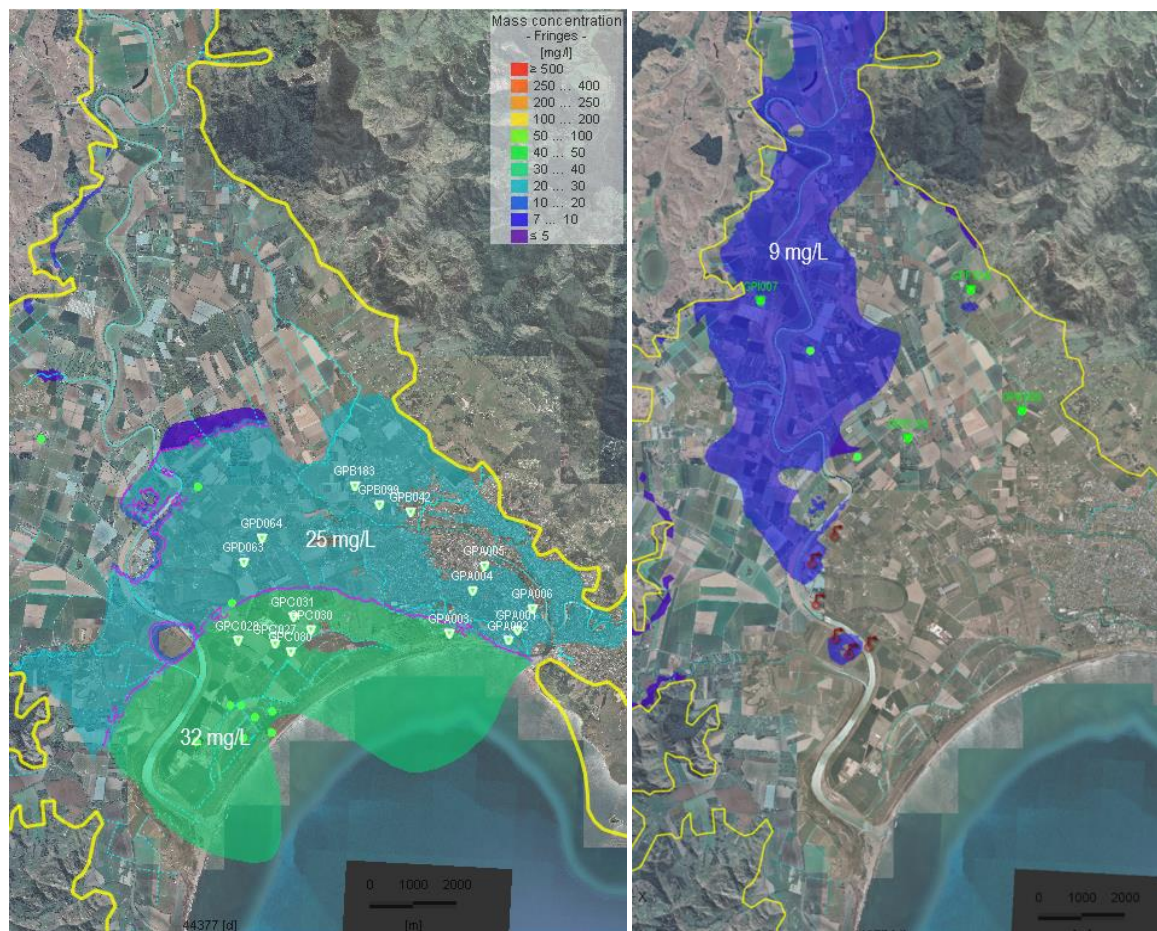


Figure 6-6: Initial distribution of Cl concentration and concentration of rainfall recharge assigned to Te Hapara Sands and Shallow Fluvial aquifers.



Figure 6-7: Initial distribution of Cl concentration and concentration of rainfall recharge assigned to Waipaoa aquifer.

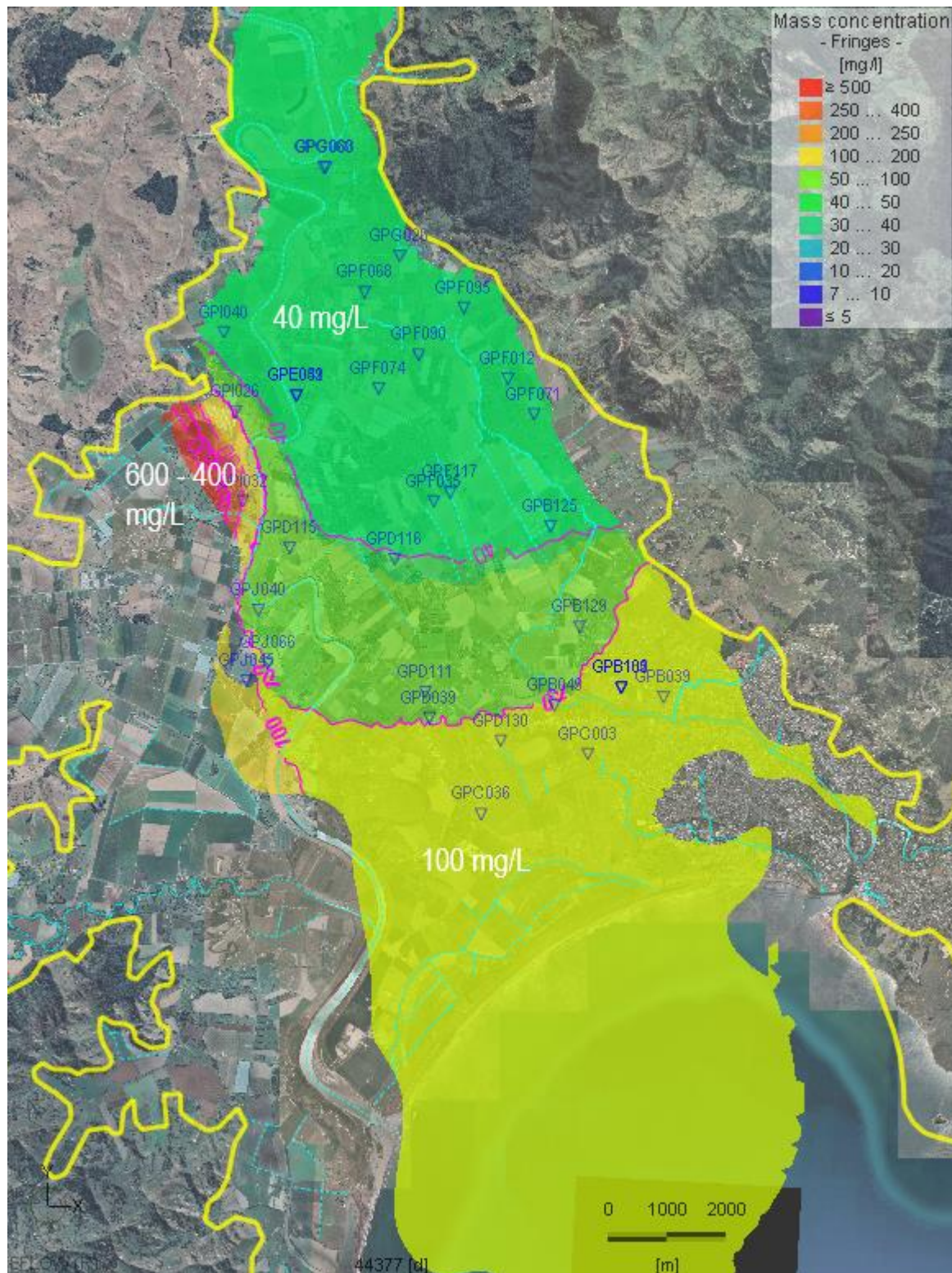


Figure 6-8: Initial distribution of Cl concentration assigned to Makauri aquifer.

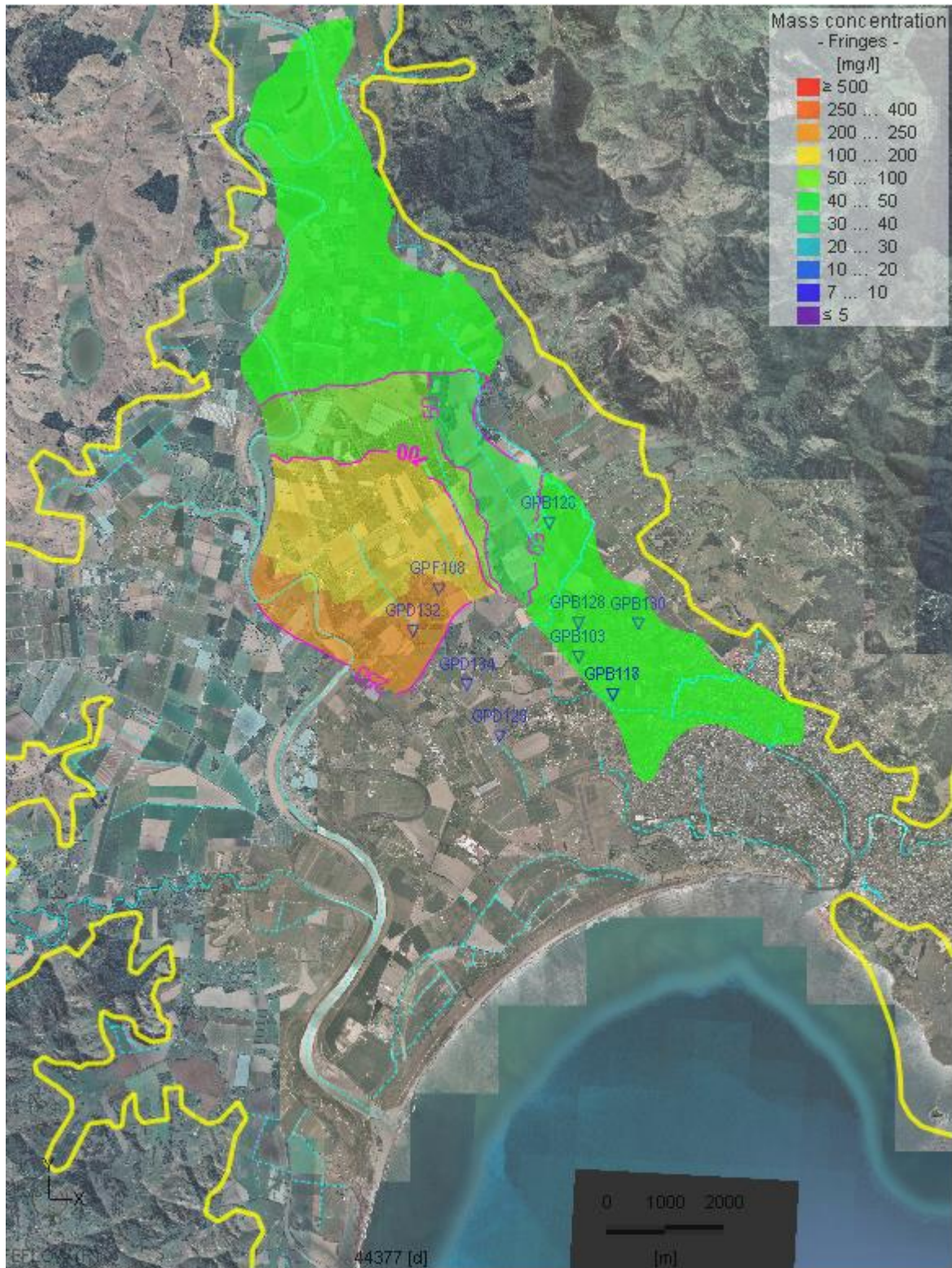


Figure 6-9: Initial Cl concentration assigned Matokitoki aquifer.

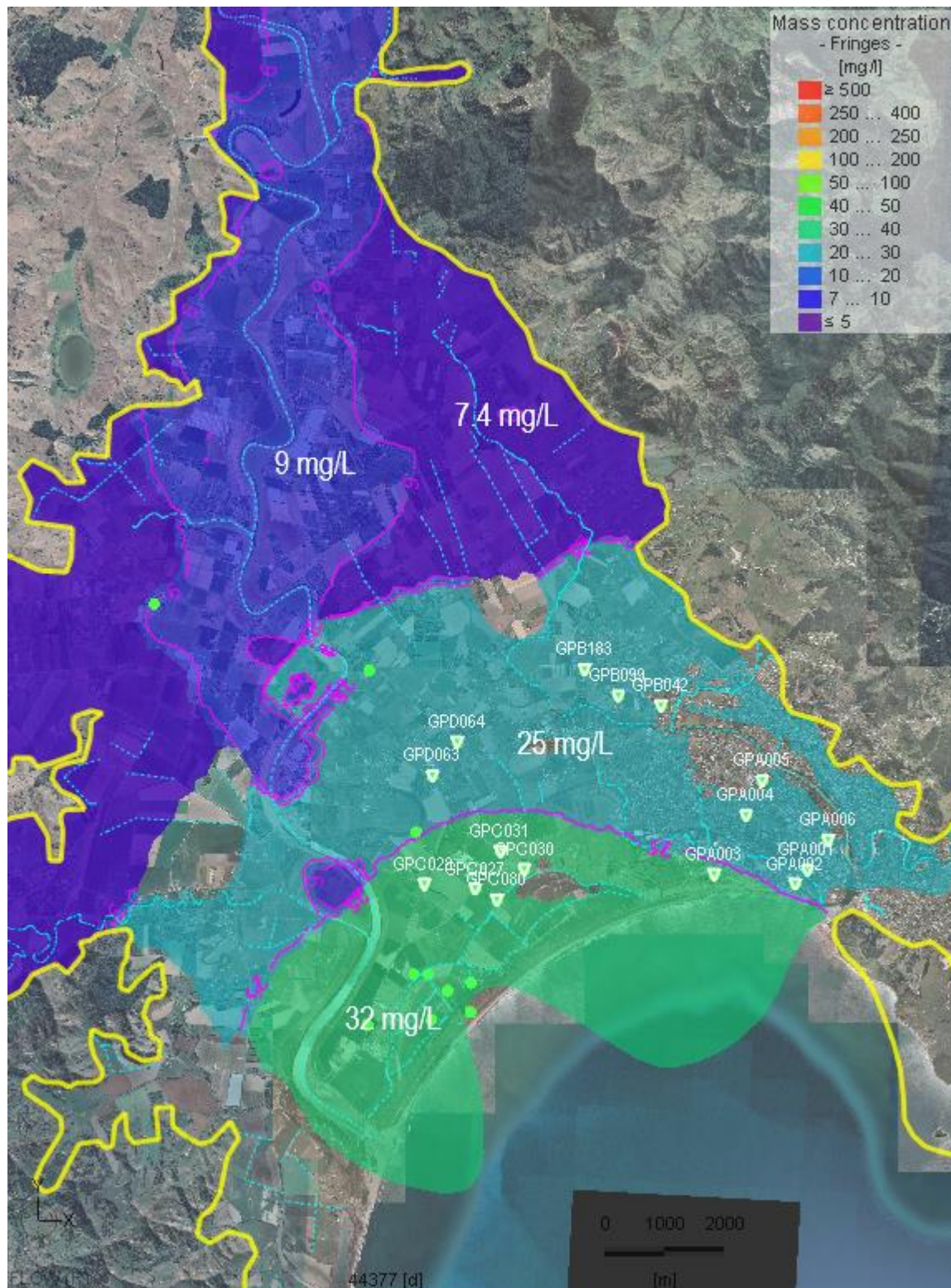


Figure 6-10: Initial distribution of Cl concentration and concentration of rainfall recharge assigned to User Data distribution RechargeConcentration in the top model layer.

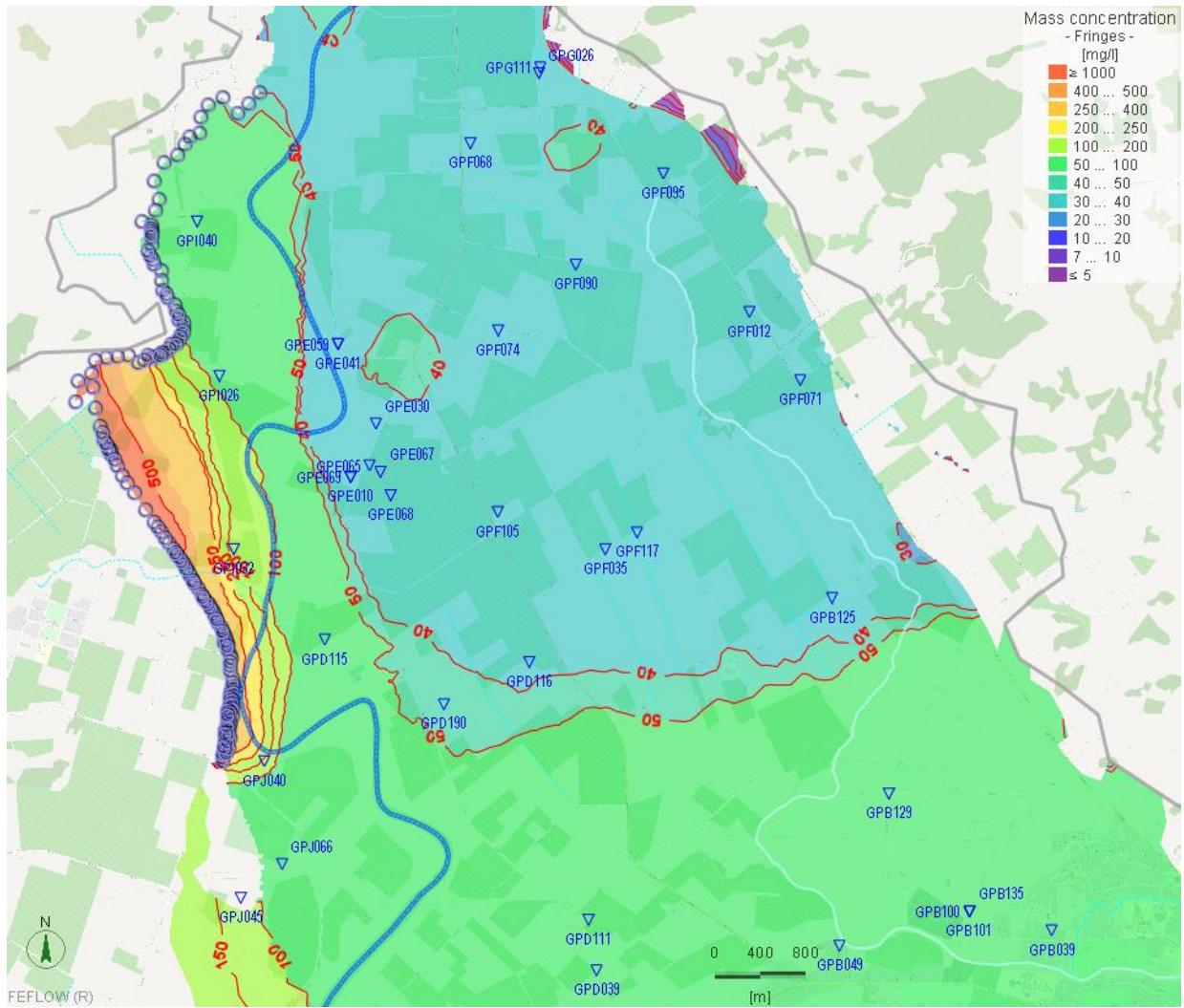


Figure 6-11: Cl concentration boundary conditions for Makauri Aquifer along its north-western boundary

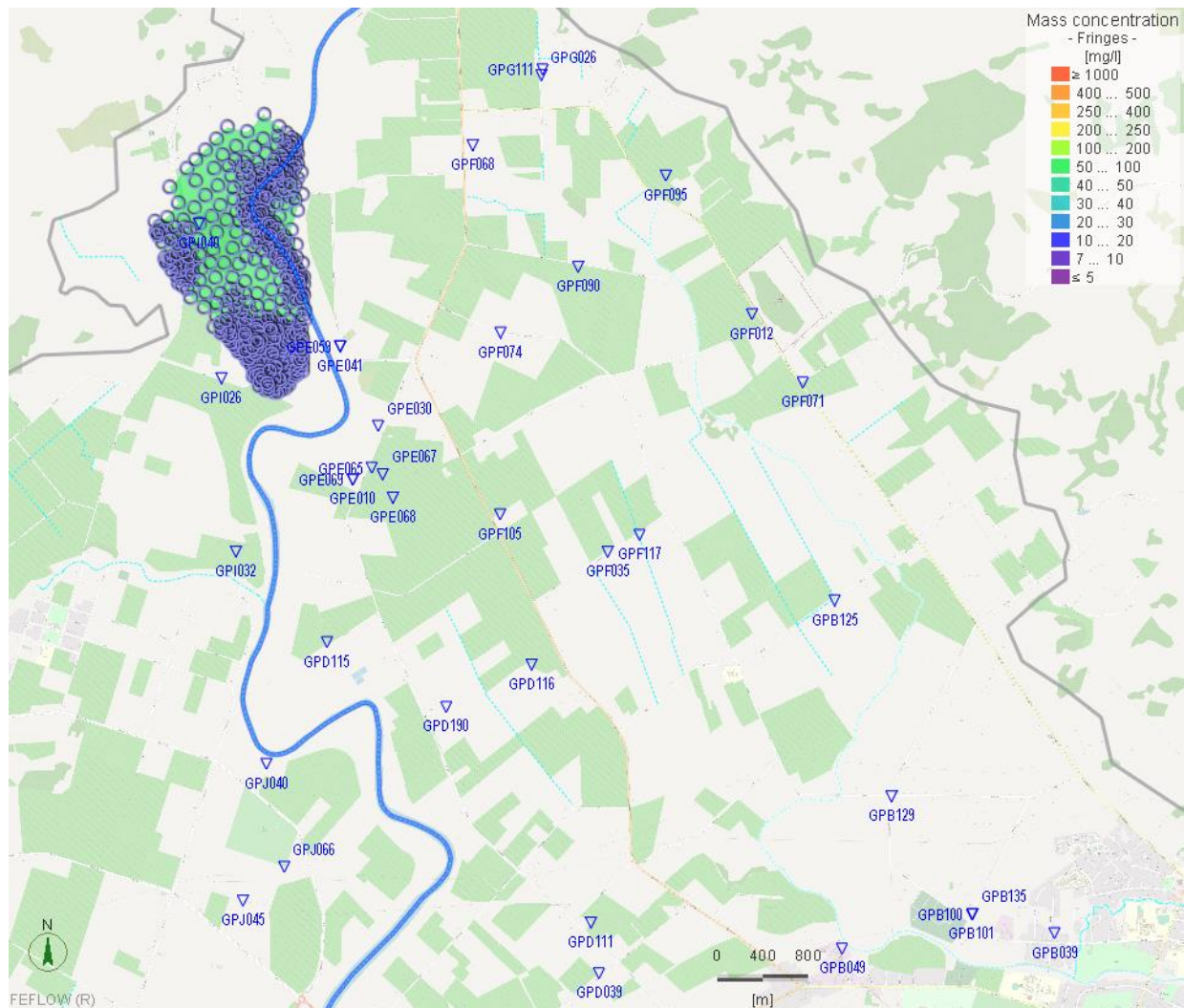


Figure 6-12: Cl concentration boundary conditions for Aquitard 2 in the north-west, above the Makauri aquifer

6.3. Salinity Simulation for the calibration and validation period 2008-2021

Based on the parameters described above, a salinity simulation for the calibration and validation period 2008 - 2021 is carried out firstly, aimed at checking plausibility of simulation results that will be used as initial Cl concentrations for the salinity scenarios simulations described in next Chapter 6.4.

Figure 6-13 through Figure 6-16 show plausibility checking of simulated Cl concentrations of selected bores with their available measured Cl concentrations in Makauri, Matokitoki, Waipaoa and Te Hapara Sands aquifer. The figures show that the simulation results, though as expected, match measurements not well, yet are useable as initial Cl concentrations for the salinity scenario simulations.

Figure 6-17 through Figure 6-20 outline simulated Cl concentrations and groundwater levels on 30 June 2021 for the Makauri, Matokitoki, Waipaoa and Shallow Fluvatile and Te Hapara Sands aquifer respectively. They are used as initial Cl concentrations and groundwater levels for the salinity scenario simulations.

Figure 6-21 shows locations of observation points which are assigned along three transects as fictive observation points for recording simulation results perpendicular to the coastline.

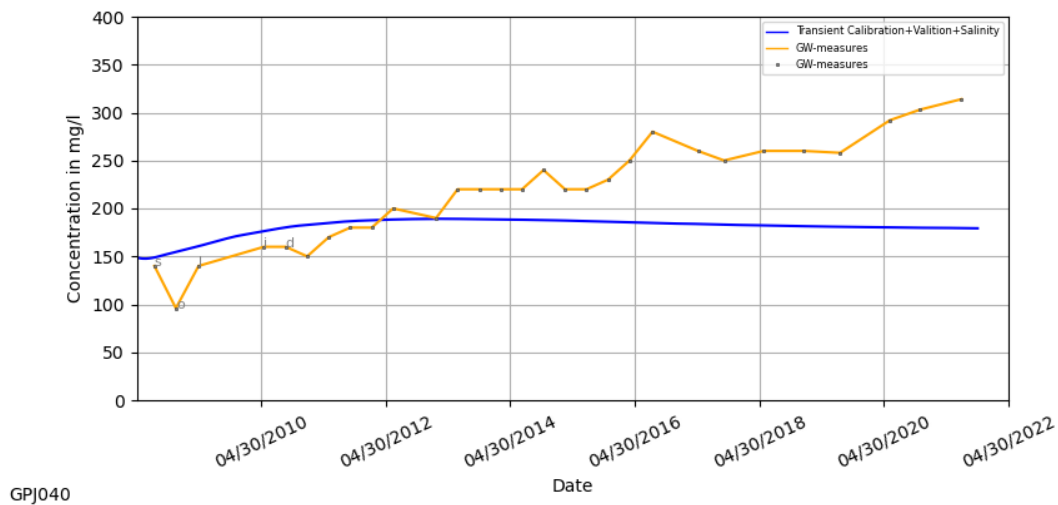
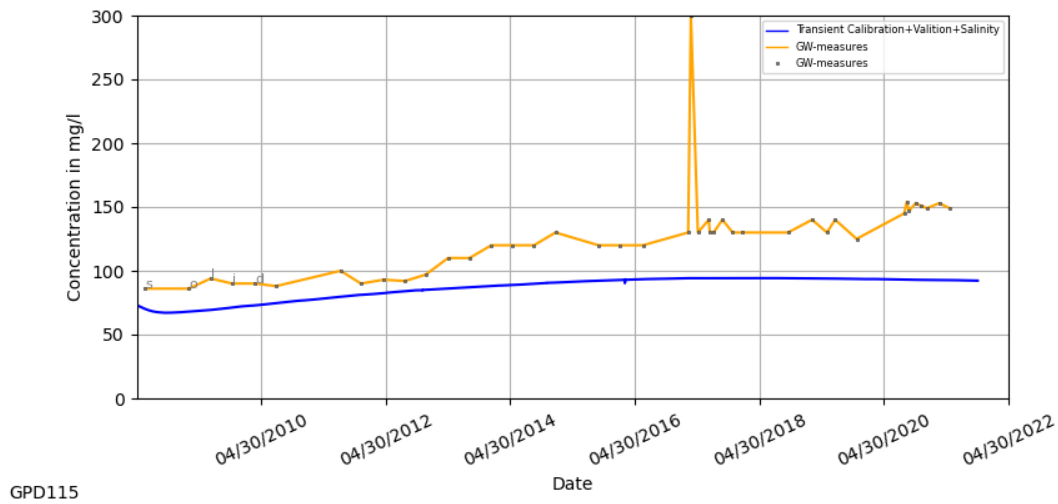
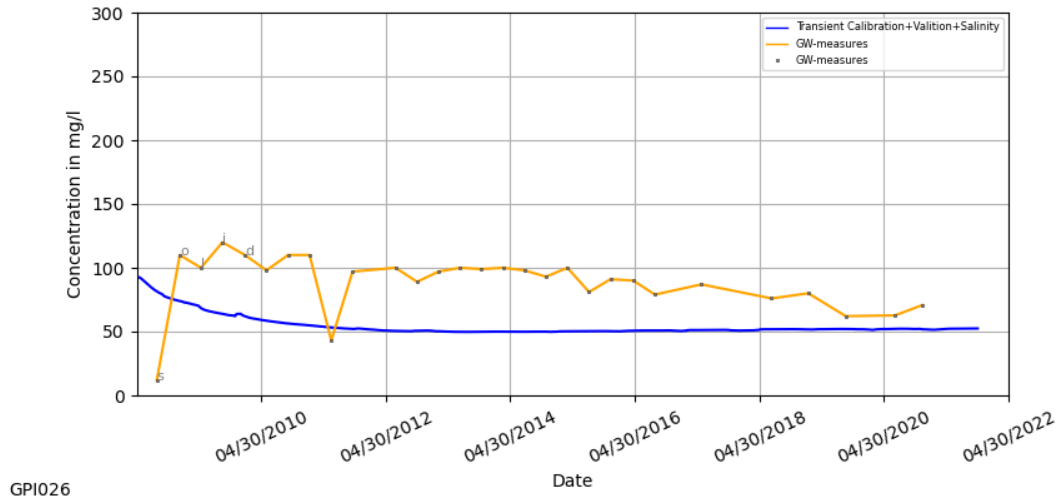


Figure 6-13: Simulated vs measured Cl concentrations of selected bores in the Makauri aquifer.

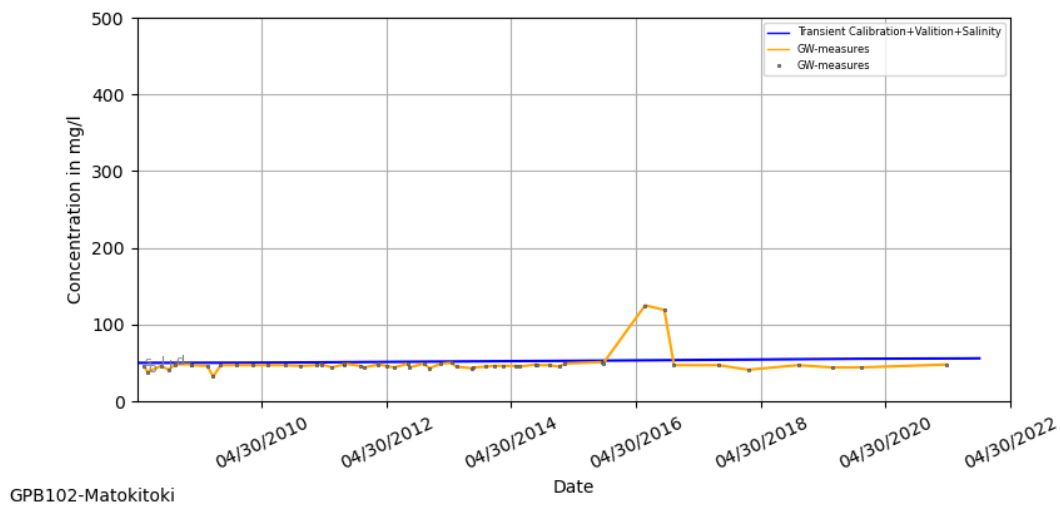
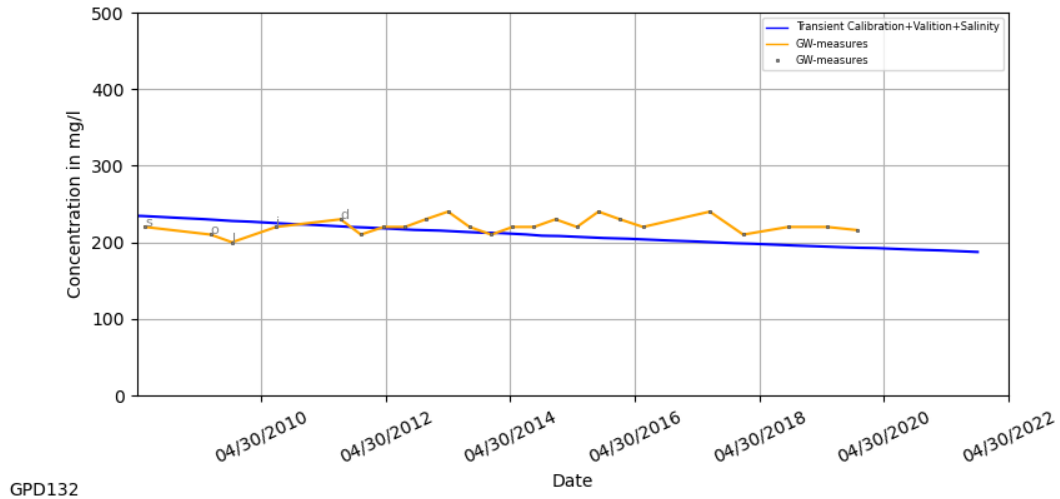


Figure 6-14: Simulated vs measured Cl concentrations of selected bores in the Matokitoki aquifer

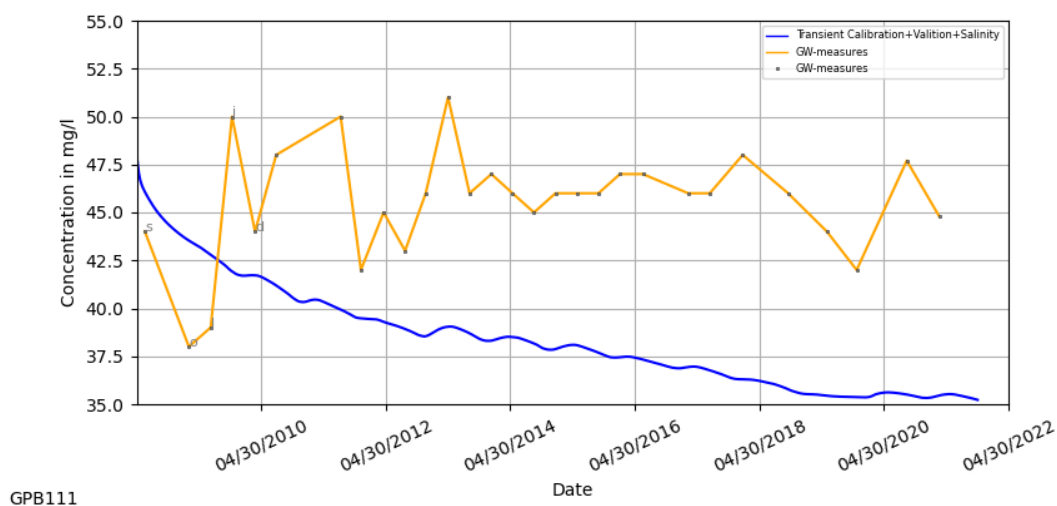
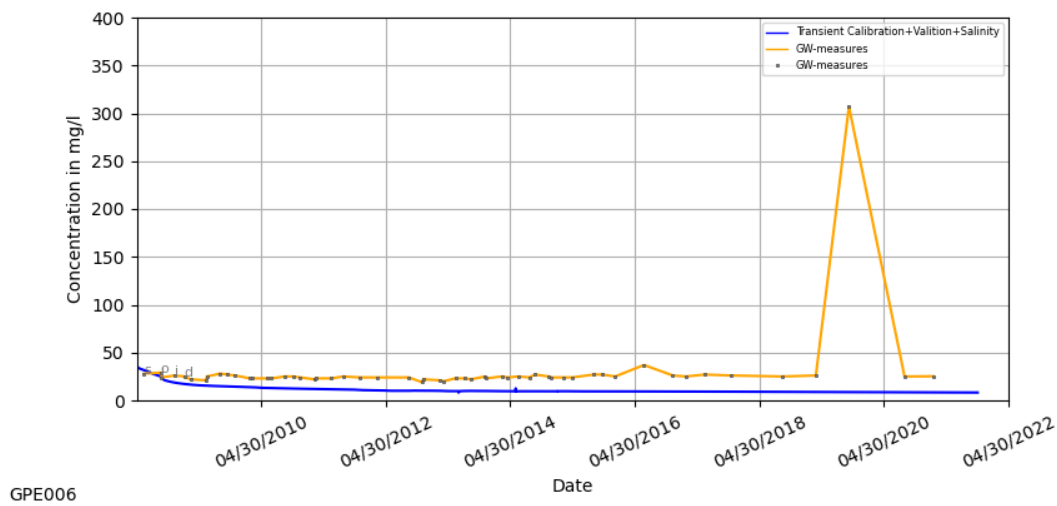
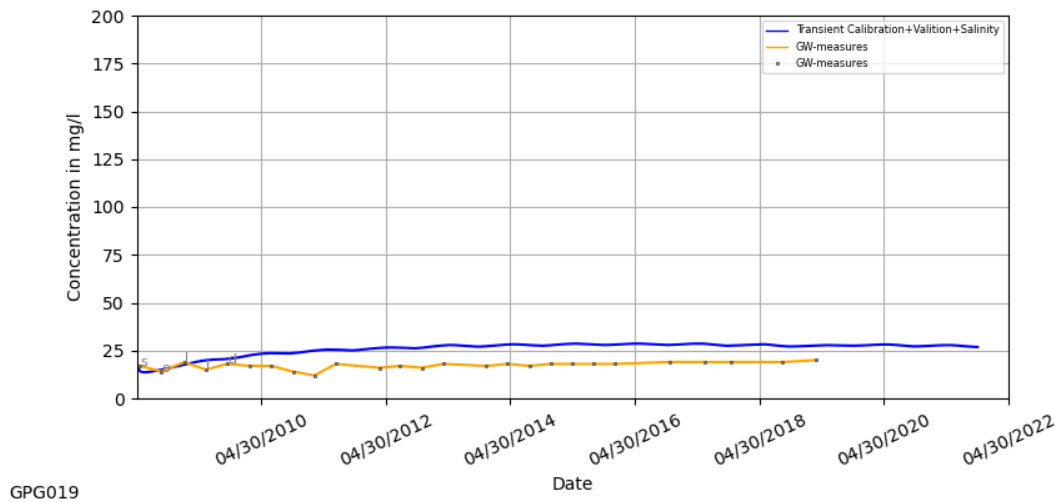


Figure 6-15: Simulated vs measured Cl concentrations of selected bores in the Waipaoa Aquifer

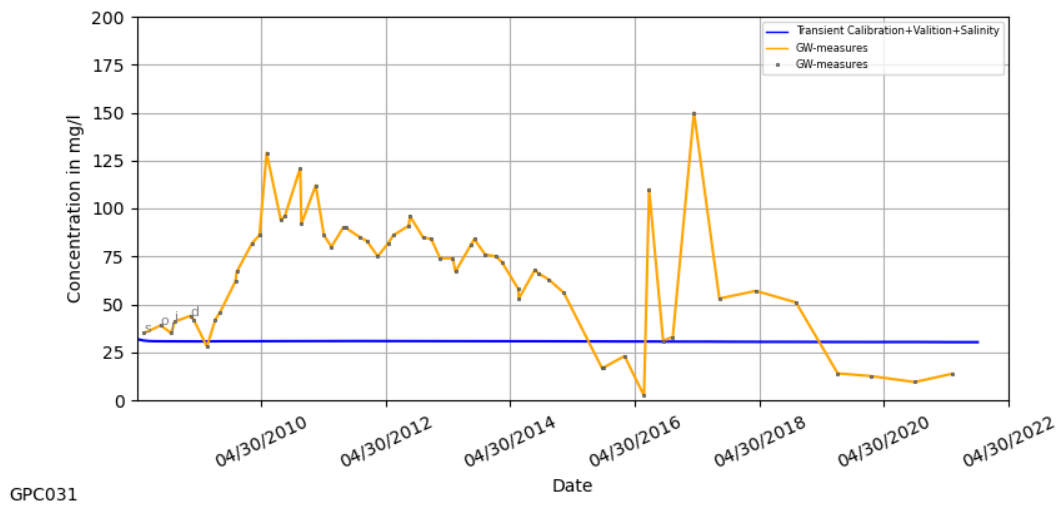
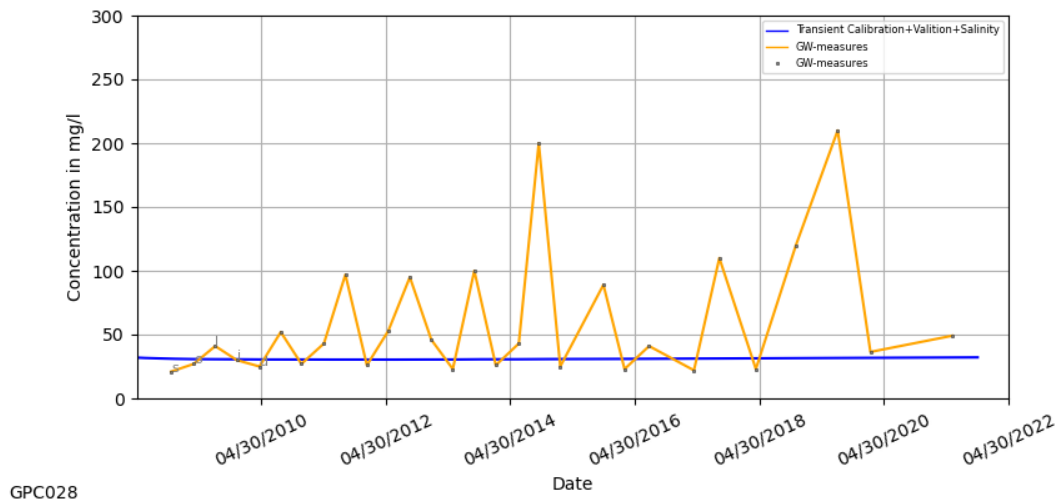
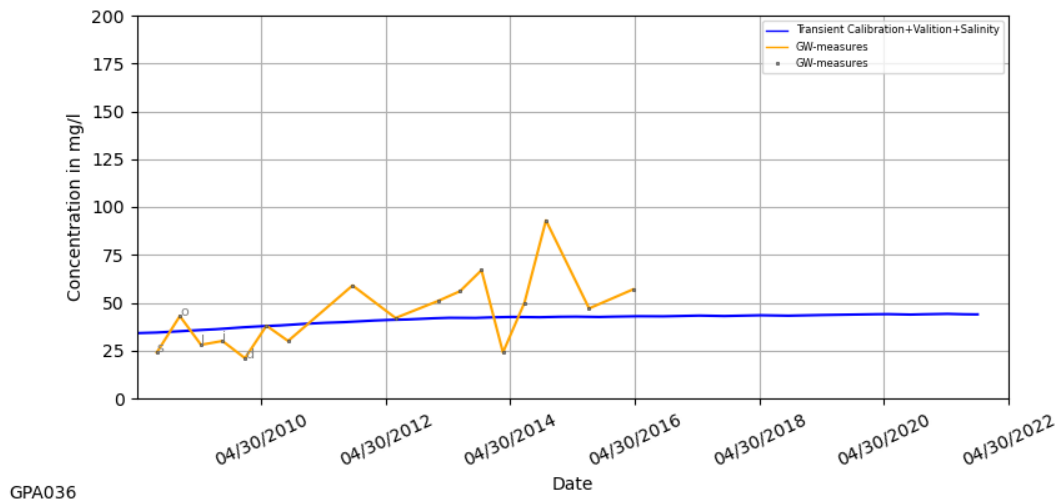


Figure 6-16: Simulated vs measured Cl concentrations of selected bores in the Te Hapara Sand Aquifer.

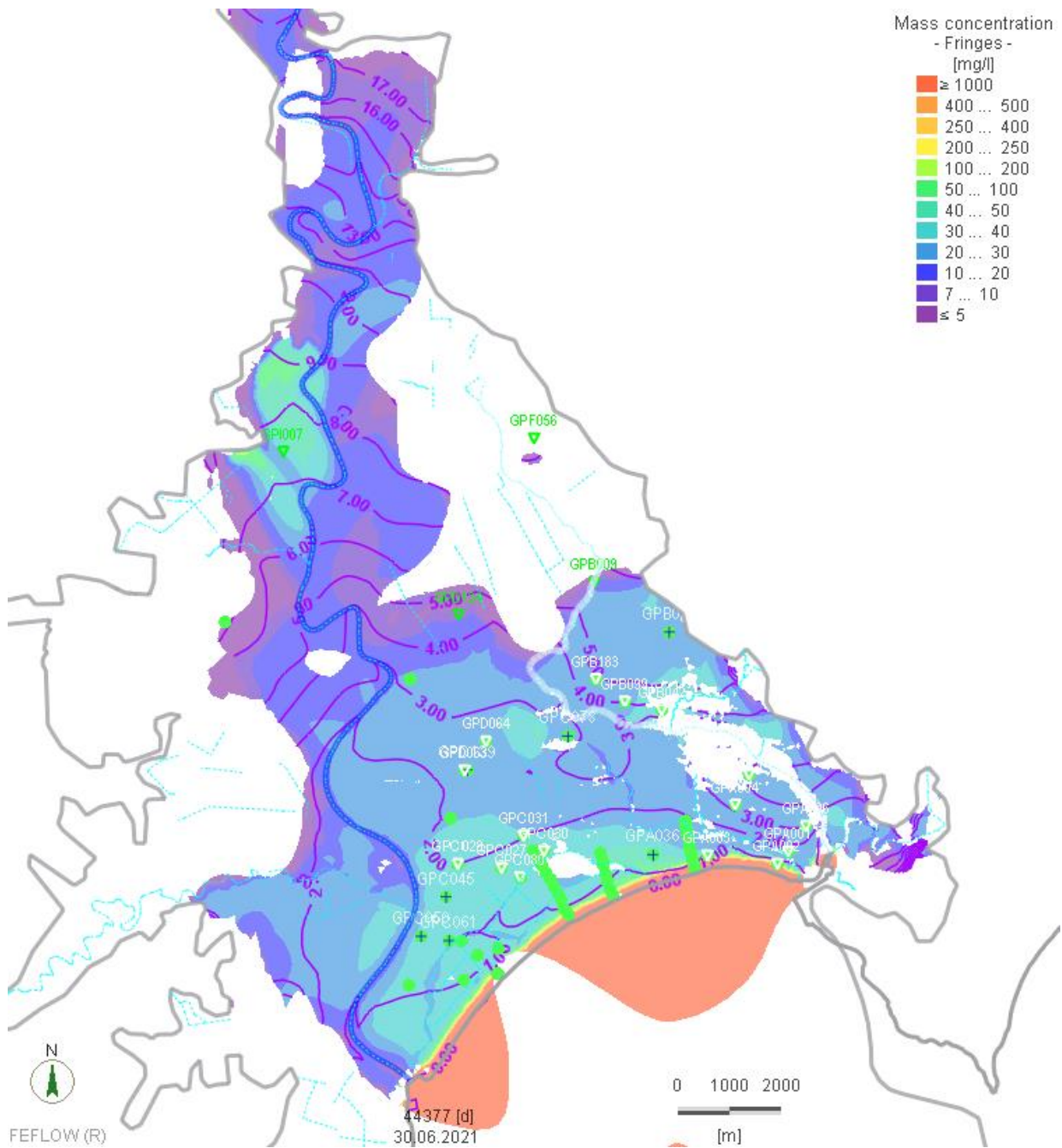


Figure 6-17: Simulated Cl concentrations and groundwater levels on 30 June 2021 in Te Hapara Sands / Shallow Fluvial aquifer.

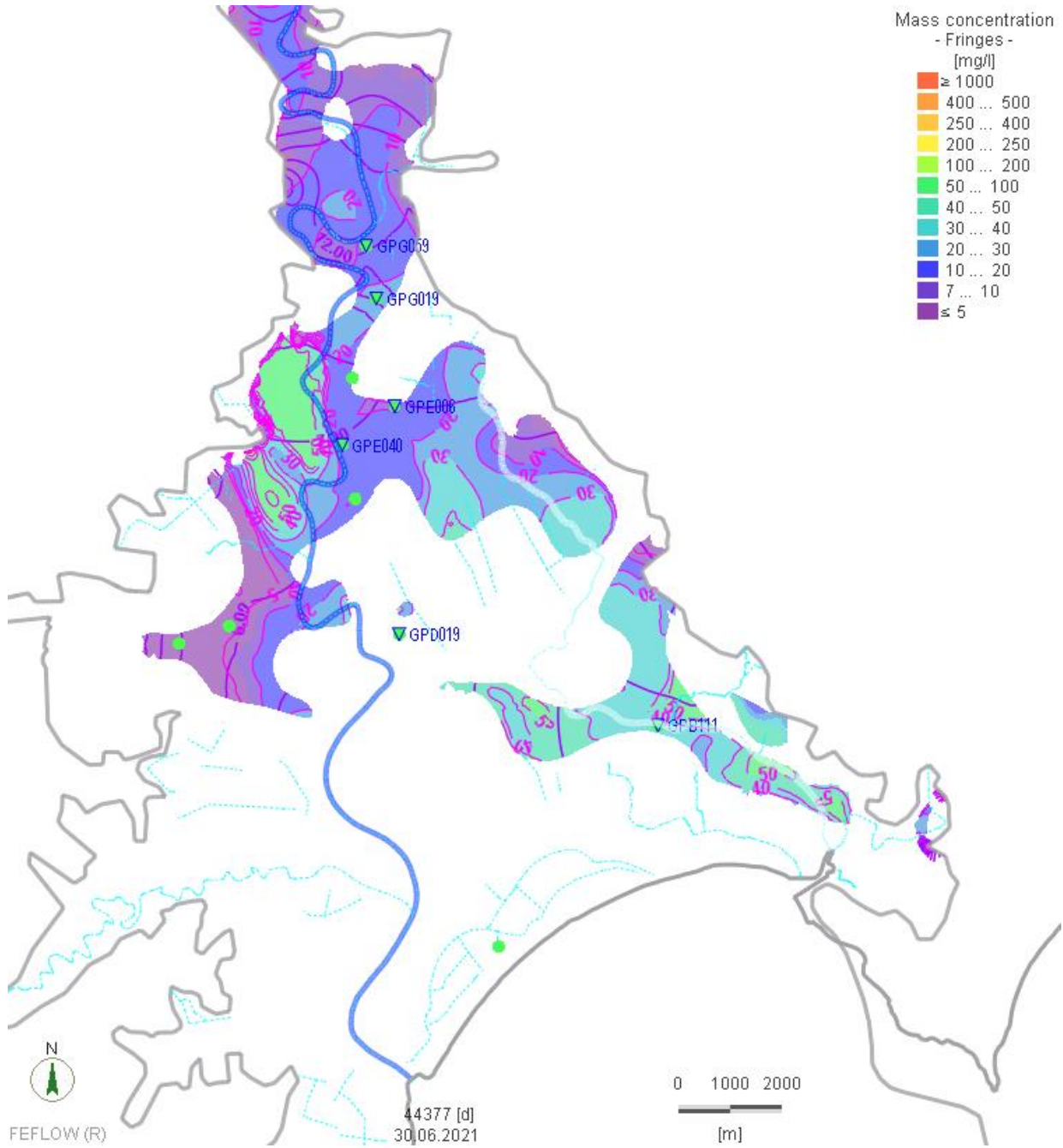


Figure 6-18: Simulated Cl concentrations and groundwater levels on 30 June 2021 in Waipaoa aquifer.

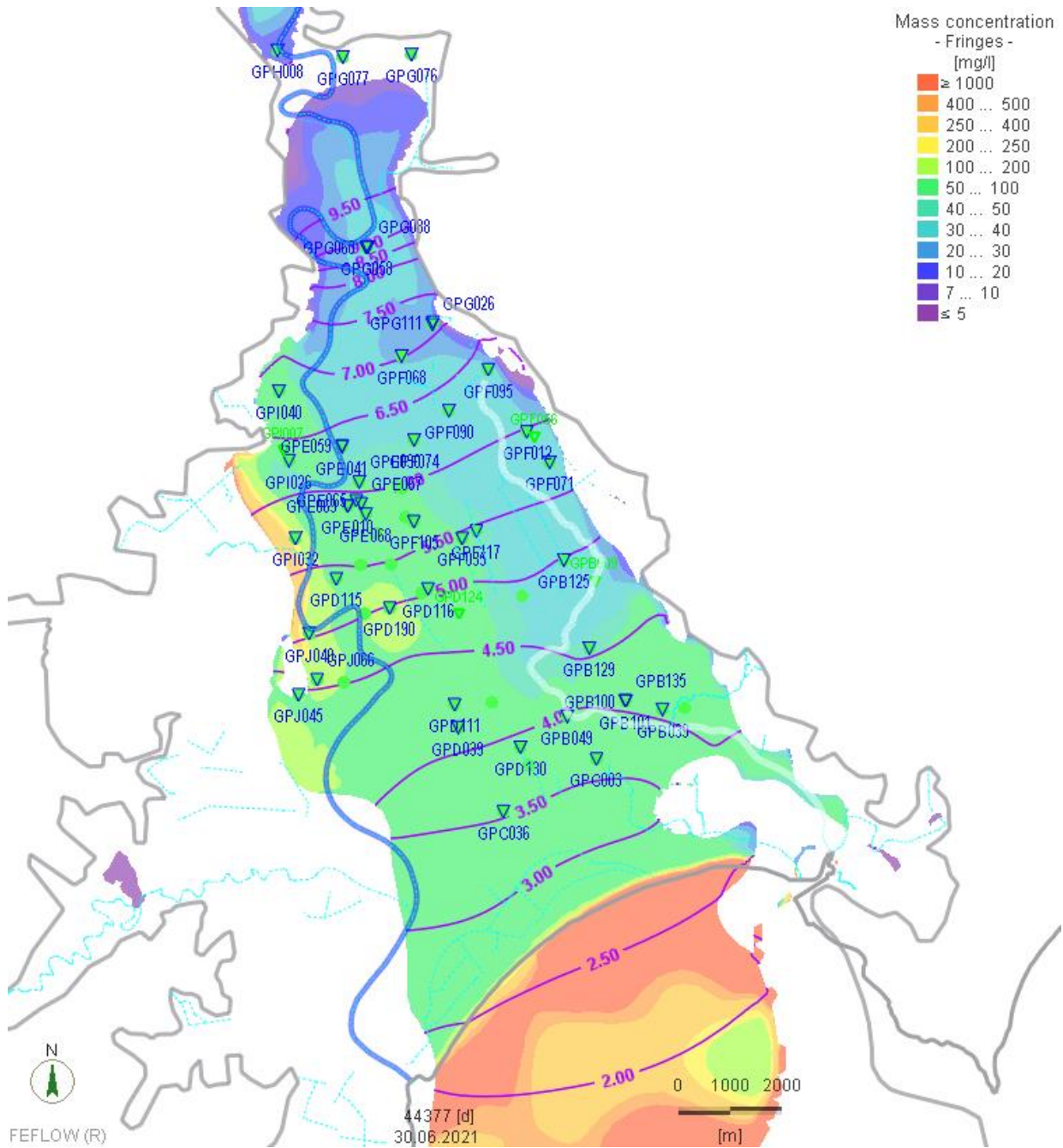


Figure 6-19: Simulated Cl concentrations and groundwater levels on 30/06/2021 in Makauri aquifer

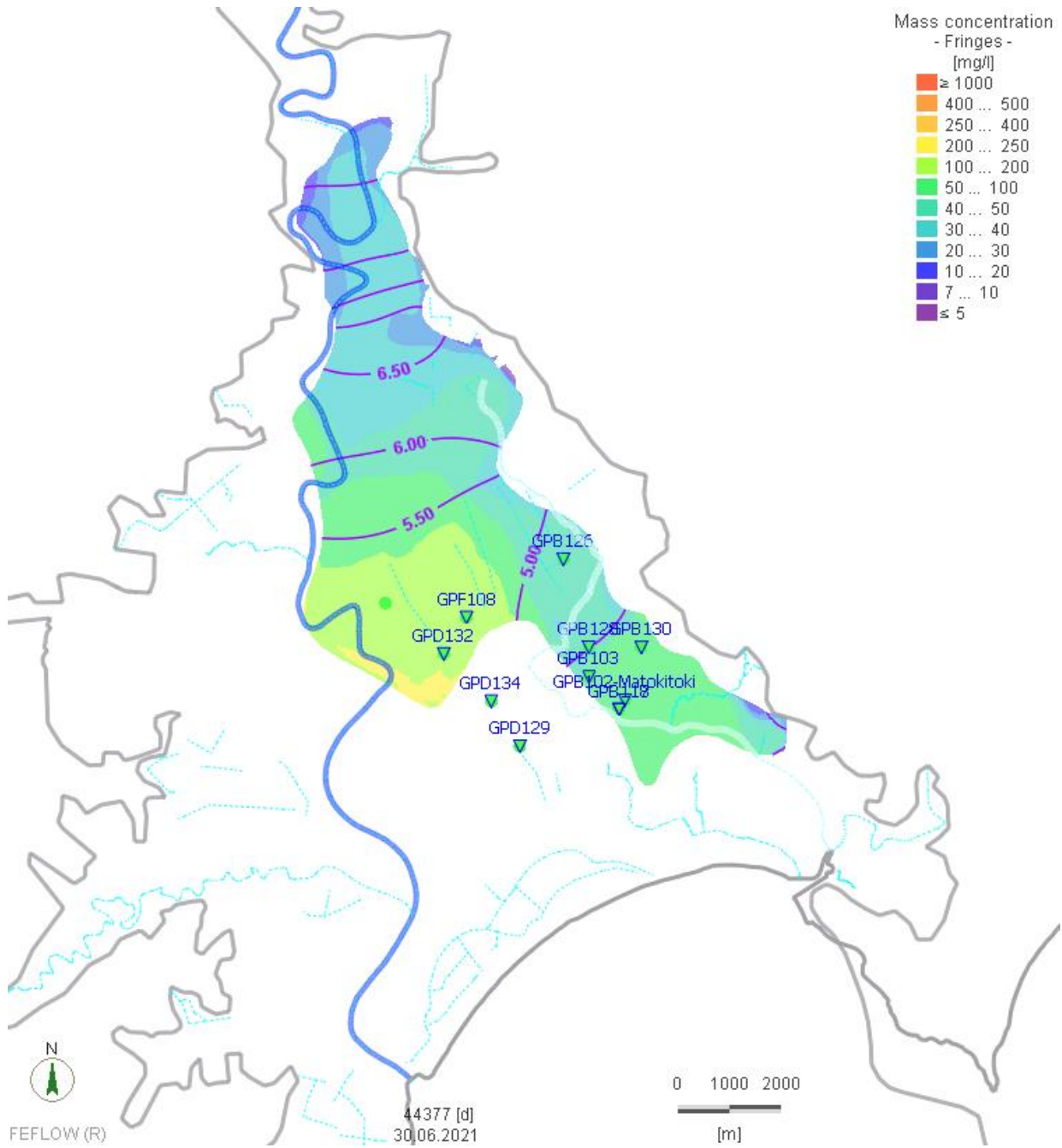


Figure 6-20: Simulated Cl concentrations and groundwater levels on 30/06/2021 in Matokitoki aquifer

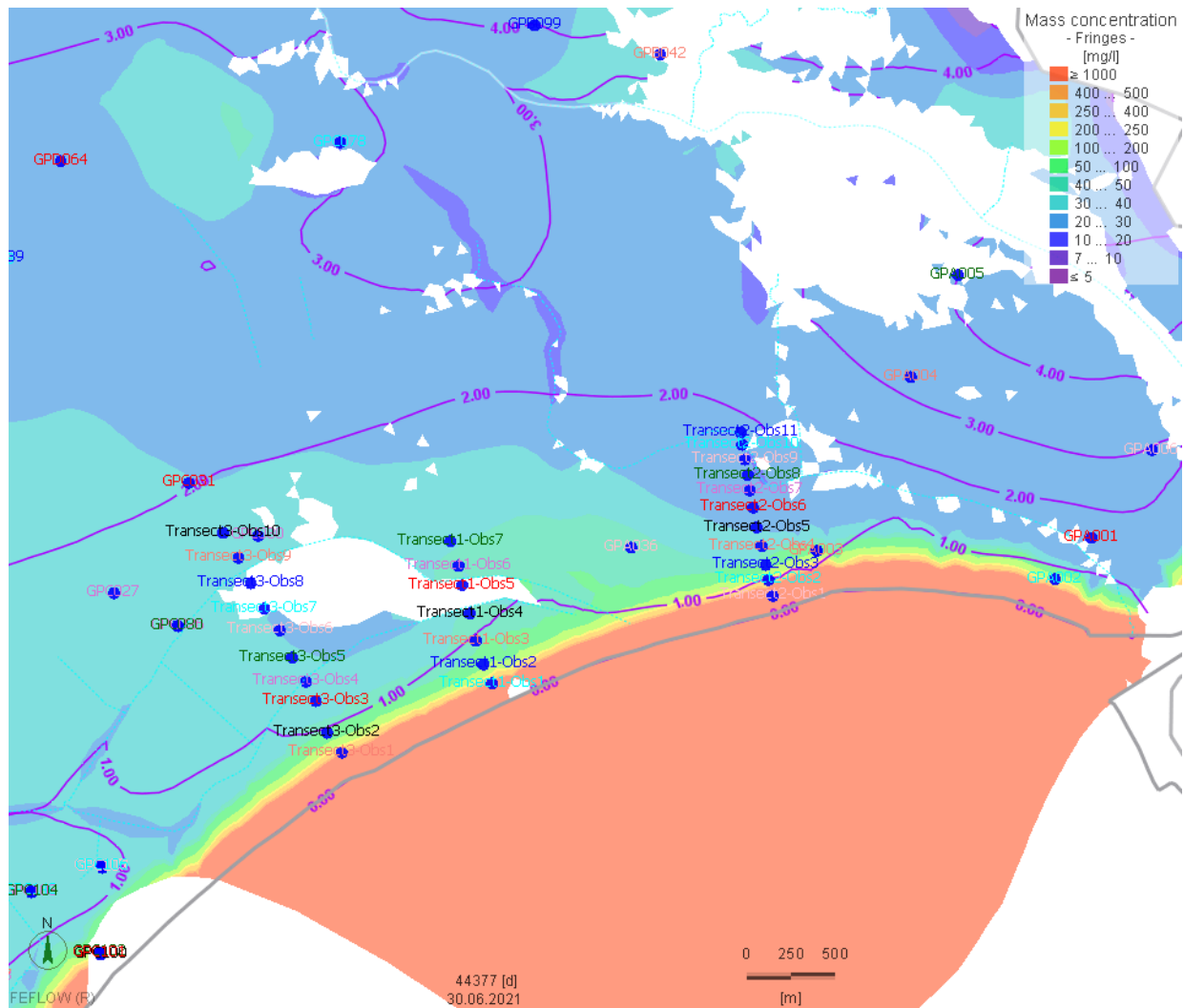


Figure 6-21: Locations of fictive observation points along three transects.

6.4. Scenario simulation results

The salinity simulation, though conceptually not complete, shows that the groundwater model is in general, and especially from a technical perspective, able to simulate salt transport. The comparison between different scenarios shows the expected behaviour. Some examples are provided here.

In the shallow aquifers along the coastline, there is a balance in between freshwater flowing towards the coast, and saltwater moving from the sea into groundwater. This balance mainly depends on the groundwater and sea-water levels, and therefore can also be influenced by tidal effects. The concentration curves shown in Figure 6-22 refer to an artificial monitoring point set in the model at Awapuni Sports Stadium. At this location, it can be seen that salinity stays about constant in scenarios where the level difference between the sea and groundwater does not change much, while with rising groundwater levels (scenario 3.1, 5.1) salinity decreases, and with even only slightly decreasing groundwater levels (about 4 cm in scenario 4.1) salinity can rise. It has to be kept in mind that this only illustrates basic processes, as a detailed prediction is not possible, also because there is a concentration drop from 20,000 mg/l to close to 0 mg/l over a very small distance.

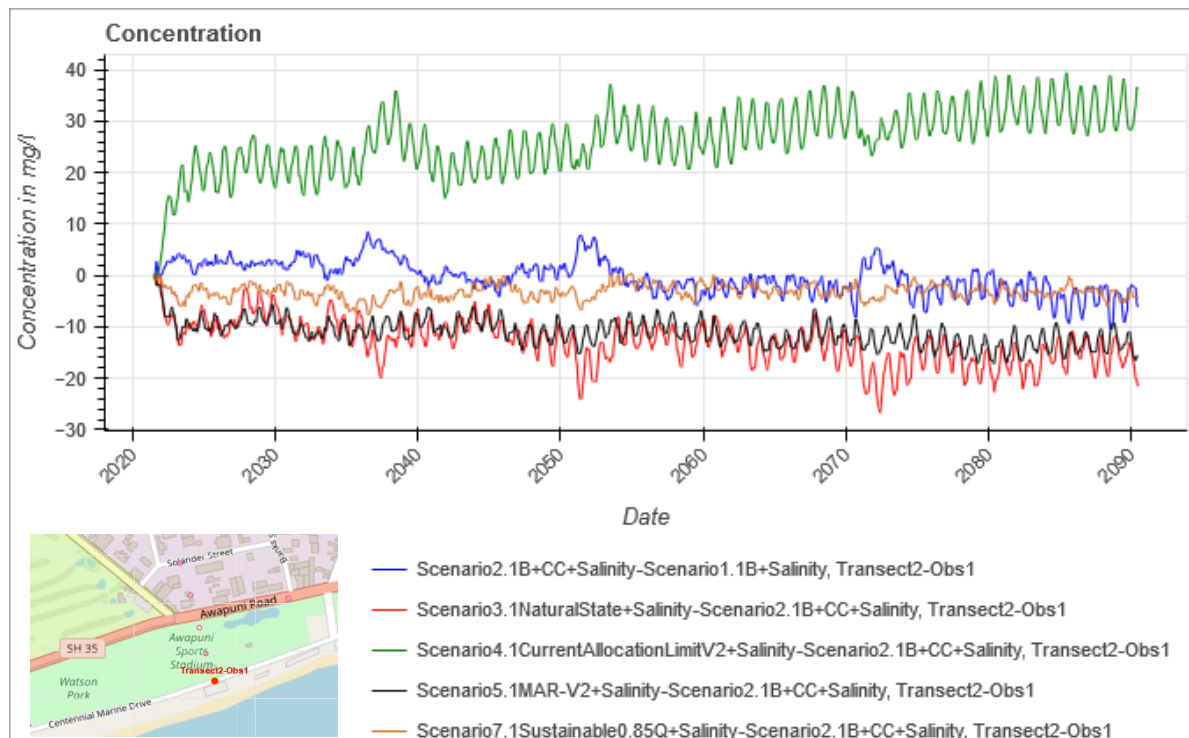


Figure 6-22: Difference between scenarios 2.1 and 2.1 and scenarios 3.1, 4.1, 5.1, 7.1 and scenario 2.1, Transect2-Obs1.

Looking at concentration in the Makauri aquifer in the centre of the model (Figure 6-23), it is visible that the groundwater freshens over time. The reason for this is lacking salt sources in the conceptual and numerical models. Therefore, inflow into the deeper aquifers is always fresher than the water pumped by abstraction. Freshening is the main process in the simulation results, and differences between the scenarios become minor. Furthermore, the differences will highly depend on initial conditions that might not reflect the actual conditions in the aquifers and aquitards.

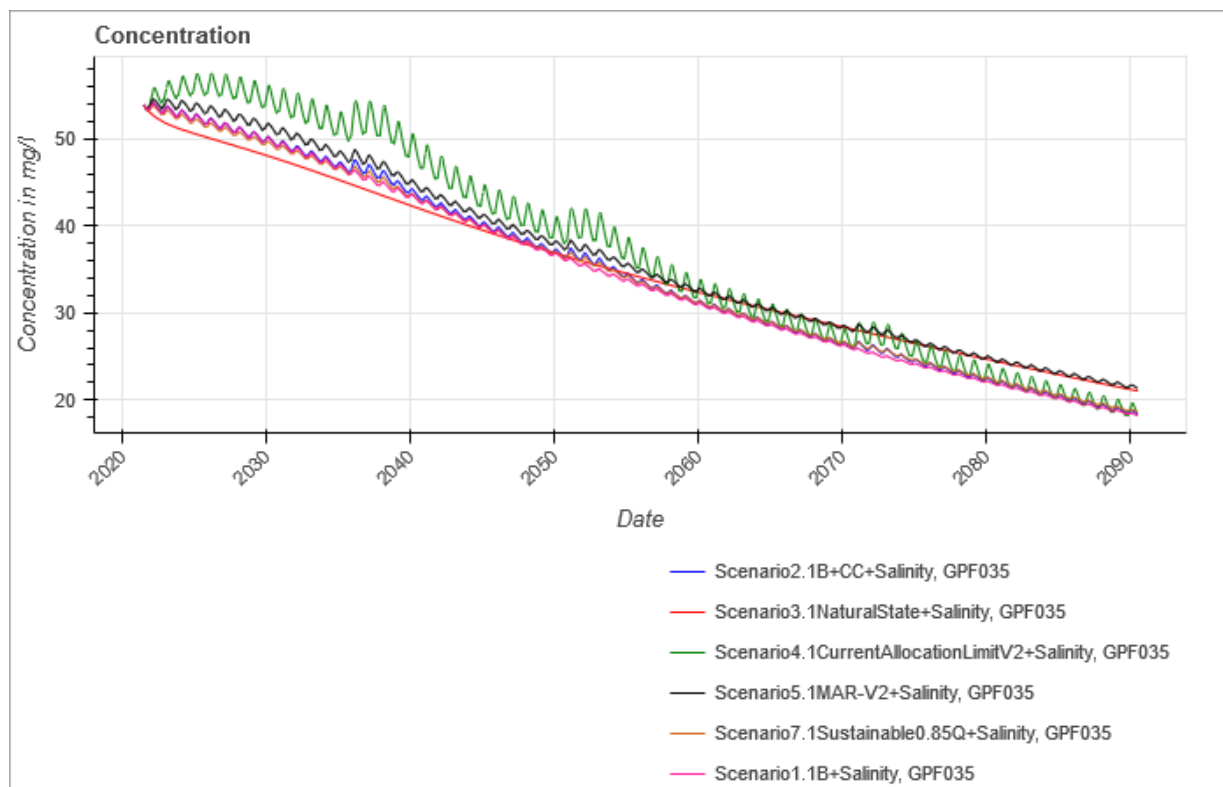


Figure 6-23: Simulated chloride concentration in scenarios 1.1-7.1 over time, observation bore GPF035 (Makauri).

6.5. Salinity simulation summary

There is limited knowledge about the conceptual processes influencing observed salinity in the Poverty Bay Flats aquifer system. Uncertainty mainly encompasses:

- the role of the western part of the Makauri aquifer (not contained in the geological model)
- the process of replenishing salinity that leads to increasing salinity levels with depth of the aquifer
- the role of coastal drains and tidal effects in influencing the salinity of the shallow aquifers close to the coastline

Because of the unknowns, it was decided to run the salinity simulations on a simplified conceptual model of the salt transport (see chapter 6.1). For this reason, no quantitatively irreproachable results can be expected from the model runs. The scenario outcomes are rather to be read as indications of what the expected development of salinity could be under different climatical and groundwater management conditions. Once again – as for results of the groundwater flow scenario runs – all results have to be interpreted based on the underlying conceptual model and the overall process understanding of the Poverty Bay Flats aquifer system.

The following systematic behaviour of salinity can be taken as reliable:

- The saltwater/freshwater front along the coastline is pushed further inland at higher abstraction levels / higher seawater rise (the former prevailing)
- The saltwater/freshwater front is pushed back towards the sea considering lower/no abstraction

The following model outcomes depend on uncertain aspects of the underlying conceptual model and therefore are uncertain themselves:

- All the scenarios show a freshening of the groundwater system over time, caused by the conceptually lacking salt replenishment. Depending on how conceptually the salt gets into the system, a

freshening may or may not be realistic – but the model very likely overestimates this process. Assuming a possible dissolution of geogenic salt from marine deposits in the aquitards, for example, lower salinity could result from higher flow velocities through the aquitards at higher abstraction rates. Though the freshening might correspond to observed decreasing salinity in some areas, without further knowledge the entire process remains speculative.

- Results show an additional saltwater inflow from the western side of the Makauri aquifer at increased abstraction. This outcome is based on intentionally higher initial salinity in this area and a fixed-concentration boundary at the western end of the Makauri in the model, forcing higher concentrations there. While this corresponds to some observations showing increasing salinity levels, the underlying process remains speculative.

In general, the salinity simulation can prove that the model is able to simulate salt transport within the aquifer system, including the sharp saltwater-freshwater interface along the coastline. When at a later stage there is deeper knowledge about the structure of the western part of the Makauri aquifer and the source of salt in the system, corresponding processes can be added to the model, and the scenario runs can be repeated.

7. Summary and recommendations

The groundwater model for the Poverty Bay Flats multi-aquifer system has been successfully set up and calibrated. A number of prognosis / scenario runs have been done to delineate the effects of climate change on the aquifer system, and to determine potential strategies to fight back negative effects. The model reflects the behaviour of the aquifer system very well, and predictions of general trends under different climatic and management circumstances are assessed as reliable. In case more precise predictions are needed in the shallow aquifer system that is closely linked to the surface water system, more detail should be added to the groundwater model. This could be adding additional smaller drains, active or passive management of drains etc., but could also result in a fully coupled groundwater-surface water model. Basic requirement for this would be measurements on the flows in the system, e. g., by installing flow loggers for each drain.

A salinity model has been set up which has been proven to be technically working. As major conceptual factors such as the source of salt in groundwater and the process of salinisation are unknown as of now, this model currently can neither reproduce the current distribution of salt over long time spans, nor can it be used to predict salinity precisely for long-term scenario runs. Once conceptual questions have been resolved, there is the possibility to incorporate the identified processes into the model. This then would have to be run for a very long simulation period to come up with a process-based initial distribution of salinity (as levels at monitoring wells are not sufficient). The resulting model can then be used to do reliable predictions for the future.

8. Literature

Barnett et al, 2012:


Barnett B, Townley LR, Post V, Evans RE, Hunt RJ, Peeters L, Richardson S, Werner AD, Knapton A and Boronkay: Australian groundwater modelling guidelines, Waterlines report, National Water Commission, Canberra, 2012.

Berlin, 24/10/2022

The authors:



P. Schätzl



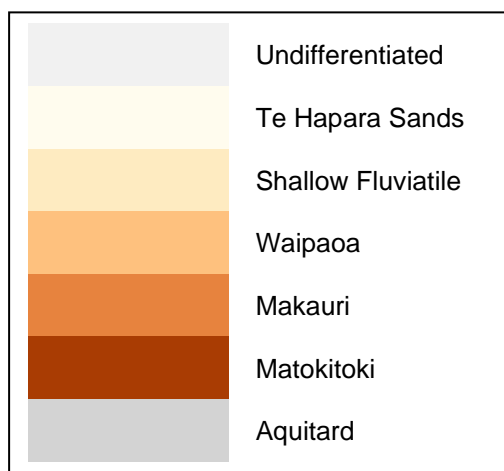
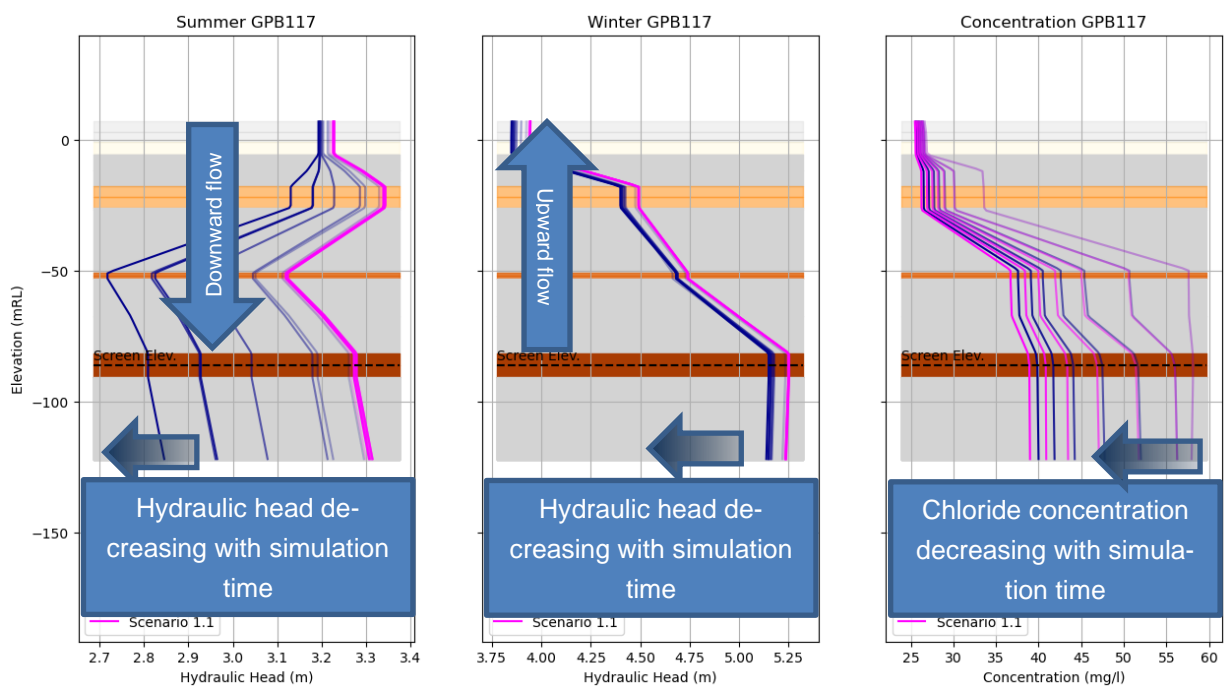
by order, Dr. J. Luo

Appendix

A1 Plot style: vertical distribution of hydraulic head and concentration

The vertical distribution plots are intended to show hydraulic head and concentration in vertical diagrams at locations of observation bores, possibly for a number of time stages in the simulation results and a number of different scenarios. Increasing opacity of the curves corresponds to increasing simulation time (10-year intervals from 2025 to 2085 for scenario simulations). Hydraulic-head diagrams are shown separately for summer (28 February) and winter (30 September) situations, concentrations are only shown for winter. Different colours of the lines are used to distinguish and compare different scenarios (typically two scenarios, scenario numbers in legend).

The aquifers are shown in different colours as depicted below; aquitards are uniformly displayed in grey. Elevations correspond to elevations in the model at the location of the bore. A black line indicates the elevation of the screen in the FEFLOW model (single elevation rather than real top/bottom).



A2 Steady-state calibration: calculated vs. observed hydraulic head

Table A1-1: Comparison of measured and simulated water levels at available monitoring bores, steady state calibration

Name	Aquifer	Measure date		Water level (mRL)			num-ber of measu-res	Simulated	Simu. - Meas.
		from	to	Min	Mean	Max			
GPA003	Te Hapara Sands	16.05.2011	16.04.2012	0.30	0.62	0.95	20	1.28	0.66
GPC031	Te Hapara Sands	16.06.2011	14.03.2012	-0.38	0.56	1.23	3	2.28	1.72
GPC030	Te Hapara Sands	16.05.2011	16.04.2012	-0.42	0.20	0.91	20	1.92	1.72
GPA005	Te Hapara Sands	16.05.2011	16.04.2012	3.78	4.10	4.47	20	4.85	0.75
GPD064	Te Hapara Sands	01.05.2011	16.04.2012	1.06	1.86	2.31	16	3.03	1.17
GPB099	Te Hapara Sands	01.05.2011	02.04.2012	3.82	4.57	5.42	16	4.91	0.34
GPA004	Te Hapara Sands	16.05.2011	16.04.2012	2.79	3.10	3.51	20	3.97	0.87
GPA006	Te Hapara Sands	16.05.2011	16.04.2012	2.89	3.16	3.39	20	3.66	0.50
GPC027	Te Hapara Sands	16.05.2011	16.04.2012	0.97	1.58	2.37	19	1.81	0.23
GPD063	Te Hapara Sands	16.05.2011	16.04.2012	1.60	2.37	3.42	20	2.95	0.58
GPB042	Te Hapara Sands	01.05.2011	16.04.2012	4.60	4.79	5.02	18	4.31	-0.48
GPA002	Te Hapara Sands	16.05.2011	16.04.2012	0.31	0.61	0.90	20	1.07	0.46
GPA001	Te Hapara Sands	25.07.2011	16.04.2012	0.87	1.17	1.54	16	2.01	0.84
GPC080	Te Hapara Sands	16.05.2011	16.04.2012	-0.26	0.08	0.63	20	1.46	1.38
GPB183	Te Hapara Sands	01.05.2011	16.04.2012	4.25	5.09	5.65	17	5.59	0.50
GPC028	Te Hapara Sands	16.05.2011	16.04.2012	1.11	2.12	3.28	20	2.04	-0.08
GPD124	Shallow Fluvial Deposits	01.05.2011	16.04.2012	-0.25	3.77	5.27	17	4.88	1.11
GPI007	Shallow Fluvial Deposits	16.05.2011	16.04.2012	3.54	7.87	9.85	20	7.99	0.12
GPF056	Shallow Fluvial Deposits	01.05.2011	16.04.2012	10.81	12.07	13.28	17	12.93	0.86
GPB009	Shallow Fluvial Deposits	01.05.2011	16.04.2012	5.04	5.60	5.95	17	5.49	-0.11
GPG059	Waipaoa Gravel	25.07.2011	16.04.2012	11.15	11.95	13.12	16	12.17	0.22
GPB111	Waipaoa Gravel	01.05.2011	16.04.2012	3.06	3.51	3.87	18	4.48	0.97
GPH030	Waipaoa Gravel	16.05.2011	16.04.2012	23.00	24.16	26.36	20	26.04	1.88
GPG019	Waipaoa Gravel	25.07.2011	16.04.2012	9.12	10.10	11.74	16	10.52	0.42
GPE040	Waipaoa Gravel	25.07.2011	16.04.2012	6.75	7.34	8.34	16	7.58	0.24
GPH022	Waipaoa Gravel	25.07.2011	16.04.2012	17.78	18.43	18.94	16	18.28	-0.15
GPE006	Waipaoa Gravel	16.06.2011	14.03.2012	8.47	10.63	13.73	3	7.61	-3.02
GPE032	Makauri Gravel	25.07.2011	16.04.2012	6.65	7.33	8.42	16	6.62	-0.71
GPD019	Waipaoa Gravel	01.05.2011	16.04.2012	2.49	3.55	4.63	17	3.97	0.42
GPG058	Makauri Gravel	25.07.2011	16.04.2012	8.14	9.12	10.64	16	9.21	0.09
GPF074	Makauri Gravel	01.05.2011	16.04.2012	3.32	5.80	7.84	18	6.40	0.60
GPF068	Makauri Gravel	01.05.2011	16.04.2012	4.11	6.36	8.05	17	7.31	0.95
GPG026	Makauri Gravel	01.05.2011	16.04.2012	3.84	6.72	8.34	17	7.42	0.70
GPI026	Makauri Gravel	16.05.2011	16.04.2012	4.07	6.10	7.49	20	6.41	0.31
GPG060	Makauri Gravel	16.05.2011	16.04.2012	7.83	9.05	10.39	20	9.22	0.17
GPG088	Makauri Gravel	25.07.2011	16.04.2012	7.03	8.69	10.43	16	9.21	0.52
GPB100	Makauri Gravel	01.05.2011	16.04.2012	3.90	4.34	5.19	17	4.62	0.28

Name	Aquifer	Measure date		Water level (mRL)			number of measu res	Simulated	Simu. - Meas.
		from	to	Min	Mean	Max			
GPB101	Makauri Gravel	01.05.2011	16.04.2012	3.86	4.43	5.16	18	4.62	0.19
GPB135	Makauri Gravel	01.05.2011	16.04.2012	3.80	4.40	4.75	17	4.62	0.22
GPJ045	Makauri Gravel	16.05.2011	16.04.2012	4.72	5.24	6.01	20	4.20	-1.04
GPF090	Makauri Gravel	16.06.2011	14.03.2012	-0.90	2.19	7.06	3	6.52	4.33
GPI032	Makauri Gravel	16.05.2011	16.04.2012	3.25	5.30	6.94	20	6.14	0.84
GPG077	Makauri Gravel	16.05.2011	16.04.2012	15.71	16.98	18.38	20	17.28	0.30
GPF117	Makauri Gravel	01.05.2011	16.04.2012	3.97	8.54	11.54	18	5.77	-2.77
GPJ040	Makauri Gravel	16.05.2011	16.04.2012	3.85	5.41	6.91	20	5.41	0.00
GPC036	Makauri Gravel	16.05.2011	16.04.2012	3.55	4.34	4.72	20	3.99	-0.35
GPB129	Makauri Gravel	01.05.2011	16.04.2012	4.91	5.26	5.54	17	4.97	-0.29
GPD111	Makauri Gravel	01.05.2011	16.04.2012	3.83	5.31	6.23	15	4.65	-0.66
GPI040	Makauri Gravel	13.06.2011	16.04.2012	5.29	6.58	7.99	17	7.17	0.59
GPD039	Makauri Gravel	01.05.2011	16.04.2012	0.27	1.36	4.09	17	4.55	3.19
GPE041	Makauri Gravel	25.07.2011	16.04.2012	6.72	7.34	8.49	16	6.62	-0.72
GPE059	Makauri Gravel	25.07.2011	16.04.2012	5.84	6.87	8.37	16	6.62	-0.25
GPB039	Makauri Gravel	01.05.2011	16.04.2012	6.86	7.35	7.63	18	4.56	-2.79
GPB125	Makauri Gravel	01.05.2011	16.04.2012	4.93	5.76	6.40	16	5.36	-0.40
GPD130	Makauri Gravel	16.06.2011	14.03.2012	2.33	3.75	5.13	4	4.36	0.61
GPF095	Makauri Gravel	01.05.2011	16.04.2012	3.86	6.52	8.22	17	6.66	0.14
GPD116	Makauri Gravel	01.05.2011	16.04.2012	3.65	5.87	7.42	17	5.44	-0.43
GPH008	Makauri Gravel	25.07.2011	16.04.2012	16.47	17.45	18.33	16	18.26	0.81
GPB049	Makauri Gravel	01.05.2011	16.04.2012	3.41	4.21	4.92	18	4.42	0.21
GPO021	Makauri Gravel	16.05.2011	16.04.2012	32.39	32.91	33.46	20	33.23	0.32
GPF012	Makauri Gravel	01.05.2011	16.04.2012	1.11	5.41	7.52	17	6.26	0.85
GPC003	Makauri Gravel	01.05.2011	16.04.2012	3.46	4.35	4.99	17	4.15	-0.20
GPD115	Makauri Gravel	01.05.2011	16.04.2012	3.80	5.61	7.43	16	5.76	0.15
GPF035	Makauri Gravel	01.05.2011	16.04.2012	5.06	5.76	6.66	17	5.73	-0.03
GPJ066	Makauri Gravel	16.05.2011	16.04.2012	3.79	4.97	6.15	20	4.99	0.02
GPO024	Makauri Gravel	16.05.2011	16.04.2012	32.88	33.47	34.09	20	33.29	-0.18
GPF071	Makauri Gravel	01.05.2011	16.04.2012	2.92	5.78	7.56	17	6.06	0.28
GPG076	Makauri Gravel	16.05.2011	16.04.2012	13.75	14.68	15.38	20	18.30	3.62
GPD134	Matokitoki Gravel	01.05.2011	16.04.2012	1.72	2.84	4.17	17	4.62	1.78
GPD132	Matokitoki Gravel	01.05.2011	16.04.2012	3.78	4.82	6.54	17	5.76	0.94
GPB102	Matokitoki Gravel	16.06.2011	14.03.2012	7.44	7.84	8.31	4	4.61	-3.23
GPB118	Matokitoki Gravel	01.05.2011	16.04.2012	7.88	8.38	8.75	17	4.87	-3.51
GPB117	Matokitoki Gravel	01.05.2011	16.04.2012	3.92	4.49	5.22	18	4.87	0.38
GPB130	Matokitoki Gravel	01.05.2011	16.04.2012	9.84	10.65	10.97	17	4.92	-5.73
GPB128	Matokitoki Gravel	01.05.2011	16.04.2012	8.15	8.58	8.89	17	5.07	-3.51
GPB126	Matokitoki Gravel	01.05.2011	16.04.2012	8.34	8.73	9.11	17	5.49	-3.24
GPF108	Matokitoki Gravel	01.05.2011	16.04.2012	3.44	5.05	5.99	17	5.76	0.71
GPD129	Matokitoki Gravel	01.05.2011	16.04.2012	3.88	4.87	6.27	17	4.36	-0.51
GPB103	Matokitoki Gravel	01.05.2011	16.04.2012	6.15	7.13	9.01	18	4.94	-2.19

A3 Parameter specification of scenario simulations

Scenario #	Scenario Name	Background Modelling Scenarios	Paper Allocation (m ³ /year)	Average seasonal metered Usage (m ³ /year)	MAR (m ³ /year)	Rainfall Rate (Section 5.1. NIWA, 2020)	PED (Section 6.1. NIWA, 2020)	PED converted to percentage increase in average seasonal metered usage	Sea Level Rise	Droughts
2.1	Baseline (B+CC) + Climate Change	Current seasonal metered usage, no MAR, climate change included	0	Makauri = 847,000 Matokitoki = 62,000 Te Hapara Sands = 103,000 Waipaoa Gravel = 69,000 Shallow Fluviatile = 107,000	0					
3.1	Natural State V2	Current seasonal metered usage turned off, no MAR, with climate change	0	0	0					
4.1	Current Allocation Limit V2	Increase usage to full paper allocation (2021 regional rules)	Makauri = 1,906,362 Matokitoki = 343,900 Te Hapara Sands = 613,346 Waipaoa Gravel = 535,400* Shallow Fluviatile = 581,860* Total = 3,980,908 *Based on annual paper allocation of individual bores	0	0	Decrease <5% of actual until 2040 (RCP4.5) Decrease Summer 5-15% of actual until 2040 (RCP4.5) Decrease Spring and Summer 5-15% of actual 2040-2090 (RCP4.5)	PED to increase +125 mm (Mid-range of NIWA prediction, +100-150 mm until 2090. RCP 4.5)	Takes to increase: 5% at 2030	Table 10 RCP4.5	3 Year drought period (from 2013, 2014, 2015 historical event) replicated 2036 2051 2071
5.1	Managed Groundwater Replenishment V2	Current seasonal metered usage, increase recharge (e.g., ~600,000 m ³ /year)	0	Makauri = 847,000 Matokitoki = 62,000 Te Hapara Sands = 103,000 Waipaoa Gravel = 69,000 Shallow Fluviatile = 107,000	Makauri = 600,000 injection to increase: 5% at 2030 15% at 2045 24% at 2060 33% at 2075 42% at 2090					
7.1	Sustainable Allocation V2	Decrease usage until decline in aquifers (B) is no longer predicted, with climate change	0	Variable rate, 85% of Scenario 2.1	0					

A4 Scenario simulations: Results of abandoned setups

The first set of scenarios has been abandoned during the course of the project in favour of the second set documented in chapter 0 of this report. Nevertheless, a basic set of result tables and images is documented here, as well as are diagram plots in digital appendix DA 3.3.

Table A3-1: Legacy Scenarios: Overview of scenarios
Table A3-1 shows an overview of the abandoned / legacy scenarios. In Table A3-1 and

Table A3-2 the results of the scenarios at the end of the simulation time are compared for summer and winter conditions.

Table A3-1: Legacy Scenarios: Overview of scenarios

Scenario	Basis	Abstraction	Recharge	River Levels	MAR
1 Baseline (B)		B*	2017/18	2017/18	-
2 Baseline + Climate Change (B+CC)	B	B	-5% in 2040 -15% in Sept in 2090	B	-
3 Natural State	B+CC	-	B+CC	B	-
4 Paper Allocation	B+CC	full PA**	B+CC	B	-
5 MAR (M1)	B+CC	B	B+CC	B	6 bores, 600,000 m ³ /a
6 MAR (M2)	B+CC	B	B+CC	B	6 bores, 1,200,000 m ³ /a
7 Sustainable Allocation	B+CC	85% B	B+CC	B	-
8 Extreme events RCP8.5	B+CC	Increase Takes incl.3*3Y-draughts > B	-10% in 2040 -15% in Sept in 2040 -15% in 2040-2090	B + SeaRCP8.5	-
9 Climate Change RCP4.5	B+CC	Increase Takes > B	B+CC	B + SeaRCP4.5	-

Table A3-1: Legacy Scenarios: Changes of Average of Simulated Water Level (m) between scenarios

Changes of Average of Simulated Water Level (m) in comparison to								
Scenario	Scenarios	Matokitoki	Makauri	Waipaoa	Shallow	Te Hapara Sands	Overall	Remark

1	Baseline B							
2	B+CC, Climate Change	-0.01	-0.01	-0.02	-0,06	-0,04		comp. to Scenario B
3	Natural State with CC	+0.71	+0.70	+0.30	+0.07	+0.06		comp. to Scenario B+CC
4	A1+CC Paper Allocation	-1.54	-1.15	-0.66	-0.06	-0.07		comp. to Scenario B+CC
5	MAR M1 (+600,000 m³)	+0.41	+0.48	+0.18	-0.02	-0.02		comp. to Scenario B
7	Sustainable incl. CC and 1/2 Takes of Baseline	+0.36	+0.35	+0.14	+0.01	+0.01		comp. to Scenario B+CC
	Number of Obs. Bores	12	65	13	12	36	137	

Table A3-2: Legacy Scenarios: Changes of Average of Simulated Water Level (m) between scenarios

Scenario #	Scenarios	Changes of Average of Simulated Water Level (m) in comparison to					Overall	Remark
		Matokitoki	Makauri	Waipaoa	Shallow	Te Hapara Sands		
1	Baseline B							
2	B+CC , Climate Change	-0.01	-0.01	-0.02	-0,06	-0,04		comp. to Scenario B
3	Natural State with CC	+0.71	+0.70	+0.30	+0.07	+0.06		comp. to Scenario B+CC
4	A1+CC Paper Allocation	-1.54	-1.15	-0.66	-0.06	-0.07		comp. to Scenario B+CC
5	MAR M1 (+600,000 m ³)	+0.41	+0.48	+0.18	-0.02	-0.02		comp. to Scenario B
7	Sustainable incl. CC and 1/2 Takes of Baseline	+0.36	+0.35	+0.14	+0.01	+0.01		comp. to Scenario B+CC
	Number of Obs. Bores	12	65	13	12	36	137	

Scenario 2

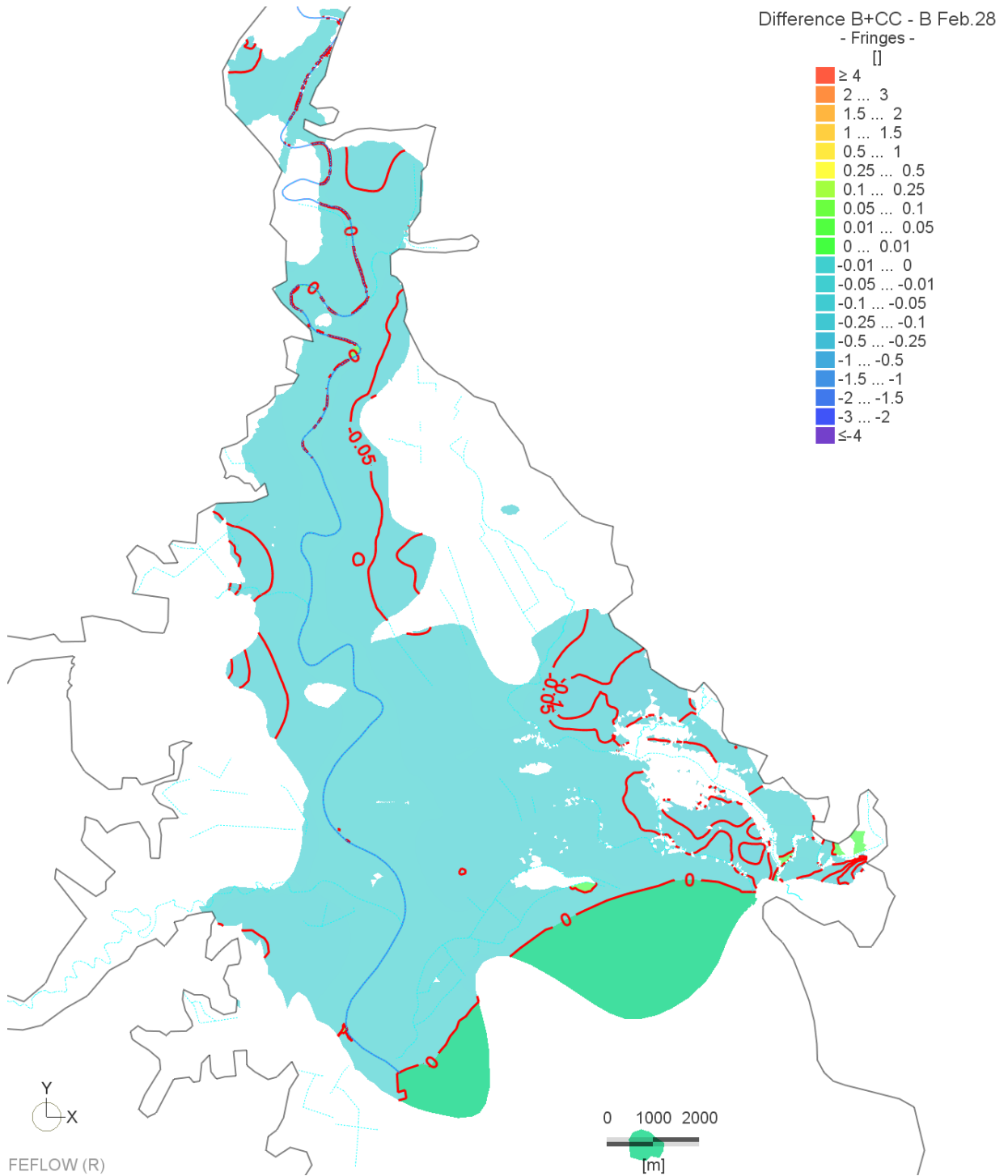


Figure A3-1: Legacy scenarios: Difference between scenarios 2 and 1, shallow aquifers, summer

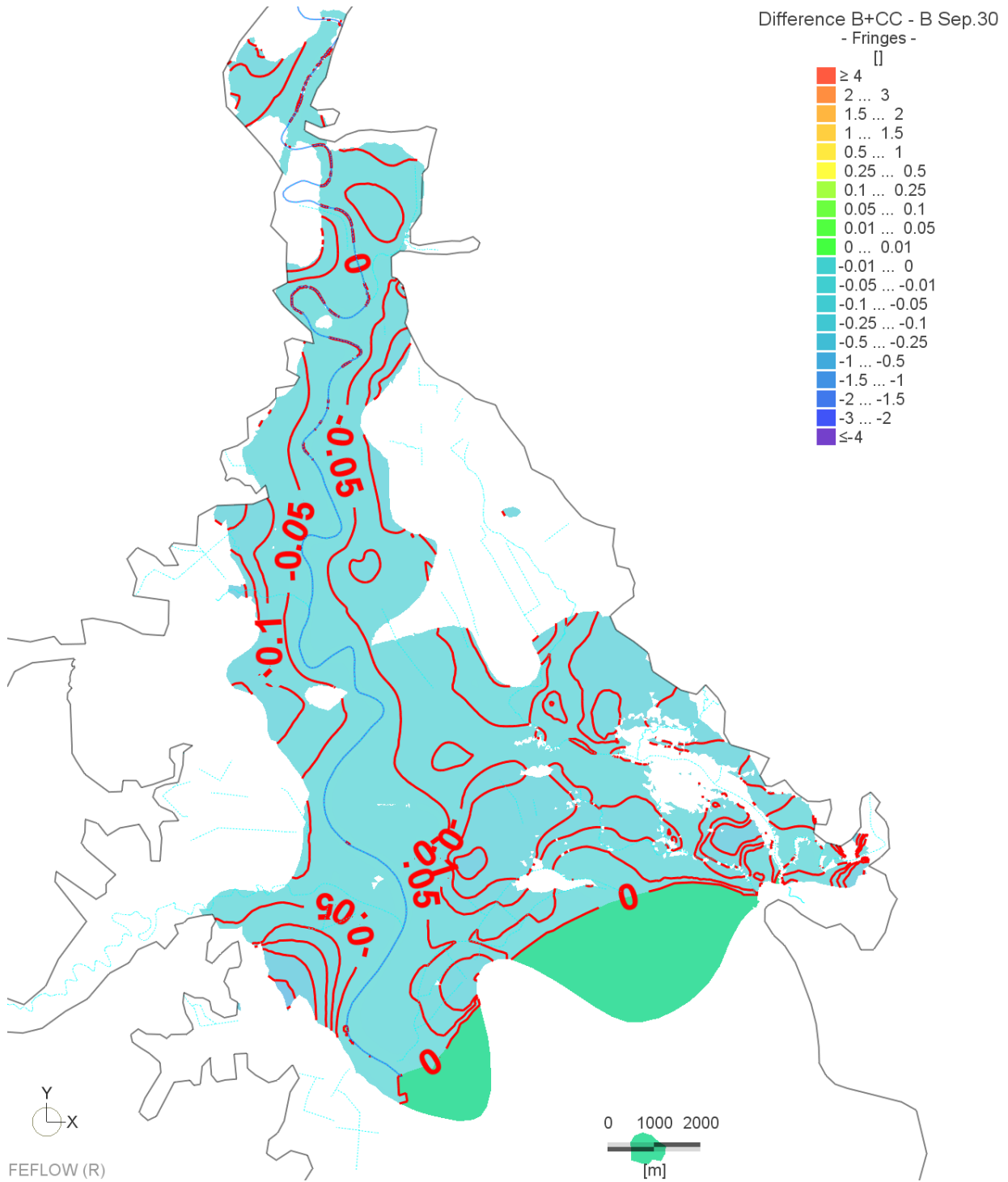


Figure A3-2: Legacy scenarios: Difference between scenarios 2 and 1, shallow aquifers, winter

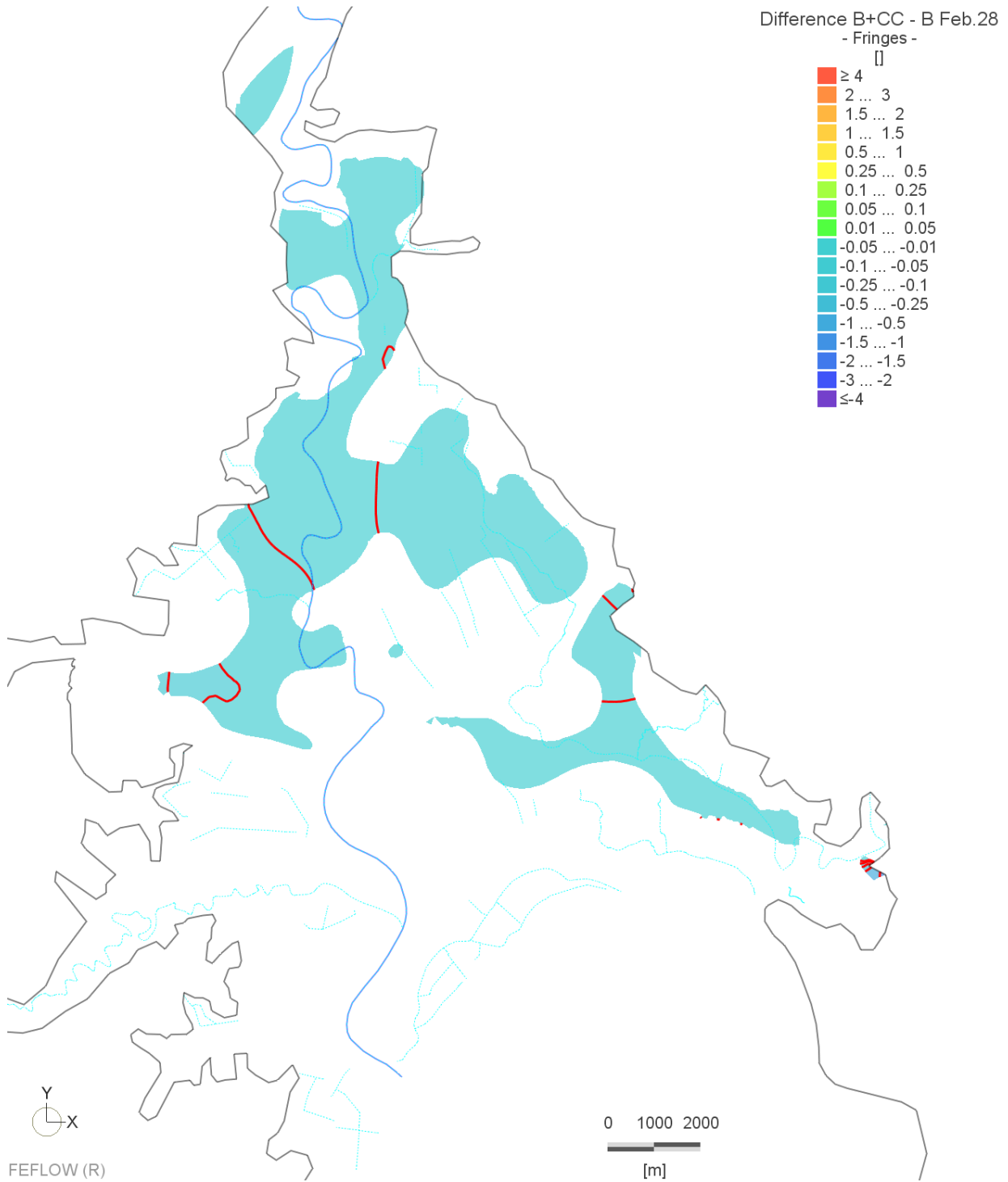


Figure A3-3: Legacy scenarios: Difference between scenarios 2 and 1, Waipaoa aquifer, summer

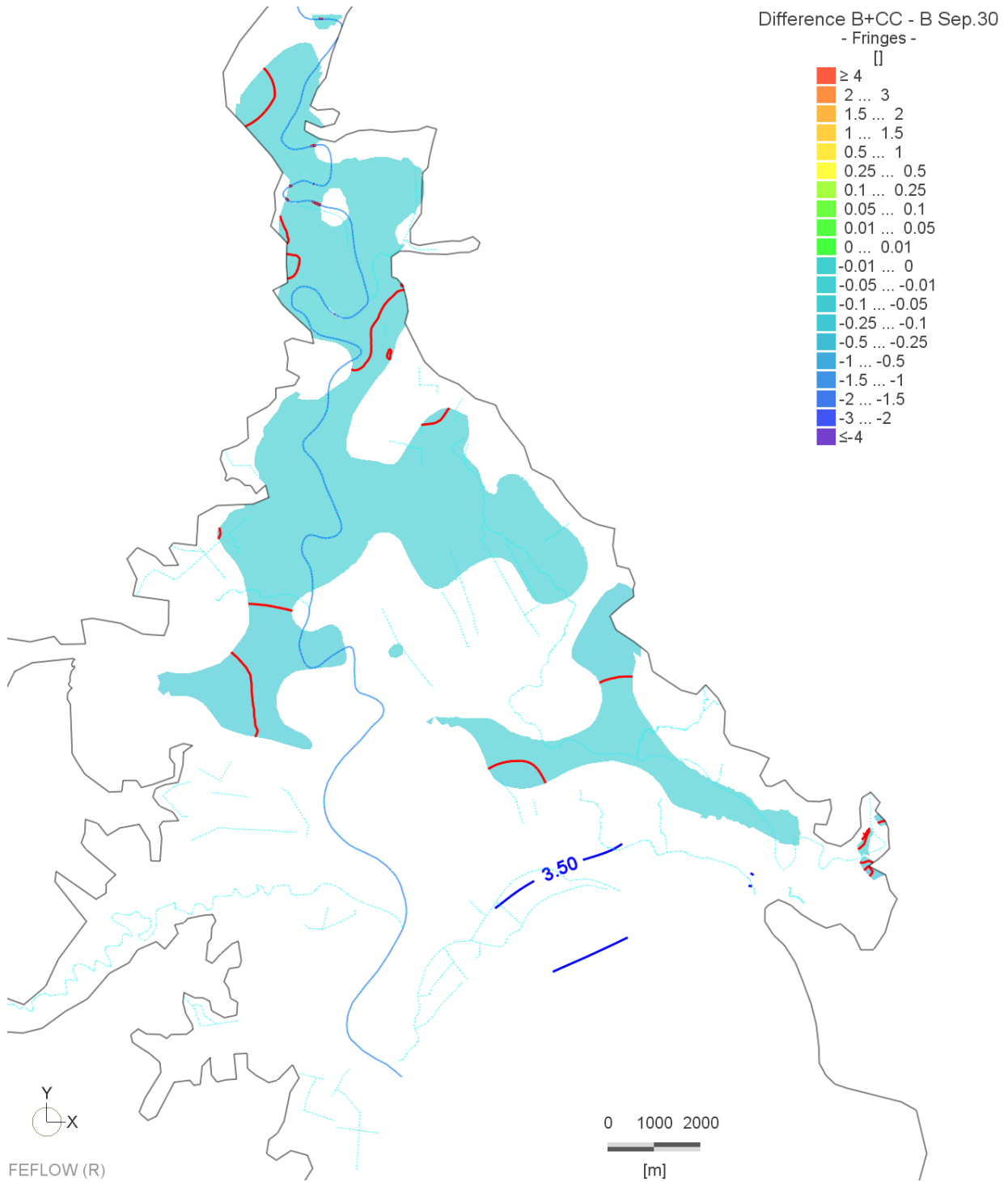


Figure A3-4: Legacy scenarios: Difference between scenarios 2 and 1, Waipaoa aquifer, winter

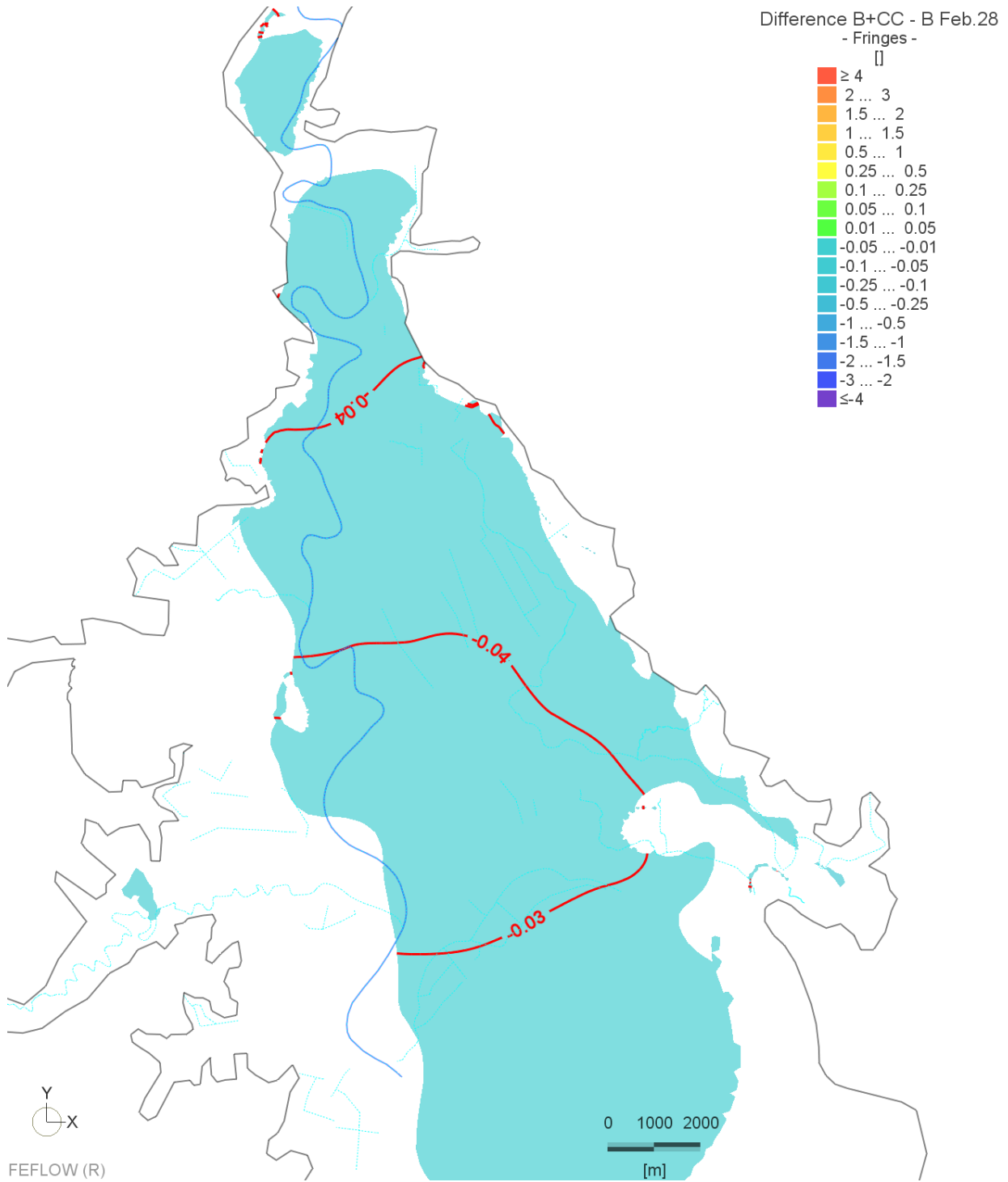
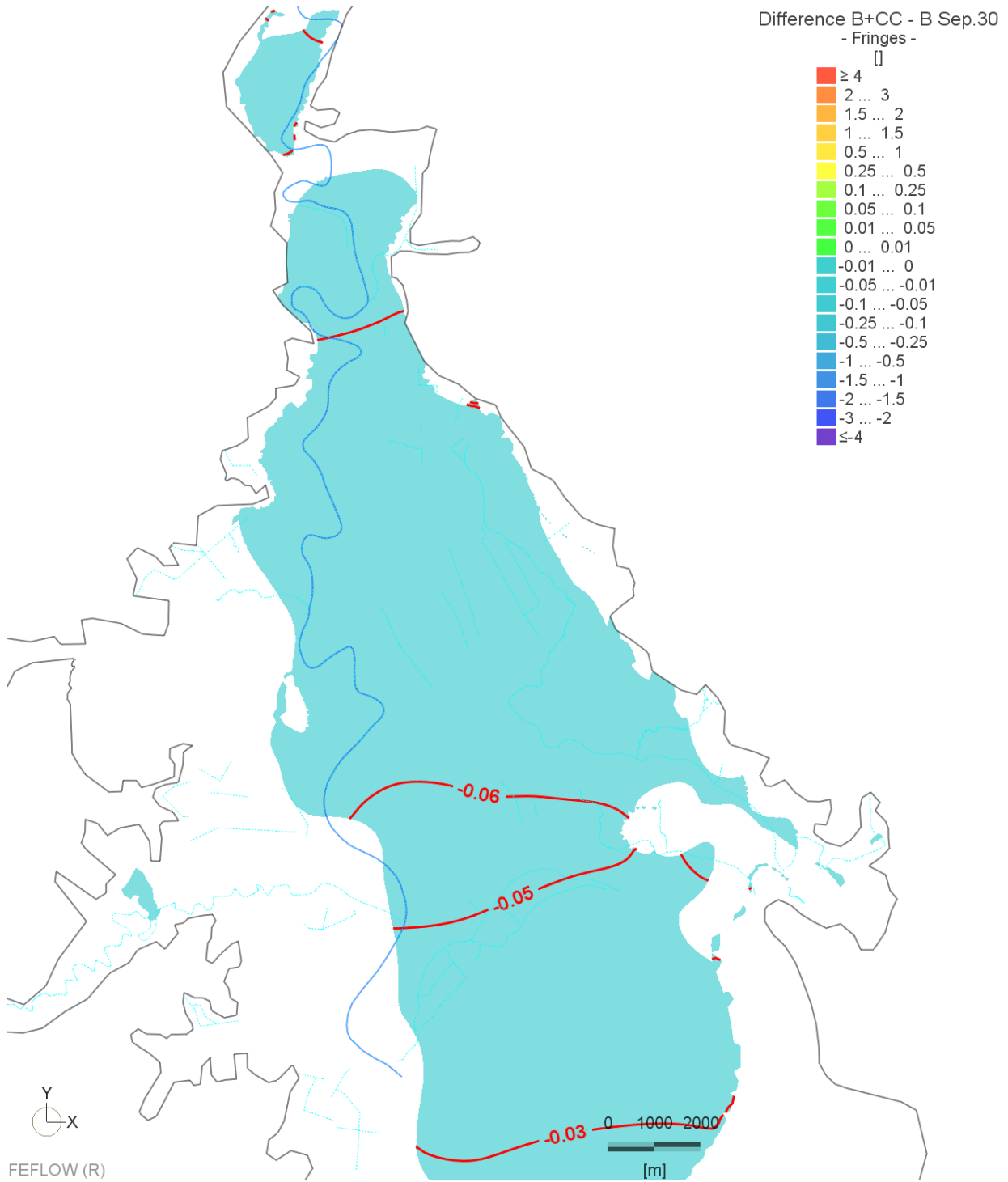


Figure A3-5: Legacy scenarios: Difference between scenarios 2 and 1, Makauri aquifer, summer



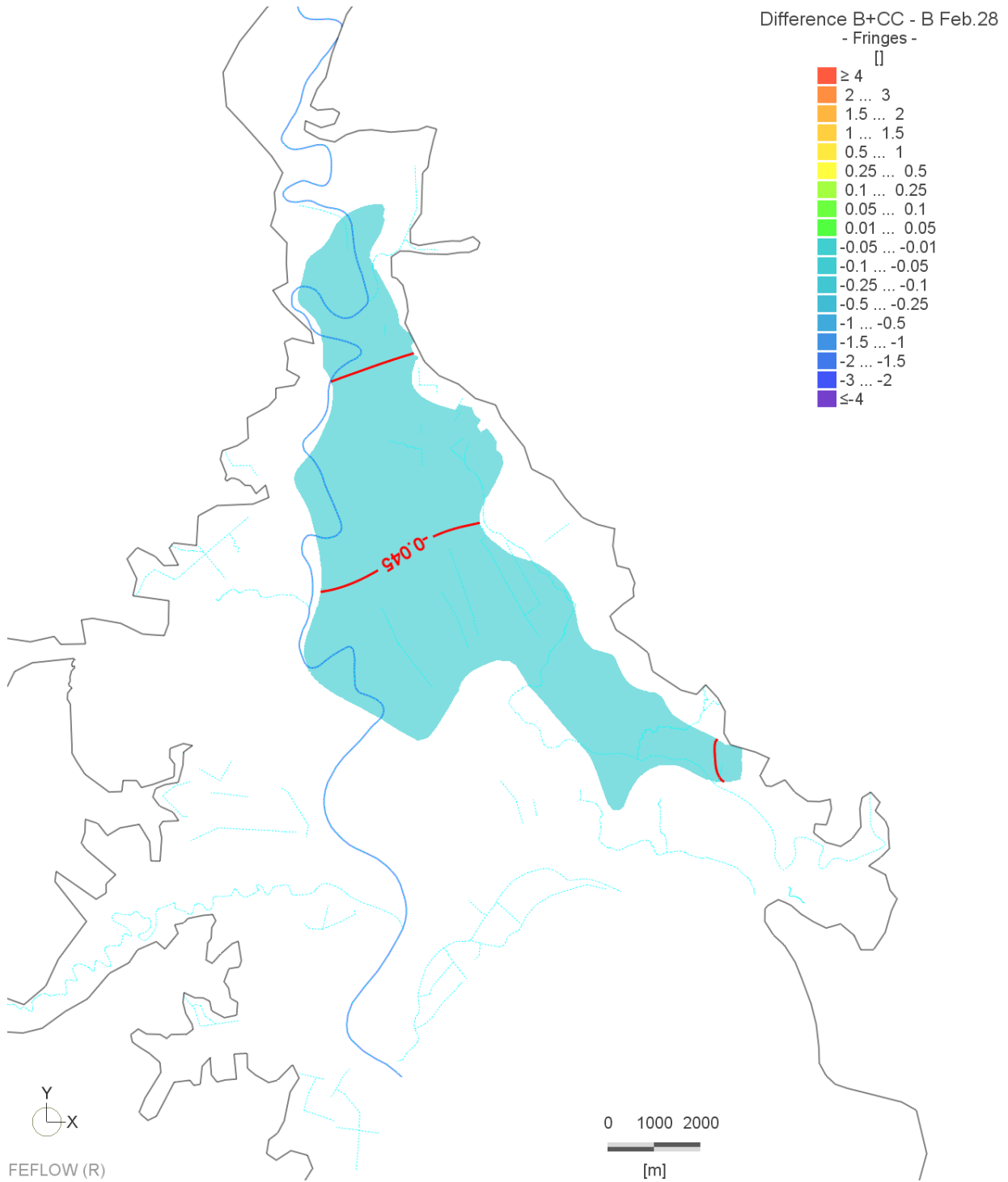


Figure A3-7: Legacy scenarios: Difference between scenarios 2 and 1, Matokitoki aquifer, summer

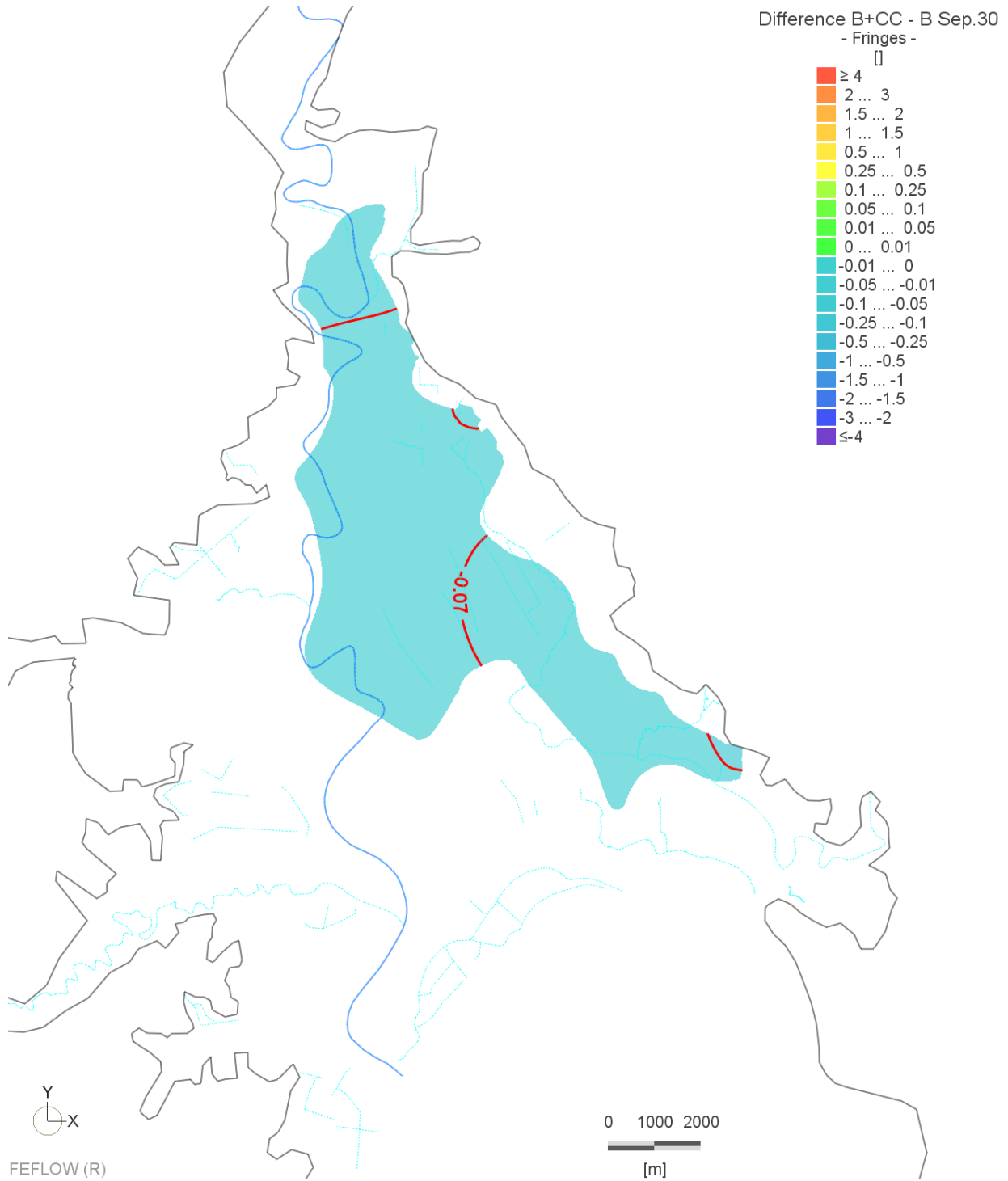


Figure A3-8: Legacy scenarios: Difference between scenarios 2 and 1, Matokitoki aquifer, winter

Scenario 3

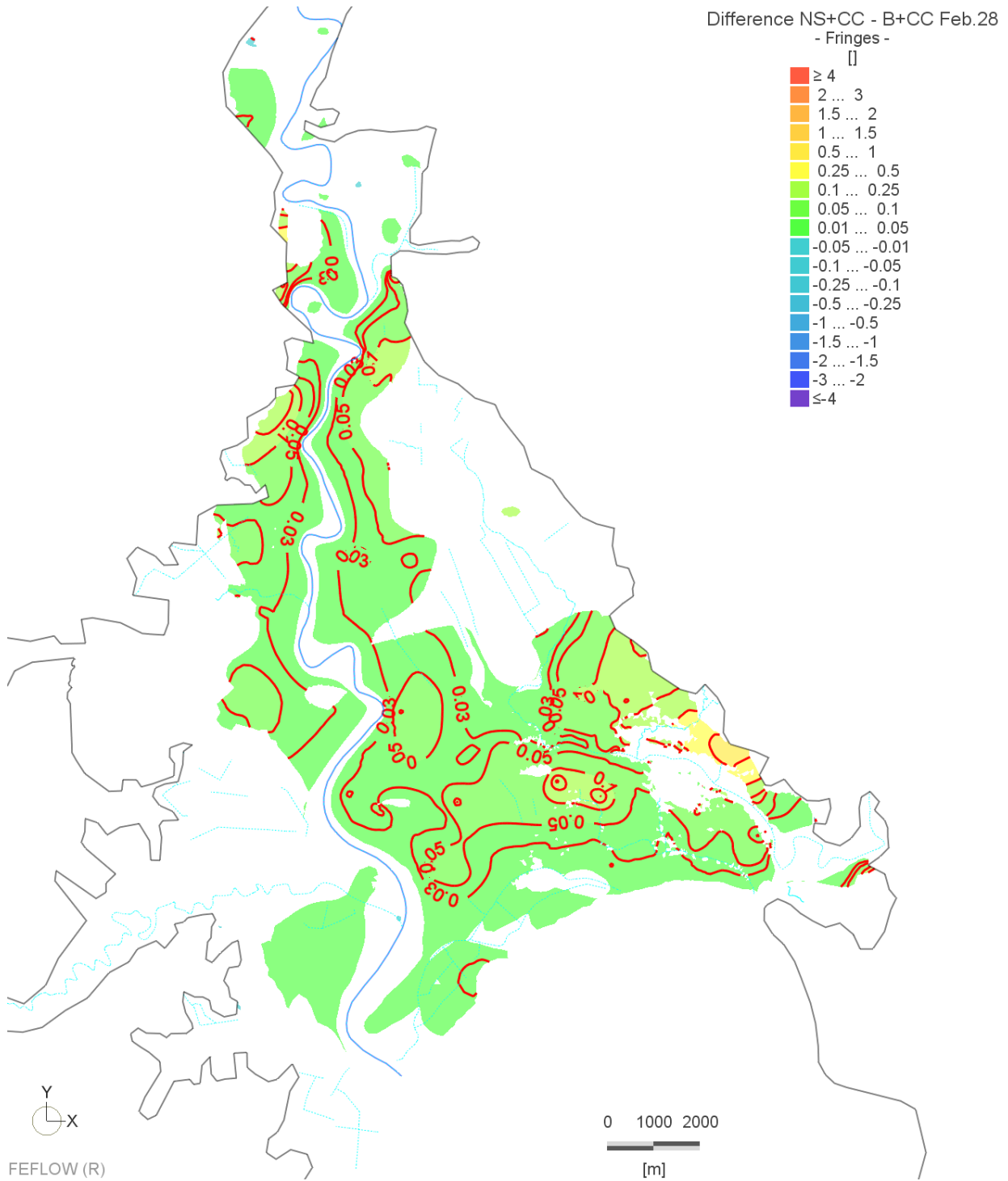


Figure A3-9: Legacy scenarios: Difference between scenarios 3 and 2, shallow aquifers, summer

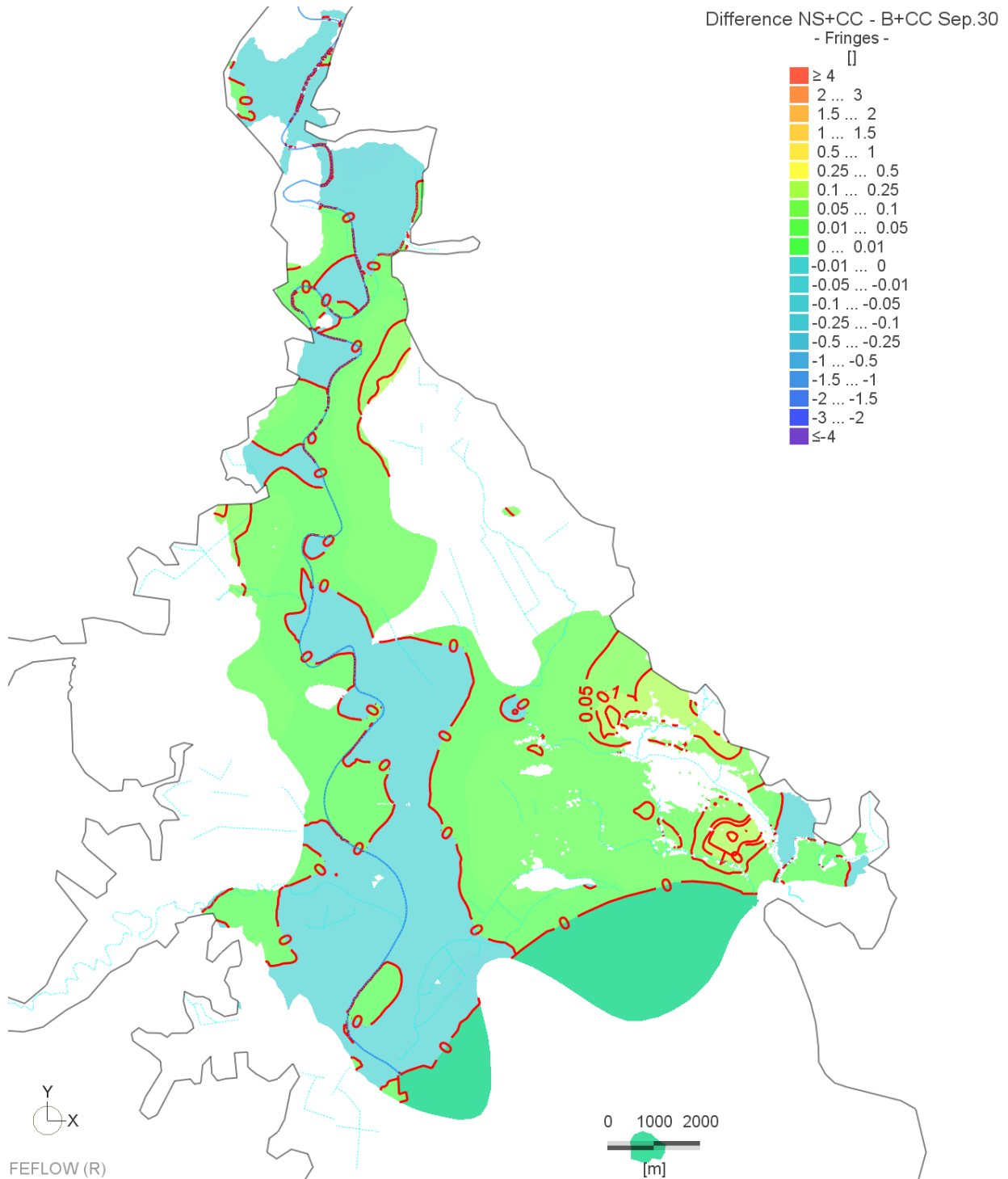


Figure A3-10: Legacy scenarios: Difference between scenarios 3 and 2, shallow aquifers, winter

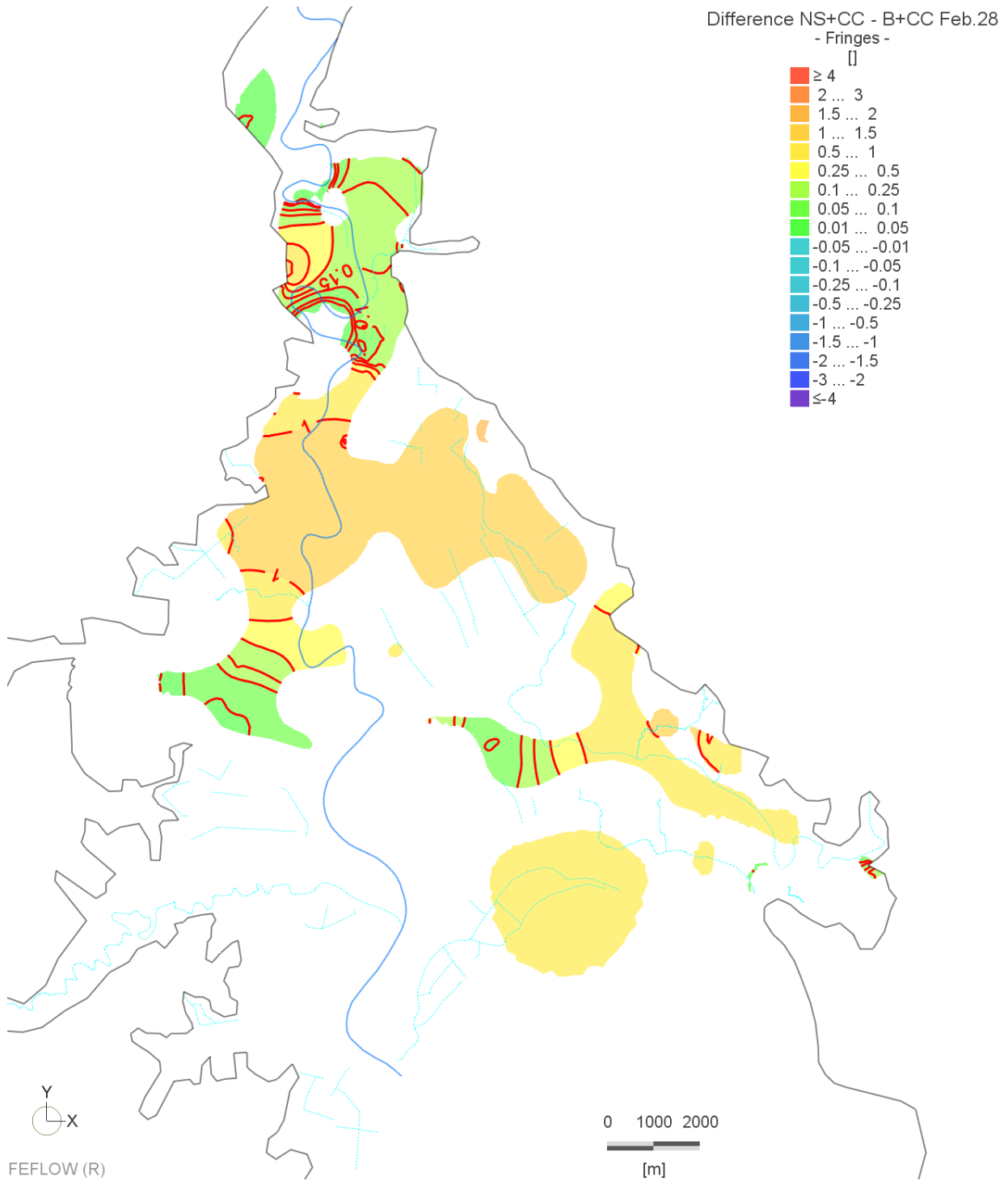


Figure A3-11: Legacy scenarios: Difference between scenarios 3 and 2, Waipaoa aquifer, summer

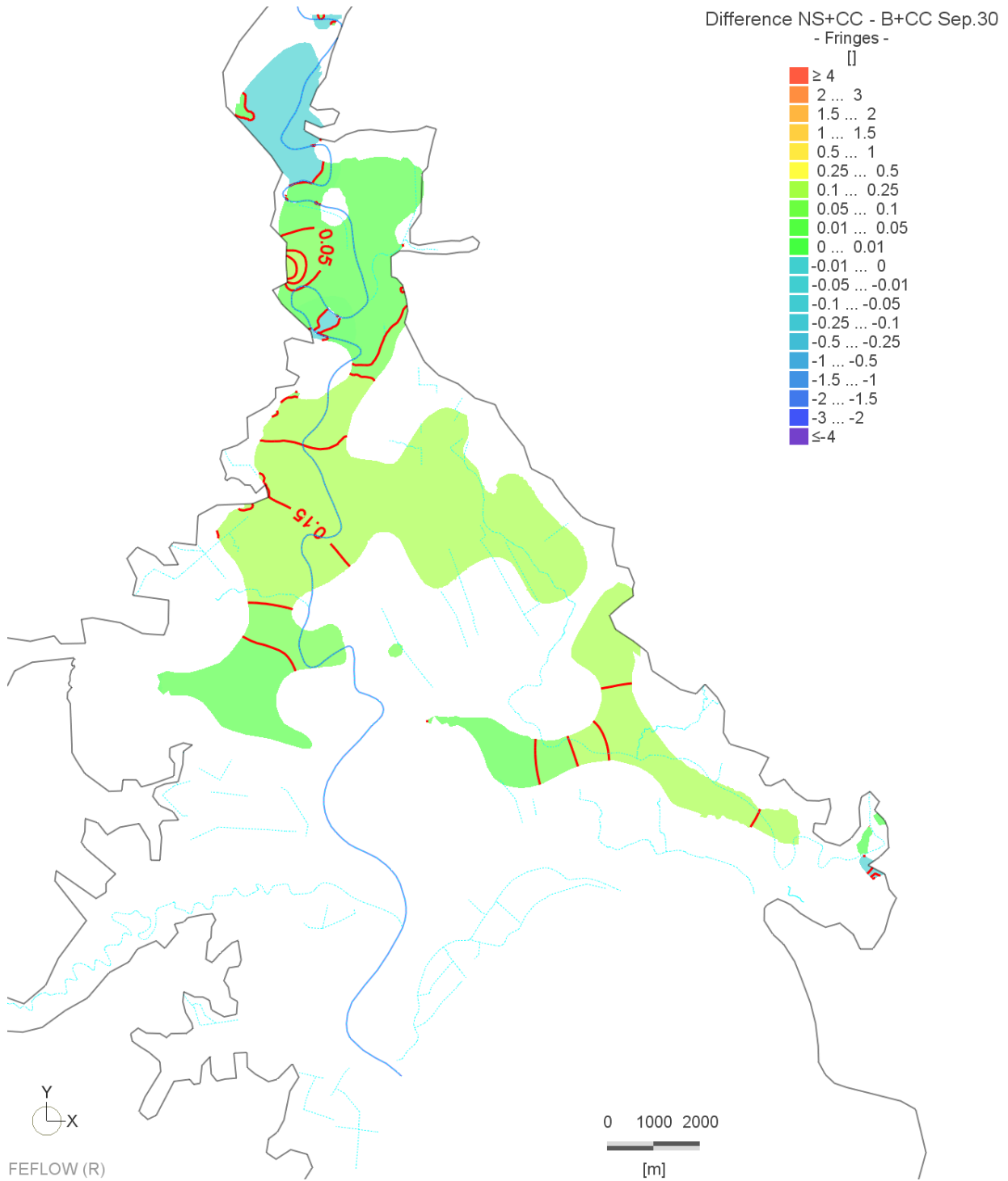


Figure A3-12: Legacy scenarios: Difference between scenarios 3 and 2, Waipaoa aquifer, winter

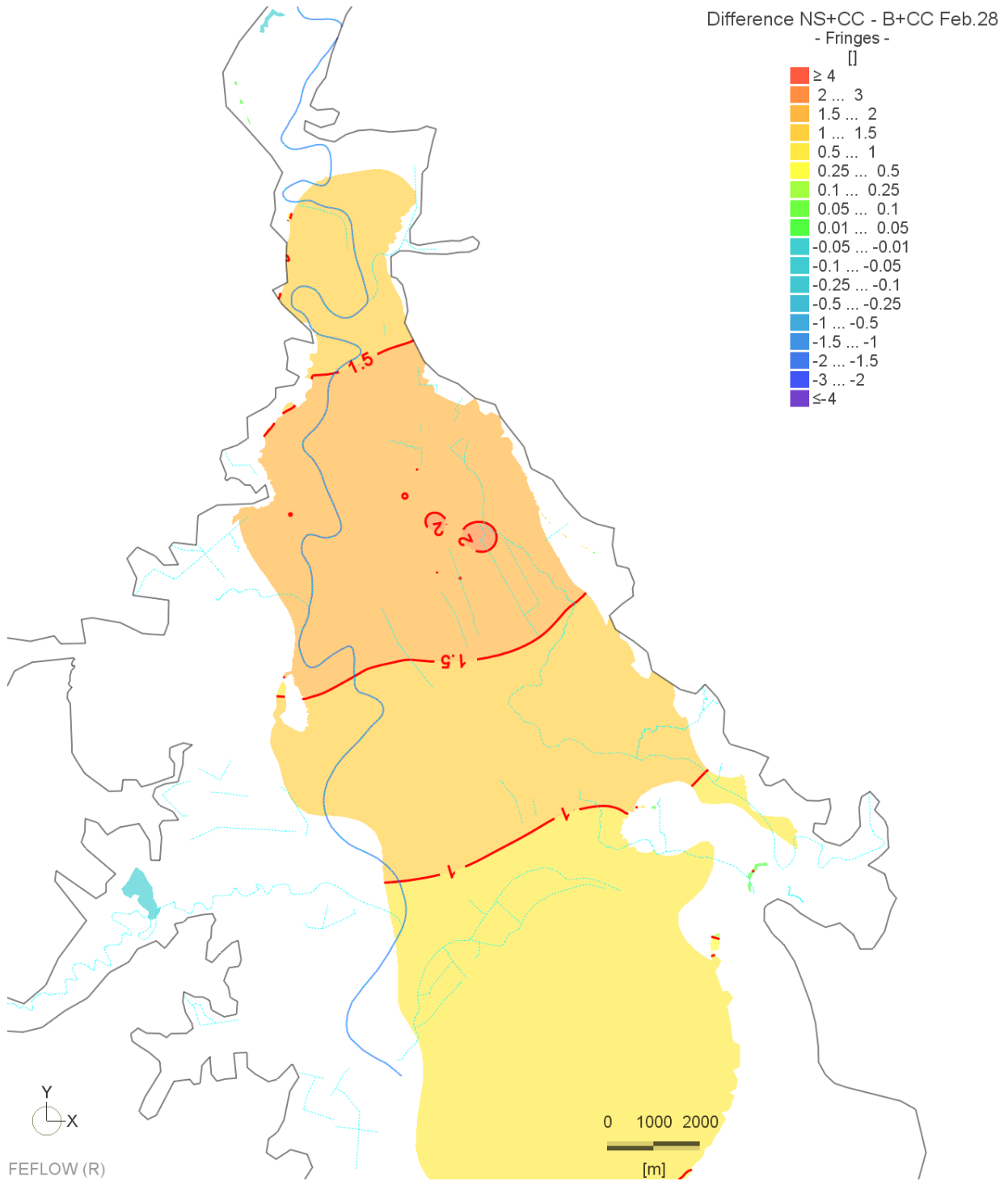


Figure A3-13: Legacy scenarios: Difference between scenarios 3 and 2, Makauri aquifer, summer

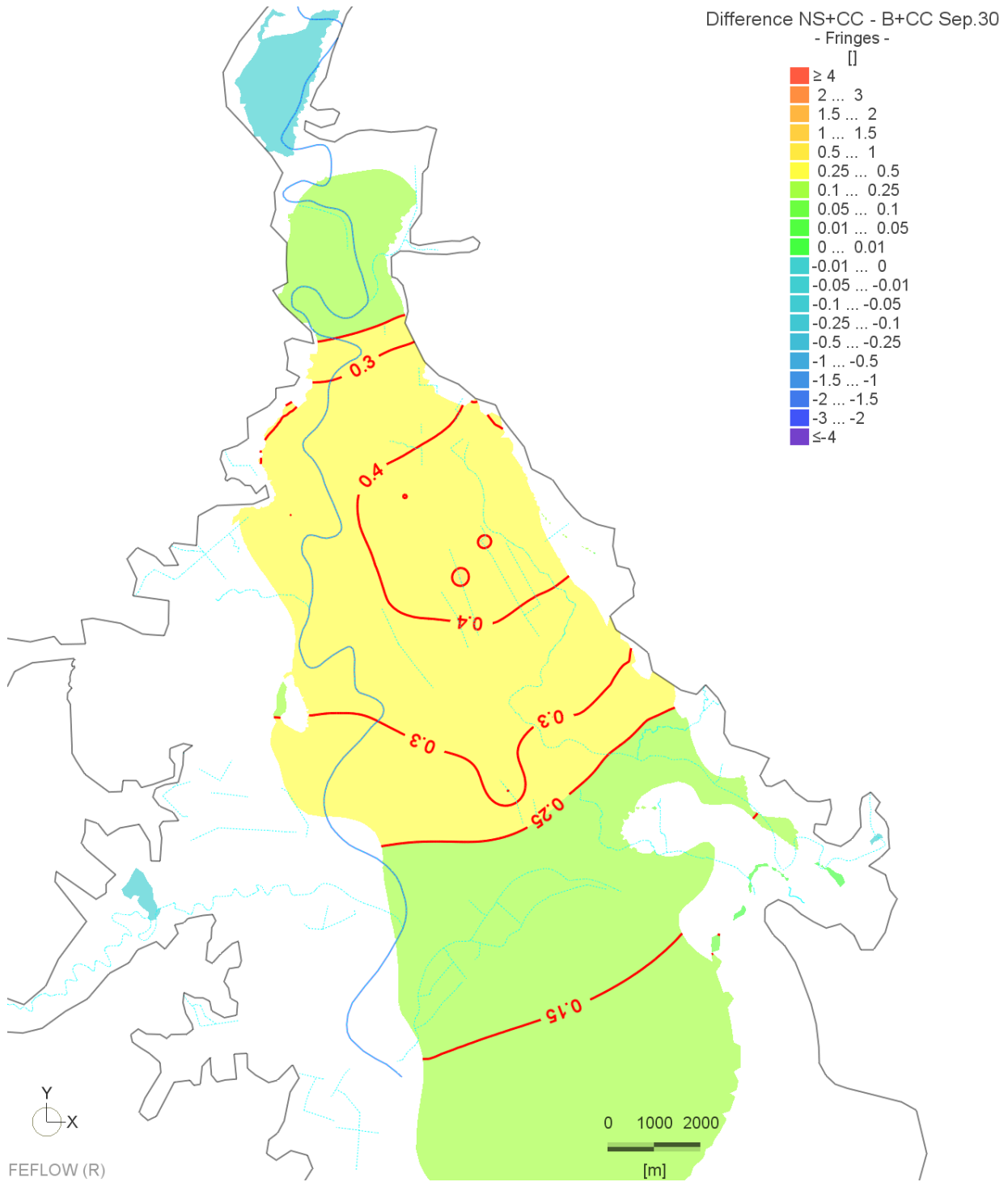


Figure A3-14: Legacy scenarios: Difference between scenarios 3 and 2, Makauri aquifer, winter

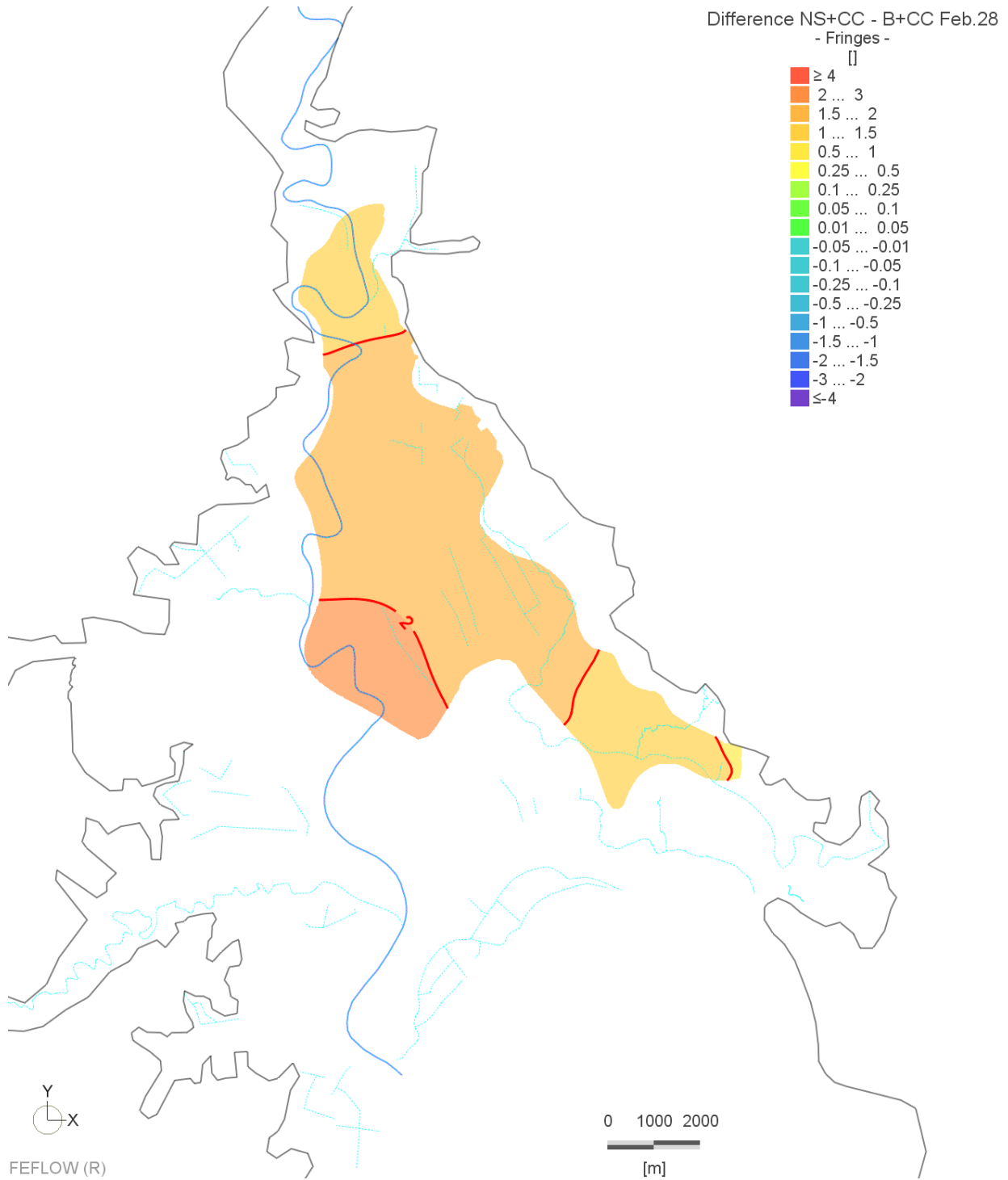


Figure A3-15: Legacy scenarios: Difference between scenarios 3 and 2, Matokitoki aquifer, summer

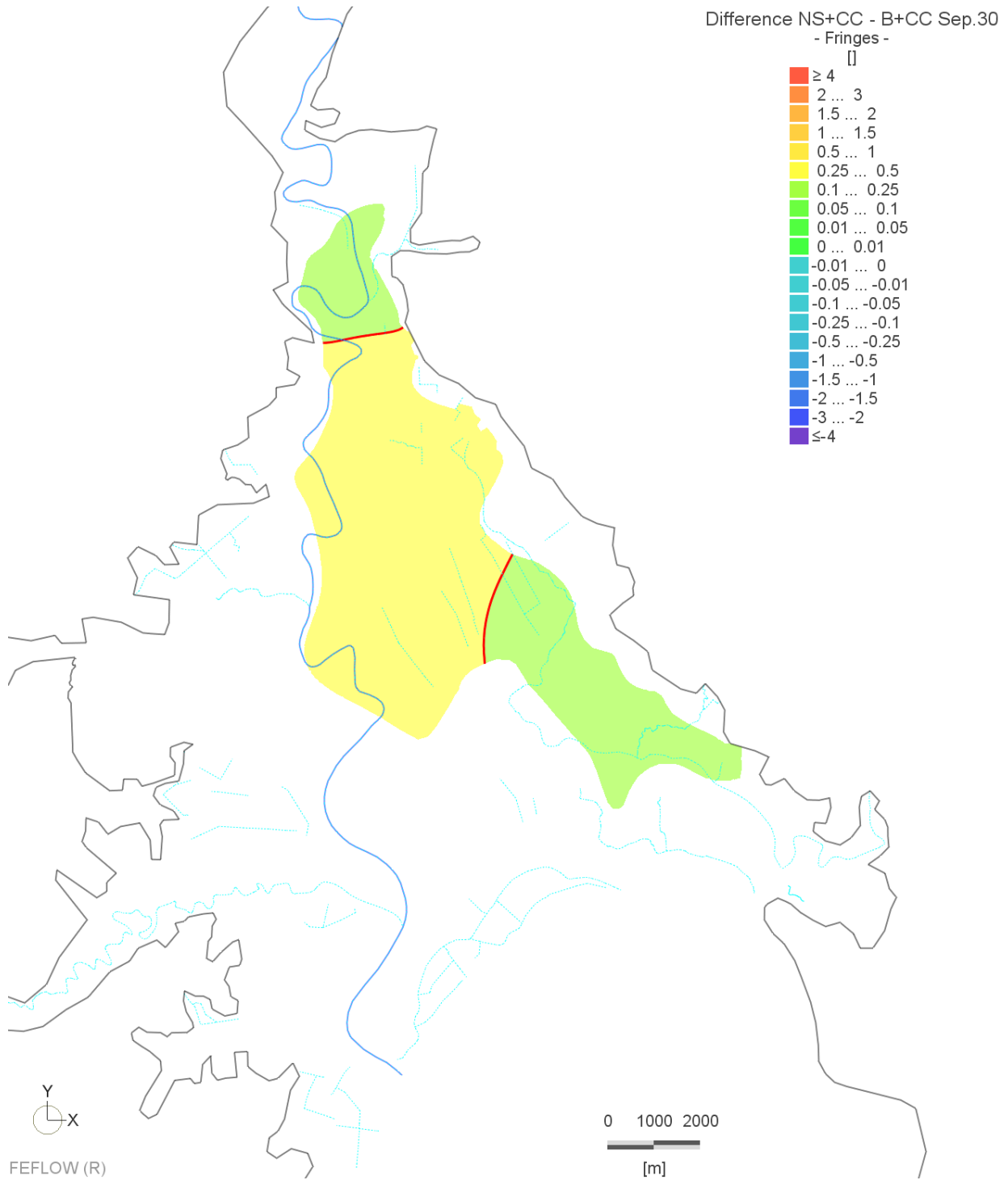


Figure A3-16: Legacy scenarios: Difference between scenarios 3 and 2, Matokitoki aquifer, winter

Scenario 4

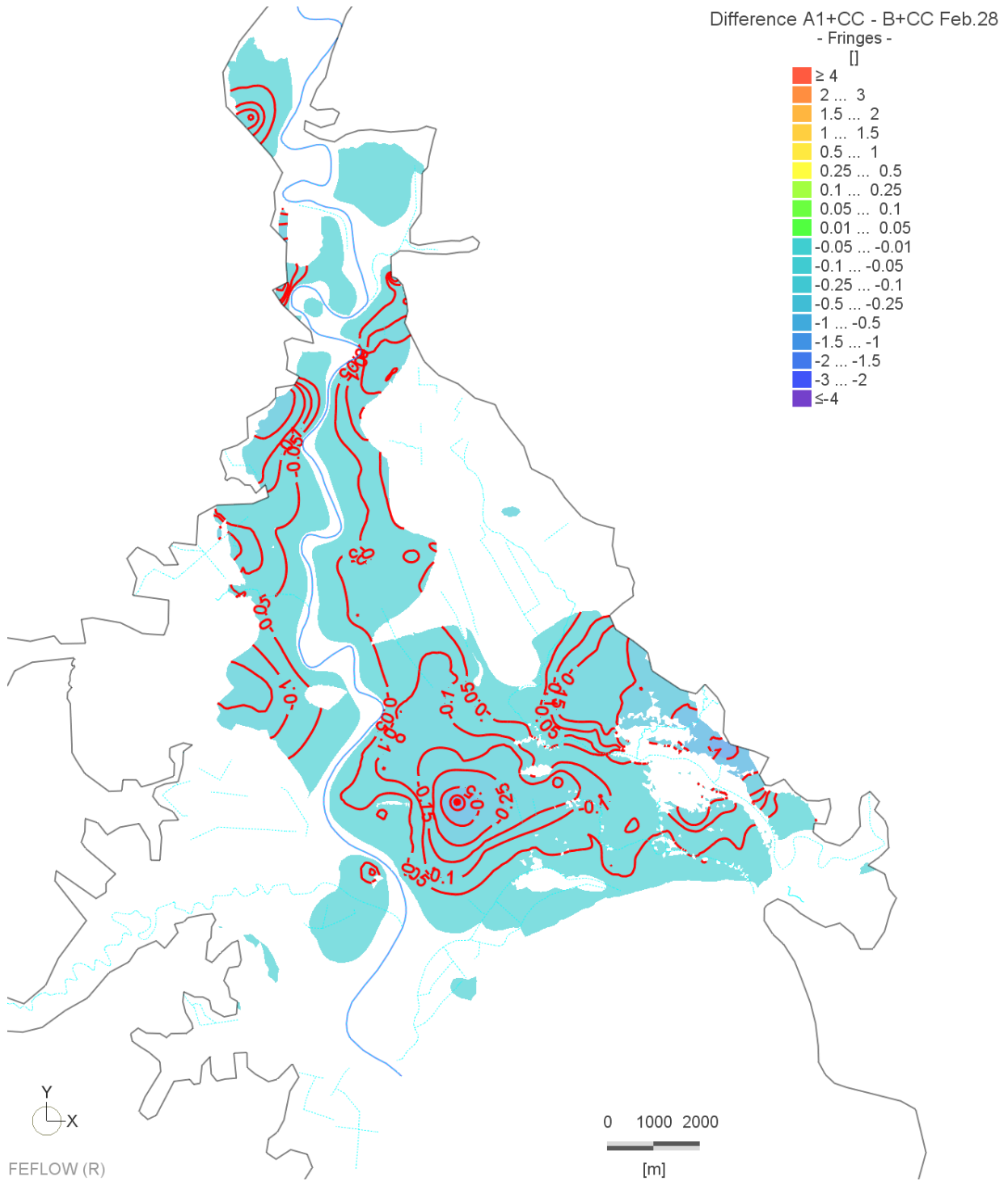


Figure A3-17: Legacy scenarios: Difference between scenarios 4 and 2, shallow aquifers, summer

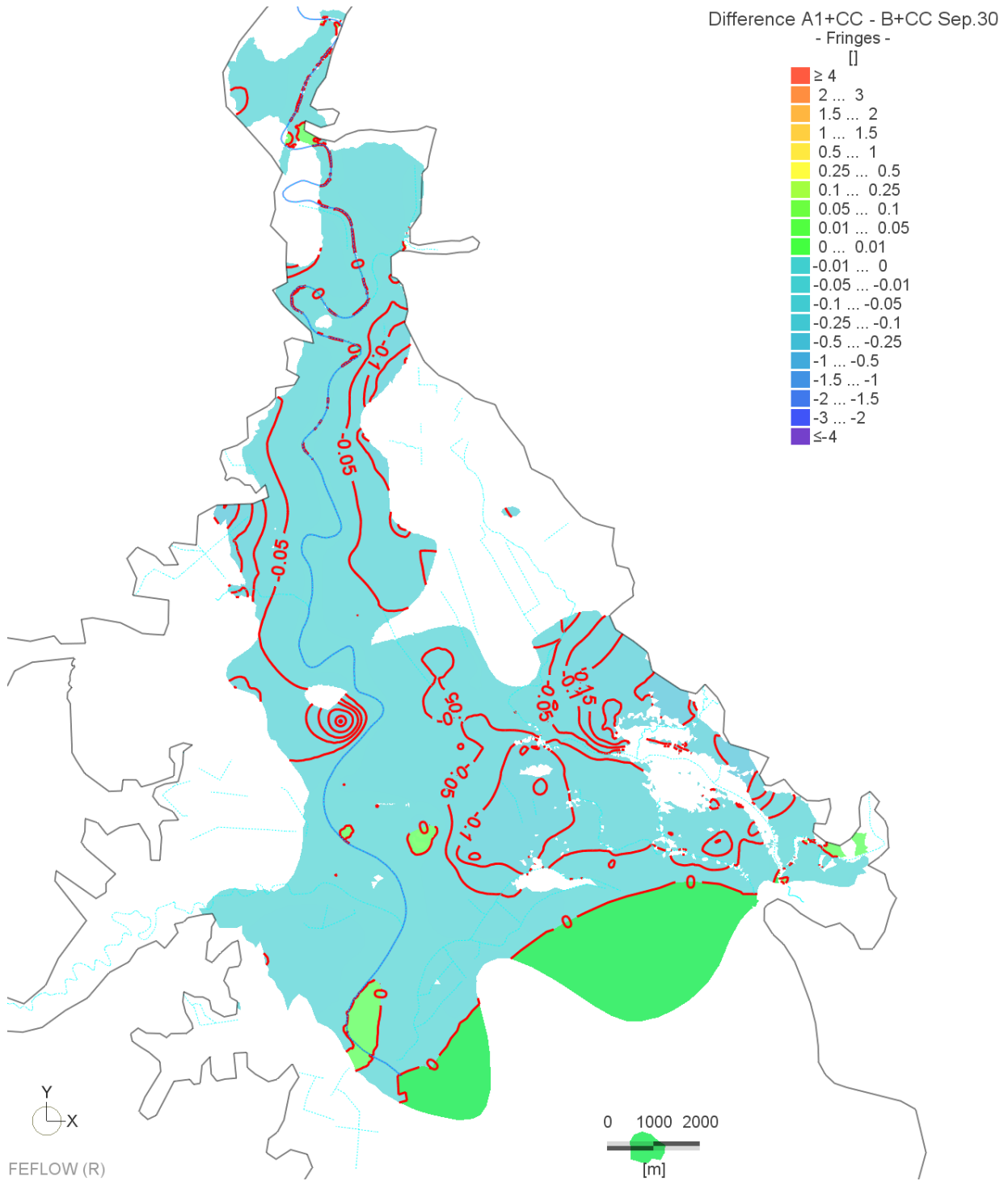


Figure A3-18: Legacy scenarios: Difference between scenarios 4 and 2, shallow aquifers, winter

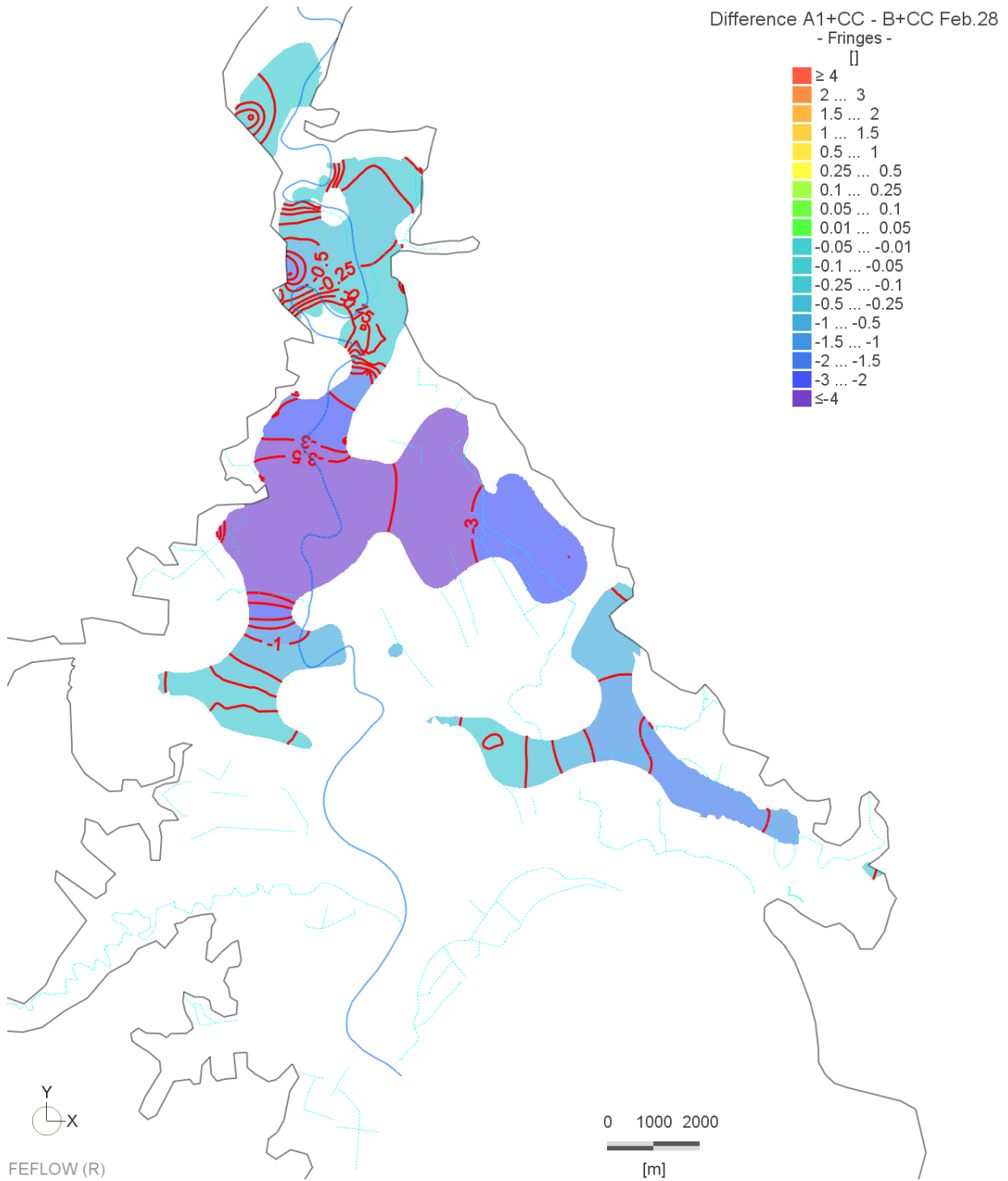


Figure A3-19: Legacy scenarios: Difference between scenarios 4 and 2, Waipaoa aquifer, summer

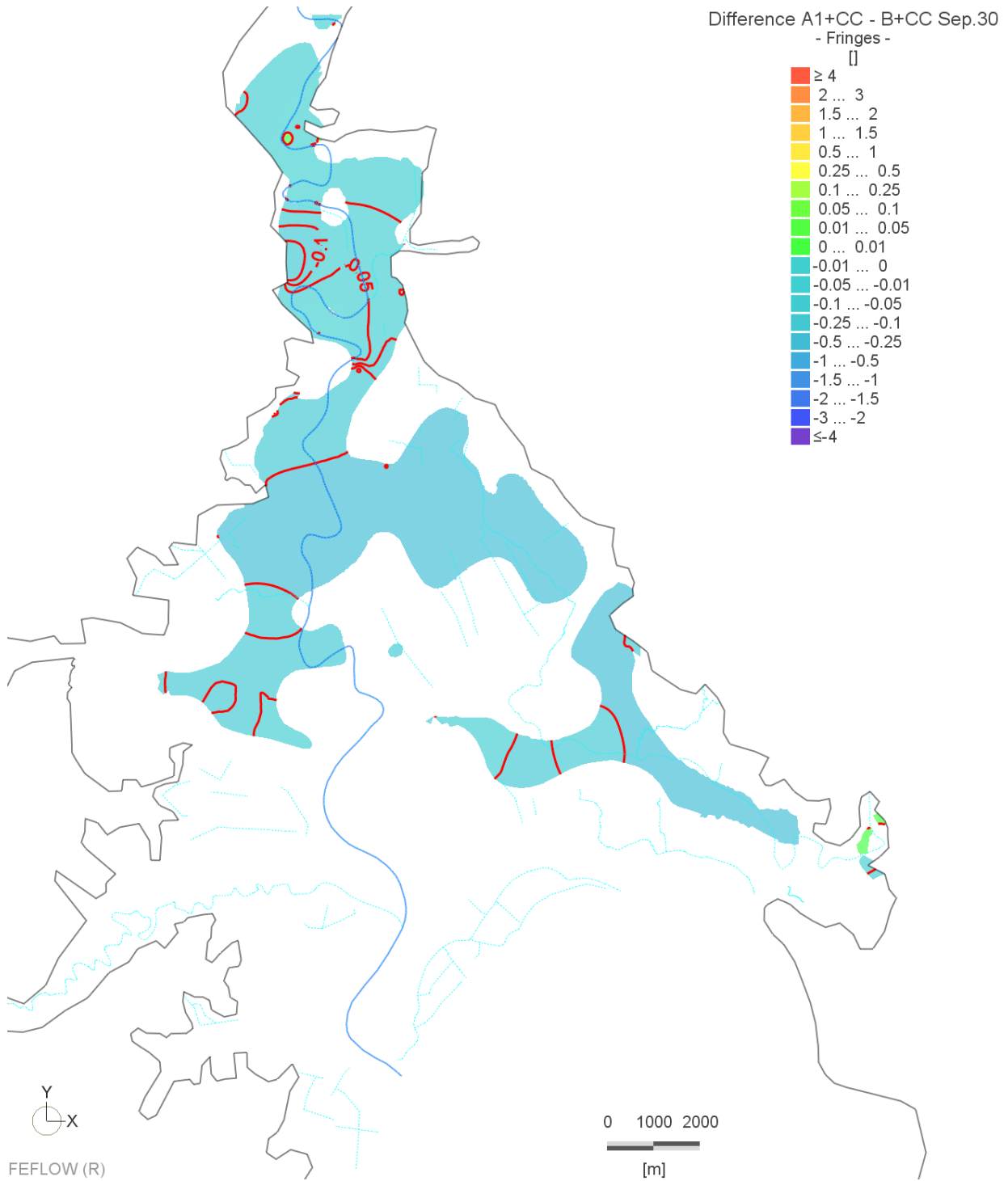


Figure A3-20: Legacy scenarios: Difference between scenarios 4 and 2, Waipaoa aquifer, winter

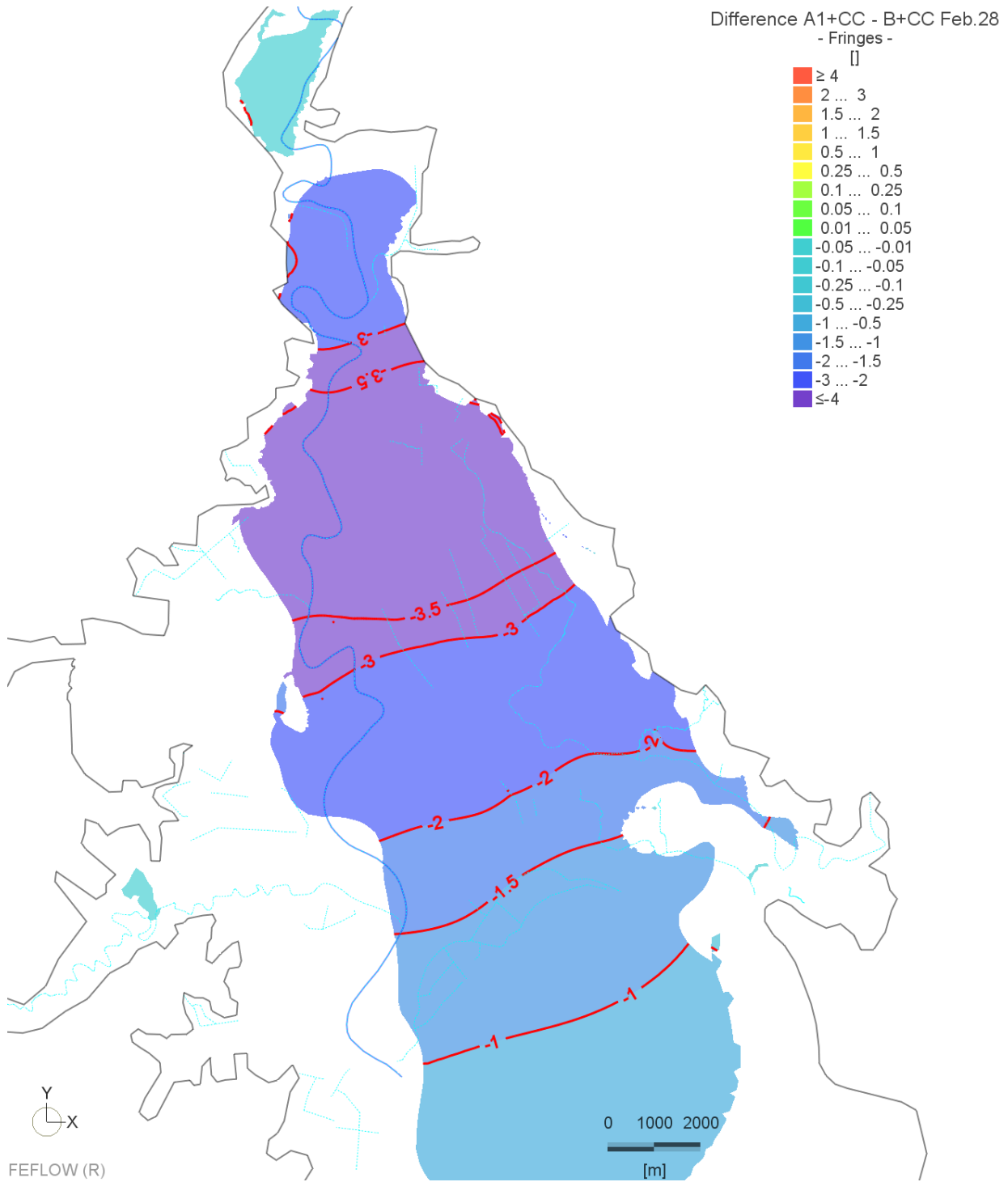


Figure A3-21: Legacy scenarios: Difference between scenarios 4 and 2, Makauri aquifer, summer

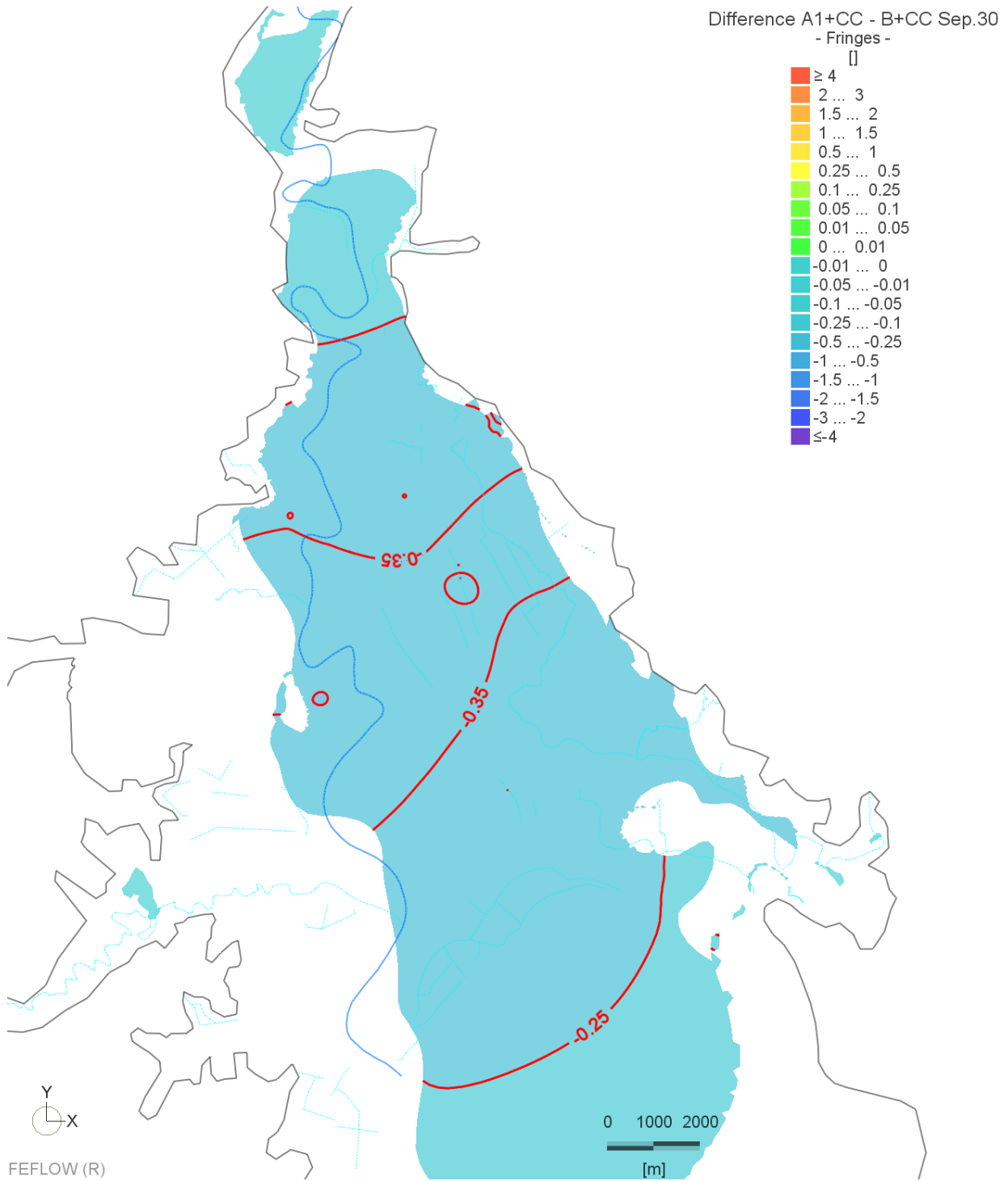


Figure A3-22: Legacy scenarios: Difference between scenarios 4 and 2, Makauri aquifer, winter

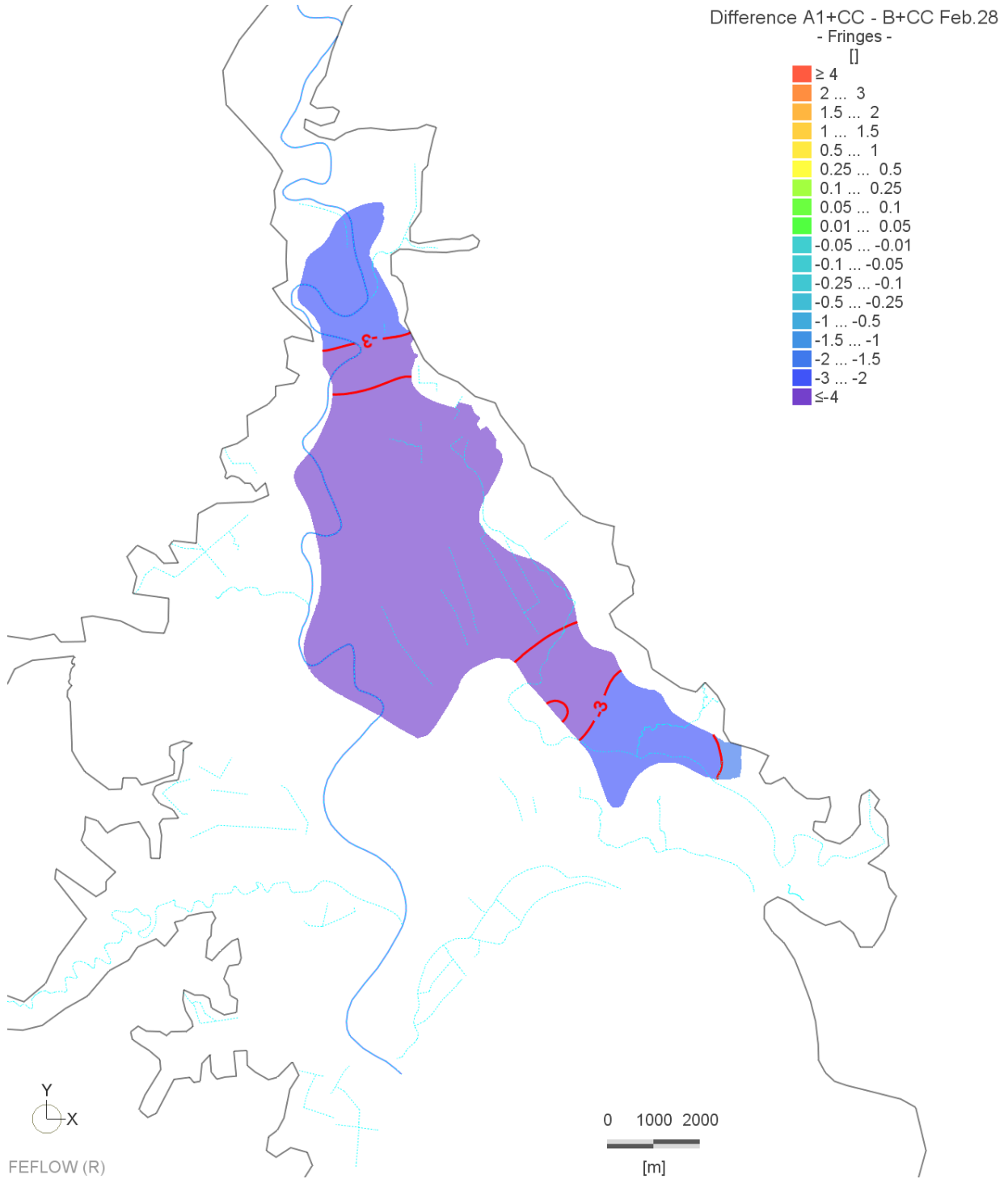


Figure A3-23: Legacy scenarios: Difference between scenarios 4 and 2, Matokitoki aquifer, summer

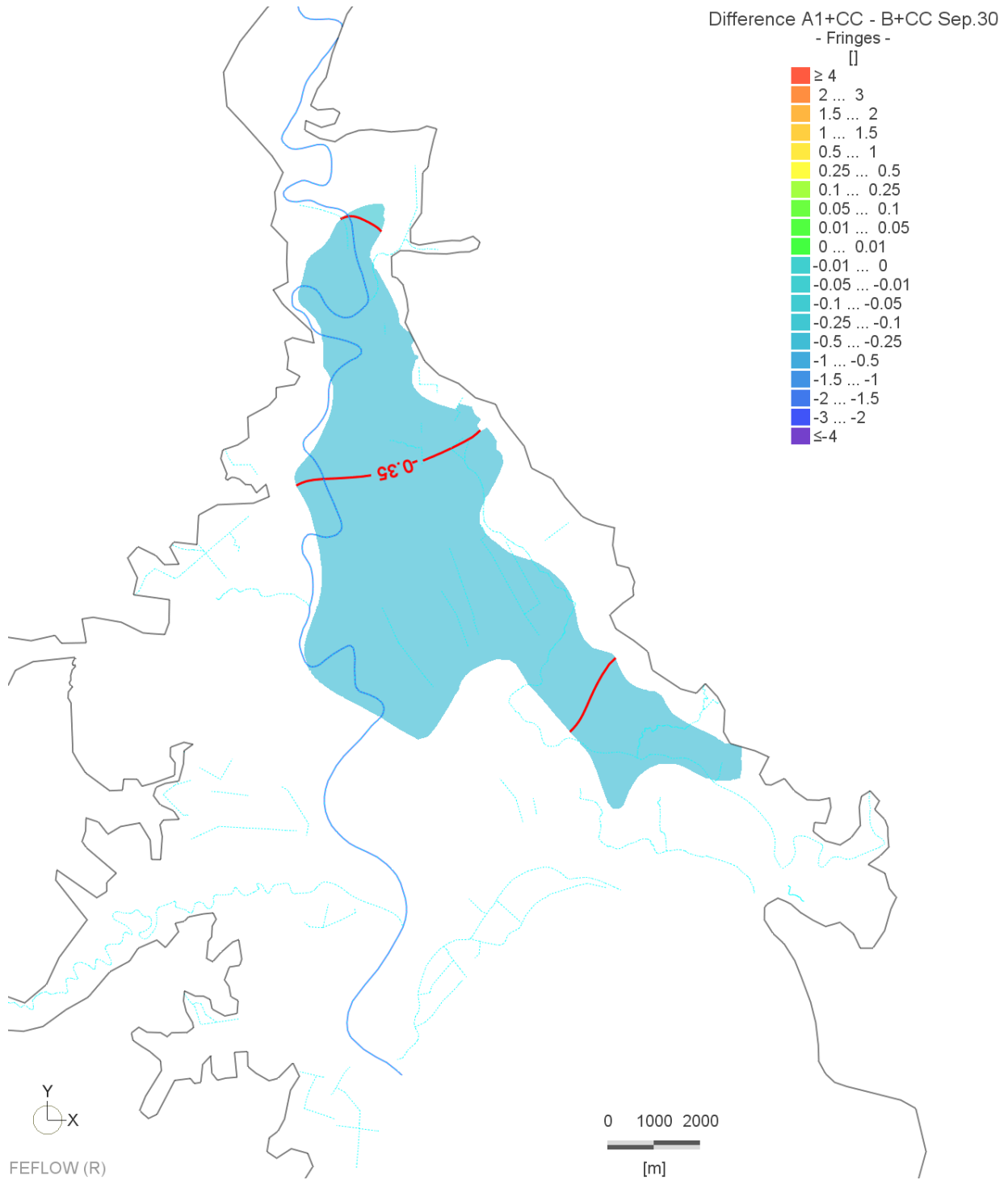


Figure A3-24: Legacy scenarios: Difference between scenarios 4 and 2, Matokitoki aquifer, winter

Scenario 5

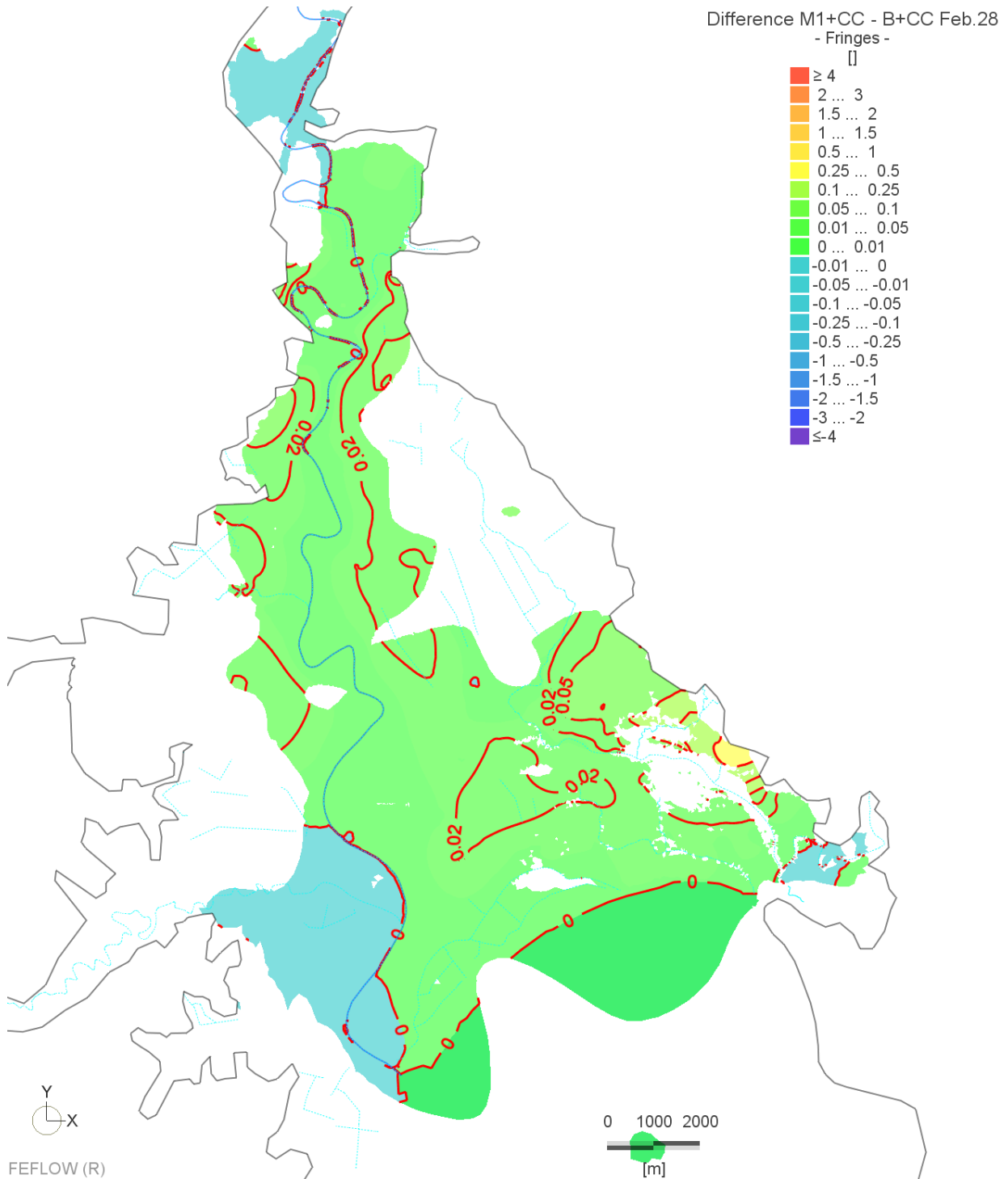


Figure A3-25: Legacy scenarios: Difference between scenarios 5 and 2, shallow aquifers, summer

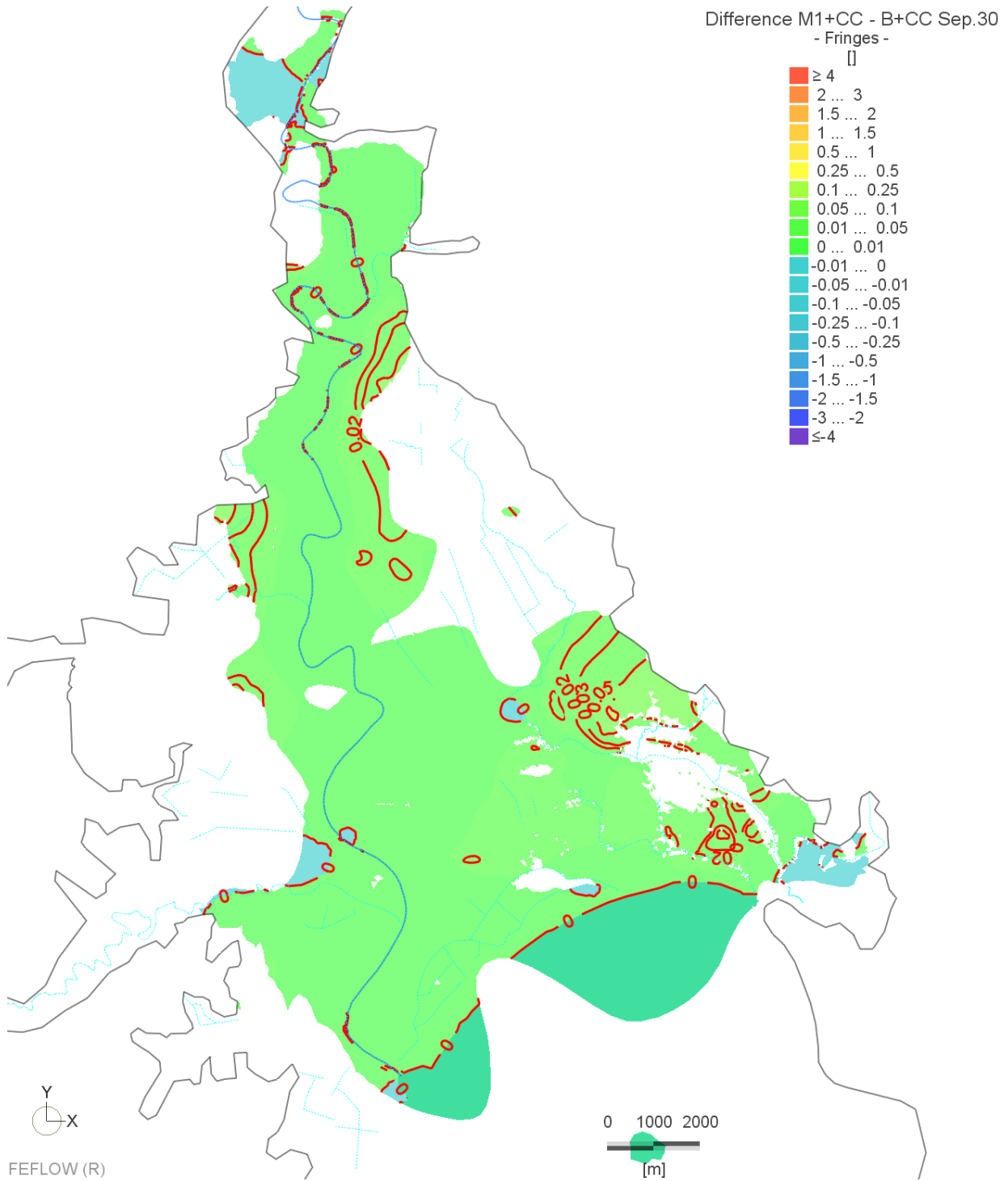


Figure A3-26: Legacy scenarios: Difference between scenarios 5 and 2, shallow aquifers, winter

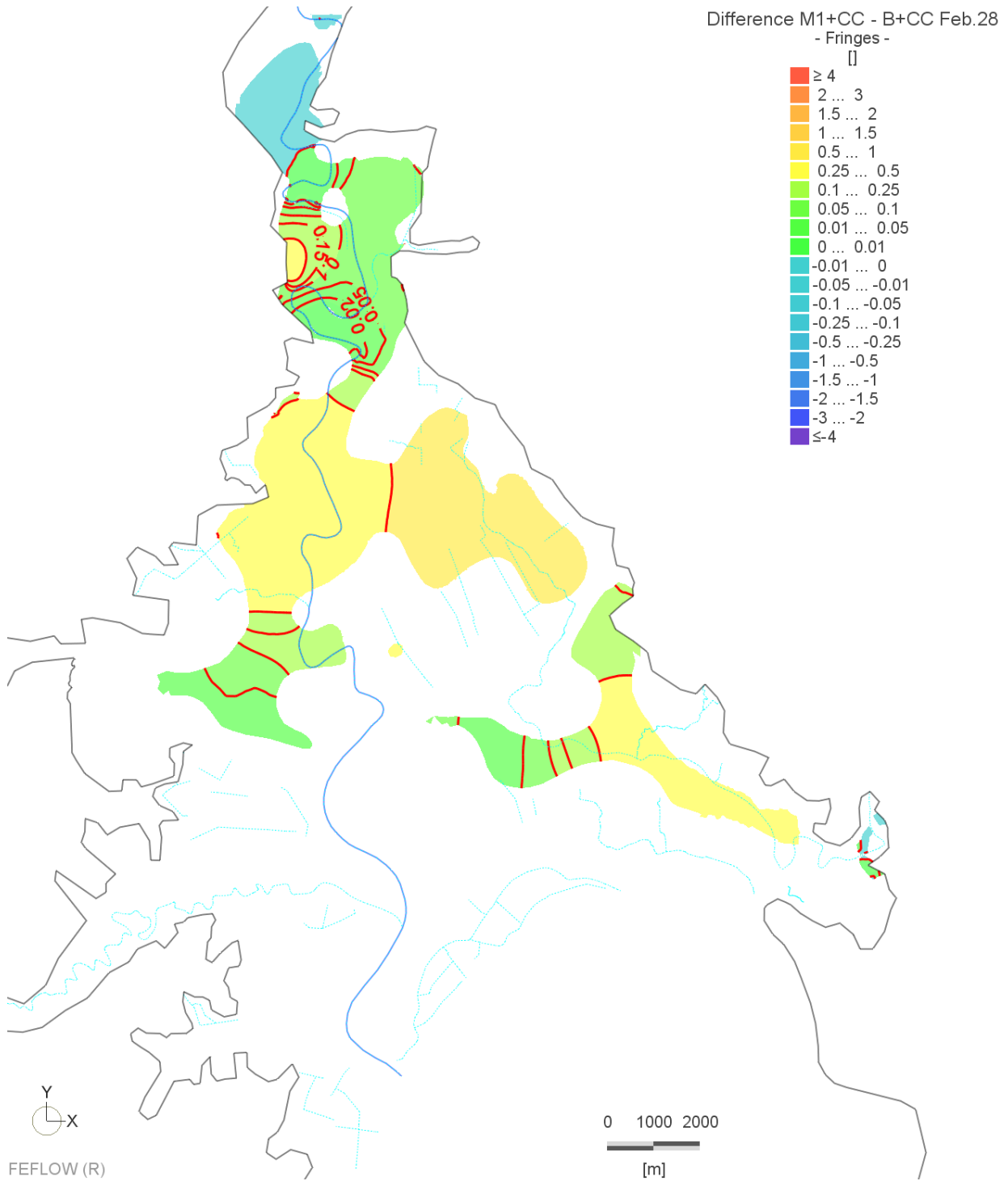


Figure A3-27: Legacy scenarios: Difference between scenarios 5 and 2, Waipaoa aquifer, summer

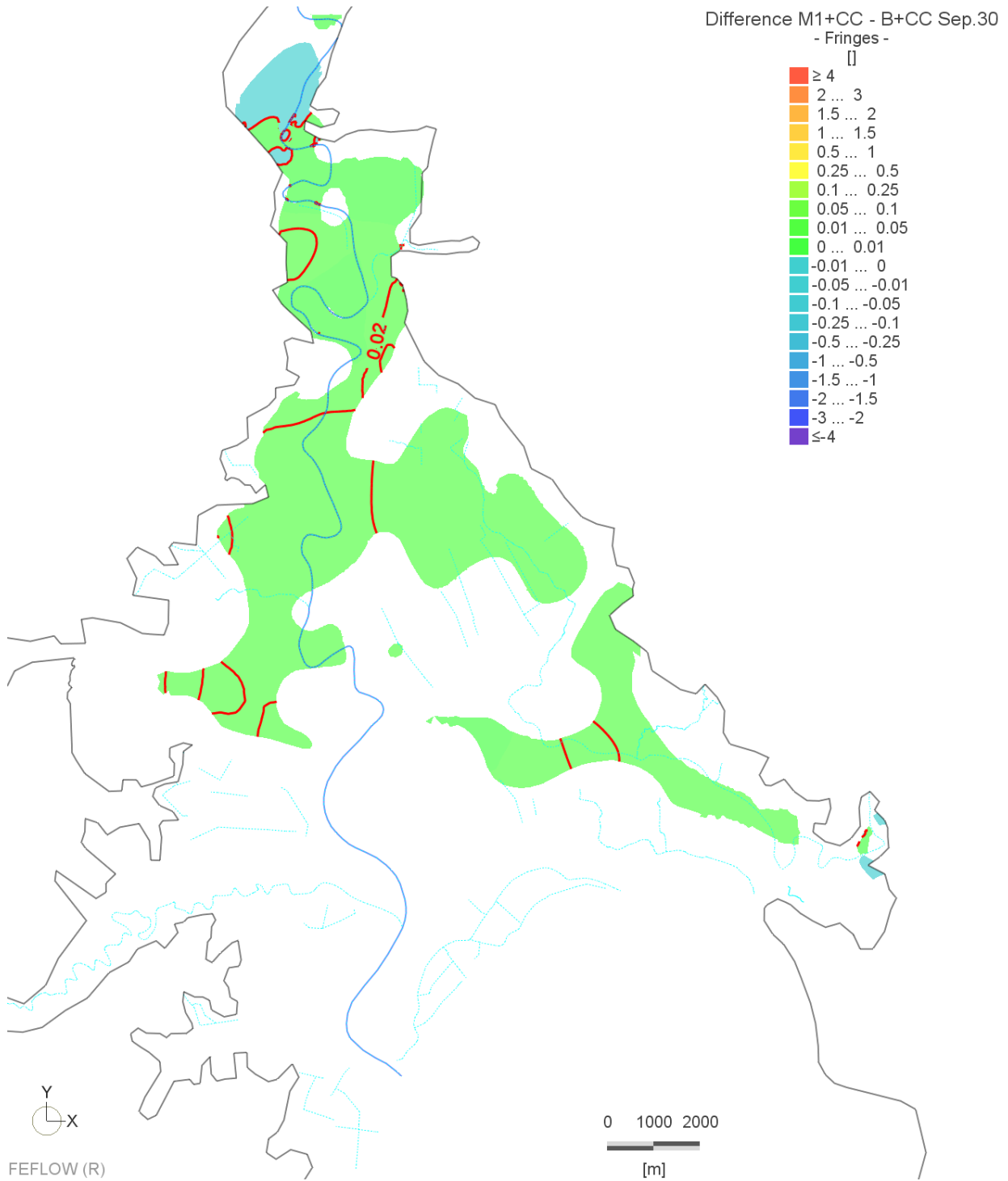


Figure A3-28: Legacy scenarios: Difference between scenarios 5 and 2, Waipaoa aquifer, winter

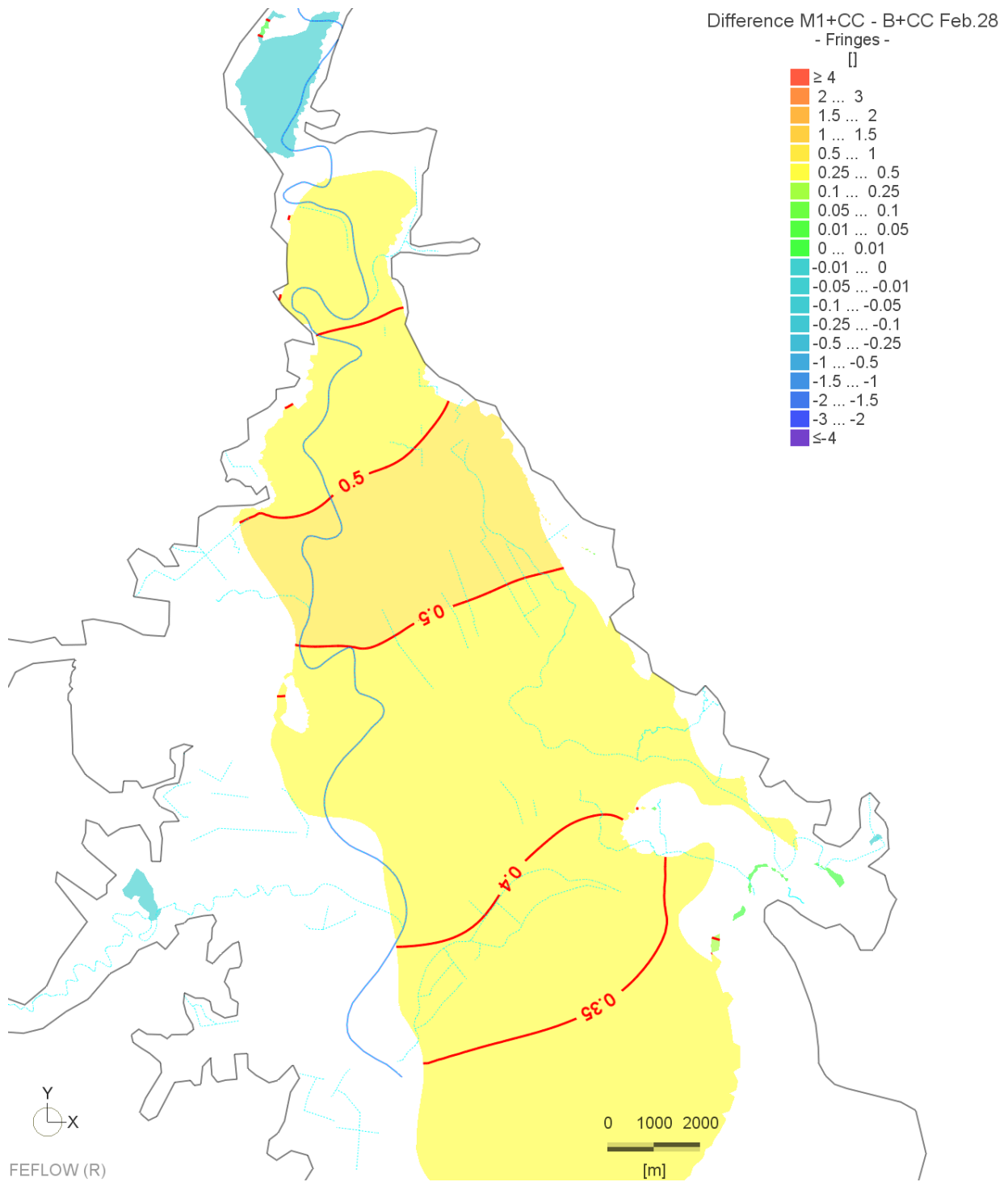


Figure A3-29: Legacy scenarios: Difference between scenarios 5 and 2, Makauri aquifer, summer

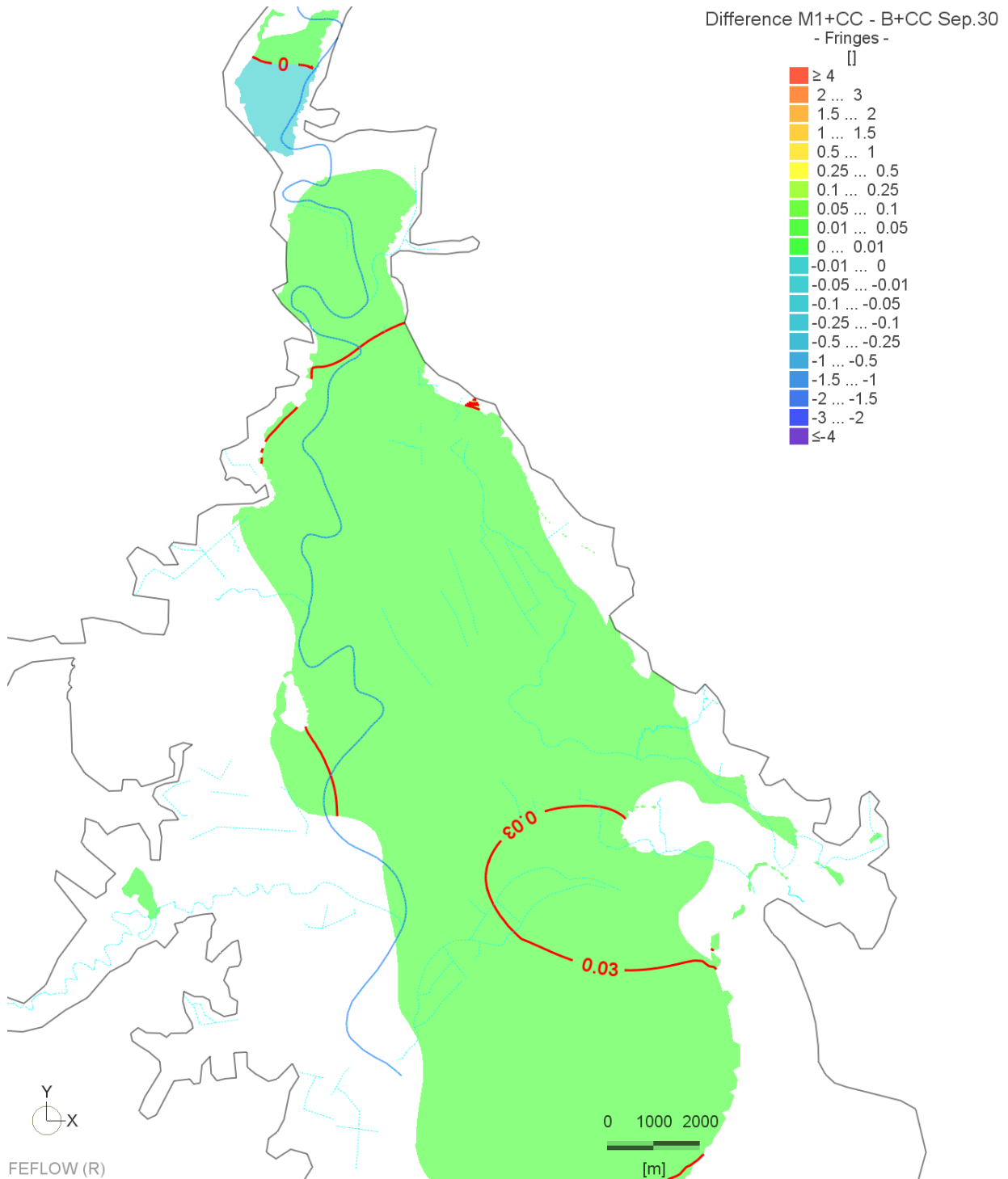


Figure A3-30: Legacy scenarios: Difference between scenarios 5 and 2, Makauri aquifer, winter

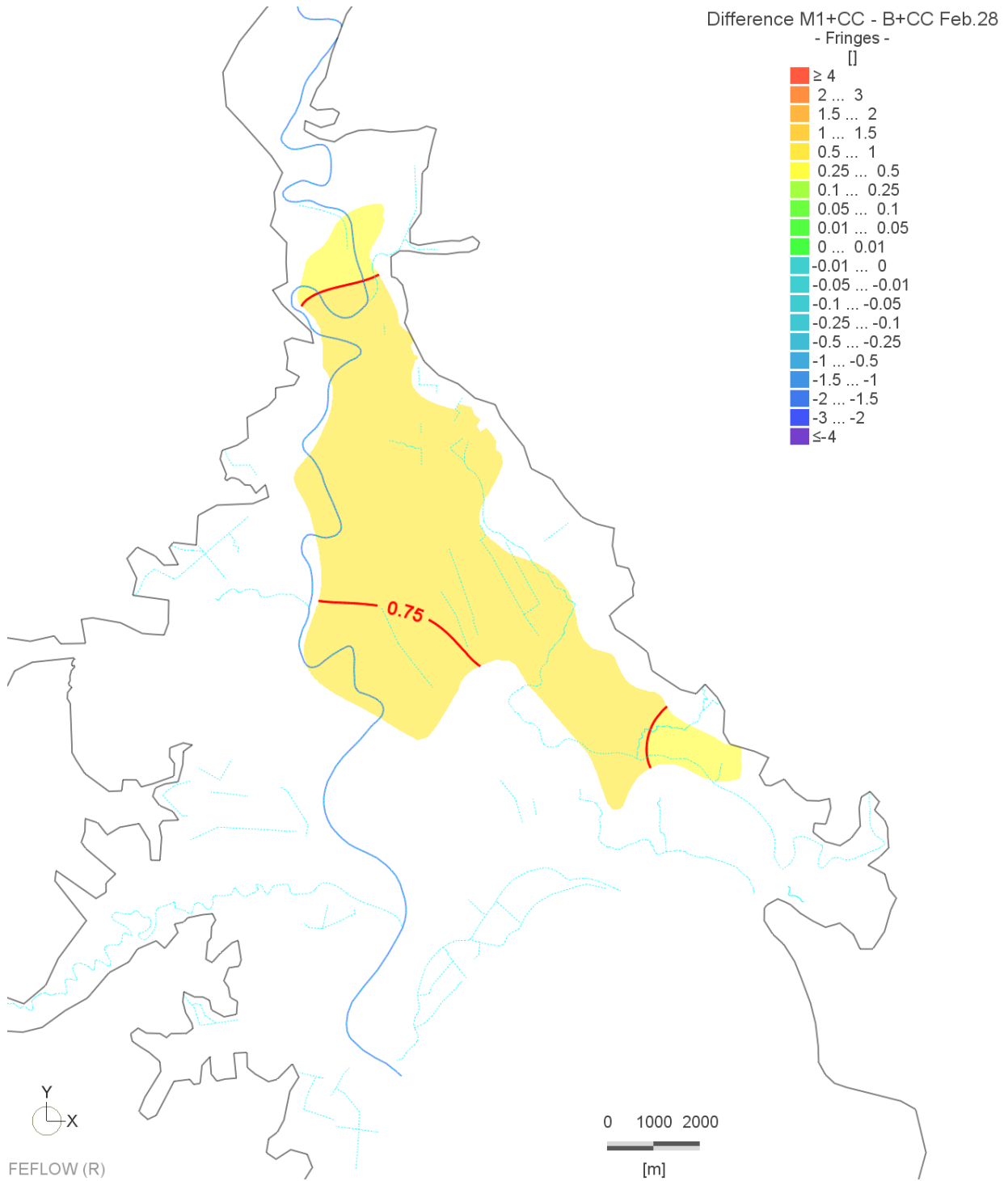


Figure A3-31: Legacy scenarios: Difference between scenarios 5 and 2, Matokitoki aquifer, summer

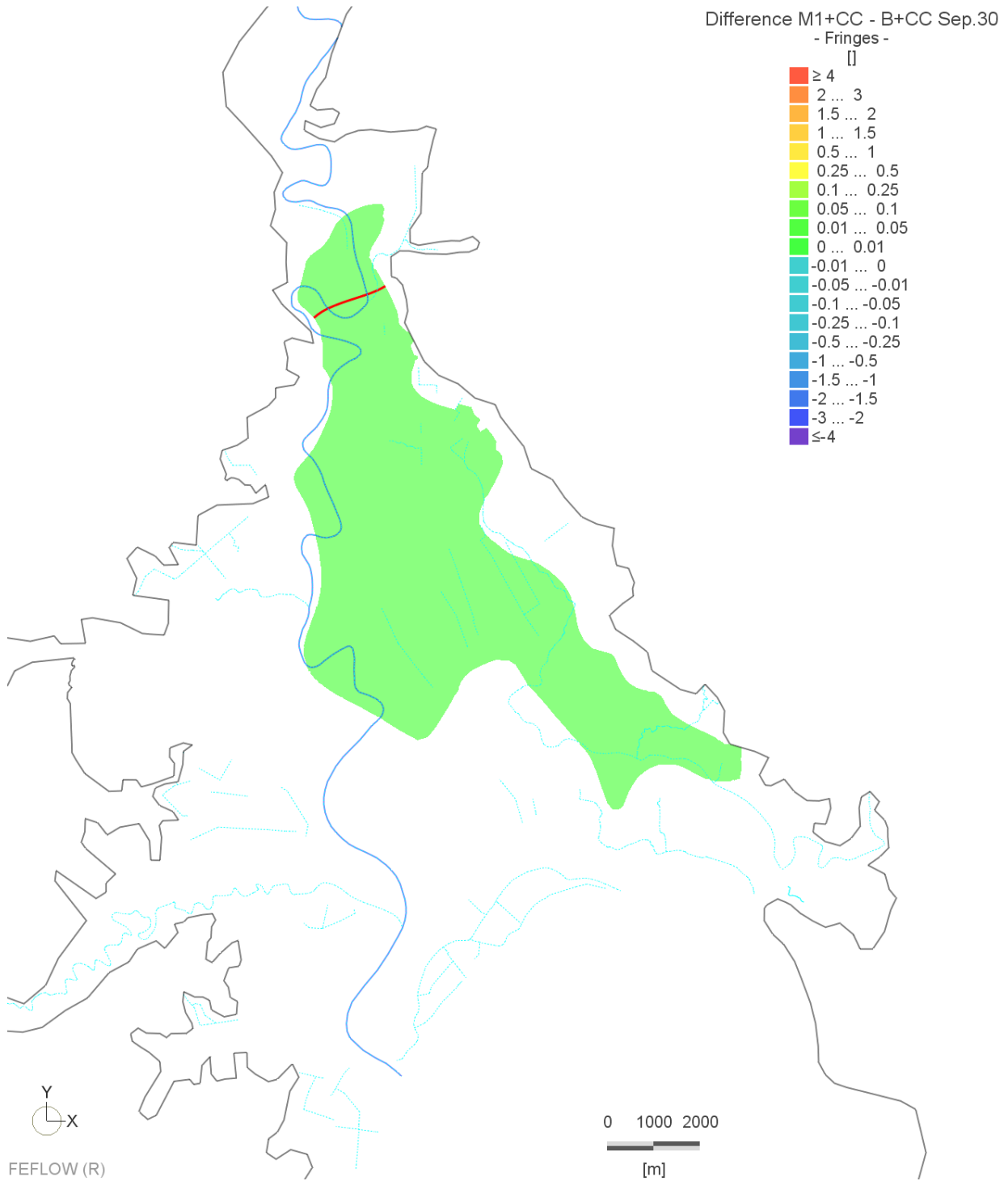


Figure A3-32: Legacy scenarios: Difference between scenarios 5 and 2, Matokitoki aquifer, winter

Scenario 6

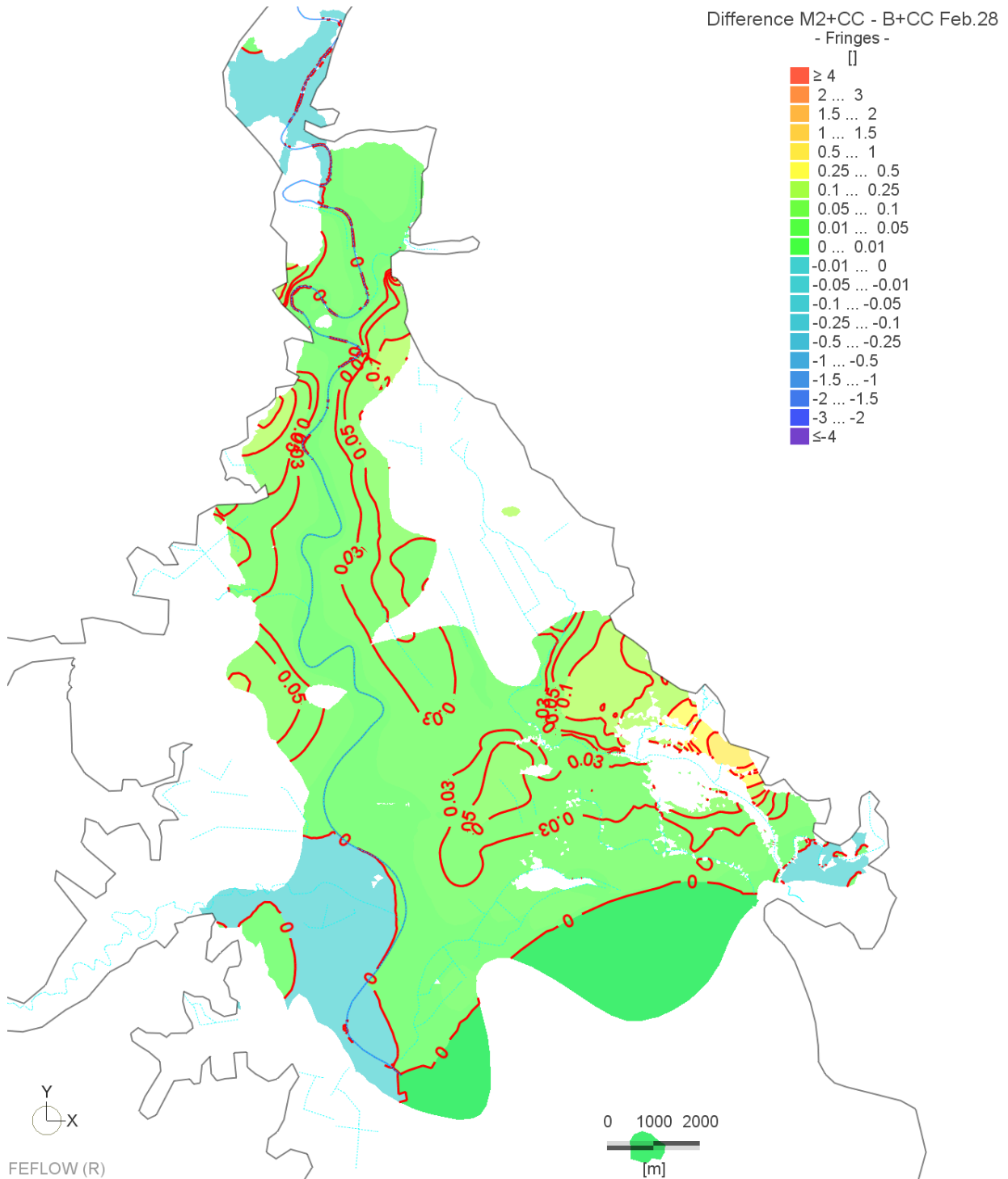


Figure A3-33: Legacy scenarios: Difference between scenarios 6 and 2, shallow aquifers, summer

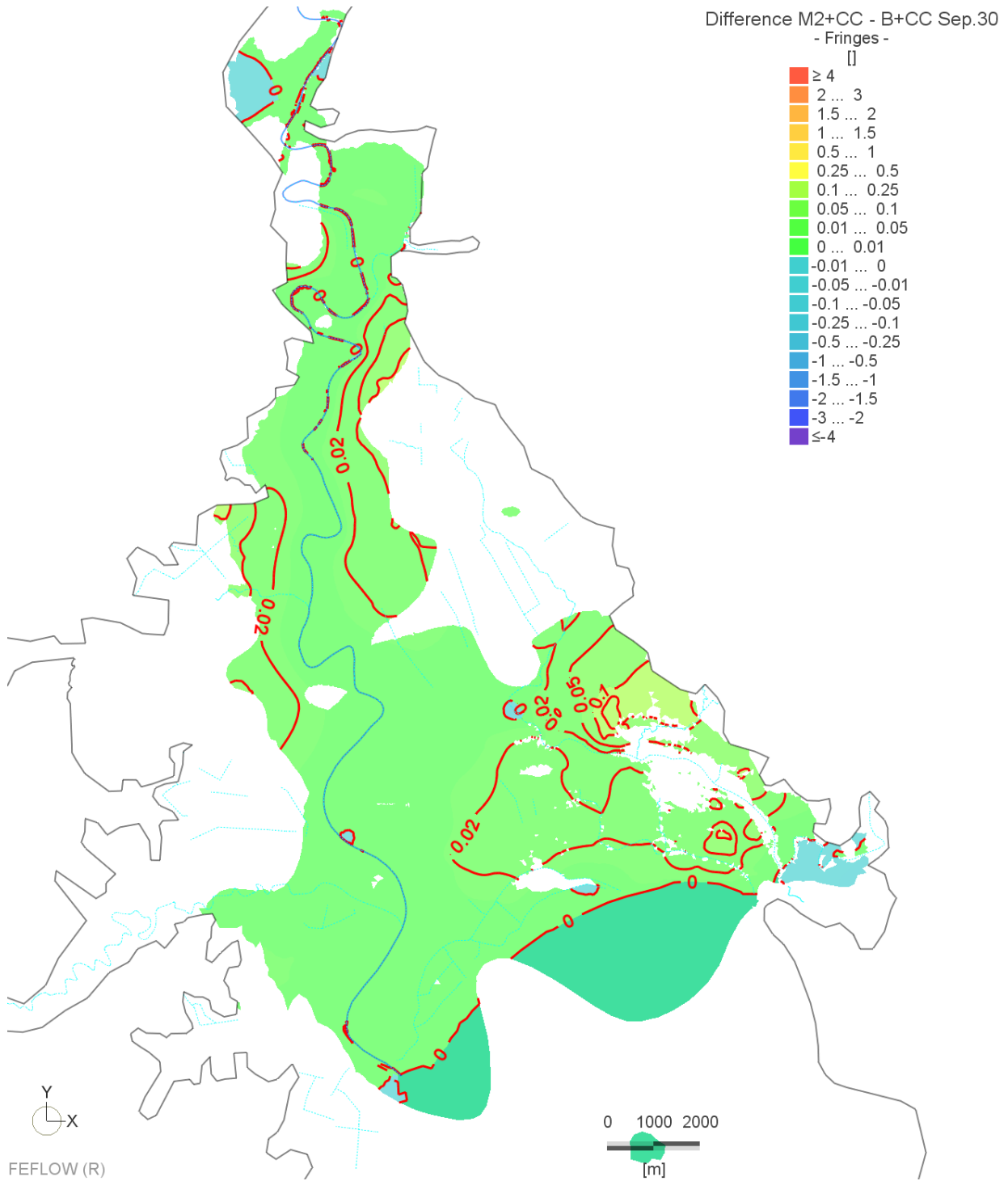


Figure A3-34: Legacy scenarios: Difference between scenarios 6 and 2, shallow aquifers, winter

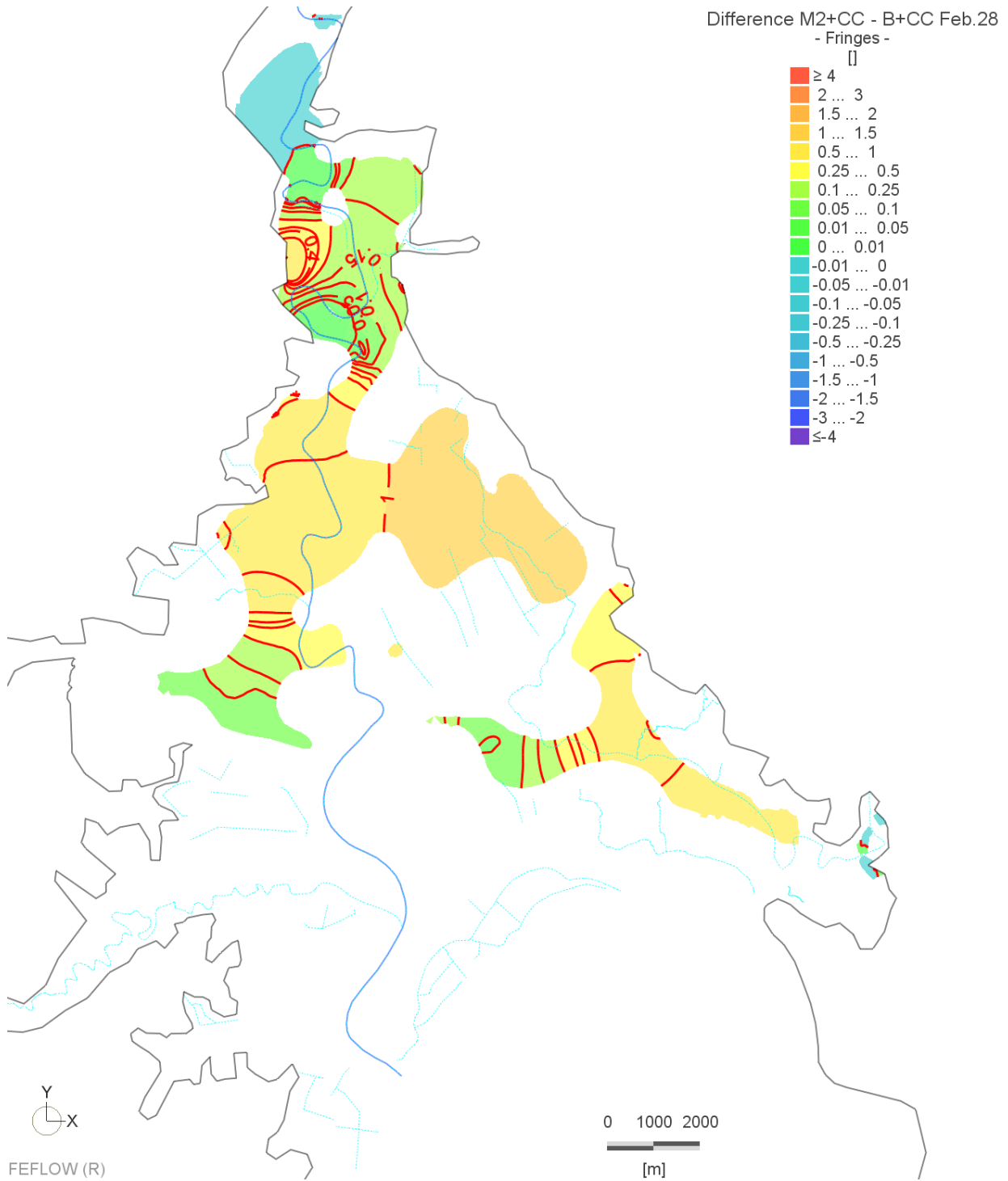


Figure A3-35: Legacy scenarios: Difference between scenarios 6 and 2, Waipaoa aquifer, summer

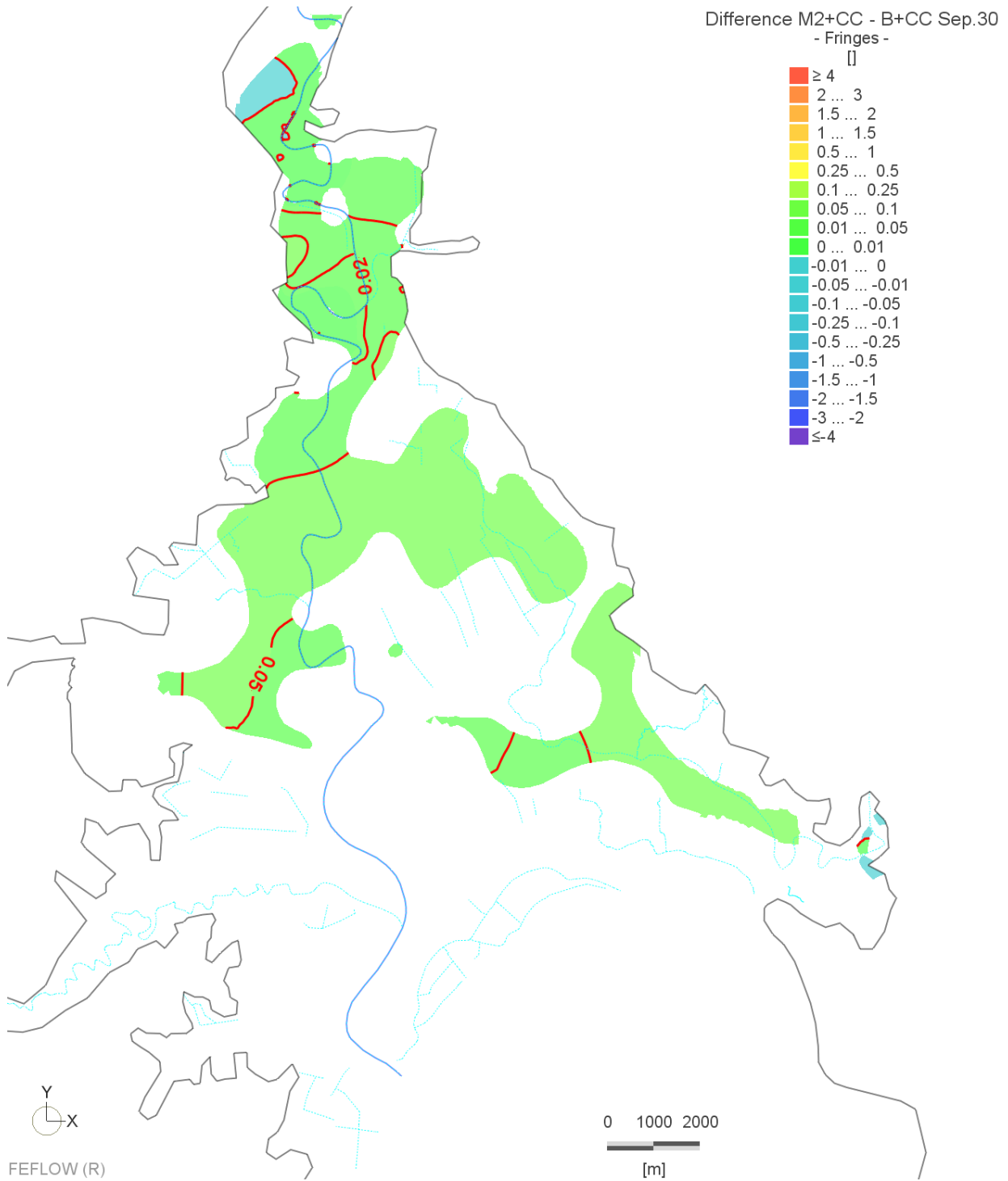


Figure A3-36: Legacy scenarios: Difference between scenarios 6 and 2, Waipaoa aquifer, winter

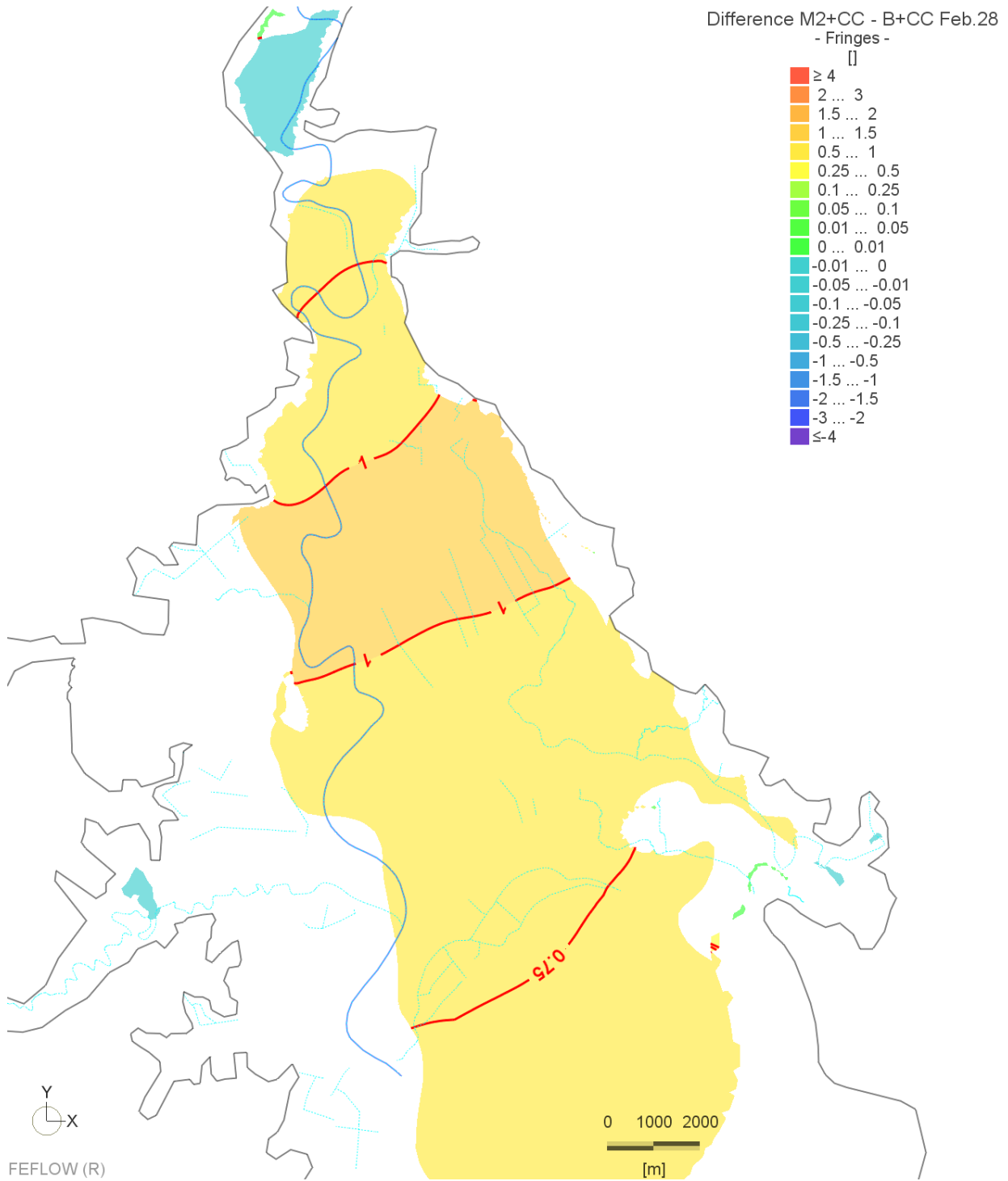


Figure A3-37: Legacy scenarios: Difference between scenarios 6 and 2, Makauri aquifer, summer

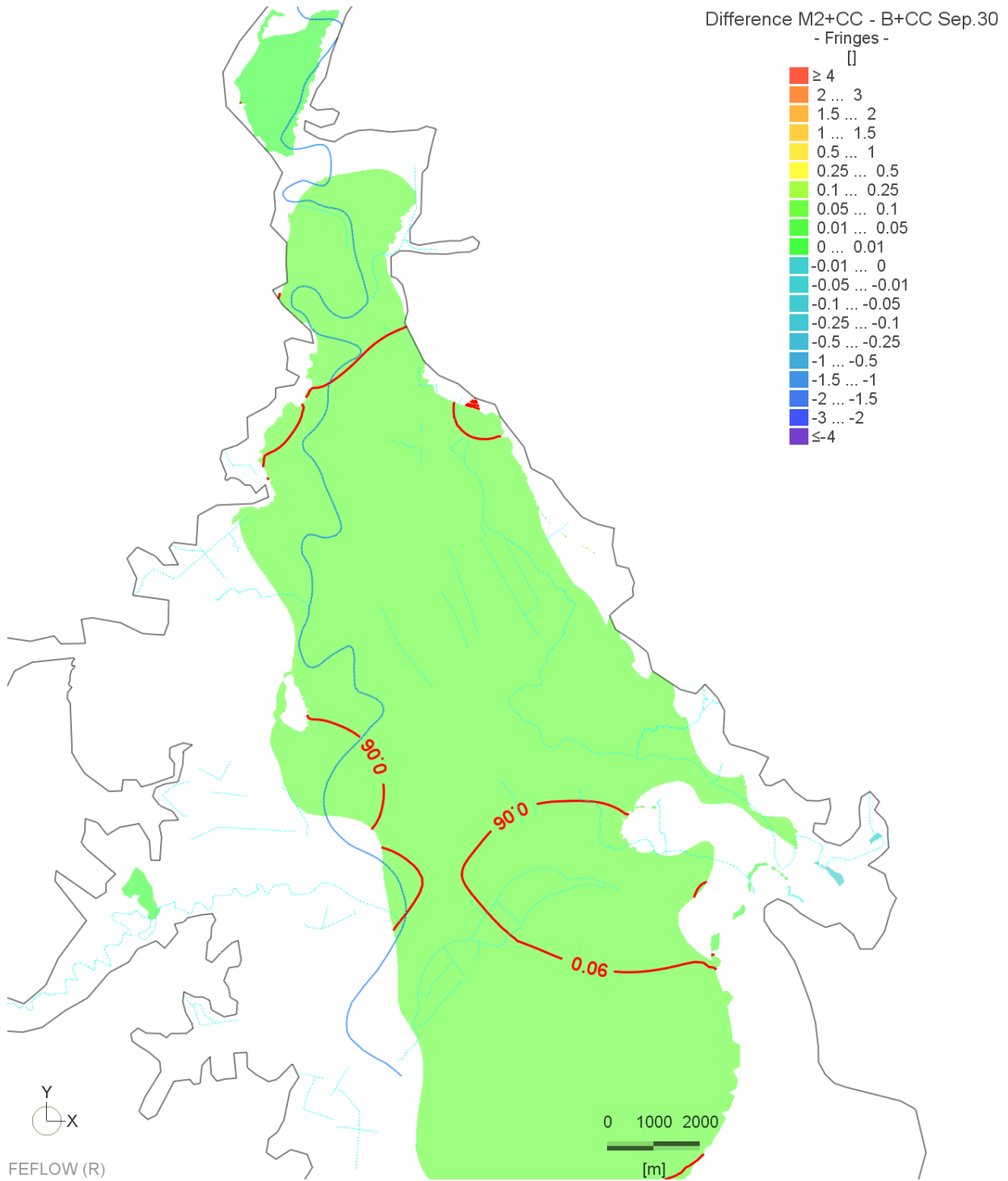


Figure A3-38: Legacy scenarios: Difference between scenarios 6 and 2, Makauri aquifer, winter

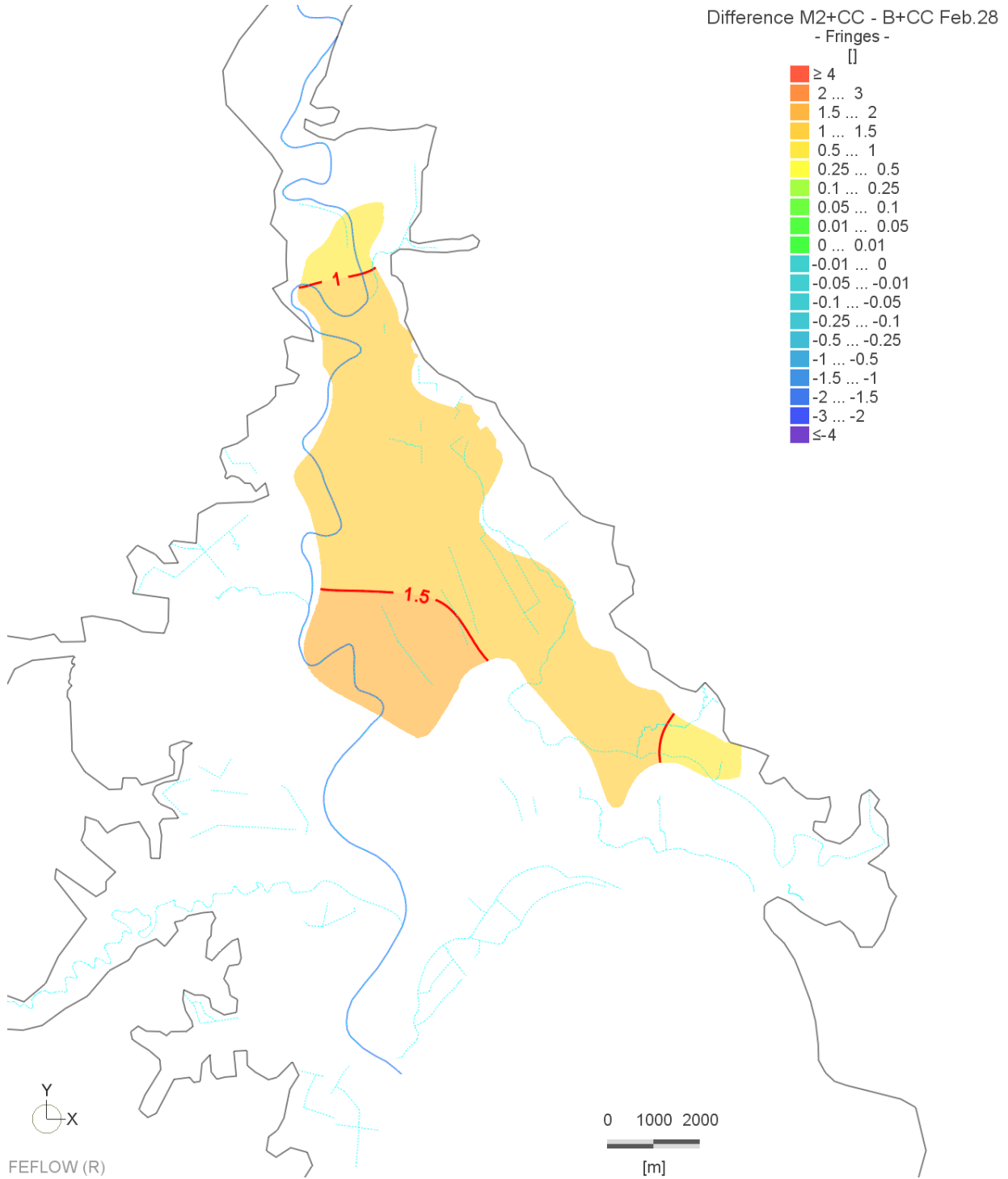


Figure A3-39: Legacy scenarios: Difference between scenarios 6 and 2, Matokitoki aquifer, summer

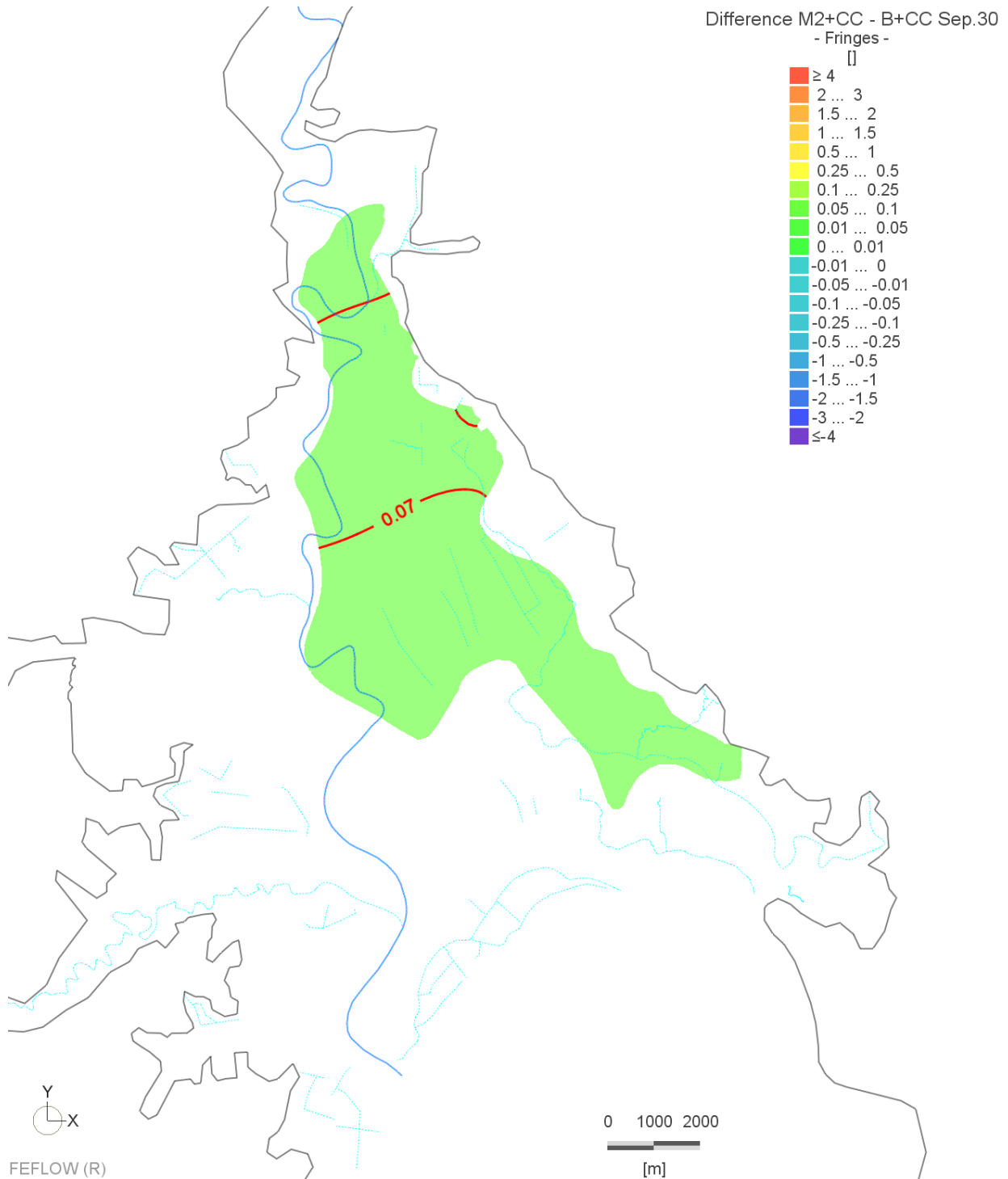


Figure A3-40: Legacy scenarios: Difference between scenarios 6 and 2, Matokitoki aquifer, winter

Scenario 7

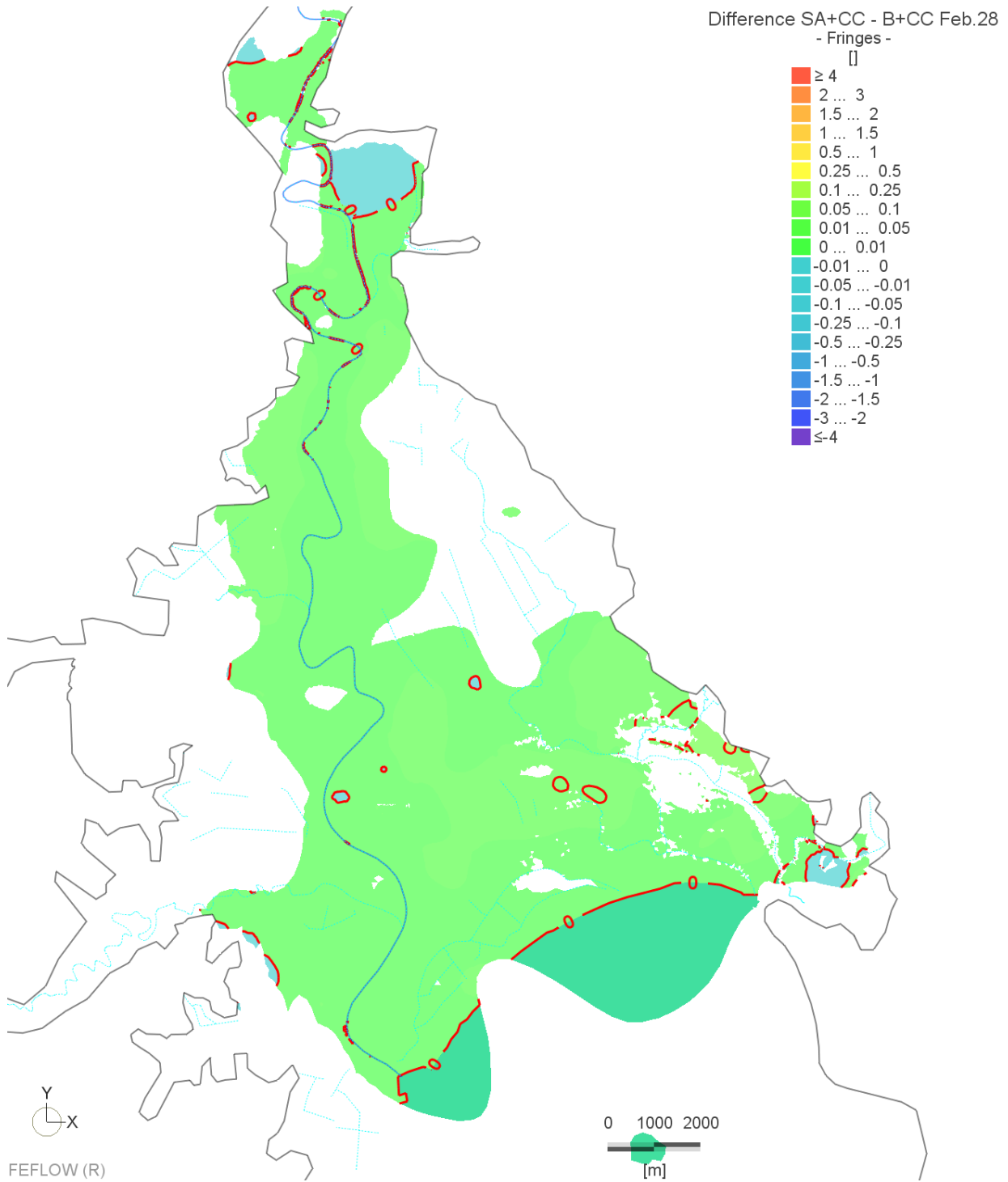


Figure A3-41: Legacy scenarios: Difference between scenarios 7 and 2, shallow aquifers, summer

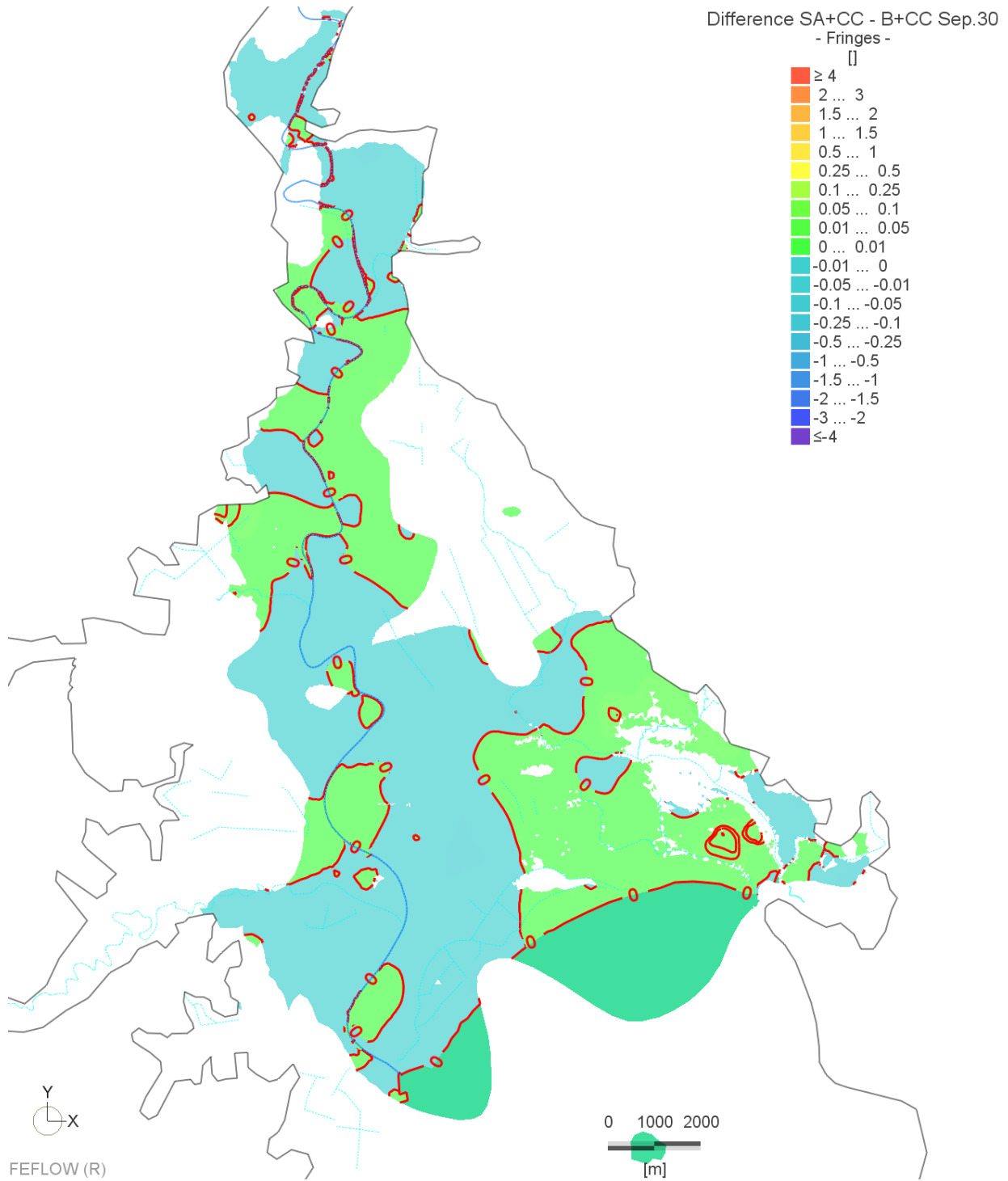


Figure A3-42: Legacy scenarios: Difference between scenarios 7 and 2, shallow aquifers, winter

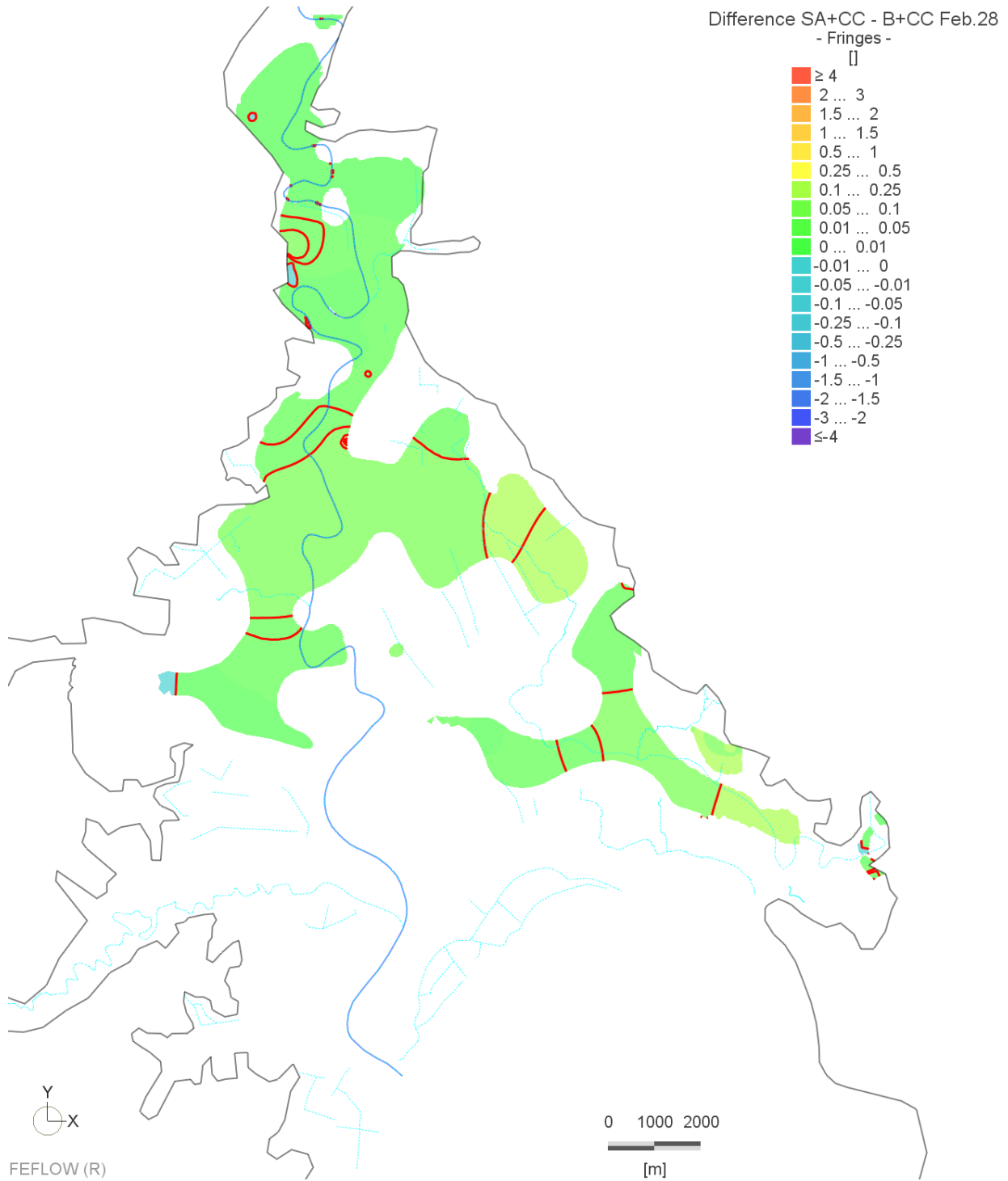


Figure A3-43: Legacy scenarios: Difference between scenarios 7 and 2, Waipaoa aquifer, summer

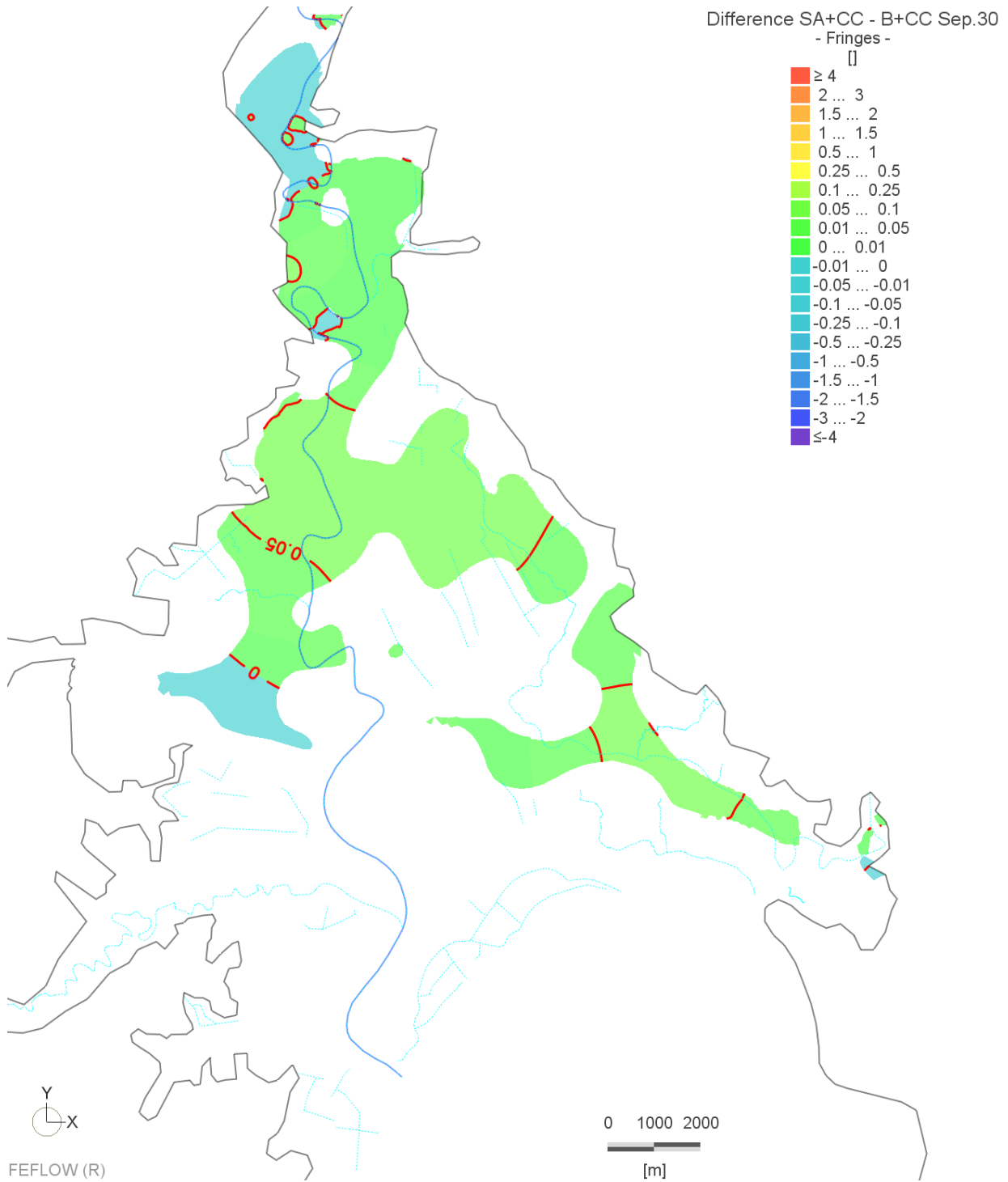


Figure A3-44: Legacy scenarios: Difference between scenarios 7 and 2, Waipaoa aquifer, winter

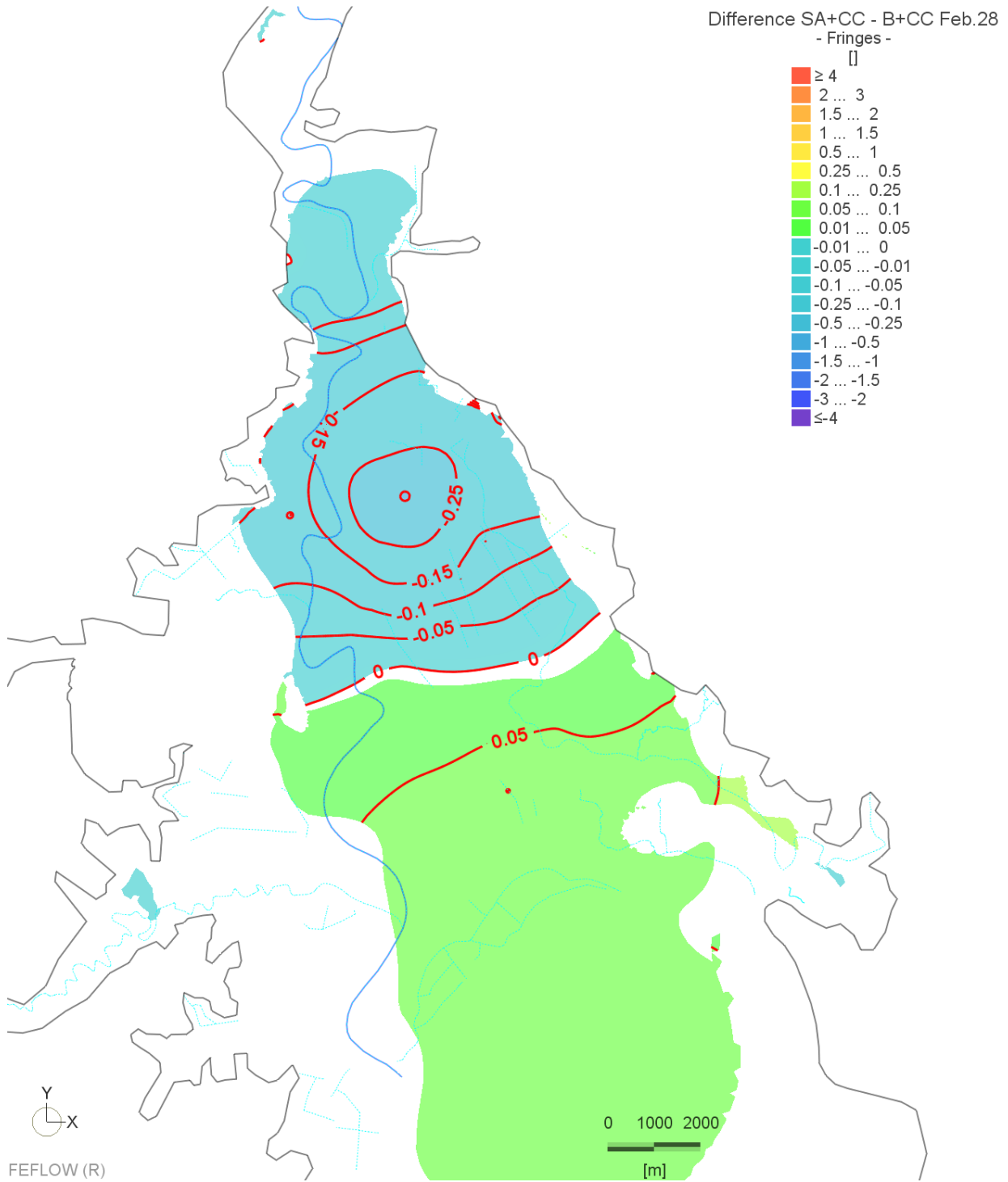


Figure A3-45: Legacy scenarios: Difference between scenarios 7 and 2, Makauri aquifer, summer

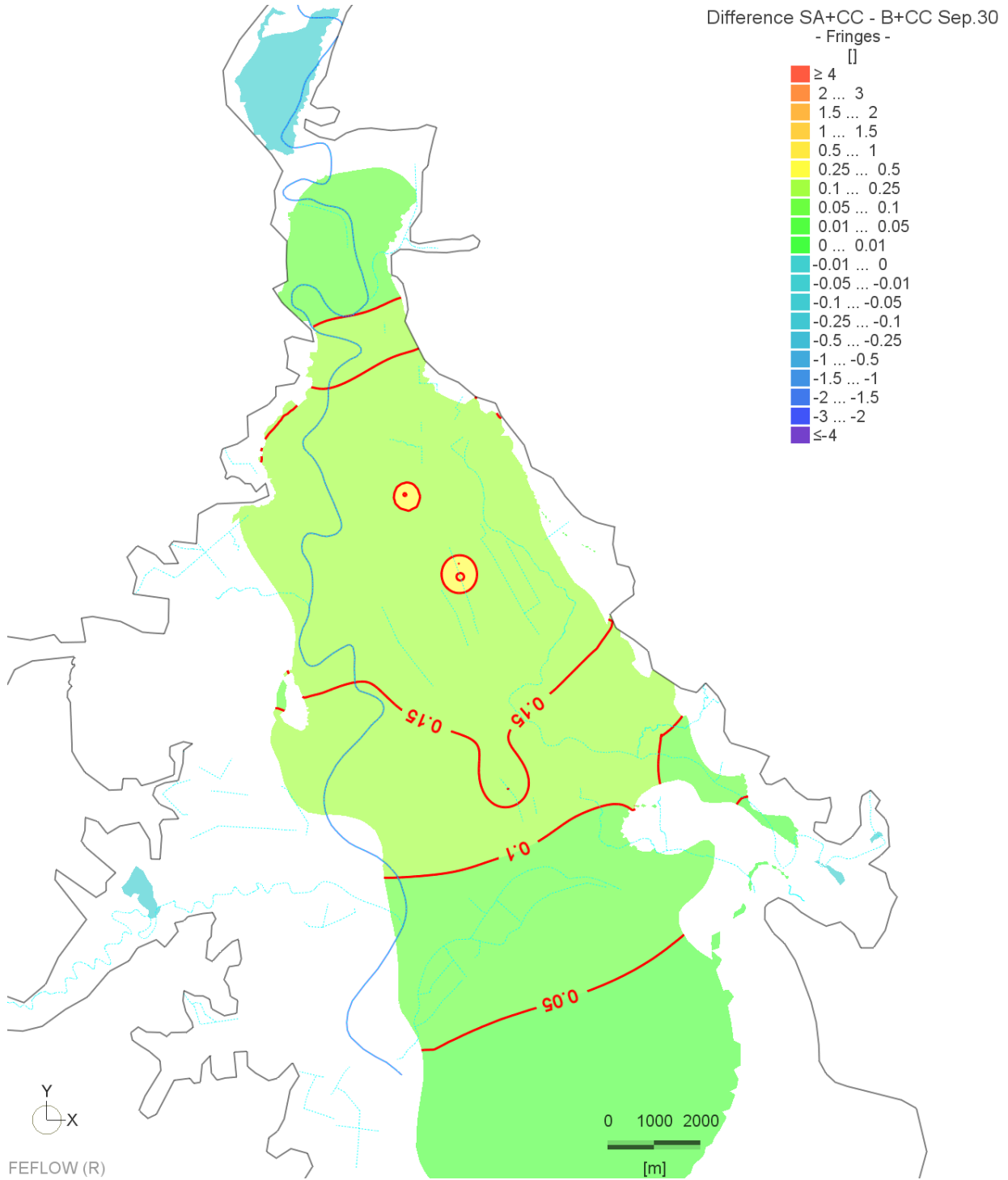


Figure A3-46: Legacy scenarios: Difference between scenarios 7 and 2, Makauri aquifer, winter

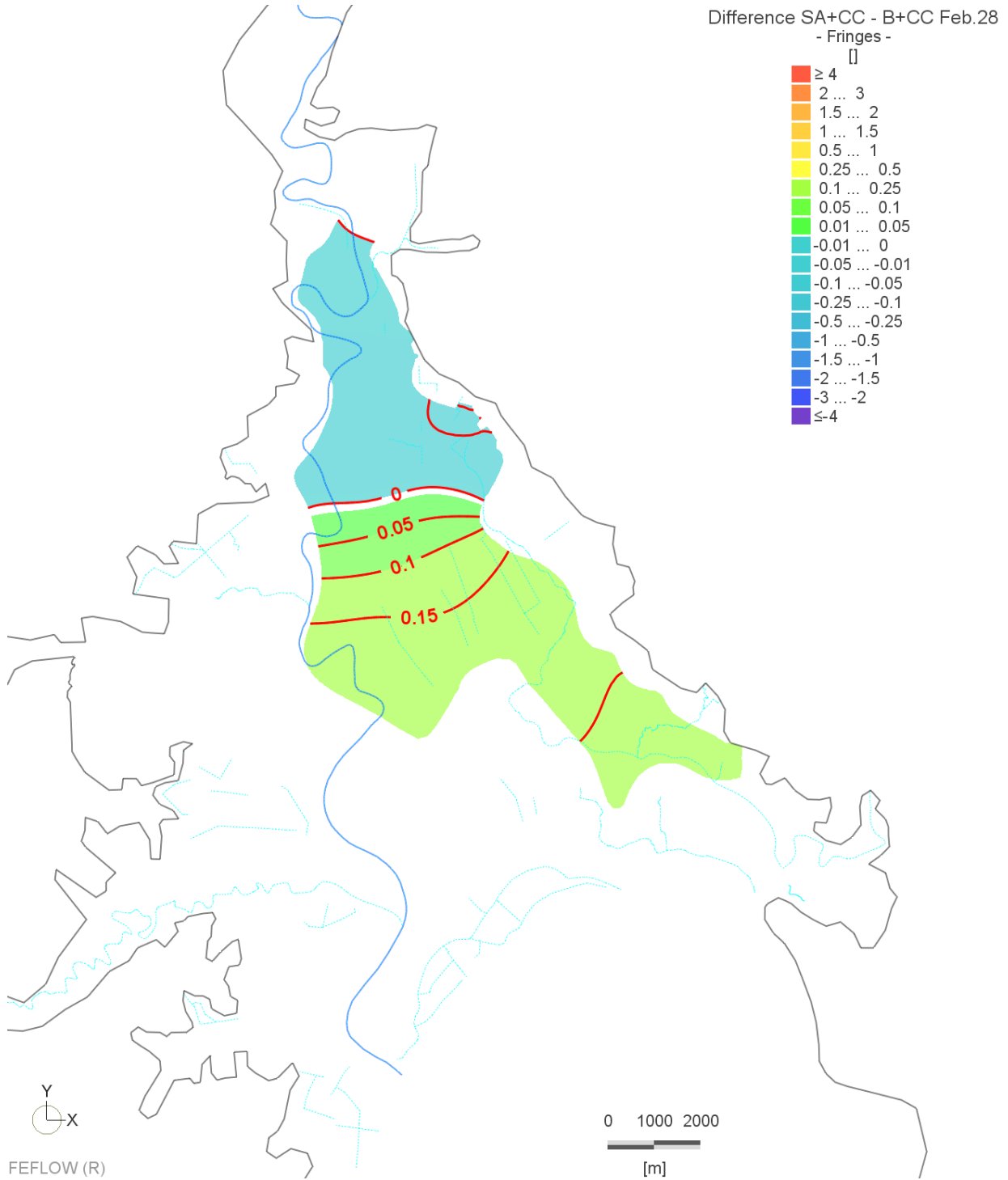


Figure A3-47: Legacy scenarios: Difference between scenarios 7 and 2, Matokitoki aquifer, summer

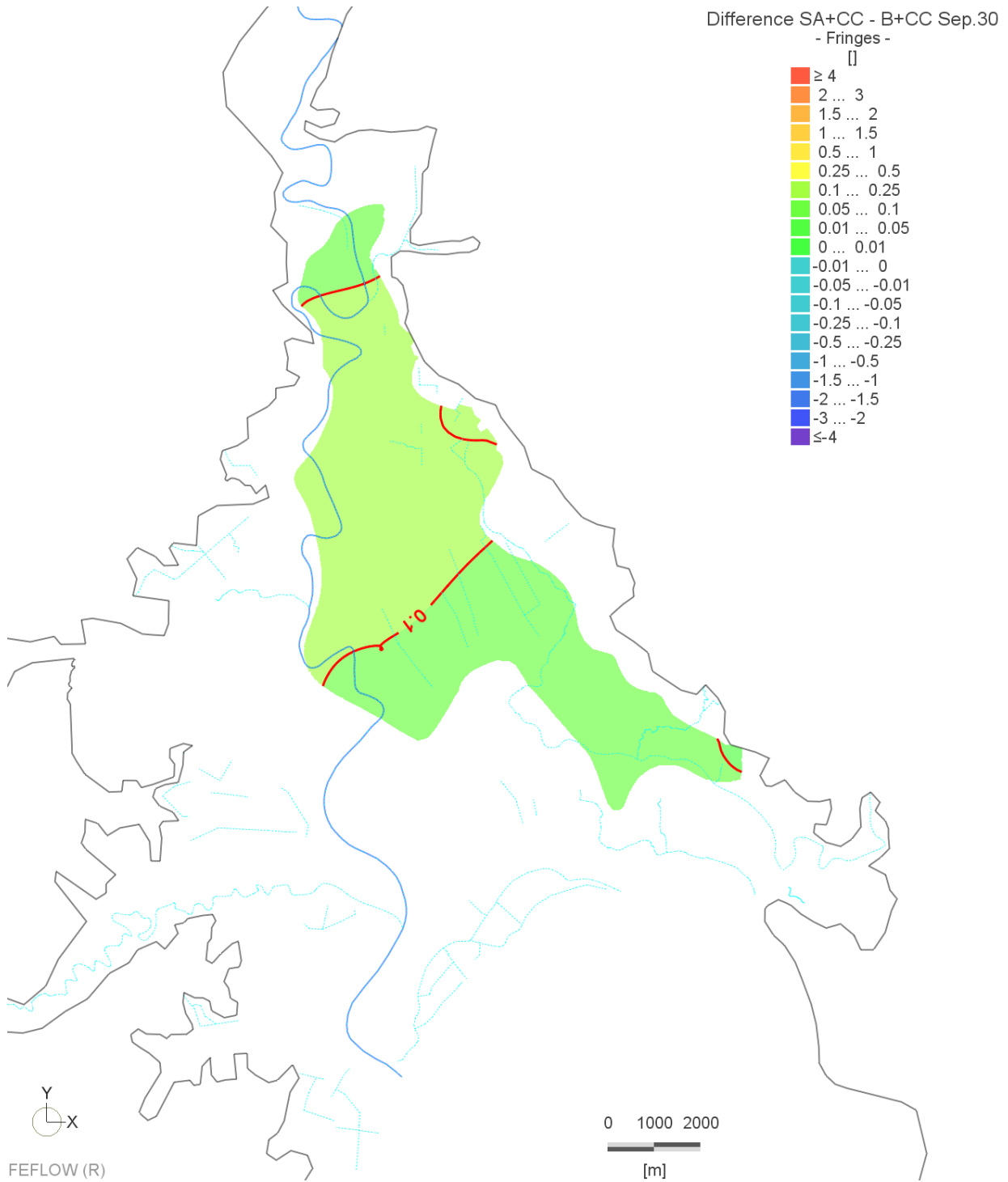


Figure A3-48: Legacy scenarios: Difference between scenarios 7 and 2, Matokitoki aquifer, winter

Scenario 8

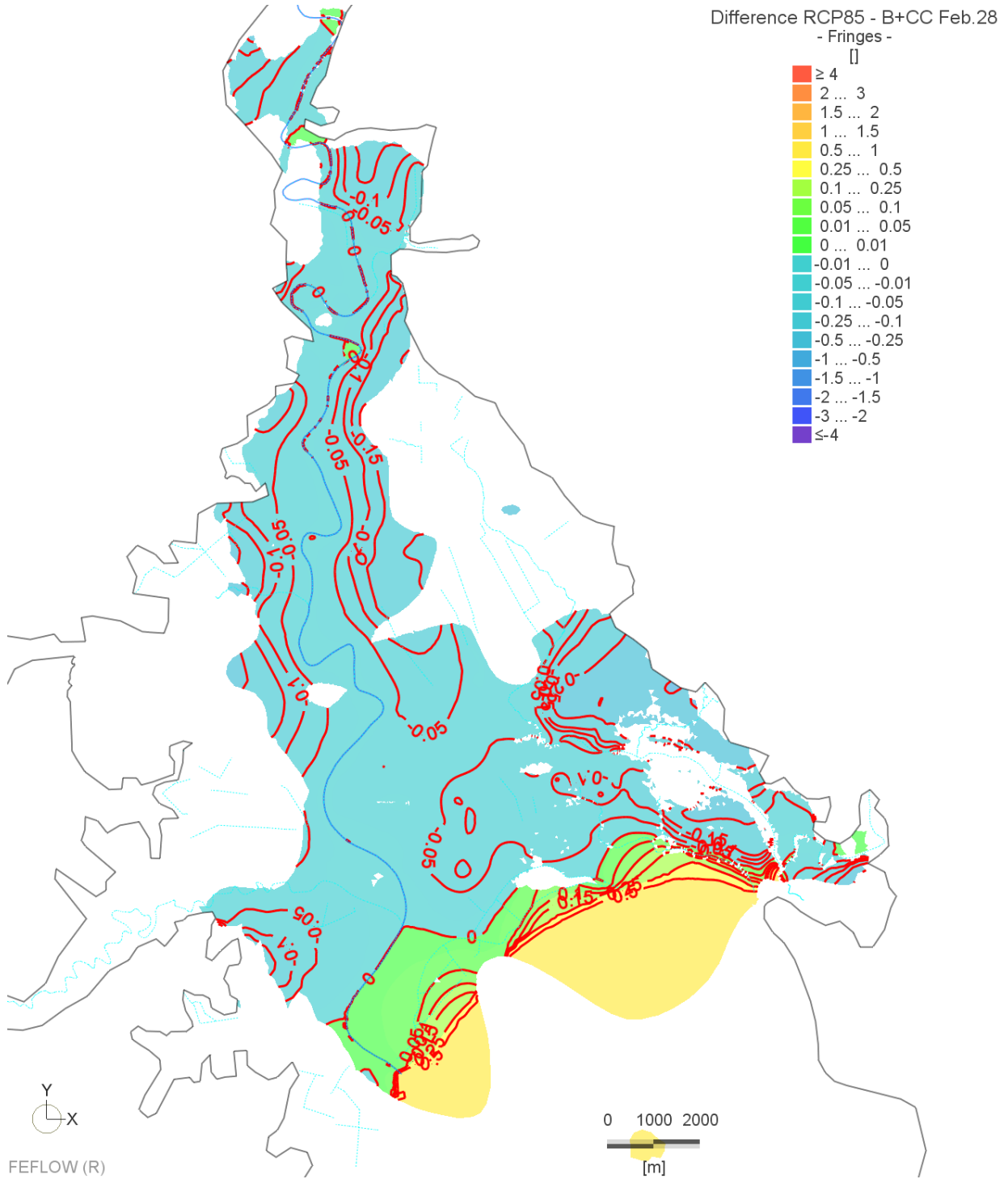


Figure A3-49: Legacy scenarios: Difference between scenarios 8 and 2, shallow aquifers, summer

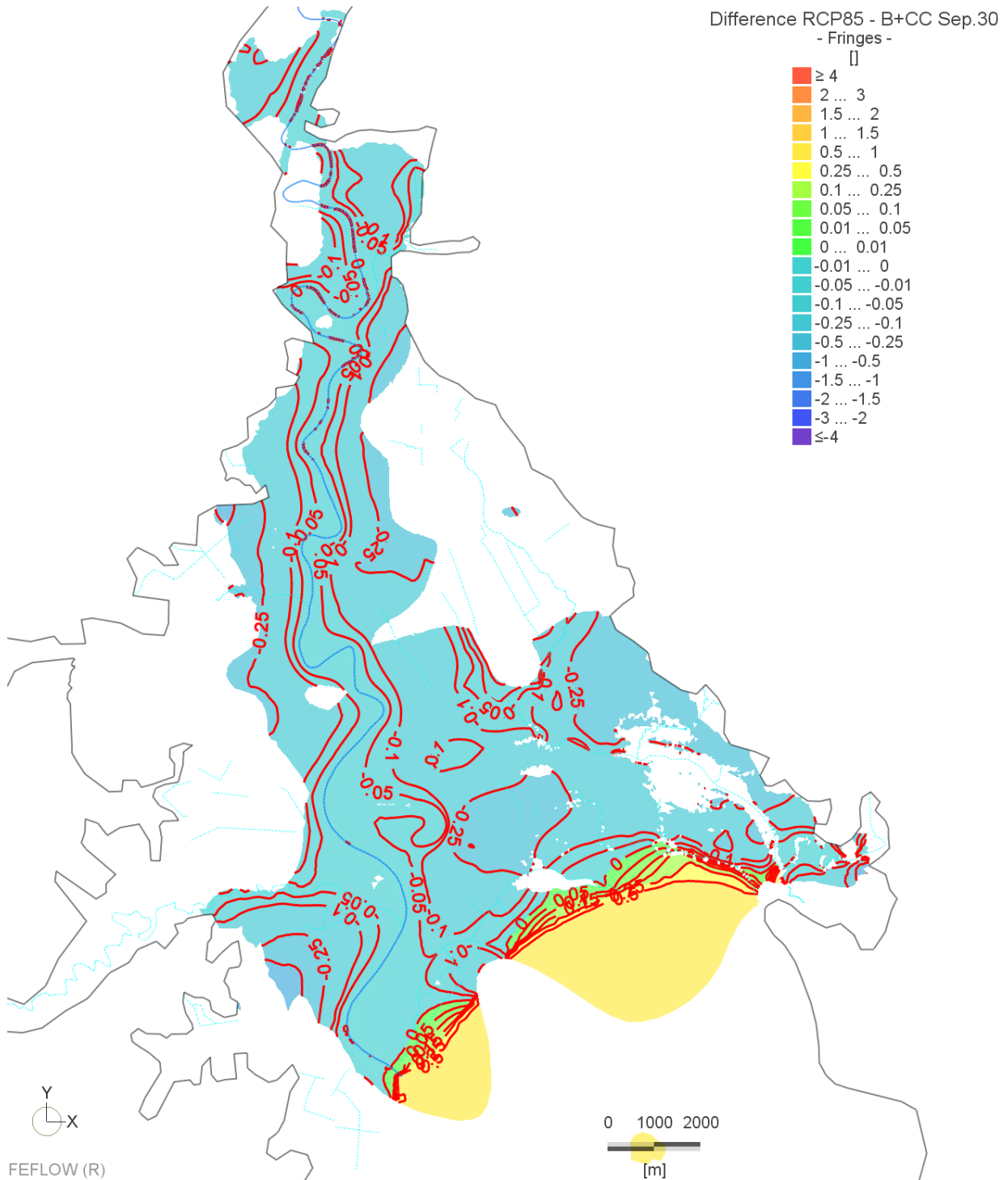


Figure A3-50: Legacy scenarios: Difference between scenarios 8 and 2, shallow aquifers, winter

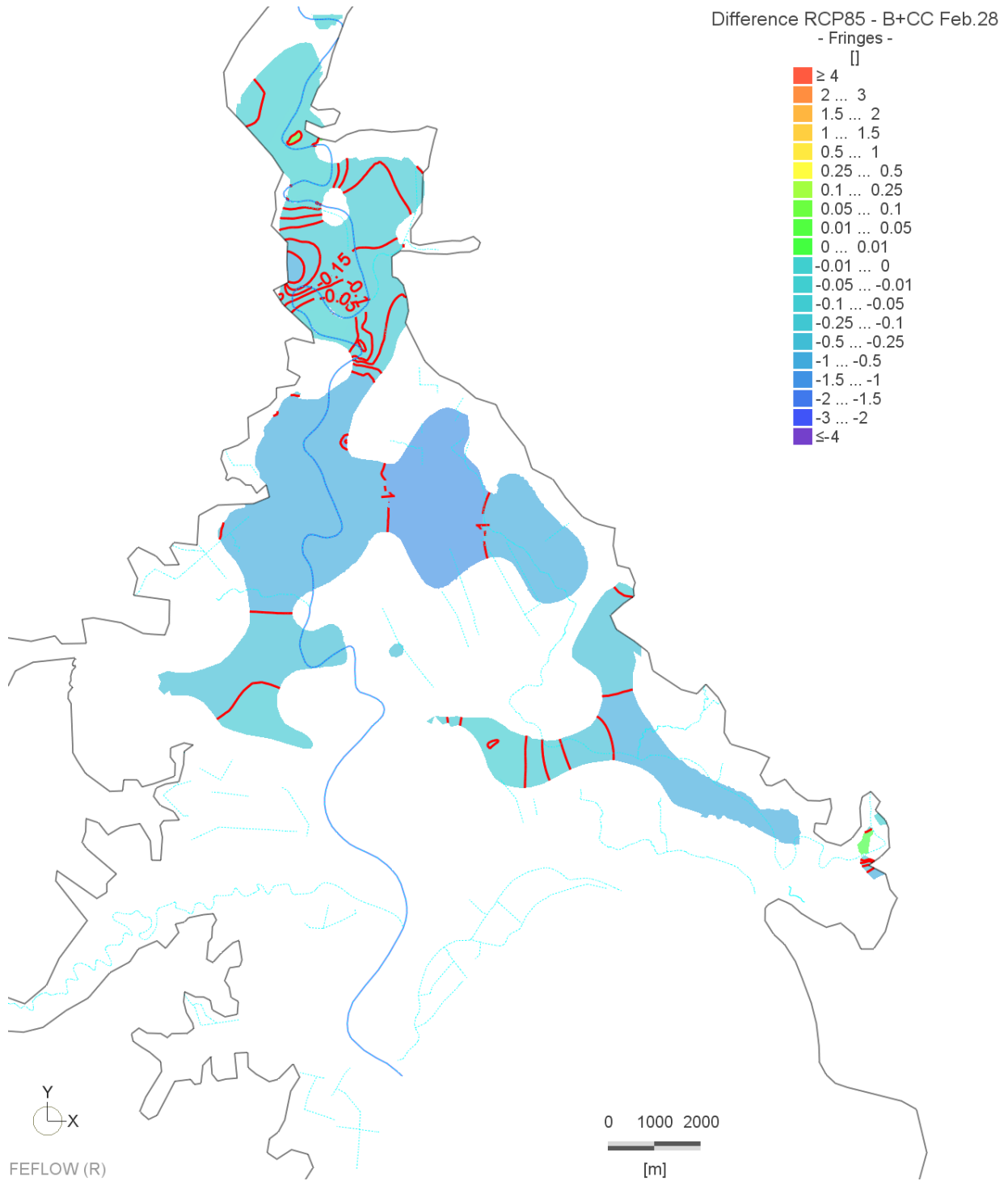


Figure A3-51: Legacy scenarios: Difference between scenarios 8 and 2, Waipaoa aquifer, summer

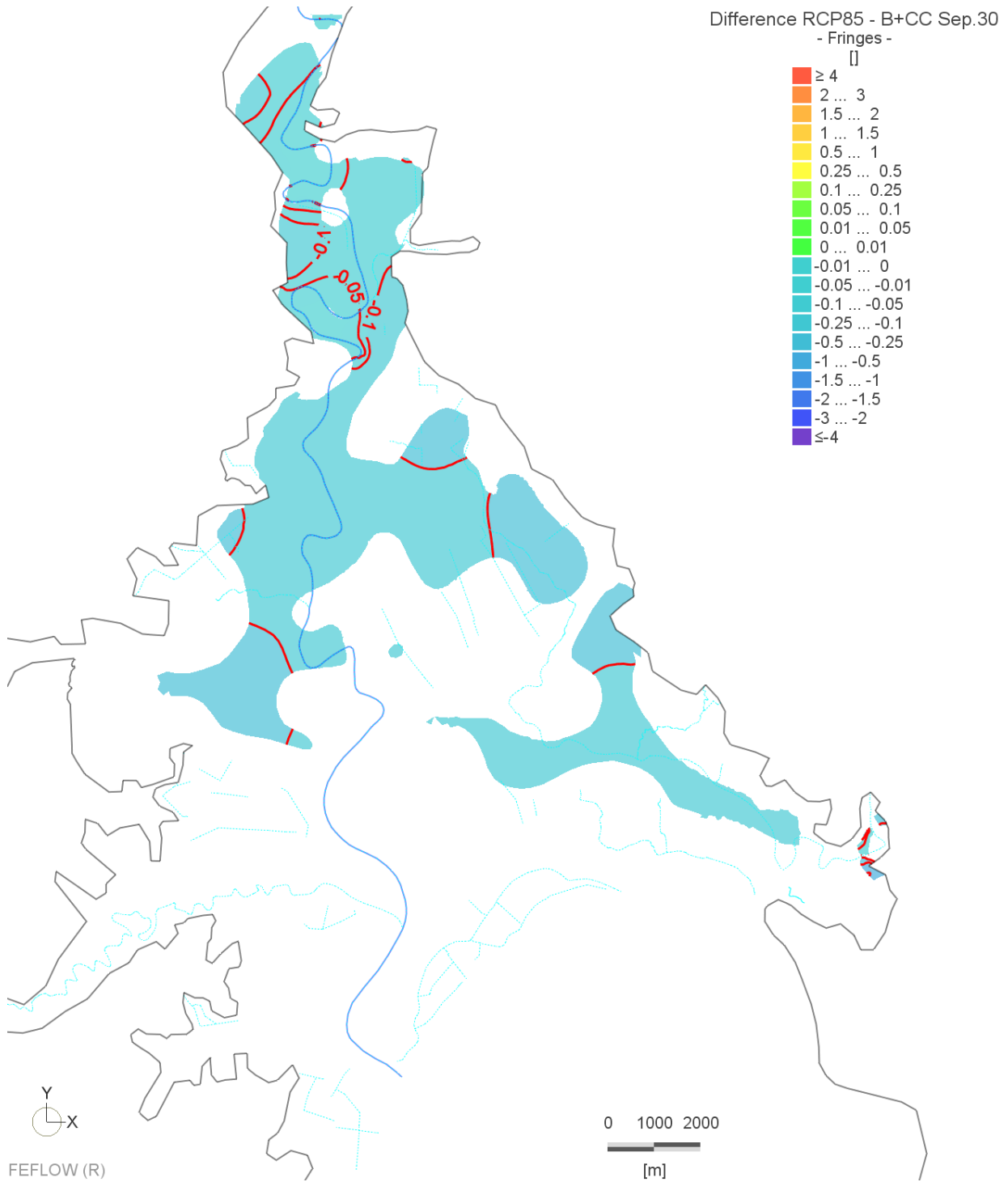


Figure A3-52: Legacy scenarios: Difference between scenarios 8 and 2, Waipaoa aquifer, winter

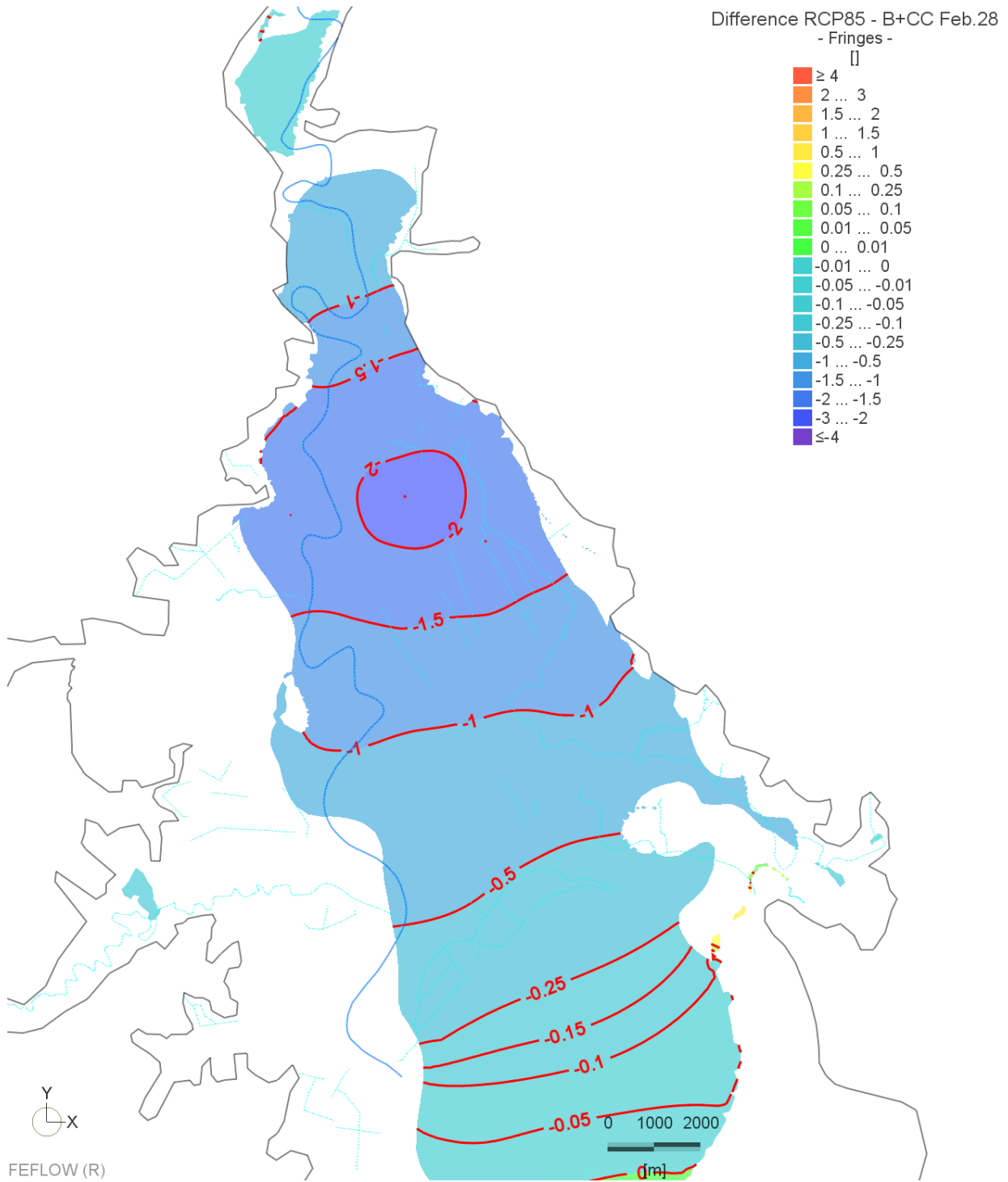


Figure A3-53: Legacy scenarios: Difference between scenarios 8 and 2, Makauri aquifer, summer

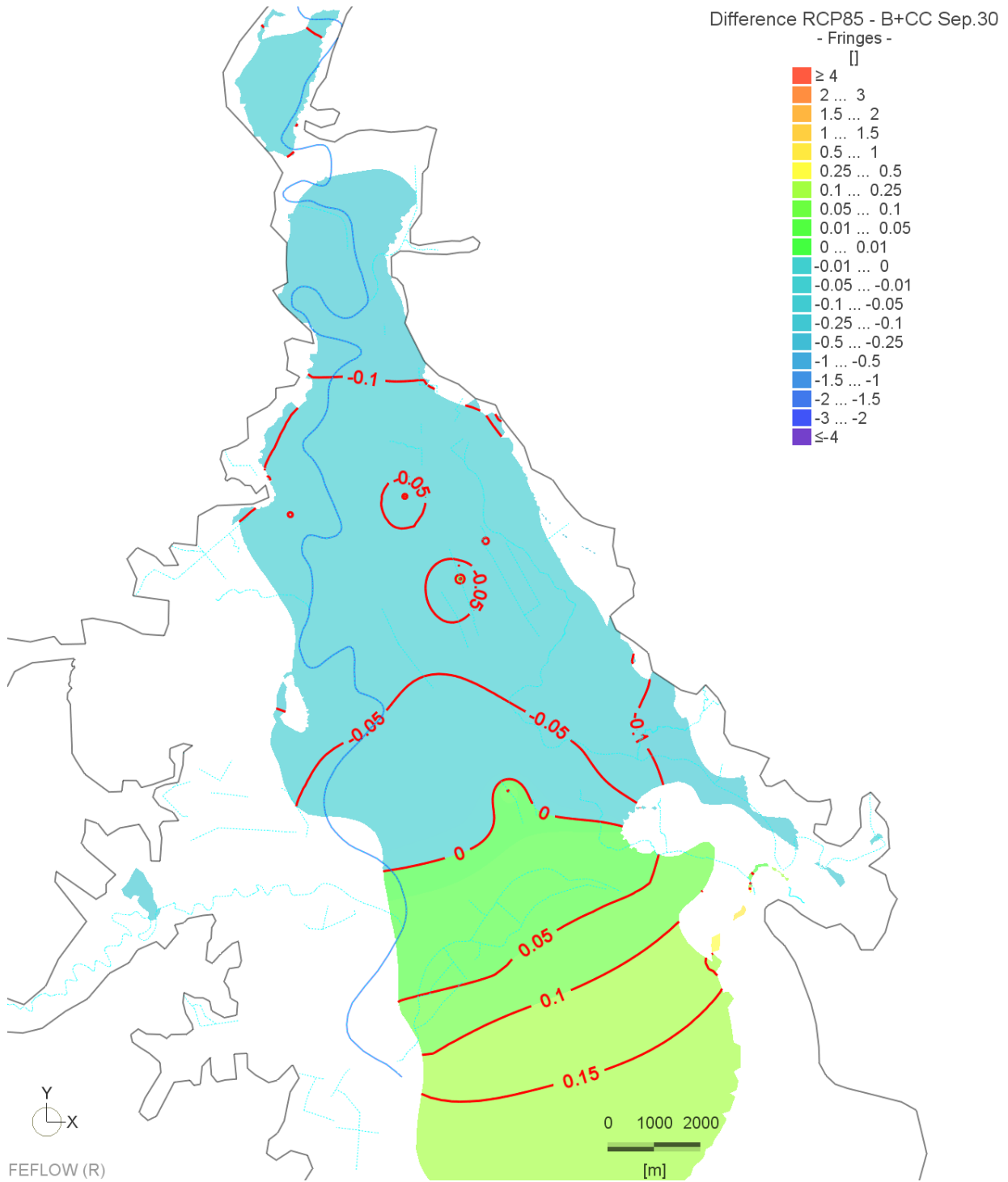


Figure A3-54: Legacy scenarios: Difference between scenarios 8 and 2, Makauri aquifer, winter

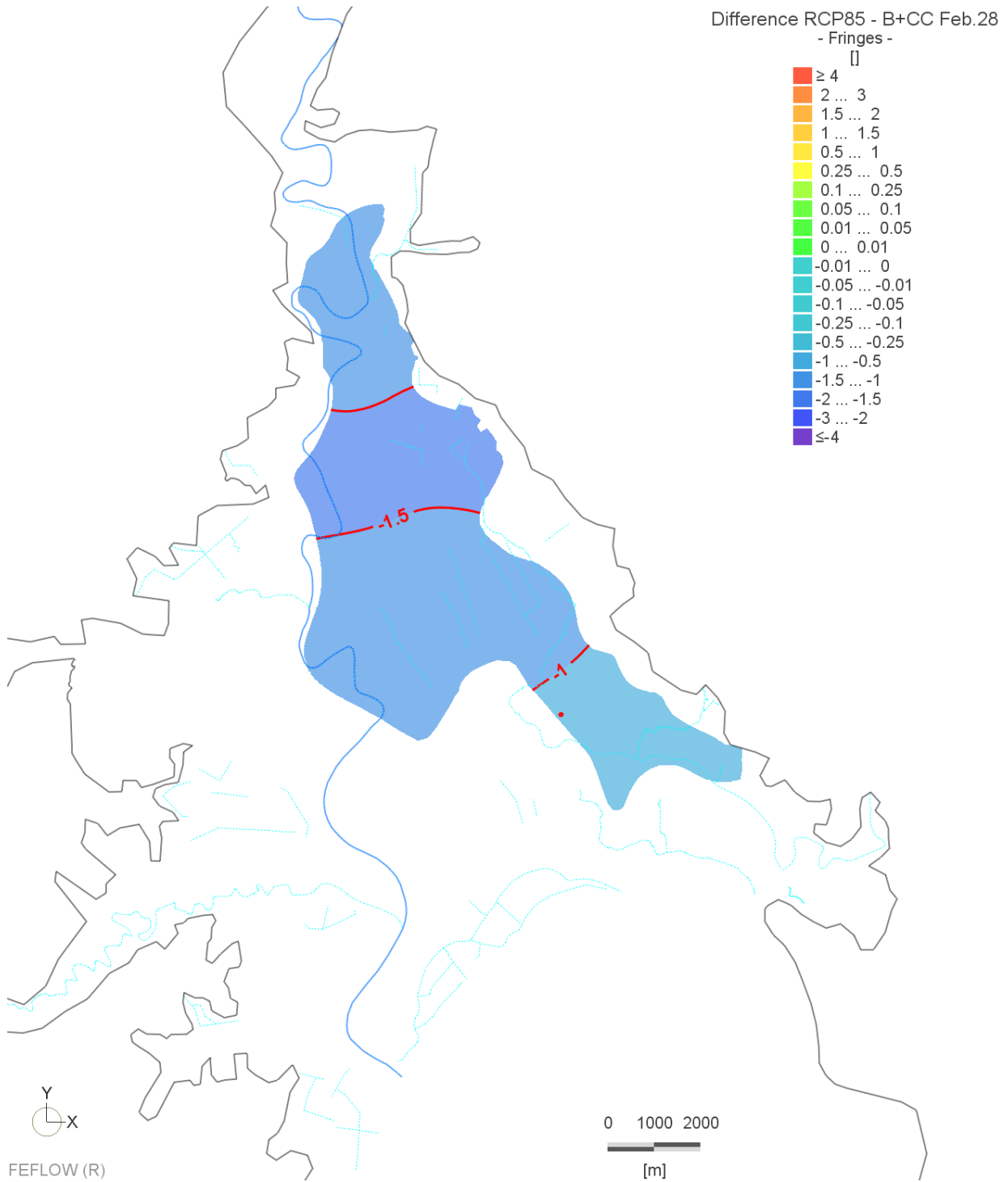


Figure A3-55: Legacy scenarios: Difference between scenarios 8 and 2, Matokitoki aquifer, summer

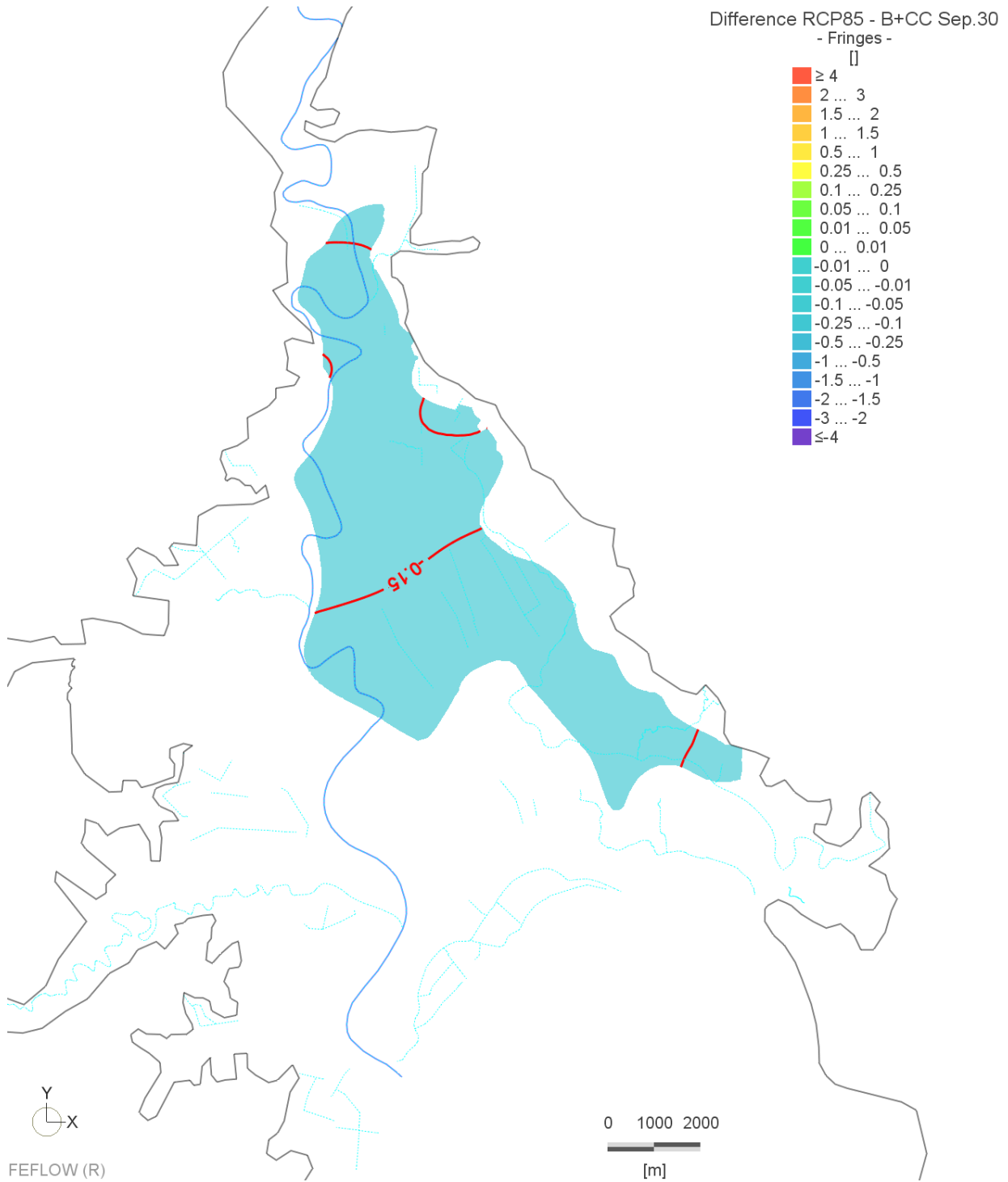


Figure A3-56: Legacy scenarios: Difference between scenarios 8 and 2, Matokitoki aquifer, winter

Scenario 9

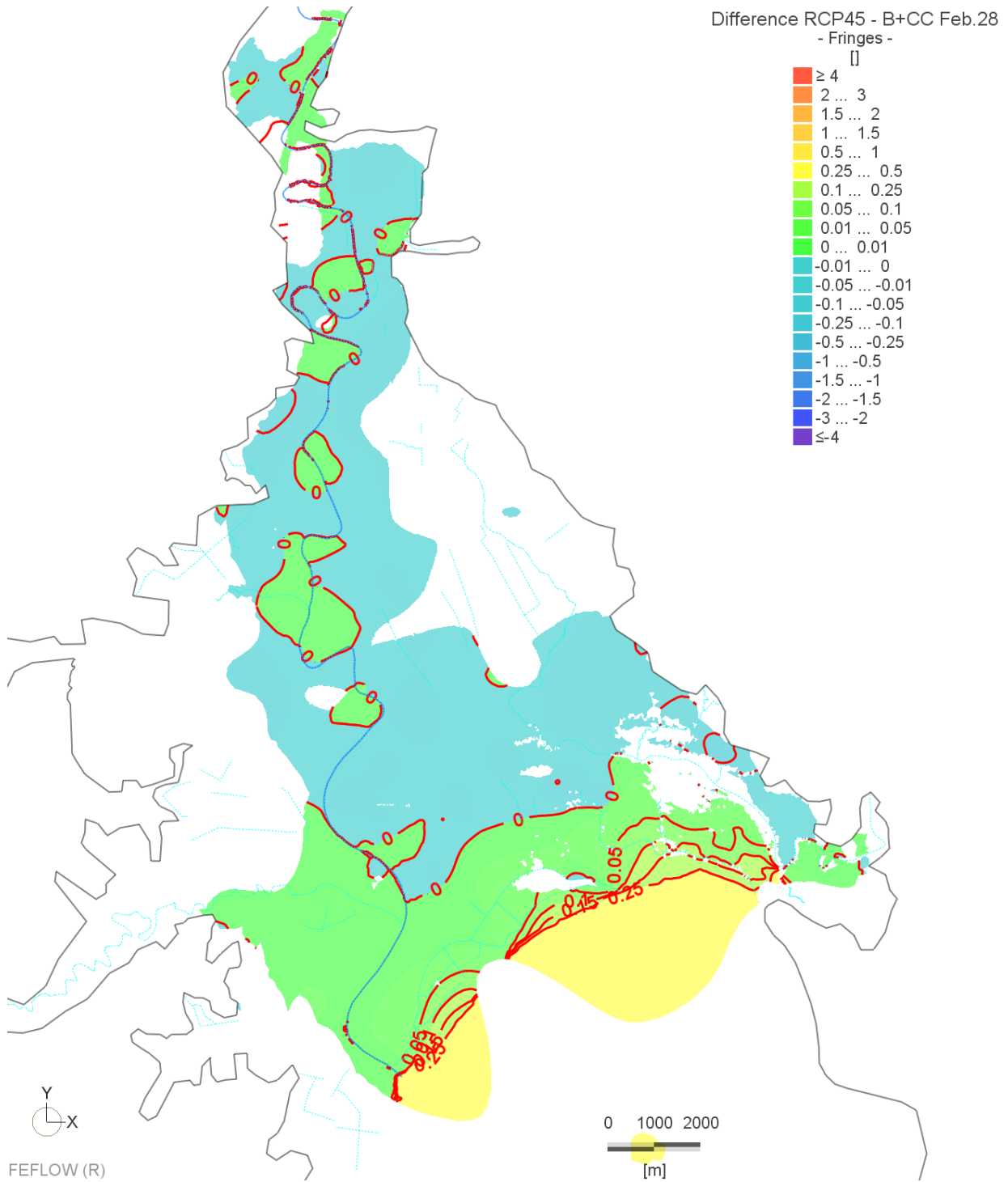


Figure A3-57: Legacy scenarios: Difference between scenarios 9 and 2, shallow aquifers, summer

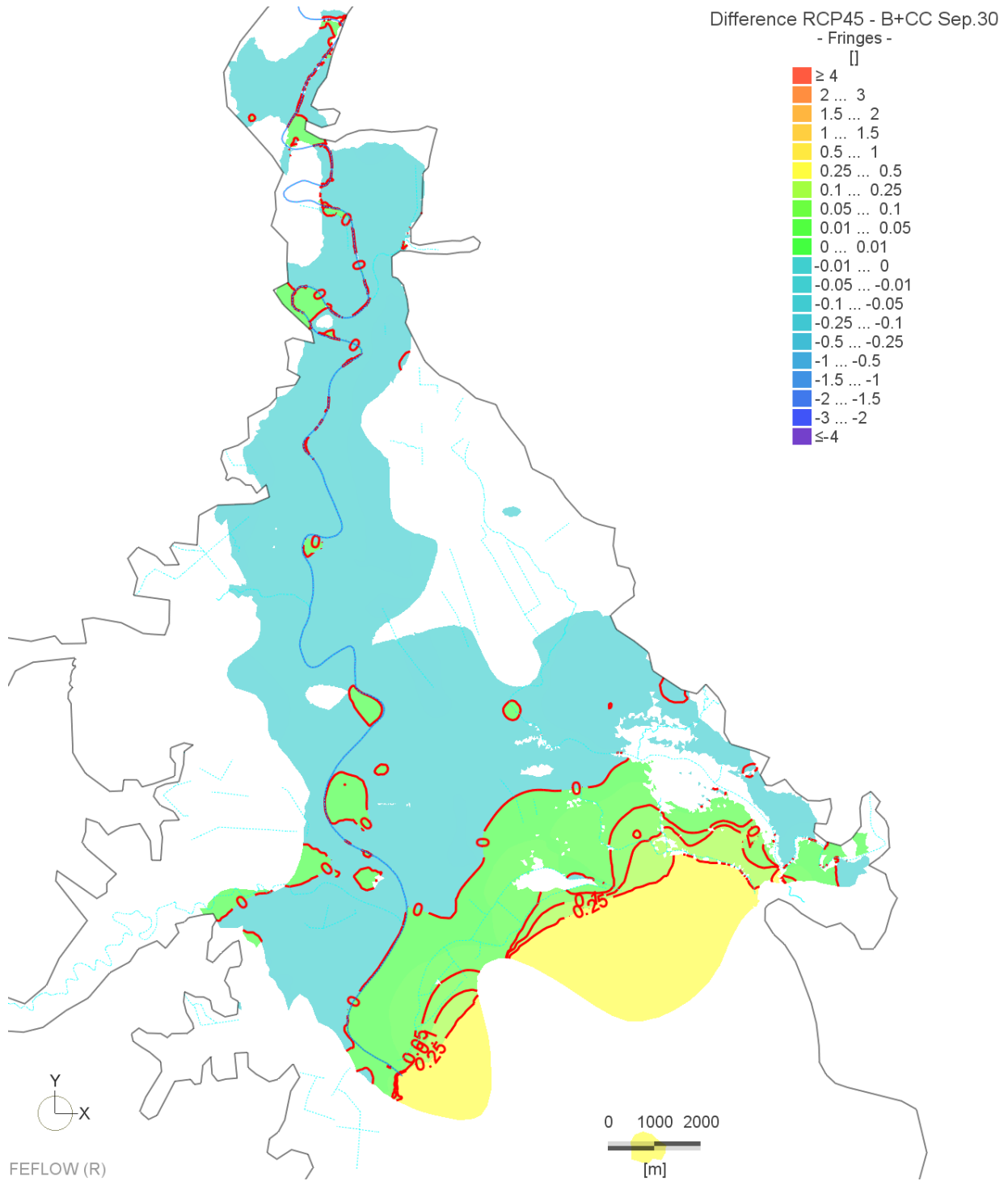


Figure A3-58: Legacy scenarios: Difference between scenarios 9 and 2, shallow aquifers, winter

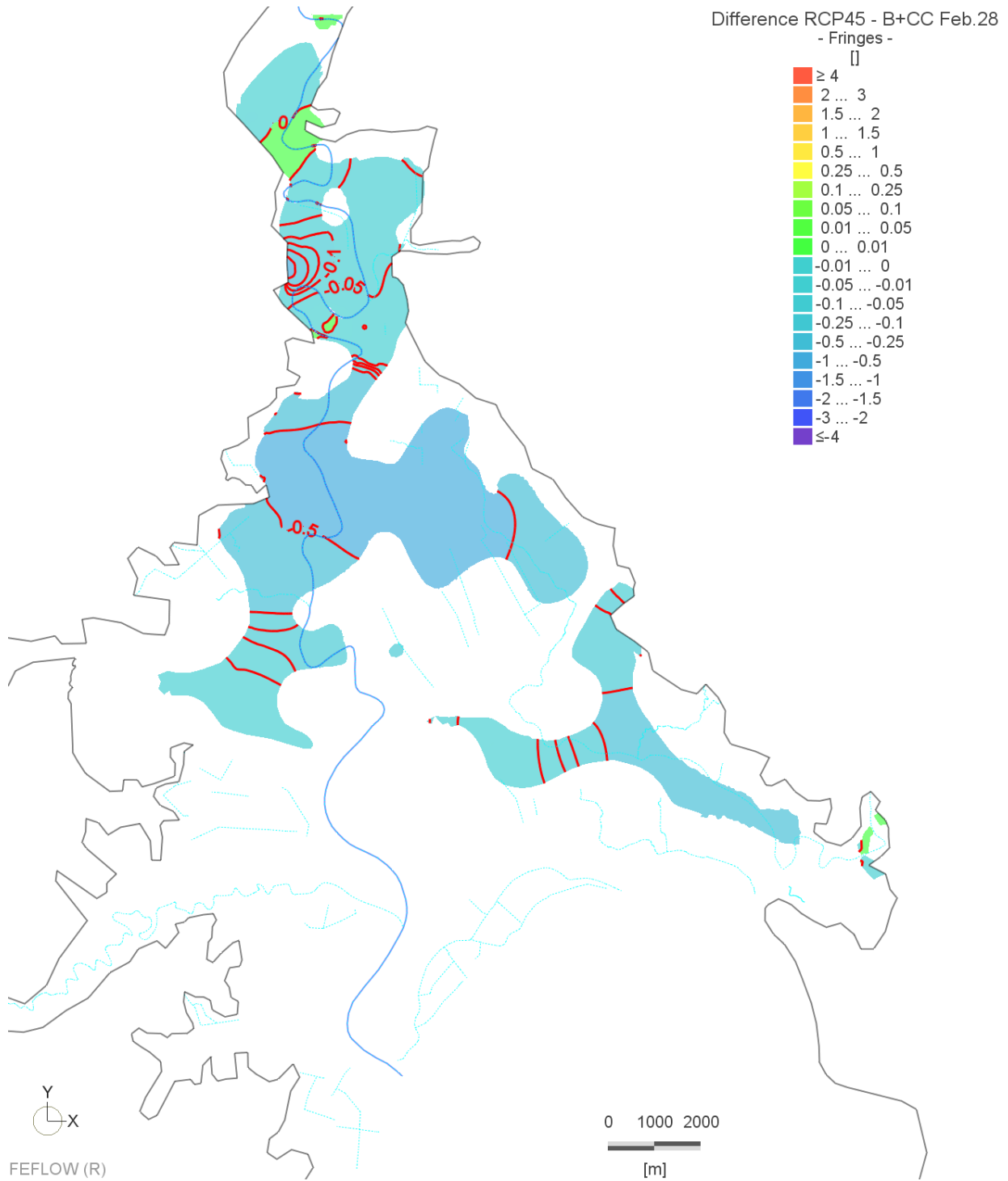


Figure A3-59: Legacy scenarios: Difference between scenarios 9 and 2, Waipaoa aquifer, summer

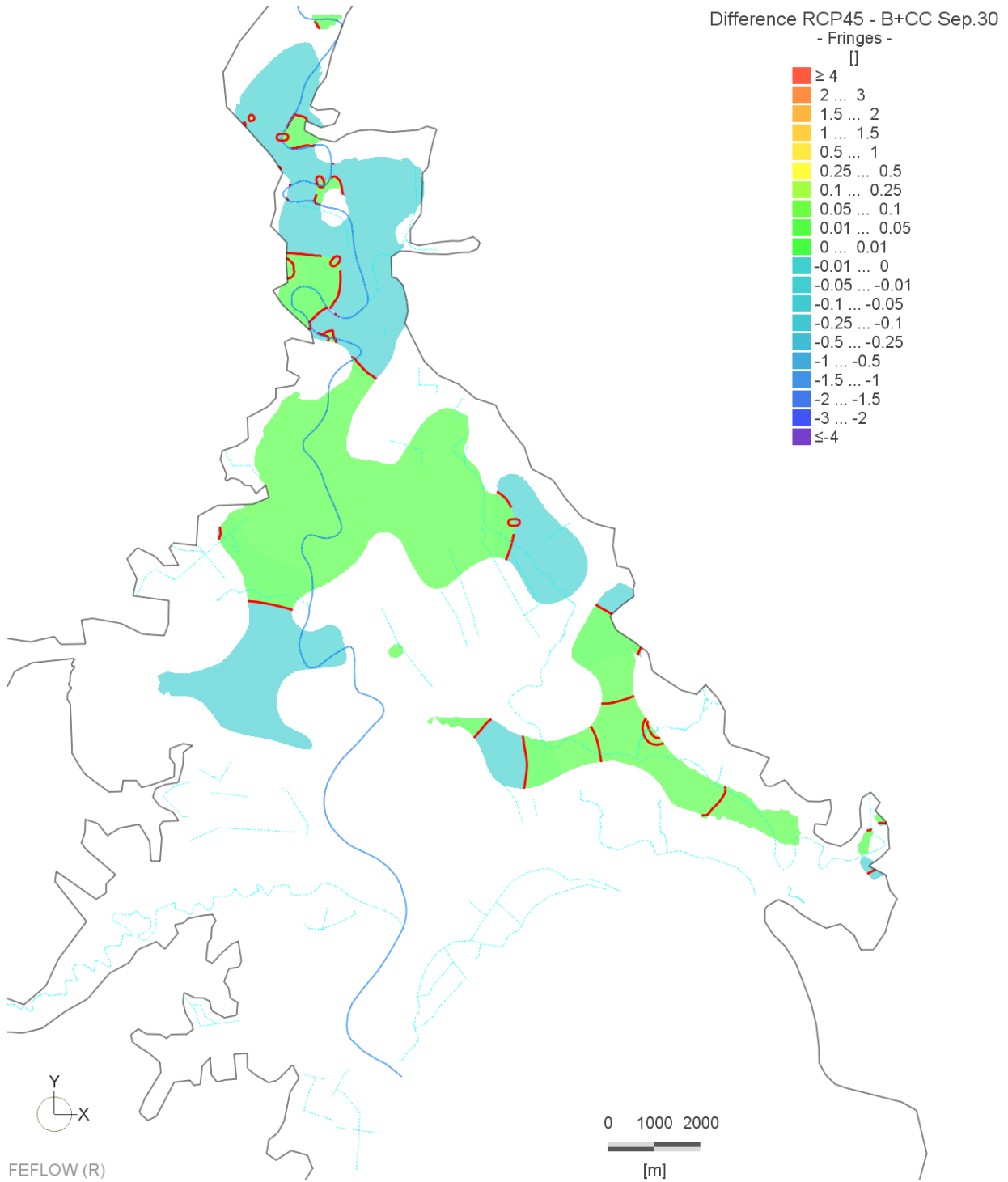


Figure A3-60: Legacy scenarios: Difference between scenarios 9 and 2, Waipaoa aquifer, winter

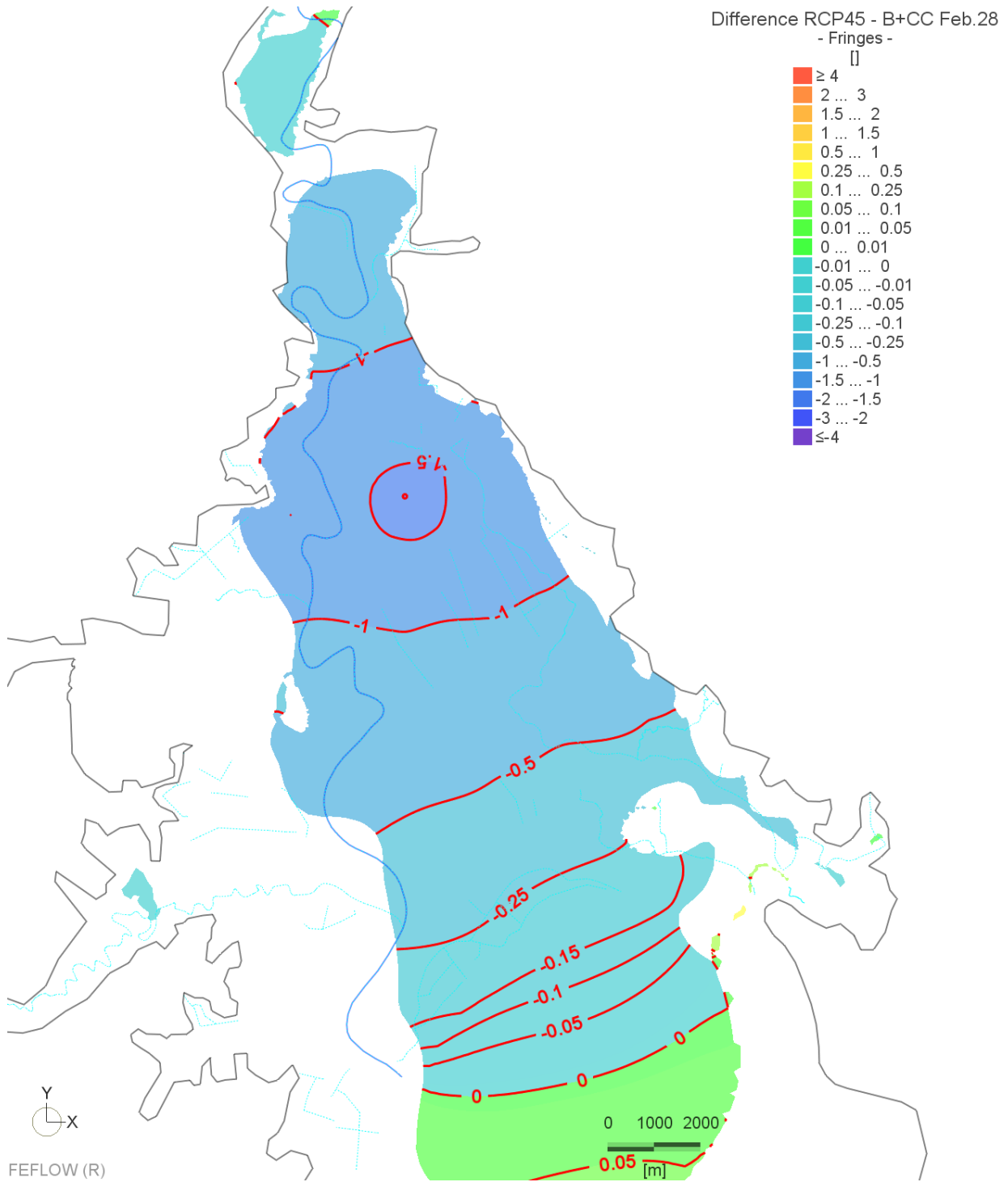


Figure A3-61: Legacy scenarios: Difference between scenarios 9 and 2, Makauri aquifer, summer

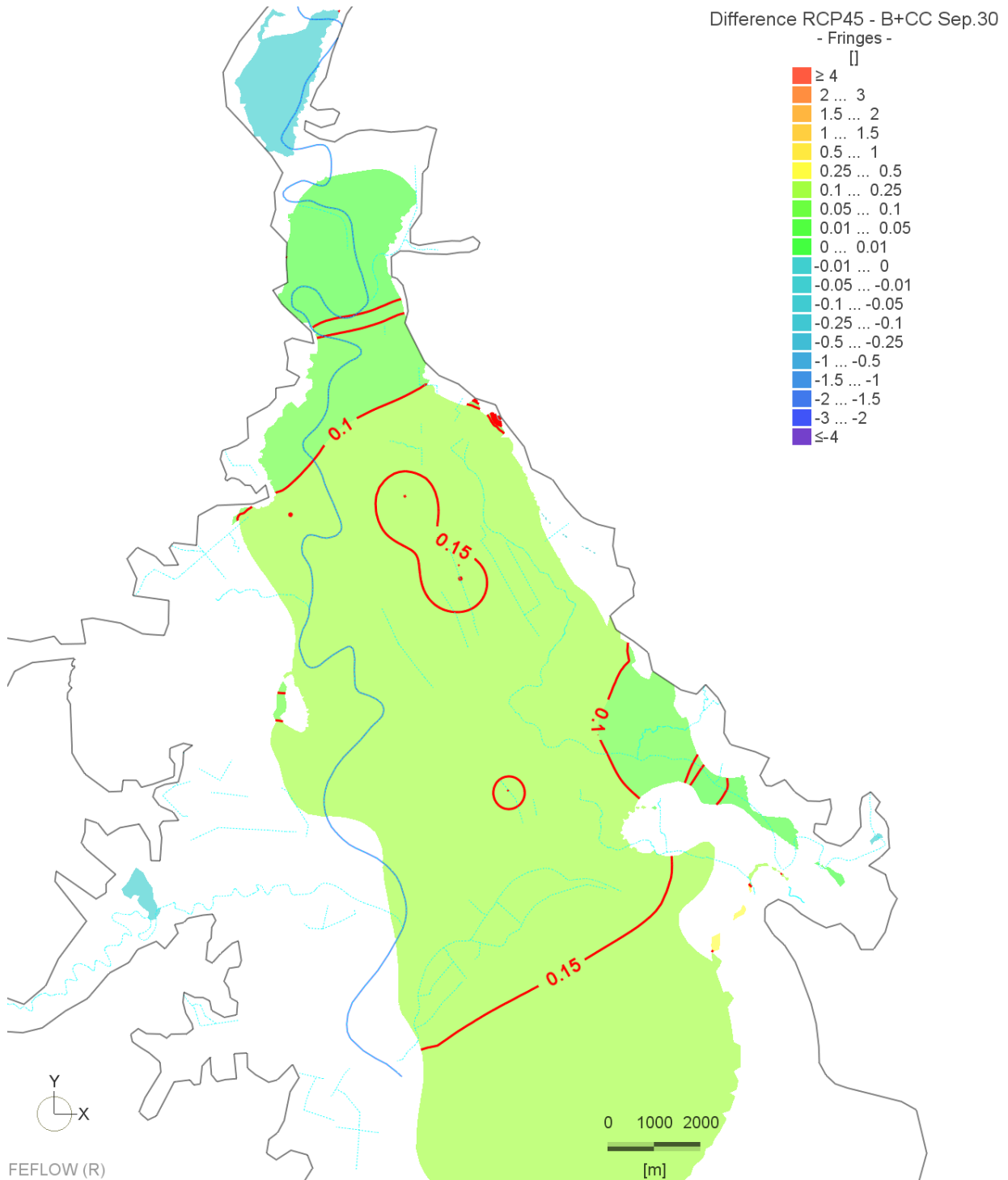


Figure A3-62: Legacy scenarios: Difference between scenarios 9 and 2, Makauri aquifer, winter

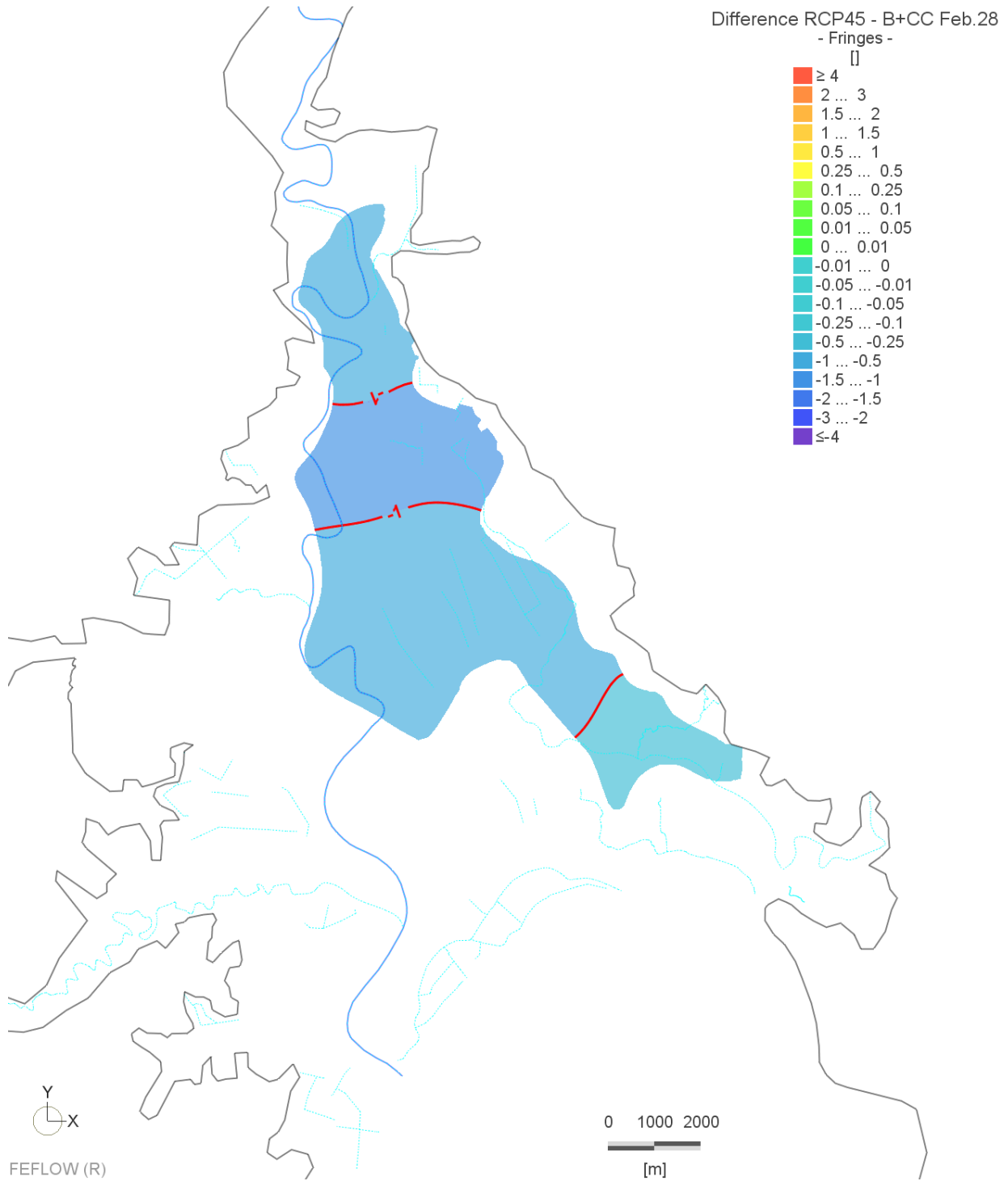


Figure A3-63: Legacy scenarios: Difference between scenarios 9 and 2, Matokitoki aquifer, summer

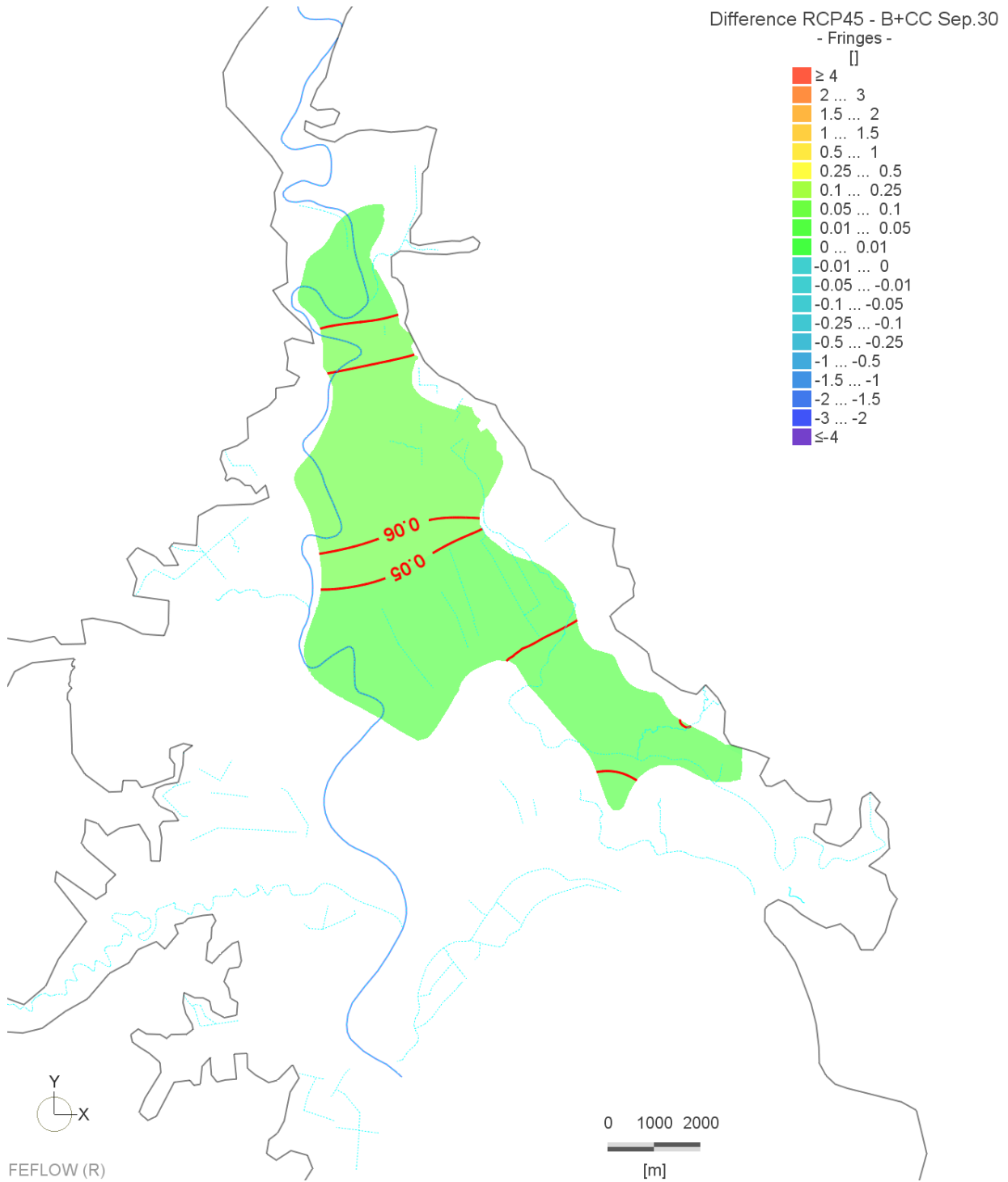


Figure A3-64: Legacy scenarios: Difference between scenarios 9 and 2, Matokitoki aquifer, winter